SPACE RESEARCH CENTRE
POLISH ACADEMY OF SCIENCES

OBSERVATOIRE DE PARIS
SYSTÈMES DE RÉFÉRENCE TEMPS-ESPACE
UMR8630 / CNRS

Earth dynamics and reference systems: five years after the adoption of the IAU 2000 Resolutions

Dynamique de la Terre et systèmes de référence : cinq ans après l'adoption des résolutions UAI 2000

Edited by

A. BRZEZIŃSKI
N. CAPITAINE
B. KOŁACZEK

JOURNÉES 2005 ☆

SYSTÈMES DE RÉFÉRENCE SPATIO - TEMPORELS

☆ WARSAW, 19-21 SEPTEMBER

ISBN 2-901057-53-5

ISBN 83-89439-60-3

TABLE OF CONTENTS

PREFACE

The "Journées 2005, Systèmes de référence spatio-temporels", with the sub-title "Earth dynamics and reference systems: five years after the adoption of the IAU 2000 Resolutions" have been held at the Space Research Centre of the Polish Academy of Sciences in Warsaw from 19 to 21 September 2005. These Journées were the seventeenth conference in this series, organized in Paris (1988 to 1992 and 1994 1996, 1998, 2000 and 2004), and the following European cities: Warsaw (1995), Prague (1997), Dresden (1999), Brussels (2001), Bucharest (2002) and St. Petersburg (2003). These Journées were organized for the second time in Warsaw, after ten years. The conference was organized in close cooperation between the Space Research Centre of PAS and Paris Observatory. The Journées 2005 were held under the patronage of the French Minister of European Affairs.

In 2005, we have received financial support from the Scientific Council of Paris Observatory, the French Embassy in Warsaw, the Committee of Geodesy of the Polish Academy of Sciences. The Space Research Centre of PAS offered the conference rooms and all facilities of the Space Research Centre building where the conference was held, free of charge. The Proceedings have been published thanks to the financial support of Department SYRTE of Paris Observatory. We are grateful to these institutions for their support.

There were 93 participants from 19 countries, among which 13 received a financial support for their participation in the conference. A financial support was also provided to PhD and post-doc researchers in the framework of the European "Descartes-nutation" project, who were invited to present their results in a special session of the conference. During the reception offered to the participants at the Polish Academy of Sciences, "Descartes-nutation" diploma were given to those young researchers by V. Dehant, Chair of the project Committee.

In agreement with the the sub-title of the Journées 2005, the main goal of the Conference was to discuss Earth dynamics and reference systems, five years after the adoption of the IAU 2000 Resolutions. The five sessions were devoted to:

1. Celestial and terrestrial reference systems;
2. Precession, nutation and polar motion;
3. Excitation of Earth rotation by geophysical fluids;
4. Time and time transfer: recent developments and projects;
5. Global reference frames and Earth rotation: impact of the gravitational satellite missions, new techniques, new international projects.

The scientific programme of the meeting included 15 invited papers, 33 oral and 35 poster presentations. The proceedings are divided into 5 sections corresponding to the sessions of the meeting. The Table of Contents is given on pages iii to vi, the list of participants on pages viii and ix and the scientific programme on pages x to xv. The Postface on page 297 gives the announcement of the "Journées 2007" in Paris.

The Proceedings of the Journées 2005 are also available on electronic form at:
http://jsr2005.cbk.waw.pl and http://syrte.obspm.fr/journees2005/.

We express our thanks to the Scientific Organizing Committee for its valuable help in preparing the scientific programme and chairing the sessions, and to all the authors of papers for their valuable contributions. We thank the Local Organizing Committee for their very efficient work before and during the meeting, especially Dr. Jolanta Nastula, Secretary of the LOC, and the staff of the the Space Research Centre of PAS as well for their kind welcome in their institute. We are grateful to Olivier Becker and Anna Korbacz for their efficient technical help for the publication.

The organizers of the "Journées 2005",

A. BRZEZIŃSKI, N. CAPITAINE, B. KOŁACZEK

October 2006

List of Participants

Altamimi Zuheir, *Institut Géographique National, LAREG, France*, altamimi@ensg.ign.fr
Andersen Per Helge , *FFI, Norway*, per-helge.Andersen@ffi.no
Andrei Alexandre Humberto, *Observatório Nacional / MCT, Brasil*, oat1@on.br
Arias Felicitas Elisa , *BIPM, France*, farias@bipm.org
Badescu Octavian, *Astronomical Institute of Romanian Academy, Romania*, octavian@aira.astro.ro
Baran Włodzimierz, *University of Warmia and Mazury in Olsztyn, Poland*, baran@uni.olsztyn.pl
Barkin Yury, *SAI MSU, Russia*, yuri.barkin@ua.es
Bizouard Christian, *Observatoire de Paris - SYRTE, France*, christian.bizouard@obspm.fr
Boboltz David, *U.S. Naval Observatory, USA*, dboboltz@usno.navy.mil
Bolotin Sergei, *Main Astronomical Observatory of NAS, Ukraine*, bolotin@mao.kiev.ua
Bouquillon Sebastien, *Observatoire de Paris - SYRTE, France*, sebastien.bouquillon@obspm.fr
Bourda Geraldine, *Observatoire de Paris - SYRTE, France*, bourda@syrte.obspm.fr
Brzeziński Aleksander, *Space Research Centre of PAS, Poland*, alek@cbk.waw.pl
Capitaine Nicole, *Observatoire de Paris - SYRTE, France*, nicole.capitaine@obspm.fr
Chapanov Yavor, *Central Laboratory for Geodesy, Bulgaria*, chapanov@clg.bas.bg
Charlot Patrick, *Observatoire de Bordeaux, France*, charlot@obs.u-bordeaux1.fr
Damljanovic Goran, *Astronomical Observatory, Serbia*, gdamljanovic@aob.bg.ac.yu
Débarbat Suzanne, *Observatoire de Paris - SYRTE, France*, suzanne.debarbat@obspm.fr
Defraigne Pascale, *Royal Observatory of Belgium, Belgium*, p.defraigne@oma.be
Dehant Veronique, *Observatoire Royal de Belgique, Belgium*, v.dehant@oma.be
Dermanis Athanasios, *The Aristotle University of Thessaloniki, Greece*, dermanis@topo.auth.gr
Englich Sigrid, *Institute of Geodesy and Geophysics, Austria*, senglich@mars.hg.tuwien.ac.at
Fey Alan, *U.S. Naval Observatory, USA*, afey@usno.navy.mil
Folgueira Marta, *Universidad Complutense de Madrid, Spain*, martafl@mat.ucm.es
Fukushima Toshio, *National Astronomical Observatory, Japan*, Toshio.Fukushima@nao.ac.jp
Gambis Daniel, *Observatoire de Paris - SYRTE, France*, daniel.gambis@obspm.fr
Grzyb Małgorzata, *Institute of Geodesy and Cartography, Poland*, malgorzata.grzyb@igik.edu.pl
Hestroffer Daniel, *IMCCE - Observatoire de Paris, France*, Daniel.Hestroffer@imcce.fr
Hilton James, *U.S. Naval Observatory, USA*, jhilton@aa.usno.navy.mil
Hohenkerk Catherine, *HM Nautical Almanach Office, RAL, United Kingdom*, cyh@nao.rl.ac.uk
Kalarus Maciej, *Space Research Centre of PAS, Poland*, kalma@cbk.waw.pl
Klügel Thomas, *BKG, Fundamentalstation Wettzell, Germany*, kluegel@wettzell.ifag.de
Kołaczek Barbara, *Space Research Centre of PAS, Poland*, kolaczek@cbk.waw.pl
Koot Laurence, *Royal Observatory of Belgium, Belgium*, laurence.koot@oma.be
Korsun' Alla , *Main Astronomical Observatory of NAS, Ukraine*, akorsun@mao.kiev.ua
Kosek Wiesław, *Space Research Centre of PAS, Poland* , kosek@cbk.waw.pl
Kovalevsky Jean, *Observatoire de la Côte d'Azur, France*, jean.kovalevsky@obs-azur.fr
Krankowski Andrzej, *Institute of Geodesy, University of Warmia and Mazury in Olsztyn, Poland*, kand@uwm.edu.pl
Kruczyk Michał, *Warsaw University of Technology, Poland* , kruczyk@gik.pw.edu.pl
Kryński Jan, *Institute of Geodesy and Cartography, Poland*, krynski@igik.edu.pl
Kudlay Oleksandr, *Main Astronomical Observatory of NAS, Ukraine*, kudlay@mao.kiev.ua
Kudryashova Maria, *Astronomical Institute of Saint-Petersburg University, Russia*, kudryashova@mercury.astro.spbu.ru
Kurzyńska Krystyna, *Astronomical Observatory of AMU, Poland*, kurzastr@amu.edu.pl
Kuzin Sergey, *Institute of Astronomy, RAS, Russia*, sk uzin@inasan.rssi.ru
Lemoine Jean-Michel, *CNES / GRGS, France*, jean-michel.lemoine@cnes.fr
Lewandowski Włodzimierz, *BIPM, France*, wlewandowski@bipm.org
Liwosz Tomasz, *Warsaw University of Technology, Poland*, tl@gik.pw.edu.pl
Luzum Brian, *U.S. Naval Observatory, USA*, bjl@maia.usno.navy.mil
Lytvyn Mykhaylo, *Main Astronomical Observatory of NAS, Ukraine*, misha@mao.kiev.ua
Lytvyn Svitlana, *Main Astronomical Observatory of NAS, Ukraine*, slytvyn@mao.kiev.ua
Masaki Yoshimitsu, *Geographical Survey Institute, Japan*, ymasaki@gsi.go.jp

McCarthy Dennis, *U.S. Naval Observatory, USA*, dmc@maia.usno.navy.mil
Medvedsky Mykhaylo, *Main Astronomical Observatory of NAS, Ukraine*, medved@mao.kiev.ua
Mouret Serge, *IMCCE - Observatoire de Paris, France*, mouret@imcce.fr
Nastula Jolanta, *Space Research Centre of PAS, Poland*, nastula@cbk.waw.pl
Nawrocki Jerzy, *Space Research Centre of PAS, Poland*, nawrocki@cbk.poznan.pl
Nedelcu Dan Alin, *Astronomical Institute of Romanian Academy, Romania*, nedelcu@aira.astro.ro
Oszczak Stanisław, *University of Warmia and Mazury in Olsztyn, Poland*, oszczak@uni.olsztyn.pl
Pashkevich Vladimir, *Astronomical Observatory of RAS, Russia*, pashvladvit@yandex.ru
Pesek Ivan, *Czech Technical University in Prague, Czech Republic*, pesekt@fsv.cvut.cz
Petrov Sergei, *Astronomical Institute of Saint-Petersburg University, Russia*, petrov@sp14272.spb.edu
Popescu Petre, *Astronomical Institute of the Romanian Academy, Romania*, petre@aira.astro.ro
Popescu Radu, *Astronomical Institute of the Romanian Academy, Romania*, pradu@aira.astro.ro
Popov Aleksey, *Astronomical Institute of Saint-Petersburg University, Russia*, aleksej@AP3678.spb.edu
Pozo Jose Maria, *Observatoire de Paris - SYRTE, France*, pozo@danof.obspm.fr
Rogowski Jerzy, *Warsaw University of Technology, Poland*, jbr@gik.pw.edu.pl
Ron Cyril, *Astronomical Institute AS CR, Czech Republic*, ron@ig.cas.cz
Rothacher Markus, *GeoForschungsZentrum Potsdam (GFZ), Germany*, rothacher@gfz-potsdam.de
Rutkowska Miłosława, *Space Research Centre of PAS, Poland*, Milena@cbk.waw.pl
Rzeszótko Alicja, *Space Research Centre of PAS, Poland*, alicja@cbk.waw.pl
Salstein David, *Atmospheric and Environmental Research Inc., USA*, salstein@aer.com
Schillak Stanisław, *Space Research Centre of PAS, Poland*, sch@cbk.poznan.pl
Sekido Mamoru, *Institute of Information and Communications Technology, Japan* , sekido@nict.go.jp
Sękowski Marcin, *Institute of Geodesy and Cartography, Poland*, msek@igik.edu.pl
Shuksto Aleksey, *Saint-Petersburg State University, Russia*, shuksto@ntc-it.ru
Shuygina Nadia, *Institute of Applied Astronomy of the RAS, Russia*, nvf@quasar.ipa.nw.ru
Sidorenkov Nikolay, *Hydrometcenter of Russian Federation, Russia*, sidorenkov@mecom.ru
Šnajdrová Kristýna, *Institute of Geodesy and Geophysics, TU-Vienna, Austria*, ksnajd@mars.hg.tuwien.ac.at
Soffel Michael, *Lohrmann Observatory, TU-Dresden, Germany*, soffel@rcs.urz.tu-dresden.de
Sokolova Julia, *Institute of Applied Astronomy of RAS, Russia*, jrs@ipa.nw.ru
Soma Mitsuru, *National Astronomical Observatory of Japan, Japan*, Mitsuru.soma@nao.ac.jp
Souchay Jean, *Observatoire de Paris - SYRTE, France*, jean.souchay@obspm.fr
Stefka Vojtech, *Astronomical Institute, Czech Republic*, Stefka.Vojtech@seznma.cz
Thorandt Volkmar, *Federal Agency for Cartography and Geodesy, Germany*, volkmar.thorandt@bkg.bund.de
Titov Oleg, *Geoscience Australia, Australia*, oleg.titov@ga.gov.au
Varga Peter, *Geodetic and Geophysical Institute, Seismological Observatory, Hungary*, varga@seismology.hu
Vondrák Jan, *Astronomical Institute AS CR, Czech Republic*, vondrak@ig.cas.cz
Wallace Patrick, *Rutherford Appleton Laboratory, United Kingdom*, ptw@star.rl.ac.uk
Weber Robert, *Institute of Geodesy and Geophysics, TU-Vienna, Austria*, rweber@mars.hg.tuwien.ac.at
Wooden William, *U.S. Naval Observatory, USA*, wooden.william@usno.navy.mil
Yatskiv Yaroslav, *Main Astronomical Observatory of NAS, Ukraine*, yatskiv@mao.kiev.ua
Zieliński Janusz, *Space Research Centre of PAS, Poland*, jbz@cbk.waw.pl
Zotov Leonid, *Sternberg Astronomical Institute of Moscow State University, Russia*, tempus@sai.msu.ru

SCIENTIFIC PROGRAMME

Scientific Organizing Committee: A. Brzeziński (Poland, Co-chair), N. Capitaine (France, Chair), P. Defraigne (Belgium), T. Fukushima (Japan), D. D. McCarthy (USA), M. Soffel (Germany), J. Vondrák Czech Republic), Y. Yatskiv (Ukraine)

Local Organizing Committee: W. Baran, A. Brzeziński (Vice Chair), B. Kołaczek (Chair), J. Kryński, J. Nastula (Secretary), J. Nawrocki, S. Oszczak, J. Rogowski, M. Rutkowska, S. Schillak, J. B. Zieliński

Opening Session of the Journées 2005

Monday 19 September, 10h00-10h45

Opening by Chairperson of the Local Organizing Committee : Prof. Barbara Kołaczek

Welcome addresses:

- Director of the Space Research Centre : Prof. Zbigniew Kłos
- Chairman of the Division III of the Polish Academy of Sciences - Prof. Henryk Szymczak
- Attaché pour la Science et la Technologie of French Embassy - Monsieur Pierre Michel
- Chairman of the Committee of Geodesy of the Polish Academy of Sciences - Prof. Włodzimierz Baran

Introduction to the Journées 2005:

- Scope of the history of the Journées Systèmes de Référence Spatio-Temporels - Prof. Barbara Kołaczek
- Scientific cooperation of the Paris Observatory and the Space Research Centre - Prof. Nicole Capitaine
- Presentation of the scientific programme of the Journées 2005 - Prof. Aleksander Brzeziński

Monday 19 September, 11h15-13h00

SESSION 1: CELESTIAL AND TERRESTRIAL REFERENCE SYSTEMS

1.1. Astrometry / The International Celestial Reference Frame

Chairperson: T. Fukushima

Invited

A. L. Fey - *Recent and future extension of the International Celestial Reference Frame*

J. Kovalevsky - *Prospects for an optical celestial reference frame using GAIA*

Oral

O. Titov - *On the selection of radiosources for the next ICRF realization*

Y. Yatskiv, A. Kuryanova and S. Lytvyn - *New combination solution for RS position RSC (GAO UA) 05 C 05*

A. H. Andrei, R. Vieira Martins, M. Assafin and D.N. Silva Neto - *Astrometric detection of faint companions*

Posters

M. Sekido and T. Fukushima - *VLBI delay model for radio sources at finite distance*

S. Lytvyn - *Comparison of various runs of combination solutions for constructing the GAO UA combined catalogue of RS positions*

P. Popescu, R. Popesku and A. Nadelcu - *Contribution to the establishment of local reference frames around ICRF optical sources*

G. Damljanovic - *Method of calculation to improve proper motions in declination of HIPPARCOS stars observed with Photographic Zenith Tubes*

A. V. Popov, A. S. Tsvetkov and V. V. Vityazev - *Spectral parallaxes of the TYCHO-2 stars*

S. Mouret, F. Mignard and D. Hestroffer – *Asteroid mass determination with the GAIA mission*

A. H. Andrei, V. A. D'Avila, E. Reis Neto, J. L. Penna, S. C. Boscardin and M. Assafin - *The Heliometric Astrolabe, a new instrument for solar diameter observations*

R. Popescu, P. Popescu and O. Badescu - *Comparative study between two astrogeodetic methods used in determining vertical deflection*

A. Shuksto and V. Vityazev - *Vectorial harmonics: from link of frames to stellar kinematics*

Monday 19 September, 14h00-18h00

1.2. Realization of the systems and scientific applications

Chairperson: D.D. McCarthy

Invited

Z. Altamimi - *Status of the ITRF 2004*

P. Charlot - *The European VLBI Network: a powerful instrument for high-resolution science*

Oral

S. Debarbat - *Public and scientific time at Paris Observatory: evolution over three centuries*

D. Gambis, Ch. Bizouard and M. Sail - *Earth orientation monitoring at IERS, current situation and prospects*

R. Biancale, D. Gambis, J.-M. Lemoine, J.-C. Marty, S. Loyer, L. Soudarin, T. Carlucci, N. Capitaine, Ph. Berio, D. Coulot, P. Exertier, P. Charlot and Z. Altamimi - *Global combination from Earth geodetic techniques*

Chairperson: P. Defraigne

Oral (cont.)

S. Bouquillon, J. Chapront and G. Francou - *Contribution of satellite laser ranging results to lunar laser ranging analysis*

S. Schillak and P. Michałek - *Monitoring the International Terrestrial Reference Frame 2000 by Satellite Laser Ranging in 1999-2003*

Posters

M. O. Lytvyn and O. V. Bolotina – *Determination of the collocated IERS sites coordinates with combination of GPS and SLR data*

S. P. Kuzin and S. K. Tatevian - *Determination of seasonal geocenter variations from DORIS, GPS and SLR data*

T. V. Ivanova and N. V. Shuygina - *Variations of the geopotential second order harmonics from the Lageos SLR data*

J. Kostelecky and I. Pesek - *Determination of the Earth orientation parameters and station coordinates from combination of IERS CPP data - internal comparisons*

V. Mioc, E. Pérez-Chavela and M. Stavinschi - *Equatorial satellite dynamics in Fock's relativistic model*

M. Soma - *Results from the recent lunar occultations of Upsilon Geminorum and Antares*

M. Medvedsky and V. Pap - New system for building telescope error model

K. Kurzyńska and R. Janicki - *Some remarks on accuracy of atmospheric model used in laser ranging observations*

M. Rutkowska – *The orbit estimation of Larets satellite*

Tuesday 20 September, 9h00-12h30

SESSION 2: PRECESSION, NUTATION AND POLAR MOTION

2.1. Recent developments of observation and modeling

Chairperson: A. Brzeziński

Invited

M. Rothacher, P. Steigenberger and D. Thaller - *Earth Orientation Parameters from reprocessing and combination efforts*

J. L. Hilton and N. Capitaine, J. Chapront, J.M. Ferrandiz, A. Fienga, T. Fukushima, J. Getino, P. Mathews, J.-L. Simon, M. Soffel, J. Vondrák, P. Wallace, and J. Williams - *Progress report of the IAU Working Group on Precession and the Ecliptic*

Oral

P. Wallace and N. Capitaine - *P03-based precession-nutation matrices*

T. Fukushima - *Application of manifold correction methods to numerical integration of rotational motion*

V. Pashkevich and G. Eroshkin – *Choice of the optimal spectral analysis scheme for the investigation of the Earth rotation problem*

A. Dermanis - *Compatibility of the IERS Earth rotation representation and its relation to the NRO conditions*

Chairperson: M. Soffel

Oral (cont.)

N. Capitaine, M. Folgueira and J. Souchay - *Earth rotation based on the celestial coordinates of the celestial intermediate pole*

M. V. Kudryashova and S. D. Petrov - *Diurnal/semidiurnal polar motion from VLBI observations*

W. Kosek, A. Rzeszótko and W. Popiński - *Phase variations of oscillations in the Earth Orientation Parameters detected by the wavelet technique*

Posters

J. Sokolova - *Influence of the unstable radiosources on the nutation offset estimation*

J. M. Ferrandiz and Yu. V. Barkin - *Nutations and precession of elastic Earth in angle-action variables*

Ya. Chapanov - *On the long-periodical variations of the Earth rotation*

A. Korsun' and G. Kurbasova - *Nonstability of the Earth rotation in 1833-2000 yy*

M. Soma and K. Tanikawa - *Abrupt changes of the Earth's rotation speed in ancient times*

R. R. Dasaev - *Research of evolution of oscillation of the Earth's pole*

V. V. Perepelkin - *Rotationally-oscillatory motion of the deformable Earth in case of a three body problem*

L. V. Zotov and S. L. Pasynok - *Analysis of discrepancies of the nutation theories MHB2000 and ZP2003 from VLBI observations*

Ya. Chapanov, J. Vondrák and C. Ron - *On the accuracy of the trigonometric solution for the periodical components of the polar motion*

W. Kosek and W. Popiński - *Forecasting pole coordinates data by combination of the wavelet decomposition and autocovariance prediction*

Tuesday 20 September, 13h30-17h00

2.2. Implementation of the IAU 2000 Resolutions and new nomenclature

Chairperson: J. Vondrák

Invited

N. Capitaine and C. Hohenkerk, A.H. Andrei, M. Calabretta, V. Dehant, T. Fukushima, B.Guinot, G. Kaplan, S. Klioner, J. Kovalevsky, I. Kumkova, C. Ma, D.D. Mccarthy, K.Seidelmann, P. Wallace - *Latest proposals of the IAU Working Group on Nomenclature for fundamental astronomy*

S. A. Klioner and M.H. Soffel - *Recent progress in astronomical nomenclature in the relativistic framework*

Oral

C. Hohenkerk and G. Kaplan - *Progress on the implementation of the new nomenclature in 'The Astronomical Almanac'*

M. Sękowski - *Astronomical Almanac of Institute of Geodesy and Cartography against the IAU 2000 Resolutions*

Discussion

On the status of the implementation of the IAU 2000 Resolutions and on the latest proposals of the IAU Working Group on "Nomenclature for fundamental astronomy"

Posters session

Wednesday 21 September, 9h00-12h15

2.3. Presentations of progress in the "Descartes-Nutation" projects

Chairperson: Ya. Yatskiv

Invited

V. Dehant - *Next decimal for nutation modeling*

Oral

M. Folgueira, N. Capitaine and J. Souchay - *On the research progress of Descartes-Subproject: "Advances in the integration of the equations of the Earth's rotation in the framework of the new parameters adopted by the IAU 2000 Resolutions"*

S. Bolotin - *Computation of the 'geodetic' excitation function of nutation*

M. Kalarus, B. Luzum, S. Lambert and W. Kosek - *Modelling and prediction of the FCN*

Posters

M. Folgueira, J. Souchay and N. Capitaine - *Discussion on the most adequate sets of variables for the study of the Earth's rotation in the framework of IAU 2000 Resolutions*

L. Koot, O. De Viron and V. Dehant - *Nutation model with Earth interior parameters adjusted on the time series data*

G. Bourda, J. Boehm, R. Heinkelmann and H. Schuh - *Analysis and comparison of precise long-term nutation series, strictly determined with OCCAM 6.1 VLBI software*

L. Fernandez and H. Schuh - *Polar motion excitation analysis due to global continental water redistribution*

SESSION 3: EXCITATION OF EARTH ROTATION BY GEOPHYSICAL FLUIDS

Chairperson: N. Capitaine

Invited

D. A. Salstein and J. Nastula - *Excitation of Earth rotation by geophysical fluids*

Oral

M. Thomas, H. Dobslaw and M. Soffel - *The ocean's response to solar thermal and gravitational tides and impacts on polar motion and nutation*

J. Nastula, B. Kołaczek and W. Popiński - *Comparisons of regional Hydrological Angular Momentum (HAM) of the different models*

A..Brzeziński and S. Bolotin - *Atmospheric and oceanic excitation of the free core nutation: observational evidence*

J. Vondrák and C. Ron - *Resonance effects and possible excitation of Free Core Nutation*

Yu. V. Barkin - *Pole trend due to the core ocean rising bulge and tectonic process*

Wednesday 21 September, 13h15-18h15

Chairperson: D. Salstein

Oral (cont.)

N. Sidorenkov - *Long term changes of the variance of the Earth orientation parameters and of the excitation functions*

Ch. Bizouard - *Influence of the earthquakes on the polar motion with emphasis on the Sumatra event*

P. Varga, D. Gambis, Ch. Bizouard, Z. Bus and M. Kiszely - *Tidal influence through LOD variations on the temporal distribution of earthquake occurrences*

L. Zotov - *Excitation functions reconstruction using observations of the polar motion*

Posters

Y. Masaki - *Comparison of two AAM functions calculated from NCEP/DOE and ERA-40 reanalyses data sets*

Yu. V. Barkin - *Explanation of nontidal acceleration of the Earth axial rotation*

E. A. Spiridonov and Y. V. Akimenko - *Modeling of the polar motion from data on the atmospheric and oceanic angular momenta*

O. G. Kudlay - *About excitation of wobble for 3-axis body rotation*

SESSION 4: TIME AND TIME TRANSFER: RECENT DEVELOPMENTS AND PROJECTS

Chairperson: B. Kołaczek

Invited

D. D. McCarthy - *Evolution of time scales*

E. F. Arias - *Recent improvements in international time keeping*

P. Defraigne and C. Bruyninx - *GPS time transfer: state of the art*

W. Lewandowski and J. Nawrocki - *Satellite time-transfer: recent developments and projects*

Posters

V. Solovyov, O. Tkachuk and A. Korsun' - *On local atomic time scale TA(UA)*

J. Nawrocki, P. Nogaś, R. Diak, A. Foks and D. Lemański - *TTS-3, multi-channel, multi-system GPS/GLONAS/WAAS/EGNOS receiver*

SESSION 5: GLOBAL REFERENCE FRAMES AND EARTH ROTATION: impact of the gravitational satellite missions (CHAMP, GRACE, GOCE), new techniques (ring laser etc.), new international projects (IAG-GGOS, GALILEO)

Chairperson: V. Dehant

Invited

T. Klüegel, U. Schreiber, A. Velikoseltsev, W. Schlüter and M. Rothacher - *Estimation of diurnal polar motion terms using ring laser data*

Oral

J. Kryński, A. Brzeziński and J. Nastula - *Recent development in the Global Geodetic Observing System at the IUGG Dynamic Planet 2005*

M. Rothacher - *Present status and future of the IAG Project GGOS*

J. M. Pozo and B. Coll - *Some properties of emission coordinates*

A. Krankowski, W. Kosek, T. Hobiger and H. Schuh - *Wavelet analysis in TEC measurements obtained using dual-frequency space and satellite techniques*

Posters

R. Weber and S. Englich - *Potential contribution of GALILEO to the TRF and the determination of ERPs*

CLOSING SESSION

Session 1.1

CELESTIAL AND TERRESTRIAL REFERENCE SYSTEMS:
Astrometry / The International Celestial Reference Frame

SYSTEMES DE REFERENCE CELESTE ET TERRESTRE :
Astrométrie / Le Système International de Référence Céleste

THE STATUS AND FUTURE OF THE ICRF

A.L. Fey
U.S. Naval Observatory
3450 Massachusetts Avenue, NW
Washington, DC 20392-5420 USA
e-mail: afey@usno.navy.mil

ABSTRACT. The International Celestial Reference Frame is currently defined by the radio positions of 212 extragalactic objects. Since its inception there have been two extensions to the ICRF. These extensions included revised positions of ICRF candidate and "other" sources, based on inclusion of additional observations, as well as positions of an additional 109 "new" sources. With continued applicable VLBI observations and improvements in analysis a better realization of the ICRF is now possible and an even better realization is feasible in the foreseeable future. Planning for a second realization of the ICRF is currently underway with a projected completion date concurrent with the 2009 IAU General Assembly. Within the next decade, optical astrometric satellites will present serious competition to the radio based ICRF. Reevaluation of the spectral regime at which the ICRF is defined will then be necessary.

1. THE STATUS OF THE ICRF

At the XXIII General Assembly of the International Astronomical Union (IAU) held on 20 August 1997 in Kyoto, Japan, the International Celestial Reference Frame (ICRF) [9] was adopted as the fundamental celestial reference frame. As a consequence, the definitions of the axes of the celestial reference system are no longer related to the equator or the ecliptic but have been superseded by the defining coordinates of the ICRF. The ICRF is currently defined by the radio positions of 212 extragalactic objects obtained using the technique of Very Long Baseline Interferometry (VLBI) at frequencies of 2.3 and 8.4 GHz over the past 20+ years. The positional accuracy of the ICRF sources is better than about 1 mas in both coordinates. The ICRF "defining" sources set the direction of the ICRS axes and were chosen based on their observing histories and the stability and accuracy of their position estimates. The sky distribution of the ICRF defining sources is shown in Figure 1. In addition to the 212 defining sources, positions for 294 less observed candidate sources along with 102 less suitable "other" sources were also given by [9] to densify the frame. The final orientation of the frame axes was obtained by a rotation of the positions into the system of the International Celestial Reference System (ICRS) [1] and is consistent with the FK5 J2000.0 optical system, within the limits of the latter system accuracy.

There have been two extensions [6] of the ICRF since its initial definition in 1998. The primary objectives of extending the ICRF were to provide positions for the extragalactic radio sources observed since the definition of the ICRF and to refine the positions of candidate and "other" sources using additional observations. There were 59 new sources in ICRF-Ext.1 and 50

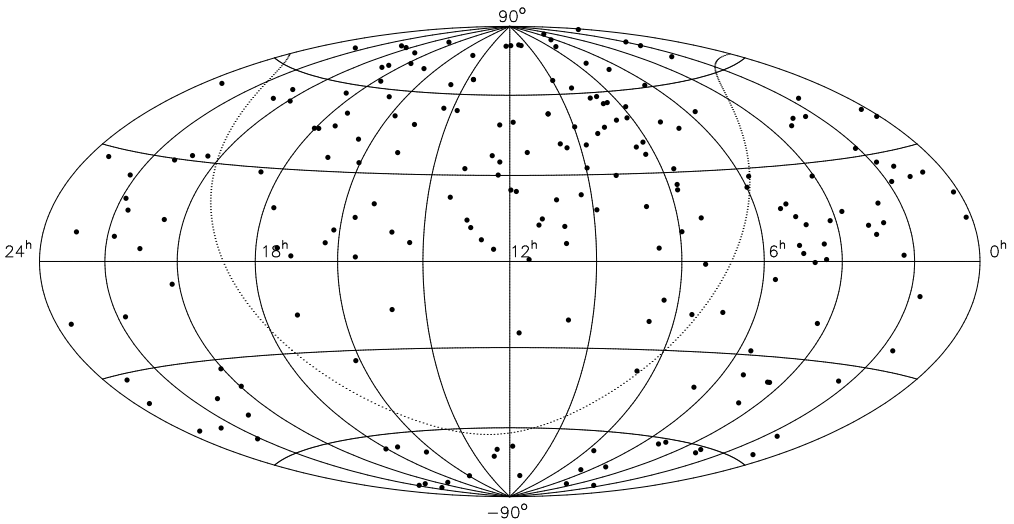

Figure 1: Distribution of the 212 ICRF Defining sources on an Aitoff equal-area projection of the celestial sphere. The dotted line represents the Galactic equator.

new sources in ICRF-Ext.2. Coordinates consistent with the ICRF were estimated for these 109 new sources. The distribution on the sky of the new sources is shown in Figure 2. Positions of the ICRF defining sources have remained unchanged.

2. ICRF MAINTENANCE

The International Astronomical Union (IAU) has charged the International Earth Rotation and Reference Systems Service (IERS) with the maintenance of the ICRF. Maintenance activities are run jointly by the IERS ICRS Product Center and the International VLBI Service (IVS).

The IERS ICRS Product Center is directly responsible for the maintenance of the ICRS and ICRF. The Center is run jointly by the Observatoire de Paris and the U.S. Naval Observatory (USNO). More information can be obtained from the Product Center Web page at `http://www.iers.org/iers/pc/icrs/`.

The IVS is an international collaboration of organizations which operate or support VLBI. The IVS provides a service which supports geodetic and astrometric work on reference systems, Earth science research, and operational activities. Many of the observing programs for maintenance of the ICRF are coordinated by the IVS. More information about the IVS can be obtained from the IVS Web page at `http://ivscc.gsfc.nasa.gov/`.

Various observing programs contribute astrometric data for maintenance of the ICRF. These include but are not limited to:

- *IVS CRF Experiments:* These $24^{\rm hr}$ duration VLBI experiments, coordinated by the IVS, concentrate primarily on observation of southern hemisphere ICRF sources for monitoring and to increase the sky density of ICRF defining sources.

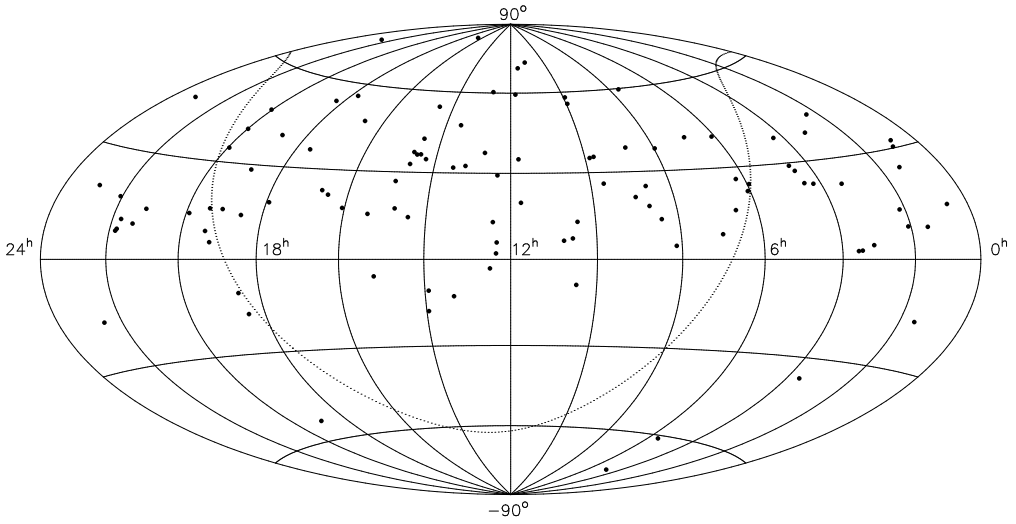

Figure 2: Distribution of the 109 new sources in ICRF-Ext.1 and ICRF-Ext.2 on an Aitoff equal-area projection of the celestial sphere. The dotted line represents the Galactic equator.

- *VLBA RDV Experiments:* These $24^{\rm hr}$ duration VLBI experiments are part of a collaborative program of geodetic and astrometric research between the USNO, Goddard Space Flight Center (GSFC) and the National Radio Astronomy Observatory (NRAO). These Very Long Baseline Array (VLBA) experiments concentrate primarily on observation of northern hemisphere ICRF sources ($\delta > -30^\circ$). Intrinsic source structure information is also obtained from these experiments.

- *IVS Geodetic/Astrometric Experiments:* These $24^{\rm hr}$ duration VLBI experiments, coordinated by the IVS, concentrate primarily on observation of sources for geodetic purposes and for Earth Orientation Parameter estimation but are also useful for astrometric purposes.

- *VLBA Calibrator Surveys:* These $24^{\rm hr}$ duration VLBI experiments are part of a joint NRAO/GSFC program to expand both the list of high quality geodetic sources and the list of phase reference calibrators for imaging.

- *EVN Experiments:* These $24^{\rm hr}$ duration VLBI experiments are part of a Bordeaux Observatory program to expand the list of ICRF defining sources in the northern hemisphere using the European VLBI Network (EVN).

- *LBA:* These $24^{\rm hr}$ duration VLBI experiments are part of a joint USNO/ATNF program to expand the list of ICRF defining sources in the southern hemisphere using the Australia Telescope National Facility (ATNF) Long Baseline Array (LBA). Intrinsic source structure information is also obtained from these experiments. The distribution on the sky of 74 new southern hemisphere sources added by this program is shown in Figure 3.

3. ASTROMETRIC ANALYSIS IMPROVEMENTS

Modeling and analysis capabilities have advanced significantly since the ICRF was defined, particularly for handling the troposphere and source structure. While the charged particle media propagation effects are effectively calibrated using two observing frequencies, the modeling of the troposphere has improved in discrete steps associated with development of new troposphere mapping algorithms [11, 12] and modeling of asymmetry and variability [10]. Current research

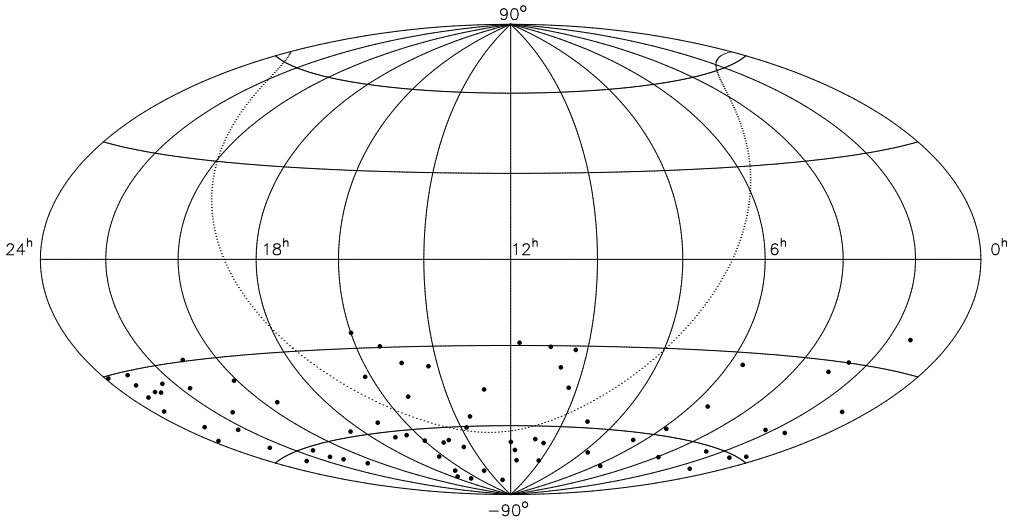

Figure 3: Distribution of 74 new southern hemisphere sources with milliarcsecond accurate astrometric VLBI positions which are now available for inclusion in the next realization of the ICRF.

is directed toward the use of global weather data in computing the mapping function through ray tracing or a proxy.

Source structure and changes in source structure put a floor on the stability of source positions. Modeling such effects has been tested on massive scales by [13]. Results of this analysis showed that the effects of intrinsic source structure on astrometric position estimation amounts to a significant fraction of the systematic error budget, thus confirming that source structure does affect VLBI analysis even though it is not currently the dominant error. An investigation of the astrometric suitability of a large sample of ICRF sources based on intrinsic source structure by [3, 4] found correlations between the observed radio structure and the astrometric position accuracy and stability of the sources indicating that the more extended sources have larger position uncertainties and are less positionally stable than the more compact sources.

Refinements in modeling the motion of the stations, especially in various loading effects, should permit the unification of analysis for the celestial reference frame, the terrestrial reference frame and Earth orientation parameters, which were separated in the ICRF analysis. As shown by [2], it should now be possible to include the station positions and velocities as global parameters (i.e. parameters dependent upon the data from all observing sessions) in the analysis without contamination of the celestial reference frame.

About one-third of the ICRF defining sources were found by [3, 4] to be somewhat spatially-extended and thus may not be appropriate for defining the celestial frame with the highest level of accuracy. This suggests that revision of source categories would be mandatory upon realization of a new ICRF. In order to address the question of finding an improved method of selecting stable and potential defining sources in a subsequent ICRF realization, [2] used position time series, computed in parallel with the ICRF-Ext.2 analysis, to derive a global source stability index based on the repeatability of the source positions from epoch to epoch. This analysis showed that over long time intervals the ICRF defining sources are not as positionally stable as could be hoped. The analysis also identified a set of sources that could potentially be better and which could be used to improve the next realization of the ICRF.

As a consequence of changes in observing strategy and networks over the lifetime of astrometric/geodetic VLBI, the stability of source positions derived from individual year data sets has improved significantly since about 1990 [7]. A considerable improvement in the ICRF can be

expected by using only the data obtained after 1990. The source stability analysis of [2] found that only about half of the available sources had sufficient data for a time series analysis. The lack of data for stability analysis is most pronounced in the southern hemisphere. Consequently, special emphasis by the IVS is now being placed on observations of the stable and potentially stable sources, especially in the southern hemisphere, identified as possible defining sources for a next realization of the ICRF.

Technical innovations incorporated into newer VLBI recording systems now allow the use of both wider spanned bandwidths and higher recorded data rates. The consequent increased sensitivity will allow observations of weaker sources not previously accessible. As these systems are more widely deployed, much higher sensitivity observations will become the norm, increasing the number of observations and increasing the number of observable radio sources.

4. THE NEXT RADIO REALIZATION OF THE ICRF

The institution of the IVS has significantly improved the organization and coordination of global geodetic/astrometric VLBI observations. With continued applicable VLBI observations and improvements in analysis, a better realization of the ICRF is now possible and an even better realization is feasible in the foreseeable future. Under the direction of the ICRS Product Center, which is responsible for the maintenance of the ICRF, planning for a second *radio* realization of the ICRF is currently underway with a projected completion date concurrent with the 2009 IAU General Assembly.

5. THE FUTURE OF THE ICRF

VLBA observations to extend the ICRF to radio frequencies of 24 GHz and 43 GHz began in 2002 May. The use of this frequency pair was motivated by the National Aeronautics and Space Administration (NASA) decision to move future spacecraft telemetry from the current 8.4 GHz to 32 GHz and the availability of 24 GHz and 43 GHz receivers on the VLBA. One of the goals of these observations was to study whether the sources were more compact at 24 GHz and 43 GHz in order to improve the astrometric accuracy at these frequencies. Initial imaging results [5] show that sources are indeed more spatially compact at these higher frequencies than those currently used for the ICRF. The initial reference frame derived from these data [8] shows agreement with the ICRF to roughly the 0.3 mas level with zonal errors dominating the differences. The accuracy of a celestial reference frame defined at these higher observing frequencies has the potential of exceeding that of the current ICRF.

In the coming decades, there will be significant advances in the area of space-based optical astrometry. Planned missions such as the NASA SIM PlaneQuest and the European Space Agency GAIA will achieve positional accuracies well beyond that presently obtained by any ground-based radio interferometric measurements. SIM PlaneQuest will be a space-based optical interferometer that will be able to determine the positions of stars with a precision approaching the microarcsecond (μas) level but is a pointed mission with a limited number of target objects and limited sensitivity. The SIM astrometric grid, which will consist almost entirely of stellar sources (and of order 100 extragalactic objects to remove the global rotation of the stellar frame), will ultimately be more accurate than the current ICRF but will not be quasi-inertial as the stars that will be observed are nearby objects in comparison to the quasars that make up the radio frame. GAIA on the other hand is planned as a survey mission and will make observations of order 10^9 objects and, with a limiting magnitude of $m_v \approx 20$, will be able to observe almost all known extragalactic sources. Because of the large number of extragalactic objects accessible by GAIA, the astrometric grid defined by GAIA can be constructed in such a way as to be quasi-inertial. If the projected accuracies for GAIA are realized, the GAIA astrometric grid will

be serious competition for the radio realization of the ICRF and must prompt reevaluation of the spectral regime at which the ICRF is defined.

References

[1] Arias, E. F., Charlot, P., Feissel, M., & Lestrade, J. –F. 1995, "The extragalactic reference system of the International Earth Rotation Service, ICRS.," A&A, 303, 604

[2] Feissel-Vernier, M. 2003, "Selecting stable extragalactic compact radio sources from the permanent astrogeodetic VLBI program," A&A, 403, 105

[3] Fey, A. L., & Charlot, P. 1997, "VLBA Observations of Radio Reference Frame Sources. II. Astrometric Suitability Based on Observed Structure," ApJS, 111, 95

[4] Fey, A. L., & Charlot, P. 2000, "VLBA Observations of Radio Reference Frame Sources. III. Astrometric Suitability of an Additional 225 Sources," ApJS, 128, 17

[5] Fey, A. L. & Boboltz, D. A., Charlot, P., Fomalont, E. B., Lanyi, G. E., Zhang, L. D. & the K-Q VLBI Survey Collaboration 2003, "Extending the ICRF to Higher Radio Frequencies - First Imaging Results," presented at Future Directions in High Resolution Astronomy: A Celebration of the 10th Anniversary of the VLBA held June 8-12, 2003, in Socorro, New Mexico, USA, to be published in the ASP Conference Series

[6] Fey, A. L., Ma, C., Arias, E. F., Charlot, P. Feissel-Vernier, M., Gontier, A. -M., Jacobs, C. S., Li, J., and MacMillan, D. S. 2004, "The Second Extension of the International Celestial Reference Frame: ICRF-EXT.2," AJ, 127, 3587

[7] Gontier, A. -M., Le Bail, K., Feissel, M., Eubanks, T. M. 2001, "Stability of the extragalactic VLBI reference frame," A&A, 375, 661

[8] Jacobs, C. S. et al. 2003, "Extending the ICRF to Higher Radio Frequencies: Astrometry," presented at Future Directions in High Resolution Astronomy: A Celebration of the 10th Anniversary of the VLBA held June 8-12, 2003, in Socorro, New Mexico, USA, to be published in the ASP Conference Series

[9] Ma, C., Arias, E. F., Eubanks, T. M., Fey, A. L., Gontier, A. –M., Jacobs, C. S., Sovers, O. J., Archinal, B. A., & Charlot, P. 1998, "The International Celestial Reference Frame as Realized by Very Long Baseline Interferometry," AJ, 116, 516

[10] MacMillan, D. S., & Ma, C. 1997, "Atmospheric gradients and the VLBI terrestrial and celestial reference frames," Geophys. Res. Lett., 24, 453

[11] Niell, A. E. 1996, "Global mapping functions for the atmosphere delay at radio wavelengths," JGR, 101, 3227

[12] Niell, A. E. & Tang, J. 2002, "Gradient Mapping Functions for VLBI and GPS," in International VLBI Service for Geodesy and Astrometry 2002 General Meeting Proceedings, edited by Nancy R. Vandenberg and Karen D. Baver, NASA/CP-2002-210002, p. 215

[13] Sovers, O. J., Charlot, P., Fey, A. L., & Gordon, D. G. 2002, "Structure Corrections in Modeling VLBI Delays for RDV Data," in International VLBI Service for Geodesy and Astrometry 2002 General Meeting Proceedings, edited by Nancy R. Vandenberg and Karen D. Baver, NASA/CP-2002-210002, p. 243

PROSPECTS FOR AN OPTICAL REFERENCE FRAME USING GAIA

J. KOVALEVSKY
Observatoire de la Côte d'Azur
Avenue Copernic, 06130 Grasse, France
jean.kovalevsky@obs-azur.fr

ABSTRACT. It is expected that at least half a million of objects, mostly QSOs, will be observed by GAIA. However, in order to build a celestial reference frame, it is necessary to identify among observations those that are without doubt extragalactic remote objects. An important effort is under way by the ESA Relativity and Reference Frames Working Group to produce tests, which will allow such an identification. About 50 000 objects will contribute to determine the reference frame and one expects to limit the remaining time dependent rotation to 0.3 μas/yr. There is a secular deformation of the frame due to the non-linear motion of the Sun. This raises the question whether the GAIA stellar positions will be in a barycentric or in a galacto-centric reference system and, in both cases, what corrections should be applied and published. Another difficulty will be to link it to the present ICRF.

1. WHAT CAN ONE EXPECT FROM GAIA?

The reduction of the cost of the GAIA project, requested by ESA in 2002, led to a major re-design of the spacecraft and the payload. The consequences are some adjustments of the expected performances as initially publicized (ESA, 2000). Although they affect only marginally the overall program, there is a significant increase of the expected uncertainties in the final astrometric parameters that will influence the final results. Let me state them.

- *Parallaxes and yearly proper motions.* For magnitude V=15, the expected accuracy is no more 10μas, but 12μas for M6V stars, increasing to 24μas for G to B stars on the main sequence. However a 20% margin is accounted for.
- *Bright stars.* The best attainable results are now 7μas rather than 4μas in positions, but, if the mission duration is 5 years, an accuracy of 10μas per year in proper motions remains possible up to magnitude 10.
- *Faint objects.* The limiting magnitude 20 may not be reached because of radiation damage.
- *Spectroscopy.* It is still expected an accuracy of 10 km/s for radial velocities at the limiting magnitude 17.
- *Photometry.* One or two channels for the medium band photometry are descoped or re-designed.

2. WHAT DID WE LEARN FROM HIPPARCOS?

The Hipparcos reference frame was constructed from the observations of 40 000 well observed single stars. The reduction procedure referred consistently the positions and proper motions to a well defined, but arbitrary, reference frame. This frame was defined in position and rotation yearly rate with a precision of 0.003 mas (ESA, 1997). This number is consistent with the 0.6 mas median error in position and 0.7 mas median error in the proper motions.

The next step was to link this reference frame to extragalactic objects so that it represents the extragalactic reference system ICRS. The problem was that no extragalactic object was observed by Hipparcos, with the exception of some 50 stars in the Magellanic clouds, which we knew have significant proper motions. It was necessary to realize independent connections between Hipparcos stars and extragalactic objects. This was essentially done using VLBI and other radio-interferometers to connect Hipparcos radiostars to ICRS, and by two epoch photographic plates to ensure the stability with respect to Galaxies (Kovalevsky and Lindegren, 1997). The final accuracy of the link was 0.25 mas/yr for each component of the rotation vector an 0.6 mas for the position of the axes at epoch.

3. CONSTRUCTION OF THE GAIA REFERENCE FRAME

As in the case of Hipparcos, the reduction procedure will provide an internally consistent, but arbitrary, reference frame. One might think that the presence of some 500 000 quasars (QSO) and active galactic nuclei (AGN) would permit to construct directly this frame in such a way that it is fixed with respect to the extragalactic objects. This should not be the case for two reasons.

1. There are almost no QSOs in a band of about $\pm 15^\circ$ width around the galactic plane, while there are stars all over the celestial sphere, thus avoiding possible systematic errors in connecting the two galactic hemispheres.

2. Because of the crucial importance of the reference frame, it is desirable to use the best observed objects, which, in this case, would be single bright stars, for instance, magnitude 13 or brighter.

This implies that, like for Hipparcos, there must be a second step, which will provide the link of the established reference frame to the assumed fixed extragalactic objects, essentially QSOs and AGNs. In what follows, I shall consider only this second step.

Since the stellar reference frame will not be fixed, the extragalactic objects will have an apparent proper motion. Assuming that these objects have either no, or randomly distributed proper motions, the apparent proper motion will have a systematic behavior produced by two different effects.

The first effect is an aberration in proper motion due to the motion of the Sun in the Galaxy (GAIA Science Advisory Group, 2000). Let $l(t)$ and $b(t)$ be respectively the galactic longitude and latitude of an object, and l and b their values at a reference time t_0. Then, one has

$$\begin{aligned} l &= l(t) - s(t-t_0) \mid \sin l(t) \mid, \\ b &= b(t) - s(t-t_0) \cos l(t) \sin b(t), \end{aligned} \tag{1}$$

where s is the coefficient of the aberration effect due to the curvature of the motion of the Sun around the center of the Galaxy. If its velocity is V, the distance of the Sun to the center of the

Galaxy is R, and c is the speed of light, then s is given by

$$s = \frac{V^2}{cR}. \tag{2}$$

The second correction represents the rotation of the reference axes. Let ω_x, ω_y, and ω_z be the rectangular components of the rotation vector Ω of the stellar system with respect to the galaxies. The total equations, including (1) written in terms of proper motions μ_l and μ_b are

$$\begin{aligned} \mu_l &= s \mid \sin l \mid \cos b - \omega_x \sin b \cos l - \omega_y \sin b \sin l + \omega_z \cos b, \\ \mu_b &= s \cos l \sin b + \omega_x \sin l - \omega_y \cos l. \end{aligned} \tag{3}$$

4. EXPECTED ACCURACY

Simulations were performed, in particular by M. Froeschlé (Kovalevsky *et al.*, 1999), to assess accuracy of the determination of the rotation of the stellar reference frame with respect to an extragalactic one. A random distribution in positions was simulated taking into account the zone of absence of $\pm 20^\circ$ on both sides of the galactic plane. A total of 170 000 QSOs and AGNs were simulated with a magnitude distribution that conformed to the actual counts, while the uncertainties of observations were those announced in 2000. The results are presented in figure 1. The

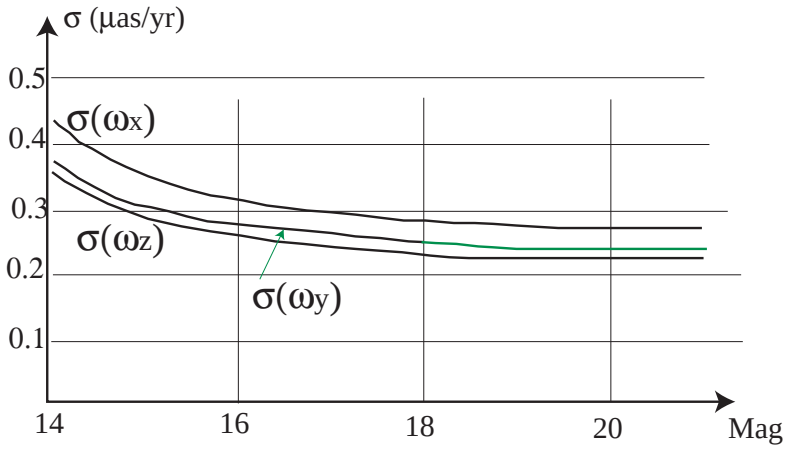

Figure 1: Uncertainties of the three components ω_x, ω_y, and ω_z of the rotation vector Ω as functions of the upper limit in magnitude.

uncertainties remain almost constant for magnitudes larger than V=18.5 despite the dramatic increase of the number of QSOs observed. Although there are about 3 times more objects than in the simulation, the conclusions remain unchanged. Table 1 gives an evaluation of the number of extragalactic objects suitable for the determination of the frame and the expected astrometric accuracy for proper motions for magnitudes larger than V= 14 with the re-designed payload. The number of stars is also given. The conclusion of the simulation is that adding objects of magnitudes larger than 19 does not change the accuracy of the results. The contribution between 18.5 and 19 is marginal. This means that taking only the 40 000 to 60 000 objects with V$<$ 18.5 is sufficient to obtain the best possible results. Taking into account that in reality there will be three times more objects than in the simulation, but that the quality of the observations is degraded, one may expect an uncertainty of 0.3 μas/yr. It is to be noted, however, that one

Table 1: Number of suitable extragalactic objects and stars and the expected accuracy in yearly proper motions

Magnitude range	Number of QSOs and AGNs	Number of stars	Expected accuracies in proper motions in μas/yr
14-15	100	15 000 000	15
15-16	700	40 000 000	25
16-17	3000	80 000 000	40
17-18	35 000	140 000 000	70
18-19	150 000	250 000 000	140
19-20	300 000	450 000 000	300

assumes that there are no systematic motions of the extragalactic large structures.

5. SORTING OUT SOURCES

A major challenge will be to ensure that the objects used in the determination of the extragalactic frame are indeed QSOs and not stars (Mignard, 2002). In the magnitude range identified in the preceding section, the ratio between the number of stars and QSOs is of the order of 5000, so that the rejection tests must be particularly effective. Evidently, a preliminary elimination will be performed by rejecting objects whose observed proper motions or parallaxes are larger than 2.5 to 3 times the expected uncertainty given in table 1, depending upon the accepted risk of rejecting quasars. But this will be by far not sufficient. The ESA Relativity and Reference Frame Working Group made considerable efforts to design efficient rejection criteria. They are based on photometric properties of QSOs (Claeskens *et al.* 2005). Actually, they are just as important for the reference frame determination as for astrophysical studies of quasars.

The tests are based on the two photometric filter systems on-board of GAIA:

1. The 5 broad band (100-150 nm) interferometry filters situated in front of the five last CCD columns of the astrometric focal plane.

2. The 11 medium band (10-80 nm) filters are situated in front of 16 CCDs in two detection areas of the focal plane of the dedicated telescope for photometry and spectroscopy (Jordi and Høg, 2005).

The main signatures of quasars are:

1. Strong emission lines, whose position in the spectrum depends on the radial velocity of the QSO;

2. An important ultra-violet excess;

3. The Lyman α break absorption.

In order to prepare the tests, a catalog of 100 000 synthetic spectra of quasars was prepared, together with samples of spectra of all types of stars, including white dwarfs and double or multiple stars. These tests were applied to simulated quasar and star observations. The main results are as follows:

- White dwarfs are efficiently rejected.

- 92% of quasars are identified at magnitude 18 and only 55% at magnitude 20.
- At magnitude 18, the star rejection rate is 99.99%. This seems very good, but as table 1 shows, more than 1000 stars may still pollute the list. The other tests will then be essential.

6. WHAT REFERENCE SYSTEM?

The first question one can ask is whether the ICRF as realized at present by VLBI is suitable to remain the defining extragalactic reference system. Originally, ICRF was stable to 0.1 mas/yr. It is still being improved and extended (Fey *et al.*, 2004) but the asymmetric and often irregular shapes limit the precise definition of a photocenter. In some cases, the shape is even changing with time (Shaffer and Marscher, 1987). So, it is very unlikely that more than an order of magnitude can ever be gained in its stability. This is far from almost three that would be necessary to match the expected accuracy of the GAIA reference frame. To link the latter to ICRF cannot be done to better than the actual accuracy of the ICRF, and this would not be acceptable.

So one is led to define a new ICRS as realized by GAIA. The intrinsic expected stability of the GAIA reference frame (0.3μas) argues in favor of such a solution. But this will imply that it will be the realization of a completely new reference system, which will coincide with the present ICRS to the accuracy of the link to the ITRF (that is to the uncertainty of the ITRF). This is not really critical since the same problem existed with the Hipparcos system versus the FK5.

As shown in section 3, in determining the reference frame, the observed positions were reduced to some fixed time t_0 by applying the time-dependent aberration due to the non-linear motion of the barycenter of the Solar system. If the result is published as such, in order to obtain the coordinates of a source at a time t one will have to apply the correction (1) for $(t_0 - t)$. This is because the system is barycentric so that it undergoes the deformation due to this effect. If the coordinates of the sources are obtained for $t = t_0$, then the GAIA reference system will be galacto-centric. The positions of the QSOs will be those that would be seen from the center of the Galaxy. So, in the publication of the positions of the extragalactic objects one must either let the user to apply the correction (1), or to include in the catalog the annual variation of their positions. In my view, the second solution is the most sensible because this applies also to stars.

Indeed, the proper motions of stars as determined with respect to the GAIA reference system must also be corrected by the same quantity. But this not all because star positions undergo a similar effect, due to the non-linear motion of the stars, so that a similar correction must be added, depending on their velocity (Kovalevsky, 2005). In the vicinity of the Sun, galactic orbits are close to that of the Sun so that the two effects cancel. But at distances from the galactic center smaller than 4-5 kiloparsecs, the stellar aberration in proper motion becomes predominant, reaching 40 μas/yr. It must be corrected. But this will be a difficult task because the velocity of the star is a function of its three dimensional position, and will have a large uncertainty at such distances from the Sun for which the parallaxes are poorly determined. Furthermore, the correction depends also upon the kinematic model of the Galaxy. Hence, in addition to the classical astrometric parameters, one will have to give an evaluation of the correction, because the user will generally not be in a position to compute it.

In conclusion, the GAIA reference system will be galacto-centric, and all corrections necessary to transform the positions and proper motions to the usual barycentric system will have to be provided for all objects of the final catalogs.

REFERENCES

Claeskens, J.-F., Smette, A. and Surdej, J., 2005, in *The Three-dimensional Universe with GAIA*, Proceedings of the Meudon Symposium, 4-7 October 2004, ESA SP-576, 667-673

ESA, 1997, *The Hipparcos and Tycho Catalogues*, ESA SP-1200, Vol. 3, 350-353

ESA, 2000, *GAIA, Composition, Formation and Evolution of the Galaxy*, ESA Report ESA-SCI (2000)4, 16-18

Fey, A.L., Ma, C., Arias, E.F., *et al.*, 2004, AJ ., 127, 3587-3608

Frey, S., 2005, in *The Three-dimensional Universe with GAIA*, Proceedings of the Meudon Symposium, 4-7 October 2004, ESA SP-576, 683-686

GAIA Science Advisory Group, 2000, in *GAIA; Composition, Formation and Evolution of the Galaxy*, ESA-SCI(2000)4, section 1.8.10, page 110

Jordi, C. and Høg, E.,2005, in *The Three-dimensional Universe with GAIA*, Proceedings of the Meudon Symposium, 4-7 October 2004, ESA SP-576, 43-50

Kovalevsky, J.,2005, in *The Three-dimensional Universe with GAIA*, Proceedings of the Meudon Symposium, 4-7 October 2004, ESA SP-576, 675-679

Kovalevsky, J., Lindegren, L., Froeschlé, M., 1999, in *Journées 1999 Systèmes de référence spatio-temporels*, Observatoire de Paris, 119-130

Kovalevsky, J., Lindegren, L., Perryman, M.A.C. *et al.*, 1997, A&A , 3230, 620-633

Mignard, F., 2002, in *GAIA: a European Space Project*, ESA Publ. Series, 2, O.Bienaymé and C. Turon *Eds*, 327-339

Shaffer, D. and Marsher, A.P., 1987, in *Superluminal radio-sources*, J.A. Zensus and T.J. Pearson (Eds), Cambridge Univ. Press, Cambridgs, 67-71

ON THE SELECTION OF RADIOSOURCES FOR THE NEXT ICRF REALIZATION

O. A. TITOV
Geoscience Australia
PO Box 378, Canberra, ACT 2615 Australia
e-mail: oleg.titov@ga.gov.au

ABSTRACT. The International Celestial Reference Frame (ICRF) is realised by high precision coordinates of a catalogue of the extragalactic radiosources observed with Very Long Baseline Interferometry (VLBI). Only radiosources with stable positions should be used in the ICRF catalogue to maintain long-term stability of the reference system. Several selection schemes have been proposed using different stability criteria. However, the problem is still open. Current daily position time series of frequently observed quasars were analysed to check the existing stability criteria. It appears that in some cases the radiosources, previously treated as 'stable', show significant variations in position on different time scales. The motions are confirmed by independent astrophysical observations. A more advanced scheme is needed for better selection of stable radiosources.

1. INTRODUCTION

Distant radiosources, quasars, are used as reference points. The radiosource positions are supposed to be stable over the long period (at least, 25 years of VLBI observations). Due to their large distance from the Earth, the quasar proper motions are negligible. However, many of the quasars demonstrate apparent positional instability. On milliarcsec level the quasars are seen as extended objects with a central core and, sometimes, several radiojets. The astrometric coordinates of an extended radiosource are treated as the centroid of its radiobrightness. Usually the radiojets move from the quasar core with superluminal velocity and rapid changes in flux density. As a result, the quasar radiobrightness centroid also varies its position. It causes apparent proper motions of the quasar on the sky plane. In this paper we show that, in opposition to the star proper motions modeled by linear function the quasar has complex apparent proper motion. Therefore, the linear approximation does not fit to the observed changes of the radiosource positions.

The apparent proper motions of radiosources, if they are not treated properly, will reduce the accuracy of the celestial reference frame. Therefore radiosources can be divided into two groups: stable and unstable objects. Positions of the 'stable' radiosources are considered as constant (global parameters) through the period covered by VLBI data. Positions of the 'unstable' radiosources are fitted independently as daily parameters. Several schemes have been developed to select stable radiosources (Ma et al., 1998; Feissel-Vernier, 2003; Fey and Charlot, 1997; Fey and Charlot, 2000). Unfortunately, many quasars are referred as 'stable' radiosources by one

criteria and 'unstable' by another one. Therefore, the determination of 'stable' radiosource is ambiguous up to now.

For operational Earth Orientation Parameter (EOP) services all radiosources imposed by their ICRF coordinates or treated as global parameters. It means that positional changes in the radiosources are not taken into account. As a result, the instability corrupts other estimated parameters due to the insufficient matrix of partials. The bias is proportional to the range of instability and the number of each radiosource scans throughout 24 hour VLBI session.

The radiosources time series of daily positions, discussed below, were estimated with OCCAM 6.1 software (Titov et al., 2001) by least squares collocation technique.

2. 2201+315

The quasar 2201+315 was classified as 'other' radiosource in the official ICRF catalogue (Ma et al., 1998) and 'stable' by Feissel-Vernier (2003). Fey and Charlot (2000) evaluated the quasar as unstable (structure index 3). The historical records used by Feissel-Vernier did not show any evidence of the 2201+315 positional instabilites. However, more recent results demonstrate the synchronous change in both coordinates after 2001.0 (Fig 1). Fig 2 shows the evolution of the 2201+315 coordinates in 2001-2004 on the sky plane as well as its approximation by 3d order polynom. The centroid of radiobrightness had moved on 500 microarcsed from its original position by the end of 2003 and returned back by the end of 2004. The positional evolution is explained by jet motion in the south-west direction over 2001-2004. The direction is confirmed by the 2201+315 radiomages in the USNO Radio Reference Frame Image Database (RRFID) (Fey and Charlot, 1997; Fey and Charlot, 2000)

3. 2145+067

The quasar 2145+067 was classified as 'defining' radiosource in the official ICRF catalogue (Ma et al., 1998) and 'unstable' by Feissel-Vernier (2003). Fey and Charlot (2000) evaluated the quasar as stable (structure index 1 or 2 for different scans). However, in the ICRF-Ext.2 it was counted as one of five unstable ICRF radiosources (Fey et al. 2004). The set of radioimages is available in the RRFID after 1994. They show a long jet in the south-east direction, moreover, structure of the jet is variable. The time series of the 2145+067 right ascension component show linear trend and quasiperiodical variations of 1.5 mas range (Fig 3), whereas its declination shows clear proper motion.

4. IMPACT ON THE NUTATION TIME SERIES

In spite of its reported positional instability the quasar 2145+067 is commonly used as geodetic radiosource for operational VLBI sessions (IRIS-A, NEOS-A, IVS-R1, IVS-R4) started in 1983. For the operational EOP analysis this radiosource is fixed or treated as 'stable', so that its coordinates are believed to be constant through the whole observational period. This approach could lead to appearance of false effects in the nutation time series with period of several years. Two different solutions have been calculated to estimate an effect of the 2145+067 instability on the nutation time series. In the first solution treated the 2145+067 positions were fixed by its ICRF2000 coordinates, in the second solution - were approximated by linear trend and harmonic variations, as shown on Fig 3. Positions of all other radiosources were fixed in both solutions. Fig 4 shows differences between the nutation time series due to the 2145+067 instability.

5. CONCLUSION

In contrast to stellar proper motions, the quasar apparent proper motions have a more complex character. The linear approximation, commonly used to model the stellar proper motions, is not suitable for modeling of the radiosource position variations.

Compactness of radiosource is usually considered as a stability criterion. However, in some cases even compact radiosources can be unstable. It is necessary to develop a combination of the statistical and astrophysical criteria for the procedure of stable radiosource selection. Unstable radiosource, being treated as stable, could bias other estimated parameters, primarily, the daily nutation offsets.

REFERENCES

Feissel-Vernier M., 2003 "Selecting stable extragalactic compact radio sources from the permanent astrogeodetic VLBI program" A&A 403, pp 105–110.

Fey A. L., Charlot P., 1997, "VLBA observations of radio reference frame sources. II. Astrometric suitability based on observed structure", AJSS 111, pp. 95–142.

Fey A. L., Charlot P., 2000, "VLBA observations of radio reference frame sources. III. Astrometric suitability of an additional 225 sources", AJSS 128, pp. 17–83.

Fey A. L., Ma C., Arias E. F., Charlot P., Feissel-Vernier M., Gontier A.-M., Jacobs C. S., Li J., MacMillan D. S., 2004, "The second extension of the international celestial reference frame: ICRF-Ext.1", AJ 127, pp. 3587–3608.

Ma C., Arias E. F., Eubanks T. M., Fey A. L., Gontier A.-M., Jacobs C. S., Sovers O. J., Archinal B. A., Charlot P., 1998, "The international celestial reference frame as realised by very long baseline interferometry", AJ 116, pp. 516–546.

Titov O., Tesmer V., Boehm J., 2001 "OCCAM Version 5.0 Software User Guide", AUSLIG Technical Report, 7, AUSLIG, Canberra.

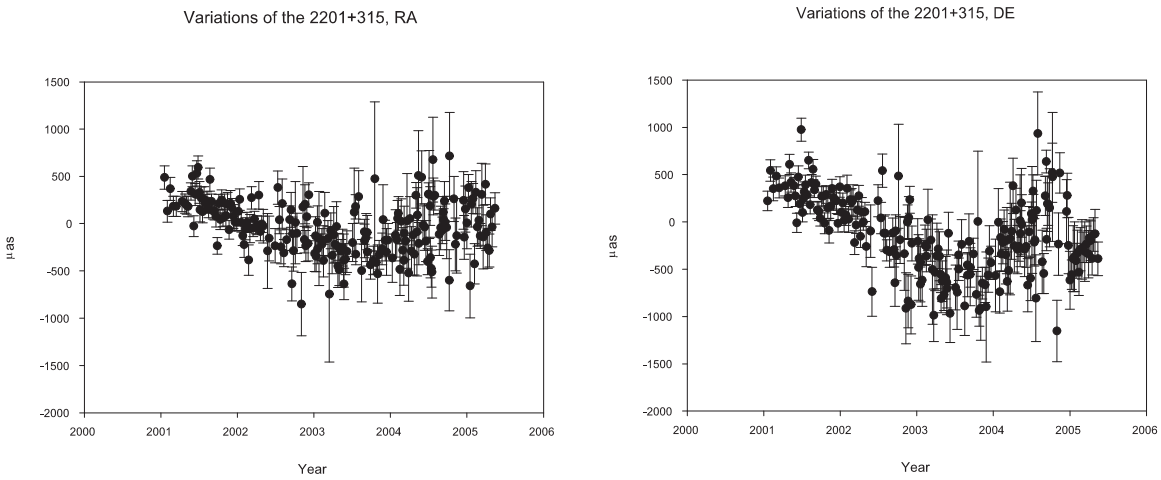

Figure 1: Time series of the quasar 2201+315 coordinates

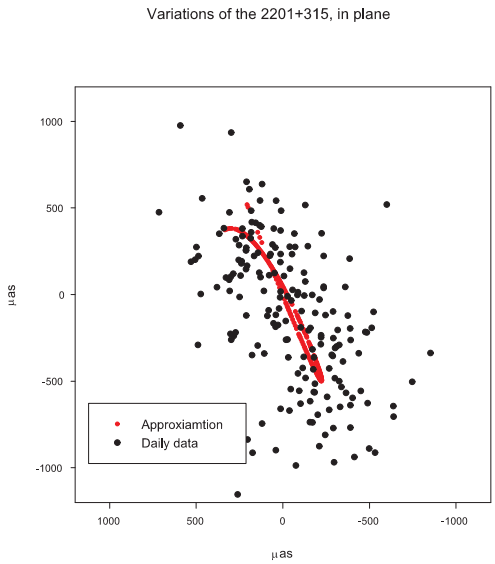

Figure 2: Evolution of the quasar 2201+315 positions on the sky plane

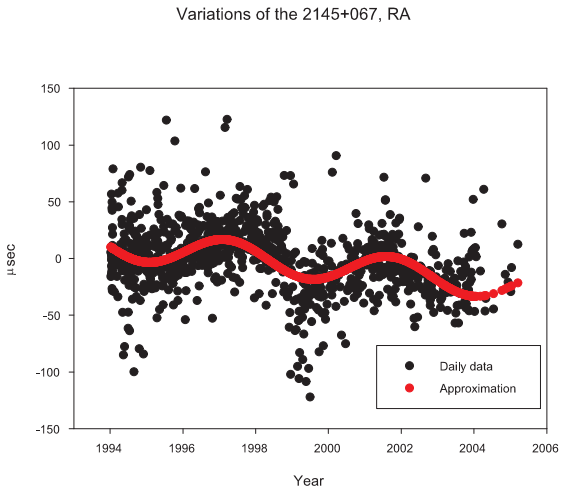

Figure 3: Time series of the quasar 2145+067 coordinates

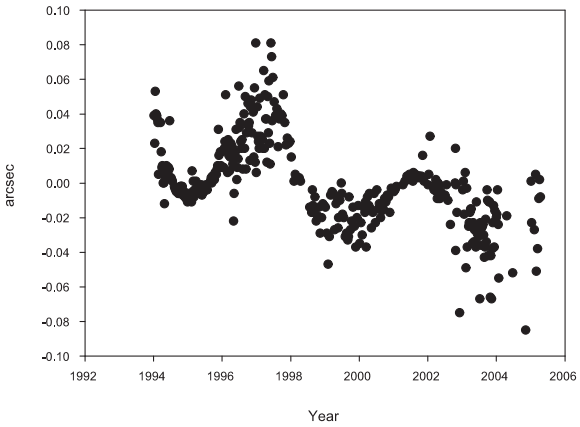

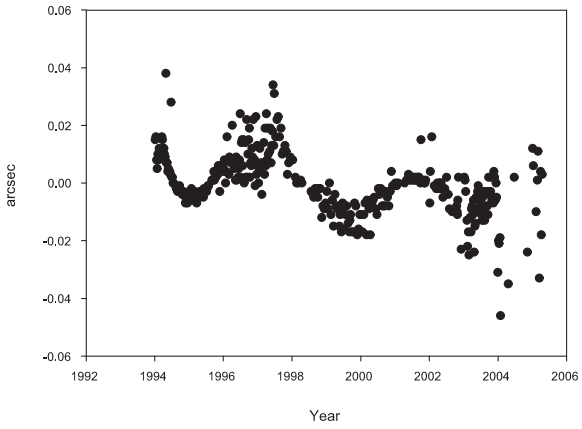

Figure 4: Effect of the quasar 2145+067 instabilities in the nutation offset time series (details in text)

NEW COMBINATION SOLUTION FOR RS POSITIONS RSC(GAOU UA)05 C 03

Y.S. YATSKIV[1], A.N. KUR'YANOVA, S.O. LYTVYN[2]
Main Astronomical Observatory National Academy of Sciences of Ukraine
27 Akademika Zabolotnoho St, 03680 Kiev, Ukraine
e-mail: [1]yatskiv@mao.kiev.ua, [2]slytvyn@mao.kiev.ua

ABSTRACT. Main Astronomical Observatory of the NAS of Ukraine is involved in the work of a redetermination of the ICRF, that was initiated by the IVS. We have carried out several combination runs based on individual catalogues provided by 8 IVS Analysis Centers and have selected the final version RSC(GAO UA)05 C 03. In comparison with the ICRF and other combined catalogues, orientation parameters and uncertainty of this new combined catalogue are given.

1. INITIAL CATALOGUES OF RS POSITIONS

In 2004 the IVS began a program to redeterminate the ICRF. The first step in February 2005 was the generation of RS catalogues in a configuration similar to the 1995 ICRF analysis. There are currently 8 initial catalogues provided by the IVS Analysis Centers (see Fig.1).

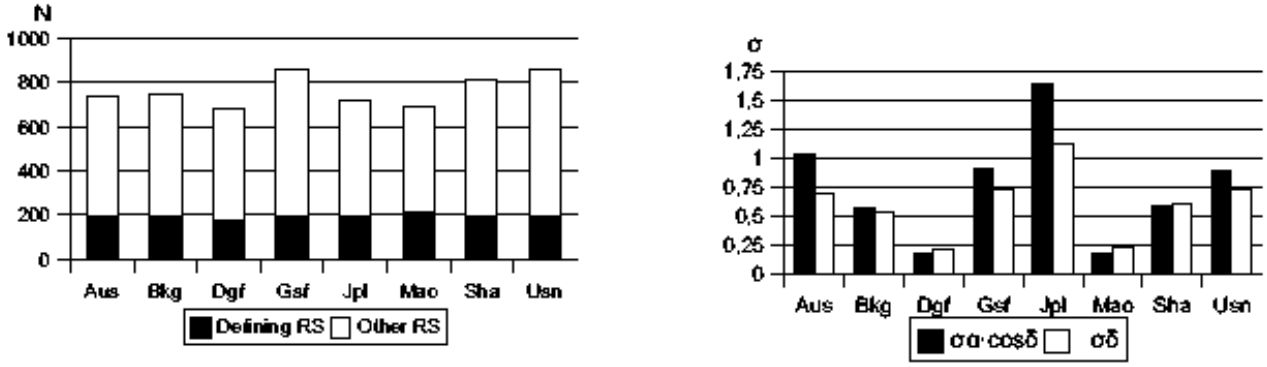

Figure 1: Number of RS (left side) and internal uncertainties (right side) for initial catalogues

2. NEW VERSION OF THE COMBINED CATALOGUE RSC(GAO UA)05 C 03

The Kyiv arc length method proposed by Y.Yatskiv and A. Kur'yanova, 1990 was used for construction of new combined catalogue. For this purpose several runs of combination solution based on initial catalogues mentioned above have been conducted and the catalogue RSC(GAO UA)05 C 03 has been selected as a final solution (see Lytvyn S., 2006).

This catalogue contains the positions of 953 RS, including 212 defining sources. The average values of positional uncertainties of defining RS are about 0,03 and 0,04 mas for RA and DEC respectively. The relative orientation and deformation parameters between the catalogue and the ICRF-Ext.1 are the following (in μas)

$$A_1 = -1 \pm 27 \quad A_2 = 2 \pm 27 \quad A_3 = -21 \pm 32.$$
$$D_\alpha = -2 \pm 1 \quad D_\delta = 0 \pm 1 \quad B_\delta = 12 \pm 24.$$

To check the quality of the RSC (GAO UA) 05 C 03 we have compared it with the ICRF-Ext.1 and the RSC(GAO UA)03 C 02 (see Yatskiv, Bolotin and Kur'yanova, 2004).

In Table 1 r.m.s. differences d_{ij}, coefficients of correlation r_{ij} between the frames, and estimated "external" uncertainties σ_i of the ICRF(σ_1), RSC(GAO UA)O3 C O2(σ_2) and the RSC(GAO UA)05 C 03(σ_3) are given.

	r.m.s.differences d_{ij}, mas			correlations r_{ij}			uncertainties, mas, on condition $r_{ij} \neq 0$		
	d_{12}	d_{13}	d_{23}	r_{12}	r_{13}	r_{23}	σ_1	σ_2	σ_3
All 584 common RS									
RA	0.54	0.44	0.39	-0.74	-0.45	-0.26	0.30	0.28	0.21
Decl	0.62	0.42	0.55	-0.73	-0.15	-0.56	0.31	0.36	0.25
211 common defining RS									
RA	0.32	0.35	0.26	-0.56	-0.69	-0.22	0.21	0.15	0.18
Decl	0.31	0.30	0.30	-0.52	-0.51	-0.47	0.18	0.17	0.17

Table 1: "External" estimations of uncertainties of the reference frames. R.M.S. differences d_{ij}, correlations r_{ij}, and uncertainties, σ_i calculated for all and for defining RSs. Indexes are used as follows: 1- ICRF, 2- RSC (GAOUA)03 C 02, 3- RSC(GAOUA)05 C 03

3. CONCLUSION

We have constructed a new combined catalogue which is internally more consistent as compared with other realisations of the ICRF.

REFERENCES

Lytvyn S., 2006. Comparison of various runs of combination solution for constructing the GAOUA combined catalogue of RS positions., Proc. Journees System de Reference Spation-Temporals, 2005. Warsaw(this volume)

Yatskiv Ya., Kur'yanova A. and Bolotin S., 2004. ICRF consistency check by comparison of the ICRF-Ext.1 with the GAOUA series of RS catalogues., Proc. Journees 2003, Astrometry, Geodynamics and Solar SyStem Dynamics: from milliarcseconds to microarcseconds, St. Petersburg (Russia), pp. 39-46.

Yatskiv Ya.S., Bolotin S.L., Kur'yanova A.N., 2004. GAOUA - realizations of celestial reference frame, Kinenatics and Phisics of Celestial Bodies, Vol. 20, No 4, pp. 291-299.

ASTROMETRIC DETECTION OF FAINT COMPANIONS

A.H. ANDREI[1,2,a], R. VIEIRA MARTINS[1,3,b] , M. ASSAFIN[2,c],
D.N. da SILVA NETO[2,d], V. ANTUNES FILHO[2,e]

[1] Observatório Nacional / MCT
R. Gal. José Cristino 77, RJ, Brasil
[2] Observatório do Valongo / UFRJ
Ladeira do Pedro Antônio 43, RJ, Brasil
[3] Observatoire de Paris / IMCCE
61 Avenue de l'Observatoire, Paris, France
e-mail: (a) oat1@on.br; (b) rvm@on.br; (c) massaf@ov.ufrj.br; (d) dario@ov.ufrj.br;
(e) valdir@ov.ufrj.br

ABSTRACT. The resolution of pairs of objects closer then the scale of seeing, and of difference of magnitude larger then ten percent is unreliable by direct imaging. The resulting image FWHM differs from a true PSF by no more then four percent. Yet, the peak of the associated Gaussian is shifted to a larger proportion. Here we present the description of the FWHM and peak location shifts as function of the seeing scale, the centers separation, and of the magnitudes difference. The shifts are hence compared to the astrometric precision nowadays derived from ground observations and reference catalogues. As case study, observations of the Pluto-Charon system are analyzed. A 0.6m telescope was used, under seeing conditions around 1.5 arcseconds, and the UCAC2 catalogue furnished the reference frame. The maximum separation of the system is 1 arcsecond and the magnitudes difference is about 2. The orbit of Charon was reconstructed from an uneven sample of 493 observations, distributed along four years.

1. THEORETICAL APPROACH

The observed flux distribution from a pointlike source can be associated to a normal distribution. Although it is not the only one possible, the Gaussian representation is of competitive efficiency, possessing the advantage of easy analytical handling. It will be used here throughout to discuss the composite image of two close sources merged by the seeing. As case test, the Pluto-Charon system is used. This was motivated by the recent campaign on the occasion of the UCAC2 2625 7135 star occultation (Sicardy et al., 2005).

Treating the Gaussian representation, without loss of generality, in one dimension, the Pluto and Charon composite flux $\mathbf{f_{P+C}(x)}$ is given by

$$f_{P+C}(x) = A_P\ exp(-x^2/(2\sigma^2))[1 + k\ exp(-{d_{PC}}^2/(2\sigma^2))\ exp((xd_{PC})/\sigma^2)] \qquad (1)$$

Where indexes **P** and **C** refer to Pluto and Charon respectively; **d** is their mutual distance; σ is the standard deviation, assumed common for the two intervening pointilike sources, as given

by the seeing (here the FWHM equal to 2.35σ); $\mathbf{A}$ is the amplitude and $\mathbf{k}$ is the Charon to Pluto amplitude ratio.

Now deriving on $\mathbf{x}$ to obtain the maximum amplitude, say, at $\mathbf{x_M}$, it is obtained

$$k(x_M - d_{PC})\ exp(d_{PC}(2x_M - d_{PC})/(2\sigma^2) + x_M = 0 \tag{2}$$

Figure 1 depicts the different Gaussians that describe the image of the Pluto-Charon pair for the condition of $\mathbf{x_M}$, and their differences. There, the data for a separation $\mathbf{d_{PC}}$=1.092 is adopted. Henceforth, $\mathbf{x_M}$=0.098; σ=1.079; and the intensity at maximum $\mathbf{I_M}$=1.093.

$$I = 1.093\ exp(-(x - 0.098)^2/(2{\times}1.079^2)) \tag{3}$$

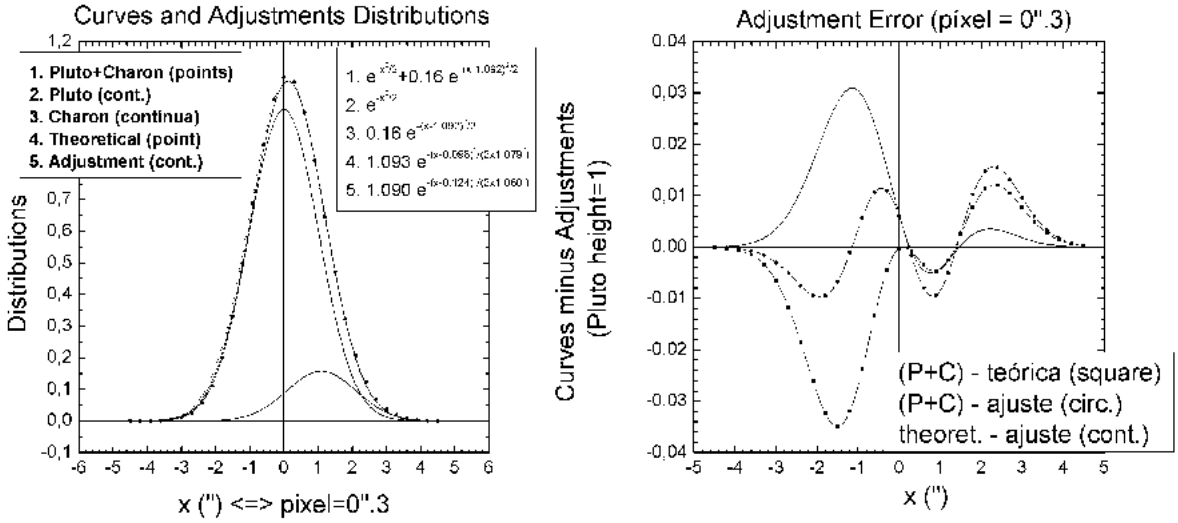

Figure 1: On the left, the intensity map (on $\mathbf{x}$) of the combined Pluto-Charon pair, plus the Gaussian curves for the Charon image, for the Pluto image, for the theoretical combination of the images, and the one adjusted to the combined images. On the right the differences between the intensity map and Gaussians relative to the combined images.

2. OBSERVATIONAL DATA

The observational data comprises 493 observations made at the LNA (Laboratório Nacional de Astrofísica/MCT, ϕ= -22° 32' 04", λ= +45° 34' 57", and h=1864m). The telescope is a 0.6m Boller & Chivens cassegrain, the pixel scale is 0".61, and the equivalent field is 10'.44 across. The typical seeing was 1".5. The data was gathered in 6 missions from 2003 to 2005. The astrometrical precision was at 45mas ($\mathbf{\Delta}\alpha\mathbf{cos}\delta$) and 44mas ($\mathbf{\Delta}\delta$).

For each observation the O-E (observed minus ephemeris) right ascension and declination residuals relatively to Pluto were calculated. The residuals distribution clearly trace the Charon orbit, as shown in the next figure.

The expressions (1) to (3) then enable to obtain the correction to go from the observed photocenter to Pluto's photocenter. Applying the photocenter correction the residuals dispersion drops from 82mas to 52mas in right ascension and from 117mas to 31mas in declination, after removing 14 observations above the 2.5σ threshold. These values are well within the astrometric

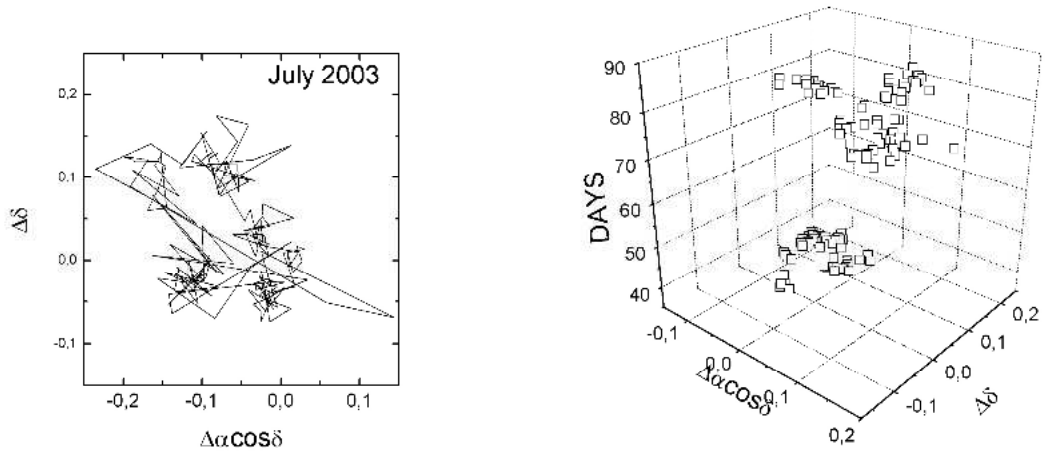

Figure 2: On the left, O-E residuals distribution for a mission covering the complete Charon orbit. On the right, time evolution of the O-E residuals along the observations.

limit stated above, indicating that the model is correct within the validity of the Pluto-Charon system data precision, that is 20mas (DE405, Standish 2005).

3. RESULTS AND CONCLUSIONS

The modern techniques of image analysis combined with the present accuracy level of the astrometric methods and reference frames open new possibilities to derive relative positions of close, dynamically tied bodies. The image analysis can reveal the small periodic variations on the amplitude, on the width, and on the location of the center from an intensity distribution seemingly created by a pointlike source.

In the present paper we discuss the simplest case where the intensity distribution is adjusted to a Gaussian distribution, and the twist of the center of the distribution is analyzed. As case study the Pluto-Charon system is examined. This was motivated by the campaign regarding the occultation of a bright, astrometrically and photometrically stable star. 493 observations, from 2003 to 2005, encompassing six missions where the period of Charon orbit was covered were either reviewed or reduced. The results show that the application of the photocenter correction effectively reduces the observed minus ephemeris residuals. The improvement is from 82mas to 52mas on right ascension and from 117mas to 31mas on declination. Charon orbit is clearly seen on the obtained plots.

Further studies are on course to establish the limits of the method, to develop analytical tools using other model distributions, and to tackle the variation on the standard deviation in two orthogonal directions. This effect drops rapidly for separations smaller than the seeing measure, but is nearly insensitive to motions of the system baricenter. Also the very Pluto-Charon case is going to be further studied by recovering and re-analyzing former observations.

REFERENCES

Sicardy B., Bellucci A., Gendron E., Lacombe F., Lacour S., Lecacheux J., Lellouch E., Renner S., Pau S., Roques F., Widemann T., Colas F., Vachier F., Ageorges N., Hainaut O., Marco O., Beisker W., Humme E., Feinstein C., Levato H., Maury A., Frappa E., Gaillard B., Lavayssière M., Di Sora M., Mallia F., Masi G., Behrend R., Carrier F., Mousis O., Rousselot P., Alvarez-

Candal A., Lazzaro D., Veiga C., Andrei A.H., Assafin M., da Silva Neto D.N., Vieira Martins R., Jacques C., Weaver D., Lecampion J.-F., Doncel F., Momiyama T., Tancredi G., 2006, "Charon: size and constraints on the atmosphere from a stellar occultation", Nature (to appear).

Standish, M., 2005, JPL DE413/Plu013 ephemeris, JPL Solar System Dynamics Group web site.

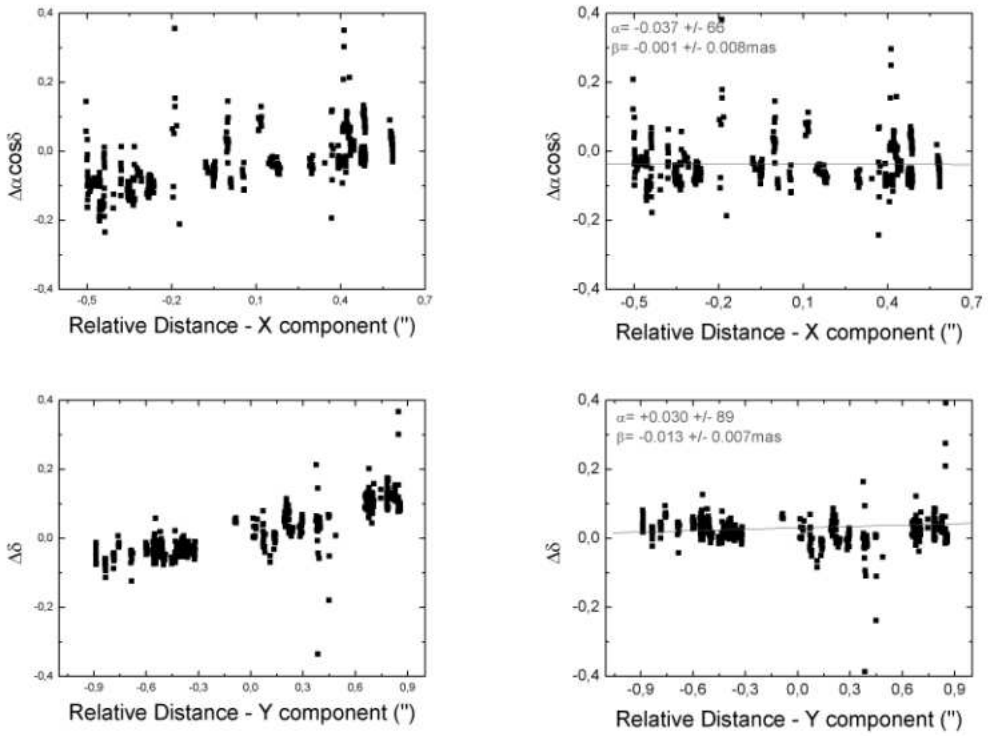

Figure 3: Plots of the O-E residuals against the relative distance Pluto-Charon, either on right ascension (X on top) or declination (Y on bottom). On the left the raw residuals are shown. On the right, the residuals after the photocenter correction; the linear (α) and angular (β) coefficients of a line fit are shown to be close to the zero level horizontal.

VLBI DELAY MODEL FOR RADIO SOURCES AT FINITE DISTANCE

M. SEKIDO[1] and T. FUKUSHIMA[2]
[1] National Institute of Information and Communications Technology
893-1 Hirai Kashima Ibaraki 314-8501, Japan
e-mail: sekido@nict.go.jp
[2] National Astronomical Observatory
2-21-1 Osawa Mitaka Tokyo, 181-8588 Japan
e-mail: Toshio.Fukushima@nao.ac.jp

ABSTRACT. A relativistic VLBI delay model for radio sources at finite distance was derived as an expansion of standard VLBI delay model (consensus model). The effect of curved wave front was taken into account up to the second order of the term $(V_2(T_2 - T_1)/R)$ by solving the delay equation with Halley's method. The VLBI observation delay in Terrestrial Time is expressed with terrestrial coordinates of observation stations and with radio source coordinates in a TDB-frame. The precision of the new delay model is 1 ps for all the Earth-based VLBI observations from Earth satellites to galactic objects. In case the radio source is farther than 10 pc away, an approximated expression of the delay model provides correction terms to adapt the consensus model for finite-distance radio sources very easily.

1. INTRODUCTION

The Very Long Baseline Interferometry (VLBI) is a powerful tool of astronomy and space geodesy with the highest angular resolution. The VLBI technique has been also used for the spacecraft navigation as its engineering application (e.g. Border, 1982). The consensus model, which is currently used as the standard VLBI delay model in the world VLBI community (MacCarthy and Petit, 2003), was derived based on the plane-wave approximation by ignoring the effect of sources' distance (Eubanks, 1991). Therefore it is inaccurate if the radio sources are at finite distance, e.g. pulsars, maser sources in our galaxy, and the difference is intolerable in the solar system. An iterative scheme to obtain the VLBI delay for finite-distance radio sources were investigated Fukushima(1994). Klioner (1991) proposed VLBI delay model with analytical formula with 1 ps accuracy. Although the delay time and the baseline vectors of these models are described in the solar system Barycentric Celestial Reference Frame (BCRF), whose time like argument is TCB (Seidelmann and Fukushima, 1992). Thus user have to convert the quantity of delay time and baseline vectors between the reference frame consistent with Terrestrial Time (TT) to that in the BCRF in that model. Although the 4-dimensional transformation is not always so simple and obvious for non-specialist. Moyer (2000) provides a VLBI delay equation for spacecraft observation, which need to be solved via numerical procedure. His model is composed of a series of procedure to get time of flight by numerical iterative solution of light time equation in BCRF or GCRF. Thus the epoch in BCRF have to be converted to station time, whose time scale is TT. However, the approach taking numerical difference of two legs of ray paths from radio sources to observers is not practical for extra solar radio sources to get accuracy of 1 ps. Motivated by potential needs to analyze the VLBI observation of interplanetary missions and

galactic sources, we developed a purely analytical model of VLBI delay for radio sources at finite distance expressed by TT time scale.

2. VLBI DELAY MODEL REPRESENTED IN TERRESTRIAL TIME

The new VLBI delay model for radio source as extension of consensus model is given by

$$(\mathrm{TT}_2 - \mathrm{TT}_1)_{\mathrm{Finite}} = \frac{-\left[1 - 2\frac{U_{\mathrm{E}}}{c^2} - \frac{\vec{V}_{\mathrm{E}}^2 + 2\vec{V}_{\mathrm{E}}\cdot\vec{w}_2}{2c^2}\right]\frac{\vec{K}\cdot\vec{b}}{c} - \frac{\vec{V}_{\mathrm{E}}\cdot\vec{b}}{c^2}\left[1 + \widehat{\vec{R}}_2\cdot\frac{\vec{V}_2}{c} - \frac{(\vec{V}_{\mathrm{E}} + 2\vec{w}_2)\cdot\vec{K}}{2c}\right] + \Delta T_{g,21}}{(1 + \widehat{\vec{R}}_2\cdot\frac{\vec{V}_2}{c})(1+H)}, \quad (1)$$

where the effect of curved wavefront is concentrated in the pseudo unit vector $\vec{K}$ defined by $\vec{K} = (\vec{R}_1 + \vec{R}_2)/(R_1 + R_2)$, $\vec{R}_i = \vec{X}_0(T_0) - \vec{X}_i(T_1)$, $i = 1, 2$. Notation 0,1, and 2 are radio source, station 1 and 2, respectively. Due to limited space of this article, please refer to a paper (Sekido and Fukushima 2005) for definitions of variables and detail of the derivation. For practical reasons, our model is intended to express delay time interval in Terrestrial Time (TT) with the baseline vector obtained by rotation transformation from that in Terrestrial Reference Frame (TRF), which is fixed to the earth, to the celestial reference system (CRS) as described in IERS conventions (MacCarthy and Petit, 2003). Radio source coordinates used in eqn. (1) are supposed to be represented in a planetary ephemeris. The precision of the delay is 1 ps for the Earth-based observation of any radio source in the "space", i.e. at the height above 100 km and more. The effect of curved wavefront was approximated up to the second order of $V_2(T_2 - T_1)/R_2$ by using Halley's method (Danby, 1988), where V_2 and R_2 is geometrical distance between station 2 and the radio source in BCRF.

When the distance to the radio source is more than 10 pc, 1 ps precision of delay prediction is available with the consensus model by just adding following correction terms.

$$c\,[(\mathrm{TT}_2 - \mathrm{TT}_1)_{\mathrm{Finite}} - (\mathrm{TT}_2 - \mathrm{TT}_1)_{\mathrm{IERS}}] = (\vec{b}\cdot\vec{p}_M)(1 - \frac{\vec{k}\cdot\vec{V}_2}{c}) - (\vec{k}\cdot\vec{b})\frac{\vec{p}_M\cdot\vec{V}_2}{c} + O(b\varepsilon^2), \quad (2)$$

where $\vec{p}_{\mathrm{M}} \equiv \{\vec{X}_M - (\vec{X}_M\cdot\vec{k})\vec{k}\}/R$, $\vec{X}_M = (\vec{X}_1(T_1) + \vec{X}_2(T_1))/2$, and R is distance to the radio source from solar system barycenter.

REFERENCES

Border J. S., F. F. Donivan, S. G. Finley, C. E. Hildebrand, B. Moultrie, and L. J. Skjerve, 1982, " Determining Spacecraft Angular Position with Delta VLBI: The Voyager Demonstration" AIAA/AAS Astrodynamics Conference Aug. 9-11, 1982 San Diego, California, AIAA-82-1471.

Danby J.M.A., 1988, "Fundamentals of Celestial Mechanics second edition", Willimann-Bell.Inc (Richmond, Virginia): p. 151.

Eubanks, T. M. , 1991, "A Consensus Model for Relativistic Effects in Geodetic VLBI", Proc. of the USNO workshop on Relativistic Models for Use in Space Geodesy, pp. 60–82.

Fukushima, T., 1994, "Lunar VLBI observation model" A&A 291, pp. 320–323.

McCarthy, D. D. and Petit, G., 2003, "IERS Conventions" Moyer, T. D., 2000, "Formulation for Observed and Computed Values of Deep Space Network Data Types for Navigation", JPL Monograph 2 (JPL Publication 00-7).

Seidelmann P. K. and Fukushima T., 1992, "Why new time scale?", A&A 265, pp. 833-838.

Sekido M., & T. Fukushima, 2005, "VLBI Delay Model for Radio Source at Finite Distance", submitted to J. Geophys. Res.

COMPARISON OF VARIOUS RUNS OF COMBINATION SOLUTION FOR CONSTRUCTING THE GAOUA COMBINED CATALOGUE OF RS POSITIONS

S.O. LYTVYN
Main Astronomical Observatory National Academy of Sciences of Ukraine
27 Akademika Zabolotnoho St, 03680 Kiev, Ukraine
e-mail: slytvyn@mao.kiev.ua

ABSTRACT. Several versions of the GAOUA type combined catalogue of radio source positions were constructed using the so-called Kiev arc length method. As a result of comparative analysis of these versions the catalogue RSC (GAOUA) 05 C 03 has been selected as final one and it was compared with previous combined catalogue of this type.

1. RESULTS OF COMPARISON

Currently the new realization of the International Celestial Reference Frame is under preparation. For this reason the construction of combined catalogue of radio source (RS) positions based on initial catalogues provided by various Analysis Centres of the IVS may be of interest. Based on eight such catalogues we have conducted several runs of combination solution for constructing the GAOUA combined catalogues using the so-called Kiev arc length method.

Different numbers of "basic" initial catalogues (see Ya. Yatskiv, et al. 2002) were used in combination process.

Frame	**N**	N_b	$\sigma_\alpha \cdot cos\delta$, **mas**	σ_δ, **mas**	Number of "basic" catalogues
RSC(GAOUA)05 C 01 (GAOUAc1)	953	212	0.03375	0.038	3
RSC(GAOUA)05 C 02 (GAOUAc2)	953	212	0.03495	0.039	4
RSC(GAOUA)05 C 03 (GAOUAc3)	953	212	0.03345	0.038	5
RSC(GAOUA)05 C 04 (GAOUAc4)	953	212	0.03315	0.038	5

Table 1: List of combined catalogues of RS positions. The first 3 catalogues have been constructed using the VLBI data since 1990, the last one is based on all available observations (since 1979). N is number of RS in frame, N_b is number of defining RS, $\sigma_\alpha cos\delta$ and σ_δ are internal uncertainties for α and δ in mas

Table 1 shows that average values of positional uncertainties do not depend on number of "basic" catalogues used in combination solutions as well as on the data collected before 1990.

Therefore we have selected the catalogue RSC(GAO UA)05 C 03 as a final solution. This catalogue has been compared with the RSC (GAOUA)03 C 02 (see Figure 1).

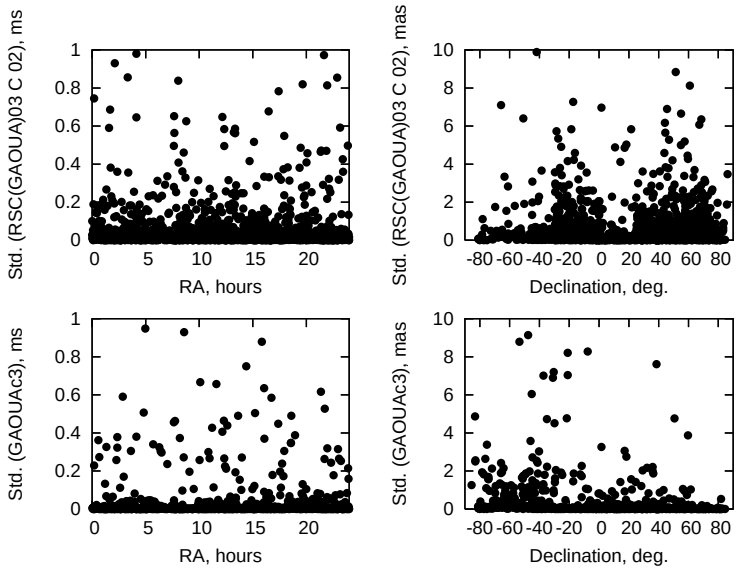

Figure 1: Positional uncertainties of RS for GAOUAc3 and RSC(GAOUA)03 C 02

2. CONCLUSIONS

The estimated uncertainties of the combined catalogues do not depend on number of "basic" catalogues used in combination solution.

The internal consistency of the combined catalogue RSC (GAOUA)05 C 03 proved to be better than for combined catalogue RSC (GAOUA)03 C 02.

REFERENCES

IVS: International VLBI Service products available electronically at ftp://ivsopar.obspm.fr/vlbi/ivs-special/icrf-next/

Kur'yanova A.N., Yatskiv Ya.S., 1993."The compiled catalogue of positions of extragalactic radio sources RSC(GAOUA)91 C 01", Kinematics and Physics of Celestial Bodies, 9, No.2, pp.15-25.

Ya.Yatskiv, O.Molotaj, A. Kur'yanova and V. Tel'nyuk-Adamchuk, 2002. "Resent compiled catalogue of radio source positions RSC(GAOUA)01 C 01", Proc. Journees Systemes de Reference Spatio-Temporels, Astrometry from Ground and Space, Bucharest (Romania), pp.60-65.

CONTRIBUTION TO THE ESTABLISHMENT OF LOCAL REFERENCE FRAMES AROUND ICRF OPTICAL SOURCES

R. POPESCU[1], P. POPESCU[1], A. NEDELCU[1]
[1] Astronomical Institute of the Romanian Academy
Str. Cuţitul de Argint, no. 5, sect. 4, RO-040558 , Bucharest, Romania
e-mail: [pradu, petre, nedelcu@aira.astro.ro]

ABSTRACT. At Bucharest Observatory we started an observational program aiming the improvement of positions for optical counterparts of ICRF radiosources by narrow-field CCD observations carried out in Belogradchik Observatory, Bulgaria (43°37′36″ E, 22°40′06′ N) using the 60-cm telescope. First results are presented in this paper.

1. INTRODUCTION

International Celestial Reference Frame is the radio realization of International Celestial Reference System and is formed by VLBI radio positions of 212 extragalactic radiosources distributed over the entire sky. In addition to the 212 defining sources were also reported : 294 candidate sources less-observed, potentially defining as more observations will become available, 102 other sources less-stable, included primarily to densify the frame and 109 new sources, based on recently VLBI observation (Fey et al. 2004).

Realization of ICRS at optical wavelengths is given by HIPPARCOS Celestial Reference Frame (HCRF). Relatively low density of objects in HCRF - 3 objects per square degree require its densification and extension to fainter magnitudes by means of ground based astrometry to allow an easier and direct access to the frame.

We started an observational program aiming:

- Improvement of positions for optical counterparts of ICRF radiosources by narrow-field CCD observation
- Accurate densification of the optical frame and extension to fainter magnitudes
- Estimation of errors in UCAC2, USNO B1.0 and 2MASS catalogs by CCD observations of ICRF sources
- Building a catalog of intermediary reference stars around ICRF optical counterparts
- Studies concerning the non-coincidence between radio and optical centers at least for ICRF extended sources.

2. OBSERVATIONS AND RESULTS

Observations were carried out in Belogradchik Observatory, Bulgaria (43°37′36″ E, 22°40′06′ N) using the 60-cm telescope equiped with 1k×1k Apogee 47P CCD camera (13μm pixel size, QE > 92% at 650 nm, Peltier cooled) leading to a resolution of 0.721”/pixel when 2×2 binned mode was used and an image size of 6.15’×6.15’. During 4 observations runs (October 2004,

February, April, July 2005) with a total of 15 clear sky nights, 101 objects have been observed.In order to derive a good statistic of data, 30 images were acquired (on average) for each object.

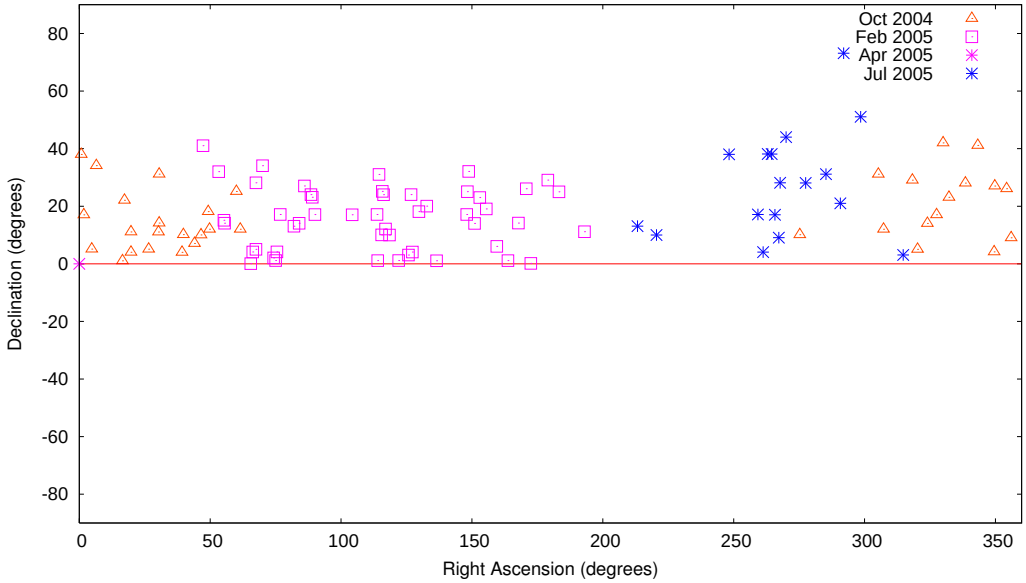

Figure 1: Sky distribution of 101 optical counterparts of ICRF sources observed during 4 runs

ICRF	USNO B1.0 - ICRF		2MASS - ICRF		UCAC2 - ICRF	
Source	$\Delta\alpha^*$	$\Delta\delta$	$\Delta\alpha^*$	$\Delta\delta$	$\Delta\alpha^*$	$\Delta\delta$
0400+258	$-260_{\pm 170}$	$260_{\pm 140}$	$-160_{\pm 160}$	$160_{\pm 160}$	$-120_{\pm 170}$	$80_{\pm 160}$
1633+382	$31_{\pm 22}$	$186_{\pm 23}$	$28_{\pm 19}$	$72_{\pm 29}$	-	-
1749+096	$29_{\pm 13}$	$151_{\pm 17}$	$6_{\pm 16}$	$77_{\pm 19}$	$13_{\pm 18}$	$-11_{\pm 19}$
1928+738	$11_{\pm 20}$	$298_{\pm 27}$	$3_{\pm 19}$	$155_{\pm 30}$	-	-
1954+513	$44_{\pm 50}$	$281_{\pm 57}$	$27_{\pm 50}$	$-27_{\pm 45}$	-	-
2059+034	$-30_{\pm 40}$	$243_{\pm 57}$	$-44_{\pm 35}$	$95_{\pm 55}$	$-100_{\pm 39}$	$40_{\pm 67}$
2200+420	$29_{\pm 41}$	$129_{\pm 34}$	$1_{\pm 28}$	$17_{\pm 31}$	$14_{\pm 29}$	$33_{\pm 35}$
2319+272	$-53_{\pm 49}$	$198_{\pm 62}$	$-56_{\pm 49}$	$86_{\pm 65}$	$-27_{\pm 48}$	$-18_{\pm 67}$

Table 1: Means and standard deviations, in *mas*, of the observed (reduced using USNO B1.0, 2MASS, UCAC2) minus ICRF coordinates for a set of data. $\Delta\alpha^* = \Delta\alpha\ cos\delta$.

For all stages of data reduction we have chosen Image Reduction and Analysis Facility - IRAF (http://iraf.noao.edu) used in batch mode analysis of data.

REFERENCES

Feissel-Vernier, M., 2003, "Selecting stable extragalactic compact radio sources from the permanent astrogeodetic VLBI program", A&A 403, 105

Fey, A. L., Ma, C., Arias, E. F., et al. 2004, " The second extension of the international celestial reference frame: ICRF-EXT.1", AJ , 127, 3587

Popescu, P., Popescu, R., et al. 2005, "Astrometry Test of MSCRED IRAF Software Package", Serb. Astron. J 170, 123

METHOD OF CALCULATION TO IMPROVE PROPER MOTIONS IN DECLINATION OF HIPPARCOS STARS OBSERVED WITH PHOTOGRAPHIC ZENITH TUBES

G. DAMLJANOVIĆ
Astronomical Observatory
Volgina 7 , 11160 Belgrade, Serbia and Montenegro
e-mail: gdamljanovic@aob.bg.ac.yu

ABSTRACT. The first astronomical satellite mission, HIPPARCOS ESA one (ESA, 1997), was less than 4 years long and finished there are more than ten years before (1991.25 is the epoch of the HIPPARCOS Catalogue). At the other hand, there are a long series of ground – based optical observations of some HIPPARCOS stars, as a different Earth rotation programmes made during interval 1899.7 – 1992.0 (Vondrák et al., 1998), useful to check or to improve some HIPPARCOS data (Vondrák, 2004). Also, the Earth Orientation Catalogue – EOC (Vondrák and Ron, 2003), based on these data, is finished. Here, the data of Photographic Zenith Tubes (PZT) were used to give better proper motions in declination than HIPPARCOS ones, and results are in good agreement with the ARIHIP ones. The ARIHIP proper motions (a combination of the HIPPARCOS and some ground – based data) are more accurate than the HIPPARCOS ones. Because of it, our calculated results were compared with the ARIHIP ones.

1. CALCULATIONS AND RESULTS

The ICRF materializes the ICRS from 1998 via a catalogue of 608 compact radio sources (Ma et al., 1998), and the HIPPARCOS Catalogue is the optical counterpart of the ICRF. The HIPPARCOS was linked to ICRS in orientation and in rotation (Kovalevsky et al., 1997).

The ARIHIP (Wielen et al., 2001) contains 90842 stars and is a selection of the best stars from the catalogues: FK6(I), FK6(III), GC+HIP, TYC2+HIP, and HIPPARCOS. The proper motion data are more accurate than the HIPPARCOS one, and because of it we compared our results with the ARIHIP ones.

As the input data, we used here the Richmond two PZTs data (RCP and RCQ), Vondrák's A00 solution (Vondrák private communication, 2002; Ron and Vondrák, 2001), and first at all removed the polar motion in line with Kostinski formula (Kulikov, 1962) and some systematic variations (local, instrumental, etc.). The residuals were averaged and got about one averaged point per year. The Least Squares Method was used. The steps of method are described in few papers (Damljanović, 2005; Damljanović and Vondrák, 2005; Damljanović and Pejović, 2005).

Calculated results were checked with the ARIHIP ones; for the stars with a long observational history (few decades) the consistency is good. For these stars, it is possible to get valid corrections of proper motions in declination of HIPPARCOS ones. For some other cases, to confirm the HIPPARCOS data. This means, the long history ground – based observations of the Earth

rotation programmes are good enough for the task to improve even the HIPPARCOS satellite data and the corresponding reference frame.

Acknowledgements. This work is a part of projects No 1468 “Structure, Kinematics and Dynamics of the Milky Way” and No 1221 “Investigations of Double and Multiple Stars” supported by the Ministry of Science and Environmental Protection of the Republic of Serbia.

REFERENCES

Damljanović, G., Pejović, N., 2005, in the Proc. of the IAU Coll. 197 "Dynamics of Populations of Planetary Systems", 469.

Damljanović, G., 2005, Serb. Astron. J., 170, 127.

Damljanović, G., Vondrák, J., 2005, in the Proc. of the Journées 2004 Systèmes de Référence Spatio – Temporels, ed. N.Capitaine, Observatoire de Paris, 230.

ESA, 1997, The Hipparcos and Tycho Catalogues, ESA SP - 1200.

Kulikov, A.K., 1962, Izmenyaemost' sirot i dolgot, Moskva.

Kovalevsky, J., Lindegren, L., Perryman, M.A.C. et al., 1997, Astron. Astrophys., 323, 620.

Ma, C. et al., 1998, Astron. J., 116, 516.

Ron, C., Vondrák, J., 2001, in Journées 2000 Systèmes de Référence Spatio – Temporels, ed. N. Capitaine, Observatoire de Paris, 201.

Vondrák, J., Pešek, I., Ron, C., Čepek, A., 1998, Earth orientation parameters 1899.7 – 1992.0 in the ICRS based on the HIPPARCOS reference frame, Astron. Inst. of the Academy of Sciences of the Czech R., Publ. No. 87.

Vondrák, J., Ron, C., 2003, in Journées 2002 Systèmes de Référence Spatio – Temporels, ed. N. Capitaine, Observatoire de Paris, 49.

Vondrák, J., 2004, Serb. Astron. J., 168, 1.

Wielen, R., Schwan, H., Dettbarn, C. et al., 2001, Veröff. Astron. Rechen – Inst. Heidelberg No. 40 (Karlsruhe: Kommissions – Verlag G.Braun).

SPECTRAL PARALLAXES OF THE TYCHO-2 STARS

A.V. POPOV, A.S. TSVETKOV, V.V. VITYAZEV
Saint-Petersburg State University
198504 Petrodvorets, Universitetsky pr., 28., S.Petersburg, Russia
e-mail: aleksej@AP3678.spb.edu

ABSTRACT. We present the spectral parallaxes for about 150 thousand stars derived from spectral types and luminosity classes of the Tycho-2 Spectral Type Catalogue. The interstellar absorption was taken into account. The comparison of the derived spectral parallaxes with trigonometric parallaxes from Hipparcos catalogue was made. For the majority of stars the accuracy of the spectral parallaxes was found to be 1-5 mas depending on the spectral type.

1. PROCEDURE.

In this paper, the Hipparcos catalogue [1]is a source of the trigonometrical parallaxes. The Tycho-2 catalogue [2] provides the m, $B-V$, positions and proper motions. The Tycho-2 Spectral Type catalogue [3] contains the spectral types and luminosity classes of the stars. Combination of these catalogues gives us a good opportunity to derive the spectral parallaxes for at least the subset of the Tycho-2 catalogue.

To obtain the spectral parallax of a star one must have its absolute and visual magnitudes. In our case, the high precision visual magnitudes are listed in the Tycho-2 catalogue. The absolute magnitude as a function of the spectral type and luminosity class can be interpolated from the figures and tables taken from [4], and [5]. To estimate the spectral parallax of a star we use the equation

$$\lg \pi_{sp} = 0.2 * (M_{tab} - m_{cat}) - 1 + 0.2 * A, \quad (1)$$

where $A = 3 * [(B-V)_{cat} - (B-V)_{tab}]$ is the interstellar absorption coefficient. Following this technique we derived the spectral parallaxes for 165 thousand stars in the Tycho-2 Spectral Type catalogue with available luminosity classes.

2. COMPARISON OF TRIGONOMETRIC AND SPECTRAL PARALLAXES

To evaluate the accuracy of the obtained spectral parallaxes, we calculated the differences

$$\Delta\pi = \pi_{sp} - \pi_{tr}, \quad (2)$$

where π_{tr} are the trigonometric parallaxes taken from 64 thousand stars of the HIPPARCOS catalogue. Of them 2243 stars with too large $\Delta\pi$ were rejected according to the "3-sigma" rule. Since both the parallaxes are absolutely independent, the r.m.s.e. of the spectral parallaxes may

be evaluated according to equation

$$\sigma_{sp} = \sqrt{(\sigma^2 - \sigma_{tr}^2)}, \tag{3}$$

where σ^2 is the variance of the $\Delta\pi$ and σ_{tr} is the r.m.s.e. of the trigonometric parallaxes. The σ_{sp} (estimated with $\sigma_{tr} = 1$ mas) as well as the mean value, asymmetry and excess of the random values $\Delta\pi$ for stars of different spectral types and luminosity classes are shown in Table 1. The mean values reveal the systematic shifts of spectral parallaxes with respect to the trigonometric ones, while the values of asymmetry and excess measure the deviation of the found probability densities from the probability density of the normal distribution.

Table 1: Mean value, σ_{sp}, asymmetry and excess of the differences $\Delta\pi$ for each spectral type

L	Sp	Mean, *mas*	σ_{sp}, *mas*	Asymmetry	Excess	Number of stars
I, III, V	OB	-0.5	0.6	-0.2	0.5	5426
I, III, V	A	0	2.4	0.3	1.4	6285
I, III, V	F	1.8	3.6	0.2	1.2	11974
I, III, V	G	1.8	4.6	0.7	2.6	10768
I, III, V	K	0.5	3.0	0.3	7.4	16226
I, III, V	M	0	1.4	0	4.2	1943
V	all	1.3	2.9	0.3	0.1	26237
V	OB	-0.3	1.0	0	0.6	3526
V	A	0.4	2.2	0.6	1.3	5145
V	F	1.9	2.9	0	0	10867
V	G	2	3.6	0	-0.4	5525
V	K	2.8	5.7	0.2	0.8	1277
III	all	0.1	2.1	-0.2	2.4	24024
III	OBA	-0.9	1.2	-0.2	0.2	2 409
III	GKM	0.3	2.1	-0.1	2.6	20865
I	all	-1.2	0.7	-0.8	1.2	928

3. RESULTS

1. The spectral parallaxes of about 165 000 Tycho-2 stars have been derived from the astrophysical data taken from the Tycho-2 Spectral Type catalogue.

2. For the majority of the stars the accuracy of the obtained spectral parallaxes was evaluated to be 1-5 mas depending on the spectral type.

Acknowledgements. The authors appreciate the support of this work by the grant 05-02-17047 of the Russian Fund of Fundamental Research and by the grant 37552 of the Ministry of Education and Science.

REFERENCES

[1] ESA, 1997, The Hipparcos and Tycho catalogues, ESA SP-1200

[2] Hog E., C. Fabricius, V.V. Makarov, U. Bastian, P. Schwekendiek, A. Wicenec, S. Urban, T. Corbin, and G. Wycoff., 1999-2000, Tycho-2 catalogue.

[3] Wright et al., 2003, Tycho-2 Spectral Type

[4] Mihalas and Binney, 1981, Galactic Astronomy, W.H.Freeman and Company, pp. 108

[5] 2000, Allen‘s astrophysical Quantities, fourth Edition, Arthur N.Cox Editor, Springer-Vereag NY, Berlin Heidelberg, pp. 381–393.

ASTEROID MASS DETERMINATION WITH THE GAIA MISSION

S. MOURET[1], D. HESTROFFER[1], F. MIGNARD[2]
[1] IMCCE-Paris observatory
77, avenue Denfert-Rochereau, 75014 PARIS, France
mouret@imcce.fr, hestroffer@imcce.fr
[2] OCA/Cassiopée
Boulevard de l'Observatoire, B.P 4229, 06304 NICE CEDEX 4, France
francois.mignard@obs-nice.fr

ABSTRACT. The ESA astrometric mission Gaia, due for launch in late 2011, will observe a very large number of asteroids ($\sim$ 500,000 brighter than V = 20) with an unprecedented positional precision (at the sub-milliarcsecond level). This precision will play an important role for the mass determination of about hundred minor planets. Presently, due primarily to their perturbations on Mars, the uncertainty in the masses of the largest asteroids is the main limiting factor in the accuracy of the solar system ephemerides[1]. Here we present the main features of the astrometric observations of asteroids with Gaia. The high precision astrometry will enable to considerably improve the orbits of almost all observed asteroids, yielding masses of the largest from mutual approaches. As an illustration we apply the overall procedure under development to the close approaches between Ceres and smaller targets observable with GAIA and assess the expected precision on the mass of Ceres at mission completion.

1. SOLAR SYSTEM OBJECTS OBSERVATIONS

Gaia is an astrometric cornerstone mission of the European Space Agency. With a launch due in late 2011, Gaia will have a much more ambitious mission than its precursor Hipparcos: obtain a "3D census" of our galaxy with astrometric, photometric and spectroscopic observations. It will pinpoint its sources with an unprecedented positional precision (at the sub-milliarcsecond level for single observation) which will allow it to observe about 500,000 asteroids (mainly main belt asteroids) brighter than V = 20. The scanning law of the satellite is very specific (Hipparcos-like) yielding observation sequences much different from the classical ground-based ones, with no observation at opposition and solar elongations symmetrically distributed around the quadratures. These elongations will range from $L_1 = 45°$ to $L_2 = 135°$. There is no dedicated observation mode for these resolved and moving targets which are observed like any other stellar source, but quickly identified from their motion. Their size and motion degrades the astrometry compared to stars, but it essentially remains a function of the target brightness. The astrometric precision σ_λ is found from simulation with GIBIS [2] and Pyxis [3] of the focal plane images for these objects. These estimates represent the precision for a single 'observation' in the along-scan direction (the astrometry in the perpendicular direction is much less precise so that the measure is essentially one dimensional).

The astrometric precision is defined by the approximations: $\sigma_\lambda \sim 0.2 - 0.3$ for $V < 14$, and $\sigma_\lambda \sim 10^{0.15V-2.7}$ elsewhere. This precision is one of the key factor impacting on the mass determination of minor planets.

2. METHOD FOR ASTEROID MASS DETERMINATION

The technique used here for the mass determination is based on the gravitational perturbation during a close approach [4] from which it is expected to obtain about 100 asteroids masses with Gaia. The present simulation considers close approaches during the mission operations between the perturber asteroid Ceres and 19 smaller and massless target asteroids, which belong to the 20,000 first main belt asteroids. These 19 targets will be perturbed by Ceres and observed by Gaia. The aim is to find the formal precision, the best precision $\sigma(m_p)$ that we expect, on the mass determination of Ceres from the Gaia astrometry of the targets.

The mass of the perturber is derived by least-squares together with a correction to the initial conditions of each target orbit. The vector *(O-C)* gives the difference between the observed and calculated position for each observation of every target asteroid. It can be written $(O - C) = A\Delta u_0 + B\Delta m_p$ where A is a matrix representing the partial derivatives, for each observation time, of the Gaia-centred longitude of asteroids relative to their initial positions and velocities while B is a matrix depending on the partial derivatives of the longitude of asteroids with respect to the perturbing mass m_p. The unknowns of the problem Δu_0 and Δm_p are respectively the correction to the initial conditions of each asteroid $\Delta u_0 = (\Delta x, \Delta y, \Delta z, \Delta \dot{x}, \Delta \dot{y}, \Delta \dot{z})$ and to the mass of perturber Ceres Δm_p.

We computed the matrices A and B by numerically integrating the motion of the targets and their variational equations. Then we assessed the formal precision $\sigma(m_p)$ from matrices A and B.

3. RESULT AND PROSPECT

The formal precision that we find is $\sigma(m_p) \sim 4.8 \times 10^{-14} M_\odot$, which represents 0.01 % of the mass of Ceres ($4.5 \times 10^{-10} M_\odot$), two orders of magnitude better than the latest ground-based estimates [4]. This method will be further extended to solve for many perturbers simultaneously. The plan is to consider ∼300 perturbers and ∼10,000 targets observed with Gaia conditions. A future work will be devoted to apply this mass determination to all these perturbers and will consider the cases where certain perturbers are also targets. Besides, other global parameters will be added, like the PPN parameter β, the solar quadrupole $J2$, and the rotation W of the ecliptic.

REFERENCES

[1] Standish E.M.Jr., A. Fienga (2002), A&A , 384,322

[2] Babusiaux C. (2004). The Gaia Instrument and Basic Image Simulator. ESA SP-576, p.417. Scientific Data Handling. ESA SP-576, p.335.

[3] Arenou F., C. Babusiaux, F. Chéreau, S. Mignot (2004). The Gaia On-Board Scientific Data Handling

[4] Hilton J., (2002). Asteroid masses and densities. In: Asteroids III, W.F. Bottke, A. Cellino, P. Paolicchi & R. P. Binzel, University of Arizona Press, p.103.

THE HELIOMETRIC ASTROLABE, A NEW INSTRUMENT FOR SOLAR DIAMETER OBSERVATIONS

A.H. ANDREI[1,2,a], E. REIS NETO[1] , V.A. D'ÁVILA[1], J.L. PENNA[1], M. ASSAFIN[2], S.C. BOSCARDIN[2], K.N. de ÁVILA[1]

[1] Observatório Nacional / MCT
R. Gal. José Cristino 77, RJ, Brasil
[2] Observatório do Valongo / UFRJ
Ladeira do Pedro Antônio 43, RJ, Brasil
e-mail: (a) oat1@on.br

ABSTRACT. The Observatório Nacional takes part in the Réseau de Suivi au Sol du Rayon Solaire (the international solar diameter monitoring network) which co-participates in the PICARD micro satellite, to be launched in 2008 to study the Earth climate and Sun variability relationship. A new instrument, a heliometer, was devised in order to minimize the atmospheric turbulence and reach data accuracy compatible with PICARD's. The heliometer principle of double images will be added to the astrolabe metrological quality, and fully digitized acquisition. The objective is to obtain two simultaneous images from the Sun, with fixed angular separation of about $30'$, which variation will contain the signature of the diameter variation.

1. INTRODUCTION

From 1998 to 2003, 16,511 measurements effective measurements were obtained by the Rio de Janeiro station of the international consortium for monitoring the solar diameter (R2S3), sweeping the heliolatitudes up to about 80°. Their standard deviation is 0".564, however, the evolution of the results is evident, in good report with the solar cycle and major burst events (Andrei et al., 2005).

At present, the solar diameter is measured along the vertical line of the observer, what restricts the heliolatitude range of observation. It is also worth to point out that the measure of the solar diameter through the reference to almucantar will always be an indirect measure. The differential refraction can be relevant, since the two borders are not observed simultaneously. Variations in refraction would imply in errors on the measure of the solar diameter.

2. THE PROPOSED HELIOMETRIC ASTROLABE

Heliometers are instruments designed to measure the solar diameter. The measurement technique relies on displacing the solar disk image by a known amount. Then the truly observed distance the limbs provides the measure of the diameter. Best results are obtained when the doubling is made larger than the diameter itself and variations are surveyed instead of the diameter itself. The double solar images to be obtained are morphologically alike to those obtained from the present instrument. On the other hand, the larger attained precision requires

improvements for topological description of the solar limb. At the same time, improvements are as well made on the determination of the loci of the solar limb points. The most crucial point relates to the definition of the center-to-limb darkening, in scales of the order of 1. The most recent measurements, air-borne made, reveal that the intensity drop only reaches to zero at a considerable distance from the visible boundary.

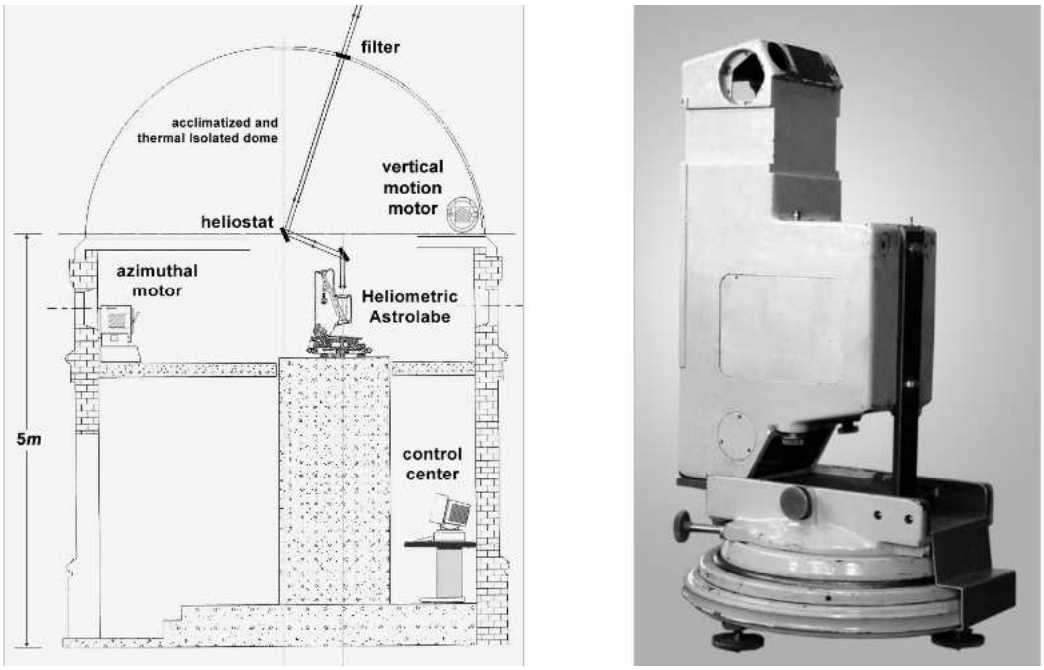

Figure 1: On the left a schematic view of the operation of the heliometric astrolabe. On the right, the instrument in its new attitude.

In the proposed technique several problems of the present method are avoided. The mercury basin is no longer necessary once the measurement is made directly from the distance between the opposite limbs, making the two image of the same quality. Since there is no more reference to the almucantar, the solar diameter measurements can be made at will towards any heliolatitude, enabling to obtain the solar figure in a very short interval of time (instead of months as presently). This is accomplished by spinning the divided objective around its focal axis (D'Ávila et al., 2005). Anomalous and differential refraction errors are effectively nullified, since the two (double) solar limbs are simultaneously observed. The instrument operation leads to automation and a very fast regimen of data acquisition, all day along. It is to be remarked that the proposed instrument will keep the output characteristics and can even keep the present data handling routines. This is a very important feature, which provides continuity to the measurements, and full comparison to the nearby solar astrolabe in the Observatório Nacional campus, as well as to the other stations of the Réseau de Suivi au Sol du Rayon Solaire international network of monitoring.

REFERENCES

Andrei A.H., Boscardin S.C., Penna, J.L., Reis Neto E., D'Ávila V.A., and Assafin M., 2005, 4th Annual Meeting of the Réseau de Suivi au Sol du Rayon Solaire, CRAAG/Alger.

D'Ávila V.A., Reis Neto E., Penna, J.L., de Ávila K.N., Boscardin S.C., and Andrei A.H., 2005, Proc. of the XXXI Annual Meeting of the Brazilian Astronomical Society-SAB, p.64.

COMPARATIVE STUDY BETWEEN ASTROGEODETIC METHODS USED IN DETERMINING VERTICAL DEFLECTION

O. BĂDESCU[1], R. POPESCU[2], P. POPESCU[2]
[1] Technical University of Civil Engineering, Faculty of Geodesy
B-dul. Lacul Tei, no.124, sect.2, Bucharest, Romania
e-mail: octavian@aira.astro.ro
[2] Astronomical Institute of the Romanian Academy
Str. Cuţitul de Argint, no. 5, sect. 4, RO-040558 , Bucharest, Romania
e-mail: [pradu,petre]@aira.astro.ro

ABSTRACT. The determination of the geoid-ellipsoid relative position is one of the main tasks of geodesy. This can be performed by many methods but we tried to do by astronomical determination of the deviation of the vertical. In this sense we realized two sets of measurements one of them with an electronic total station (the method was already described in precedent articles of Journées) and another, for safety and comparisons, with a CCD astrolabe. The results show that the actual geodetic devices can be used with success to this type of works.

1. INTRODUCTION

How the geocentric coordinates are determined respect to the Earth's center, the geodetic coordinates respect to the reference ellipsoid, the astronomical coordinates are determined respect to the local vertical from observation's point. The deviation of the vertical is usually decomposed in two orthogonal components: one component on the north-south direction (ξ) and an east-west or prime vertical component (η). The relations between astronomical coordinates and geodetic coordinates are: $\xi = \Phi - \mathrm{B}$ and $\eta = (\Lambda - \mathrm{B})\cos \mathrm{B}$. The next relation, on the base of these two components, gives the total deviation of the vertical: $\varepsilon^2 = \xi^2 + \eta^2$. The deviation of the vertical on some azimuthally direction (α) is: $\varepsilon_\alpha = \xi \cos\alpha + \eta \sin\alpha$ that is a frequently relation in geodetic calculations.

The main task was to perform some comparative studies between two methods concerning astro-geodetical determination of vertical deflection:

- First method (A): a classical method using the modernized astrolabe (CCD camera and GPS time measurement);

- Second method (B): a completely new method (already described in earlier articles in Proceedings of Journées 2002, Journées 2004) using Leica TC 2002 geodetic total station.

The both methods were applied to Astronomical Institute of Romanian Academy (GPS coordinates - WGS84 ellipsoid: latitude N 44°24'43".05955; longitude = E 26°07'38".02430

Targets:

- Studies concerning the benefits, limitations and drawbacks of both methods, comparative statistical analysis between methods;

- Testing Leica instrument and the specific mathematical algorithm for vertical deflection determination versus an unambiguous, well-known method and secure devices;

- Preparing of Leica TC 2002 total station for mounting a micro CCD camera to the optical system and GPS time receiver for fully automation of the method.

2. RESULT AND STATISTICAL ANALYSIS

The mean values from the next tables were obtained from 25 nights of observations with astrolabe and 5 nights of observation with Leica TC 2002 total station.

CCD Astrolabe (A)	Mean value	Max value	Min value	Δ=Max - Min
ξ (arcsec)	11.707	12.252	10.669	1.583
η (arcsec)	4.801	5.592	4.187	1.405
u (arcsec)	12.655	13.399	11.461	1.938
Leica TC 2002 (B)	Mean value	Max value	Min value	Δ=Max - Min
ξ (arcsec)	11.150	11.455	10.661	0.794
η (arcsec)	4.422	4.869	3.460	1.409
u (arcsec)	12.006	12.447	11.639	0.808

Table 1: Comparative results

The statistical analysis required:

- Comparison between the results obtained from night to night of observations, separately for each method;

- Comparison between the results obtained from the two methods;

The statistical analysis was performed for:

- Evaluation of the global precision of the methods

- Evaluation of the accuracy of the methods (relieved of the systematic errors)

The results of statistical analysis demonstrate that:

- Bartlett test (verification of the variance homogeneity) do not confirm the hypothesis of the variance homogeneity in this case it was used the weight arithmetic average and the standard deviation as weight average of the individual standard deviations;

- F test (comparison of the variances of the two methods) between of the precisions of the methods exist a significant difference. Method A is more precise for evident reasons;

- Student test (comparison of the average of the methods) between of the precisions of the methods exist a significant difference. Both methods do not present systematic errors at an significant level. The differences between method A and method B are the consequence of the random errors, both in ξ and η components;

- Successive differences test (verification of the existence of some factors with a systematic action on the results) does not exist a source of systematic errors at a significant level, both in ξ and η components.

REFERENCES

Archinal B.A.: 1992, "Explanatory Supplement to the Astronomical Almanac", University Science Books, Mill Valley, California, USA

Rüeger J.M., Featherstone W.E.: "The importance of using deviations of the vertical for the reduction of survey data to a geocentric datum",
http://www.cage.curtin.edu.au/∼will/devertfinal.pdf

VECTORIAL HARMONICS: FROM LINK OF FRAMES TO STELLAR KINEMATICS

A.K. SHUKSTO, V.V. VITYAZEV
Saint-Petersburg State University
198504 Petrodvorets, Universitetsky pr., 28., S. Petersburg, Russia
e-mail: shuksto@ntc-it.ru

1. OUTLINE OF THE METHOD

In astrometry, the vectorial spherical functions were used for the first time for determination of the orientation and spin between the FK5 and HIPPARCOS reference frames [1]. The present paper is devoted to elaboration of this approach to the kinematical analysis of the proper motions.

Let the proper motions in galactic coordinate system be $\mu_l(l,b)\cos b$ and $\mu_b(l,b)$. We are looking for decomposition of the proper motions in such a way that

$$\mu_l(l,b)\cos b\,\vec{e}_l + \mu_b(l,b)\,\vec{e}_b = \sum_{j=1}^{\infty}\left[t_j\vec{T}_j(l,b) + s_j\vec{S}_j(l,b)\right], \tag{1}$$

where $\vec{e}_l$ and $\vec{e}_b$ are the unit vectors in the directions of longitude and latitude, and $\vec{T}_j(l,b)$ and $\vec{S}_j(l,b)$ are given in [1].

In case of the Ogorodnikov–Milne model [2] the stellar velocity field is given by expression

$$\vec{V} = \vec{V}_0 + M^+\,\vec{r} + M^-\,\vec{r}, \tag{2}$$

where the following notations are used:

$\vec{V}_0$ — the velocity of the Sun with respect to given centroid of stars. This velocity is defined by components U, V, W in the directions of the principal galactic axes x, y, z;

M^+ — the diverging matrix with the dilation coefficients M^+_{11}, M^+_{22}, M^+_{33}, and M^+_{12}, M^+_{13} M^+_{23} standing for shears in the galactic planes (x,y), (x,z), (y,z). Since proper motions reflect tangential motions only, we set $M^+_{22} = 0$. In this case the unknowns M^+_{11} and M^+_{33} are replaced with $M^*_{11} = M^+_{11} - M^+_{22}$ and $M^*_{33} = M^+_{33} - M^+_{22}$ respectively;

M^- — the rotation matrix with the components ω_1, ω_2 è ω_3 about axes x, y, z;

The crucial point of our method is that the elements of M^+ and M^- are connected to the low-order coefficients of the decomposition (1) by the following equations (with R_j standing for the normalization factor of corresponding vectorial harmonic $\vec{T}_j$ or $\vec{S}_j$):

$$t_1 = \frac{\omega_3}{R_1}, \qquad t_2 = \frac{\omega_2}{R_2}, \qquad t_3 = \frac{\omega_1}{R_3}, \tag{3}$$

$$s_4 = \frac{M^*_{33} - \frac{1}{2}M^*_{11}}{2R_4}, \tag{4}$$

$$s_5 = \frac{M^+_{23}}{R_5}\,, \qquad s_6 = \frac{M^+_{13}}{R_6}\,, \tag{5}$$

$$s_7 = \frac{M^+_{12}}{2R_7}\,, \qquad s_8 = \frac{M^*_{11}}{4R_8}\,, \tag{6}$$

whereas the rest of harmonics does not belong to the Ogorodnikov–Milne model and may be used to study the effects that are beyond the model.

2. "EXTRA-MODEL" COMPONENTS OF THE PROPER MOTIONS

When applied to stellar kinematics of HIPPARCOS catalogue, the main advantage of the vectorial harmonics over traditional approach is a chance to detect the motions which are not included in the Ogorodnikov–Milne model. Indeed, in the global solution the method of vectorial functions detected the terms $(-12.9 \pm 4.6) \times \vec{S}_{10}$, $(12.2 \pm 4.4) \times \vec{S}_{14}$, $(-12.7 \pm 4.6) \times \vec{S}_{20}$, $(11.1 \pm 4.3) \times \vec{S}_{34}$ (all in km s^{-1} kps^{-1}). Besides the global solution we applied our method to several samples of stars with different distances and spectral classes. The "extra-model" terms specified by the functions $\vec{T}_4$, $\vec{T}_6$, $\vec{S}_{10}$ and $\vec{S}_{14}$ were found to be common to all examined samples including the global solution.

In conclusion, we state that contribution of the "extra-model" components to the proper motions is comparable with the contribution of the "classical" terms (see Figure 1). The next paper will be devoted to the physical properties of the "extra-model" terms detected here.

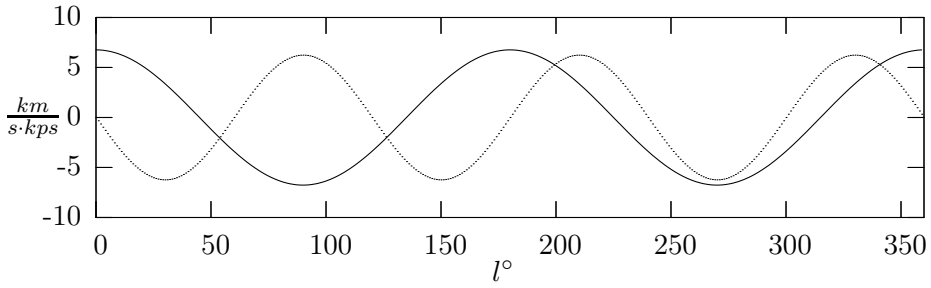

Figure 1: Contribution to the proper motions in longitude from the model harmonic $\vec{S}_7$ (Oort's coefficient $A = M^+_{12}$, solid line) in comparison to the significant "extra-model" harmonic $\vec{S}_{14}$ (dashed line).

Acknowledgements. The authors appreciate the support of this work by the grant 05-02-17047 of the Russian Fund of Fundamental Research and by the grant 37552 of the Ministry of Education and Science.

REFERENCES

[1] Mignard F., Morando B., Analyse de catalogues stallaires au moyen des harmoniques vectorelles, Journees 90. Systemes de reference spatio-temporels. Paris, pp.151-158, 1990.

[2] du Mont B., A three-dimensional analysis of the kinematics of 512 FK4 Sup. stars. A&A, 61, N 1. pp. 127-132, 1997.

Session 1.2

CELESTIAL AND TERRESTRIAL REFERENCE SYSTEMS: Realization of the systems and scientific applications

SYSTEMES DE REFERENCE CELESTE ET TERRESTRE : Réalization des systèmes et applications scientifiques

STATUS OF THE ITRF2005

Z. ALTAMIMI[1], X. COLLILIEUX[1], J. LEGRAND[1], C. BOUCHER[2]
[1]Institut Géographique National, LAREG
6-8 Avenue Blaise Pascal, 77455 Marne-la-Vallée, France
e-mail: altamimi@ensg.ign.fr, collilieux@ensg.ign.fr, jlegrand@ensg.ign.fr
[2] Conseil Général des Ponts et Chaussées
Tour Pascal B, 92055 La Défense, France
e-mail: cbpro@club_internet.fr

ABSTRACT. Unlike the previous realization of the International Terrestrial Reference System (ITRS), the ITRF2005 input data are time series of station positions (weekly solutions from satellite techniques and daily solutions from VLBI) and daily Earth Orientation parameters (EOPs). This paper summarizes the current status of the ITRF2005 in terms of submitted input data and the methodology used to construct the ITRF2005. Since this the first time that EOPs are included in the ITRF combination, we show some EOP preliminary results and in particular comparison to the IERS C04 series. These preliminary EOP results show a significant bias in the Y pole component (of the order of 200 micro-arc-second) between our combination and the C04 series. The ITRF2005 will be the occasion to re-calibrate the C04 results in order to make it consistent with the ITRF2005.

1. ITRF2005 INPUT DATA

The ITRF2005 input data are under the forme of time-series solutions, provided in a weekly sampling by the IAG International Services of satellite techniques (the International GNSS Service-IGS, the International Laser Ranging Service-ILRS and the International Doris Service-IDS) and in a daily (VLBI session-wise) basis by the International VLBI Service (IVS). Each per-technique time-series is already a combination, at a weekly basis, of the individual Analysis Center (AC) solutions of that technique, except for DORIS for which individual analysis center time-series were submitted to the ITRF2005. Local tie vectors in about 100 sites will be used in the ITRF2005 combination that allow connection between the 4 techniques. The ITRF2005 will comprise about 800 stations located at about 500 sites. Figure 1 shows the distribution of ITRF2005 sites underlying the co-located ones.

2. DATA ANALYSIS

The strategy adopted for the ITRF2005 generation consists in the following steps :

- Remove original constraint (if any) and apply minimum constraints equally to all solutions
- Use as they are minimally constrained solutions
- Form per-technique combinations (TRF + EOP)

- Identify and reject/de-weight outliers and properly handle discontinuity using piece-wise approach
- Combine if necessary all solutions of a given technique into a unique solution
- Combine per-technique combination adding local ties in co-location sites

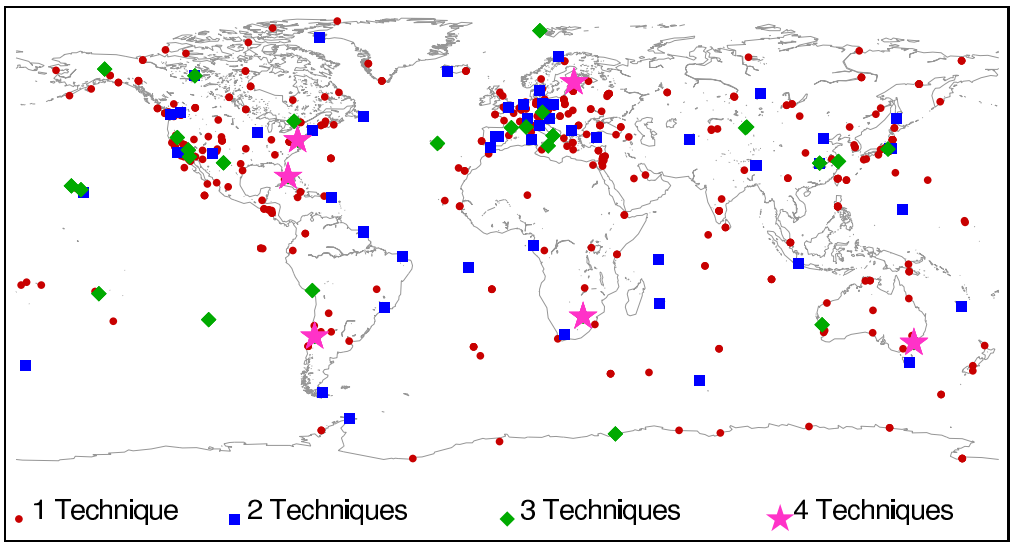

Figure 1: ITRF2005 Co-located sites

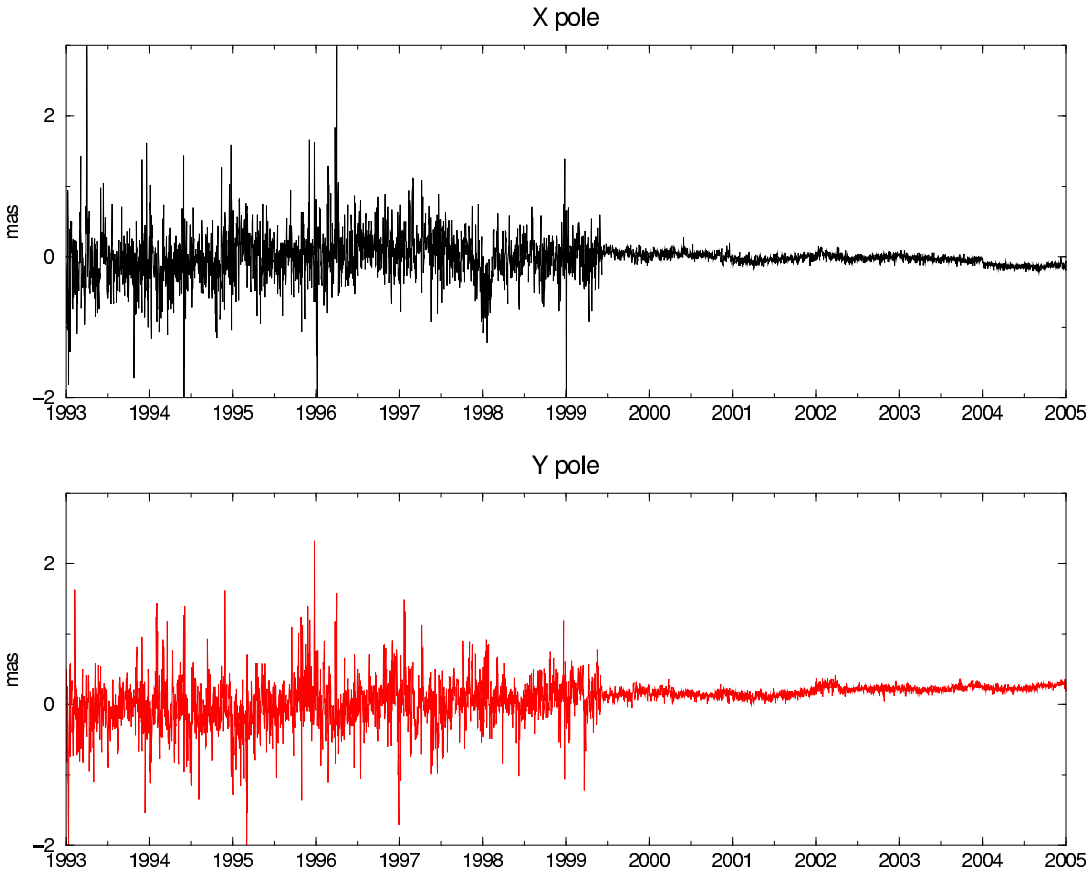

Figure 2: Polar motion differences between ITRF2005 preliminary solution and IERS C04.

3. SOME PRELIMINARY RESULTS

For the purpose of this paper we select to show EOP preliminary results since this is the first time that the EOPs are included in the ITRF combination.

As results from a preliminary global combination, similar to what will be the ITRF2005 solution, Figure 2 shows Polar Motion differences between our combination and the IERS C04 series. The mean of these differences indicates a significant bias of about 200 micro-arc-second in the Y component between our EOP series (expressed in ITRF2000) and the IERS C04. Therefore the ITRF2005 will be the occasion to re-calibrate the IERS C04 to make it consistent with the ITRF2005.

More preliminary results are published in (Altamimi et al., 2005).

REFERENCES

Altamimi Z., Collilieux X., Boucher C., 2005, Preliminary Analysis in view of the ITRF2005, Proceedings of IAG Symposium, the Dynamic Planet, submitted.

THE EUROPEAN VLBI NETWORK: A SENSITIVE AND STATE-OF-THE-ART INSTRUMENT FOR HIGH-RESOLUTION SCIENCE

P. CHARLOT
Observatoire de Bordeaux (OASU) – CNRS/UMR 5804
BP 89, 33270 Floirac, France
e-mail: charlot@obs.u-bordeaux1.fr

ABSTRACT. The European VLBI Network (EVN) is an array of 18 radio telescopes located throughout Europe and beyond that carry out synchronized very-long-baseline-interferometric (VLBI) observations of radio-emitting sources. The data are processed at a central facility located at the Joint Institute for VLBI in Europe (JIVE) in the Netherlands. The EVN is freely open to any scientist in the world based on peer-reviewed proposals. This paper outlines the current capabilities of the EVN and procedures for observing, highlights some recent results that have been obtained, and puts emphasis on the future development of the array.

1. INTRODUCTION

The European VLBI Network (EVN)[1] was formed in 1980 by a consortium of five of the major radio astronomy institutes in Europe (the European Consortium for VLBI). Since then, the EVN and the Consortium has grown to include 12 institutes in Spain, UK, the Netherlands, Germany, Sweden, Italy, Finland, Poland and China (Table 1). In addition, the Hartebeesthoek Radio Astronomy Observatory in South Africa and the Arecibo Observatory in Puerto Rico are active Associate Members of the EVN.

The EVN members operate 18 individual antennae, which include some of the world's largest and most sensitive telescopes (Fig. 1). Together, these telescopes form a large scale facility, a continent-wide radio interferometer with baselines ranging from 200 km to 9000 km. The angular resolution of the array is 5 mas at 1.6 GHz and 0.3 mas at 22 GHz, hence providing astronomers with the sharpest view of the observed target sources.

The Joint Institute for VLBI in Europe (JIVE), located in Dwingeloo (Netherlands), was formed by the EVN in 1993 to build and operate the current 16-station EVN data processor (also referred to as the EVN correlator) and to provide central support for EVN users. The new EVN correlator has been operational since 1999, increasingly taking most of the load of EVN data processing. A small portion of the EVN data is also processed by the 9-station correlator of the Max-Planck Institut für Radioastronomie in Bonn.

The overall policy of the EVN is set by the *Consortium Board of Directors* (CBD) whose membership consists of the Directors of the member institutes of the EVN. It meets twice a year to discuss operational, technical and strategic issues.

[1]See http://www.evlbi.org/

Table 1: Member institutes of the European Consortium for VLBI.

Institute	Name	Location	Country
	Full members		
Nether. Found. for Research in Astronomy	ASTRON†	Dwingeloo	Netherlands
Istituto di Radioastronomia	IRA†	Bologna	Italy
Jodrell Bank Observatory	JBO†	Jodrell Bank	UK
Joint Institute for VLBI in Europe	JIVE	Dwingeloo	Netherlands
Max-Planck Institut für Radioastronomie	MPIfR†	Bonn	Germany
Metsähovi Radio Observatory	MRO	Espoo	Finland
Observatorio Astronómico Nacional	OAN	Alcalá de Henares	Spain
Onsala Space Observatory	OSO†	Onsala	Sweden
Shanghai Observatory	SHAO	Shanghai	China
Toruǹ Centre for Astronomy	TCfA	Toruǹ	Poland
Urumqi Astronomical Observatory	UAO	Urumqi	China
Bundesamt für Kartographie und Geodäsie	BKG	Wettzell	Germany
	Associate members		
Hartebeesthoek Radio Astron. Observatory	HartRAO	Hartebeesthoek	South Africa
National Astronomy and Ionosphere Center	NAIC	Arecibo	Puerto Rico

†Founding institutes.

2. EVN OBSERVING

The EVN observes for three periods per year known as "VLBI sessions". Each of these sessions is approximately 3–4 weeks long and typically involves 3–4 different observing frequencies[2]. The EVN is also linked on a regular basis to the 7-element MERLIN interferometer (located in the southern half of the UK) to create a very sensitive "regional network", and to the US NRAO Very Long Baseline Array (VLBA) and the NASA Deep Space Network (DSN) to create a "Global Network". The EVN in stand-alone or global mode, also observed together with the orbiting radio telescope HALCA launched in February 1997 by the Institute of Space and Astronautical Science (ISAS) in Japan as part of the first dedicated Space VLBI mission VSOP (VLBI Space Observatory Programme).

The EVN *scheduler* ensures that all telescopes follow the same observing schedule during the VLBI sessions. Engineering issues related to EVN operations are considered by the *Technical and Operations Group* (TOG) whole role is to ensure that all telescopes are delivering good quality data during VLBI observing. At each EVN telescope, the data are recorded on disks with data rates up to 1 Gb/s using the Mark V recording system (which replaced traditional VLBI magnetic tape recording two years ago). After each observing programme is completed, the disks are shipped to JIVE where the data are replayed and combined at the EVN correlator to produce the VLBI observables.

Astronomers who wish to use the EVN must submit observing proposals to the EVN *Programme Committee* (PC). A *Call for proposals* is distributed three times a year with proposal deadlines of 1st February, 1st June and 1st October. The EVN PC is an independent body appointed by the CBD to assess all EVN, joint EVN plus MERLIN and Global VLBI requests for

[2]The available frequencies are 0.3, 0.6, 1.2–1.6, 2.3, 5.0, 6.7, 8.4, 22 and 43 GHz, including the standard dual-frequency observing setup (simultaneous 2.3 and 8.4 GHz) used in astrometry and geodesy. The 6.7 GHz frequency (tracing methanol maser emission) is unique to the EVN. Not all frequencies are available at all telescopes.

Figure 1: Pictorial representation of the 18 telescopes of the European VLBI Network.

observing time. The EVN is an open facility and the PC awards observing time based only on scientific merit and technical feasibility.

EVN users can obtain assistance and support from JIVE via its support scientists. These scientists are funded through the European Commission's IHP Programme *Access to Research Infrastructures* and are able to advise on many different aspects of EVN observations and data analysis, including the technical feasibility of a proposed observing programme, the creation of EVN and Global VLBI experiment schedules, support of observations and data correlation, data calibration and image analysis at JIVE.

3. SCIENCE WITH THE EVN

The range of scientific projects carried out with the EVN covers a wide variety of areas, reflecting the growing applications of the VLBI technique. These include studies of masers in star forming regions, individual stars and X-ray binaries, pulsars and interstellar scattering, supernovae remnants in nearby galaxies, weak Seyfert nuclei, environment of active galaxies through OH and HI absorption lines and megamasers, the "classical" monitoring of jets in active galactic nuclei, and extragalactic and galactic astrometry.

Two recent highlights of the EVN are illustrated by the images in Figs. 2 and 3. Figure 2 shows the spatial distribution of the methanol maser emission in the candidate high-mass protostar G23.657–0.127 (Bartkiewicz et al. 2005). The striking nearly-circular ring structure seen in this image suggests a common origin for the maser components. A possibility is that the methanol maser emission arose in a shock initiated by a young, massive star at the centre of the ring, which yields a new perspective on the problem of the origin of methanol masers and star formation. Figure 3 shows a sequence of 24 images of the supernova 1993J obtained with the Global VLBI

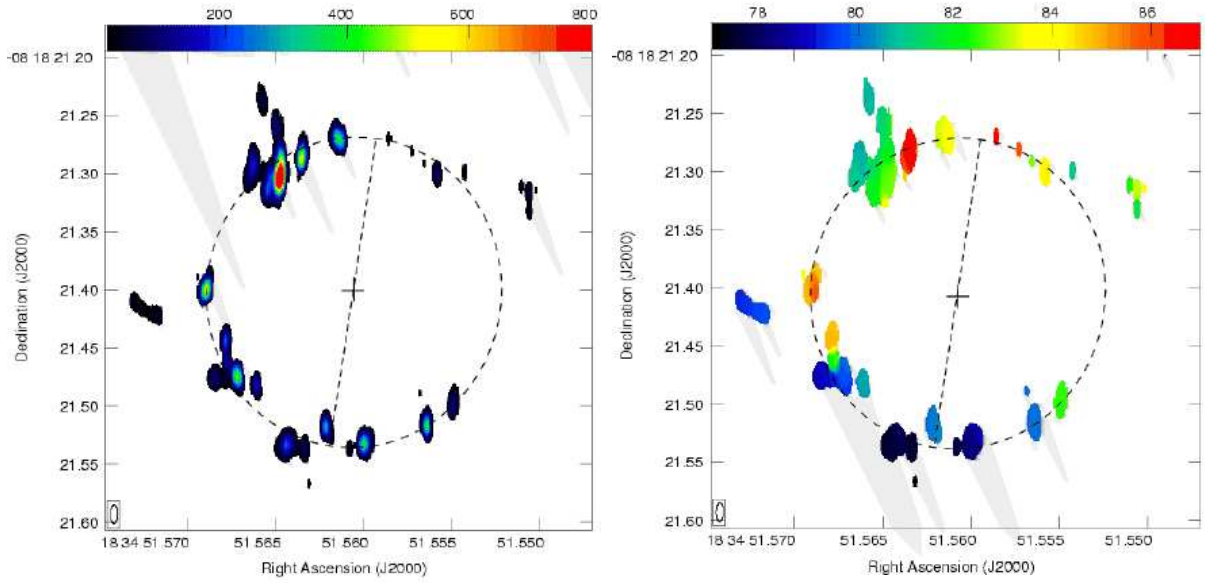

Figure 2: A 6.7 GHz EVN image of the galactic radio source G23.657–0.127 showing the spatial geometry (left panel) and velocity field (right panel) of the methanol maser emission in this young high-mass star (reproduced from Bartkiewicz et al. 2005). (See the website version of Proceedings for the color version of this figure.)

array over a range of 7.5 years starting shortly after the shock breakout in 1993 (Bietenholz et al. 2003). The sequence of images shows the expanding radio shell of the exploded star in detail, permitting a direct measurement of the angular expansion of the shell and studies of the interaction of the ejected material with the circumstellar medium around the progenitor star.

Another recent scientific highlight of the EVN was the precision VLBI tracking of the Huyguens probe as it descended on to the surface of Titan on 2005 January 14 (Lebreton et al. 2005). Combined with Doppler data, the VLBI astrometric measurements will provide a full three-dimensional trajectory of the probe during its descent, enabling planetary scientists to study Titan's winds and to put measurements of the physical and chemical structure of the Titan atmosphere in perspective (Bird et al. 2005). The EVN has also been recently used to measure sub-milliarcsecond accurate astrometric positions for 150 new reference frame sources, as part of a project to densify the International Celestial Reference Frame (ICRF) towards weaker sources (Charlot et al. 2004). As noted above, the EVN is especially adapted to observe such weak sources due to its high sensitivity.

4. THE FUTURE OF THE EVN

Looking ahead, future developments will be targeted primarily at increasing further the sensitivity of the EVN. Disk-based recording with the Mark 5 system (yielding data rates up to 1 Gb/s) has already provided a gain by a factor of 4 compared to the standard 256 Mb/s data rate used until a few years ago when recording was still on magnetic tapes. A gain by an additional factor of two will be possible when Mark 5B units are available (two of these used in parallel will support up to 2 Gb/s), while the introduction of modern digital videoconverters opens up hope for recording rates up to 4–8 Gb/s on the longer term. New large antennas that are being constructed, e.g. in Spain (40 m telescope in Yebes to be available by 2006), Italy (64 m telescope in Sardinia planned for 2008) or China (50 m telescope in Miyun and 40 m in

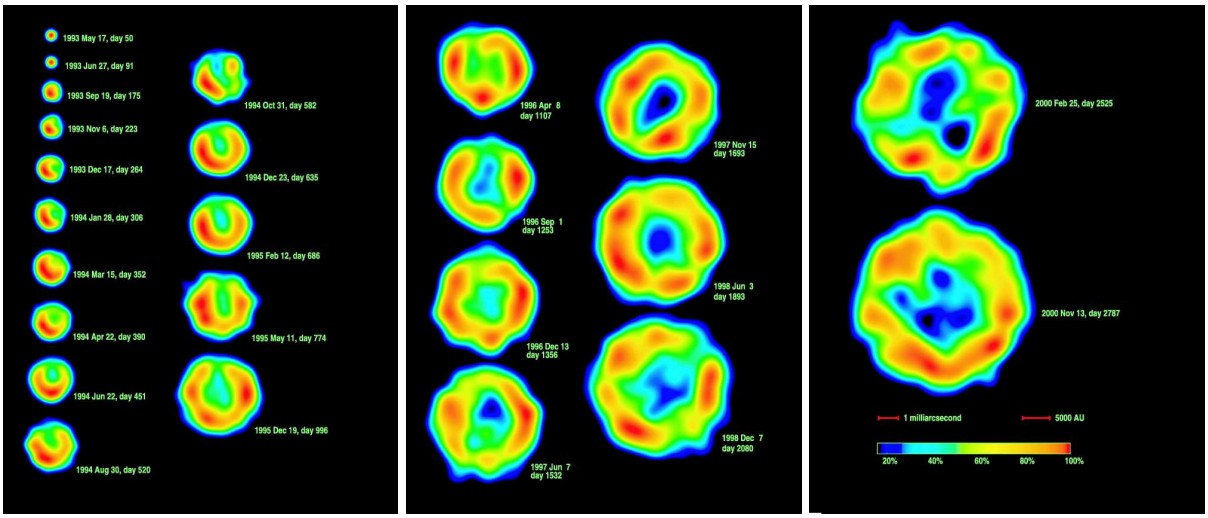

Figure 3: The evolution of the supernova 1993J which exploded on 1993 March 28 in the nearby galaxy M81. The observations were made with the global VLBI array at 8.4 GHz and cover a period from 50 to 2287 days after the explosion (reproduced from Bietenholz et al. 2003). (See the website version of Proceedings for the color version of this figure.)

Kunming to be available within about a year) will also directly and significantly improve the sensitivity of the EVN.

Another rapidly-developing area is the connection of EVN telescopes through high-speed networks (like the Pan-European Research Network GÉANT–2) to transfer and correlate VLBI data in real time. Such real-time experiments are usually referred to as "e-VLBI" experiments. As of September 2005, telescopes at Onsala, Westerbork, Jodrell Bank, Cambridge, Torun and Arecibo have already been connected to JIVE, while the Medicina antenna is expected to be connected soon. Subsequent to technical tests, a first e-VLBI science experiment[3] was conducted on 2004 September 22 and proved to be a great success. Notably, this experiment demonstrated real-time transfer and correlation over a 8200 km baseline between the EVN telescopes in Arecibo and Torun.

In the next 4 years, such e-VLBI developments will be coordinated through the EXPR*e*S (EXpress Production Real-time *e*-VLBI Service) project, an Integrated Infrastructure Initiative (I3) proposal submitted to the European Commission under the 6$^{\text{th}}$ Framework Program. This proposal was rated No. 1 out of 43 submitted proposals and was awarded 3.9 Million Euros. The objective of EXPR*e*S is to make e-VLBI an operational instrument by connecting 16 EVN telescopes (including those in China and South Africa) to JIVE at 1 Gb/s (the current e-VLBI transfer is only reliable to about 128 Mb/s), by integrating the antennas from e-MERLIN (an upgrade of the present MERLIN interferometer) transparently within the e-EVN and by offering a Target of Opportunity capability to the EVN users, i.e. a rapid response of the array allowing one to observe transient astronomical phenomenons like flaring stars, gamma-ray bursts,...etc...

With these developments, the EVN is likely to remain a state-of-the-art radio interferometer instrument in the forefront of astronomical research for high-resolution studies of galactic and extragalactic targets through the next decade.

[3]See http://www.evlbi.org/evlbi/first_science/first_science.html

Acknowledgements. The author wishes to thank Anna Bartkiewicz and Leonid Gurvits for providing material prior to publication. He is also grateful to Mike Garrett for information about the EXPR*e*S project. The European VLBI Network is a joint facility of European, Chinese, South African and other astronomy institutes funded by their national research councils.

REFERENCES

Bartkiewicz, A., Szymczak, M., and van Langevelde, H. J., 2005, "Ring shaped 6.7 GHz methanol maser emission around a young high-mass star", A&A 442, pp. L61–L64.

Bietenholz, M. F., Bartel, N., and Rupen, M. P., 2003, "SN 1993J VLBI. III. The evolution of the radio shell", ApJ 597, pp. 374–398.

Bird, M. K., Allison, M., Asmar, S. W., et al., 2005, "The vertical profile of winds on Titan", Nature, 438 pp. 800–802.

Charlot, P., Fey, A. L., Jacobs, C. S., Ma, C., Sovers, O. J., and Baudry, A., 2004, "Densification of the International Celestial Reference Frame: Results of EVN+ Observations", Journées 2004 Systèmes de référence spatio-temporels, Fundamental Astronomy: New concepts and models for high accuracy observations, Ed. N. Capitaine, pp. 21–25.

Lebreton, J.-P., Witasse, O., Sollazo, C., et al., 2005, "An overview of the descent and landing of the Huyguens probe on Titan", Nature 438, pp. 758–764.

PUBLIC AND SCIENTIFIC TIME AT PARIS OBSERVATORY : EVOLUTION OVER THREE CENTURIES

S. DÉBARBAT
SYRTE/UMR8630 - Observatoire de Paris
61, avenue de l'Observatoire - 75014 Paris
suzanne.debarbat@obspm.fr

ABSTRACT. When the *Académie Royale des sciences* is created in 1666, and the following year the Observatoire Royal, by Louis the XIVth, several improvements had appeared during the past millenium. Time and determinations by sundials, between sunrise and sunset had led to intervals of twelve unequal hours and to a special reference, the time the shadow was the shortest one, later known as to represent the meridian line. The two aspects of time were also seen : - the date as an instant of time ; - the duration between two dates.

1. WHAT IS TIME ?

What is behind the expression "the measure of time" ? A quantity which indeed cannot be measured. In 1858 Le Verrier (1811-1877) had written : *"Bien que nous ne puissions savoir ce qu'est en lui-même le temps, nous concevons néanmoins qu'on peut, par la répétition de phénomènes identiques, s'assurer de l'égalité de certains intervalles de temps"*. Almost one century later, in 1949, Danjon (1890-1967) could write : *"On n'a rien fait quand on a dit que c'est* [il s'agit de la durée] *l'intervalle de temps compris entre deux instants, puisque cette affirmation reporte le problème sur le mot temps. Mais l'expérience permet d'atteindre une certaine quantité susceptible d'une représentation numérique à laquelle on donne le nom de temps"*. Fortunately, as written by Le Verrier, there are periodical phenomena leading to a certain estimation of time: the rotation of the Earth around the Polar Star, its revolution around the Sun.

Another related problem concerns the necessity of maps to travel from one place to another one. In that case, latitude is easily obtained from the altitude of the Polar Star but for longitude, related to the rotation of the Earth, it needs time determinations. In any case time, whatever it is, needs to be determined and to be kept with the best possible accuracy. In the past sundials could give it at about a minute and various types of clepsydra, sand-glass, hour candles could keep it in between.

The major evolution of clocks which appeared in the bell-towers, as early as during the 13th century, will come with Huygens (1629-1695), in the Low Countries by 1655. He introduced a pendulum leading to pendulum clocks, later to be named regulators. While old clocks could vary of one hour per day, the new ones will be able to keep the second over 24 hours.

Due to the quality of his clocks, Huygens was invited by the Sun-King to come to Paris and he stayed in France from 1666 to 1681/82. From good clocks for time, the longitude problem appeared to be possibly solved for cartography.

2. TIME BY THE END OF THE 17th CENTURY

The 17th century will be, for astronomy and related fields in general, for time in particular, a very decisive one. On the other hand, mural sectors will be equipped with refractors, themselves having filar micrometers, after the works by Auzout (1622-1691) and Picard (1620-1682). Murals are installed, at the Paris Observatory, along its thick meridian walls. Clocks, designed, under Huygens, in Paris by the horologer Thuret (Figure 1), are placed in their vicinity and they can beat the half-second allowing time to be recorded at about a quarter of a second.

In 1668, the French astronomers had to check Cassini's table allowing to predict eclipses of the nowadays named galilean satellites of Jupiter. Due to their quality Cassini (1625-1712), from Bologna, was invited to come to Paris where he arrived in spring 1669, the Observatoire Royal being under construction. In 1673 he decided to stay in France. In 1669, Picard designed three new instruments, a sector with a short limb for zenith observations, a portable quadrant with two refractors for azimuth measurements, a level equipped with a refractor. This year and the following one, he worked on the measurement of a meridian arc centered on the Paris Observatory latitude. From its length he could deduce the circumference, the diameter and the radius of the Earth with a very high accuracy for the time.

Between 1671 and 1672, Picard experienced the method of determination of longitude in using eclipses of Jupiter satellites and good pendulum clocks. He went to Danemark where he received the help of young Roemer (1644-1710) with whom he came back to France in 1672. The corresponding observations were made in Paris, by Cassini. In 1676, Picard began to use the eclipses of the galilean satellites for longitude determination along the French coasts. He was working with La Hire (1640-1718) determining the timings by clocks, Cassini doing the same from the Observatory meridian line. The corresponding map, including this meridian for the first time, was presented to the Academy in 1682, and published in 1693.

Astronomy, which will give birth to astrometry, geodesy, topography, cartography and other related domains, had gained powerful instruments, introduced new methods and obtained fundamental results. The astronomers had obtained accurate positions of celestial bodies; they were able to perform terrestrial astro-geodetic measurements; they had proved the value of the pendulum clocks, given the data concerning the figure of the Earth, established a reference for local time determinations and, more generally, for longitude campaigns.

3. 18th CENTURY INSTRUMENTS, METHODS AND RESULTS

Using a vertical sector, similar to the one designed by Picard, Bradley (1693-1762), the third *Astronomer Royal* at Greenwich Observatory (established in 1675) published, in 1728, the discovery of aberration and two decades later nutation. The first phenomenon could confirm the discovery of Roemer concerning the velocity of light. The second will affect the celestial pole.

Portable quadrants will not change so much. But, by the end of the century, astronomers had large mural quadrants for determination of time and meridian observations of celestial bodies. While the portable quadrants were made by the French Langlois (ca 1730/1750), the Paris Observatory was equipped with a mural one made by the British maker Bird (1709-1776). It was installed on the east side of the Observatory at about 35 meters from the meridian of reference. They had at their disposal clocks made by the horlogers Julien Leroy (1686-1759) and Berthoud (1729-1807). They had improved their pendulum part in using two different metallic pieces and one, from Berthoud (Figure 2), is still in the collections of the Paris Observatory.

The astronomers from Paris Observatory, upon request of Colbert, Louis the XIVth, later Louis the XVth, were asked to develop geodesy in view of a general map of France. They established a reference for longitude (the Paris Observatory meridian line, from the northern to the southern border), and a reference for latitude perpendicular to the reference meridian at the latitude of the building. The issued map, achieved in 1790, is - one can assume - the first one,

at the level of a country, established under a scientific cartographic method. By the end of the century appeared small portable transit instruments for field observations.

For the public, and before his departure from the Observatory in 1793, Cassini IV (1748-1845) submitted the proposal to fire a canon, from its upper level, every day at noon. But in case it could affect the building the project was abandoned.

4. 19th CENTURY EVOLUTION

Due to the improvements in the mechanical domain, larger instruments could be built. Under the influence of Arago (1786-1853), a large east wing is built, around 1835, to house three new ones : - a meridian circle for declination measurements ; - a transit instrument for right ascension and time determinations ; - a meridian circle to perform both types of observations (Figure 3).

Their regulators, under the form of two clocks, one for mean solar time, the other for sidereal time are placed in the same room close to the instruments due to the method of the time (ear and eye) being used. As soon as electricity was available, such clocks were equipped with a new design to insure a better regularity. To give profit to the public of accurate time determinations, Arago had in mind to install a Chappe (1763-1805) telegraph on the Observatory. With the electricity he moved to the use of the electric telegraph.

But what time will be given to the public ? According to Arago, in Paris - from 1816 - the clocks had to be settled upon the one given by the Paris Observatory meridian. While, in the past, public clocks gave the local solar time, from 1839, they had to give the mean local solar time, in using the *Annuaire du Bureau des longitudes*, created in 1795. By 1881 and during the following years, mean solar time of Paris was provided to the main harbors beginning with Le Havre, Rouen and others ; later on came the main towns under the influence of the railway.

A decision studied in Roma in 1883, was taken in 1884 in Washington, to divide the Earth into 24 time zones, referred to Greenwich meridian; it was not immediately adopted in France. By the end of the century, with the discovery of wireless, the very first time signals were sent, from Hamburg in Germany, in 1899. A few years earlier a phenomenon, suspected by Picard but not yet found in the observations, was discovered, in the US by Chandler (1846-1913) : the 1.2 periodical motion of the pole which will play an important role during the following century.

At Paris Observatory, the clocks were still installed in the vicinity of the time measurement instruments. From 1891, time was unified in France, being the mean solar time of the Paris Observatory meridian of reference.

5. UNIFICATION OF TIME DURING THE 20th CENTURY

Ferrié (1868-1932) to become later general, took into consideration what is called in French TSF (*Télégraphie Sans Fil*). In cooperation with Paris Observatory, he set-up a laboratory at the bottom of the Eiffel Tower. He had in mind to sent time signals from its very high summit. Poincaré (1854-1912), then president of the *Bureau des longitudes*, was affected by the delay which had occurred due to the flood of the river Seine in January 1910. Fortunately he could show, to the the French government, the equipment in June and, in November, the very first efficient time signals could be sent up to 5 000 kilometers. Accurate values of time were sent, from Paris Observatory to the tower, every day at given hours.

The following year, 1911, France decided to adopt the time zone system referenced to Greenwich. An international conference was held in Paris, upon invitation launched by the *Bureau des longitudes*, in 1912. It was decided to consider the general unification of time at the international level and to create some special bureau to take care of it. But World War I stopped the projects.

During the war Baillaud (1848-1934), then director of the Observatory, and Bigourdan (1851-

1932) succeeded in pursuing some sort of continuation of the project. When the International Astronomical Union was created, in 1919, the *Bureau des longitudes* took this opportunity to propose the creation of a time commission and what was named *Bureau International de l'Heure* (BIH). From the beginning of the century new clocks under constant temperature and pressure were designed. At Paris Observatory they were installed in the basement at minus 27 meters from the courtyard level (temperature stable between 12°5 and 13°), in thick metallic cylindars in which a very low pressure is obtained (Figure 4). Bips issued from the clocks were send to the time division, later to the BIH.

A new meridian instrument had been installed in a special building of the park and two small more modern transit instruments took place in two other ones. After World War I a new instrument appeared, the Claude (1858-1938) and Driencourt (1858-1940) prismatic astrolabe, able to provide data for the simultaneous determination of time and latitude. The bips af all theses instruments were registered through printing chronometers up to the hundredth of the second. After World War II a new instrument, issued by Danjon from the Claude and Driencourt model, was set up in the park in October 1952. More efficient printing chronometers were installed in order to register the bips up to the thousandth of the second, and, in the eighties, more electronics was introduced. Time was given at ± 0,005 second. Observations with this last instrument were stopped, in Paris, on 1987 December 31, new instruments being used for time and latitude determinations.

Meanwhile, by 1930, came quartz clocks and, in 1937, seasonal irregularities of the rotation of the Earth were discovered in Berlin and, in Paris, with Stoyko (1894-1976). For time scales, this new phenomenon had to be taken into account together with the effect of the polar motion. The comparison of clocks scales from various observatories was made under the leadership of the BIH and an international scale was established. In 1985 the time part of the BIH was moved to the Bureau International des Poids et Mesures and, from 1988 January the first, was created the International Earth Rotation Service (IERS).

On the other hand, in 1955, in Great Britain, atomic clocks were designed that were so successful that they can provide time scales independent from the irregularities of the Earth rotation. In 1967, the atomic second replaced the astronomical one based, after the rotation of the Earth (UT), on its revolution (ET). Whatever is the origin of the second, official time is still given to the public, in France, by the Paris Observatory through the speaking or talking clocks, taking benefit of the evolution of time during the 20th century having been created and put into service on 1933.

REFERENCES

Danjon A., *Astronomie générale*, Blanchard Ed., Paris, 1952, 1959, réédité avec notes en 1980.

Delambre J.-B., *Histoire de l'astronomie*, Paris, 1817 à 1827.

Cassini J., *Eléments d'astronomie, Tables astronomiques*, Paris, 1740.

Lalande J.-J. (Lefrançois de), *Astronomie*. Paris, 1764, 1771, 1792.

Toulmonde M., *A propos de l'année zéro*, Les Cahiers Clairaut, nř 89 (printemps 2000), p. 11.

Conférence internationale des étoiles fondamentales de 1896, Paris, 1896.

Constantes fondamentales de l'astronomie, Colloque international du CNRS (Paris, 1950), in Bull. Astron., 15, fascicules 3 et 4, Paris CNRS Ed., 1950.

Le système de constantes astronomiques, IAU Symposium $n°21$ (Paris 1963), Kovalevsky J. (Resp. d'éd.), Gauthier-Villars, Paris, 1965.

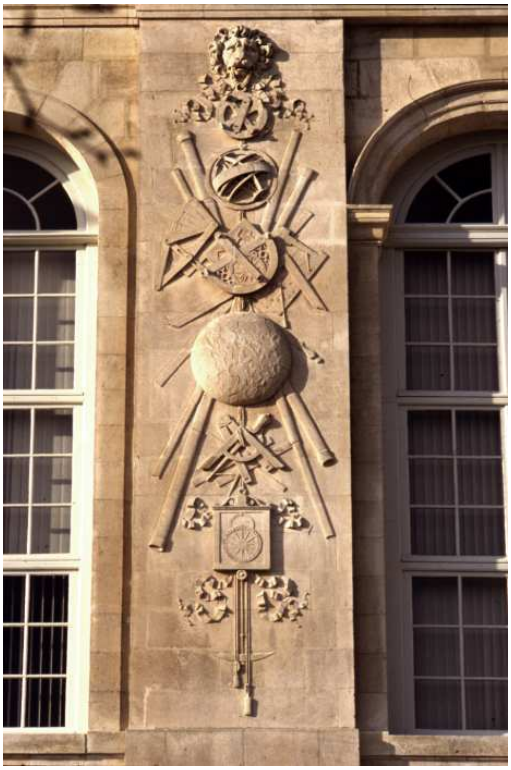

Figure 1: Thuret's clock represented on the southern facade of the Paris Observatory.

Figure 2: A Berthoud's reflactor, the oldest clock still preserved in the collections of Paris Observatory.

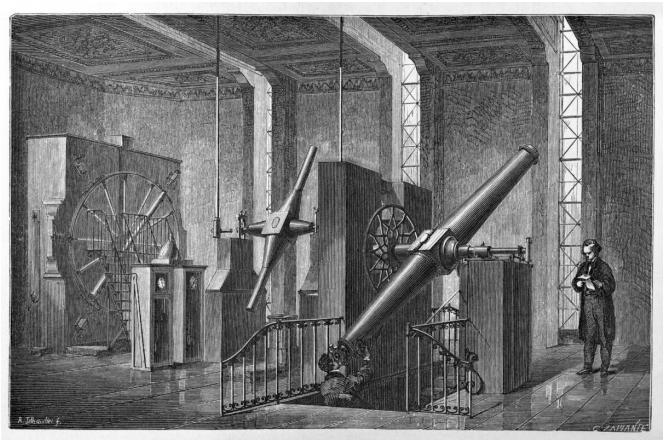

Figure 3: The meridian room as installed when Arago was "directeur des observations" at Paris Observatory.

Figure 4: A fundamental clock installed, by the beginning of the 20th century, in the basement of the Paris Observatory.

EVOLUTION OF EARTH ORIENTATION MONITORING AT IERS

D. GAMBIS, C. BIZOUARD, M. SAÏL
Earth Orientation Product Center
Observatoire de Paris, France
e-mail: daniel.gambis@obspm.fr

ABSTRACT. The dramatic improvement in the accuracy of Earth Orientation Parameters (EOP) over the last decades have lead to the requirement of new concepts and new models in the softwares used to perform time series combinations (McCarthy and Petit, 2004). These softwares themselves have been improved to take advantage of the quality of series independently derived from the various geodetic techniques. However, if the level of precision of combined EOP solutions is now reaching unprecedent values, i.e. 40 μas for polar motion and 8 ms for UT1, the overall accuracy reflecting inconsistencies between EOP and reference frames is significantly larger, 300 μas for polar motion and 20 μs for UT1. This is now not acceptable for various applications needing a high level of consistency. We summarize here the state-of-art concerning the current EOP monitoring and address the new procedure to be applied in order to yield a better consistency between Earth orientation parameters and Reference frames, celestial (CRF) and terrestrial (TRF). For a detailed description of the reference solution IERS Bulletin b and C04 see Gambis (2002, 2004, 2005), Gambis and Wooden (2005).

1. CURRENT CHARACTERISTICS OF EOP ESTIMATES

Precision gives an estimation of the agreement of various individual solutions with respect to other combined solutions, it can be seen as a short-term stability. The current values derived from the internal comparisons are the following:

- Polar motion: 40 μas
- Universal Time: 4 - 10 ms
- Nutation offsets: 70 μas

Accuracy reflects the real uncertainties of the solutions. It takes into account systematic errors of the EOP system with respect to the terrestrial and celestial frames; it is more critical than precision:

- Polar motion: 200-300 μas
- Universal Time: 15-20 ms
- Nutation offsets: 70 μas

2. INCONSISTENCY OF IERS EOP SERIES WITH RESPECT TO ITRF AND ICRF REALIZATIONS

Individual EOP series determined from the analyses of the various techniques present mutually systematic errors, generally limited to biases and drifts which can be attributed to the adoption of different references frames and models. The consistency between EOP and reference frames characterizes the “closure" when making the transformation between CRF and TRF via EOP. Due to the separate computation of EOPs and TRF, it is not surprising that inconsistencies arise after several years. (Altamimi et al., 2005, Gambis et al., 2006). Monitoring inconsistencies is a main task of the EOP Center (Gambis et al. 2002, Gambis and Bizouard, 2003)

At 2006.0 inconsistencies are at the level of 250 μas which is small but significant at the present level of precision brought by the various geodetic techniques (Figure 1). Rigorous methods based on a simultaneous determination of EOP and reference frames TRF and CRF will replace the current combination procedure in the future (Rothacher, 2002) . But it is urgent now to re-align the present reference solution Bulletin B and C04 to the ITRF frame. This will be done in the course of 2006 as soon as the new realisation of ITRF, i.e ITRF2005 will be available to the community. Over 2000 to 2005 C04 polar motion will be adjusted to ITRF2005 System. Corrections consist mainly in a bias which is at 2006.0 in the range of -60 μas. and 250 μas in respectively X and Y-Pole.

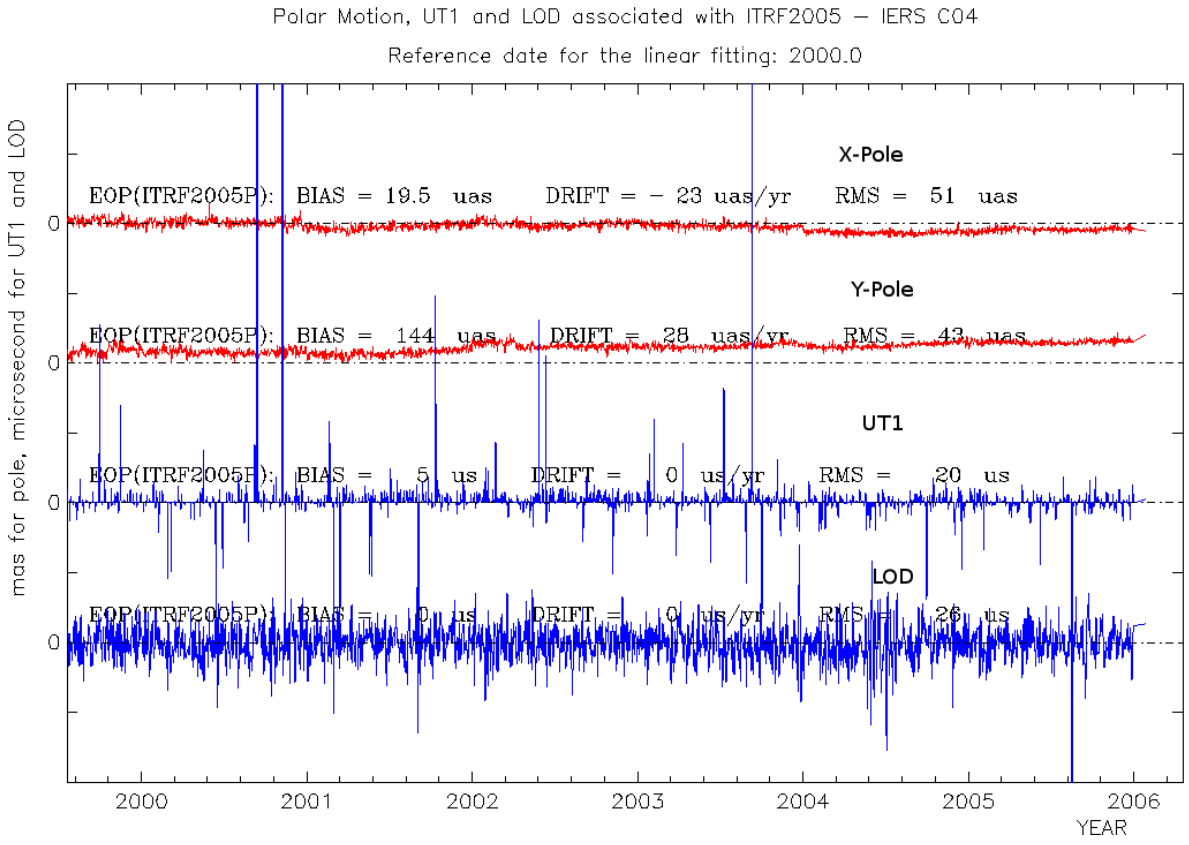

Figure 1: Due to the separate determination of EOP and the International Terrestrial Reference Frame of which the last realization is ITRF2005, small but significant discrepancies appear between the IERS C04 and the EOP solution associated with the ITRF2005. At 2006.0, the values reach - 60 μas and 300 μas in respectively X and Y-Pole.

REFERENCES

Altamimi Z, Sillard P, Boucher C, 2002, ITRF2000: "A new release of the International Terrestrial Reference Frame for Earth Science Applications". JGR, VOL. 107, NO. B10, 2214.

Altamimi Z., Boucher C and D. Gambis, 2005, "Long-term Stability of the Terrestrial Reference Frame", Adv. Space Res 33(6) : 342-349, DOI: 10.1016/j.asr.2005.03.068

Gambis D., 2002, "Allan Variance analysis applied to Earth Orientation Analysis", Adv. Space Research, 30/2, 207-212.

Gambis D., 2004, "Monitoring Earth Orientation at the IERS using space-geodetic observations", J. of Geodesy, 78, pp 295-303.

Gambis D., 2005, "Earth Orientation Monitoring, State-of-the-art and prospects", Artificial Satellite, Journal of Planetary Geodesy, 40, 1, part3, Earth rotation, pp61-69.

Gambis D. and Wooden W., 2005, "Explanatory Supplement for Bulletins A and B", Observatoire de Paris, also available by electronic access (http://hpiers.obspm.fr/eop-pc).

Gambis, D.; Carlucci, T.; Saï, M.; Bizouard, C; Altamimi, Z., 2006, "Towards the improvement of the consistency between the ITRF and the IERS EOPs", EGU General Assembly, Vienne, Austria, 2-7 April 2006, Geophys. Res. Abs., Vol 8.

Gambis D., Bizouard C., Carlucci T., "Jean-Alexis D., 2002, Comparative Study of the EOP Series Derived for the Second IVS Pilot Project", IVS 2002 General meeting proceedings (Vandenberg and Baver, eds))

Gambis D., C. Bizouard, 2003, "Consistency analysis between EOP series and reference frames", in IERS Technical Note 30, Richter (ed.), ISBN 3-89888-877-0, pp 57-62.

McCarthy D.D. and G. Petit (ed.), 2004, "IERS Conventions 2003", IERS Technical Note 32, Verlag des Bundesamts für Kartofraphie und Geodäsie, Frankfurt Am Main, ISBN 3-89888-884-0, 127 p.

Rothacher M.: 2002, "Future IERS products, Implementation of the IAU 2000 resolutions", IERS TN29, Capitaine et al. (eds.), 77-84

GLOBAL COMBINATION FROM SPACE GEODETIC TECHNIQUES

D. GAMBIS , R. BIANCALE, J.-M. LEMOINE, J.-C. MARTY, S. LOYER *,
L. SOUDARIN **, T. CARLUCCI, N. CAPITAINE, PH. BÉRIO, D. COULOT,
P. EXERTIER, P. CHARLOT AND Z. ALTAMIMI
Groupe de Recherche de Géodésie Spatiale, FRANCE
* Noveltis, Ramonville St-Agne, FRANCE
** CLS, Ramonville St-Agne, FRANCE

ABSTRACT. We have demonstrated the possibility of deriving both station coordinates and Earth Orientation Parameters (EOP) using weekly normal equations derived from the processing of different space-geodetic techniques: VLBI, SLR, LLR, DORIS and GPS. The work is performed in the frame of a joint project within the GRGS, Groupe de Recherches de Géodésie Spatiale, federation of French institutes. Observations of the different techniques: VLBI, SLR, LLR, DORIS and GPS are processed separately at the different institutes where in addition expertise can be found for the specific technique. Before such products are adopted as references, different problems concerning the stabilization of the terrestrial reference frame have to be solved in addition to upgrading the individual techniques processing to the best possible level of accuracy.

1. INTRODUCTION

Earth Orientation Parameters (EOP) provide the transformation between the International Terrestrial Reference Frame (ITRF) and the International Celestial Reference Frame (ICRF). The reference EOP series computed at the Earth Orientation Centre at Paris Observatory is obtained from the combination of individual EOP time series derived from the various astro-geodetic techniques: Laser Ranging to the Moon (LLR) and to dedicated artificial satellites (SLR), Very Large Baseline Interferometry on extra-galactic sources (VLBI) and more recently from GPS and DORIS systems.

Although the current determination of reference frames and EOP temporal series are both derived from the same observations processing, the rigorous approach allowing a simultaneous determination of station coordinates and EOP is not currently applied. This is however more satisfactory to ensure consistency between the EOP system and both reference frames. Different approaches are now carrying out within the IERS. The first one is based on combination of SINEX matrices derived from the various techniques (Altamimi et al, 2002; Altamimi et al., 2005). An alternative approach is the combination at the observation equation level. Observations of the different techniques are processed separately by the unique software package: GINS/DYNAMO. The normal matrices derived from the analyses of individual techniques are stacked to give both the terrestrial frame materialized by station positions and Earth Orientation Parameters (EOP). The project started in January 2005 on an operational mode. Results are available on the ftp/Web of the IERS Central bureau (http://www.iers.org).

The a priori dynamical and geometrical models used in the GINS DYNAMO package include: GRIM5-C1 gravity field model and the three body point mass attraction from the Sun, the Moon (in addition J2 Earth's indirect effect) and planets. A priori models include: Earth tides, FES-2004 ocean tide, 6h-ECMWF atmospheric pressure fields. DTM94bis thermospheric model, albedo and infra-red grids from ECMWF, station coordinates derived from ITRF 2000, EOP

from IERS C04 series.

DYNAMO is a set of numerical codes used for normal equations handling: permutation, solving, and stacking. It also can generate a normal equation matrix from a set of constraint parameters.

2. CONSTRAINTS

When solving for parameters, i.e. EOP and station coordinates, the normal equation matrices might not be invertible; it is then necessary to apply constraints. Two kinds of constraints can be applied in the procedure:

II- 1 - Minimum constraints:

Minimum constraints concern transformation parameters: translation, rotation parameters and a scale factor. Their application allows to inverse normal equations matrices suffering from rank deficiencies, which is initially not invertible.
The basic expression used in the transformation of two reference frames X1 and X2 can be written as:

$$X_2 = T + \lambda R X_1,$$

where T is the vector translation $T = (T_x, T_y, T_z)$, R the vector rotation $R = (R_x, R_y, R_z)$ and λ a scale factor.

The minimum constraints applied in the present analysis are translations in X, Y, Z for the VLBI and rotation in Z for the satellite techniques GPS, SLR and DORIS. For more details about minimum constraints, see Sillard and Boucher (2001).

II-2 - Local ties constraints

The combination of EOP and station coordinates derived from the various techniques requires a good link between the terrestrial reference frames. This link is brought by local surveys at collocation sites where two or more techniques are simultaneously observing. Classical surveys are usually direction angles, distances, and levelling measurements between reference points of the instruments or geodetic markers. This is commonly referred to as local ties (3D coordinate differences between the reference points). Adjustments of local surveys are performed by national geodetic agencies operating space geodesy instruments to provide local ties connecting the collocated instruments. An accuracy level of 1-2 mm is required for reference frames combination, however real estimates can reach several centimetres. A local tie file is derived from the computation of the ITRF (Altamimi et al, 2002). DYNAMO allows generating a normal equation matrix from such a local ties file. 23 local ties constraints (ITRF2000 file) were used in the present analyses i.e. 3 SLR-VLBI, 6 SLR- GPS, 6 SLR-DORIS, 1 GPS-VLBI and 7 GPS-DORIS stations.

II-3 -EOP continuity constraints

In addition, to stabilize the EOP time series and remove the short-term noise, continuity constraints on EOP have to be applied. This leads to smooth the corresponding time series. Piece-wise linear fits are applied over 6 h time intervals for deriving daily pole components.

3. WEEKLY COMBINATION PROCESS, ESTIMATION AND VALIDATION

Normal equations derived from the different techniques are stacked on a weekly basis over the six first months of 2005. The constraints previously presented are applied: minimum variance, EOP continuity constraints, local ties (ITRF2000); piece-wise linear fits are applied over 6 h time intervals for pole components in order to derive a daily estimates. The mean measurement residuals lead to determine the weighting of each technique in the global combination (Table 1).

The weighting procedure is based on the variance component estimation method as suggested by Helmert (Sahin et al., 1992). The relative weights are used in the matrices combinations. They should be carefully considered since contributions to EOP and stations coordinates are different according to techniques. Changes in the weights can have significant effects on the final estimation quality.

	Number of observations per week	Mean measurement residuals	Weighting (expressed in measurement units)
GPS (phase)	600 000	4.5 mm	6.8 mm
SLR	1500 - 4000	1.0 cm	1.3 cm
DORIS	100 000	0.40 mm/s	0.27 mm/s
VLBI	2000 - 5000	1.5 - 3.5 cm	1.0 cm
LLR	0 - 20	11. cm	46. cm

Table 1: Statistics concerning the processing of the various techniques

III-1 - Multi-technique EOP combined solution EOP are computed with respect to the IERS EOP C04 (Gambis, 2004] corrected with the diurnal and sub diurnal model (Ray et al, 1994). Station position corrections are computed with respect to ITRF2000 positions (Altamimi et al, 2002) corrected with models of IERS conventions Table 2 gives for pole components and UT1 the differences between this multi-technique combined solution, referred as EOP (GRGS) and the IERS C04 with the corresponding statistics, biases and RMS. External results derived from the different techniques also referenced to IERS C04 are also given. RMS values are good compared to the various international services contributions but are so far not at the level of accuracy of these solutions. This comes from the fact that individual techniques observations processed by GINS need to be improved to match the best products given by GPS for polar motion and VLBI for UT1.

III-2 - Assessment of the quality of the global reference frame derived
Weekly sets of station coordinates are expressed in a frame consistent with the ITRF2000 used as the reference. Levels of 3-5 mm in positions and 3-8 mm in the height component are reached with fair time stability.

The quality of the multi-technique combined terrestrial reference frame (GRGS) depends on the relative qualities of the contributing solutions per technique as well as on the combination strategy which is applied. The overall quality indexes of the individual solutions included in the GRGS combination is given via the transformation components: translation and scale.

Table 3 represents the transformation between these reference frames expressed in the form of translation, rotation and scale factor parameters. It gives the accuracy of the origin and scale. All results and in particular those relative to the multi-technique combination show a general fair stability of terrestrial reference frames compared to ITRF2000. We can note that SLR results present some significant discrepancies larger than one centimetre in the translation components.

	Bias			R M S		
	X_p (μas)	Y_p (μas)	$UT1$ (μs)	X_p (μas)	Y_p (μas)	$UT1$ (μs)
IGS	-31	320		36	31	
IVS	-221	231	1	195	122	8
ILRS	-226	242		180	213	
IDS	21 265	14 657		459	744	
GRGS	-21	30	1	73	74	15

Table 2: Earth rotation parameters: differences of the global combined solution referred as to GRGS with IERS C04 used as the reference. Comparisons with solutions derived from International Services are also given

	T_X (mm)	T_Y (mm)	T_Z (mm)	Scale (ppb)	R_X (mm)	R_Y (mm)	R_Z (mm)
GPS	6	7	-4	11	-3	-1	-3
SLR	-14	-11	-21	1	-6	7	-7
VLBI	1	-3	-1	2	-1	0	2
DORIS	3	30	31	-8	-7	2	10
GRGS	-7	6	-4	6	-3	0	1

Table 3: Reference frame solution: 7-parameter transform / ITRF2000 translation and rotation components in mm. Scale factors are in ppb (6 mm in station heights)

4. CONCLUSIONS

The combination process is performed on a routine basis since the beginning of 2005 in the frame of GRGS. We already demonstrated the good quality of the results for EOP as well as station coordinates. Better results are expected after the improvement in the processing of the different techniques. It appears that the EOP and station coordinate solutions are sensitive to a number of critical parameters mostly linked to the terrestrial reference frame realization i.e. station minimum constraints, local ties, EOP continuity constraints for the Earth Orientation Parameters. Before EOP and station coordinates be derived on an operational basis with an optimal accuracy different problems have to be studied and solved. Another critical point which needs to be carefully studied concerns the optimization of the weighting of the different techniques using the Helmert's method. Other improvements will likely come from the upgrade in the processing of the various techniques such as the use of GPS double differences with integer ambiguities resolution, the use of JASON DORIS data taking care of SAA correction, the homogenization of tropospheric corrections per site using dry and wet delays derived from ECMWF. We also expect to be able to reduce the delivery delay to less than 8 weeks.

REFERENCES

Altamimi, Z., Sillard, P., and Boucher, C., 2002, A new Release of the International Terrestrial Reference Frame for Earth Science Applications J Geophys Res 107(B10), 2214, doi 10.1029/2001JB000561

Altamimi Z., Boucher C and D. Gambis, 2005, Long-term Stability of the Terrestrial Reference Frame, Adv. Space Res 33(6) : 342-349, DOI: 10.1016/j.asr.2005.03.068

Gambis D., 2004, Monitoring Earth Orientation at the IERS using space-geodetic observations., J. of Geodesy, 78, pp 295-303. state-of-the-art and prospective, J Geod 78(4-5):295-303, doi: 10.1007/s00190-004-0394-1

IERS Conventions, 2003, McCarthy and Petit (eds), BKG, Frankfurt am Main.127p.

Ray, R. D., Steinberg, D. J., Chao, B. F. et al. 1994, Science, 264, 830

Sahin, M., Cross, P. A. and Sellers P. C. 1992, Bull. Géod., 66, 284

Sillard, P., and C. Boucher, 2001, Review of algebraic constraints in terrestrial reference frame datum definition, J. Geod., 75, 63- 73.

CONTRIBUTION OF SLR RESULTS TO LLR ANALYSIS

S. BOUQUILLON, J. CHAPRONT, G. FRANCOU
Observatoire de Paris
77, avenue Denfert Rochereau, 75014 Paris, FRANCE
e-mail: sebastien.bouquillon@obspm.fr

ABSTRACT. Terrestrial stations of Satellite Laser Ranging (SLR) can be used for Lunar Laser Ranging (LLR). Currently, Moon's echoes are regularly provided by the two stations : OCA (Grasse, France) and McDonald observatory (Texas, USA). The quality of the density and the distribution of SLR global tracking network associated with the sub-centimeter precision of this technique allows to determine the time series for positions of the stations in the International Terrestrial Reference Frame (ITRF). The global accuracy is better than 5 mm (Coulot et al. 2003). We show here different attempts we tried to improve the Lunar Laser Ranging residuals (O-C) by taking account of time series for the positions of Grasse and McDonald LLR stations determined by SLR technique.

1. INTRODUCTION

LLR data of the last decade have a sub-centimeter accuracy. Hence, to compute LLR residuals, we need to have the coordinates of the laser ranging stations in a terrestrial reference system with at least the same accuracy. The coordinates of laser ranging stations that we currently use are ITRF coordinates. Each of these ITRF coordinates are the sum of a constant value corresponding to the position of the station at J2000 and a time derivative coefficient corresponding to the tectonic plate motions. But some other local motions can also occur (seasonal motions, non predictable motions, ...). For this reason a new ITRF representation is evolving towards time series for the coordinates of terrestrial stations together with time series of Earth's orientation parameters. The work started by GEMINI team of OCA (Coulot et al. 2003) is a first step to determine these time series by SLR technique. We try here to implement these series in our model for the computation of the LLR residuals.

First, we rapidly remind the laser ranging technique and we illustrate the LLR residuals that we got when we do not take account of the time series for the positions of the stations. Next, we use the time series of Grasse determined by SLR technique and we derive a simple model that we have to add to the classical ITRF coordinates of Grasse to reduce LLR residuals. At last, we show the consequences of this implementation on LLR residuals.

2. LASER RANGING TECHNIQUES

Satellite laser ranging and lunar laser ranging techniques are very similar. The principle of these techniques is based on measurements of the time propagation of a light pulse between a station on the Earth and a target which is either a satellite or one of the four retro-reflectors settled on the lunar surface by Apollo and Lunakhod missions. A laser pulse is emitted through a telescope in the direction of one of these targets and the starting time of the pulse is measured. The Moon's retro-reflectors are corner cube arrays. A satellite which allows us to perform laser ranging measurements has also one corner cube at least on its surface. The interest of glass corner cube is to reflect the laser pulse in the precise opposite direction of its arrival. In our case, it reflects the laser pulse toward the Earth. Some of these return laser photons are detected by the same telescope and the returning time is measured. The time interval between the starting and returning times allows us to deduce the distance between the terrestrial laser station and the target. The main difference between LLR and SLR techniques is due to the distance between the Earth and the Moon which is larger than between the Earth and a satellite. For instance, Lageos is fifty times closer to the Earth than the Moon. This difference in the distances, the laser divergence and the atmosphere effects, explain that the number of returning photons from the Moon's retro-reflectors is drastically smaller than from a satellite. It is why only few laser stations are able to shoot the Moon's retro-reflectors.

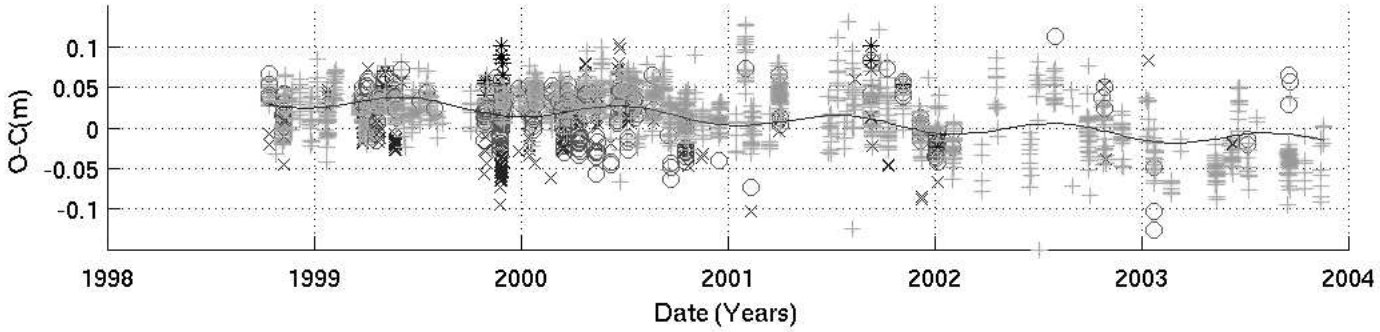

Figure 1: Lunar laser ranging O-C (Grasse station)

Figure 1 shows our LLR residuals for the period 1998-2004. The used LLR observations are data from Grasse station. The corresponding LLR residuals obtained with McDonald are not shown on Figure 1 but are very similar to Grasse's ones. The computed part of these LLR residuals are provided by a software developed by J. Chapront, M. Chapront-Touzé and G. Francou. It is based on ELP/MPP02 ephemeris for the orbital motion of the Moon and on M. Moons' libration model with some analytical and numerical complements for the orbital and rotational motions of the Moon. See Chapront et al. (2002) for more details. In this paragraph, the laser ranging station positions used in this modelling are usual ITRF coordinates. The "O", "X", "+" and "$\star$" marks on Figure 1 represent LLR residuals obtained with Apollo XI, Apollo XIV, Apollo XV and Lunakhod 2 retro-reflectors respectively. The line crossing on Figure 1 is a very simple model fitted to LLR residuals (O-C) derived from a weighted least squares software. Using the year as a time unit and $t = 0$ at J2000, the resulting model in meter is :

$$(O-C)_{aj.1} = 0.02266 - 0.01028 * t - 0.00913 \cos(2\pi t) + 0.00139 \sin(2\pi t)$$

The number of LLR data, the mean values and the RMS of our LLR residuals for each retro-reflectors and for both Grasse and McDonald are given in Table 1. The total mean values are not really centred on zero because it was resulting from a fit performed on a much longer interval of time.

	Grasse station data			McDonald station data		
Retro-reflectors	Data Nb.	Mean value(m)	RMS(m)	Data Nb.	Mean value(m)	RMS(m)
Apollo XI	241	0.012	0.034	188	-0.013	0.058
Apollo XIV	165	-0.009	0.040	222	-0.001	0.048
Apollo XV	1899	0.018	0.032	1881	-0.004	0.043
Lunakhod 2	19	0.057	0.032	10	-0.018	0.022
Total	2324	0.015	0.034	188	-0.004	0.045

Table 1: Mean values and RMS of Lunar laser ranging residuals for each retro-reflector provided by Grasse laser station since 1998 and by McDonald laser station since 1994.

3. TIME SERIES OF GRASSE SATELLITE LASER RANGING STATION POSITIONS

Here, we do not explain how the time series for the positions of satellite laser ranging stations were determined by GEMINI team (see Coulot et al. (2003) for this) but we simply display the results for Grasse. On Figure 2, we show the X,Y and Z coordinates of Grasse station in ITRF determined by SLR technique each eight days since 1998. This date corresponds to the begining of satellite laser ranging with Lageos at Grasse.

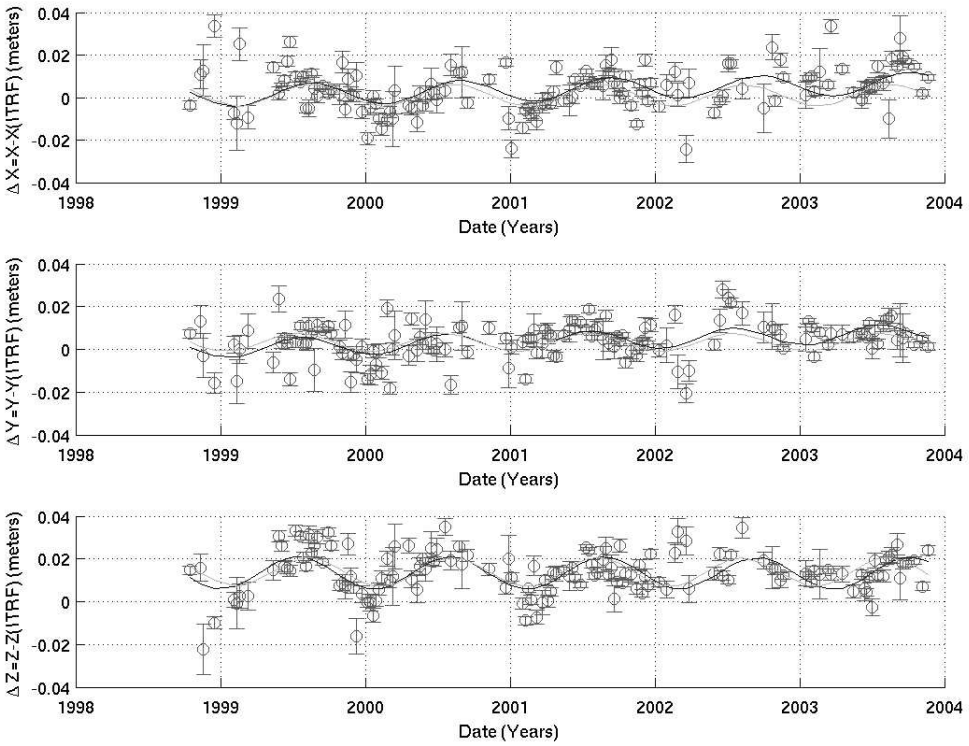

Figure 2: Time series of Grasse station positions in ITRF 2000

By a frequency analysis performed with the software named FAMOUS (Mignard, 2003). We find as a main periodic term in each time series of the station coordinates a term close to a one year period. We find, for X, Y and Z respectively, periodic terms: 1.0324 ± 0.0249 years, 0.9944 ± 0.0251 year and 1.0584 ± 0.0694 years and with signal-to-noise ratios: 4.7, 4.0 and 4.9. The annual periodic term is probably due to seasonal variations of continental water storage . To take account of the uncertainties of each eight days determination of station positions into the model of these time series, we fit a one order polynomial in time and an annual term, with

the aid of a weighted least squares. The resulting models for each coordinates of Grasse station are :

$$\begin{aligned}
\Delta X &= 0.00104 + 0.00173 * t - 0.00357 \cos(2\pi t) - 0.00353 \sin(2\pi t) \\
\Delta Y &= 0.00327 + 0.00103 * t - 0.00399 \cos(2\pi t) - 0.00100 \sin(2\pi t) \\
\Delta Z &= 0.01385 - 0.00057 * t - 0.00517 \cos(2\pi t) - 0.00415 \sin(2\pi t)
\end{aligned}$$

We first add this model to the ITRF coordinates of Grasse station and we compute once again LLR residuals. This operation does not really improve RMS of LLR residuals. If we try to fit a model as in paragraph 2 to these new residuals, we get the following resulting approximation that we must compare with the previous one above:

$$(O-C)_{aj.2} = 0.02266 - 0.00836 * t - 0.01218 \cos(2\pi t) + 0.00565 \sin(2\pi t)$$

We see, that we don't have any improvement of annual term coefficients. Nevertheless, we have an improvement of the time derivative coefficient of 2 mm/year on the 7 years of this analysis.

We perform the same analysis with time series of McDonald positions. The fit is more complicated mainly because the frequency analysis of McDonald series doesn't display similar frequencies in each of its three coordinates. As for Grasse data, the RMS of McDonald lunar laser ranging residuals are not significantly improved by taking account of the time series of McDonald obtained by SLR techniques.

4. CONCLUSION

The introduction of time series for the positions of SLR stations into the LLR reductions is justified by two main reasons: The first one is that since 1993 for McDonald and since 1998 for Grasse, Lageos Satellite laser ranging observations (used to get time series of station positions) and LLR observations have been done in a concomitant way with the same instrument and the same laser ranging technique. The second one is that the amplitude of variation for the positions of the laser stations are of the same order that the actual LLR residuals RMS (the annual amplitude of Grasse laser station position is about 2 cm and the Grasse LLR residuals RMS between 1998 and 2004 is around 3.4 cm).

Unfortunately, this first attempt to take into account the local variations of laser station positions do not really improve the RMS of LLR residuals. One reason could be that some larger effects (as lunar librations, retro-reflector orientations, atmosphere effects, etc ...) are not modelized with a sufficient accuracy. One another reason could be that we don't take account of geocenter motion in LLR reduction while it is taken into account in the deterrmination of the station positions.

However, it remains an interesting result: the time derivative coefficient of LLR residuals is reduced by 2 mm/year between 1998-2004 when taking account of time series for the positions of SLR stations determined by SLR analysis.

REFERENCES

Coulot, D. et al.: 2003, SF2A "Semaine de l'Astrophysique française", Eds.: Combes, F. et al., EdP-Sciences, Conference Series, p.51.

Chapront J., Chapront-Touzé, M., Francou G.: 2002, Astron. & Astroph., 387, p.700.

Mignard, F.: 2003, FAMOUS (Frequency Analysis Mapping On Unusual Sampling)

MONITORING THE INTERNATIONAL TERRESTRIAL REFERENCE FRAME 2000 BY SATELLITE LASER RANGING IN 1993–2003

S. SCHILLAK, P. MICHAŁEK
Space Research Centre of the Polish Academy of Sciences
Astrogeodynamic Observatory
Borowiec

ABSTRACT. Monitoring of terrestrial reference frames in the long time periods is important task for control of the correctness of the stations coordinates. The laser technique give the absolute positioning which permit detection of all instabilities of each station on the Earth surface. The paper presents results of determination of positions and velocities of all SLR stations in comparison to ITRF2000 in the five years period 1999-2003. The coordinates were determined individually for each station from one month orbital arcs of Lageos-1 and Lageos-2 satellites for first day of every arc and for epoch 1997.0. The stability of station coordinates determined for the same epoch 1997.0 in the five year period varied from 5 mm to 7 cm. In the period of study two real position changes were detected; for station Tateyama in 2000 and Arequipa in 2001. The orbital RMS and range bias separately for Lageos-1 and Lageos-2 were determined for each station. The results for both satellites for the most stations were in very good agreement which confirm correctness of orbital analysis. The stations velocities as result mainly of tectonic plate motion were determined by regression analysis from five years period. For the most stations is a good agreement with model of tectonic plate motion NUVEL1A. Several stations had significant differences in comparison to position and velocity in ITRF2000.

1. INTRODUCTION

The paper presents results of monitoring of the satellite laser ranging (SLR) station positions and velocities determined from satellite laser observations performed in the period 1999-2003. All results were compared with ITRF2000. The calculations included all SLR data in the period of study with exception five stations with too small number and quality of data. The positions of 50 SLR points and stations for epoch 1997.0 were determined for the period from 1^{st} January 1999 to 31^{st} December 2003. The velocities of the SLR stations were determined for 29 stations including only points with time span longer then two years.

2. ORBITAL ANALYSIS

The calculations were performed in Borowiec Analysis Centre (BAC) by NASA orbital program GEODYN-II (McCarty et al. 1993). The program included the following models and parameters: Earth gravity field: EGM96 (Lemoine et al. 1998) or EIGEN-GRACE02S (Reigber et al. 2005) 20x20, polar motion IERS C04, arc length 1 month, satellites LAGEOS-1 and LAGEOS-2, 15–17 reference stations in ITRF2000 (Boucher et al. 2004) for orbit determina-

tion; estimated parameters: satellite state vector, station geocentric coordinates, acceleration parameters along-track, cross-track and radial at 5 days intervals.

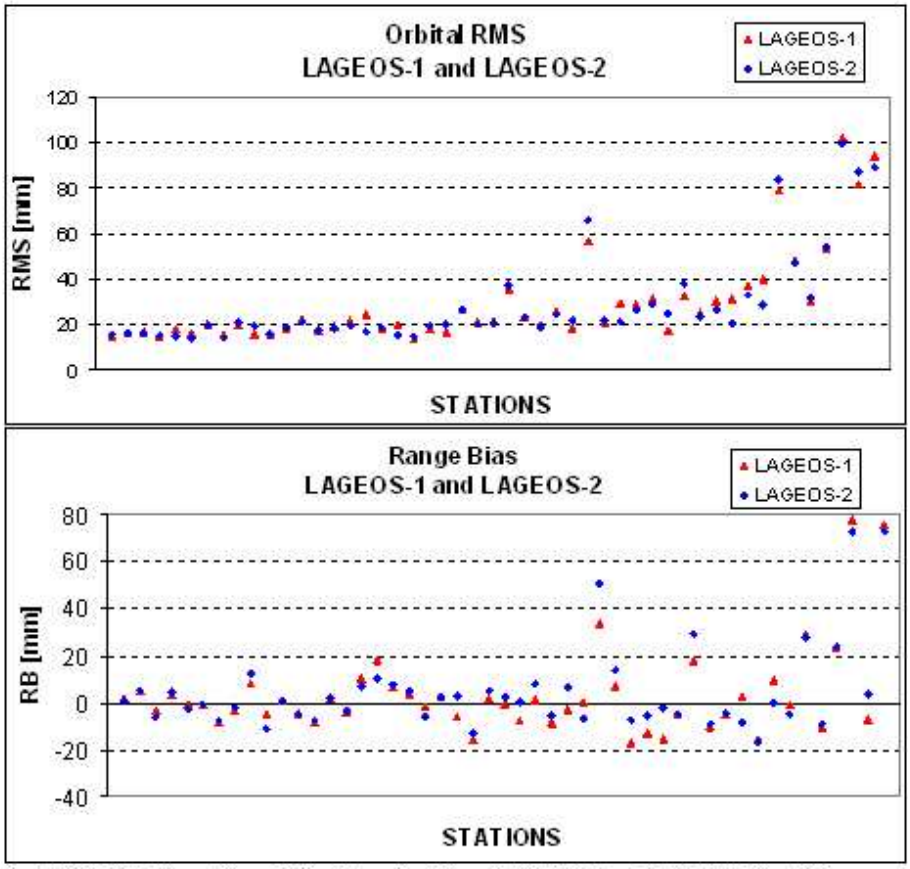

Figure 1: Orbital RMS and Range Bias determined from LAGEOS-1 and LAGEOS-2 satellites for all SLR stations in 1999-2003

The influence of observations data on the quality of the orbit determination is presented in Fig.1. The orbital RMS-of-fit and Range Bias for each station were determined independently from orbit of LAGEOS-1 and LAGEOS-2. High agreement of the results for both satellites indicate that sources of errors are mainly from SLR stations. The improvement of accuracy of the orbital analysis was achieved by change of used models: polar motion from model IERS C01 to IERS C04 (Schillak, 2005-2) and gravity field model from model EGM96 to model EIGEN-GRACE02S (Fig. 2). The mean orbital RMS-of-fit for 5 years was equal to 15 mm.

3. STABILITY OF STATION COORDINATES

The stability of 50 stations and points were calculated from scatter of positions determined per each month. The real change of position due to earthquake were detected for two stations: Tateyama (7339), 4.5 cm in June–August 2000 (Schillak et al. 2005) and Arequipa (7403), 62 cm in 23 June 2001 (Schillak and Wnuk, 2002). The results for two stations: Zimmerwald and Concepcion were calculated independently for two colors: blue-423 nm and infrared-846 nm. The best station stability was on the level 5 to 10 mm (16 points and stations). The stability of the most stations (30) was in the range 1-3 cm. Several stations had significant technical problems.

36 stations had coordinates ITRF2000. The differences of the station positions between

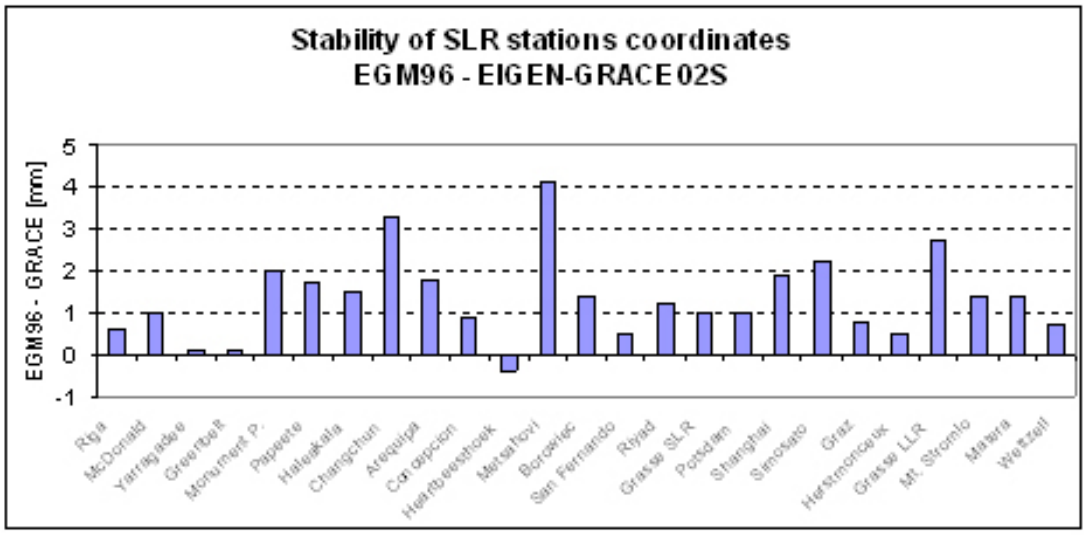

Figure 2: Stability of the SLR station coordinates for gravity field EGM96 and EIGEN-GRACE02S in 1999-2003

ITRF2000 and results of Borowiec Analysis Centre (BAC) were in the range 3-15 mm. Some stations had incorrect ITRF2000 coordinates, specially Riyad (7832), several stations had significant technical problems in the period of study (Maidanak-2, Beijng, Cagliari, Kunming, San Fernando, Simosato) or too small number of observations (Tokyo, Helwan).

4. STATION VELOCITIES

The station velocities were determined only for stations with data time span longer than 20 months, it means for 29 stations and points. The best accuracy of station velocities determination was obtained for span of 5 years. The accuracy for two years is three times lower. The difference of station velocities between ITRF2000 and the results of BAC were in the range 0-5 mm/year. Only for four stations differences were significant (Maidanak-2, Beijng, Arequipa after earthquake and Riyad). The comparison of station velocities with tectonic plates motion model NUVEL1A shows similar agreement with exception of Arequipa, Concepcion, Shanghai and Simosato. The model NUVEL1A is insufficient for South America plate and Japan.

5. CONCLUSIONS

The paper shows a good agreement between positions and velocities of the SLR stations determined by Borowiec Analysis Centre and ITRF2000 and tectonic plate motion model NUVEL1A. The ITRF2000 position and velocity of Riyad station need a correction. The station position stability for the best station achieve 5 mm in the 5 year period of study but for the most stations is in the range 1-3 cm and need improvement of the quality of SLR data of these stations. The determination of the SLR station velocities is possible with sufficient accuracy only for periods longer than two years, the longer time period significantly improve results. The long time series are very important for velocity determination. The velocities of South America tectonic plate and Japan (Arequipa, Concepcion, Simosato) and wave character changes in vertical component for several station should be explain. The positions and velocities of new points in Tateyama and Arequipa after earthquakes should be included in the new ITRF2005 solution. The near-real time monitoring of the SLR station coordinates is necessary for quick detection

of real position changes and stations instrumental systematic errors. The improvement of accuracy of stations coordinates need further upgrading of the orbital programs: new or improved models of satellite and station position perturbations (atmosphere, loading effects, new models of Earth gravity field, geocenter motion...), new International Terrestrial Reference Frame (ITRF2005), new precession-nutation model (IAU2000), new celestial and terrestrial reference system (IAU2000).

Acknowledgements. The authors wish to thank NASA geodesy group from the Goddard Space Flight Center, Greenbelt, for providing the GEODYN-II program. Also, we like to thank Danuta Schillak from the Borowiec Astrogeodynamic Observatory for her assistance in calculations and preparing the data for the program GEODYN-II. We would like to thank all ILRS (International Laser Ranging Service) stations and data centers for their continuous efforts to provide high-quality global SLR data for this work.

REFERENCES

Boucher C, Altamimi Z, Sillard P, Feissel-Vernier M, 2004, "The ITRF2000", IERS Technical Note No. 31, BKG, Frankfurt am Main

Lemoine FG, Kenyon SC, Factor JK, Trimmer RG, Pavlis NK, Chinn DS, Cox CM, Klosko SM, Luthcke SB, Torrence MH, Wang YM, Williamson RG, Pavlis EC, Rapp RH, Olson TR, 1998, "The development of the joint NASA GSFC and the National Imagery and Mapping Agency (NIMA) Geopotential Model EGM96", NASA/TP-1998-206861, Goddard Space Flight Center, Greenbelt

McCarthy JJ, Moore D, Luo S, Luthcke SB, Pavlis DE, Rowton S, Tsaousi LS, 1993, "GEODYN-II", Vol. 1-5, Hughes STX Systems Corporation, Greenbelt

Reigber C, Schmidt R, Flechtner F, Koenig R, Meyer U, Neumayer KH, Schwintzer P, Zhu SY, 2005, "An Earth gravity field model complete to degree and order 150 from GRACE: EIGEN-GRACE02S", Journal of Geodynamics 39 (1): 1-10

Schillak S, Wnuk E, 2002, "The SLR stations coordinates determined from monthly arcs of LAGEOS-1 and LAGEOS-2 laser ranging in 1999-2001", Adv Space Res 31 (8): 1935-1940

Schillak S., Wnuk E., Kunimori H., Yoshino T., 2005-1, "Crustal deformation in the Key Stone network detected by satellite laser ranging", Journal of Geodesy, DOI:10.1007.s00190-005-0020-x

Schillak S., 2005-2, "Ocena dokladnosci wyznaczania wspolrzednych stacji technika laserowa", 2005, Seminarium "Satelitarne metody wyznaczania pozycji we wspolczesnej geodezji i nawigacji", Poznan, 23-24.06.2005, (CD-ROM Proc., in Polish).

DETERMINATION OF THE COLLOCATED IERS SITES COORDINATES WITH COMBINATION OF GPS AND SLR DATA

M.O. LYTVYN, O.V. BOLOTINA
Main Astronomical Observatory of the National Academy of Sciences of Ukraine
27, Akademika. Zabolotnoho St., 03680 Kiev, Ukraine
e-mail: misha@mao.kiev.ua, olga@mao.kiev.ua

ABSTRACT. The year data series of GPS and SLR observations from European collocated IERS sites were processed. The analyses were performed with the *GAMIT/GLOBK ver. 10.2* and *Kiev-Geodynamics-5.2* respectively. The coordinate time series were obtained. Combination of results obtained from two techniques are carried out at normal equations level. The comparison of sites positions derived from single technique and from combined solution are discussed.

1. OBSERVATIONS PROCESSING

The Lageos-1 and Lageos-2 observations from 36 SLR stations over the period of 2000.12.18 – 2002.01.26 were used. The apriori coordinates and velocities were taken from the solution SSC(GAOUA)01L01. The data processing has been carried out according to the models and methods recomended by IERS Conventions (1996) (McCarthy, 1996). The frame of GPS_SLR were transformed to ITRF2000.

The GPS data have been processed with *GAMIT 10.2* software package (King, 2003) for GAO_GPS solution. The data from 13 GPS weeks (every fifth week from GPS week 1095 to 1147) obteined at 7 permanent GPS stations (GLSV, WTZR, CRAO, ZIMM, BOR1, MATE, METS) were used for obtaining GAO_SLR solution. Apriori coordinates are taken from ITRF2000. The procesing has been carried out according to EPN standards using IGS products (Beutler, 1990) (precise satellite orbits, antennas phase center variations, etc.).

2. OBTAINING THE COMBINED SOLUTION

The combined solution GPS_COMB was obtained with *GLOBK ver 10.2* software. The combination has been carried out using the stored VCV matrices and apriori values for estimated parameters from GAO_GPS and GAO_SLR solutions. The good positions agreement from GPS and SLR data were obtained for 3 stations – Zimmerwald, Wettzel, Borowiec. For this reason only this sites were treated as sites with collocated techniques.

Table 1 gives the transformation parameters between the solutions and ITRF2000.

Parameters	ITRF-GAO_SLR	ITRF-GAO_GPS	ITRF-GAO_COMB
T1, m	1.376	0.079	0.080
T2, m	3.654	-0.307	-0.306
T3, m	-2.003	0.399	0.400
D, mm/km	0.0128	-0.0094	-0.007
R1, mas	0.098	-0.010	0.007
R2, mas	-0.076	0.006	-0.006
R3, mas	-0.069	0.005	0.015

Table 1: Transformation parameters between the frames

3. CONCLUSIONS

- Selected SLR and GPS stations are iregularly distributed around the globe.
- The number of SLR observations in a two order smaller than number of GPS observations.
- SLR observations has been carried out irregularly.
- The solutions are distorbed by errors of processing software.

For these reasons there are big differences in reference points positions for 2 sites with collocated techniques.

- The year data span is not enough to obtain reliable SLR stations positions.
- Combining the data from different techniques we have to provide wheight function whith account for not only precision of observations but also their number and regularity.
- If there are a small number of SLR data it is possible to strenthen solution adding a GPS data.

Acknowledgements. This work is supported by the grant No. F7/256-2001 by the Ministry of Science and Education of Ukraine.

REFERENCES

Ge L., H.-Y. Chen, S. Han, Ch. Rizos et. al., 2000, "The integration of collocated GPS, VLBI and SLR results", ION GPS, 19-22 September 2000, Salt Lake Sity.- pp. 1525-1535

McCarthy D. (Ed.), 1996, "IERS Conventions, IERS Tech. Note 21", Paris: Observatoire de Paris

Boucher C. (Ed.) et. al., 2004, "The ITRF2000, IERS Tech. Note 31", Frankfurt am Main: Verlag des Bundesamts fur Kartographie und Geodasie

King R., Y. Bock, 2003, "Documentation for the GAMIT GPS Analysis Software", Massachusets Institute of Technology

Beutler G., M. Rothacher, S. Schaer, et. al., 1990, "The International GPS Service (IGS): An Interdisciplinary Service in Support of Earth Sciences", Adv. Space Res. Vol. 23, No. 4, pp. 631-635

DETERMINATION OF SEASONAL GEOCENTER VARIATIONS FROM DORIS, GPS AND SLR DATA

S.P. KUZIN, S.K. TATEVIAN
Institute of Astronomy, RAS
48, Pyatnizkaya st., Moscow, Russia
e-mail: skuzin@inasan.rssi.ru
e-mail: statev@inasan.ru

The gravitational center of the Earth plays a crucial role as the origin of the terrestrial reference system and should be determined and monitored with highest accuracy.

Physically, the geocenter is defined as center of mass (CM) of the whole Earth, including oceans, atmosphere and surface groundwater.

Practically, the geocenter is realized by the coordinates of the tracking network on the solid Earth. If a set of tracking stations has sufficient global coverage, the variations of the center of network (CN) will be a good representation of the geocenter variations [Dong et al., 2003].

Geocenter variations caused both surface and internal mass redistribution. Theoretically the spectrum of the geocenter oscillations is a sum of spectra from all geophysical processes capable of causing mass redistribution. In this investigation we pay our attention on seasonal geocenter variations (annual and semiannual) as the most significant compare with other periods [Montag, 1999].

5 time series of geocenter solutions were used for comparison:
- two DORIS solutions using data on SPOT2, SPOT3, SPOT4, SPOT5, TOPEX-POSEIDON and ENVISAT satellites;
- one GPS global solution;
- two SLR solutions.

The seasonal geocenter variations were derived by least squares method using the next approximation:

$$J(t) = a_0 + b_0 t + A_0 \sin\left[\frac{2\pi(t - t_0)}{P} + \varphi_0\right], \qquad (1)$$

A_0 - amplitude of the signal;
P - period of the signal (in years);
φ_0 - initial phase of the signal;
a_0 - offset;
b_0 - trend;
t - time;
t_0 - arbitrary initial time (we take t_0 - 1st January).

Table 1 shows the seasonal geocenter variations derived from Doris, GPS and SLR data and predicted values from surface mass redistribution (atmosphere, oceans, continental hydrology). The SLR solutions (Lageos1,2 and Topex/Doris) are in good agreement with the geophysical predictions for amplitudes. The phases are mainly different. The amplitudes of the Doris and GPS x and y components are a bit larger compare with the SLR and predicted solutions. The phases again are different. The amplitudes of z component for Doris and GPS geocenter variations are significantly bigger (4-7 times) then in the mean SLR solutions.

For IGN/JPL DORIS geocenter time series, the biases and trends are 2.7±0.6, 9.4±0.6, -35.4±3.3 mm, -1.9±0.1, 0.1±0.1, 5.1±0.4 mm/yr, for x, y and z, respectively. For INASAN DORIS geocenter time series, the biases and trends are 2.9±0.5, 11.5±0.5, -32.4±2.4 mm, -1.2±0.1, -0.4±0.1, 3.7±0.5 mm/yr, for x, y and z, respectively. For JPL GPS geocenter time series, the biases and trends are 5.4±0.6, 13.5±0.5, -37.1±1.3 mm, -0.2±0.1, -1.6±0.1, 3.8±0.2 mm/yr, for x, y and z, respectively. For CSR SLR (Lageos1,2) geocenter time series, the biases and trends are -0.7±0.5, -0.9±0.5, -6.8±0.6 mm, -0.2±0.1, 0.7±0.1, 1.2±0.2 mm/yr, for x, y and z, respectively. For CSR SLR (Topex/Doris) geocenter time series, the biases and trends are -0.4±0.3, 0.5±0.3, -2.2±0.9 mm, 0.1±0.1, 0.2±0.1, 0.6±0.2 mm/yr, for x, y and z, respectively.

Table 1: Measured and predicted seasonal variations of geocenter motion

MEASURED

SOLUTION		Span	X				Y				Z			
			Annual		Semiannual		Annual		Semiannual		Annual		Semiannual	
			A, mm	Ph, deg	A, mm	Ph, deg	A, mm	Ph, deg	A, mm	Ph, deg	A, mm	Ph, deg	A, mm	Ph, deg
DORIS	IGN/JPL (weekly)	1993.0-2005.4	6.2 ±0.3	91.6 ±3.2	1.2 ±0.3	1.8 ±15.2	5.5 ±0.1	314.9 ±5.3	4.4 ±0.5	199.4 ±2.9	30.6 ±1.2	288.8 ±4.7	18.4 ±1.5	347.8 ±7.3
	INASAN (weekly)	1993.0-2004.5	5.5 ±0.3	104.9 ±5.1	2.0 ±0.4	5.1 ±10.4	4.3 ±0.3	352.6 ±6.0	1.9 ±0.5	205.2 ±5.7	23.7 ±1.2	286.8 ±5.6	11.0 ±1.6	353.7 ±10.7
GPS	JPL (daily)	1993.0-2004.7	3.0 ±0.1	302.5 ±7.1	14.1 ±0.2	354.9 ±1.2	5.0 ±0.1	288.8 ±3.8	3.3 ±0.3	12.0 ±3.2	13.2 ±0.4	109.5 ±3.4	6.0 ±0.4	106.8 ±7.2
SLR	CSR-Lag1,2 (monthly)	1993.0-2000.2	3.1 ±0.5	17.6 ±4.9	1.1 ±0.5	19.2 ±13.2	5.5 ±0.5	197.9 ±2.6	0.8 ±0.5	16.0 ±18.5	3.6 ±0.5	82.8 ±6.5	1.4 ±0.6	197.1 ±12.2
	CSR-T/P (monthly)	1993.0-2000.1	1.8 ±0.4	47.8 ±0.5	1.5 ±0.2	170.7 ±11.7	2.8 ±0.1	130.3 ±6.1	0.4 ±0.1	295.1 ±38.0	2.3 ±0.8	66.0 ±8.0	3.8 ±0.8	195.4 ±6.8

PREDICTED

Dong et al.[1997]	4.2	224	0.83	30	3.2	339	0.43	26	3.5	235	1.1	313
Chen et al.[1999]	2.4	244	0.75	181	2.0	270	0.89	221	4.1	228	0.5	238
Bouille et al.[2000]	1.6	236			1.8	309			3.1	254		

CONCLUSIONS

SLR, Doris and GPS space geodesy techniques are sensitive to the variations of geocenter in different degree. The SLR solution has results the closest compare with the predicted solutions. GPS and Doris solutions have a slightly higher amplitudes for x and y components compare with the SLR and considerably higher for z component. It is confirm the lower quality geocenter determination from the geometric method, though degree-1 deformation approach gives more reasonable estimates for amplitudes and phases of GPS geocenter time series, which are consistent with SLR results and geophysical predictions [Dong et al., 2003].

REFERENCES

Bouille F., Cazenave A., Lemoine J.M., and Cretaux J.F., 2000, "Geocentre motion from DORIS space system and laser data on Lageos satellites: Comparison with surface loading data", Geophys. J. Int. , 143, pp.71-82.

Chen J.L., Wilson C.R., Eanes R.J. and Nerem R.S., 1999, " Geophysical interpretation of observed geocenter variations", J. Geophys. Res. , 104, pp. 2683-2690.

Dong D., Fang P., Dickey J.O., Chao Y., and Cheng M.K., 1997, "Geocenter variations caused by atmosphere, ocean and surface ground water", Geophys.Res.Lett., 24, 1867-1870.

Dong D., Yunck T., and Heflin M., 2003, "Origin of the International Terrestrial Reference Frame", J. Geophys. Res. , 108(B4), 2200, doi:10.1029/2002 JB002035.

Montag H., 1999, "Geocenter motions derived dy different satellite methods, IERS Technical Note 25, IERS Analysis Campaign to Investigate Motions of the Geocenter", J.Ray (Ed.) , Observatorie de Paris, pp.71-74.

VARIATIONS OF THE SECOND ORDER HARMONICS OF GEOPOTENTIAL FROM THE ANALYSIS OF THE LAGEOS SLR DATA FOR 1988-2003

T.V. IVANOVA, N.V. SHUYGINA
Institute of Applied Astronomy of the RAS
10 Kutuzov quay, 191187 St. Petersburg, Russia
e-mail: itv@ipa.nw.ru, nvf@ipa.nw.ru

The paper is devoted to study of the second order harmonics of the geopotential from the analysis of satellite laser ranging to LAGEOS 1 and LAGEOS 2. All available observations for 1988-2003 (about 2000000) are taken from the Crustal Dynamics Data Informational System (CDDIS) and the European Data Center (EDC). These observational data were analyzed by means of the programming system ERA (Krasinsky, 1996). Initial site positions were taken from ITRF2000 solution. Transformation from the Terrestrial Reference Frame to Celestial Reference Frame is carried out using IAU (1976) precession, IAU (1980) nutation, celestial pole offsets and Earth rotation parameters taken from EOP (IERS) C04 series.

The main aim is to estimate the in-phase amplitude of the K_1 tidal wave in the tesseral harmonics C_{21} and S_{21} which manifest themselves as sinusoidal oscillations ΔC_{21} and ΔS_{21} with the period of one sidereal day, given in IERS Conventions 2000 for the normalized coefficients $\overline{C}_{21}$ and $\overline{S}_{21}$ in the form

$$\left(\Delta\overline{C}_{21}\right)_{K_1} = K_1 \sin(\Theta_g + \pi)\,, \qquad \left(\Delta\overline{S}_{21}\right)_{K_1} = K_1 \cos(\Theta_g + \pi)\,,$$

with Θ_g being the Greenwich Mean Siderial Time and $K_1 = 471.8 \times 10^{-12}$. This wave is caused by the differential rotation of the Earth's fluid core.

The data analysis has been performed into two steps. The whole time span was divided into 7-day arcs. It turned out that 7-day interval is the optimal period of time for which there are sufficient numbers of normal points. At the first step six coordinates and velocities, along-track acceleration and reflectance coefficients were adjusted by the least-squares data fitting. At the second step simultaneously with these parameters the K_1 amplitude and the correction to the normalized zonal harmonic $\overline{C}_{20}$ have been estimated. The last values are regarded as global parameters for the time interval of one year, while the orbital parameters are considered as the local ones on each arc. As a result:

$$K_1 = (415.4 \pm 23.7) \times 10^{-12}\,, \qquad \Delta\overline{C}_{20} = (-1.9 \pm 2.1) \times 10^{-11}.$$

One can see that the estimated K_1 is slightly different from the given above convention value $K_1 = (471.3 \pm 21.7) \times 10^{-12}$ and rather different from the value $K_1 = (634.8 \pm 81.4) \times 10^{-12}$ estimated from the analysis of the Etalon SLR data (Ivanova, 2003) by the same procedure that for Lageos SLR data. It should be noted that the error for the amplitude K_1 obtained from the Lageos observations is less than that of determined from the Etalon data. These results are shown in figures 1 and 2 respectively.

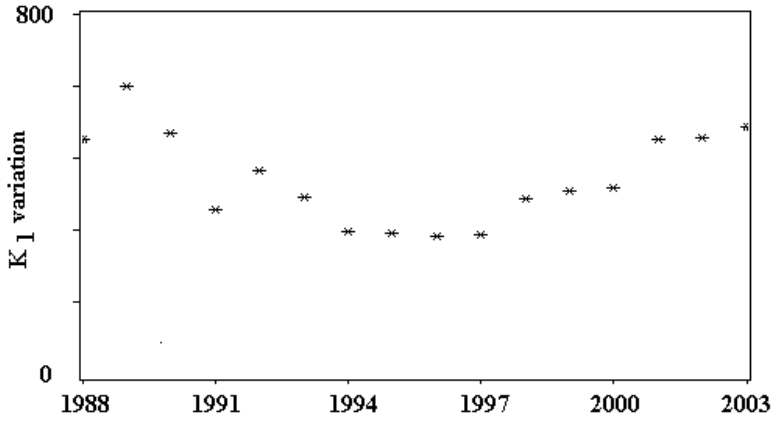

Figure 1: Variation of the amplitude of the tidal wave $K_1 \times 10^{12}$

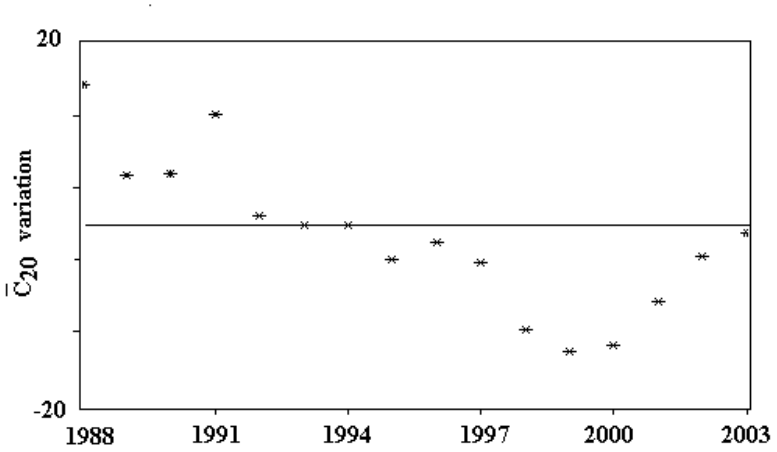

Figure 2: Variation of the geopotential harmonic $\Delta\overline{C}_{20} \times 10^{11}$

This investigation will be continued using the new theory of rotation of deformable Earth with the viscous fluid core which is developing now in the Institute of Applied Astronomy by G. Krasinsky (Krasinsky, 2005).

REFERENCES

Ivanova T. V., N. V. Shuygina, 2003, Variations of the second order harmonics of geopotential from the analysis of the Etalon SLR data for 1992–2001. Proc. Journees-2003 "Astrometry, geodynamics and Solar system dynamics: from milliarcseconds to microarcseconds", A.Finkelstein, N.Capitaine (eds.), 207-208.

Krasinsky G. A., M. V. Vasilyev, 1996, ERA: knowledge base for ephemeris and dynamical astronomy, Proc. of IAU Colloquium 165, 239.

Krasiniky G. A., 2005, Rotation of the deformable Earth with the viscous fluid core. 1. Mathematical model, Submitted to the Celestial Mechanics and Dynamical Asrtronomy.

DETERMINATION OF EARTH ORIENTATION PARAMETERS AND STATION COORDINATES FROM COMBINATION OF IERS CPP DATA (INTERNAL COMPARISONS)

J. KOSTELECKÝ[1,2], I. PEŠEK[1]
[1] Dept. of Advanced Geodesy, Faculty of Civil Engineering, CTU in Prague
Thakurova 7, CZ-16629 Prague
e-mail: pesekt@fsv.cvut.cz
[2] Research Inst. of Geodesy, GO Pecny
CZ-25165 Ondrejov
e-mail: kost@fsv.cvut.cz

ABSTRACT. A method for non-regular combination of solutions for different techniques is applied to the data collected for the "IERS Combination Pilot Project" (CPP). The method is based on combining station position vectors transformed to the celestial reference frame, in which they are functions of both the station coordinates and the Earth orientation parameters. These position vectors are treated as fictitious observations.

The equation system is stabilised by a no-net rotation constraint. The EOP at the adjacent epochs are tied by adding pseudo-observations, a weighting of whose controls smoothness of the solution.

Results of the particular techniques enter the common adjustment as the input data. For VLBI the EOP were derived from session combined normal equations (as given in the CPP database) taking station coordinates over from the VTRF2005 IVS Conventional Reference Frame.

High quality of the GPS and VLBI data collected in the CPP database allowed to study effects of various modes of the method on the combination results. Especially, it was proved that the method is able to reflect the short periodic variations present in the data to both the station coordinates and the EOP when they are combined as a series of successive one monthly solutions, while the long-term effects became distinct when the data from the whole time interval is combined in one common adjustment.

(The full text will be published in IERS Technical Note – Proceedings of the IERS Workshop on Combination, GFZ Potsdam, Germany, 10–11 October 2005)

EQUATORIAL SATELLITE DYNAMICS IN FOCK'S MODEL

V. MIOC[1], E. PÉREZ-CHAVELA[2], M. STAVINSCHI[1]
[1] Astronomical Institute of the Romanian Academy
Str. Cuţitul de Argint 5, RO-040557 Bucharest, Romania
e-mail: vmioc@aira.astro.ro, magda@aira.astro.ro
[2] Universidad Autonoma Metropolitana - Iztapalapa, Departamento de Matematicas
Apdo. Postal 55-534, Mexico, D.F., C.P. 09340, Mexico
e-mail: epc@xanum.uam.mx

ABSTRACT. We transpose the problem in McGehee-type blow-up coordinates and fully depict the phase-space structure. We find a much more rich phase portrait than in the case of the standard Kepler problem.

1. BASIC EQUATIONS

The equatorial satellite motion in Fock's relativistic field is described (in configuration-momentum coordinates) by

$$\dot{\mathbf{q}} = \mathbf{p}, \qquad \dot{\mathbf{p}} = -\sum\nolimits_{n=1}^{4} (n a_n / |\mathbf{q}|^{n+2}) \mathbf{q},$$

where a_n have well-known expressions (Fock 1959). The equations admit the integrals of angular momentum and energy, respectively:

$$\mathbf{q} \times \mathbf{p} = L \text{ (constant)}; \qquad |\mathbf{p}|^2 / 2 - \sum\nolimits_{n=1}^{4} a_n / |\mathbf{q}|^n = h/2 \text{ (constant)}.$$

Passing to standard polar coordinates (r, θ), and using the McGehee-type transformations (McGehee 1974) $x = r^2 \dot{r}$, $y = r^3 \dot{\theta}$, $ds = r^{-3} dt$, we obtain regular equations of motion (blowing up the singularity at $\mathbf{q} = (0, 0)$), and the first integrals

$$y = Lr; \qquad x^2 + y^2 = hr^4 + 2 \sum\nolimits_{n=1}^{4} a_n r^{4-n}.$$

2. RESULTS

Starting from the first integrals above, we fully describe the phase portrait in the (r, x)-plane: Figure 1 for $h < 0$, Figure 2 for $h \geq 0$. The corresponding physical orbits in Figure 1 are: M/N = ejection/collision; UE/SE = unstable/stable circular orbit; 1, 2, 4 = ejection-collision orbits; 3a = ejection - unstable circular orbit; 3b = unstable circular orbit - collision; 3c = the very special

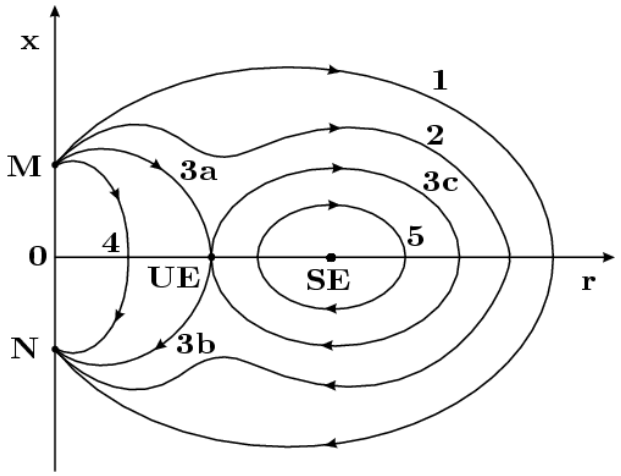

Figure 1: Phase portrait for negative energy

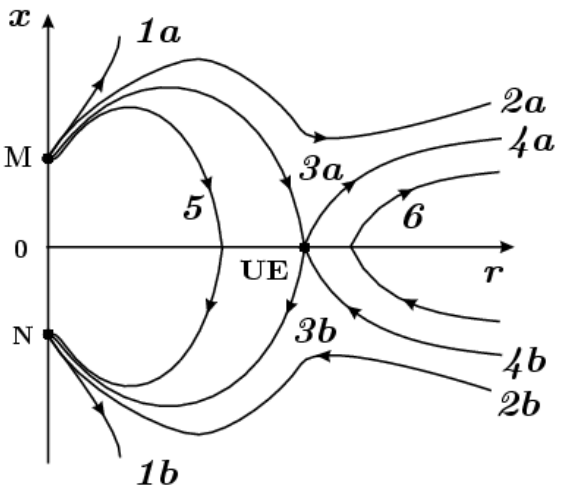

Figure 2: Phase portrait for nonnegative energy

homoclinic orbit; 5 = quasiperiodic and periodic orbits. For Figure 2: 1, 2 (a/b) = ejection-escape / capture-collision; UE, 3a, b = like in Figure 1; 4 (a/b) = UE-escape / capture-UE; 5 = ejection-collision orbits; 6 = capture-escape orbits.

Of course, for satellites, the characteristic trajectories are SE, periodic orbits, UE, quasiperiodic orbits (the two latter ones being met only in Fock's field). But, given the perturbations, any other behaviour described above becomes possible.

REFERENCES

Fock V. A., 1959, " The Theory of Space, Time and Gravitation" , Pergamon Press, London.

McGehee R., 1974, "Triple collision in the collinear three-body problem" , Inventiones Math. 27, pp. 191-227.

RESULTS FROM THE RECENT LUNAR OCCULTATIONS OF UPSILON GEMINORUM AND ANTARES

M. SÔMA
National Astronomical Observatory of Japan
Mitaka, Tokyo 181-8588, Japan
e-mail: Mitsuru.Soma@nao.ac.jp

ABSTRACT. The lunar grazing occultation of υ Geminorum was observed on 2005 April 16 in the U.S.A. and from its observations it was found that the star is a hitherto unknown double star. The lunar occultation of Antares was observed in March this year in Japan and in the U.S.A., and from the observations the separation of the companion of Antares from the primary was precisely obtained. We present here the results of them.

1. LUNAR GRAZING OCCULTATION OF UPSILON GEM ON 2005 APRIL 16

On 2005 April 16 there was a lunar grazing occultation of the 4th magnitude star υ Geminorum in California, U.S.A., and 14 observers participated in the observations. Among the observers Derek C Breit, Ed Morana, and Richard Nolthenius reported several faint events (mostly just before and after the bright events) which corresponded to events of a star of about 10th magnitude. The star's angular diameter had been estimated to be about 0.006 arcseconds (Ochsenbein & Halbwachs 1982; Wesselink et al. 1972), and therefore the faint events cannot be attributed to the effect of the stellar size or the effect of the Fresnel diffraction. On the other hand if we assume that the faint events were caused by a faint companion of the star, all of the observations can be analyzed consistently. From the analysis of the observations the positions of the companion relative to the primary are estimated to be
separation $0''.04 \pm 0''.01$, and position angle $70^\circ \pm 20^\circ$.

Since the star has been listed in the Catalogue of Stellar Diameters (Pasinetti Fracassini et al. 2001), it should be emphasized that one should notice that this star is a close binary when they use it as one of the standard stars for the stellar diameters.

2. LUNAR OCCULTATIONS OF ANTARES IN MARCH 2005

In March, 2005, the lunar occultation of Antares (α Scorpii, 1.0 magnitude) was observed in the U.S.A. (on Mar 3) and in Japan (on Mar 30). The star has a companion, whose magnitude is 5.4, and at the reappearance of the lunar occultation the companion appeared prior to the primary by several seconds.

The orbits of the binary have been determined by several authors, and the positions of the companion relative to the primary at the times of the occultations were calculated as follows:

Author	Sep	PA
	arcsec	deg
Heintz (1960)	2.215	276.9
Baize (1978)	2.527	273.7
Pavlovic & Todorovic (2005)	2.677	276.6

(These values are for the 2005 Mar 30 event. For the 2005 Mar 3 event the separation should be larger by 0.001 arcsec for all of the orbits.)

We use here only the observations whose event times were obtained precisely with videos. The observations were analyzed using the latest orbit (Pavlovic & Todorovic 2005), and for each event the position of the lunar limb with its position angle was obtained. The analysis not only shows the large errors in Watts' (1963) data, but also shows that the lunar limb points obtained from the companion are systematically lower than those from the primary. Since the position angles of the events measured counterclockwise from the north point of the Moon's disk range from 255° to 292°, which are not much different from the position angle of the companion relative to the primary, the systematic differences in the analysis indicate that the angular separations of the companion from the primary used in the analysis are too small. This fact indicates that, while the errors of the older orbits were greater than that of the latest one among the three because the latest one gives the largest separation, the latest orbit still has an error in the separation. By averaging the differences between the companion's and primary's reduced results, the correction to the separation obtained from Pavlovic & Todorovic's (2005) orbit is

$$\Delta\mathrm{Sep} = +0''.062 \pm 0''.014.$$

The lunar occultation of Antares will be occurring for a few years, and combining the results of them the positions (both the separation and position angle) of the companion relative to the primary will be improved.

3. CONCLUSION

From the observations of its lunar grazing occultation on 2005 April 16 the occulted star v Geminorum is found to be a hitherto unknown double star. This fact is especially important because this star has been used as a standard star for estimating the stellar diameters. The separation of its companion relative to Antares was precisely determined from its lunar occultations observed in March 2005.

The details of the present analyses will be published elsewhere.

REFERENCES

Baize, P., 1978, Inf. Circ. 76.
Heintz, W.D., 1960, Veröff. Sternw. München 5, 87.
Ochsenbein, F., Halbwachs, J.L., 1982, A&AS 47,523.
Pasinetti Fracassini L.E., Pastori L., Covino S., and Pozzi A., 2001, A&A 367, 521.
Pavlovic, R. & Todorovic, 2005, Inf. Circ. 156.
Watts C.B., 1963, Astron. Papers Am. Ephemeris 17, U.S. Government Printing Office, Washington, D.C.
Wesselink, A.J., Paranya, K., De Vorkin, K.: 1972, A&AS 7, 257.

SOME REMARKS ON ACCURACY OF ATMOSPHERIC MODEL USED IN LASER RANGING OBSERVATIONS

K. KURZYŃSKA, R. JANICKI
Astronomical Observatory, A. Mickiewicz University, Poznań, Poland
e-mail: kurzastr@amu.edu.pl

ABSTRACT. The presently used Marini-Murry model of atmospheric corrections in laser ranging observations takes into account an influence of atmosphere only up to 25 km. Our studies indicate that atmosphere is dense enough up to 100 km to slow down significantly electromagnetic waves. Systematic differences between delay values in the zenith direction calculated according to the Marini-Murry formula and those of our model equal even 10 cm. It is striking that various parameters determined from laser observations do not show such errors. Some suggestions of elucidation of this fact are proposed.

With the use of laser ranging observations, a station position is determined at present with accuracy of several millimeters. This accuracy is supposed to be limited by method of taking into account the influence of atmosphere. To check a possibility of improving corrections for the zenith delay in laser observations, we have considered a two-layer model of atmosphere which describes a density discontinuity on tropopause (*Sugawa and Kikuchi*, 1974). We have also looked for the limit height of atmosphere above which contributions to the delay are negligible. We found that the influence of atmosphere can be neglected only above 100 km over the Earth surface. Basing on the actual aerological soundings, we have found by numerical integration values of the zenith delay and compared them with those obtained with the help of the commonly used Marini-Murray formula (*Marini and Murray*, 1973). Figure 1 shows the result obtained on the base of ten years aerological data.

Surprising are the systematic differences between the both values varying from 6 cm in summer up to 11 cm in winter. In our opinion these differences are a consequence of cutting atmosphere up in the Marini-Murray model on 25 km which is the maximum height of aerological soundings. Indeed, results obtained with the help of our model practically coincide with those of the Marini-Murray model if we finish the numerical integration on the height of 25 km (Fig. 2). In Figure 2, the solid line describes values of the zenith delay calculated with the help of the Marini-Murray model, the dashed line corresponds to values calculated by numerical integration up to 22 km and the dashed-dotted line to values calculated up to 25 km.

A question arises why the station coordinates are determined with the millimeter accuracy though the atmospheric delay is taken into account only with several centimeters accuracy? At present, we cannot strictly answer this question. We plan to check a supposition that the millimeter accuracy is only a selfconsistent property of the GEODYN program and an actual accuracy can be worse.

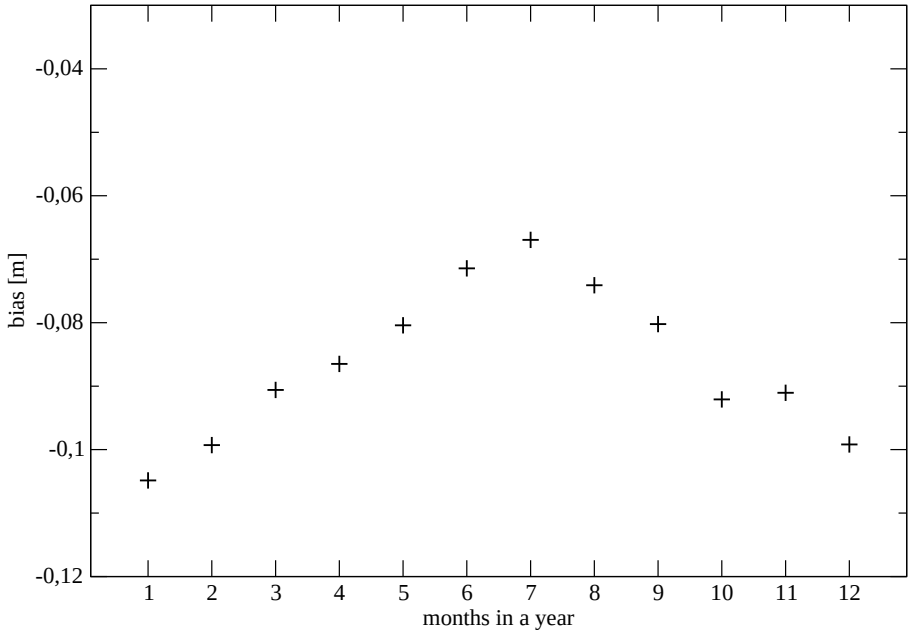

Figure 1: Differences between delay values in the zenith direction calculated according to the Marini-Murry formula (*Marini and Murray*, 1973) and those of our model.

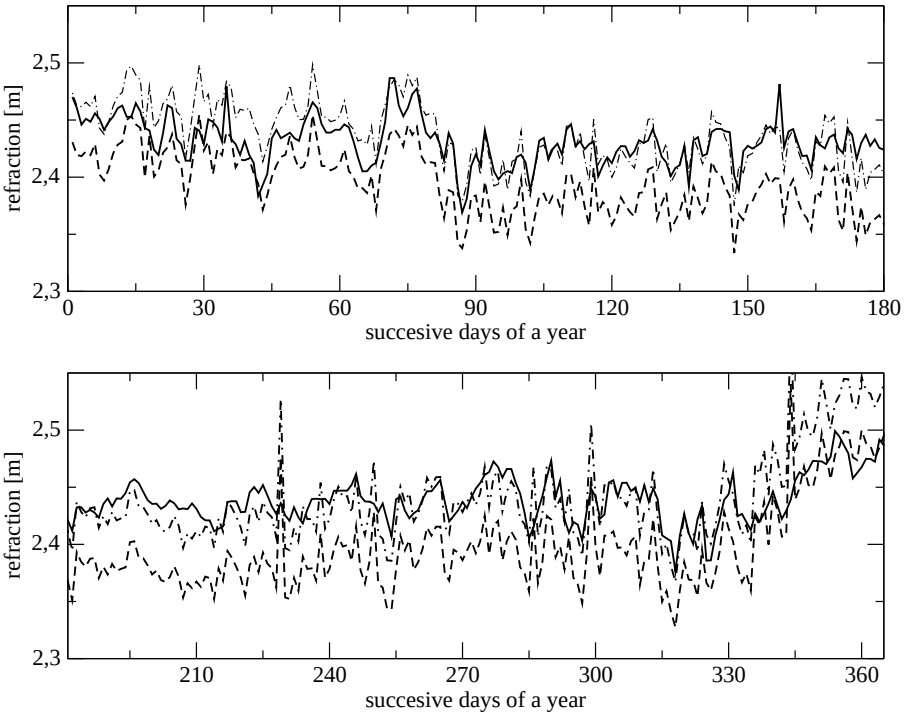

Figure 2: Delay values in the zenith direction calculated according to various methods using the aerological sounding data. See text for details.

REFERENCES

Sugawa C., N. Kikuchi, Pub. Astr. Observ., Beograd (1974).
Marini J. W., C. W. Murray, NASA Tech. Rep. X-591-73-351 (1973).

THE ORBIT ESTIMATION FOR LARETS SATELLITE

M. RUTKOWSKA
Space Research Centre, PAS, Bartycka 18A, 00-716, Warsaw, Poland
e-mail: Milena@cbk.waw.pl

1. INTRODUCTION

The LARETS satellite was launched on September 26, 2004 into a circular orbit at an altitude of 690 km and with an inclination of 98.2 degree. The aim of this study is the computation of the orbit of the satellite LARETS with the highest accuracy possible. The paper discusses the influence of the modelling of different physical effects on the motion of LARETS, in particular in terms of orbit quality. All computations are performed with the NASA program GEODYN II (Eddy et al.,1990).

2. METHOD OF ANALYSIS AND CONCLUSIONS

The study is based on the observations taken by the global network of laser stations during the period from December 30, 2003 to May 15, 2004. Four and half-month period of measurements (5706 normal points) was divided into 18 7.5-day arcs with half day overlaps between successive arcs. In this study three test cases were analyzed.

1. The computation model described in (Rutkowska and Noomen, 2002), gravity field GRGS/ GFZ GRIM-5S1(99,99) (Biancale and Schwintzer, 2000), atmospheric density MSIS 86 with solved for half-day intervals used for LARETS.
2. As above, but atmospheric density MSIS 86 with solved for 8-hour intervals.
3. The computation model which uses the CSR gravity field TEG-4(200,200) (Tapley et al., 2002) and the atmospheric density model MSIS 86 with solved for the 8-hour intervals.

The black triangle represent the estimated rms values for LARETS in this case 1 (Figure 1).The average value of rms-of-fit is equal to 7.05 cm. The plot with white diamonds (case 2) represents rms values solved for 8-hour intervals. The plot with solid diamonds (case 3) represents rms values for LARETS obtained with the gravity field model TEG-4 up to degree and order (200,200) and atmospheric density model MSIS 86 with solved for 8-hour intervals. It has been verified that the modeling of the gravity field up to degree and order (100,100) which gives the same rms-of-fit value. The average rms-of-fit value is equal to 3.73 cm for case 3. Generally, it can be concluded that the best solution obtained here for LARETS is for case 3. The example of residuals for the case 3 are shown in Figure 2. The frequency of solving parameters (atmospheric drag) have a big influence on the accuracy of orbit determination. The changes of the solved parameters for the half-day intervals by the 8-hour intervals is a reason of diminish of rms-of-fit about 0.4 cm for each arc separately. The estimated (for 8-hour intervals) are shown in Fig. 3. For LARETS (case 3), 18 successive data arcs were solved, of 7.5-day length each and with 12-hour overlaps.

REFERENCES

Biancale, R., and P. Schwintzer, The GRIM5-S2/C2 Earth Gravity Field Models, paper presen ted at the EGS XXV General Assembly, Nice, France, 2000.

Eddy, W.F, J.J. McCarthy, D.E. Pavlis, J.A. Marshall, S.B. Luthce, L.S. Tsaoussi ; GEODYN II System Operations Manual, Vol. 1-5, ST System Corp., Lanham MD, USA 1990.

Hedin, A.E., MSIS-86 Thermospheric Model, J. Geophys. Res., 92, A5, 4649-4662,1987.

Rutkowska, M,. R. Noomenn, Global orbit analysis of the satellite WESTPAC, Advances in Space Rese arch, Vol. 30, No. 2, 2002, pp 265-270, GREAT BRITAIN, 2000.

Tapley, AGU Fall 2001Š 01 Meeting, Abstract G51A-0236. USA 2002.

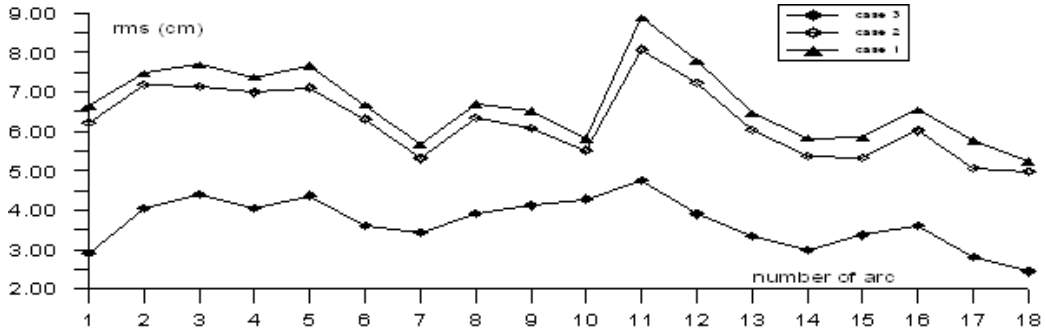

Figure 1: The rms values for LARETS for the total 4.5-month interval.

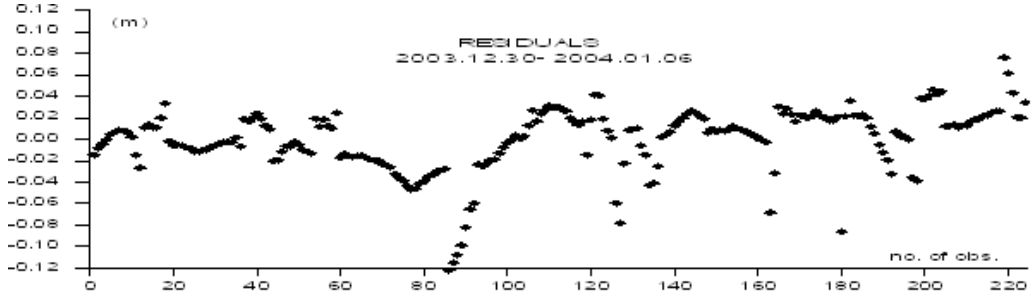

Figure 2: Residuals for 7.5-day arc (example 1).

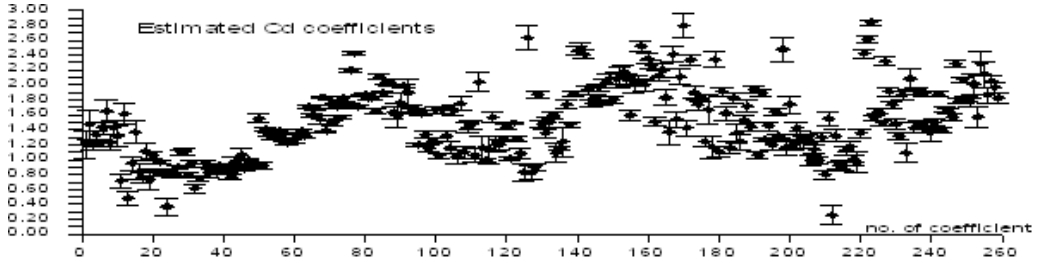

Figure 3: The atmospheric drag coefficients estimated for LARETS (case 3).

Session 2.1

PRECESSION, NUTATION AND POLAR MOTION:
Recent developments of observation and modeling

PRÉCESSION, NUTATION ET MOUVEMENT DU PÔLE :
Développements récents relatifs aux observations et à la modélisation

EARTH ORIENTATION PARAMETERS FROM REPROCESSING AND COMBINATION EFFORTS

M. ROTHACHER, P. STEIGENBERGER, D.THALLER
GeoForschungsZentrum Potsdam
Telegrafenberg, D-14473 Potsdam, Germany
e-mail: rothacher@gfz-potsdam.de

ABSTRACT. In the last few years two major improvements have been achieved concerning the determination of Earth Orientation Parameters (EOP):

(1) A few GPS analysis centers started to reprocess long time intervals (≈10 years) of global GPS data to obtain very homogeneous and much refined time series of EOPs, considerably improving the modeling of the observations (ionospheric corrections of higher order, satellite and receiver antenna phase center patterns, atmospheric mapping function, etc.). The effect of these reprocessing and modeling efforts on polar motion, LOD and nutation rates will be shown.

(2) With various activities (IERS SINEX Combination Campaign, IERS Combination Pilot Project, IERS Call for Long Time Series) the IERS has promoted the rigorous combination of the different space geodetic techniques. Such a combination is not only important to guarantee EOP results referring to a unique reference frame, but it also allows to make use of the complementarity of the space techniques (e.g., UT1 from VLBI densified in time using LOD from GPS). We show results from the CONT02 campaign to illustrate the benefits but also the critical issues of such a rigorous combination of the different observation techniques.

Finally, we will give an outlook at what might be a future, very consistent and highly accurate set of IERS products, resulting from the combination of the space geodetic techniques.

REFERENCES

Angermann, D., D. Thaller, M. Rothacher, 2003, IERS SINEX Combination Campaign. *IERS Technical Note No. 30, eds. B.Richter, W. Schwegmann and W. Dick*, Bundesamt für Kartographie und Geodäsie, Frankfurt am Main.

Thaller, D., R. Schmid, M. Rothacher, V. Tesmer, D. Angermann, 2004, Rigorous combination of VLBI and GPS using the CONT02 campaign. *Proc. 23rd IUGG General Assembly 2003, June 30 - July 11, Sapporo, Japan, IAG Symposia Series*, Springer-Verlag, (accepted).

PROGRESS REPORT OF THE IAU WORKING GROUP ON PRECESSION AND THE ECLIPTIC

J.L. HILTON[1], N. CAPITAINE[2], J. CHAPRONT[3], J.M. FERRANDIZ[4], A. FIENGA[5], T. FUKUSHIMA[6], J. GETINO[7], P. MATHEWS[8], J.-L. SIMON[9], M. SOFFEL[10], J. VONDRAK[11], P. WALLACE[12], J. WILLIAMS[13]

[1]Astron. Applications Dept., U.S. Naval Observatory
3450 Massachusetts Ave., NW, Washington, DC 20392, USA
e-mail: jhilton@aa.usno.navy.mil

[2]SYRTE, Observatoire de Paris
61 avenue de l'Observatoire, 75014 Paris, FRANCE
e-mail: nicole.capitaine@obspm.fr

[3]SYRTE, Observatoire de Paris
61 avenue de l'Observatoire, 75014 Paris, FRANCE
e-mail: Jean.Chapront@obspm.fr

[4]Dpt. Matematica Aplicada, EPS Univ de Alicante
Aptdo. 99, 03080 Alicante, SPAIN
e-mail: jm.ferrandiz@ua.es

[5]IMCCE, Observatoire de Paris
77 Av Denfert Rochereau, 75014 Paris, FRANCE
e-mail: fienga@imcce.fr

[6]Public Relation Center, Ntl. Astronomical Observ. (NAOJ)
2-21-1 Osawa, Mitaka, Tokyo 181-8588, JAPAN
e-mail: Toshio.Fukushima@nao.ac.jp

[7]Grupo Mecanica Celeste, Facultad de Ciencias
47005 Valladolid, SPAIN
e-mail: getino@maf.uva.es

[8]Dept. Theoretical Physics, Univ. of Madras, Guindy Campus
Chennai 600025, INDIA
e-mail: indi4272@yahoo.com

[9]IMCCE, Observatoire de Paris
77 Av Denfert Rochereau, 75014 Paris, FRANCE
e-mail: simon@imcce.fr

[10]Inst. Planet Geodaesie Dresden Tech Universität
Mommsenstraße 13, 01062 Dresden, GERMANY
e-mail: soffel@rcs.urz.tu-dresden.de

[11]Astronomical Inst., Czech Academy of Sciences
Bocní II 1401, 141 31 Praha 4, Czech Rep.
e-mail: vondrak@ig.cas.cz

[12]Space Science & Technology Dept. CCLRC, RAL
Chilton, Didcot, Oxfordshire OX11 0QX, UK
e-mail: ptw@star.rl.ac.uk

[13]JPL, CALTECH
4800 Oak Grove Dr, MS 238 332, Pasadena, CA 91109, USA
e-mail: James.Williams@jpl.nasa.gov

ABSTRACT. The IAU Working group on Precession and the Ecliptic looked at several solutions for replacing the precession part of the IAU 2000A precession-nutation model, which is not dynamically consistent. These comparisons show that the Capitaine et al. (2003) precession theory, P03, is both dynamically consistent and the solution most compatible with the IAU 2000A nutation model. The two greatest sources of uncertainty in the precession theory are the rate of change of the Earth's dynamical flattening, ΔJ_2, and the precession rates (i.e. the constants of integration used in deriving the precession). The combined uncertainties limit the accuracy in the precession theory to approximately 2 mas cent^{-2}.

Given that there are difficulties with the traditional angles used to parameterize the precession, z_A, ζ_A, and θ_A, the working group has decided that the choice of parameters should be left to the user. We shall provide a consistent set of parameters that may be used with either the traditional rotation matrix, or those rotation matrices described in Capitaine et al. (2003) and Fukushima (2003).

We recommend that the ecliptic pole be explicitly defined by the mean orbital angular momentum vector of the Earth-Moon barycenter in an inertial reference frame, and explicitly state that this definition is being used to avoid confusion with previous definitions of the ecliptic.

Finally, we recommend that the terms *precession of the equator* and *precession of the ecliptic* replace the terms *lunisolar precession* and *planetary precession*, respectively.

1. INTRODUCTION

Precession or, more precisely, precession of the equinox is the result of the motions of two planes in inertial space. The first motion is that of the plane of the Earth's equator. The second is the motion of the ecliptic, the mean plane of the Earth's orbit about the Sun. These two planes have been chosen because the equinox has historically provided a convenient fiducial point in the observation of the heavens and the passage of time. For example, the civil calendar year is tuned to follow the tropical year from equinox to equinox rather than any other definition of the year such as perihelion passage or the complete revolution of the Earth about the Sun in inertial space. These planes are also both dynamically involved in the motion of the Earth's pole. By definition, the mean latitude of the Sun with respect to the ecliptic is 0°, and, averaged over the 18.6 year period of the motion of its node, the average plane of the Moon's orbit is nearly coincidental with the ecliptic.

In the past, the motion of the Earth's equator in inertial space has been called *lunisolar precession* while the motion of the ecliptic has been called *planetary precession*. The names of the individual components are based on the dominant source for each of the motions. However, the accuracy to which the precession can now be measured has reached the point where the contribution of the planets to the motion of the Earth's equator is significant. Thus, these names have become misleading. Capitaine et al. (2003) proposed the terms *precession of the equator* and *precession of the ecliptic*. We recommend that these terms be adopted for general use.

Since its adoption, it has become apparent the IAU 1976 theory of general precession (Lieske et al., 1977) (henceforth Lieske) is in error by approximately 300 mas cent^{-1}, where 1 mas = $0\overset{''}{.}001$ and the century consists of 36525 Julian days TT. In addition, Williams (1994) showed there should also be a secular motion in the latitude of the Earth of about $\tilde{\text{U}}24$ mas cent^{-1}. This motion in latitude is caused by the slight inclination of the lunar orbit to the ecliptic when averaged over the period of its node. When the IAU 2000 precession-nutation theory (IERS 2004) was adopted (IAU 2001) the emphasis of the analysis was on the periodic nutations and correcting the linear portion of the precession observable in VLBI observations. The effect of these changes on the higher-order terms in the precession theory were ignored. Ignoring the higher-order terms results in an error in the precession of about 6.4 mas cent^{-2} in longitude. Thus, the precession theory was not dynamically consistent.

Furthermore, Fukushima (2003) showed that the values of ζ_A and z_A, two of the traditional angles for parameterizing the precession, are complementary and highly dependent on the precise values that are adopted for the offset between the dynamical frame and the GCRS at J2000.0. Thus, they are unsuited to polynomial representation.

Finally, the ecliptic in use was defined by Lieske using a simplified variant for the determination of proper elements devised by Newcomb (1894). However, Resolution A4, Recommendation VII, Note 3 of IAU (1992) recommends determining the ecliptic from the mean values as derived from a planetary ephemeris for the Earth.

The IAU Working Group on Precession and the Ecliptic was formed at the XXVth General Assembly of the IAU in Sydney, Australia to address these topics and make recommendations regarding them to the IAU.

2. PRECESSION OF THE EQUATOR

Three high precision precession theories (Bretagnon et al. 2003, Capitaine et al. 2003, and Fukushima 2003) have been published recently to address the shortcomings of the precession portion, including the ecliptic, of the IAU 2000A precession-nutation theory. In addition, Harada & Fukushima (2004) examined the definition of the ecliptic alone. All four of these theories are designed to be dynamically consistent, but took different approaches in their methods for determining the higher-order terms in the precession theory and/or ecliptic definition.

The initial task of the working group was to determine if these precession theories actually are physically consistent, and which is the best suited to complement the nutation portion of the IAU 2000A precession-nutation theory. Capitaine et al. (2004) provides just such a comparison.

Regarding the equatorial precession the most important results of Capitaine et al. (2004) are:

- The equator of precession is the plane perpendicular to the celestial intermediate pole.
- The accuracy of the expression for the precession is limited by the uncertainty in the long term change of J_2, ΔJ_2, as a function of time. More recently, Bourda & Capitaine (2004) estimate the uncertainty in ΔJ_2 limits the accuracy of the rate of precession to about 1.5 mas cent^{-1}.
- A new precession theory for the equator should be based on the most recent precession rates and geophysical model determined from VLBI observations.
- VLBI observations do not yet span a long enough period of time to discriminate between the different solutions.
- Only the Capitaine et al. (2003) solution includes both an Earth model that is realistic and integration constants that are realistic. More recently, Capitaine et al. (2005) has determined Mathews et al.'s (2002) use of the Lieske ecliptic in determining the precession requires a small correction of approximately 1 mas cent^{-1} in the equatorial precession.

Since both the uncertainty in the long-term rate of change in J_2 and the ability to discriminate between the different theories will require VLBI observations over an extended period of time, the only true discriminant is whether the Earth model is realistic. Only the Capitaine et al. (2003) model meets this criterion. Thus, the working group recommends the adoption of the Capitaine et al. (2003) theory, designated P03, for the precession of the equator.

3. THE ECLIPTIC AND PRECESSION OF THE ECLIPTIC

The equinox is the intersection of the equator and the ecliptic, two non-inertial planes. Both the equinox and the ecliptic are still of use. The equinox serves as the basis of the civil calendar,

and is frequently used when describing astronomical phenomena. However, this application does not require high accuracy. Many celestial mechanics problems with lesser accuracy requirements, such as the dynamics of asteroids, find the ecliptic useful as a slowly changing fiducial plane for solar system dynamics work. However, some celestial mechanics problems have reached the level of accuracy ($\sim$1 mas or less) where knowledge of the instantaneous angular momentum of the Earth-Moon barycenter about the solar system barycenter is required instead of the mean angular momentum of the Earth about the solar system barycenter, represented by the plane of the ecliptic.

Before an expression for the ecliptic can be agreed upon, two problems regarding the definition of the ecliptic had to be addressed.

First, whether the ecliptic should be defined with respect to inertial space or the geometric path of the Sun as seen from the Earth (the so called "rotating" ecliptic). This question arises because the ecliptic has been realized as a plane perpendicular to the Earth's orbital angular momentum vector. Prior to the establishment of the ICRS, it was impossible to establish a truly inertial reference system. Thus, rather than try to separate out the non-inertial component, Newcomb (1894) chose to use geometric path of the Sun. The ICRS, however, established a quasi-inertial coordinate system. Thus, inclusion of the motion of the ecliptic in its realization is no longer an expedient.

Second, how the equinox can be defined as the intersection of the Earth's equator, a plane defined in the geocentric reference system, and the ecliptic, a plane defined in the barycentric reference frame. This second question arises because solar system dynamics has reached the point where general relativistic considerations are significant, and the gauge transformation does not allow a plane in one reference system to be transferred to another reference system. The details of these considerations are discussed in Hilton (2006). The main conclusion is that the ecliptic is still useful in low precision applications. In higher precision applications, certain arbitrary decisions have to be made concerning the position of the ecliptic and the equinox. However, the regime in which the equinox and ecliptic become arbitrary is also the regime in which the instantaneous rather than mean angular momentum of the Earth-Moon barycenter is required. Thus, those arbitrary decisions required to realize the ecliptic do not impair the physical models.

The working group recommends the precession of the ecliptic included in the P03 precession theory. More specifically, we recommend that the ecliptic pole should be explicitly defined by the mean orbital angular momentum vector of the Earth-Moon barycenter in an inertial reference frame to simplify the dynamics. We also recommend that both the definition used and the process by which the ecliptic has been determined be made explicit when any future definition is adopted, to avoid confusion.

4. RECOMMENDATIONS

The Working Group on Precession and the Ecliptic has reached a consensus on its recommendations and has submitted its report for publication. The working group will recommend:

The Working Group on Precession and the Ecliptic, recognizing:

1. the need for a precession theory consistent with dynamical theory compatible with the IAU 2000A nutation theory,

2. the gravitational attraction of the planets make a significant contribution to the motion of the Earth's equator (thus making the terms *lunisolar precession* and *planetary precession* misleading),

3. the need for a definition of the ecliptic for both astronomical and civil purposes, and

4. the ecliptic has, in the past, been defined both with respect to an observer situated in inertial space (inertial definition) and an observer comoving with the ecliptic (rotating definition),

recommends:

1. The terms *lunisolar precession* and *planetary precession* be replaced by *precession of the equator* and *precession of the ecliptic*, respectively.

2. The IAU adopt the P03 precession theory, of Capitaine et al. (2003) for the precession of the equator (Eqs. 37) and the precession of the ecliptic (Eqs. 38); the same paper provides the polynomial developments for the P03 primary angles and a number of derived quantities for use in both the equinox based and CIO based paradigms.

3. The choice of precession parameters be left to the user.

4. The recommended polynomial coefficients for a number of precession angles shall be given in Table 1 of the report, including the P03 expressions set out in Tables 3Ũ5 of Capitaine et al. (2005), and those of the alternative Fukushima (2003) parameterization, including the corresponding matrix representations.

5. The ecliptic pole should be explicitly defined by the mean orbital angular momentum vector of the Earth-Moon barycenter in an inertial reference frame, and this definition should be explicitly stated to avoid confusion with older definitions.

The official report of the working group, Hilton et al. (2006), was submitted for publication in October 2005 and should be available shortly.

REFERENCES

Bourda, G. & Capitaine, N. 2004, A&A , 428, 691

Bretagnon, P., Fienga, A., & Simon, J.-L. 2003, A&A , 400, 785

Capitaine, N., Wallace, P.T., & Chapront, J. 2003, A&A , 412, 567

Capitaine, N., Wallace, P.T., & Chapront, J. 2004, A&A , 421, 365

Capitaine, N., Wallace, P.T., & Chapront, J. 2005, A&A , 432, 355

Fukushima, T. 2003, AJ , 126, 494

Harada, W. & Fukushima, T. 2004, AJ , 127, 531

Hilton, J.L. 2006, in preparation

Hilton, J.L., Capitaine, N., Chapront, J., Ferrandiz J.M., Fienga, A., Fukushima, T., Getino, J., Mathews, P., Simon, J.-L., Soffel, M., Vondrak, J., Wallace, P., & Williams, J. 2006, Celest. Mech., submitted

IAU 1992, *Proceedings of the Twenty-First General Assembly, Buenos Aires 1991*, in Transactions of the International Astronomical Union, Vol. XXIB, J. Begeron, ed., (Dordrecht: Kluwer 1992), pp. 49-50

IAU 2001, *Proceedings of the Twenty-Fourth General Assembly, Manchester 2000*, in Transactions of the International Astronomical Union, Vol. XXIVB, H. Rickman, ed., (Provo, UT: Astronomical Society of the Pacific 2001), pp. 43-44

IERS 2004, "IERS Conventions (2003)," IERS Technical Note 32, D.D. McCarthy and G. Petit eds., Frankfurt am Main: Verlag des Bundesamts für Kartographie und Geodäsie

Lieske, J.H., Lederle, T., Fricke, W., & Morando, B. 1977, A&A , 58, 1

Mathews, P.M., Herring, T.A., & Buffet, B.A. 2002, J. Geophys. Res. , 107, B4, 10.1029/2001JB000390

Newcomb, S. 1894, Astron. Papers Am. Ephemeris, 5, Part 4, pp. 301-378

Williams, J.G. 1994, AJ , 108, 711

P03-BASED PRECESSION-NUTATION TRANSFORMATIONS

P.T. WALLACE[1], N. CAPITAINE[2]

[1] HMNAO, CCLRC / Rutherford Appleton Laboratory,
Chilton, Didcot, OX11 0QX, United Kingdom
e-mail: P.T.Wallace@rl.ac.uk

[2] SYRTE/UMR8630-CNRS, Observatoire de Paris
61, avenue de l'Observatoire, 75014 - Paris, France
e-mail: n.capitaine@obspm.fr

ABSTRACT. The IAU WG on precession and the ecliptic has recommended the adoption of the P03 models of Capitaine et al. (2003). We discuss methods for generating the rotation matrices that transform celestial to terrestrial coordinates, taking into account frame bias (B), P03 precession (P), P03-adjusted IAU 2000A nutation (N) and Earth rotation. The NPB portion can refer either to the equinox or the celestial intermediate origin (CIO), requiring either the Greenwich sidereal time (GST) or the Earth rotation angle (ERA) as the measure of Earth rotation. The equinox based NPB transformation can be formed using various sequences of rotations, while the CIO based transformation can be formed using series for the X, Y coordinates of the celestial intermediate pole (CIP) and for the CIO locator s; also, either matrix can be computing using series for the x, y, z components of the "rotation vector". Common to both methods is the CIP, which forms the bottom row of the transformation matrix. In the case of the CIO based transformation, the CIO is the top row of the NPB matrix, whereas in the equinox based case it enters via the GST formulation in the form of the equation of the origins (EO). The EO is the difference between ERA and GST and equivalently the distance between the CIO and equinox. The choice of method is dictated by considerations of internal consistency, flexibility and ease of use; the different ways agree at the level of a few microarcseconds over several centuries, and consume similar computing resources.

1. INTRODUCTION

At the 2003 IAU General Assembly, a working group was formed to select models for the precession of the ecliptic and equator that are consistent with dynamical theories to replace the simple rate corrections adopted in 2000 (see Hilton et al. 2005). The new precession will be used with the existing IAU 2000A nutation, and in order to be consistent with the new precession, this requires small (~ 10 μas) corrections for the effects of (i) the change in obliquity from the IAU 1980 ecliptic to the P03 ecliptic and (ii) the secular variation in the Earth's dynamical flattening, not taken into account in the IAU 2000A model. In this paper, based on the recent study of Capitaine & Wallace (2005), we review methods for using the new precession-nutation in practical applications.

The following matrix:

$$\mathbf{M}_{class} = \mathbf{N}\,\mathbf{P}\,\mathbf{B} \tag{1}$$

is needed in two forms, namely the classical form based on the equinox and the new form based on the celestial intermediate origin (CIO). The matrices $\mathbf{B}$, $\mathbf{P}$ and $\mathbf{N}$ are the successive contributions of the frame bias, precession and nutation. In order to predict terrestrial coordinates, or hour angles, formulations for both Greenwich sidereal time and Earth rotation angle are needed. The end-to-end transformation for both forms is between celestial and terrestrial coordinates, represented by the matrix $\mathbf{R}$ in:

$$\begin{aligned} \mathbf{R} &= R_3(ERA) \cdot \mathbf{M}_{CIO} && (2) \\ &= R_3(ERA) \cdot R_3(-EO) \cdot \mathbf{M}_\Upsilon \\ &= R_3(GST) \cdot \mathbf{M}_\Upsilon. && (3) \end{aligned}$$

The link between the two methods is the equation of the origins, EO, a quantity somewhat akin to the equation of the equinoxes but including precession as well as nutation. Note that in the equinox based version, (3), the R_3 rotation is a function both of Earth rotation and time, whereas in the CIO based version, (2), the rotation-related and time-related components are kept separate.

2. PRECESSION-NUTATION

The two types of NPB matrices, $\mathbf{M}_{CIO}$ and $\mathbf{M}_\Upsilon$, can be generated in a number of ways, including semi-analytical expressions for the CIP location $X(t), Y(t)$ and CIO locator $s(t)$, classical methods using precession and nutation angles, and models for the Euler axis and angle (the "r-vector"). The matrices $\mathbf{M}$ can both be expressed in terms of three Euler angles E, d, $E + \beta$, where E, d are the GCRS polar coordinates of the CIP and the angle β selects the origin of right ascension:

$$\mathbf{M} = R_3(-E - \beta) \cdot R_2(d) \cdot R_3(E), \tag{4}$$

or:

$$\mathbf{M}_\beta = R_3(-\beta) \cdot \mathbf{M}_\Sigma, \tag{5}$$

where the matrix $\mathbf{M}_\Sigma$ is a function of the CIP X, Y, Z:

$$\begin{aligned} \mathbf{M}_\Sigma &= R_3(-E) \cdot R_2(d) \cdot R_3(E) \\ &= \begin{pmatrix} 1 - aX^2 & -aXY & -X \\ -aXY & 1 - aY^2 & -Y \\ X & Y & 1 - a(X^2 + Y^2) \end{pmatrix}, && (6) \end{aligned}$$

with:

$$a = 1/(1 + \cos d) = 1/(1 + Z) = 1/[1 + (1 - X^2 - Y^2)^{1/2}], \tag{7}$$

For the CIO-based matrix $\mathbf{M}_{CIO}$, $\beta = s$; for the equinox-based matrix $\mathbf{M}_\Upsilon$, $\beta = -EO + s$. Another convenient way of writing the $\mathbf{M}$ matrices is as three unit vectors $\mathbf{v}$:

$$\mathbf{M}_{CIO} \equiv \begin{pmatrix} \mathbf{v}_{CIO} \\ \mathbf{v}_{CIP} \times \mathbf{v}_{CIO} \\ \mathbf{v}_{CIP} \end{pmatrix}, \qquad \mathbf{M}_\Upsilon \equiv \begin{pmatrix} \mathbf{v}_\Upsilon \\ \mathbf{v}_{CIP} \times \mathbf{v}_\Upsilon \\ \mathbf{v}_{CIP} \end{pmatrix}. \tag{8}$$

In each case the top row ($\mathbf{v}_{CIO}$ and $\mathbf{v}_\Upsilon$) is the the RA origin of date, namely the CIO or the equinox respectively. The bottom row is the GCRS position of the CIP, which of course is common to both formulations.

The most conservative method of forming the equinox based matrix $\mathbf{M}_\Upsilon$ is to provide individual rotation matrices for each of the three stages, delivering successively mean place of epoch and mean place of date. In this scheme, the precession stage can use four angles that come directly from P03, or alternatively the traditional z, ζ and θ, giving a total of either ten or nine rotations respectively. The Fukushima-Williams method (Fukushima 2003) instead condenses these into only four rotations, different uses of which deliver the full transformation or stop short at one of the earlier stages.

For the CIO based matrix, the starting-point is the CIP position and the CIO locator s. By (8), any of the above classical methods can be used to obtain X, Y simply by evaluating only the matrix elements $\mathbf{M}(3,1)$ and $\mathbf{M}(3,2)$. However, an efficient and foolproof alternative is semi-analytical series for the coordinates themselves, that deal with frame bias, precession and nutation in a single step.

A radically different approach, capable of generating both $\mathbf{M}_\Upsilon$ and $\mathbf{M}_{CIO}$, is to use semi-analytical series to generate the x, y and z coordinates of the "rotation vector". This is the Euler axis unit vector scaled by the amount of rotation, from which the more familiar rotation matrix can be derived.

3. EARTH ROTATION AND THE ORIGIN OF RIGHT ASCENSION

The choice of equinox or CIO as the longitude zero affects how Earth rotation is expressed, namely as sidereal time or Earth rotation angle. These two measures are related through the equation of the origins (EO), which is the distance between the CIO and the equinox, so that $GST = ERA - EO$.

The CIO is located by the quantity s, through (5) and $\beta = s$. It can be obtained quite readily by numerical integration, but for much faster results in practical applications a series is always used. Series for s itself exist, but a much more concise result is obtained by evaluating the expression $s + XY/2$: see Table 1. Even fewer terms are needed to compute $s + XY/2 + D$, where $D = -Y_2 t^2 (X_1 t/3 + X_{nut})$, but this involves intermediate results from evaluating the X, Y series, a complication that probably outweighs the small performance gains. Comparable numbers of terms are needed to compute the periodic part of the equation of the origins, once the precession and nutation in right ascension are known.

quantity	t^0	t	t^2	t^3	t^4
s	24	125	21	2	0
$s + XY/2$	33	3	25	4	1
$s + XY/2 + D$	33	3	1	1	0
$\Delta\psi \cos\epsilon + EO$	33	1	0	0	0

Table 1: Sizes of the series of periodic terms for generating s and the EO.

4. COMPUTING CONSIDERATIONS

We have compared the different approaches for numerical consistency and the consumption of computing resources. Fig. 1 shows the residual rotation that remains after taking the product of (i) the equinox based transformation using the Fukushima-Williams NPB matrix with GST

with (ii) the inverse of the transformation using series for X, Y and s with ERA. Similar levels of consistency are achieved by the r-matrix method. The costs, in both lines of code and computing time, are similar for all the methods, with perhaps a slight edge in favour of the X, Y, s approach.

The best formulation depends on the application. For a very focused application such as IERS VLBI analysis, where only the CIO based paradigm is required and the accuracy objectives are clear, direct use of series for X, Y and s is the most straightforward option. Where a collection of utility software components is to be developed, as for SOFA, a good approach is to select a set of core components – the nutation series, the Fukushima-Williams precession angles and the equation of the origins for example (see Fukushima 2004) – and use it to build the full range of products, both equinox based and CIO based. This not only minimizes the total amount of code required, but also ensures that numerical consistency depends only on rounding errors.

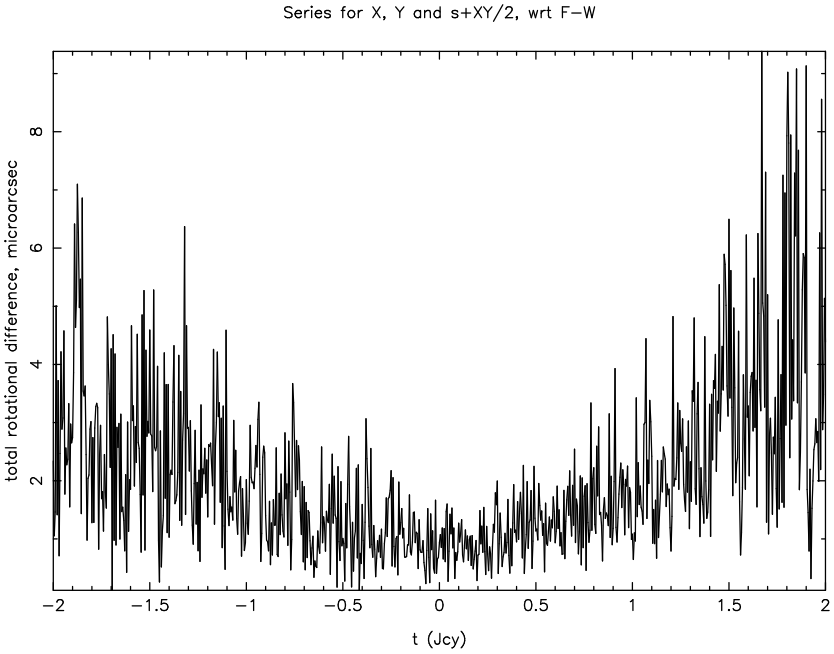

Figure 1: A numerical comparison, based on the P03/IAU 2000A precession-nutation, of two methods of transforming celestial coordinates into terrestrial: (a) series for X, Y and s, with Earth rotation angle compared with (b) precession-nutation angles and sidereal time. The total rotational difference, a product of the resolutions of the expressions used, remains within a few microarcseconds for four centuries.

REFERENCES

Capitaine, N., Wallace, P.T, Chapront J., 2003, "Expressions for IAU 2000 precession quantities," A&A 412, pp. 567–586.

Capitaine, N., Wallace, P.T, 2005, "High precision methods for locating the celestial intermediate pole and origin", submitted to A&A .

Fukushima, T., 2003, AJ, 126, pp. 494–534.

Fukushima, T., 2004, "New formulae of relations among UT1, GAST and ERA", in Proc. of the Journées Systèmes de référence spatio-temporels 2003, ed. A. Finkelstein & N. Capitaine, St. Petersburg, 114–119.

Hilton, J. et al., 2005, in Reports on Astronomy 2002-2005, IAU Transaction XXVIA, 2005, O. Engvold (ed.).

EFFICIENT INTEGRATION OF TORQUE-FREE ROTATION BY ENERGY SCALING METHOD

T. FUKUSHIMA
National Astronomical Observatory of Japan
2-21-1, Ohsawa, Mitaka, Tokyo 181-8588, Japan
e-mail: Toshio.Fukushima@nao.ac.jp

ABSTRACT. As a first trial of the manifold correction methods applied to rotational motions, we adapted its simplest technique, the energy scaling method, to the torque-free rotational motion in terms of Serret-Andoyer variables. The key point is to keep rigorously the consistency of the kinetic energy relation by applying a scaling to L, the C-axis component of the rotational angular momentum at every integration step. As a result, the new method suppress the growth rate of the integration errors in the combined rotational angles, $g + \ell$, from quadratic to linear in time.

1. ENERGY SCALING METHOD

Originally developed by Nacozy (1971), and extended to the restricted three body problem by Murrison (1989), the manifold correction methods have revived recently in orbital integrations. As for the list of our works on the manifold correction methods, see the references of our latest paper (Fukushima, 2005). Very recently, we extended the method to cover the case of conservative potential and succeeded in reducing the error growth of the two-body problem perturbed by J_2 and other zonal harmonics (Umetani and Fukushima, 2005).

Now, let us apply it to the torque-free rotational motion, the equation of motion of which is described by the well-known Serret-Andoyer canonical variables (L, G, H, ℓ, g, h) (Andoyer, 1923; Deprit, 1967; Kinoshita, 1972; 1977; 1992) as

$$\frac{\mathrm{d}L}{\mathrm{dt}} = -\left(\frac{a+b}{2}\right)\left(G^2 - L^2\right)\sin 2\ell, \tag{1}$$

$$\frac{\mathrm{d}\ell}{\mathrm{dt}} = -L\left[\left(\frac{a+b}{2} - c\right) - \left(\frac{a-b}{2}\right)\cos 2\ell\right], \tag{2}$$

$$\frac{\mathrm{d}g}{\mathrm{dt}} = G\left[\left(\frac{a+b}{2}\right) - \left(\frac{a-b}{2}\right)\cos 2\ell\right], \tag{3}$$

and

$$\frac{\mathrm{d}G}{\mathrm{dt}} = \frac{\mathrm{d}H}{\mathrm{dt}} = \frac{\mathrm{d}h}{\mathrm{dt}} = 0. \tag{4}$$

Here $a \equiv 1/A$, $b \equiv 1/B$, and $c \equiv 1/C$ are the reciprocals of the principal moments of inertia, A, B, and C, respectively. Note that conserved are G, H, h, and the kinetic energy,

$$T \equiv \frac{1}{4}\left[(a+b)G^2 - (a+b-2c)L^2 - (a-b)\left(G^2 - L^2\right)\cos 2\ell\right]. \tag{5}$$

In order to maintain the consistency condition of T, we modify the integrated L by the scaling $L \to sL$ at every integration step. Here the scaling factor s is determined uniquely as

$$s = \sqrt{\frac{G_0^2\left[(a+b)-(a-b)\cos 2\ell\right]-4T_0}{L^2\left[(a+b-2c)-(a-b)\cos 2\ell\right]}}. \tag{6}$$

where G_0 and T_0 are their initial values while L and ℓ are the integrated values. Note that we do not correct any other integrated variables, ℓ nor g.

2. NUMERICAL EXPERIMENTS

In order to examine the effectiveness of the energy scaling method, we conducted test integrations of three typical cases; a triaxial rigid Earth, a triaxial rigid Moon, and the asteroid Ida. The rotational motion of an oblate spheroidal rigid body, where $A = B$ and therefore $a = b$, in terms of the Serret-Andoyer variables reduces to be trivial linear motions in g and ℓ and a constant L. Therefore, it cannot be used as a practical test of numerical integrations.

In the below, we will show the case of the so-callede short-axis mode, namely the case where the polhode is a curve circulating around the axis of the largest principal moment of inertia, the C-axis. In this mode, the solution in g and ℓ are circulating while L is librating (Kinoshita, 1992). Namely the first two angle-like variables, g and ℓ become quasi-linear functions of time with relatively small periodic terms while the action-like variable L is a purely periodic function with a constant offset. Then the numerical integration errors most significantly appear in the sum of two angle-like variables, $g + \ell$.

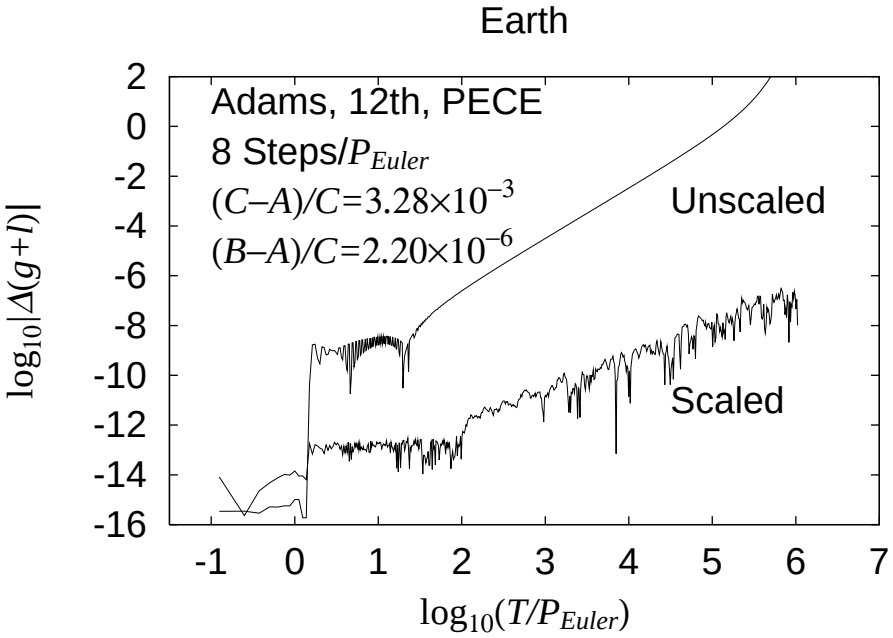

Figure 1: The numerical integration errors in the combined rotational angles $g + \ell$ of the torque-free rotation of a rigid triaxial Earth are shown as functions of time in a log-log scale. The initial angle of inclination, J_0, is chosen as small as 10^{-6} radian. The step size was as large as 1/8 of the Eulerian period, ~ 300 days.

See Figure 1, which compares the error growth of the torque-free rotation of a rigid triaxial Earth obtained by the standard method to integrate the equation of motion directly and that

with the aforementioned energy scaling with respect to the kinetic energy, T. This is the case of almost oblately spheroidal body, i.e. $B - A \ll C - A \ll C$.

In the figure, we illustrated the errors in the combined rotational angles $g + \ell$ as functions of time in a log-log scale. We compared the error growth of the torque-free rotation of a rigid triaxial Earth integrated by two methods; (1) the standard method to integrate directly the canonical equation of rotational motion in terms of Serret-Andoyer variables, and (2) the energy scaling method described in the previous section.

We adopted the 12th order implicit Adams method in the PECE mode (predict, evaluate, correct, evaluate), fixed the step size through the integration, and set it as large as 1/8 the Eulerian period. As for the starting tables needed for Adams method, we prepared them by Gragg's extrapolation method. We measured the errors by comparing with the reference solutions obtained by the same method, the same integrator, and the same model parameters but with half the step size. Since the order of the integrators are sufficiently high, halving the step size eliminates almost all the truncation errors.

We set the initial conditions as $g_0 = \ell_0 = 0$, and $L_0 = G_0 \cos J_0$ where G_0 is taken as unity after an appropriate adustment of units. Also we chose the initial value of the amplitude of polar motion, J_0, as small as 10^{-6} radian to resemble the actual Earth rotation.

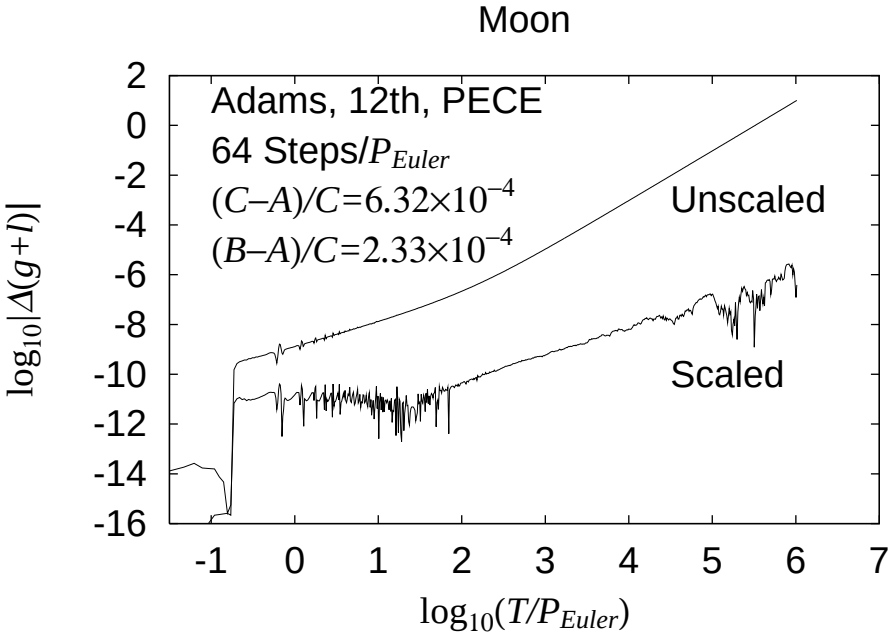

Figure 2: Same as Figure 1 but for the torque-free rotation of a rigid Moon. The initial angle J_0 was taken as 10^{-5} radian. The chosen step size was relatively small as 1/64 of its Eulerian period.

Figure 2 shows the case of Moon. This is an example of triaxial but almost spherical case, i.e. $B - A \sim C - A \ll C$.

Figure 3 depicts the case of an illustration of truly triaxial body, i.e. $A \sim B \sim C$, namely that of the asteroid Ida.

The curves in these three graphs show that the quadratic increase of the integration errors by the standard method is reduced to a linear growth, which has been observed for a limited type of integration scheme; the symplectic integrator and the symmetric linear multistep method. The observed difference in the rate of error growth lead to a large difference in the magnitude of

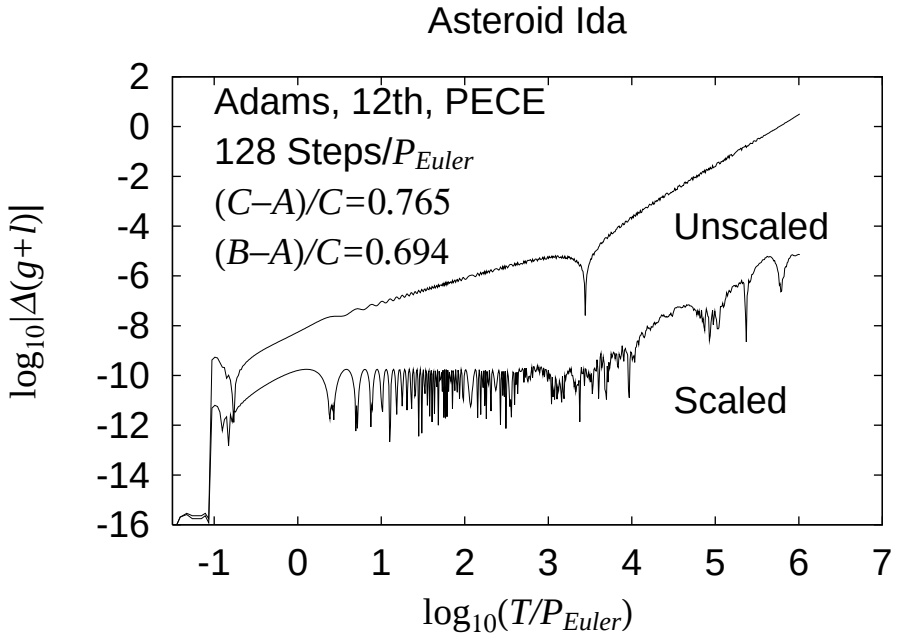

Figure 3: Same as Figure 1 but for the asteroid Ida. The initial angle J_0 was taken as relatively large 0.1 radian. The chosen step size was 1/128 of its Eulerian period.

integration error in the long run as shown in the graphs.

The next target of our study is, of course, the rotational motion under torques. In those perturbed cases, T is no longer a constant of integration. Then we should follow its time development simultaneously as we did for the Kepler energy in the first scaling method of ours (Fukushima, 2003).

REFERENCES

Andoyer, H., 1923, Mécanique Céleste, Gauthier-Villars, Paris
Deprit, A., 1967, Am. J. Physics, 35, 424
Fukushima, T., 2003, AJ , 126, 1097
Fukushima, T., 2005, AJ , 129, 2496
Kinoshita, H., 1972, PASJ, 24, 423
Kinoshita, H., 1977, Celest. Mech. , 15, 277
Kinoshita, H., 1992, Celest. Mech. Dyn. Astr. , 53, 365
Murison, M.A. 1989, AJ , 97, 1496
Nacozy, P.E. 1971, Astrophys. and Space Sci., 14, 40
Umetani, M., and T. Fukushima, 2005, submitted to Celest. Mech. Dyn. Astr.

CHOICE OF THE OPTIMAL SPECTRAL ANALYSIS SCHEME FOR INVESTIGATION OF THE EARTH ROTATION PROBLEM

V.V. PASHKEVICH, G.I. EROSHKIN
Central (Pulkovo) Astronomical Observatory of Russian Academy of Science
Pulkovskoe Shosse 65/1,196140, St. Petersburg, Russia
e-mails: pashvladvit@yandex.ru, eroshkin@gao.spb.ru

ABSTRACT. The spectral analysis algorithms for the research and elaboration of numerical and semi-analytical models of the rigid Earth rotation are studied. The optimal algorithm scheme, in respect to the computational time and to the accuracy is determined. It is ALGORITHM - 1A (Figure 1), which investigates the arrays of the differences between the semi-analytical solution and the numerical one using method - A of the spectral analysis (Figure 2) in which the power spectrum is constructed only one time.

1. ALGORITHMS

In this investigation the numerical and semi-analytical models of the rigid Earth rotation are studied by means of four algorithmic schemes. These schemes include two types of the algorithms (Figure 1) and two variants of the spectral analysis methods (Figure 2).

The first type algorithm (ALGORITHM - 1) includes one of two spectral analysis schemes for processing the differences between the Numerical Solution and the Semi-analytical Solution.

The second type algorithm (ALGORITHM - 2) includes one of two spectral analysis schemes for the investigation of the Numerical Solution or the Semi-analytical Solution.

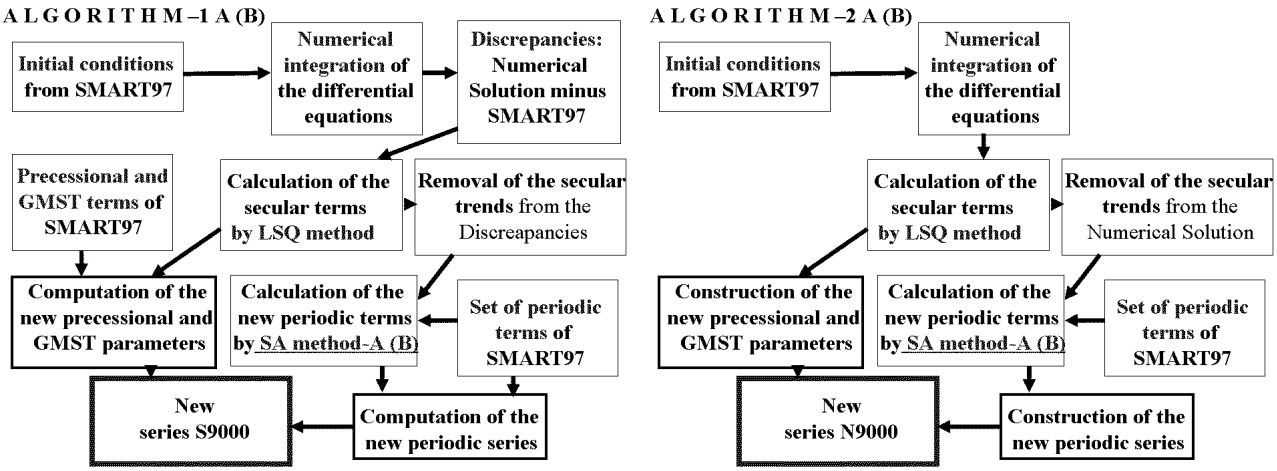

Figure 1: Two types of algorithms

The numerical solution of the rigid Earth rotation problem is the result of the quadruple precision numerical integration of the differential equations of the problem (Eroshkin *et al.*, 2004). The initial conditions are determined by SMART97 solution (Bretagnon *et al.*, 1998). The numerical solution is compared with SMART97 semi-analytical solution over the time interval of 2000 years time interval from AD 1000 to AD 3000 with one-day spacing. The arrays of the differences are constructed only for ALGORITHM - 1. For shortness, the term "ARRAYS" will be used instead of "DIFFERENCES" for ALGORITHM - 1 and "NUMERICAL SOLUTION" for ALGORITHM - 2. The investigation of ARRAYS is carried out by the least squares (LSQ) method and by the spectral analysis (SA) methods:

1. The secular parts of ARRAYS are processed by the LSQ method and are represented by the temporal polynomials of the 6-th degree.

2. New precessional and GMST polynomials are derived as the sums of the calculated secular terms and the precessional and GMST polynomials of SMART97 in the case of ALGORITHM - 1. In the case of ALGORITHM - 2 the computed secular terms are the new precessional and GMST polynomials.

3. The determined polynomials are removed from ARRAYS.

4. The periodic parts of ARRAYS are processed by one of two variants of the SA methods, A or B (Figure 2):

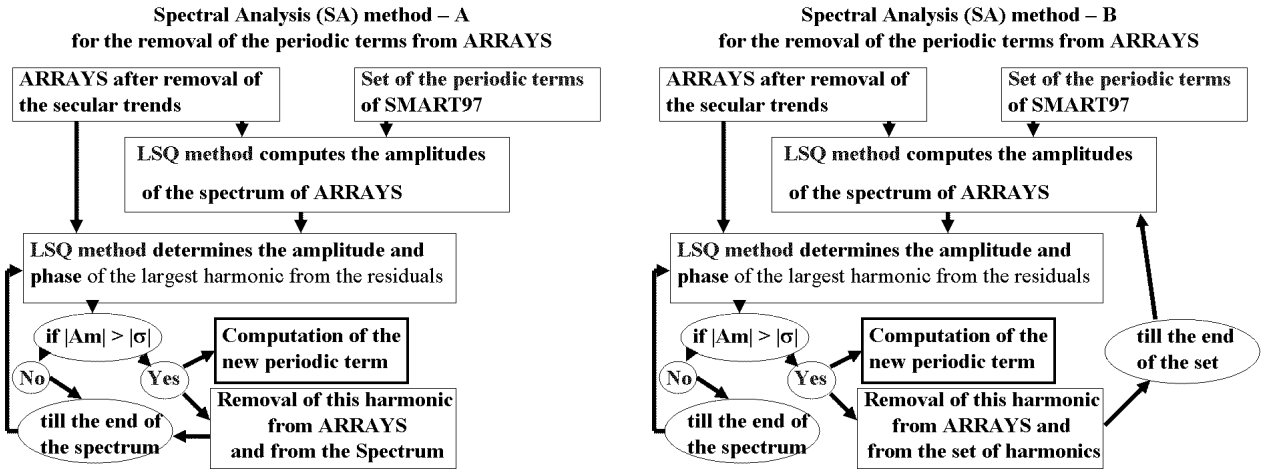

Figure 2: Two variant Spectral Analysis Methods. "Am" means the value of each amplitude of the spectrum and "σ" is the value of its root-mean-square error.

The spectrum of the periodic parts of ARRAYS for SA method - A (ALGORITHMS - 1A, 2A) is constructed one time only. The coefficient of the new periodic term equals the sum of the calculated periodic term coefficient and the coefficient of the corresponding periodic term of the SMART97 in the case of ALGORITHM - 1. In the case of ALGORITHM - 2 the periodic term coefficient is determined directly. The harmonic is removed from ARRAYS and from the spectrum. Starting from the maximum term of the spectrum the procedure is accomplished successively till its least term. The spectra represented in Figure 3 are ranged by terms with the periods from 1.0003 days to 1000 years.

The spectrum of the periodic parts of ARRAYS for SA method - B (ALGORITHMS - 1B, 2B) is constructed anew after every removal of the largest harmonic from ARRAYS. Each constructed spectrum is used for the determination of the new coefficient of the periodic term as for SA method - A. This procedure is performed to the end of the set. The spectra of the terms with periods between 6700 and 6900 days, are shown in Figure 5.

The amplitudes of this spectra are computed by the LSQ method using the argument of the periodic terms of SMART97.

5. New secular and periodic terms form the new high-precision rigid Earth rotation series S9000 in the case of ALGORITHM - 1A (Pashkevich *et al.*, 2004). In the case of ALGORITHM - 2A they are named N9000 series.

Spectra of the harmonic terms, which are close to the main nutational term are depicted in Figure 3 - ψ, θ, ϕ.

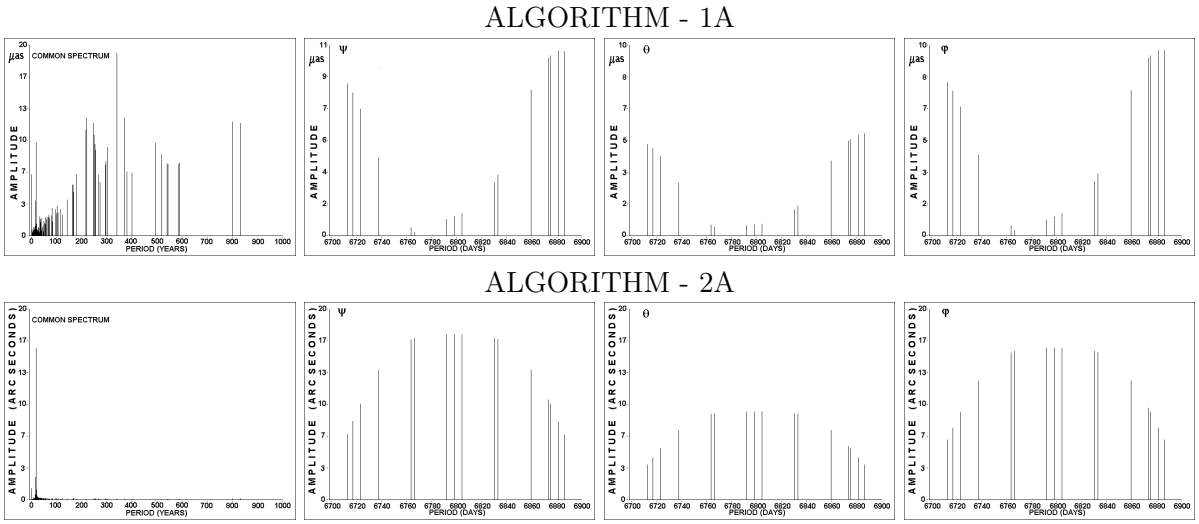

Figure 3: Common spectrum and spectra for Euler angles

Naturally, the values of the amplitudes of the spectra for ALGORITHM - 1A are essentially less than ones for ALGORITHM - 2A. The difference of the spectra for Euler angles (ψ, θ, ϕ)in any chosen algorithm is only values of the amplitudes of the harmonics. The order of removal of the harmonics are similar (Figure 3 - ψ, θ, ϕ). So, the common spectrum can be constructed only once for each of the Euler angles. It makes the process of computation shorter. In each spectrum of ALGORITHM - 2A, there is a set of the harmonics with close frequencies and close amplitudes. This fact reduces essentially the efficiency of ALGORITHM - 2A for the construction of the semi-analytical solution.

The new Numerical Solution (NS) of the problem is performed with the initial conditions determined by S9000 series and N9000 series. The differences between the new NS and S9000 series are less than the differences between the new NS and N9000 series. In the first case they do not surpass 10 μas over 2000-year time interval while in the second case they do not surpass 15 μas over the same time interval (Figure 4). Hence, ALGORITHM - 1A is more accurate than ALGORITHM - 2A.

In Figure 5 the iteration spectrum of the proper rotation angle (ϕ) for ALGORITHM - 2B is depicted for the harmonics with the frequencies close to that of the main nutational term. The amplitudes of the spectrum for ALGORITHM - 2A (Figure 3 - ϕ) are by more than 3 orders of magnitude larger than those for ALGORITHM - 2B. Therefore ALGORITHM - 2B is more accurate than ALGORITHM - 2A. It means that SA method - B is more accurate that SA method - A. The time of a construction of the common spectrum of the periodic terms of ARRAYS (Figure 3) on the computer Intel Pentium IV (2.4 GHz) amounts to 12 hours, with double precision representation of real numbers. The time increases as an exponential function of number of the harmonics.

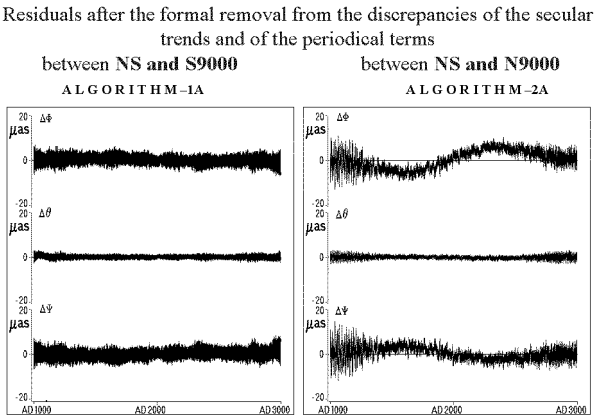

Figure 4

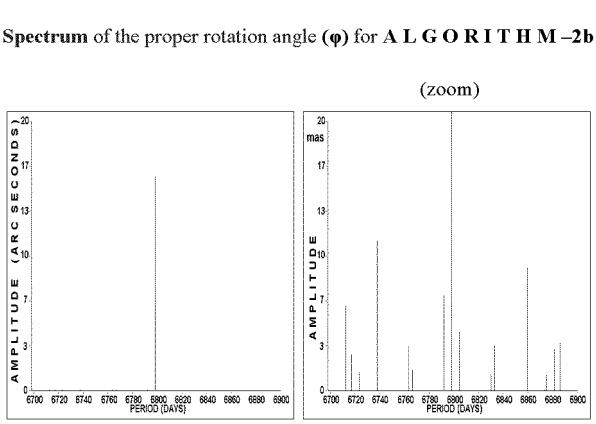

Figure 5

2. SUMMARY AND CONCLUSIONS

1. The secular and periodic terms representing the rigid Earth rotation series S9000 were determined by ALGORITHM - 1A. The differences between NS and S9000 do not surpass 10 μas over 2000 years.

2. The secular and periodic terms representing the rigid Earth rotation series N9000 were determined by ALGORITHM - 2A. The differences between NS and N9000 do not surpass 15 μas over 2000 years.

3. ALGORITHMS - 1B, 2B are very time-consuming, consequently they are not suitable for the investigation of the long time series.

It is proved that ALGORITHM - 1A is optimal with respect to the computational time and the accuracy.

Acknowledgments. The investigation was carried out at the Central (Pulkovo) Astronomical Observatory of Russian Academy of Science and the Space Research Centre of Polish Academy of Science, under a financial support within the program of cooperation between Polish and Russian Academies of Sciences, Theme No. 31.

REFERENCES

Bretagnon P., Francou G., Rocher P. and Simon J. L.: 1998, A&A , 329, No.1, pp. 329–338.

G.I.Eroshkin, V.V.Pashkevich and A.Brzeziński: 2004, Arcificial Satellites, 39, No.4, Space Res. Centre PAS, Warsaw, pp. 291–304.

Pashkevich V. V., Eroshkin G. I.: 2004, Proc. Journees 2004, N. Capitaine (ed.), Observatoire de Paris, pp. 82–87.

COMPATIBILITY OF THE IERS EARTH ROTATION REPRESENTATION AND ITS RELATION TO THE NRO CONDITIONS

A. DERMANIS
Department of Geodesy and Surveying, The Aristotle University of Thessaloniki
Univ Box 503, 54124 Thessaloniki, Greece
e-mail: dermanis@topo.auth.gr

The rotation of the earth is mathematically represented by an orthogonal rotation matrix $\mathbf{R}(t)$, which relates coordinates $\mathbf{x}_C$ in a Celestial Reference System $\vec{\mathbf{e}}^C$ with coordinates $\mathbf{x}_T$ in a Terrestrial Reference System $\vec{\mathbf{e}}^T$ according to

$$\mathbf{x}_C = \mathbf{R}\mathbf{x}_T \,, \qquad \vec{\mathbf{e}}^T = \vec{\mathbf{e}}^C\mathbf{R} \,, \tag{1}$$

where any row-matrix $\vec{\mathbf{e}} = [\vec{e}_1\, \vec{e}_2\, \vec{e}_3]$ contains the elements $\vec{e}_1$, $\vec{e}_2$, $\vec{e}_3$ of a corresponding geocentric orthonormal basis and $\mathbf{x} = \left[x^1\, x^2\, x^3\right]^T$ is the column-matrix of the relevant coordinates. The orthogonal matrix $\mathbf{R}(t)$ can be adequately defined by 3 parameters (functions of time), e.g. Euler angles. Consequently any representation involving k parameters must be accompanied by $k-3$ conditions between these parameters. Once $\mathbf{R}(t)$ is given by a particular representation, the rotation of the earth (in fact of the chosen terrestrial reference system) is completely defined and so is the corresponding earth rotation vector (vector of instantaneous angular rotation) $\vec{\omega} = \vec{\mathbf{e}}^T\boldsymbol{\omega}_T = \vec{\mathbf{e}}^C\boldsymbol{\omega}_C$. In fact $\vec{\omega}$, is defined by its terrestrial coordinates $\boldsymbol{\omega}_T$, which can be derived from $\mathbf{R}$ by the generalized Euler's kinematic equations

$$[\boldsymbol{\omega}_T\times] = \mathbf{R}^T\frac{d\mathbf{R}}{dt} \,, \tag{2}$$

where $[\boldsymbol{\omega}_T\times]$ denotes the antisymmetric matrix having ω_T as its axial vector. Both the classical astronomical representation and the new one provided by IERS in accordance with the IAU 2000 resolutions involve a separation of $\mathbf{R}$ into 3 parts $\mathbf{R} = \mathbf{QDW}$. The precession-nutation part $\mathbf{Q}$, the diurnal rotation part $\mathbf{D}$ and the polar motion part $\mathbf{W}$, are realized with the use of two intermediate systems, the Intermediate Celestial (IC) system $\vec{\mathbf{e}}^{IC} = \vec{\mathbf{e}}^C\mathbf{Q}$ and the Intermediate Terrestrial (IT) system $\vec{\mathbf{e}}^{IT} = \vec{\mathbf{e}}^C\mathbf{QD} = \vec{\mathbf{e}}^T\mathbf{W}^T$ with a common third axis, defined by the unit vector

$$\vec{p} = \vec{e}_3^{IC} = \vec{e}_3^{IT} \,, \tag{3}$$

which we will loosely call the "celestial pole". In fact the diurnal part is simply a rotation around the celestial pole $\vec{p}$

$$\mathbf{D} = \mathbf{R}_3(-\theta) \,. \tag{4}$$

The question arises about the coincidence or not of the celestial pole (CP) $\vec{p}$ used in a specific representation with the (mathematically) "compatible celestial pole" (CCP) defined through (2) and represented by the unit vector

$$\vec{n} = \frac{1}{|\vec{\omega}|}\,\vec{\omega} \,. \tag{5}$$

In addition to the directional coincidence, the question arises about the magnitude coincidence between the compatible angular velocity $\omega = |\vec{\omega}|$ and the angular velocity of the diurnal rotation $\dot{\theta} = d\theta/dt$.

A three-part earth rotation representation involves at least 5 parameters according to the scheme (Dermanis, 1977) $\mathbf{R} = \mathbf{Q}(\Xi, \mathrm{H})\mathbf{D}(\psi)\mathbf{W}(\xi, \eta)$, which however suffers from the fact that the separation between diurnal rotation on one part and precession-nutation or polar motion on the other, strongly depends on the explicit parameterizations used. For example the three possible choices $\mathbf{Q} = \mathbf{R}_1(\Xi)\mathbf{R}_2(\mathrm{H})$, $\mathbf{Q} = \mathbf{R}_2(B)\mathbf{R}_1(A)$, $\mathbf{Q} = \mathbf{R}_3(-E)\mathbf{R}_2(-d)\mathbf{R}_3(E)$, lead to a different position of the "celestial origin" $\vec{e}_1^{\,IC}$ (starting direction for the "diurnal" angle ψ), while the same is true for the "terrestrial origin" $\vec{e}_1^{\,IT}$ (terminal direction for ψ) with respect to the possible choices $\mathbf{W} = \mathbf{R}_1(-C)\mathbf{R}_2(-D)$, $\mathbf{W} = \mathbf{R}_2(-\Pi)\mathbf{R}_1(-\Sigma)$, $\mathbf{W} = \mathbf{R}_3(-F)\mathbf{R}_2(g)\mathbf{R}_3(F)$. To avoid this problem the IAU2000 resolutions introduce a separation $\psi = s + \theta - s'$, including s in precession-nutation $\mathbf{Q}$ and s' in polar motion $\mathbf{W}$, in such a way that the positions of the celestial $\vec{e}_1^{\,IC}$ and terrestrial origin $\vec{e}_1^{\,IT}$ are independently defined with the ingenious introduction of the 2 Non Rotating Origin (NRO) conditions.

More details can be found in the IERS conventions 2003 (McCarthy and Petit, 2004), as well as in a series of relevant papers (Capitaine, N., 1986, Capitaine & Gontier, 1993, Capitaine et al. 2000, 2002, IERS, 2001, Johnston et al., 2000, Lambert & Bizouard, 2002, McCarthy, 1996, Seidelmann & Kovalevsky, 2002). The specific IERS representation has the form

$$\begin{aligned} \mathbf{R} &= \mathbf{Q}(E, d, s)\mathbf{D}(\theta)\mathbf{W}(F, g, s') \\ &= \mathbf{R}_3(-E)\mathbf{R}_2(-d)\mathbf{R}_3(E)\mathbf{R}_3(s)\mathbf{R}_3(-\theta)\mathbf{R}_3(-s')\mathbf{R}_3(-F)\mathbf{R}_2(g)\mathbf{R}_3(F) \end{aligned} \tag{6}$$

where the appearing 7 parameters are in fact reduced to 5, by means of the NRO conditions $\dot{s} = \dot{E}(\cos d - 1)$, $\dot{s}' = \dot{F}(\cos g - 1)$ (dots denote derivatives with respect to time), which give the dependence relations $s = s(E, d)$, $s' = s'(F, g)$.

Generalizing and extending previous work (Dermanis, 2003), we will examine here the possibility of reducing the 7 parameters of the earth rotation representation (6) to the minimum required of 3 independent parameters, by introducing 4 appropriate conditions. Three candidate conditions are the 2 *direction conditions* implied by

$$\vec{p} = \vec{n}\,, \qquad \left(\vec{e}_3^{\,IC} \equiv \vec{e}_3^{\,IT} = \frac{1}{|\vec{\omega}|}\,\vec{\omega}\right) \tag{7}$$

and the *magnitude condition*

$$\omega \equiv |\vec{\omega}| = \dot{\theta} \equiv \frac{d\theta}{dt}\,. \tag{8}$$

The one condition which is still missing can be associated with the choice of the origin $\vec{e}_1^{\,IC}$ of the diurnal rotation angle θ. Note that once this choice is made, the value $\theta = \int \omega dt$ resulting from (8) defines uniquely the terminating direction $\vec{e}_1^{\,IT}$. For any choice of E, d, s, θ, s', F, g, replacement of s and s' with $\bar{s} = s + \Delta s$ and $\bar{s}' = s' - \Delta s$, respectively, provides exactly the same rotation matrix $\mathbf{R}$. Thus the 4th condition is implicitly provided by the arbitrary choice of the function $\Delta s(t)$, with every choice corresponding to a different choice of $\vec{e}_1^{\,IC}$ (and consequently of $\vec{e}_1^{\,IT}$).

In order to find 4 explicit conditions we need to resort to the NRO conditions, which we will present in a geometric form, by using the decomposition

$$\vec{\omega} = \vec{\omega}_Q + \vec{\omega}_D + \vec{\omega}_W\,. \tag{9}$$

The relative rotation vectors $\vec{\omega}_Q = \vec{\mathbf{e}}^{\,IC}(\boldsymbol{\omega}_Q)_{IC}$ of $\vec{\mathbf{e}}^{\,IC}$ with respect to $\vec{\mathbf{e}}^{\,C}$, $\vec{\omega}_D = \vec{\mathbf{e}}^{\,IT}\,(\boldsymbol{\omega}_D)_{IT}$ of $\vec{\mathbf{e}}^{\,IT}$ with respect to $\vec{\mathbf{e}}^{\,IC}$ and $\vec{\omega}_W = \vec{\mathbf{e}}^{\,T}\,(\boldsymbol{\omega}_W)_T$ of $\vec{\mathbf{e}}^{\,T}$ with respect to $\vec{\mathbf{e}}^{\,IT}$, are uniquely defined by their components determined respectively from relations similar to (2)

$$\left[(\boldsymbol{\omega}_Q)_{IC}\times\right] = \mathbf{Q}^T\frac{d\mathbf{Q}}{dt}\,, \quad \left[(\boldsymbol{\omega}_D)_{IT}\times\right] = \mathbf{D}^T\frac{d\mathbf{D}}{dt}\,, \quad \left[(\boldsymbol{\omega}_W)_T\times\right] = \mathbf{W}^T\frac{d\mathbf{W}}{dt}\,. \tag{10}$$

The two NRO conditions take the geometric form $\vec{\omega}_Q \perp \vec{p}$, $\vec{\omega}_W \perp \vec{p}$ or

$$\vec{\omega}_Q \bullet \vec{p} = 0\,, \qquad \vec{\omega}_W \bullet \vec{p} = 0\,, \tag{11}$$

which impose "no component" along the diurnal rotation direction $\vec{p}$, for both the precession-nutation and polar motion relative rotation vectors $\vec{\omega}_Q$ and $\vec{\omega}_W$, respectively. Now we have altogether 5 conditions, the 2 direction conditions (7), the magnitude condition (8) and the 2 NRO conditions (11), among which we must isolate the desired 4 independent conditions. To do this we need to switch from the geometric to a mathematical form by employing components in the most advantageous intermediate celestial system $\vec{\mathbf{e}}^{IC}$. Since $\vec{p} = \vec{\mathbf{e}}^{IC}\mathbf{p}_{IC} \equiv \vec{e}_3^{IC}$ has components $\mathbf{p}_{IC} = [0\,0\,1]^T \equiv \mathbf{i}_3$ and $\vec{n} = \vec{\mathbf{e}}^{IC}\mathbf{n}_{IC} = \omega^{-1}\vec{\omega}$, the *direction conditions* $\vec{n} = \vec{p}$ take the form $n^1_{IC} = p^1_{IC} = 0$, $n^2_{IC} = p^2_{IC} = 0$, or in terms of the rotation vector components

$$\omega^1_{IC} = 0\,, \qquad \omega^2_{IC} = 0\,. \tag{12}$$

Setting $\vec{\omega}_Q = \vec{\mathbf{e}}^{IC}(\boldsymbol{\omega}_Q)_{IC}$, $\vec{\omega}_W = \vec{\mathbf{e}}^{IC}\,(\boldsymbol{\omega}_W)_{IC}$ the NRO conditions become accordingly

$$\big(\omega_Q\big)^3_{IC} = 0\,, \qquad (\omega_W)^3_{IC} = 0\,. \tag{13}$$

For the remaining *magnitude condition* $\omega \equiv |\vec{\omega}| = \sqrt{\boldsymbol{\omega}^T_{IC}\boldsymbol{\omega}_{IC}} = \dot{\theta}$ we have according to (9) $\boldsymbol{\omega}_{IC} = (\boldsymbol{\omega}_Q)_{IC} + (\boldsymbol{\omega}_D)_{IC} + (\boldsymbol{\omega}_W)_{IC}$, where , $(\boldsymbol{\omega}_D)_{IC} = (\boldsymbol{\omega}_D)_{IT} = \dot{\theta}\mathbf{i}_3$ and $\omega^3_{IC} = (\omega_Q)^3_{IC} + (\omega_D)^3_{IC} + (\omega_W)^3_{IC}$, where $(\boldsymbol{\omega}_D)^3_{IC} = \dot{\theta}$. Thus the *magnitude condition* in the form $\omega^2 = \boldsymbol{\omega}^T_{IC}\boldsymbol{\omega}_{IC} = \dot{\theta}^2$, becomes

$$\begin{gathered}\omega^2 = [\omega^1_{IC}]^2 + [\omega^2_{IC}]^2 + [\omega^3_{IC}]^2 = \\ = [\omega^1_{IC}]^2 + [\omega^2_{IC}]^2 + [(\omega_Q)^3_{IC} + \dot{\theta}^2 + (\omega_W)^3_{IC}]^2 = \dot{\theta}^2\,.\end{gathered} \tag{14}$$

From the above relation it is obvious that when the direction conditions $\omega^1_{IC} = 0$, $\omega^2_{IC} = 0$ and the NRO conditions $(\omega_Q)^3_{IC} = 0$, $(\omega_W)^3_{IC} = 0$ are satisfied, then the magnitude condition (14) is also trivially satisfied. Therefore we arrive at the following conclusion:

> *The 2 direction conditions (12) and the 2 NRO conditions (13), provide the desired set of 4 independent conditions, which reduce the 7 parameters E, d, s, θ, s′, F, g, to the required 3 independent parameters that suffice for the description of the orthogonal rotation matrix* **R**.

The current IERS representation implements the NRO conditions but not the direction conditions and consequently $\vec{n} \neq \vec{p}$ and $\omega \neq \dot{\theta}$. Thus the compatible celestial pole (CCP) $\vec{n}$ does not coincide with the celestial pole $\vec{p}$, which in this case is the Celestial Intermediate Pole (CIP). The CIP results by removing from the theoretical solution to the precession-nutation problem, high frequency terms of (celestial) periods smaller than 2 days. Unlike precession-nutation, polar motion and length-of-the-day variation cannot be predicted by theory and therefore the rotation matrix **R** is constructed from observations, which have a resolution limited by the corresponding sampling rate. The removal of high frequency terms from the formerly used Celestial Ephemeris Pole (CEP), has thus brought the CIP closer to the CCP but a difference still remains. Apart from the direction problem, the compatible angular velocity ω provides the means for defining a compatible diurnal rotation angle $\theta_{CCP} = \int \omega dt$, which will in turn defines a compatible Universal Time $\mathrm{UT}_{CCP} = A\theta_{CCP} + B$, using appropriate constants A and B in order to conveniently choose the origin and unit of this new time system. The IERS provided parameters can be used for determining the direction of the corresponding CCP and compatible angular velocity ω. Setting $\mathbf{n}_C = [X_{CCP}\,Y_{CCP}\,Z_{CCP}]^T$ for the celestial components,

while $\mathbf{p}_C = [X\,Y\,Z]^T$ and $\mathbf{p}_T = [\xi\,\eta\,\zeta]^T$, then with X, Y, $\xi \approx x_P$, $\eta \approx -y_P$ and θ provided by the IERS, we may compute first $\boldsymbol{\omega}_C = \mathbf{R}\boldsymbol{\omega}_T$, with $\boldsymbol{\omega}_T$ from (2) and next $\omega = \left(\boldsymbol{\omega}_C^T\boldsymbol{\omega}_C\right)^{1/2}$ and $\mathbf{n}_C = \omega^{-1}\boldsymbol{\omega}^C$. After rather lengthy computations, which also implement the NRO conditions, we arrive at

$$\omega^2 = \dot\theta^2 + \left(b_Q^1\right)^2 + \left(b_Q^2\right)^2 + \left(b_W^1\right)^2 + \left(b_W^2\right)^2 - 2\cos\psi\left(b_Q^1 b_W^1 + b_Q^2 b_W^2\right) + 2\sin\psi\left(b_Q^1 b_W^2 - b_Q^2 b_W^1\right) \quad (15)$$

$$\begin{bmatrix} X_{CCP} \\ Y_{CCP} \end{bmatrix} = \frac{\dot\theta}{\omega}\begin{bmatrix} X \\ Y \end{bmatrix} + \frac{1}{\omega}\begin{bmatrix} 1-\alpha X^2 & \alpha XY \\ -\alpha XY & 1-\alpha Y^2 \end{bmatrix}\left\{\begin{bmatrix} b_Q^1 \\ b_Q^2 \end{bmatrix} - \begin{bmatrix} \cos\psi & \sin\psi \\ -\sin\psi & \cos\psi \end{bmatrix}\begin{bmatrix} b_W^1 \\ b_W^2 \end{bmatrix}\right\} \quad (16)$$

where $\psi = -s + \theta + \dot s$ and

$$\begin{bmatrix} b_Q^1 \\ b_Q^2 \end{bmatrix} = \frac{Y\dot X - X\dot Y}{X^2+Y^2}\begin{bmatrix} X \\ Y \end{bmatrix} + \frac{X\dot X + Y\dot Y}{(X^2+Y^2)\sqrt{1-X^2-Y^2}}\begin{bmatrix} -Y \\ X \end{bmatrix}, \quad (17)$$

$$\begin{bmatrix} b_W^1 \\ b_W^2 \end{bmatrix} = \frac{\eta\dot\xi - \xi\dot\eta}{\xi^2+\eta^2}\begin{bmatrix} \xi \\ \eta \end{bmatrix} + \frac{\xi\dot\xi + \eta\dot\eta}{(\xi^2+\eta^2)\sqrt{1-\xi^2-\eta^2}}\begin{bmatrix} -\eta \\ \xi \end{bmatrix}. \quad (18)$$

REFERENCES

Capitaine, N. (1986): The earth rotation parameters: conceptual and conventional definitions. Astron. Astrophys., 162 (1986), 323-329.

Capitaine, N. and A.-M. Gontier (1993): Accurate procedure for deriving UT1 at a submilliarcsecond accuracy from Greenwich Sidereal Time or from the stellar angle. Astron. Astrophys., 275 (1993), 645-650.

Capitaine, N., B. Guinod, D.D. McCarthy (2000): Definition of the Celestial Ephemeris Origin and of UT1 in the International Celestial Reference Frame. Astron. Astrophys., 355 (2000), 398-405.

Capitaine, N., D. Gambis, D.D. MacCarthy, G. Petit, J. Ray, B. Richter, M. Rotacher, E. Myles Standish, J. Vondrak (eds.) (2002): IERS Technical Note No. 29: Proceedings of the IERS Workshop on the Implementation of the New IAU Resolutions. Observatoire de Paris, 18-19, April 2002. Verlag des Bundesamts fur Kartographie und Geodasie, Frankfurt am Main 2002.

Dermanis, A. (1977): Design of Experiment for Earth Rotation and Baseline Parameter Determination from Very Long Baseline Interferometry. Report No. 245, Department of Geodetic Science, The Ohio State University, Columbus, Ohio.

Dermanis, A. (2003): Some remarks on the description of earth rotation according to the IAU 2000 resolutions. In: "From Stars to Earth and Culture". Honorary volume in memory of Professor Alexandros Tsioumis, pp. 280-291. School of Rural & Surveying Engineering, The Aristotle University of Thessaloniki.

IERS (2001): IERS Annual Report 2001. Verlag des Bundesamts fur Kartographie und Geodasie, Frankfurt am Main 2002.

Johnston, K.J., D.D. MacCarthy, B.J. Luzum, G.H. Kaplan (eds.) (2000): Proceedings of IAU Colloquium 180: Towards Models and Constants for Sub-Microarcsecond Astrometry. Washington, DC, 27-30 March 2000. U.S. Naval Observatory, Washington, DC, 2000.

Lambert, S. and C. Bizouard (2002): Positioning the Terrestrial Ephemeris Origin in the International Terrestrial Reference Frame. Astron. Astrophys., 394 (2002), 317-321.

McCarthy, D.D. (ed.) (1996): IERS Conventions 1996. IERS Technical Note 21, Central Bureau of IERS, Observatoire de Paris.

McCarthy D.D. and G. Petit (eds.), 2004: IERS Conventions (2003). IERS Technical Note No. 32, Verlag des Bundesamts fur Kartographie und Geodasie, Frankfurt am Main 2004.

Seidelmann P.K. and J. Kovalevsky (2002): Application of the new concepts and definitions (ICRS, CIP and CEO) in fundamental astronomy. Astron. Astrophys., 392 (2002) 341-351.

EARTH ROTATION BASED ON THE CELESTIAL COORDINATES OF THE CELESTIAL INTERMEDIATE POLE

N. CAPITAINE[1], M. FOLGUEIRA[2,1] and J. SOUCHAY[1]

[1] Observatoire de Paris, SYRTE, UMR 8630/ CNRS,
61 avenue de l'Observatoire, 75014 Paris, France.
e-mail: nicole.capitaine@obspm.fr; jean.souchay@obspm.fr

[2] Instituto de Astronomía y Geodesia (UCM-CSIC),
Facultad de CC. Matemáticas, Universidad Complutense de Madrid,
Plaza de Ciencias, 3. Ciudad Universitaria, 28040 Madrid, Spain.
e-mail: martafl@mat.ucm.es

ABSTRACT. We report on the semi-analytical part of the Descartes-nutation project (see Folgueira et al. 2005, and this Volume, Session 2.3) devoted to the integration of the dynamical equations of Earth's rotation in terms of the X, Y celestial coordinates of the Celestial Intermediate Pole (CIP) and Earth Rotation Angle (ERA). We first explain how the Earth's rotational equations have been developed as functions of those variables. We then describe the integration method that has been used to get the semi-analytical solution for an axially symmetric Earth (Capitaine et al. 2006a) and we report on tests of the efficiency of the method. We finally describe how this approach has be used (Capitaine et al. 2006b) to get new series for the X, Y CIP coordinates that best represent the rigid Earth precession-nutation of the CIP equator.

1. INTRODUCTION

The series for the X, Y coordinates of the celestial intermediate pole (CIP) unit vector in the geocentric celestial reference system (GCRS) that are currently available have been derived from expressions for the IAU 2000A nutation for the classical nutation angles (Mathews et al. 2002) and either the IAU 2000 precession (Capitaine et al. 2003a and IERS Conventions 2003) or P03 precession (Capitaine et al. 2003b) for the classical precession angles.

The work described in this paper aims at obtaining the X, Y series directly as solutions of the equations for Earth rotation (Capitaine et al. 2006a and b). The first part has consisted in (i) establishing the equations in terms of X, Y, (ii) developing an integration method, (iii) testing the efficiency of the method and the accuracy of the solution and (iv) extending the approach to a non-rigid Earth. The second part has consisted in computing the rigid Earth solution using the expression for the external torque acting on the Earth based on the best currently available semi-analytical solutions for the orbital motions of the Moon, the Sun and the planets. All the semi-analytical computations performed in this work have been based on the software package GREGOIRE developed by Chapront (2003) devoted to Fourier and Poisson series manipulations.

2. THE EQUATIONS OF EARTH ROTATION AS FUNCTION OF X AND Y

The equations for Earth rotation are based on the equations for the Earth's angular momentum balance in space but require, for obtaining a rigorous solution in an appropriate way, to be written explicitly as function of the components ω_1, ω_2, ω_3 of the instantaneous rotation vector in the terrestrial system (i.e. Euler's kinematical equations) where the inertia momenta A, B and C, have the simplest formulations.

Expressing $\omega_1, \omega_2, \omega_3$ as functions of the transformation parameters between the International Terrestrial System (ITRS) and the GCRS, allows us to obtain the rigorous equations of Earth rotation in terms of X, Y and ERA ($= \theta$). This requires using the GCRS-to-ITRS transformation as recommended by IAU 2000 Resolution B1.8 (IAU Transactions 2000), based on the Celestial Intermediate Origin (CIO) (i.e. the new name recommended by the IAU NFA Working Group (2006) for the Celestial Ephemeris Origin, also called "non-rotating origin" (Guinot 1979)). As we are looking for the solution relative to the motion in space of the CIP and we are considering the axially symmetric case, the ITRS motion of the CIP can be omitted, which reduces the relationship to:

$$\begin{pmatrix} \omega_1 \\ \omega_2 \\ \omega_3 \end{pmatrix} = \begin{pmatrix} 0 \\ 0 \\ \dot{\Theta} \end{pmatrix} + \frac{\mathbf{R}}{Z} \begin{pmatrix} -\dot{Y} - X\,\dot{s} \\ \dot{X} - Y\,\dot{s} \\ Z\,\dot{s} \end{pmatrix}. \tag{1}$$

where $\mathbf{R} = R_3(\Theta)$, $Z = \sqrt{1-(X^2+Y^2)}$ and $\Theta = \theta - s$, with $\dot{\theta} = \Omega$ (the mean angular velocity of the Earth) and s is the distance along the CIP equator between the point Σ and the CIO (see Fig. 1). We denote CIRS' the intermediate system defined by the CIP and the point Σ.

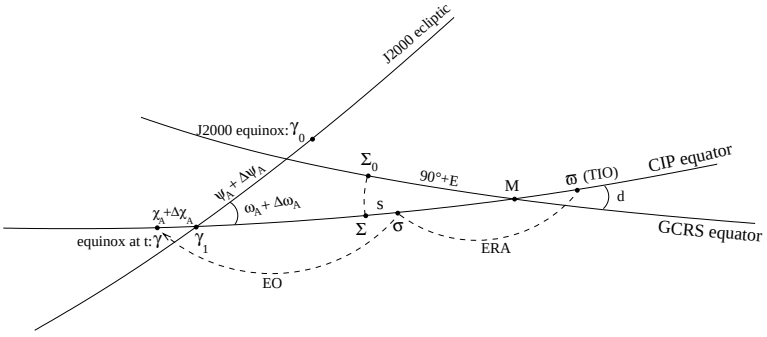

Figure 1: Relationship between various points: Σ_0 is the GCRS origin, M is the ascending node of the CIP equator on the GCRS equator, Σ is the point on the CIP equator such that $\widehat{\Sigma M}$=$\widehat{\Sigma_0 M}$, γ_0 is the J2000 equinox, γ is the equinox of date and γ_1 is the ascending node of the J2000 ecliptic on the CIP equator. ERA=$\widehat{\sigma\varpi}$ is the Earth rotation angle (θ), EO=$\widehat{\sigma\gamma}$ is the equation of the origins and $\widehat{\gamma_1\gamma}$ is the precession of the ecliptic along the CIP equator.

For an axially symmetric rigid Earth, an appropriate form for practical integration is:

$$\begin{aligned} -\ddot{Y} + (C/A)\,\Omega\,\dot{X} &= (L/A) + F'' \\ \ddot{X} + (C/A)\,\Omega\,\dot{Y} &= (M/A) + G'', \end{aligned} \tag{2}$$

where only the prominent terms have been retained in the first member, the other terms (F'' and G''), which are of the second order in the X and Y quantities, having been moved to the second member; L and M are the CIRS' components of the external torque.

3. METHOD FOR SOLVING THE EQUATIONS

Equations (2) can be integrated in a semi-analytical way by successive approximations. We have used the method of "variations of parameters" described in Woolard (1953) and Bretagnon et al. (1997). This consists in using the solution for the reduced system and get a particular solution of the general equations as an expression with the same form, but with the constants of integration transformed into time-dependent quantities.

The solutions of the reduced equations have the following form:

$$\begin{aligned} \dot{X} &= -K'_c \sin\sigma t + K'_s \cos\sigma t \\ \dot{Y} &= K'_s \sin\sigma t + K'_c \cos\sigma t \end{aligned} \tag{3}$$

where $\sigma = (C/A)\,\Omega$ is the Euler frequency in the CIRS' and K'_s and K'_c are the constants of integration of this free motion.

In order that the particular solution for $X\,, Y$ verifies Eqs (2), the quantities $K'_s(t)$ and $K'_c(t)$ should be derived from the following equations:

$$\begin{aligned} \dot{K'_s} &= -\frac{L}{A}\sin\sigma t + \frac{M}{A}\cos\sigma t - F''\sin\sigma t + G''\cos\sigma t \\ \dot{K'_c} &= -\frac{L}{A}\cos\sigma t - \frac{M}{A}\sin\sigma t - F''\cos\sigma t - G''\sin\sigma t\,. \end{aligned} \tag{4}$$

The solution for X and Y can thus been obtained by a quadrature of Eqs. (3) with substituting the expressions for $K'_s(t)$ and $K'_c(t)$ derived from Eqs. (4). The final solution results from an iterative process that ensures that the solution converges to the required level of accuracy.

4. TEST OF THE INTEGRATION METHOD

We have performed a number of semi-analytical simulations for testing the approach and the integration process described in the previous sections. These simulations have consisted in computing the expression of the (pseudo-) IAU 2000 torque using (i) the rotational equations for the Euler angles (Woolard 1953) and (ii) the IAU 2000A precession-nutation series for the Euler angles. The (pseudo-) torque components obtained in this way are in the intermediate system linked to the CIP and the point γ_1 (see Fig. 1). They have been transformed into components in the CIRS'. The rotational equations (2) based on those (pseudo-) torque components have then been integrated to get series for X and Y.

These simulations have shown that the integration method is efficient in providing a solution for $X\,, Y$ that converges at a 0.01 μas level after only a very few iterations. Comparison of this solution with respect to the current IAU 2000 expressions for $X\,, Y$ have shown that its accuracy is compliant with that of the current IAU 2000A precession-nutation model. This validates (i) the rotational equations in terms of $X\,, Y$ established in this work (c.f. Sect. 2) and (ii) the integration process described in Sect. 3.

5. EXTENSION OF THE APPROACH TO A DEFORMABLE EARTH

We have extended this approach to a model of a deformable Earth compliant with the P03 precession solution of Capitaine et al. (2003b) that includes the contribution of the secular variation of the dynamical ellipticity of the Earth. We have shown that the solutions for a deformable Earth can be obtained in a form similar to that for a rigid Earth with using dynamical equations expressed as functions of $X\,, Y$ that include the additional contributions from the tidal deformation of the Earth, the J_2 rate variation and the rotational deformation.

6. SOLUTION FOR A RIGID EARTH

In a further step, we have computed the X , Y solutions of the dynamical equations of Earth rotation for an axially symmetric rigid Earth model corresponding to the solutions VSOP87 for the orbital motions of the Earth and planets and ELP2000 for the Moon.

We have first developed the semi-analytical expressions for the components of the external torque in the CIRS', based on the solutions VSOP87 and ELP2000, and we have then integrated the dynamical equations in terms of X , Y (i.e. Eqs. (2)) using the method described in Sect. 3.

REFERENCES

Bretagnon, P. and Francou, G., 1988, "Planetary theories in rectangular and spherical variables - VSOP 87 solutions," A&A 202, pp. 309–315.

Bretagnon, P., Rocher, P., and Simon, J.-L., 1997, "Theory of the rotation of the rigid Earth," A&A 319, pp. 305–317.

Capitaine, N., Chapront, J., Lambert, S., Wallace, P.T., 2003a, "Expressions for the Celestial Intermediate Pole and Celestial Ephemeris Origin consistent with the IAU 2000A precession-nutation model," A&A 400, pp. 1145–1154.

Capitaine, N., Wallace, P. T., Chapront, J., 2003b, "Expressions for IAU 2000 precession quantities," A&A 412, pp. 567–586.

Capitaine, N., Folgueira, M., Souchay, J., 2006a, "Earth rotation based on the celestial coordinates of the celestial intermediate pole, I. The dynamical equations,", A&A 445, pp. 347–360.

Capitaine, N., Folgueira, M., Souchay, J., 2006b, 'Earth rotation based on the celestial coordinates of the celestial intermediate pole, II. The solutions for a rigid Earth", to be submitted to A&A.

Chapront, J., 2003, Notice, Paris Observatory (January 2003)

Chapront-Touzé M. and Chapront J., 1998, "The lunar ephemeris ELP 2000," A&A 124, pp. 50–62.

Folgueira, M., Capitaine, N. and Souchay, J., 2005, in Proc. Journées 2004 "Systèmes de Référence spatio-temporels", N. Capitaine (ed.), Observatoire de Paris, pp. 136-137.

Guinot, B., 1979, in *Time and the Earth's Rotation*, D.D. McCarthy, J.D. Pilkington (eds), D. Reidel Publishing Company, 7.

Report of the IAU Division 1 Working Group on "Nomenclature for Fundamental Astronomy"), IAU Transactions XXVIA, 2006, or http://syrte.obspm.fr/iauWGnfa/Explanatory.html.

IAU Transactions (2000), Vol. XXIVB; in the Proceedings of the Twenty-Fourth General Assembly; Manchester, ed. H. Rickman, Astronomical Society of the Pacific, Provo, USA, 2001, 34.

IERS Conventions (2003), IERS Technical Note 32, D.D. McCarthy and G. Petit (eds), Frankfurt am Main: Verlag des Bundesamts für Kartographie und Geodäsie, 2004.

Mathews, P.M., Herring, T.A., Buffett B.A., 2002, "Modeling of nutation and precession: New nutation series for nonrigid Earth and insights into the Earth's interior,"'", J. Geophys. Res. 107, B4, 10.1029/2001JB000390.

Woolard, E.W., 1953, in Astronomical Papers prepared for the use of the American Ephemeris and Nautical Almanac, XV, Part I, 1.

DIURNAL POLAR MOTION FROM VLBI OBSERVATIONS

M.V. KUDRYASHOVA, S.D. PETROV
Astronomical Institute of St. Petersburg State University
Universitetskii pr., 28, Petrodvorets, St. Petersburg, Russia
e-mail: kudryashova@mercury.astro.spbu.ru

ABSTRACT. A new 15-years long time series of the Earth Rotation Parameters (polar motion and $UT1 - UTC$) has been derived from the VLBI observations by the least square collocation method. Henceforward we focused our attention on the polar motion time series. It has a non-uniform time distribution and covers the time span from 1989 till 2004. The method of complex demodulation has been applied in order to extract from the series a signal in the diurnal frequency band. Amplitudes of polar motion variations at main tidal frequencies have been estimated and then compared with the model of atmospheric tidal variations.

1. INTRODUCTION

The Very Long Baseline Interferometry (VLBI) observations are used routinely to estimate the pole coordinates x and y as averages per 24-hour long observing sessions. Meanwhile, there is an interest to polar motion with sub-daily resolution. A typical VLBI session provides a few hundreds of observables per day. Thus, it is possible, in principle, to estimate polar motion with sub-diurnal resolution. The problem is that the VLBI observations are carried out normally only few times per week at most. In order to estimate polar motion time series with sub-diurnal resolution, special continuous VLBI campaigns have been organized, but they were, in turn, restricted in duration to the time intervals of two weeks.

The aim of this work is to obtain a few years long time series of diurnal polar motion by use of all available VLBI observations. This goal is achieved by applying the complex demodulation technique which allows to convert the high-frequency components of a signal into the low-frequency band.

2. VLBI DATA PREPROCESSING

In our analysis we used observations from 24-hour geodetic VLBI sessions from January 1989 till April 2004. Whole amount of the processed experiments was 987. The time span covered by these data was longer than 15 years.

In order to obtain a time series of Earth Rotation Parameters (ERP) with sub-diurnal resolution we applied the least-square collocation method (LSQM) as it is realized in OCCAM 6.0 software. In frame of this method, a model with 3 types of parameters is used (see Titov & Schuh, 2000):

$$Au + Bv + Cw + \xi = l, \tag{1}$$

where l is the vector of differences between the observed and calculated values (O-C); ξ is the vector of measurement errors; A, B, C are the matrices of partial derivatives; u, v, w are the vectors of parameters under estimation. The first group of parameters (vector u) includes only corrections to radiosourses positions. They were considered as global parameters, i.e. as having the same values for all sessions. The second group of parameters (vector v) was considered as 'daily', i.e. it was supposed that these parameters were constant during each 24-hours session. Among the parameters of this group were corrections to stations coordinates, offsets of the Celestial Ephemeris Pole as well as the statistical expectations of stochastic parameters. We treated the Earth Rotation Parameters (ERP – x, y coordinates of the pole, $UT1-UTC$), clock rates and offsets, zenith delays and tropospheric gradients as stochastic processes (vector w).

The LSQ method allows to estimate vectors u, v and w in two stages. At first step an adjustment of global parameters u is made. At the second step, the vectors of 'daily' (v) and stochastic parameters (w) are estimated.

In our study an improvement of the existing Celestial Reference Frame (CRF) was not of interest, therefore we just fixed the the CRF to a priory catalogue ICRF-Ext.1. Thus we assumed that we know radiosourses coordinates quite exactly, i.e. $u = 0$. In this case model (1) with three groups of parameters could be reduced to the model with two groups of them (v, w). Estimations of these parameters for each VLBI experiment are given by

$$\hat{v} = (B^T {Q_0}^{-1} B)^{-1} B {Q_0}^{-1} l, \tag{2}$$

$$\hat{w} = Q_w C^T (C Q_w C^T + Q_\xi)^{-1} (l - B\hat{v}), \tag{3}$$

where $\hat{v}, \hat{w}$ are estimations of v, w vectors; Q_ξ, Q_w – the covariance matrixes of observational dispersions and stochastic parameters, respectively. We denoted as Q_0 the following matrix

$$Q_0 = C Q_w C^T + Q_\xi.$$

For more details concerning this procedure see Titov (2000), Titov & Schuh (2000).

As a result of applying the LSQM we derive unevenly sampled time series of the ERP. Note that in this series the model of the diurnal and sub-diurnal variations in polar motion and $UT1$ due to oceanic tides has already been taken into account. The model contains 71 diurnal and sub-diurnal terms and was calculated by R. Eanes based on the paper by Ray et al. (1994). The time resolution of the output ERP series is three to ten minutes during one session and two to seven days-long gaps between the sessions. As a result, it is needed to apply special methods of analysis.

3. EOP ANALYSIS

Hereafter we will consider series of polar motion only. In order to extract signals in the diurnal frequency band we used the method of complex demodulation. This method has been described in details for instance in Brzezinski et al. (2002). Here we only outline the main ideas of the method. After applying the demodulation transformation, frequencies ω are transformed into $\omega' = \omega - \sigma_0$, where σ_0 is the so-called demodulation frequency which could be chosen arbitrarily. In the time domain the initial time series of polar motion $f = x - iy$ will be changed as $f' = -fe^{-i\sigma_0 t}$. But in the frequency domain, due to the Fourier transform property, such transformation just shifts spectrum of the initial series by the value σ_0 such a way that $\omega = \sigma_0$ becomes 0.

In this work we used $\sigma_0 = \Omega$ in order to extract prograde diurnal motion, where Ω is a diurnal sidereal frequency equal to 1 cycle per sidereal day.

The advantage of the transformation is that variations with frequencies from the vicinity of σ_0 become long-periodical, i.e. slowly varying with time. All other variations are removed by a low-pass filter which in addition significantly reduce an amount of values in the time series under estimation.

Here we applied different methods of smoothing in order to check how the estimated parameters depend on the chosen method. The following methods have been applied: averaging by session (as the complex demodulation have already been applied such procedure does not change spectral constitution of the analyzed series in the prograde diurnal frequency band), the Gaussian filter (with the following parameters: full width at the half of maximum equal to 20 days and output time step of seven days) and the moving average.

4. DISCUSSION AND CONCLUSIONS

Combination of complex demodulation and smoothing allows to obtain an evenly sampled time series which contains a signal of sub-daily frequency band. Applying of a such technique gives us new possibilities in sub-daily variation study because it permit to use highly developed methods of analysis of equally spaced time series.

A least square fit of most powerful tidal components as well as a constant term has been made. In diurnal frequency band these components are $K1, P1$ and $S1$ with the corresponding frequencies after demodulation $\omega'_1 = 0$ (constant), $\omega'_2 = 1/182.61$ cpsd, $\omega'_3 = 1/365.20$ cpsd. To obtain residual variations at these frequencies we applied the following model:

$$x = \sum_{i=1}^{3} A_i sin(2\pi\omega'_i t) + B_i cos(2\pi\omega'_i t),$$

$$y = \sum_{i=1}^{3} A'_i sin(2\pi\omega'_i t) + B'_i cos(2\pi\omega'_i t).$$

Estimated amplitudes A_i, B_i and A'_i, B'_i obtained after applying of different smoothing methods are summarized in Table 1 and Table 2, correspondingly.

	K1	P1		S1	
	B_1	A_2	B_2	A_3	B_3
Gaussian filter	−3.2	−0.1	0.2	0.3	−0.7
averaging by session	−3.4	0.1	0.6	0.6	−1.2
moving average	−4.4	0.9	0.6	0.8	−1.6
demodulated series	−4.4	0.6	0.9	1.1	−1.4
Atmosphere (Petrov, 1998)				0.5	−0.8

Table 1: Amplitudes of main prograde diurnal harmonics in x-component of polar motion (μas).

These tables also contain amplitudes of the tidal components derived from the demodulated series without applying of any smoothing. Amplitude of the $S1$ term estimated from the atmospheric data (Petrov, 1998) is presented in the last row of each table. One can see that the S1 amplitude derived from VLBI observations is comparable to that from the atmospheric contribution. In order to compute this term we used the longest AAM series (NCEP/NCAR reanalysis)

	K1	P1		S1	
	B'_1	A'_2	B'_2	A'_3	B'_3
Gaussian filter	2.6	−0.3	−1.3	−1.3	1.0
averaging by session	3.0	−0.1	−1.3	−1.4	0.7
moving average	3.4	−0.9	−2.1	−2.4	0.9
demodulated series	3.4	−0.1	−2.2	−2.6	0.5
Atmosphere (Petrov, 1998)				−1.8	0.7

Table 2: Amplitudes of main prograde diurnal harmonics in y-component of polar motion (μas).

available (Salstein & Rosen, 1997), though we have to admit that different AAM series give different estimations of S1 amplitudes. Moreover, the atmospheric contribution has to be combined with the non-tidal oceanic influence, see Brzezinski et al. (2004) for detailed discussion.

A most important conclusion of this work is that it is possible to extract the high frequency components of ERP extending over several years, from the standard VLBI observations, without referring to the continuous campaigns. Our estimation of the prograde diurnal components of polar motion and comparison with the atmospheric excitation indicates that the method proposed here yields meaningful results.

Acknowledgements. This work was carried out with financial support of the grant 37847 of Ministry of Education and Science of Russian Federation.

REFERENCES

Brzezinski A., Bizouard Ch. and Petrov S.D., 2002, 'Influence of the atmosphere on Earth rotation: what new can be learned from the recent atmospheric angular momentum estimates?', Surveys in Geophisics, 23, pp. 33-69.

Brzezinski A., Ponte R.M. and Ali A.H., 2004, 'Nontidal oceanic exitation of nutation and diurnal/semidiurnal polar motion revisited', J. Geophys. Res. , 109, doi: 10.1029/2004JB003054.

Petrov S.D., 1998, 'Modeling geophysical excitation of Earth rotation: stochastic and nonlinear approaches', PhD thesis, Space Research Centre PAS, Warsaw, Poland.

Ray R.D., Steinberg D.J., Chao B.F. and Cartwright D.E.,1994, 'Diurnal and Semidiurnal Variations in the Earth's Rotation Rate Induced by Ocean Tides', Science, 264, pp. 830-832.

Salstein D.A. and Rosen R.D., 1997, 'Global momentum and energy signals from reanalysis systems', Preprints, 7th Conf. on Climate Variations, American Meteorological Society, Boston, MA, pp. 344-348.

Titov O., 2000, 'Estimation of subdiurnal tidal terms in UT1-UTC from VLBI data analysis', IERS Technical Note No 28, pp. 11–14.

Titov O. and Schuh H., 2000, 'Short periods in Earth rotation seen in VLBI data analysis by least-squares collocation methods', IERS Technical Note No 28, pp. 33–41.

PHASE VARIATIONS OF OSCILLATIONS IN THE EARTH ORIENTATION PARAMETERS DETECTED BY DIFFERENT TECHNIQUES

W. KOSEK[1], A. RZESZÓTKO[1] and W. POPIŃSKI[2]
[1]Space Research Centre, Polish Academy of Sciences, Warsaw, Poland
[2]Central Statistical Office, Warsaw, Poland
e-mail: kosek@cbk.waw.pl, alicja@cbk.waw.pl, w.popinski@stat.gov.pl

ABSTRACT. The phases of oscillations in the Earth Orientation Parameters (EOP) vary in time. The wavelet transform techniques as well as other methods comprising: complex demodulation (CD), Hilbert transform (HT), Fourier transform band pass and low pass filters (FTBPF and FTLPF) and the least-squares (LS) were applied to compute the phases of the most energetic oscillations in the EOP data. The forced annual oscillations in polar motion and length of day (LOD) are related to the seasonal thermal cycle therefore their phases fluctuate around their well-defined expected values. The expected value of the phase of the Chandler wobble (CW) and of the Free Core Nutation (FCN) is not well-defined, since these oscillations are free wobble oscillations. There is a good agreement between the phases computed by different techniques in the most energetic oscillations of the EOP data.

1. COMPUTATION TECHNIQUES APPLIED

The following computation techniques were applied to determine the instantaneous phases in the EOP time series: 1) Morlet wavelet transform (MWT) (Chui 1992), 2) Harmonic wavelet transform (HWT) (Newland 1998), 3) combination of the FTBPF (Kosek 1995) and CD (FTBPF +CD), 4) combination of the FTBPF and HT (FTBPF+HT), 5) combination of CD and the FTLPF (CD+FTLPF), 6) least-squares (LS) method. All these computation techniques can be applied to complex-valued time series except for the FTBPF+HT technique.

In the MWT and HWT techniques the formula for the transform coefficients, computed as the convolution of the complex-valued signal $x(t)$ and the specific wavelet analyzing function $w(t)$, can be expressed in the frequency domain as follows (Chui 1992, Newland 1998):

$$\widehat{X}(b,T) = \frac{1}{2\pi}|T|^{\frac{1}{2}} \int_{-\infty}^{+\infty} \check{x}(\omega)\overline{\check{w}}(\omega,T)e^{ib\omega}d\omega, \tag{1}$$

where b is the translation (or shift) parameter and $T \neq 0$ is the dilation (or period) parameter, $\check{x}(\omega)$ is the continuous Fourier transform (CFT) of the signal $x(t)$ and $\check{w}(\omega,T)$ is the CFT of the wavelet function applied. In the MWT technique the CFT of the complex-valued Morlet wavelet function (Chui 1992, Schmitz-Hübsch and Schuh 1999)

$$\check{w}(\omega,T) = \sigma[e^{-(\omega T-2\pi)^2\sigma^2/2} - e^{-(\omega T-2\pi)^2\sigma^2/4} \cdot e^{-\pi^2\sigma^2}] \tag{2}$$

is applied, where σ is the parameter, which increase improves the frequency resolution. In the HWT technique the CFT of the harmonic wavelet function

$$\check{w}(\omega,T)=\begin{cases} \mid T \mid^{-\frac{1}{2}} e^{-(1/T-\omega)^2/(2s^2)} & if \quad |1/T-\omega|\le\lambda \\ 0 & otherwise \end{cases} \tag{3}$$

localized in the frequency domain near some central frequency $1/T$ is applied, which is of the boxcar type tapered by the gaussian window for better frequency resolution. The frequency resolution is controlled by the window half-width λ and the smoothing parameter s.

Interpretation of the wavelet phase spectrum

$$\widehat{\phi}(b,T)=atan[\Im(\widehat{X}(b,T))/\Re(\widehat{X}(b,T))], \tag{4}$$

where $\Re$ and $\Im$ denote the real and imaginary part of a complex number, respectively, is rather difficult. However, the phase variations can be computed from it for the particular period T_0 by the formula: $\widehat{\varphi}(b,T_0)=\widehat{\phi}(b,T_0)-2\pi t/T_0$.

To determine the instantaneous phases of an oscillation with central frequency ω_0 in time series $x(t)$ using FTBPF+CD, FTBPF+HT and CD+FTLPF techniques it is necessary to determine first the complex-valued function $z(t,\omega_0)$, from which this phase can be computed as:

$$\widehat{\varphi}(t,\omega_0)=atan[\Im(z(t,\omega_0))/\Re(z(t,\omega_0))]. \tag{5}$$

To compute the function $z(t,\omega_0)$ by the FTBPF+CD technique one must first determine the oscillation with central frequency ω_0 using one- or two-dimensional FTBPF:

$$x(t,\omega_0)=FT^{-1}[FT(x(t))\cdot A(\omega,\omega_0)], \tag{6}$$

where

$$A(\omega,\omega_0)=\begin{cases} 1-(\omega-\omega_0)^2/\lambda^2 & if \quad |\omega-\omega_0|\le\lambda \\ 0 & otherwise \end{cases} \tag{7}$$

is the parabolic transmittance function in which λ is the window half-width which controls the frequency resolution. Next, to remove the linear trend from the instantaneous phases, the oscillation $x(t,\omega_0)$ is multiplied by the monochromatic complex harmonic with the frequency $-\omega_0$: $z(t,\omega_0)=x(t,\omega_0)e^{-i\omega_0 t}$.

In order to compute the function $z(t,\omega_0)$ by the FTBPF+HT technique the oscillation with central frequency ω_0 is first filtered by one-dimensional FTBPF using eqs. (6) and (7). Next, we create the complex-valued series which consists of the oscillation and its HT in the real and imaginary parts, respectively, and from the properties of the HT it follows that it can be also expressed by the formula which involves the Fourier transform (Poularikas 1996):

$$z(t,\omega_0)=x(t,\omega_0)+i\cdot H[x(t,\omega_0)]=FT^{-1}[FT(x(t))\cdot A(\omega,\omega_0)(sign(\omega)+1)]. \tag{8}$$

In the CD+FTLPF technique the time series $x(t)$ is first multiplied (demodulated) by the complex-valued harmonic with the frequency $-\omega_0$ (Hasan 1983): $x(t,\omega_0)=x(t)\cdot e^{-i\omega_0 t}$. Next, the transformed signal $x(t,\omega_0)$ is filtered by two-dimensional FTLPF:

$$z(t,\omega_0)=FT^{-1}[FT(x(t,\omega_0))\cdot A(\omega)], \tag{9}$$

where $A(\omega)=A(\omega,0)$ is the parabolic transmittance function defined by eq. (7).

2. DATA AND RESULTS

The following EOP series were used in the analysis (IERS 2005): 1) x, y pole coordinates data and LOD data of IERS EOPC04 in 1962.0-2005.6, 2) x, y pole coordinates data of IERS EOPC01 in 1846.0-2002.0, 3) dX, dY IAU2000A nutation-precession corrections in 1979.0 - 2005.6. The x, y pole coordinates data from the EOPC01 and EOPC04 were merged in 1962 to create one data file for the analysis. From the LOD data the IERS Conventions tide model (McCarthy and Petit 2004) has been removed to get the LODR data.

Next, the phase variations of the most energetic oscillations in the EOP were computed by different techniques and to enable their comparison their mean values were subtracted. Figure 1 shows the phase variations of the Chandler and annual oscillations computed in x pole coordinate data by the MWT, CD+FTLPF and FTBPF+CD techniques. Figure 2 shows the phase variations of the semi-annual oscillations computed in complex-valued $x - iy$ pole coordinate data by the MWT, HWT and FTBPF+CD techniques. The boundary effects of the HWT technique cause irregular jumps of the computed phase at the ends of data time span. Figure 3 shows the phase variations of the annual oscillation computed in LODR data by the MWT, CD+FTLPF and FTBPF+HT techniques. Figure 4 shows the phase variations of the FCN computed in complex-valued $dX + idY$ IAU2000A nutation-precession corrections by the LS, MWT and FTBPF+CD techniques.

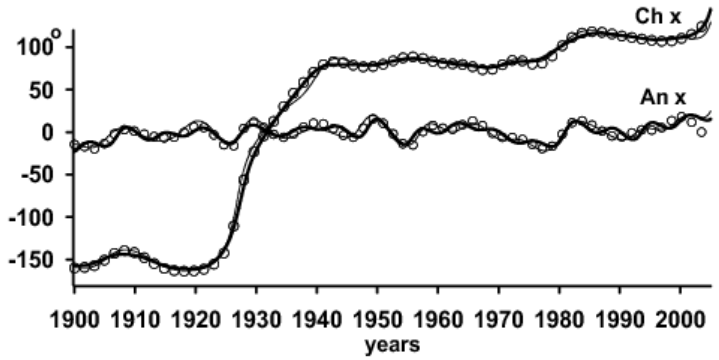

Figure 1: Phase variations of the Chandler and annual oscillations computed in x pole coordinate data by the MWT ($\sigma = 2$) (thick line), CD+FTLPF ($\lambda = 0.0004$) (circles) and FTBPF+CD ($\lambda = 0.0004$)(thin line) techniques.

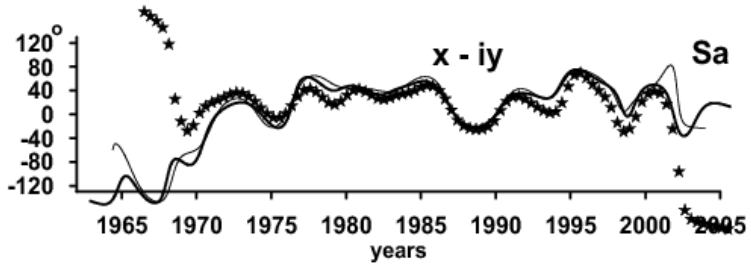

Figure 2: Phase variations of the semi-annual oscillation computed in complex-valued $x - iy$ pole coordinate data by the MWT ($\sigma = 1$)(thick line), HWT ($\lambda = 0.002, s = 0.003$) (stars) and FTBPF+CD ($\lambda = 0.001$)(thin line) techniques.

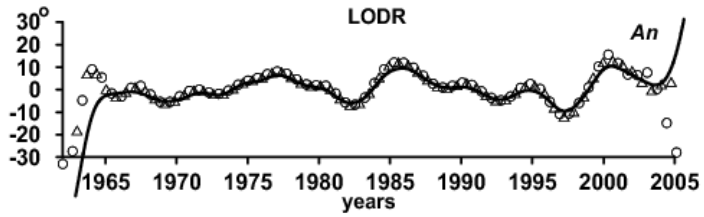

Figure 3: Phase variations of the annual oscillation computed in LODR data by the MWT ($\sigma = 1$)(thick line), CD+FTLPF ($\lambda = 0.001$) (cirles) and FTBPF+HT ($\lambda = 0.001$) (triangles) techniques.

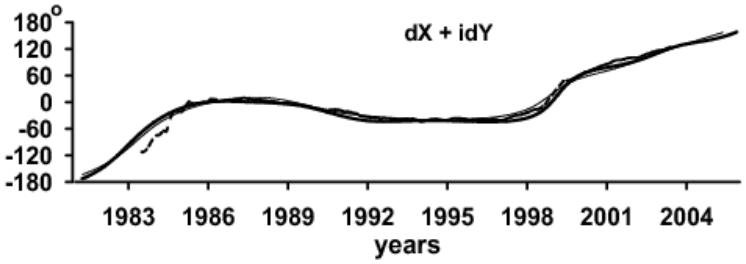

Figure 4: Phase variations of the FCN computed in complex-valued $dX + idY$ IAU2000A nutation-precession corrections by the LS in 5 year time intervals (dashed line), MWT ($\sigma = 1$)(thick line) and FTBPF+CD ($\lambda = 0.0005$) (thin line) techniques.

3. DISSCUSSION

The phase variations of the most energetic oscillations in the EOP are very important for studying the Chandler wobble excitation (Kosek 2005) or their influence on the EOP prediction errors (Kosek et al. 2002). The phases of the most energetic oscillations in the EOP computed by the presented techniques are in a good agreement, except at the ends of data time span where boundary effects occur, especially for the HWT technique.

Acknowledgments. This paper was supported by the Polish Ministry of Education and Science under the project No 4 T12E 039 29.

REFERENCES

Chui C.K., 1992, An Introduction to Wavelets, Wavelet Analysis and its Application. Vol. 1, Academic Press, Boston-San Diego.

Hasan T., 1983, Complex Demodulation: Some Theory and Applications, In Brillinger D.R. and Krishnaiah P.R. (eds), Handbook of Statistics - Vol. 3, Elsevier, Amsterdam, 125-156.

IERS, 2005, The Earth Orientation Parameters, http://hpiers.obspm.fr/eop-pc/.

Kosek W., 1995, *Artificial Satellites*, 30, 27-43.

Kosek W., McCarthy D.D., Luzum B.J., 2002, *Proc. Journees 2001*, 85-90.

Kosek W., 2005, *Proc. ECGS Chandler Workshop* Vol. 24., H.P. Plag et al.(eds), 121-126.

McCarthy D.D., Petit G. (eds), 2004, IERS Conventions (2003), *IERS Technical Note* No. 32.

Newland D.E. 1998, in: Signal Analysis and Prediction, A. Prohazka et al. (eds), Boston.

Poularikas A.D. (ed.), 1996, The Transforms and Applications Handbook, CRC Press - IEEE Press, Boca Raton 1996.

Schmitz-Hübsch H., Schuh H., 1999, in: F. Krumm and V.S. Schwarze (eds), Quo vadis Geodesia?, 421-431.

INFLUENCE OF THE UNSTABLE RADIOSOURCES ON THE CELESTIAL POLE OFFSET ESTIMATIONS

J.R. SOKOLOVA
Institute of Applied Astronomy
nab. Kutuzova, 10, St. Petersburg 191187
e-mail: jrs@ipa.nw.ru

ABSTRACT. Some of the CRF radio sources are known to have apparent proper motions at the sub-milliarcsecond level, which can lead to changes in estimates of precession or long-period nutation coefficients. The main goal of this work is to study the influence of unstable radiosources on the nutation offset estimates. Two nutation time series have been calculated from two global solutions in different modes.

1. INTRODUCTION

Since some of the CRF's radio sources are known to have apparent proper motions at the sub-milliarcsecond level, it can leads to changes in estimates of precession or long-period nutation coefficients (Feissel-Vernier et al., 2004). There are two possible ways to reduce the effect of source instability. The first way is to replace some of the ICRF defining sources by more stable ones for constraining the axes of ICRS. The second way is to model apparent proper motions for some unstable radiosources. The first way has been considered in this paper.

2. DATA ANALYSIS

Two solutions have been obtained by least squares collocation method using OCCAM 6.0 software (Titov et al., 2004). The first solution refers to the 207 'defining' radio sources (Fey et al., 2004) used for constraining the CRF axes. The second solution uses 199 'stable' radio sources proposed by Martine-Feissell (2003) for the same purpose. Improved positions of several hundred radio sources were listed in individual catalogue for each of these two solutions. After then, two nutation time series have been calculated with OCCAM/GROSS software using the source positions from the two catalogues.

Table 1: Series statistic (Unit of wrms: microarcsec)

-	Num. of points (after 1990 year)	Wrms dX	Wrms dY
Series 1	2289	151	158
Series 2	2289	144	156
Series 1 - Series 2	2197	30	32

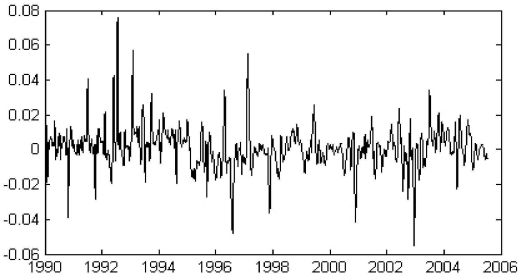

Figure 1: Smoothed differences between two offset nutation series (dX 1 - dX 2)(Unit: mas).

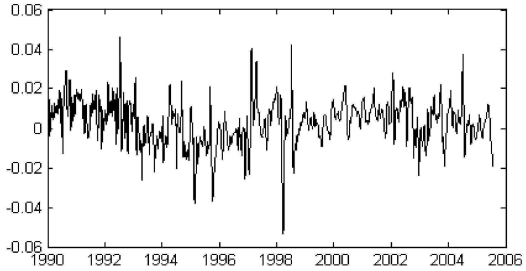

Figure 2: Smoothed differences between two offset nutation series (dY 1 - dY 2) (Unit: mas).

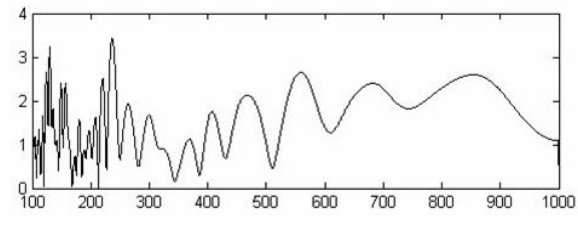

Figure 3: dX, Spectra of raw data, Ferraz - Mello method, (Unit : Solar days vs. microarcsec)(Unit: mas).

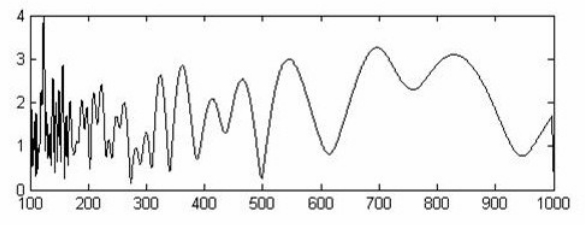

Figure 4: dY, Spectra of raw data, Ferraz - Mello method, (Unit : Solar days vs. microarcsec)(Unit: mas).

3. CONCLUSIONS

1. The differences in nutation offset estimations between two series are below 10 mas, which is below noise level (fig.1,2).
2. Changes in the period of the main harmonics are insignificant, when different source lists were used for constraining the CRF Axes.
3. Periodic signals in differences between two nutation time series, were not revealed (fig 3,4).

The first way to reduce effect of source instability, which has been considered in this paper did not show significant results, therefore the second way need to be considered.

REFERENCES

Feissel-Vernier M., et al., IVS 2004 General Meeting Proc., pp. 22-31
Titov O., et al., IVS 2004 General Meeting Proc., pp. 257-271
Fey A.L. et al., 2004, AJ. 127, 3587-3608
Feissel-Vernier, M., 2003, AA 403, 105-110

NUTATIONS AND PRECESSION OF ELASTIC EARTH IN ANGLE-ACTION VARIABLES

J.M. FERRANDIZ [1], Yu.V. BARKIN [1,2]
[1] University of Alicante, Spain
[2] Sternberg Astronomical Institute, Moscow
e-mail: jm.ferrandiz@ua.es

1. INTRODUCTION

Since the classical works of Laplace, Tisserand or Pontecoulant till the modern solutions of the Earth rotation (Kinoshita, 1977), most of the theories of the rotation of solar system bodies assume the simplest unperturbed motion, a steady rotation around the axis of largest inertia so that the angle θ between the angular momentum and the polar axis of inertia vanishes in the zeroth order approximation. Such an assumption is accurate enough in the Earth case, which justifies the usual approaches to the Earth rotation, although it is worth to remark that allowing a non-zero value of the angle θ can bring into light new dynamical effects. As an example, we can point out the paper (Barkin, 2000) in which an initial value of the angle $\theta = 0''175$ has been used to investigate long-periodic variations in the Earth pole motion.

However, the motion of some celestial bodies does not satisfy that condition. Namely, the observed orientation of the Venus pole reveals a large value of the free obliquity amplitude $\theta = 2°1$ compared to the nominal forced amplitude of $0.5°$ (Yoder, 1995). The motion of irregular asteroids or spacecrafts requires the Euler-Poinsot representation even in the zeroth approximation. Therefore, to study the later problems or enhance the available solutions to the Earth, Venus or Mars rotation, it becomes necessary or useful the development of analytical perturbation theories relying on the unperturbed Euler-Poinsot motion of a triaxial rigid body, with arbitrary tensor of inertia and initial conditions. Convenient expressions for such a solution can be found in (Kinoshita, 1977; Barkin, 1992, 1998). A generalization to the case of a body weakly deformed by its own rotation was presented in the paper (Barkin et al., 1996) and we will refer to it as Euler-Chandler motion. A perturbation solution using the angle-action variables associated to the Chandler-Euler problem was developed in (Barkin, 1998). In this presentation we report on the main effects on the free Earth rotation and the solution of the forced Earth rotation based on the said Chandler-Euler unperturbed motion.

2. EULER-CHANDLER UNPERTURBED MOTION

The unperturbed rotation of a celestial body weakly deformed by its own rotation can be reduced to the classical Euler-Poinsot motion of an ideal rigid body with suitable, different moments of inertia, referred to as Euler-Chandler motion since it gathers the Chandler polar motion. The complete solution of the problem (Andoyer's variables, components of angular velocity in the body and space frames, etc.) is expressed in terms of elliptical and Θ-functions, and Fourier series in the angle-action variables. We remark the following characteristics of the

solution: 1. The known difference between Euler and Chandler periods is recovered in it (304.4 and 433.2 days). 2. A new phenomenon is the appearance of a difference of eccentricities of Euler and Chandler polar trajectories (the corresponding geometrical eccentricities are 0.00328 and 0.00462). 3. Non-uniformity of Chandler motion. 4. Small variation of the Earth angular velocity with half a Chandler period. 5. Changes of the projection of the Earth's angular momentum on its polar axis. 6. Extreme values of the angles between relevant pairs of vectors are derived: angular momentum vector and polar axis of inertia of the Earth, angular momentum and angular velocity. 9. Variations of the moment of inertia of the Earth about rotation axis.

3. ANALYTICAL SOLUTION BY PERTURBATION METHODS

The theory of the perturbed rotation of a deformable Earth is approached using angle-action variables. The expression of the force function requires to perform real or complex expansions of quadratic functions of the direction cosines, that have been carried out in detail for the second order harmonic of the Earth-Moon (and Earth-Sun) interactions. First order perturbations caused by the lunisolar gravitational attraction are derived as trigonometric series whose arguments are linear combinations of the angles and the arguments of the lunar orbital motion. Their coefficients are expressed in terms of elliptical integrals and elliptical and hyperbolic functions of the initial values of the action variables and some elastic parameter k. The approach is useful to get more insight into the effects of the mantle elasticity on the Earth rotation and can be specialized to recover the nutation series derived in elastic Andoyer variables (Getino and Ferrandiz, 1991). The role of elasticity on polar motion, nutations and precession is discussed, focusing on the following: 1. Contribution of the gravitational attraction of Moon and Sun to the mean angular velocity and to Chandler period. 2. Influence of elasticity on the precession constant value. 3. Contribution of the mantle elasticity to the amplitudes of first order perturbations in angle-action variables. All the results are analytical and applicable to the study of the rotation of other solar system bodies (Venus, single or double asteroids, satellites with irregular shape, comets, etc.).

Acknowledgements. Barkin's work was supported by Spanish grant SAB2000-0235 and Program of Alicante University "Senior Professor" 2005. Partial support of Spanish projects AYA2005-8109 and ACOMP06/120 from Generalitat Valenciana is also acknowledged.

REFERENCES

Barkin, Yu. V., Ferrandiz, J. M. and Getino, J.(1996) About the application of action-angle variables to the rotation of deformable celestial bodies. In Dynamics, ephemerides, and astrometry of the solar system: Proc. IAU Symp. 172, S. Ferraz-Mello et al., eds., p. 243.

Barkin, Yu. V. (1998) Unperturbed Chandler Motion and Perturbation Theory of the Rotation Motion of Deformable Celestial Bodies. Astronom.& Astroph. Transac., 17, pp.179-219.

Barkin, Yu. (2000) A Mechanism of Variations of the Earth Rotation at Different Timescales. In Polar Motion: Historical and Scientific Problems, ASP Conference Series, Vol. 208, S. Dick, D. McCarthy, and B. Luzum, eds., pp.373-379.

Getino, J. and Ferrandiz, J. M. (1991) A Hamiltonian Theory for an Elastic Earth - First Order Analytical Integration. Celes. Mech. & Dyn. Astron., 51, pp. 35-65.

Kinoshita, H. (1972) First-Order Perturbations of the Two Finite Body Problem. Pub. Astron. Soc. Japan, 24, pp.423-457 .

Kinoshita, H. (1977) Theory of the rotation of the rigid earth. Celes. Mech., 15, pp. 277-326.

Yoder, C. F. (1995) Venus' free obliquity. Icarus, 117, pp. 250-286.

ON THE LONG-PERIODICAL OSCILLATIONS OF THE EARTH ROTATION

YA. CHAPANOV
Central Laboratory for Geodesy, Bulgarian Academy of Sciences
Acad. G. Bonchev Str., Bl.1, Sofia 1113, Bulgaria
e-mail: chapanov@clg.bas.bg

The most accurate time series of the length of day (LOD) variations is from the solution C04 of the IERS (Fig.1). An empirical model of the long-periodical oscillations of the Earth rotation according this time series is proposed here. The lowest frequency oscillation in the model is with period 48 years, which is closed to the period of 45-year solar asymmetry cycles. These cycles are due to the North-South asymmetry of the solar differential rotation with periodicity $45.5a \pm 11.5a$ and they have strong correlation with Earth rotation (Georgieva, 2002). The half of the 48-year oscillation is quite visible in the LOD series for the interval 1962-1986 (Fig.1) and this 24-year oscillation is closed to the period of magnetic cycle of the Sun about 22a. Other long-periodical oscillations in the model of the LOD series are with the period of the Lunar node 18.6a; the period of the solar activity - about 11a; the oscillations with period of 6.4a, which are discovered in UT1 series (Chapanov et al., 2005), and the periods of ENSO event in the band 2-4a, represented by the high harmonics of the above periodicities. The empirical model includes also a polynomial of degree 2 and seasonal oscillations. The coefficients and amplitudes of the long-periodical oscillations of the LOD are estimated and the correlation between the LOD variations and solar activity is determined by means of the proposed empirical model here.

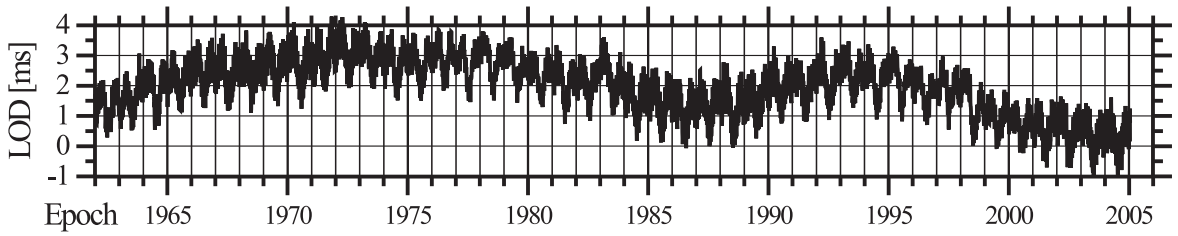

Figure 1: Variations of LOD (in ms) according the solution C04 of the IERS.

The proposed here model of the long-periodical LOD variation is

$$f = f_\circ + f_1(t - t_\circ) + f_2(t - t_\circ)^2 + \sum_{k=1}^{5} \sum_{i=1}^{n_k} a_{ik} \sin i\omega_k t + b_{ik} \cos i\omega_k t, \qquad (1)$$

where the middle epoch $t_\circ$ is 1983.5 and the frequencies $\omega_k = 2\pi/P_k$ correspond to the five periods P_k: $48a$; $18.6a$; $10.3a$; $6.4a$ and $1a$. The three solar activity cycles for the interval 1962-2005 have mean period of 10.3 year, which is used in the model (1). The number of harmonics

Table 1: Coefficients and amplitudes of the periodical oscillations of the LOD series [ms].

P_k	i	a_{ik}	b_{ik}	A_{ik}	$\sigma_{A_{ik}}$	i	a_{ik}	b_{ik}	A_{ik}	$\sigma_{A_{ik}}$
P_1=48a	1	-0.776	-0.190	2.057	±0.089	2	+0.372	-0.021	0.373	±0.027
P_2=18.6a	1	-0.495	-0.218	0.541	±0.015	3	-0.059	+0.082	0.101	±0.018
	2	+0.174	-0.034	0.178	±0.011	4	-0.048	+0.012	0.049	±0.006
P_3=10.3a	1	-0.204	+0.145	0.250	±0.011	3	+0.006	+0.061	0.062	±0.007
	2	-0.016	+0.058	0.061	±0.006	4	-0.045	-0.019	0.048	±0.009
P_4=6.4a	1	+0.174	-0.016	0.175	±0.019	3	-0.057	+0.031	0.065	±0.007
	2	-0.053	-0.046	0.071	±0.011	4	-0.015	-0.018	0.024	±0.006
P_5=1a	1	-0.176	-0.327	0.371	±0.006	2	-0.194	-0.288	0.348	±0.006

of the model (1) is as follow: 2 harmonics for the 48-year cycle, 10 harmonics for the 18.6-year cycles, 4 harmonics for the solar activity cycles, 5 harmonics for the 6.4-year cycles and 4 harmonics the seasonal changes. The successful separation of the oscillations with close periods of 18.6 and 24 years needs an observation span at least 83 years long. Here these periods are separated by a loose restriction of the solution for the coefficients of the second harmonic of the 48-year cycle. The possible hidden singularity of the normal matrix, due to close frequencies in the model is controlled by the Singular Value Decomposition solution with ratio 10^8 between the maximum and minimum values of the used singular values. Several of the estimated harmonically coefficients are shown in Table 1. The estimates of the polynomial coefficients in the model (1) are $f_\circ = 3.92ms \pm 0.07ms$, $f_1 = 0.0031ms/a \pm 0.001ms/a$, $f_2 = -0.011ms/a^2 \pm 0.0004ms/a^2$.

The decadal variations of the LOD due to the solar activity are determined as a sum of the residuals of the approximation of the LOD series by the model (1), after filtration of the high-frequencies with periods less then one year, and the 10.3-year oscillation of the LOD. The resulting curve, shown in Fig.2 is very close to the shifted with +1.6a curve of the smoothed Wolf's number. The correlation between the shifted time series is high with coefficient +0.87.

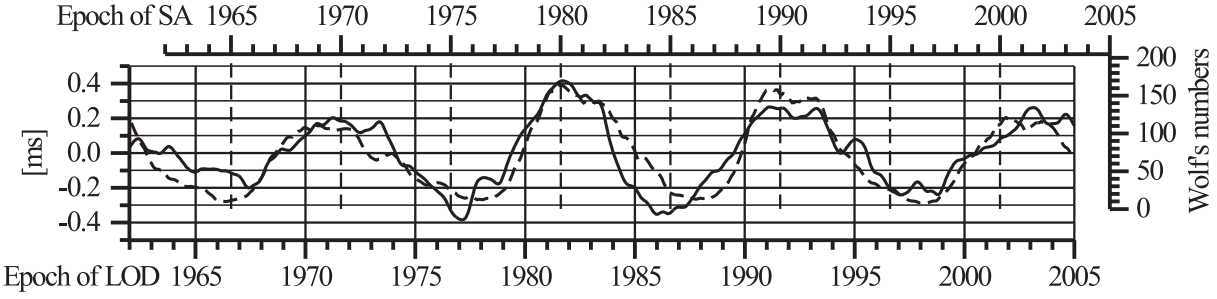

Figure 2: Comparison of the decadal variations of LOD at the solar activity frequency with mean period 10.3a (solid line) and smoothed Wolf's numbers (dashed line). The phase delay of the LOD changes is 1.6a. The correlation coefficient between the shifted time series is +0.87.

Acknowledgements. This study was supported by contract No. NZ-1213/02 with the National Council for Scientific Research at Bulgarian Ministry of Education and Science.

REFERENCES

Chapanov, Ya., Vondrák J., Gorshkov, V., Ron C., 2005, "Six-year cycles of the Earth rotation and gravity", Reports on Geodesy, No. 2(73), pp. 221–230.

Georgieva K., 2002, "Long-term changes in atmospheric circulation, earth rotation rate and north-south solar asymmetry", Physics and Chemistry of the Earth, 27, pp. 433–440.

INSTABILITY OF THE EARTH'S ROTATION IN 1833 - 2000 YEARS

A.A KORSUN'[1], G.S. KURBASOVA[2]
[1] Main Astronomical Observatory, National Academy of Sciences of Ukraine
27 Zabolotnogo Str., 03680 Kyiv, Ukraine
e-mail: akorsun@mao.kiev.ua
[2] Crimean Astrophysical Observatory
p/o Nauchny, 98677 Crimea, Ukraine
e-mail: gsk@simeiz.ylt.crimea.com

1. DATA AND METHOD OF THE ANALYSIS

We used the following series of data for analysis:
(D) - Excess of the duration of the day to 86400s (IERS Annual Report, 2000);
(EQ) - The mean annual numbers of Earthquakes with a magnitude of more than 7 in 1900-2004 (http:/neic.usgs.gov/neis/eqlists/);
(SSC) - The mean annul numbers of the geomagnetic sudden commencements in 1868-2002 (http://www.wdcb.ru/);
(GMT) - Global Temperature Anomalies (http://www.cdc.noaa.gov/ClimateIndices/);
(aa) - Geomagnetic Indices (http://www.wdcb.ru/);
(W) - Relative Sunspot Numbers (http://www.wdcb.ru/).

Calculations are based on a classical spectral methods and two-channel estimates of the autoregressions (AR) spectral power density.

2. MODEL USED AND RESULTS

We have found the basic not tidal waves with the periods near 64, 32, 21 years in the (D) - data. The (D)-data are interpreted on the base of new quasi-polynomial model:

$$s(t) = \sum_{m=1}^{n} \sum_{l=0}^{k_l-1} a_{ml} t^l e^{z_m t}, \tag{1}$$

where $n \geq 1, k_l \geq 1, z_m$ are some complex numbers.

The analytical approximation with (D)-data is accurate to better than 12 % .

According to (1) oscillations with the periods 64 year and 21 year (Figure 1, gr.3,5) are similar structure and also describe fading process. This fact will be coordinated to conclusions Braginsky's (1982) about generation by their one system torsion fluctuations in liquid core of the Earth. The oscillation with the period 32 year (Figure 1, gr.4) has well defined character of the quasi-harmonic process. It will be coordinated to the assumption Morrison (1979) about various mechanisms of generation inside the Earth of oscillations with the periods about 64 year and 32 year.

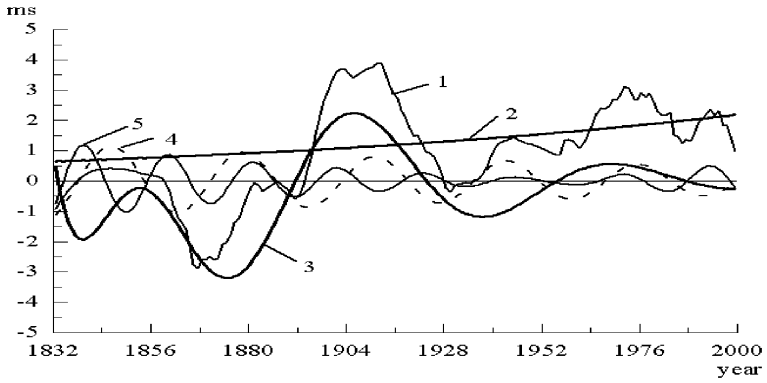

Figure 1: The basic oscillations in the structure of quasi-polynomial models
1 - initial (D)-data; 2 - trend; 3 - oscillation with the period 64 year; 4 - oscillation with the period 32 year; 5 - oscillation with the period 21 year.

3. TWO-CHANNEL AR-ANALYSIS

In table 1 results two-channel AR-analysis are presented. The basic oscillations in (D) (I the channel) are compared with similar oscillations in various geophysical and atmospheric numbers.

Table 1: Results two-channel AR-analysis of the (D)-data (I channel) and compared the data (II channel)

Name of data (II channel)	Quantity of data	Period (year)	Displacement , year (in I channel concerning II)	SMC %
aa	132	21.3	10.4	83
aa	132	22.3	-10.4	94
W	132	22.3	- 9.7	95
aa	132	32.0	10.4	92
EQ	100	32.0	0.2	85
EQ	100	64.0	-18.0	96
GMT	120	64.0	18.1	62
SSC	100	64.0	-12.9	78

That fact, that on close frequencies of oscillations in (D) - data have a high degree of coherence (the square modulus of the coherence(SMC)>80 %) with external and internal processes simultaneously, admits the possibility of the existence of the interconnected mechanism of the generation different from tidal changes.

REFERENCES

Braginsky S.I., 1982, "Analytical descriptions of secular variations of a geomagnetic field and speed of rotation of the Earth", Geomagnetizm i aeronomiya, vol.22, 1, pp.115-122.

Morrison L.V., 1979, "Re-determination of the decade oscillations in the rotation of the Earth in the period 1861 - 1978", Geophys. J. R. Astron. Soc. , vol. 58, pp.349-360.

ABRUPT CHANGES OF THE EARTH'S ROTATION SPEED IN ANCIENT TIMES

M. SÔMA and K. TANIKAWA
National Astronomical Observatory of Japan
Mitaka, Tokyo 181-8588, Japan
e-mail: Mitsuru.Soma@nao.ac.jp, tanikawa.ky@nao.ac.jp

ABSTRACT. In our recent work using ancient solar eclipse records we showed that the Earth's rotation rate changed abruptly in about AD 900 (Sôma and Tanikawa 2005). We show here that more abrupt changes in the Earth's rate of rotation occurred in about AD 500.

1. INTRODUCTION

For the past few years we have been deriving the changes of the Earth's rate of rotation using the solar eclipse records in ancient times (Tanikawa and Sôma 2002, 2004, Kawabata et al. 2004, Sôma et al. 2003, 2004), and in Journées 2004 we showed that the Earth's rotation rate changed abruptly in about AD 900 so that the ΔT (TT − UT) values decreased between the years AD 873 and 912 by more than 600 sec (Sôma and Tanikawa 2005). We concentrate here the changes in about AD 500.

2. CHANGE OF THE EARTH ROTATION RATE AROUND AD 500

Sôma et al. (2004) deduced the following ranges of the possible ΔT values from the multiple ancient solar eclipse records:

Date	Range of ΔT (sec)	Date	Range of ΔT (sec)
306 July 27 360 Aug 28	6529 – 7120	616 May 21 628 Apr 10	2278 – 2959
516 Apr 18 522 July 10 523 Nov 23	3567 – 5085	702 Sept 26 729 Oct 27 761 Aug 05	2728 – 3254

On 454 Aug 10 there was a solar eclipse in China, and it was recorded as total. As discussed by Stephenson (1997, p. 242), this record was misplaced one calendar year. It can be assumed that this eclipse was observed at Jiankang (Chien-k'ang), the capital at the time.

The 484 Jan 14 solar eclipse was recorded at Athens. The record says that the day was turned into night and the darkness was deep enough for the stars to become visible, and therefore it is clear that the eclipse was total at Athens.

From the above two records, the range of the possible ΔT values can be obtained as follows:

Date	Range of ΔT (sec)
454 Aug 10	6027 – 7858
484 Jan 14	4490 – 5463

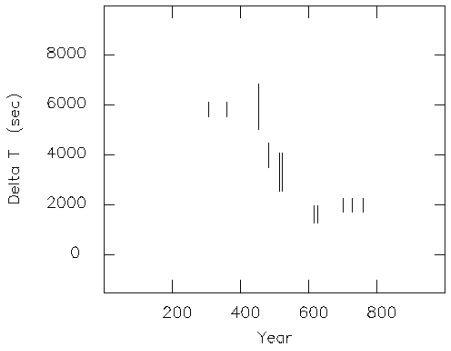

Figure 1: ΔT around AD 500

Fig. 1 shows the variation of the ΔT values in around AD 500. The figure clearly shows that the speed of the Earth's rotation increased abruptly in around AD 450, and it gradually decreased until about AD 600.

3. REFERENCES

Kawabata K., Tanikawa K., and Sôma M., 2004, "TT − UT in the Seventh Century Derived from Astronomical Records in the Nihongi, the Suishu, and the Jiu- and Xin-Tangshu", in Astronomical Instruments and Archives from the Asia-Pacific Region, W. Orchiston, F.R. Stephenson, S. Debarbat, and I.-S. Nha (eds.), pp. 113–118, Yonsei University Press, Seoul.

Sôma M., Tanikawa K., and Kawabata K., 2003, "Earth's Rotation in the 7th Century Derived from Eclipse Records in Japan and in China", in Proceedings of the "Journées 2002 Systèmes de Réffence Temps Espace" (Astronomy from Ground and from Space), N. Capitaine and M. Stavinschi (eds.), pp. 248–250, Bucharest.

Sôma M., Tanikawa K., and Kawabata K., 2004, "Earth's Rate of Rotation between 700 BC and 1000 AD Derived from Ancient Solar Eclipses", in Proceedings of the "Journées 2003 Systèms de Référence Spatio-Temporels" (Astrometry, Geodynamics and Solar System Dynamics: from milliarcseconds to microarcseconds), A. Finkelstein and N. Capitaine (eds.), pp. 122–127, St. Petersburg.

Sôma M. and Tanikawa K., 2005, "Variation of Delta T between AD 800 and 1200 Derived from Ancient Solar Eclipse Records", in Proceedings of the "Journées 2004 Systèmes de Référence Spatio-Temporels" (Fundamental Astronomy: New concepts and models for high accuracy observations), N. Capitaine (ed.), pp. 265–266, Paris.

Stephenson, F.R., 1997, Historical Eclipses and Earth's Rotation, Cambridge University Press.

Tanikawa K. and Sôma M., 2002, "Reliability of the Totality of the Eclipse in AD 628 in the Nihongi", Astronomical Herald, 95, pp. 27–37 (in Japanese).

Tanikawa K. and Sôma M., 2004, "ΔT and the Tidal Acceleration of the Lunar Motion from Eclipses Observed at Plural Sites", Publ. Astron. Soc. Japan, 56, pp. 879–885.

ANALYSIS OF DISCREPANCIES OF THE NUTATION THEORIES MHB2000 AND ZP2003 FROM VLBI OBSERVATIONS

L.V. ZOTOV, S.L. PASYNOK
Sternberg Astronomical Institute of Moscow State University
119992, Moscow, Universitetskij prospect 13, Russia
e-mail: tempus@sai.msu.ru, pasynok@sai.msu.ru

ABSTRACT. Spectral and structural analysis of discrepancies of the nutation theories for the nonrigid Earth ZP2003 and IAU2000 from VLBI observations was performed.

As a result of structural analysis it was shown that the linear parts of the equations of momentum in these theories are modeled well enough and the improvement in the future is possible only by the perfection of the models of the nonlinear parts.

As a result of spectral analysis it was derived that the main differences between ZP2003 and IAU2000 are at semiannual and main nutation 18.6-year periods. The causes of these discrepancies are under discussion. The major part of deviations of the theories from observations is determined by the free core nutation (FCN). Spectral investigation proved the existence of an unknown process, which compensates the influence of atmosphere at the semiannual frequency.

With use of SVD least squares method the empirical corrections to the main harmonic oscillations for ZP2003 were estimated.

1. INTRODUCTION, INITIAL DATA

The theory MHB2000 [Mathews et al., 2002] was adopted at the XXIV assembly of the International Astronomical Union (IAU) as the new nutation theory IAU2000. The theory ZP2003 [Pasynok, 2003] developed in Russia differs from IAU2000 by the method of calculation of the atmosphere and liquid core effects. In ZP2003 the laws of conservation of energy and momentum are taken into account during the determination of the parameters of the Earth internal structure, which are not known precisely from observations.

The series of discrepancies between the theories and observations were derived by processing of VLBI observations since 1984 till 2003 year with use of OCCAM 5.0 package. The series of discrepancies of $d\varepsilon$ and $d\psi$ in more then 2000 points were used in analysis. Weighted mean squares deviations made up 235 ($d\varepsilon$) and 829 ($d\psi$) μas for ZP2003, 199 and 480 μas for IAU2000 accordingly.

2. STRUCTURAL AND SPECTRAL INVESTIGATIONS, DISCUSSION

At the first stage the corrections to the amplitudes of the main 300 nutation harmonic oscillations were estimated by the least squares method (LSM) with use of algorithm SVD [Forsite et al., 1980].

At the second stage the corrections to the transfer function's parameters were estimated with use of SVD LSM. Attempts to approximate the amplitudes corrections by varying of the transfer function parameters do not lead to a success. This testifies that the linear parts of the equations of momentum in both theories are modeled well enough and the improvement in the future is possible only by the perfection of the models of the nonlinear effects.

Than the periodograms of the smoothed and equal-spaced series of discrepancies were calculated, wavelet-analysis was performed. Scalograms illustrate the temporal evolution of the periodical components of dε at Fig. 1. The major part of the discrepancies is determined by the

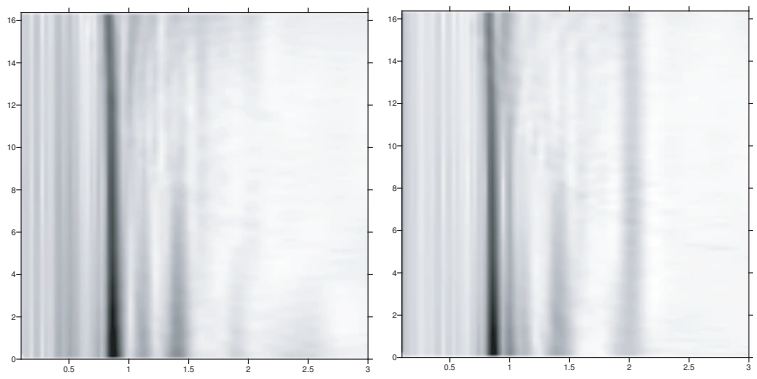

Figure 1: Scalograms of discrepancies of dε for IAU2000 (left) and ZP2003 (right) theories. The frequency in years^{-1} across, years since 1984 in vertical direction.

free core nutation FCN. The discrepancies of the theory ZP2003 from VLBI observations contain more energy at 18.6-year period, then the discrepancies of IAU2000. It can be connected with the problem of separation of harmonic oscillations with close frequencies.

The components at semiannual frequencies are present in the discrepancies of ZP2003, but are absent in those ones of IAU2000. The IAU2000 theory doesn't include the atmosphere correction at this frequency. It was suggested, that an unknown process compensates the influence of atmosphere [Mathews et al., 2002]. In ZP2003 the atmosphere was taken in account in the equations of momentum, but no other unknown processes was. So the spectral investigation proves the existence of an unknown process, which compensates the atmosphere influence at the semiannual frequency in IAU2000.

Corrections at the semiannual and 18.6-year periods for ZP2003 were estimated with use of SVD LSM. The agreement of ZP2003 became better and weighted mean squares deviations of discrepancies reached the level of 207 (dε) and 808 (dψ) μas. After estimation of corrections to 300 first harmonics weighted mean square deviations became 146 (dε) and 345 (dψ) μas.

Acknowledgements. The authors would like to thank Dr. V.E. Zharov for useful discussions. The work is supported by RFBR grants No 05-02-17091 and No 04-02-16681.

REFERENCES

Mathews P.M., Herring T.A., Buffet B.A., 2002, Modeling of nutation and precession: New nutation series for nonrigid Earth and insights into the Earth's interior, J. Geophys. Res. , 107(B4), doi.: 10.1029/2000JB000390.

Pasynok S.L., 2003, IAU2000: Comparison with VLBI observations and other nutation theories, Proc. Journees 2003, "Astrometry, geodynamics and solar system dynamics: from milliarseconds to microarcseconds", St. Petersburg, Russia, pp. 176-181.

Forsite J., Malkolm K., Mouler., 1980, Mechanical methods of mathematical calculus, Moscow.

ON THE ACCURACY OF THE TRIGONOMETRIC SOLUTION FOR THE PERIODICAL COMPONENTS OF THE POLAR MOTION

YA. CHAPANOV[1], J. VONDRÁK[2], C. RON[2]
[1]Central Laboratory for Geodesy, Bulgarian Academy of Sciences
Acad. G. Bonchev Str., Bl.1, Sofia 1113, Bulgaria, e-mail: chapanov@clg.bas.bg
[2]Astronomical Institute, Academy of Sciences of the Czech Republic
Boční II, 141 31 Prague 4, Czech Republic, e-mail: vondrak@ig.cas.cz, ron@ig.cas.cz

ABSTRACT. The classical approximation of the polar motion by trigonometric functions with constant amplitudes and phases may lead to a significant increase of the errors of the estimated parameters of the annual and Chandler oscillations. The increase of the errors of the estimated parameters of the polar motion is analyzed here by means of the simulation of the polar motion, based on the solution C04 of the IERS. The simulated model of the polar motion includes such variations of the annual and Chandler amplitude, so that the simulated motion is close to the real motion. After that, the variations of the annual and Chandler amplitude are estimated by the Least Squares Method over the spans of 6 years. The differences of the estimated and modelled variations of the amplitudes are obtained. It is shown that the errors of the estimated parameters of the periodical components of the polar motion are significantly higher than the accuracy of the modern determinations of the pole coordinates.

The mathematical models for determination of the periodical components of the polar motion consists of trigonometric functions of common type

$$\begin{aligned} x &= x_0 + x_1 t + \sum_{i=1}^{n} a_{ai} \sin i\omega_a t + b_{ai} \cos i\omega_a t + \sum_{j=1}^{m} a_{cj} \sin j\omega_c t + b_{cj} \cos j\omega_c t, \\ y &= y_0 + y_1 t + \sum_{i=1}^{n} c_{ai} \sin i\omega_a t + d_{ai} \cos i\omega_a t + \sum_{j=1}^{m} c_{cj} \sin j\omega_c t + d_{cj} \cos j\omega_c t, \end{aligned} \tag{1}$$

where x and y are the pole coordinates, x_0, y_0, x_1, y_1 - the mean coordinates and their rates in the middle of the six-year time interval respectively, $a_{ai}, b_{ai}, c_{ai}, d_{ai}, i = 1, \ldots, n$; $a_{cj}, b_{cj}, c_{cj}, d_{cj}, j = 1, \ldots, m$ - unknown harmonic coefficients of the components with known seasonal (annual) frequency w_a and Chandler frequency w_c; t is the observation epoch. Usually the number of harmonics is equal to 1 (n=m=1), for study of the semi-annual and semi-Chandler oscillations the value of harmonics n and m may increase to 2.

To estimate the real errors of the approximation of the polar motion with trigonometric functions of the type (1), a simulation of the polar motion with known variations of the parameters of the seasonal and Chandler oscillation, which are close enough to its real changes in the time,

is used here. The parameter values of the simulated polar motion are obtained by the model (1) from the solution C04 of the IERS with running 6-year observation spans. The beginning and end of the time series of the obtained parameters are lengthened with constant values, so the simulation of the polar motion is given for the period 1955-2013 (Fig.1).

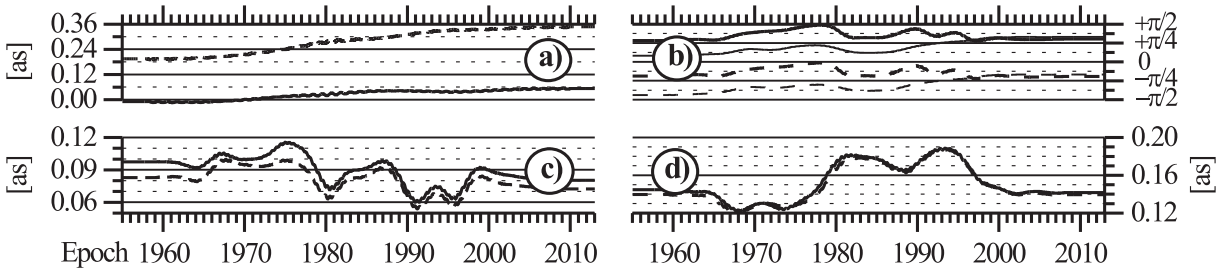

Figure 1: Parameter variations of the simulated polar motion (solid line for x-coordinate and dashed line for y-coordinate): a) - for the mean values; b) - for the annual (bold lines) and the Chandler (thin lines) phases; c) - for the annual amplitudes; d) - for the Chandler amplitudes.

The polar motion parameters are determined by means of the simulated pole coordinates. After that an estimation of the real errors of the parameters in the model (1) is made by comparisons of the obtained and original values of the parameters. The differences between the "true" and estimated annual and Chandler amplitudes and phases are shown in Figs. 2 and 3. The maximal values of the estimated "real" errors reach 11 mas for the annual amplitude and 19 mas for the Chandler amplitude and their standard deviations are 3.9 mas and 5.9 mas respectively. The maximal "real" errors for the annual and Chandler phases are $-6.9°$ and $-4.9°$ with standard deviations $2.2°$ and $1.8°$. These errors are by two – three orders higher than the accuracy of the modern determinations of the pole coordinates.

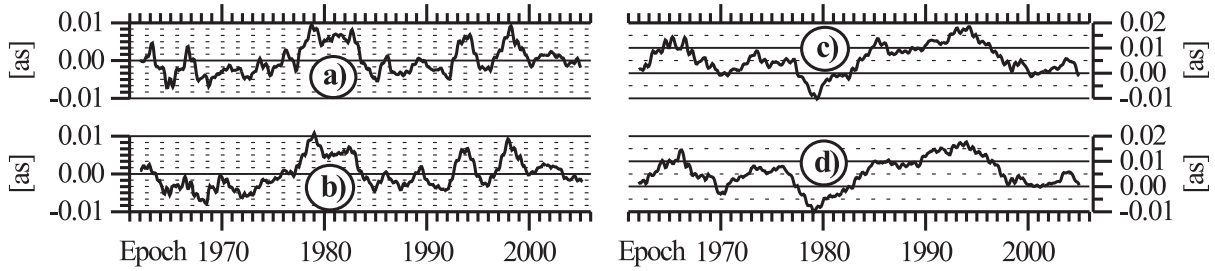

Figure 2: Estimation of the real errors of the annual amplitudes - a) for y and b) for x, and Chandler amplitudes - c) for y and d) for x pole coordinates.

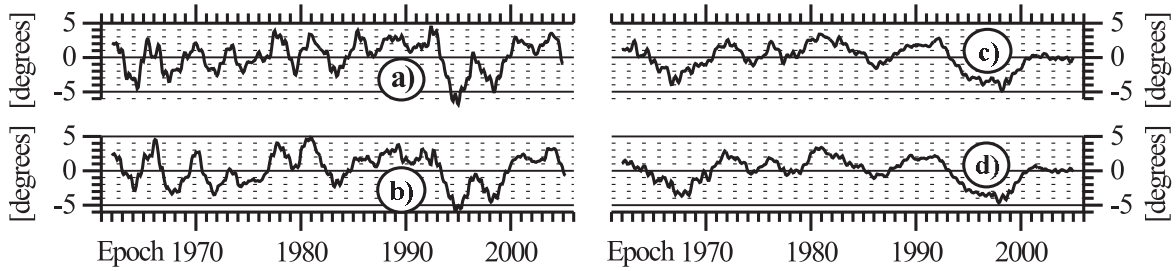

Figure 3: Estimation of the real errors of the annual phases - a) for y and b) for x, and Chandler phases - c) for y and d) for x pole coordinates.

Acknowledgements. This study was supported by contract No. NZ-1213/02 with the National Council for Scientific Research at Bulgarian Ministry of Education and Science.

FORECASTING POLE COORDINATES DATA BY COMBINATION OF THE WAVELET DECOMPOSITION AND AUTOCOVARIANCE PREDICTION

W. KOSEK[1] and W. POPIŃSKI[2]

[1]Space Research Centre, Polish Academy of Sciences, Warsaw, Poland
[2]Central Statistical Office, Warsaw, Poland
e-mail: kosek@cbk.waw.pl, w.popinski@stat.gov.pl

1. INTRODUCTION

The basic problem in forecasting a time series is the necessity of separate treatment of the low and high frequency variations. This problem can be solved by combination of the discrete wavelet transform (DWT) decomposition with the autocovariance forecast (AC) technique (DWT+AC) (Kosek et al. 2005). In this approach each frequency component determined by the DWT is predicted separately by the AC technique, and the final prediction is the sum of the predicted components (Kosek et al. 2005). Combination of the DWT+AC technique enables adaptive forecasting of time series in different frequency bands. The applied DWT decompositions were based on the Meyer (Meyer 1990, Popiński and Kosek 1995) and Shannon (Benedetto and Frazier 1994) wavelet function concepts.

2. DATA USED, THEIR ANALYSIS AND RESULTS

The following x, y pole coordinates data were used: EOPC01 in 1846 - 2002 and EOPC04 in 1962 - 2005.6 (IERS 2005). The combined pole coordinates series which consist of the EOPC01 data interpolated at 1 day sampling interval from 1880 to 1962 and the EOPC04 data from 1962 to 2005.6 was created.

Decomposition of the x, y pole coordinates data into frequency components using the DWT based on the Meyer or Shannon wavelets does not enable separation of the Chandler and annual oscillations. It was found previously that the AC forecast applied directly to the pole coordinates data attains lower accuracy than the AC forecast applied in the polar coordinate system (Kosek 2002). Thus, to solve the problem of the separation of the Chandler and annual oscillations the DWT+AC forecast was computed in the polar coordinate system using the following algorithm:
Step 1. Computation of the mean pole coordinates data by the Ormsby (1961) low pass filter and its forecast by the least-squares method.
Step 2. Transformation of x, y pole coordinates data into the radius and angular velocity data, which were then interpolated at 1 week sampling interval.
Step 3. Decomposition of the radius and angular velocity series into frequency components using the chosen DWT. In order to reduce the DWT filtration errors at the ends of these frequency components time span, the radius and angular velocity data were preliminary predicted by the AC method to extend their time span to $n = 2^{12}$ points (78.5 years) before decomposition.

Step 4. Computation of predictions of the frequency components of the radius and angular velocity data by the AC forecast. The final prediction of the radius and angular velocity series is the sum of the predicted components.
Step 5. Transformation of the predictions of the radius and angular velocity data from the polar to the Cartesian coordinate system using linear intersection formulae (Kosek 2003).
Step 6. The next prediction point of x, y pole coordinates data can be computed by repeating the Step 5 after the previously determined predictions of the pole coordinates data and of the mean pole coordinates data are added at the end of the corresponding time series, etc.

The absolute values of the difference between the x, y pole coordinates data, the radius and angular velocity data and their corresponding predictions computed by the DWT+AC method for different starting prediction epochs are shown in Figure 1.

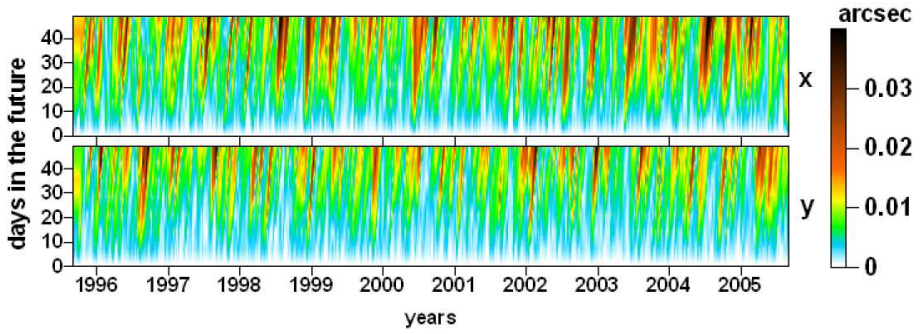

Figure 1: The absolute values of the difference between x, y pole coordinates data and their predictions for 50 days in the future, at different starting prediction epochs, obtained by the DWT+AC technique with Shannon wavelet function. Contour line at 0.01 second of arc.

3. DISCUSSION

The DWT+AC combination enables adaptive prediction of x, y pole coordinates data in different frequency bands. The transformation from the Cartesian to polar coordinate system is necessary to solve the problem of the resolution of the Chandler and annual oscillations. There are still many problems to be solved when using this forecast approach: 1) the applied prediction algorithm is very time consuming, 2) each frequency component computed by the DWT has got the errors at the end of time series due to filtration, so the preliminary extension of time series is necessary to diminish these errors, 3) for each frequency component the appropriate length of data used for the prediction computation should be found.

Acknowledgments. This paper was supported by the Polish Ministry of Education and Science under the project No 4 T12E 039 29.

REFERENCES

Benedetto J.J. and Frazier M.W., 1994, Mathematics and Applications, LRC Press, Boca Raton, 221-245.
IERS 2005, Earth Orientation Parameters, http://hpiers.obspm.fr/eop-pc/.
Kosek W., 2002, *Advances in Space Research*, 30, 375-380.
Kosek W., 2003, *Proc. Journees 2002*, Bucarest, 25-28 Sep. 2002, 125-131.
Kosek W., Kalarus M., Johnson T.J., Wooden W.H., McCarthy D.D. and Popiński W., 2005, *Artificial Satellites*, Vol. 40, No. 2, 119-125.
Meyer Y., 1990, Ondelettes et Operateurs, Vol. 1, Hermann, Paris.
Ormsby J.F.A., 1961, *J. Assoc. Compt. Mach.*, 8, 440-466.
Popiński W., Kosek W., 1995, *Proc. Journees 1995*, 121-124.

Session 2.2

PRECESSION, NUTATION AND POLAR MOTION:
Implementation of the IAU 2000 Resolutions and new nomenclature

PRÉCESSION, NUTATION ET MOUVEMENT DU PÔLE :
Implementation des résolutions UAI 2000 et nouvelle nomenclature

LATEST PROPOSALS OF THE IAU WORKING GROUP ON "NOMENCLATURE FOR FUNDAMENTAL ASTRONOMY"

N. CAPITAINE, Observatoire de Paris, France
and
C. HOHENKERK, HMNAO, UK; A.H. ANDREI, Observatorio Nacional, Brazil; M. CALABRETTA, ATNF, Australia; V. DEHANT, ROB, Belgium; T. FUKUSHIMA, NAO, Japan; B. GUINOT, Observatoire de Paris, France; G. KAPLAN, USNO, USA; S. KLIONER, Lohrmann Observatory, Germany; J. KOVALEVSKY, OCA, France; I. KUMKOVA, Sobolev Astronomical Institute, Russia; C. MA, GSFC, USA; D.D. MCCARTHY, USNO, USA; K. SEIDELMANN, Virginia University, USA; P. WALLACE, CCRLC/RAL, UK

ABSTRACT. The IAU Division 1 Working Group on "Nomenclature for Fundamental Astronomy" (NFA) was established by the 25th IAU General Assembly with the task of preparing a consistent and well defined terminology associated with the implementation of the IAU 2000 resolutions on reference systems. This WG is also intended to make related educational efforts to address the issue to the large community of scientists. In this paper, we recall the main nomenclature issues and report on the latest NFA WG recommendations on terminology choices and guidelines that have been supported by explanatory documents, including a NFA IAU 2000 Glossary. In order to introduce the astronomical community to the main NFA recommendations, a WG Resolution proposal will be submitted to the IAU 2006 General Assembly as a supplement to the IAU 2000 resolutions for harmonizing the name of the pole and origin to "intermediate" and for specifying the default orientation of the BCRS and GCRS.

1. INTRODUCTION

The IAU 2000 resolutions on reference systems, which have been implemented by the IERS (International Earth Rotation and Reference Systems Service) Conventions 2003 and SOFA (Standards Of Fundamental Astronomy) (Wallace 2004), have consequences for the whole astronomical community; these include (i) the improvement in the procedures to be used in the realization of the International Celestial Reference System (ICRS), (ii) the use of an improved precession-nutation model, (iii) the use of a new definition of Universal Time, and (iv) the abandonment of the intermediary reference to the ecliptic and equinox.

The IAU Division 1 Working Group on "Nomenclature for Fundamental Astronomy" (NFA), established by the 2000 IAU General Assembly, has worked on selecting a consistent and well defined terminology for all the quantities based on the IAU 2000 Resolutions in order that it will be understood, recognized and adopted by the astronomical community. The terminology and guidelines recommended by the WG have been described in a number of Newsletters and documents (available on a WG web page) and are supported by the NFA explanatory document.

2. THE NOMENCLATURE ISSUES

The IAU 2000 Resolutions are such that, in particular:

- Resolution B1.3 specifies that the systems of space-time coordinates as defined by IAU Resolution A4 (1991) for the solar system and the Earth within the framework of General Relativity are named the Barycentric Celestial Reference System (BCRS) with Barycentric Coordinate Time (TCB) and the Geocentric Celestial Reference System (GCRS) with Geocentric Coordinate Time (TCG), respectively (see Soffel et al. 2003).

- Resolution B1.6 recommends the adoption of the IAU 2000 precession-nutation (Dehant et al. 1999, Mathews et al. 2002) with submilliarcsecond accuracy.

- Resolution B1.7 specifies the definition of the Celestial Intermediate Pole (CIP) as an intermediate pole in the transformation from the GCRS to the International Terrestrial Reference System (ITRS), separating, by convention, nutation from polar motion (see Capitaine 2002).

- Resolution B1.8 recommends that the transformation between the ITRS and the GCRS be specified by the position of CIP in the GCRS, the position of the CIP in the ITRS, and the Earth Rotation Angle (ERA) based on the use of the "non-rotating origin" (Guinot, 1979). UT1 has been defined as linearly proportional to the Earth Rotation Angle (ERA) between these origins on the moving equator.

The implementation of the above resolutions requires using a consistent and well defined terminology associated with the use of (i) the Barycentric and Geocentric celestial reference systems, (ii) the precession-nutation of the CIP and (iii) the new origins on the CIP equator.

3. TERMINOLOGY ASSOCIATED WITH THE NEW EQUATORIAL ORIGIN

The change of the origin on the CIP equator and the use of the ERA corresponds to the use of a new paradigm for the GCRS-to-ITRS transformation that requires specific recommendations on nomenclature. The NFA WG has recognized that using the designation "intermediate" to refer to both the pole and the origins of the new systems, namely the CIP and the Celestial or Terrestrial Ephemeris origins, defined in Resolutions B1.7 and B1.8, respectively, would improve the consistency of the nomenclature. The WG have therefore recommended:

- harmonizing the name of the pole and origin to "intermediate" and therefore changing CEO/TEO to CIO/TIO,

- using "equinox based" and "CIO based" for referring to the classical and new paradigms, respectively,

- choosing "equinox right ascension" and "CIO right ascension" (or "intermediate right ascension") respectively, for the azimuthal coordinate along the equator in the classical and new paradigms, respectively,

- defining the celestial and terrestrial "intermediate systems",

- keeping the classical terminology for "true equator and equinox" and

- giving the name "equation of the origins" to the distance between the CIO and the equinox along the intermediate equator. The sign of this quantity is such that it represents the CIO right ascension of the equinox, or equivalently, the difference between the Earth Rotation Angle and Greenwich apparent sidereal time.

The CIO was originally set close to the mean equinox at J2000.0. However, as a consequence of precession-nutation the CIO moves according to the kinematical property of the non-rotating origin. Similarly, the TIO was originally set at the ITRF origin of longitude and, as a consequence of polar motion the TIO moves according to the kinematical property of the non-rotating origin. The NFA WG has adopted the following designations to locate the CIP and the TIO:

- the CIO locator (denoted s) is the difference between the GCRS right ascension and the intermediate right ascension of the intersection of the GCRS and intermediate equators,

- the TIO locator (denoted s') is the difference between the ITRS longitude and the instantaneous longitude of the intersection of the ITRS and intermediate equators.

The Celestial Intermediate Reference System (CIRS) has been specified to be the geocentric reference system related to the GCRS by a time-dependent rotation taking into account precession-nutation. It is defined by the intermediate equator (of the CIP) and CIO on a specific date. It is similar to the system based on the true equator and equinox of date, but the equatorial origin is at the CIO.

4. TERMINOLOGY ASSOCIATED WITH THE USE OF THE BCRS AND GCRS

IAU Resolution B1.3 has defined the systems of space-time coordinates in the framework of general relativity for:

a) the solar system, called the Barycentric Celestial Reference System (BCRS), which can be considered to be a global coordinate system that contains all distant regions,

b) the Earth, called the Geocentric Celestial Reference System (GCRS), which can only be considered as a local coordinate system.

However, the NFA WG has recognized that 1) the BCRS definition does not determine the orientation of the spatial coordinates and 2) the natural choice of orientation for typical applications is that of the ICRS. Moreover, the GCRS is defined such that its spatial coordinates are kinematically non-rotating with respect to those of the BCRS and consequently the orientation of the GCRS spatial coordinates is induced by that of the BCRS.

Therefore, a NFA WG Recommendation on the default orientation of the BCRS and GCRS was adopted, fixing the default orientation of the BCRS so that for all practical applications, unless otherwise stated, the BCRS is assumed to be oriented according to the ICRS axes. Once the BCRS is spatially oriented according to the ICRS, the spatial GCRS coordinates inherit an "ICRS-induced" orientation.

5. ACTIVITIES OF THE NFA WORKING GROUP

Discussion about terminology associated with the IAU 2000 Resolutions was first published by Seidelmann & Kovalevsky (2002), Capitaine et al. (2003a,b) and Kovalevsky & Seidelmann (2004).

Then there has been detailed e-mail discussion within the NFA WG on the terminology choices. The agreements reached by the WG on these choices have been reflected in the WG Recommendations, which are supported by an explanatory document. Part A of this document reports on the basis for the IAU Resolutions and their implementation and Part B provides a more detailed description of the proposed terminology. Contained in Part B is the "NFA IAU 2000 Glossary" that provides a set of detailed definitions that best explain all the terms required for implementing the IAU 2000 resolutions. Complementary and supporting material (e.g. a

chart of the transformation process from ICRS to observed places of stars) are included in order to facilitate the understanding and implementation of the IAU 2000 resolutions, as well as illustrating the Glossary. The NFA issues and documents have been discussed during international meetings in 2004 and 2005 (See the NFA web page at: `http://syrte.obspm.fr/iauWGnfa/`). The Almanac Offices have begun to implement the WG recommendations beginning with their 2006 editions (see Hohenkerk 2005).

In order to approve the proposed terminology, the WG is preparing to submit to the IAU 2006 General Assembly a Resolution entitled "Supplement to the IAU 2000 Resolutions on reference systems", including Recommendation 1 *Harmonizing the name of the pole and origin to 'intermediate'* and Recommendation 2 *The default orientation of the BCRS and GCRS*. A special page of the NFA web site http://syrte.obspm.fr/iauWGnfa/ makes available documents with educational purposes relevant to the NFA issue.

REFERENCES

Capitaine, N., 2002, "Comparison of Old and New concepts: The Celestial intermediate pole and Earth orientation parameters," IERS Technical Note 29, N.Capitaine et al. (eds), Frankfurt am Main: Verlag des Bundesamts für Kartographie und Geodäsie, pp. 35–44.

Capitaine, N., Chapront, J., Lambert, S., and Wallace, P.T. 2003a, "Expressions for the Celestial Intermediate Pole and Celestial Ephemeris origin consistent with the IAU 2000A precession-nutation model", A&A 400, pp. 1145–1154.

Capitaine, N., Wallace, P.T., and McCarthy, D.D. 2003b, "Expressions to implement the IAU 2000 definition of UT1", A&A 406, pp. 1135–1149.

Dehant, V., Arias, F., Bizouard, Ch., Bretagnon, P., Brzeziński, A., et al. 1999, "Considerations concerning the non-rigid Earth nutation theory," Celest. Mech. Dyn. Astr., 72, pp. 245–310.

Guinot, B., 1979, "Basic Problems in the Kinematics of the Rotation of the Earth," in *Time and the Earth's Rotation*, D. D. McCarthy and J. D. Pilkington (eds), D. Reidel Publishing Company, pp. 7–18.

Hohenkerk, C. 2005, in Proceedings of the "Journées 2004 Systèmes de référence spatio-temporels," N. Capitaine (ed), Observatoire de Paris, pp. 168–171.

IERS Conventions (2003) 2004, IERS Technical Note 32, D.D. McCarthy and G. Petit (eds), Frankfurt am Main: Verlag des Bundesamts für Kartographie und Geodäsie.

Kovalevsky, J. & Seidelmann P.K. 2004, Fundamentals of Astrometry, Cambridge University Press.

Mathews, P. M., Herring, T. A., and Buffett B. A., 2002, "Modeling of nutation-precession: New nutation series for nonrigid Earth, and insights into the Earth's Interior", J. Geophys. Res. 107, B4, 10.1029/2001JB000390.

Seidelmann, P.K. and Kovalevsky, J. 2002, "Application of the new concepts and definitions (ICRS, CIP, and CEO) in fundamental astronomy", A&A 392, pp. 341–351.

Soffel,M., Klioner, S., Petit, G., Bretagnon, P., Capitaine, N., et al. 2003, "Explanatory supplement for the IAU 2000 resolutions on relativity", AJ 126, pp. 2687–2705.

Wallace P.T. 2004, SOFA software support for IAU 2000, AAS Meeting 204, #28.02, May 2004.

RECENT PROGRESS IN ASTRONOMICAL NOMENCLATURE IN THE RELATIVISTIC FRAMEWORK

S.A. KLIONER and M. SOFFEL
Lohrmann Observatory,
Dresden Technical University,
Mommsenstraße, 13, 01062 Dresden, Germany
klioner@rcs.urz.tu-dresden.de

ABSTRACT. Special topics of astronomical nomenclature related with relativity are discussed: the spatial orientation of the BCRS and GCRS, the problem of barycentric time scales TDB and T_{eph} and the notions of day, Julian date and Julian year.

1. THE SPATIAL ORIENTATION OF THE BCRS

The Barycentric Celestial Reference System (BCRS) was adopted by the International Astronomical Union in the year 2000 as basis for modelling high-accuracy astronomical observations, solar system spacecraft navigation, etc. Theoretically it is fixed by the form of the barycentric metric tensor (see, IAU, 2001; Rickman, 2001; Soffel, *et al.*, 2003 for more detail)

$$\begin{aligned} g_{00} &= -1 + \frac{2}{c^2} w(t,\mathbf{x}) - \frac{2}{c^4} w^2(t,\mathbf{x}) \,, \\ g_{0i} &= -\frac{4}{c^3} w^i(t,\mathbf{x}) \,, \\ g_{ij} &= \delta_{ij} \left(1 + \frac{2}{c^2} w(t,\mathbf{x}) \right) . \end{aligned}$$

Here the scalar function w generalizes the usual Newtonian gravitational potential and the vector function w^i describes gravito-magnetic type effects due to matter currents (moving masses). The BCRS is a particular reference system in the curved space-time of the solar system. From a mathematical point of view any kind of space-time coordinate system covering the solar system could be employed for practical applications. However, to avoid confusions and provide an unambigious way to interpret numerical values of various parameters (e.g. parameters of motion) a particular reference system should be fixed. This BCRS is a standard reference system adopted by the IAU. This does not mean, however, that other reference systems cannot be used. However, if some other reference system is used, the final results (numerical values of the parameters) should be transformed into the BCRS so that one can compare and/or combine these results with other results in a consistent way.

This BCRS is a dynamical concept in the sense that its metric tensor fixes the form of equations of motion for massive bodies as well as for light rays up to certain degrees of freedom.

The BCRS coordinates, as they are defined by the Resolution B1.3 of the IAU (2000) are fixed up to *constant change of the origin of time reckoning* and a *time-independent (constant) rotation of spatial coordinates*. In this sense the adoption of the BCRS is similar to adopting Newtonian equations of motion without Coriolis and centrifugal terms (i.e., to adopting a Newtonian inertial reference system) in the Newtonian framework. Another usual degree of freedom of an inertial reference system in the Newtonian framework is the choice the origin of spatial coordinates. For the BCRS, however, the origin is fully fixed to be the post-Newtonian barycenter of the solar system.

Now, the origin of time reckoning of the BCRS coordinate time $t = \mathrm{TCB}$ is also fixed by the definition of TCB, TT and TCG given by the IAU 1991 Resolutions. According to those Resolutions, on 1977 January 1, 00h 00m 00s TAI at the geocenter, the readings of TT, TCG and TCB are 1977 January 1, 00h 00m 32s.184 (JD 2443144.5003725).

However, the orientation of spatial axes was *not* fixed in the IAU (2000) resolutions. This orientation is irrelevant for physical laws, e.g., for equations of motion. Nevertheless this orientation is of major concern for astrometric problems. It is now recommended that this orientation is fixed by the ICRS. This means that in practice the spatial orientation of the BCRS is given by the ICRF, that is by the coordinates of a set of extragalactic sources obtained by VLBI observations. In the next decade the ICRF will be realized in the optical by the final Gaia catalog (ESA, 2004).

2. THE SPATIAL ORIENTATION OF THE GCRS

The Geocentric Celestial Reference System (GCRS) was adopted by the International Astronomical Union (2000) for modelling physical processes in the vicinity of the Earth and as intermediate step for relating the BCRS with the terrestrial system ITRS. The GCRS was constructed such that the gravitational fields of external bodies is represented only in forms of relativistic tidal potentials that grow at least quadratically with coordinate distance from the geocenter. The internal gravitational field from the Earth itself "coincides" with the gravitational field of a corresponding isolated Earth (in the absence of other bodies). The metric tensor of GCRS

$$\begin{aligned} G_{00} &= -1 + \frac{2}{c^2} W(T,\mathbf{X}) - \frac{2}{c^4} W^2(T,\mathbf{X})\,, \\ G_{0a} &= -\frac{4}{c^3} W^a(T,\mathbf{X})\,, \\ G_{ab} &= \delta_{ab}\left(1 + \frac{2}{c^2} W(T,\mathbf{X})\right) \end{aligned}$$

is given by the geocentric metric potentials W and W^a. They can be split into internal-, inertial- and tidal- (external) parts. Again the GCRS is a dynamical concept and fixes the coordinates up to the degrees of freedom that we had discussed for the BCRS.

However, the IAU 2000 framework explicitly gives the complete form of the coordinate transformation between BCRS and GCRS. The implication of these coordinate transformations is that once the BCRS coordinates are fully fixed the GCRS coordinates are also fully fixed by the given coordinate transformation. If the BCRS is spatially oriented according to the ICRS the spatial coordinates of the GCRS, being kinematically non-rotating, will get an ICRS-compatible orientation.

It would be confusing and even dangerous to think that the GCRS has the *same* spatial orientation as the BCRS or ICRS. The reason is that the transformations between the BCRS and the GCRS are 4-dimensional time-dependent space-time transformations (for example, the

BCRS vector $(t, 1, 0, 0)$ is not transformed into the GCRS vector $(T, 1, 0, 0)$). The main part of the change of the GCRS spatial axes with respect to the BCRS axes comes from the Lorentz transformation. Therefore, the difference in spatial coordinates cannot simply be described by a shift in origin plus a 3-dimensional rotation. Formal differences in spatial coordinates will be of order $(v_E/c)^2 \sim 10^{-8}$ or a few mas in angle, v_E being the BCRS velocity of the Earth. These differences are automatically taken into account in high-precision relativistic models, e.g., for VLBI, astrometry etc.

3. DAY, JULIAN DATE, JULIAN YEAR AND JULIAN CENTURY

From the practical point of view it seems to be advantageous that day, Julian year and Julian century are just defined as multiples of the second: $1\,\mathrm{d} \equiv 86400\,\mathrm{s}$, 1 Julian year $\equiv 365.25\,\mathrm{d}$ and 1 Julian century $\equiv 36525\,\mathrm{d}$. With these definitions these time intervals or 'units' can be used with *any* time scale: with TCG, TT TCB and TDB or proper time of some observer.

Also the concept of Julian date can be used for any of these time scales. E.g., on 1977 January 1, $00^h00^m00^s$ TAI at the geocenter, the readings of TT, TCG and TCB are JD 2443144.5003725 (1977 January 1, $00^h00^m32^s.184$) and increase by 1 every 86400 seconds of the corresponding time scale. The equivalent $\mathrm{T_{eph}}$ reading depends upon the specific ephemeris: the same reading for TDB(DE405) is JD 2443144.5003725 $-$ 65.564518 μs. It is suggested to use the notations $\mathrm{JD_{TT}}$, $\mathrm{JD_{TCG}}$, $\mathrm{JD_{TCB}}$ and $\mathrm{JD_{TDB}}$ for the Julian dates in the corresponding time scales.

4. TDB AND $\mathrm{T_{eph}}$

Although the coordinate time TCB is a natural and physically adequate time scale for the use for solar system ephemerides for historical reasons another time scale (TDB) has been used for the same purpose. There has been a long and controversial discussion about the barycentric time scale TDB (Barycentric Dynamical Time). According to the original definition from 1976 TDB should differ from Terrestrial Time (TT) only by periodic terms. This implies, however, that TDB would not be a linear function of TCB. On the other hand the relativistic Einstein-Infeld-Hoffmann (EIH) equations of motion that form the basis of modern planetary ephemerides since about 1970 are valid only with TCB or a linear function thereof. After this was realized Standish (1998) introduced $\mathrm{T_{eph}}$ as reaction to this concern. By definition $\mathrm{T_{eph}}$ is a linear function of TCB. The rate and the offset between TCB and $\mathrm{T_{eph}}$, being dependent upon the particular ephemeris under consideration, were chosen so that $\mathrm{T_{eph}}-\mathrm{TT}$ remains as small as possible.

One can claim that TDB as defined in 1976 has never been used. Even the widely-used analytical formulas for TDB as function of TT by Hirayama et al. (1987) and by Fairhead & Bretagnon (1990) contain non-periodic terms (mixed and quadratic) while claiming that it is TDB that is realized .

The only good reason to have a scaled version of TCB is to avoid a secular drift between TT and the independent time argument of solar system ephemerides. Since TT (or TAI) is the time scale used by typical users on the Earth, the driving force for TDB is the idea to avoid in practice time scales deviating secularly. This idea, however, does not imply that the difference between that time argument and TT is purely periodic. It just means that the constants in the linear transformation between TCB and the time argument of solar system ephemerides should be chosen to minimize the differences between the latter and TT.

A natural way to relate TCB to TT and to find the optimal linear coeffients for a scaled version of TCB is a direct numerical integration of the TCB(TT) relation using some given solar system ephemeris. This way was discussed in details by Fukushima (1995) and Irwin &

Fukushima (1999). In this numerical approach it is not natural to distinguish between periodic, mixed, secular, etc. terms: TT is calculated as function of TCB.

The current situation with TDB and T_{eph} is unsatisfactory: (1) TDB as originally defined in 1976 is not compatible with widely-used equations of motion, (2) widely-used analytical realizations of TDB are not fully compatible with its original definition, (3) the linear transformation between T_{eph} and TCB is not a part of the definition of T_{eph}, but can be restored aposteriori, and, finally, (4) we have two different time scales for the same purpose. There are several ways to cure, clarify and simplify this situation. Ongoing discussions within the corresponding Working Groups of the IAU will hopefully achieve progress in this controversial question.

REFERENCES

ESA 2004, Proceedings of the Symposium "The Three-Dimensional Universe with Gaia", 4-7 October 2004, Observatoire de Paris-Meudon, France, ESA SP-576

Hirayama Th., Fujimoto M.-K., Kinoshita H., Fukushima T. 1987, Analytical expression of TDB-TDT. Proc. IAG Symposia at IUGG XIX General Assembly, Tome I, p. 91

Fairhead, L., Bretagnon, P. 1990, A&A, 229, 240

Fukushima, T. 1995, A&A, 294, 895

IAU 2001, Information Bulletin, 88 (errata in IAU Information Bulletin, 89)

Irwin, A. W., Fukushima, T. 1999, A&A, 348, 642

Rickman, H. 2001, Reports on Astronomy, Trans. IAU, XXIV B

Soffel, M., Klioner, S.A., Petit, G., *et al.* 2003, Astron. J., 126, 2687

PROGRESS ON THE IMPLEMENTATION OF THE NEW NOMENCLATURE IN THE ASTRONOMICAL ALMANAC

C. HOHENKERK[1], G. KAPLAN[2]
[1]H.M. Nautical Almanac Office
Rutherford Appleton Laboratory, Chilton, Didcot, OX11 0QX, United Kingdom
e-mail: cyh@nao.rl.ac.uk
[2]Astronomical Applications Department, U.S. Naval Observatory
3450 Massachusetts Ave NW, Washington, DC 20392, United States of America
e-mail: gkaplan@usno.navy.mil

ABSTRACT. *The Astronomical Almanac 2006*, published in January 2005, was the first edition to introduce the concepts set out in the IAU 2000 resolutions on positional astronomy. Not only was the IAU 2000A precession-nutation theory used, but the quantities and concepts relating to the Celestial Intermediate Reference System were tabulated and explained. With the preparation of the the almanac for the year 2007 (2007 edition), improvements have been made, which include the recommendations of the IAU Working Group on Nomenclature for Fundamental Astronomy.

This paper focuses on Section B of the 2007 edition of the almanac—Time-Scales and Coordinate Systems—and highlights some of the changes. A summary is also given of the checks made between SOFA and NOVAS, the software libraries that are the basis of the numbers in the almanac.

1. THE ASTRONOMICAL ALMANAC AND THE NEW NOMENCLATURE

The Astronomical Almanac (AsA) is a joint publication of the Nautical Almanac Office of the US Naval Observatory and HM Nautical Almanac Office (HMNAO) of the United Kingdom. The 2006 edition was published in January 2005 and was the first of our almanacs to implement the IAU 2000 resolutions on precession-nutation, the new Celestial Intermediate Origin (CIO), and the Earth Rotation Angle (ERA).

The AsA is a reference product that maintains international standards, so it is important that the AsA incorporate and explain new procedures that are part of those standards. At the same time, the almanac offices have a commitment to continue to serve their users by providing the data that they require. The AsA will continue for the foreseeable future to tabulate quantities and explain traditional techniques using Greenwich apparent sidereal time and right ascension measured from the equinox. For example, the tables of apparent celestial coordinates in the AsA use the traditional coordinate systems, with the equinox as the origin of right ascension. However, for those who wish to use the new techniques, based on the ERA and the CIO, Section B of the AsA—Time-Scales and Coordinate Systems—now tabulates and explains the use of these basic quantities, including a description of how to calculate an object's CIO-based right ascension. The first part of this paper describes the additions to Section B.

A problem that faced the almanac offices with the IAU 2000 resolutions, particularly the recommendation to use the CIO (Celestial Ephemeris Origin, as it was called in the text of the resolution) as the origin of right ascension, was that of nomenclature. New words and phrases were needed for the new concepts. This issue is being addressed by the IAU Working Group for Nomenclature for Fundamental Astronomy (WGNFA) (2003 GA). Although the recommendations of the working group have not yet been ratified by the IAU, many of them have been

included in the 2006 almanac and the upcoming 2007 edition. This has been an iterative process, and there have been some changes in the 2007 edition, particularly in the text, as a result.

Equinox Based		**CIO Based**
True equator and equinox of date		Celestial Intermediate Reference System
Celestial Intermediate Pole (CIP)	=	Celestial Intermediate Pole (CIP)
True equator of date	=	Celestial Intermediate equator
True equinox of date		Celestial Intermediate origin (CIO)
equation of the equinoxes		CIO locator (s)
Apparent place		Intermediate place
Apparent right ascension		Intermediate right ascension
Apparent declination	=	Intermediate declination
Greenwich apparent sidereal time (GAST)		Earth Rotation Angle (ERA)
Greenwich hour angle (GHA)	=	Greenwich hour angle (GHA)

The table above lists the various terms used in the AsA. The left-hand column gives the familiar equinox-based nomenclature while right-hand column gives the new terms that are recommended by the WGNFA. Similarly in the AsA the method for the planetary reduction to Greenwich hour angle and declination is described in parallel (see Figure 1).

Equinox Method — *CIO Method*

***5.** Apply frame bias, precession, nutation, and Greenwich apparent sidereal time to convert from the GCRS to the Terrestrial Intermediate Reference System; origin the TIO and the equator of date.

***5.** Rotate, using $\mathcal{X}$, $\mathcal{Y}$, s and θ to apply frame bias, precession-nutation and Earth rotation, from the GCRS to the Terrestrial Intermediate Reference System; origin the TIO and equator of date.

***6.** Convert to spherical coordinates, giving the Greenwich hour angle (H) and declination (δ) with respect Terrestrial Intermediate Reference System (TIO and equator of date).

Figure 1: Extract from the AsA *Planetary Reduction*

The tables of the almanac for the year 2007 are broadly the same as those for 2006, although there have been some changes in the headings. Figure 2 is an extract from the left-hand page tabulating **NPB**, the equinox-based matrix for transformation from the Geocentric Celestial Reference System (GCRS) to the true equator and equinox of date system.

B42 FRAME BIAS, PRECESSION AND NUTATION, 2007

GCRS TO TRUE EQUATOR AND EQUINOX OF DATE
FOR 0^h TERRESTRIAL TIME

Date 0^h TT	$\mathbf{NPB}_{11}-1$	$\mathbf{NPB}_{12}$	$\mathbf{NPB}_{13}$	$\mathbf{NPB}_{21}$	$\mathbf{NPB}_{22}-1$	$\mathbf{NPB}_{23}$	$\mathbf{NPB}_{31}$	$\mathbf{NPB}_{32}$	$\mathbf{NPB}_{33}-1$
Jan. 0	−14815	−1578 7515	− 685 8885	+1578 7236	−12470	−41 1824	+ 685 9526	+40 0995	−2361
1	−14838	−1580 0005	− 686 4306	+1579 9728	−12490	−40 9686	+ 686 4945	+39 8840	−2364

Values are in units of 10^{-10}. Matrix used with GAST (B12–B19). CIP is $\mathcal{X} = \mathbf{NPB}_{31}$, $\mathcal{Y} = \mathbf{NPB}_{32}$.

Figure 2: Extract showing **NPB** matrix from AsA 2007.

For those who wish to use the CIO-based method, Fig. 3 shows an extract from the corresponding right-hand page, tabulating **C**, the matrix that transforms vectors from the GCRS to the Celestial Intermediate Reference System (CIO and equator of date). The headlines for this pair of pages are identical except that the one on the right-hand page is shaded, maintaining the style adopted to highlight material relating to the CIO. Note as well the similarity of the headings and the replacement of "ICRS" used the 2006 edition by the more correct "GCRS". These matrices are identical except for the 4 elements of the top left-hand corner, which provide the position of the origin of right ascension.

GCRS TO CELESTIAL INTERMEDIATE ORIGIN & EQUATOR OF DATE
FOR 0^h TERRESTRIAL TIME

Julian Date	$\mathbf{C}_{11}-1$	$\mathbf{C}_{12}$	$\mathbf{C}_{13}$	$\mathbf{C}_{21}$	$\mathbf{C}_{22}-1$	$\mathbf{C}_{23}$	$\mathbf{C}_{31}$	$\mathbf{C}_{32}$	$\mathbf{C}_{33}-1$
4100·5	− 2353	− 40	− 685 9526	−235	− 8	−40 0995	+ 685 9526	+40 0995	− 2361
4101·5	− 2356	− 40	− 686 4945	−233	− 8	−39 8840	+ 686 4945	+39 8840	− 2364

Values are in units of 10^{-10}. Matrix used with ERA (B20–B23). CIP is $\mathcal{X} = \mathbf{C}_{31}$, $\mathcal{Y} = \mathbf{C}_{32}$

Figure 3: Extract showing **C** matrix from AsA 2007.

The equation of the origins, the difference between the ERA and GAST, is tabulated with the ERA. Symbols for the tabulated quantities have been added, with E_o, as suggested by WGNFA, representing the equation of the origins rather than the previous symbol o (a confusing choice) used in the 2006 edition.

The traditional tables are all still present: the table of Universal and Sidereal Times, containing Greenwich mean and apparent sidereal time; the position and velocity of the Earth; and the nutation in longitude and obliquity and the true obliquity of the ecliptic. But also now listed with the nutations are $\mathcal{X}$ and $\mathcal{Y}$, the coordinates of the celestial intermediate pole (CIP), and the quantity s, now called the CIO locator.

2. SOFTWARE COMPARISONS

All the quantities tabulated in Section B are calculated using IAU SOFA routines (Wallace 2002), which form the core of HMNAO's software. To ensure that the quality of the AsA is maintained, comparisons have been made between the HMNAO calculations and those of the US Naval Observatory, which are based on NOVAS (Kaplan 1990) version F2.9. The first four columns of the table below are a summary of the comparisons.

The comparisons for each quantity were made for 1101 days at 0^h UT1 or TT as tabulated in the almanac, except for s. All quantities were checked with two more decimal places than are printed. The fourth column gives the number of times the last digit checked was one unit different. Note that for **C** this excludes† elements $\mathbf{C}_{21}$ and $\mathbf{C}_{12}$, where 15% of these were different with a maximum of 5 units in the 12^{th} place. Kaplan evaluated the **NPB** and **C** matrices at 0^h TDB, and calculated s using an independent integration method that provided values every 2 days at 12^h TDB. The differences for the CIO locator s ranged between $\pm 1'' \times 10^{-6}$.

Also considered was the effect on the AsA data of the P03 model of precession (Capitaine et al. 2003) that is being recommended by the IAU Working Group on Precession and the Ecliptic (Hilton et al. 2006). The last two columns of the table give the range of the differences in the terms of the printed precision for the various quantities checked. This demonstrates that the adoption of P03 hardly affects the printed data for years 2006–2008. For this reason, and the fact that it has not yet been adopted by the IAU, it was decided that the P03 model would not be used in preparing the 2007 AsA. The large differences in the true obliquity of date (ϵ) indicated in the table results from the substantial change in the mean obliquity at J2000.0 adopted for P03; thus some ecliptic coordinates will change in the end figures.

These checks on P03 were calculated using a draft version of SOFA that was specially provided and a non-public version of NOVAS.

Comparisons were also made of the method for calculating geocentric apparent planetary positions described in Section B with that implemented in the latest version of NOVAS. This version of NOVAS includes relativistic gravitational light deflection caused by the major planets as well as the Sun. The comparison was made daily at 0^h TT from 2005 to 2015, and agreement

HMNAO (SOFA) − NOVAS 2005-2007				IAU 2000 − P03		
	Decimal Places	Decimal Places	Number of Values 1		2006	2006–2008
Item(unit)	Printed	Checked	Different	Item	in terms of printed precision	
					0.1 ms	
GMST (s)	4	6	0	GMST	$[+0.005, +0.007]$	$[+0.004, +0.008]$
GAST (s)	4	6	1	GAST	$[+0.005, +0.007]$	$[+0.004, +0.008]$
EE (s)	4	6	0			
ERA ($''$)	4	6	0	ERA	$[-0.007, -0.006]$	$[-0.008, -0.005]$
EO ($''$)	4	6	20%			
$\Delta\psi$ ($''$)	4	6	3			
$\Delta\epsilon$ ($''$)	4	6	0		0.1 mas	
ϵ ($''$)	4	6	0	ϵ	$[+41.7, +41.8]$	$[+41.7, +41.8]$
X ($''$)	4	6	15%	X	$[0.00, +0.01]$	$[0.00, +0.01]$
Y ($''$)	4	6	0	Y	$[0.04]$	$[+0.03, +0.05]$
NPB, $\mathbf{C}^\dagger$	10	12	15%	s	$[0.0]$	$[0.00]$

was generally better than $9'' \times 10^{-6}$ in right ascension and declination. However, for the Moon, the differences on a few occasions increased to 0.0003 arcseconds, due to the numeric limitations of the double-precision Julian dates used in the light-time iteration. Also, for Uranus and Neptune the difference between the methods increases to 0.0002 arcseconds when their geocentric positions pass nearly behind Jupiter, due to the difference in light deflection calculations.

3. ADDITIONAL EXPLANATORY MATERIAL

It is the intention of the UK and US almanac offices to continue to review and improve the formulas and text in Section B of the AsA, and comments and suggestions from users are always welcome. A detailed explanation of the IAU resolutions on positional astronomy passed in 1997 and 2000, along with formulas for their implementation, is given in USNO Circular 179 (Kaplan 2005). The circular, which includes the equations for the P03 precession model, is intended for AsA users and others with an interest in positional astronomy. A new edition of the *Explanatory Supplement to the Astronomical Almanac* is in the early stages of preparation.

REFERENCES

Capitaine, N., Wallace, P. T., Chapront, J., 2003, "Expressions for IAU 2000 precession quantities", A&A , 412, pp. 567-586.

Hilton, J. L., Capitaine, N., Chapront, J., Ferrandiz, J. M., Fienga, A., Fukushima, T., Getino, J., Mathews, P., Simon, J.-L., Soffel, M., Vondrak, J., Wallace, P., & Williams, J., 2006, "Report of the International Astronomical Union Division I Working Group on Precession and the Ecliptic", submitted to Celest. Mech. Dyn. Astr.

Kaplan, G., 1990, "NOVAS", Bull. AAS, 22, pp. 930-931; latest version of NOVAS at http://aa.usno.navy.mil/software/novas/.

Kaplan, G., 2005, "The IAU Resolutions on Astronomical Reference Systems, Time Scales, and Earth Rotation Models: Explanation and Implementation", USNO Circular 179, downloadable from http://aa.usno.navy.mil/publications/docs/Circular_179.html and available in print from USNO.

Wallace, P., 2002, "Update to SOFA report", Highlights of Astronomy, 12, p. 128; latest version of SOFA at http://www.iau-sofa.rl.ac.uk.

ROCZNIK ASTRONOMICZNY (ASTRONOMICAL ALMANAC) OF THE INSTITUTE OF GEODESY AND CARTOGRAPHY AGAINST THE IAU 2000 RESOLUTIONS

M. SĘKOWSKI
Institute of Geodesy and Cartography
ul. Modzelewskiego 27, Warsaw, POLAND
e-mail: msek@igik.edu.pl

ABSTRACT. Since 1945 the Institute of Geodesy and Cartography publishes an Astronomical Almanac "Rocznik Astronomiczny". The paper describes the changes made in the RA almanac (edition 2004), according to the new concepts adopted in the resolutions of the XXIV IAU General Assembly in Montreal 2000 (IAU, 2001) and recommended to be applied in astronomical almanacs starting from 1 January 2003.

As the main users of RA almanac are now students of geodesy, for educational aspects a general decision was made to switch to the new CEO concept as well as to present the ICRS – ITRS transformation according to the new paradigm based on a direct use of the CEO and the ERA. For continuity reasons, however, some tables and data were left presented in old version too.

Some problems, caused by the changes, concerning mainly the new concept terminology and the structure of data are also pointed out.

1. INTRODUCTION

There are some points that must be considered when implementing any changes to the almanacs: a) generally almanacs are to provide practical astronomical data; b) almanacs must satisfy the needs of a wide variety of user applications (i.e. navigation, ephemeris computation, planning observing sessions, pointing a telescope, research and education); c) almanacs are expected to be formally unchanged from year to year. There are also particular criteria of when or if to make the changes. The changes should then result in more accurate information, have a reliable scientific motivation and finally they must result in data relevant to the users.

The implementation of the IAU 2000 resolutions requires an adoption of: a) the concept of the Celestial Intermediate Pole (CIP) and the Intermediate Reference System (IRS) as the basis for positions of planets as well as the apparent places of stars; b) the IAU2000 precession–nutation model to replace the IAU1976 and IAU1980 ones for the motion of the Celestial Intermediate Pole (CIP) with respect to the Geocentric Celestial Reference System (GCRS); c) the conventional relationship for defining UT1 as proportional to the Earth Rotation Angle (ERA) between the Celestial and the Terrestrial Ephemeris Origins (CEO and TEO). There are also two equivalent ways for transformation between International Terrestrial and Celestial Systems (ITRS and ICRS): a) based on the new paradigm, with direct use of the CEO and the ERA and b) based

Figure 1: Example cover pages of Astronomical Almanac of IGiK

on classical paradigm, with direct use of the equinox and Greenwich Apparent Sidereal Time (GAST), and indirect use of the CEO and the ERA.

The changes in the RA almanac have been introduced starting from the edition of 2004 (Kryński J., Sękowski M., 2003). Considering the fact that the main group of users of the RA almanac are undergraduate and graduate students of geodesy, a general and fundamental decision was made to switch entirely to the new CEO concept, as well as to present the ICRS – ITRS transformation according to the new paradigm based on a direct use of the CEO and the ERA. These changes have been supplemented by switching from the FK5 system to ICRS (HCRF — Hipparcos Celestial Reference Frame) in the stars' positions and from LE200/DE200 to LE405/DE405 in Solar System ephemeris data. For continuity reasons, however, some parts of the RA almanac were left presented in the old version too.

2. THE CONTENT OF THE RA ASTRONOMICAL ALMANAC

The content of the RA astronomical almanac consists of several tables that generally can be classified into two sets of data. These are the primary data, used by a large majority of users: students, professional users but also the amateurs of astronomy; and the secondary data, mainly dedicated for specific or particular astro-geodetical applications, but also covering less important or not so often used astronomical data. The primary data are grouped into tables of sidereal time, Sun and Moon apparent equatorial co-ordinates, mean positions of stars, Besselian numbers and the apparent positions of selected stars. The secondary data are the tables of the Earth orientation parameters (x, y pole co-ordinates, UT1 − UTC), the tables of azimuth and zenith distance of Polaris, the tables for calculation of astronomical latitude from the altitude of Polaris, as well as the tables of equatorial co-ordinates of planets and tables for calculation the rises and sets of Sun, Moon and the planets. The RA almanac contains also an astronomical calendar, list of stellar constellations, set of simple sky maps, dates of introducing a daylight-saving time in Poland, a map of magnetic declination of Poland and other data. Finally the almanac is supplemented with a detailed description of the history and present of the celestial, terrestrial and time systems used with the extensive explanations, as well as practical examples

of corresponding transformations and algorithms.

Before the changes coming from the IAU 2000 Resolutions were introduced, the RA almanac Sidereal Time tables consisted of four columns. They were the GMST (Greenwich Mean Sidereal Time) data, the long- and short-period components of nutation and the GAST (Greenwich Apparent Sidereal Time) data. The data were presented for 0^h UT1 with 1 day interval. They were calculated according to the formulae adopted by IAU GA (Montreal, 1979; Patras, 1982) (IAU, 1980; 1983), IAU80 nutation theory (McCarthy, 1996) and the equation of the equinoxes in the form: $\mathrm{GAST} = \mathrm{GMST} + (\Delta\psi + \delta\psi)\cos\varepsilon_0$.

The Sun and Moon tables contain the respective apparent positions, placed in a table with 1 day interval, as well as some additional parameters including e.g. the Sun and Moon parallaxes and rises and sets in Warsaw. Before changes were made, the data were based on the DE200/LE200 planetary ephemeris, IAU76/IAU80 precession–nutation theory and were calculated for 0^h in TDT time scale. In computations the classical formula for the annual aberration was used. The equation of time values, which are also included in the tables with 1 day interval, were calculated on the basis of the formula: $E + 12^h = \mathrm{GAST} - \alpha_\odot|_{\mathrm{TDT}=0^h}$.

The tables of mean positions of stars, containing 949 stars homogeneously distributed on the northern and partially southern hemisphere, based on the data of the FK5 fundamental catalogue, were expressed in the FK5 System. The positions were computed every year for the epoch of the middle of the year using the IAU76 precession formulae (Lieske et al., 1977). Along with the mean positions the tables contained also stars' FK5 numbers, visual magnitudes, spectral types, parallaxes and the annual rate of mean position change.

The mean positions tables are followed by the tables of Besselian numbers to provide a possibility of computation an apparent position for each star starting from its mean position. The Besselian numbers which are derived from the precession constant and long- and short-period nutation series were computed according to the IAU76 system of constants and IAU80 nutation theory. The tables consist of columns presenting the Besselian number (A, A', B, B', C, D, E) as well as part of year parameter (τ) at 0^h sidereal time, in 1 sidereal day interval.

The RA almanac contains also the data of apparent places of 61 selected stars, including 56 stars of declination in the range of $-30^\circ \div 80^\circ$ and 5 northern circumpolar stars. The apparent places of stars are placed in a table with 10 days interval (1 day in the case of circumpolar stars). The data are supplemented with the double upper transit date (for circumpolar stars a lower transit date is given too). Consequently, as in the case of mean position tables from before the RA 2004 edition, the tables of apparent places were based on the data of the FK5 catalogue and were expressed in the FK5 System. The algorithm is based on a simple formula for shifts due to proper motions, transformation from the barycentric to geocentric systems with use of star parallaxes and the formulae for light deflection and annual aberration. The combined matrix of IAU76 precession and IAU80 nutation matrices was used.

3. CHANGES MADE IN THE ASTRONOMICAL ALMANAC IN 2004

Changes into the RA almanac due to the IAU Recommendations were introduced starting from the edition for the year 2004. The general decision has also been made to fully adopt the new concepts including the changes in the right ascension origin. For continuity reasons, however, most of the old tables are still kept. There are thus in the RA some new tables added and some tables that have been doubled with their new versions. There are also some tables left unchanged, some changed by adding the new data or by an application of new definition, theory or formulae.

The Sidereal Time tables were extended by adding a new column of the ERA and changed by adoption the new formula for the GMST (Capitaine et al., 2003) relating it to the ERA. The tables contain now four columns representing GMST, GAST and θ (ERA) for 0^h UT1.

CZAS GWIAZDOWY GREENWICH I KĄT OBROTU ZIEMI 2005

DATA		0^h UT1				DATA		0^h UT1			
		GMST	Eq	GST	ERA			GMST	Eq	GST	ERA
			$0^s.0001$						$0^s.0001$		
Styczeń	0	$6^h39^m02^s.3728$	−4526	$01^s.9202$	$6^h38^m47^s.0041$	Luty	15	$9^h40^m23^s.9197$	−3788	$23^s.5410$	$9^h40^m08^s.1637$
	1	6 42 58.9282	−4532	58.4750	6 42 43.5510		16	9 44 20.4751	−3783	20.0968	9 44 04.7107
	2	6 46 55.4835	−4557	55.0278	6 46 40.0980		17	9 48 17.0305	−3756	16.6548	9 48 01.2576
	3	6 50 52.0389	−4593	51.5796	6 50 36.6449		18	9 52 13.5858	−3715	13.2144	9 51 57.8046
	4	6 54 48.5943	−4627	48.1316	6 54 33.1919		19	9 56 10.1412	−3667	09.7745	9 55 54.3515
	5	6 58 45.1496	−4645	44.6851	6 58 29.7388		20	10 00 06.6966	−3623	06.3342	9 59 50.8985
	6	7 02 41.7050	−4633	41.2417	7 02 26.2858		21	10 04 03.2519	−3592	02.8927	10 03 47.4454
	7	7 06 38.2604	−4580	37.8024	7 06 22.8327		22	10 07 59.8073	−3581	59.4492	10 07 43.9924
	8	7 10 34.8158	−4484	34.3674	7 10 19.3797		23	10 11 56.3627	−3595	56.0032	10 11 40.5393
	9	7 14 31.3711	−4354	30.9357	7 14 15.9266		24	10 15 52.9180	−3635	52.5545	10 15 37.0863

Figure 2: Astronomical Almanac 2005: example of the table of Sidereal Time & ERA

The data interval of 1 day has not been changed. Former two columns of long- and short-period components of nutation have been reduced to one column of total equation of the equinoxes. The main reason of that is a recent computation algorithm. The equation of the equinoxes values are computed on the basis of new IAU2000 precession–nutation theory and the IAU2000 algorithms in their presently published form do not provide the separation between long- and short-period components.

The main subject of the Sun and Moon tables is, as in the previous RA editions, the respective apparent positions, tabulated with 1 day interval for 0^h in TT time scale. However, position computation is based now on DE405/LE405 planetary ephemeris. The IAU2000 precession–nutation model is fully applied as well as more sophisticated, relativistic formulae for annual and planetary aberrations are used. Besides, the main change is an extension of the existing data by adding new column of $\alpha_{app}^{\mathrm{CEO}}$. The equation of time values are calculated now on the basis of the formula: $E + 12^h = \mathrm{ERA} - \alpha_{\odot}^{\mathrm{CEO}}|_{\mathrm{TT}=0^h}$. Additional data including e.g. Sun and Moon rises and sets in Warsaw are presented with no changes.

The major change concerning the data of mean positions of stars is a supplement of existing tables (left unchanged, in FK5 System) by the new ones providing the ICRF (HCRF) positions of the stars for the epoch of the year (concerning only the proper motion of stars). The adoption of the ICRS which is motionless in outer space makes the mean positions data more or less redundant. Movements due to precession and nutation are now concerned jointly within the transformation from ICRS (GCRS) to IRS procedure. The old tables as well as the new ones are kept then just for continuity and educational reasons. The new tables contain the same 949 stars. The data are the Hipparcos catalogue positions, supplemented with FK6 (FK5) radial velocities. Computations from the epoch of the Hipparcos catalogue (J1991.25) are based on the Standard Model of Stellar Motion (ESA, 1997).

Tables of Besselian numbers for the reasons mentioned above have not been changed too and they are left referred to IAU76 system of constants and IAU80 nutation theory.

The RA almanac data of stars' apparent places have also been modified by adding supplementary tables realizing the new concepts. The added tables contain $\alpha_{app}^{\mathrm{CEO}}$, δ_{app} co-ordinates of the same set of stars as the old tables do. The data are presented for 0^h UT1 with 7 days interval (1 day in the case of circumpolar stars). Computations are based on the Hipparcos positional data complemented with the FK6 (FK5) radial velocities of stars. The main improvements in the algorithm for apparent places computations are due to the adoption of the Standard

Model of Stellar Motion instead of former simple formulae and the replacement of IAU76/IAU80 precession–nutation matrix with the new IAU2000 matrix.

Along the changes due to the IAU Resolutions, but also aiming to provide a complete data set for transformation between terrestrial and celestial systems for those who use the Almanac in their educational activity there are also some new tables added. These are, first of all, the table containing the components of the precession–nutation matrix (Q). The table of barycentric and heliocentric position and velocity of the Earth was also added. The data in the tables are computed on the basis of IAU2000 model and DE405/LE405 ephemeris and are tabulated with 1 day interval for 0^h TT and TDB respectively.

Finally, the new editions of RA almanac are supplemented with the extensive description of the systems and explanations of all changes coming from the recent IAU Resolutions. The text of IAU 2000 Resolutions in Polish translation have also been published in the RA almanac issue of 2004.

4. PROBLEMS TO BE SOLVED

There are still some problems remaining to be solved. The first group of them are the problems concerning a proper or standard terminology and symbolic designations, e.g. naming of α^{CEO}. In the RA almanac the term "right ascension" is applied to both α^{CEO} and α^{γ} quantities. Also the designation α^{CEO} is used instead of sometimes suggested A. There are also some abbreviation problems concerning newly introduced systems and frames. In the RA almanac the abbreviation IRS is adopted and consequently used for the Intermediate Reference System. Two other designations $\mathrm{IRS}_{CELESTIAL}$ and $\mathrm{IRS}_{TERRESTRIAL}$ are also used to distinguish between IRS before and after applying the transformation due to Earth rotation ($R_3(\theta)$).

The second group of problems concerns the interpolation of the tabularized data. Publication of the apparent places of stars with 10- or 7-days interval is not sufficient for reliable interpolation when the short-period nutation terms are not filtered out. The same concerns the interpolation of the components of precession–nutation matrix (Q). There is a need then to redesign the IAU2000 algorithms to allow separate application of long- and short-period nutation terms.

REFERENCES

Capitaine N., Wallace P. T., McCarthy D. D., 2003, "Expressions to implement the IAU 2000 definition of UT1", A&A 406, pp. 1135–1149.

ESA, 1997, "The Hipparcos and Tycho Catalogues", ESA SP–1200.

IAU, 1980, Transactions of the IAU Vol. XVII B, D. Reidel, Dordrecht, The Netherlands.

IAU, 1983, Transactions of the IAU Vol. XVIII B; D. Reidel, Dordrecht, The Netherlands.

IAU, 2001, Transactions of the IAU Vol. XXIV B, "Proceedings of the Twenty-Fourth General Assembly, Manchester, UK, August 7–18, 2000"; ed. H. Rickman, Astronomical Society of the Pacific.

Kryński J., Sękowski M., 2003, Rocznik Astronomiczny, vol. LIX.

Lieske J. H., Lederle T., Fricke W., Morando B., 1977, "Expressions for the precession quantities based upon the IAU (1976) system of astronomical constants", A&A 58, pp. 1–16.

McCarthy D. D., 1996, IERS Conventions, IERS Technical Note 21.

SUMMARY OF THE DISCUSSION ON

"The status of the implementation of the IAU 2000 resolutions and the proposals of the IAU working group on Nomenclature for Fundamental Astronomy"

N. CAPITAINE
Chair of the IAU Working Group on
Nomenclature for Fundamental Astronomy (NFA)

This discussion took place after Session 2.2 entitled "Implementation of the IAU Resolutions and new nomenclature" chaired by J. Vondrák (see the Table of contents). A few points were introduced by N.Capitaine and J. Vondrák and were submitted to the audience for comments and discussion. The discussion on these points is summarized below.

(1) The status of the implementation of the IAU 2000 resolutions in data reduction

The progress with implementing the IAU 2000 Resolutions in the reduction of VLBI and GPS data was discussed. Information was provided about the consideration of the issue within the International VLBI Service for Geodesy and Astrometry (IVS) and the International GNSS Service (IGS). A number of software projects for reducing the data were reported to be in the process of being updated accordingly (mainly based on the IERS Conventions 2003 and SOFA software packages).

(2) The status of the implementation in the astronomical almanacs

Additionally to the progress that was reported in Session 2.2 about the implementation of the IAU 2000 resolutions and new nomenclature in *The Astronomical Almanac* (by USNO/HMNAO) and in the *Astronomical Almanac* of Institute of Geodesy and Cartography (Warsaw, Poland), information was provided by a few participants about the future plan for other Almanacs, especially the Russian, Japanese and French Almanacs.

(3) The status of the WG of the American Astronomical Society on the IAU 2000 Resolutions

After the 2003 IAU General Assembly, some concern was expressed to the IAU and the IERS by the American Astronomical Society (AAS) about the impact of the IAU 2000 Resolutions on astronomers. A special session of the AAS was organized in June 2004 on "The Reference System Resolutions of the IAU" and a Working Group on "The IAU Reference Frame Resolutions" was created to look at the consequences of the recent IAU resolutions on reference systems for astronomers. The chair of that Working Group, J. Hilton (USNO), reported on the work and especially on the WG document in preparation that would provide all classes of astronomer with a sound introduction to the IAU 2000 resolutions. Moreover, a USNO Circular was prepared by G. Kaplan that would provide explanatory and implementation information concerning astronomical reference systems and the IAU resolutions.

(4) The update of the IERS Conventions

B. Luzum (USNO), co-responsible with G. Petit (BIPM) of the IERS Conventions Center, explained the plan for updating the IERS Conventions. A special page of the IERS Conventions web site at BIPM provides update of the IERS Conventions. It contains all corrections to the IERS Conventions (2003) that have been identified and a list of update changes since the last approved version. It must be considered as being a working version that is under development and is not definitive nor officially approved as a registered edition. Moreover a discussion forum has been established to receive, classify and archive comments and contributions on the update of the IERS Conventions. An update of the IERS Conventions is planned to take into account the NFA recommendations on terminology and the IAU 2006 Resolutions.

(5) The new IAU rules for the adoption of IAU Resolutions

T. Fukushima, Division 1 President, explained the foreseen process for submitting and adopting new IAU Resolutions at the next General Assembly in August 2006. Resolution proposals are being prepared by the IAU Working Groups on "Precession and the Ecliptic"' and on "Nomenclature for Fundamental Astronomy" in order to be submitted to the IAU before the IAU deadline (15 May 2006).

(6) Needs on nomenclature

Some points of the latest proposals of the IAU NFA Working Group on nomenclature that were presented during Session 2.2 were discussed. No additional need on nomenclature was identified; a few corrections were proposed to the wording of the NFA Resolution proposal.

(7) Versions of the NFA Glossary in other languages

The NFA IAU 2000 Glossary prepared by the NFA Working Group provides a set of detailed definitions (in English) that best explain all the terms required for implementing the IAU 2000 resolutions, including a few newly proposed terms. Those definitions will require translation into different languages. The NFA Working Group members will be able to translate the NFA Glossary into French. Some difficulties with translation to other languages were reported.

Session 2.3

PRECESSION, NUTATION AND POLAR MOTION:
Presentations of progress in the "Descartes-Nutation" projects

PRÉCESSION, NUTATION ET MOUVEMENT DU PÔLE :
Présentation des progrès du projet "Descartes-Nutation"

NEXT DECIMAL FOR NUTATION MODELING

V. DEHANT
Royal Observatory of Belgium
3 avenue Circulaire, B-1180 Brussels, Belgium
e-mail: v.dehant@oma.be

1. INTRODUCTION AND PRESENT SITUATION CONCERNING THE NUTATION MODELING

The nutation model adopted by the IAU and the IUGG in 2000/2003 has been elaborated on the basis of the model MHB2000, a work of Mathews et al. (2002), and the rigid Earth nutation REN2000 of Souchay et al. (1999). The differences between the very Long Baseline Interferometry (VLBI) observations and the theory are at the milliarcsecond (mas) level in the time domain. Consequently, the next decimal for modeling is at the sub-centimeter level in pole position. The adopted model is based on a seismic model for the rheological properties inside the Earth from which the deformations are computed, and the Liouville equations are derived for a three-layered Earth for computing the nutational motions. There is an elastic inner core, a liquid outer core, and an inelastic mantle. The three layers are flattened and the Earth has a uniform rotation, which is used to compute the flattening of the inner core in hydrostatic equilibrium. Deviation from the hydrostatic equilibrium is considered for the core flattening and the global Earth dynamical flattening. The ocean tides, the mantle inelasticity, and a constant atmospheric contribution to the prograde annual nutation are considered. MHB2000 has been built from a fit of some geophysical parameters on the VLBI observations. The rigid Earth nutation model REN2000 accounts for the luni-solar gravitational attraction on Earth, the direct and indirect effects of the planets, the coupling effect induced by J_2 (the so-called J_2-tilt effect), the second order terms related to the Earth precession-nutation effects on the nutations. The new model is the result of the convolution of the Earth transfer function and these rigid Earth nutations, and considers in addition, the ocean tide and atmospheric contributions. It brings the theory close to the observations. Nevertheless, when compared to the observations, remaining residuals appear at the level of the mas.

2. IMPROVEMENT IN THE EXPRESSION OF THE OBSERVATION VARIABLES

Previously and for the adopted model, the nutation variables used were $\Delta\psi$ and $\Delta\epsilon$, the so-called nutation in longitude and in obliquity respectively. However, due to the new adopted procedure to pass from the terrestrial frame to the celestial frame, based on the adopted Non Rotating Origin scheme, one uses the variables X and Y (see Capitaine et al., 1986, 2003, and Capitaine, 2005, this issue). For this reason, Folgueira et al. (2005, this issue) and Souchay et al. (2005, this issue), have examined a new formulation for the Earth Rotation Parameters (ERP). They have established and integrated the equation of the Earth rotation using the ERP as defined by the IAU in 2000, using (X, Y). They have construct the relation that shows the

equivalence between the use of $\Delta\psi$ and $\Delta\epsilon$ and the use of (X, Y).

3. IMPROVEMENTS IN OBSERVATION AND IN FITTING PROCEDURE OF THE GEOPHYSICAL PARAMETERS

Fey (2005, this issue) has mentioned the improvement in technology of VLBI observations and of their treatment, in the modeling of the phenomena which must be considered to improve the residuals such as the tropospheric corrections. Additional improvement in coverage of the sky and the increase of the number of stations participating in the networks, allows a better geometry of the VLBI networks. Titov (2005, this issue, se also Feissel-Vernier, 2003) also mentioned the corruption from source instabilities, and proposes a selection procedure. Charlot (2005, this issue) addressed as well the problems related to the source structure and showed the improvement from their knowledge.

The geophysical parameters such as the global Earth flattening, the core flattening, the dissipation at the Core-Mantle Boundary (CMB) and at the Inner Core Boundary (ICB), are generally fitted using the nutation amplitudes and phases in the frequency domain. However, this does not allow to account for the noise in the data, which is a function of time. Additionally, some of the corrections such as the atmospheric effects on nutation are not constant with time when considering each frequency component. They are better represented in the time domain. For this reason, Koot et al. (2005, this issue) have used a Bayesian approach to fit the parameters. This method is very promising.

4. IMPROVEMENT IN THE COUPLING MECHANISM AT CMB

The coupling mechanisms which could play a role in Earth rotation are the following:

1. the so-called inertial coupling related to the gravitational interaction between the flattened three layers of the Earth,
2. the gravitational coupling between the mass anomalies in the mantle and in the core,
3. the electromagnetic coupling,
4. the viscous coupling, and
5. the topographic coupling.

The first coupling mechanism, the inertial coupling, has been considered in the adopted model and thus does not need further improvement. The second coupling has been shown to be negligible by Defraigne et al. (1996). The electromagnetic coupling has already been considered for a part in MHB2000. At diurnal timescale, there exists a large relative motion of the core with respect to the mantle (see Figure 1). This motion is associated with the nutations and is particular important for nutations near the resonance at the Free Core Nutation (FCN). The magnetic field lines are following the global motion in the main part of the layer but there is a shearing of the magnetic field due to the relative rotations (see Figure 1). This interaction is not only considered at the CMB between the mantle and the fluid outer core, but also at the ICB, between the fluid outer core and the solid inner core. The magnetic field considered in the model has two components: (1) the most important part of the field, i.e. the dipole part, and (2) a uniform field representing the remaining contributions. In a recent paper, Delaplace and Cardin (2005) have recomputed the electromagnetic coupling for a global field developed in spherical harmonics. They of course used the recent values of the field as determined from the recent satellite missions.

In parallel, Huang et al. (2004, and 2006 in preparation) consider the coupling between the deformation equation and the induction equation. They have added a Lorentz force in the motion equation and considered the induction equation relating the magnetic field and the velocity field in the core. This is an ongoing very promising work.

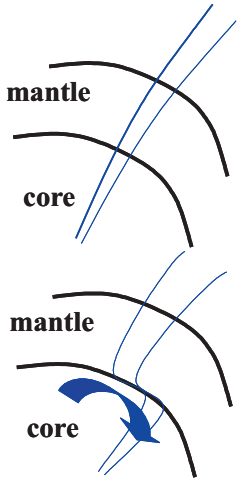

Figure 1: Magnetic field lines with and without the diurnal differential nutation of the core with respect to the mantle.

Topographic coupling must be considered in the future nutation models. It consists of considering the fluid pressure effects on the CMB topography (see Figure 2). Wu and Wahr (1997) have considered the topographic coupling and have analytically developed the torque acting on the core-mantle boundary. This needs to be evaluated in the light of new topography from seismologic tomography.

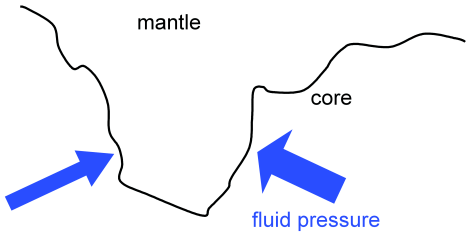

Figure 2: Representation of the topographic torque induced by the fluid pressure acting at the CMB.

Viscous coupling has been shown to be very small. However, the existence of an effective viscosity (Brito et al., 2004) has been discovered from laboratory experiment. For that reason, viscous coupling is not considered as negligible any more. Mathews and Guo (2005), on the one hand, and Deleplace and Cardin (2005), on the other hand, have computed the effects of this coupling mechanism between the core and the mantle and its influence on nutation (see Figure 3 for a representation of this coupling mechanism).

Concerning the coupling mechanisms at ICB, electromagnetic and viscous coupling must be considered, but no topographic coupling is evaluated because the inner core is considered to be

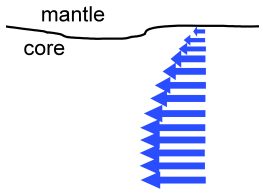

Figure 3: Viscous coupling between the core and the mantle.

in hydrostatic equilibrium.

5. CONSIDERATION OF THE INNER CORE VISCOSITY

Greff et al. (2000 and 2002) have considered the viscosity of the inner core in the computation of the nutations. They investigated the perturbations induced by the nearly-diurnal luni-solar tidal potential considering the effects of the magnetic friction at the inner core boundary (ICB) and considering the inner core viscosity. They showed that VLBI observations of the in-phase and out-of-phase components of some nutations can give information on the viscosity of the inner core and on the amplitude of the radial component of the magnetic field at the ICB. The effects are generally very small but at the level of the nutation observation precision. Generally speaking the electromagnetic field must be even larger when the inner core viscosity is considered than without considering the inner core viscosity. There is one exception to the generally small effect of the inner core viscosity: the effect on the 18.6 year nutation. The amplification due to the long period of this nutation can lead to a variation of the amplitude, induced by different viscosity and friction parameters, of a few tenths of milliarcsecond, well above the VLBI precision. In the model MHB2000, Mathews et al. (2002) do not account for the inner core viscosity but do consider the electromagnetic coupling at the CMB and ICB. They have modeled the non-elastic behaviour of the inner core with frequency dependent rheological parameters (they consider a frequency-to-the power-law for the rheology). This does not cover the whole range of viscosity possibilities but must be considered as a first step. Considering a Maxwell body rheology allows Greff et al. (2000 and 2002) to describe a completely solid inner core, a completely fluid behaviour, and all the intermediate states of the inner core rheology. This has allowed them to examine the behaviour of the forced nutations as a function of the different possible ranges of the electromagnetic frictional coupling constant as well as of the inner core viscosity.

6. PRECESSION CONSTANT

The precession constant can be deduced from the precession and nutation observation after correction of the non luni-solar contribution to precession. It is proportional to the differences of the moments of inertia of the whole Earth or the so-called dynamical flattening of the Earth. This parameter also enters in the principal nutation amplitudes. A fitting on the observation of precession and of nutation for this parameter has therefore been done by Mathews et al. (2002). A readjustment of the precession is discussed in Capitaine et al. (2003) and in Hilton (this issue). In their paper, Capitaine et al. (2003) discuss precession models consistent with the IAU2000A precession-nutation (i.e. MHB2000, provided by Mathews et al. 2002) and provide a range of expressions that implement them. They have developed new expressions for the motion of the ecliptic with respect to the fixed ecliptic using the developments from Simon et

al. (1994) and Williams (1994) and with improved constants fitted to the most recent numerical planetary ephemerides. The final precession model, designated by P03, is a possible replacement for the precession component of IAU2000A, considering the improved dynamical consistency and a better basis for future improvement.

G. Bourda in her thesis (2004) has considered the coupling between J_2 and the precession constant as based on same geophysical parameters, and their time variation. The possibility to have time variation of the precession constant is considered in the P03 solution of Capitaine et al. (2003).

7. SECOND ORDER EFFECTS

The next step for nutation is the consideration of all second order effects that have been neglected in MHB2000. Dehant and Mathews are examining these terms for their book (in preparation). I only provide here a non exhaustive list of what can be expected.

1. Second order effects due to Liouville equations developed up to the second order in the wobbles: the Liouville equations contain linear terms in the wobble amplitudes m_i and the moment of inertia components c_{ij} and first order in the small quantities such as the dynamical flattenings of the whole Earth and of the core or the so-called compliances (directly related to deformability). Second order terms in the small quantities and in m_i, in particular the coupling between m_3 and m_1, m_2, must be considered.

2. Poincaré motion is considered in the liquid core. This is a strong approximation that certainly must be studied. One possibility is to consider second order of the core relative angular momentum due to second order in Poincaré motion.

3. The geometrical flattening was considered as equal to the dynamical flattening, which is not the case as the Earth is not in hydrostatic equilibrium.

4. The torques acting at the fluid core-mantle boundary involve the normal to the surface, which is expressed at the first order and should be extended as well.

5. The expression of the initial products of inertia for the whole Earth can be considered at second order.

6. Second order effects due to triaxiality can be considered. One finds already some work in that direction in the literature. Zharkov and Molodensky (1996), Gonzalez and Getino (1997), Van Hoolst and Dehant (2002) have also examined these effects and in particular have estimated the changes in the normal modes such as the Chandler Wobble.

7. The second order in C_{nm} S_{nm} (coefficients of the Earth gravitational potential) contributions to the external torque are related to additional gravitational interaction with respect to the classical interaction between the ellipsoidal Earth (J_2-part of the Earth gravity) and the celestial bodies (the Moon, the Sun, and the other planets). These effects induce non-retrograde-diurnal contributions as well in the terrestrial frame (see Bretagnon and Mathews, 2003, see also Lambert and Mathews, 2006).

8. Additional contributions to the torque acting on the Earth from the gravitational interaction between the external celestial bodies and the tidally deformed Earth (Lambert and Mathews, 2006).

9. Effect of coupling between the gravitational potential acting on an Earth which has tides (Lambert and Mathews, 2006).

8. EFFECT OF THE GEOPHYSICAL FLUIDS

The most important contribution of which the computation must be improved is the effect of the atmosphere, the ocean, and possibly the hydrosphere.

A few remarks need to be done at this level:

1. These contributions are not constant with time. They contain seasonal modulations, but the amplitudes of the sine and/or cosine of the seasonal period are not constant with time.

2. The computation from the angular momentum approach are not yet perfect as based on not enough sampling in the time domain for representing diurnal contribution.

3. Although the torque approach for computing the response of the Earth to the loading and attraction of the geophysical fluids provides very nice insight on the physical mechanisms of transfer of angular momentum, it is less precise than the angular momentum approach.

In Figure 4, we provide the wavelet transform of the atmospheric angular momentum contribution to nutation and the residuals between the VLBI observations and the MHB2000 model.

From this figure one can see that there is much more power in the nutation residuals than in the atmosphere angular momentum. This leaves some rooms for the ocean and hydrological contributions. Particular efforts have been recently done on the FCN excitation and the FICN excitation.

Concerning the FCN excitation, many Descartes Fellows are working on it as this is an important limitation of MHB2000 model. On the other hand, the residuals that are seen in a period range between 500 and 1000 days also intrigued the scientists. They are presented in Figure 5.

The large residuals that were seen in the nutation and were not yet explained by MHB2000 were believed to be related to an excitation of the FICN. However, a white noise excitation of this mode does not provide amplitude high enough to explain this (Dehant et al., 2005). The reality must be found in the network configuration (see Feissel-Vernier and Ma, 2005).

9. CONCLUSIONS

The new adopted nutation model is precise at a couple of centimeter level at the Earth surface. The advance in analytical, numerical, and observational works will therefore have to understand the physics and to consider all the contributions at the millimeter levels. We have here summarized a few steps in these directions. They are addressing the coupling mechanisms at the core-mantle boundary and at the inner core boundary, all the second order effects that are necessary to be included, and the geophysical fluid contributions. The Advisory Board of the Descartes Nutation Prize has therefore selected proposals in these directions. The new Descartes Nutation Fellows are listed her below. The theme of their research is also provided.

1. 'Dynamical Flattening and Geophysical Fluids Combination' (with a GGOS flag), Laura Fernández, 6 months, working with Harald Schuh at Technical University of Vienna;

2. 'Relations between the EOP and the variations of the Earth gravity field, through the inertia tensor', (with a GGOS flag), Géraldine Bourda, 6 months, working with Harald Schuh at Technical University of Vienna;

3. 'Investigation of excitations of nutation from geophysical fluids', Yonghong Zhou, 6 months, working with David Salstein at AER (Atmospheric and Environmental Research), USA;

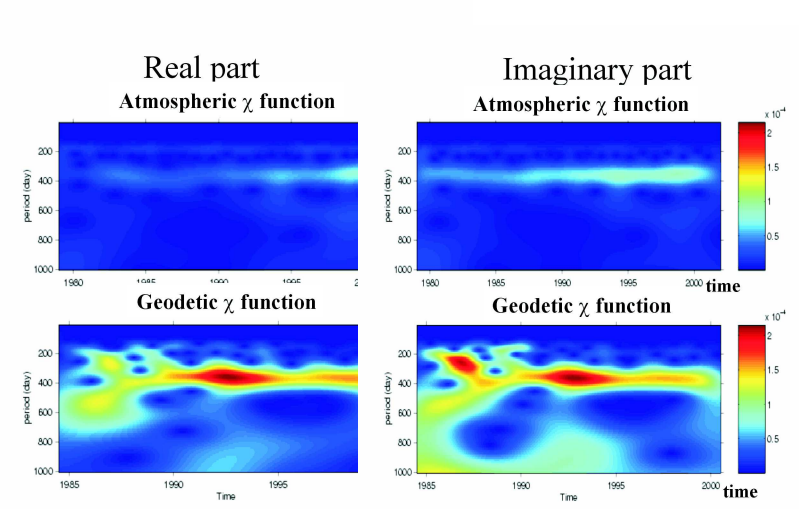

Figure 4: Real part (left) and imaginary part (right) of the atmosphere angular momentum (top graphics) and the geodetic observed residuals (bottom graphics).

4. 'Modeling and prediction of the FCN; Study of the atmospheric and non-tidal oceanic effects on nutation', Maciej Kalarus, 6 months, working with Harald Schuh at Technical University of Vienna (3 months) and with Tom Johnson at US Naval Observatory, USA (3 months);

5. 'Modeling atmospheric and oceanic contribution to nutation', Sergei Bolotin, 6 months, working with Aleksander Brzeziński at Space Research Center in Poland;

6. 'Study of the FCN and subdaily variability of polar motion and length of day', Maria Kudryashova, working with Aleksander Brzeziński at Space Research Center in Poland;

7. 'Coupling and new nutation model from observation', Laurence Koot, 2 months, working with Veronique Dehant, at Royal Observatory of Belgium;

8. 'Advances in the integration of the equations of the Earth's rotation in the framework of the new parameters adopted by the IAU 2000 Resolutions', Marta Folgueira, 6 months, working with Nicole Capitaine at Paris Observatory, France;

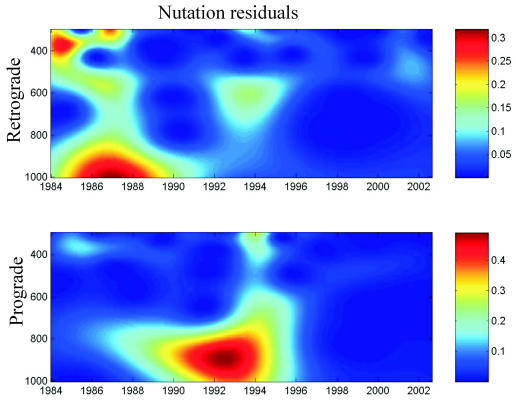

Figure 5: Nutation residuals (VLBI-MHB2000).

9. 'Geophysical effects of considering the new solutions for the Earth's rotation in the framework of the new parameters adopted by the IAU 2000 Resolutions', Marta Folgueira, 3 months, working with Veronique Dehant at Royal Observatory of Belgium;

10. 'Future of nutation from combination between GPS and GALILEO', Kristyna Snajdrova, 1.5 year, working with Harald Schuh at Technical University of Vienna (in collaboration with Veronique Dehant at Royal Observatory of Belgium);

11. 'Computation of the coupling mechanisms at the core-mantle boundary from a finite element approach; geodynamo model integration for the electromagnetic coupling', Laurent Métivier, 6 month from Descartes Prize and 6 months from a GSFC grant, working 3 months with Véronique Dehant at the Royal Observatory of Belgium and 9 months with Weijia Kuang at Goddard Space Flight Center, USA.

REFERENCES

Bourda G., 2004, "Terrestre et variations du champ de gravité : étude et apport des missions CHAMP et GRACE.", PhD thesis, Observatoire de Paris, France.

Brito D., Aurnou J., and Cardin P., 2004, "Turbulent viscosity measurements relevant to planetary core mantle dynamics.", Phys. Earth planet. Inter. 141(1), pp. 3-8.

Capitaine N., Guinot B., and Souchay J., 1986, "A non-rotating origin on the instantaneous equator: definition, properties and use.", Celest. Mech. 39, pp. 283-307.

Capitaine N., Wallace P., and Chapront J., 2003, "Expressions for IAU2000 precession quantities.", A&A 412, pp. 567-586.

Defraigne P., Dehant V., and Wahr J.M., 1996, "Internal loading of an homogeneous compressible Earth with phase boundaries.", Geophys. J. Int. 125, pp. 173-192.

Dehant V., de Viron O., Greff-Lefftz M., 2005, "Atmospheric and oceanic excitation of the rotation of a three-layer Earth.", A&A 438, pp. 1149-1161, DOI: 10.1051/0004-6361:20042210.

Deleplace B. and Cardin P., 2006, "Viscous and Electromagnetic Coupling at the Core Mantle Boundary.", Geophys. J. Int. in press.

Feissel-Vernier M. and Ma C., 2003, "Selecting stable extragalactic compact radio sources from the permanent astrogeodetic VLBI program.", A&A 403, 105.

Feissel-Vernier M., 2003, "Selecting stable extragalactic compact radio sources for the maintenance of the ICRF axes.", in: proc. 4th IVS workshop, Paris, France.

Getino J., Gonzalez A.-B., and Escapa A., 1997, "The rotation of a non-rigid, non-symmetrical Earth II: free nutations and dissipative effects.", Celest. Mech. Dyn. Astr. 76(1), pp. 1-21.

Greff-Lefftz M., Legros H., and Dehant V., 2000, "Influence of the inner core viscosity on the rotational eigenmodes of the Earth.", Phys. Earth planet. Inter. 122, pp. 187-204.

Greff-Lefftz M., Dehant V., and Legros H., 2002, "Effect of inner core viscosity on gravity changes and spatial nutations induced by luni-solar tides.", Phys. Earth planet. Inter. 129(1-2), pp. 31-41.

Huang C., Dehant V., and Liao X., 2004, "The explicit equations of infinitesimal elastic-gravitational motion in the rotating, slightly elliptical fluid outer core of the Earth.", Geophys. J. Int. 157(2), pp. 831-837, DOI: 10.1111/j.1365-246X.2004.02238.x.

Lambert S. and Mathews P.M., 2006, "Second order torque on the tidal redistribution and the Earth's rotation.", A&A submitted.

ON THE RESEARCH PROGRESS OF DESCARTES-SUBPROJECT: "Advances in the integration of the equations of the Earth's rotation in the framework of the new parameters adopted by the IAU 2000 Resolutions"

M. FOLGUEIRA[1,2], N. CAPITAINE[2] and J. SOUCHAY[2]

[1] Instituto de Astronomía y Geodesia (UCM-CSIC),
Facultad de CC. Matemáticas, Universidad Complutense de Madrid,
Plaza de Ciencias, 3. Ciudad Universitaria, 28040 Madrid, Spain.
e-mail: martafl@mat.ucm.es

[2] Observatoire de Paris, SYRTE, UMR 8630/ CNRS,
61 avenue de l'Observatoire, 75014 Paris, France.
e-mail: n.capitaine@obspm.fr; jean.souchay@obspm.fr

ABSTRACT. This paper reports on the progress of the research European DESCARTES-Subproject entitled: "Advances in the integration of the equations of the Earth's rotation in the framework of the new parameters adopted by the IAU 2000 Resolutions", describing the scientific approach, the aims and objectives of the work and its successive steps. Firstly, we give a brief overview of the role of the variables in the description of the rotational dynamics of the Earth. Then, we summarize the different mathematical methods used to carry out our investigations, which include analytical, semi-analytical and numerical approaches, in order to obtain the solution with microarcsecond accuracy.

1. INTRODUCTION

The IAU Resolutions passed in 2000 have recommended the use of the Celestial Intermediate Pole (CIP) and of the "new paradigm" to transform between the international terrestrial system (ITRS) and the geocentric celestial reference system (GCRS). The recommended form of the ITRS-to-GCRS transformation is based on the Celestial intermediate origin, CIO (originally called the Celestial ephemeris origin, CEO) to express the Earth rotation angle (ERA) instead of the classical Greenwich sidereal time, and on the ITRS and GCRS CIP coordinates. The IAU 2000A expressions for the GCRS CIP (X, Y) coordinates provided by Capitaine et al. (2003a) have been derived from the IAU 2000A expressions of Mathews et al. (2002) (denoted MHB) for the classical precession and nutation quantities. The IAU 2000A nutation expressions have been generated by the convolution of the MHB 2000 transfer function with the rigid Earth nutation series REN 2000 of Souchay et al. (1999), which are themselves solutions of the rigid Earth's dynamical equations. The IAU 2000 precession component has been derived from a fit of the precession rates in longitude and obliquity to series of Very Long Baseline Interferometry (VLBI) observations. More recently, an updated solution of the dynamical equations of the Earth's precession, denoted P03, has been obtained by Capitaine et al. (2003b) which has been used to obtain the P03 expressions for the CIP (X, Y) coordinates in a similar way.

In our work, we have used a different approach which has consisted in developing the equations for Earth rotation as function of the variables that are directly related to the parameters recommended by the IAU 2000 resolutions.

2. OBJECTIVES AND APPROACHES

The main objective of the project is to establish dynamical equations of the rigid Earth's rotation based on variables that can be *directly* related to the rectangular celestial coordinates of the CIP (X, Y) and that can be integrated in the simplest way in order to provide rigorous solutions. For this purpose, we have followed analytical, semi-analytical and numerical approaches. The comparison between the different types of solutions will allow us to evaluate the theoretical and real accuracy that can be achieved.

A further objective will be to investigate the transformation of the rigid Earth solutions to non-rigid Earth solutions and to compare the analytical and semi-analytical solutions to VLBI observations.

3. METHODOLOGY AND RESULTS

The first step of the project has been to review the sets of variables which are the most appropriate for reaching the objectives described in the previous section.

The rectangular components (ω_1, ω_2, ω_3) of the angular velocity vector along the principal axes of inertia, or alternatively the Euler angles between the figure axes and a fixed reference plane, are basic non-canonical variables (set I) that are classically used for writing the Euler dynamical equations. Expressing these variables as functions of the GCRS CIP coordinates (X, Y) will allow us to get the rotational equations of the Earth as functions of (X, Y).

Folgueira et al. (2006) have reviewed the sets of variables to be used in the Hamiltonian approach in order to get the equations in a compact form allowing us to integrate them in a simplest way and obtain analytical solutions. Two sets of canonical variables (Sets II and III) have been proposed. These variables are represented by the amplitude of the angular-momentum vector ($\overrightarrow{L}$), the X- and Y- components of this vector with respect to the inertial reference system, the x- and y-components of $\overrightarrow{L}$ with respect to the figure axes and their canonically conjugate variables.

Table 1 provides the basic variables and equations and the different techniques of integration which can be applied to solve the differential equations.

VARIABLES	BASIC EQUATIONS	METHOD OF INTEGRATION
Non-canonical: Set I	transformed Euler dynamical equations	• Variation of parameters • Runge-Kutta-Fehlberg
Canonical: Sets II and III	Hamiltonian equations	• Hori-Deprit's averaging perturbation

Table 1: Different forms of basic Earth's rotational equations and integration methods considered in this study.

In the following, we present a summary of the papers related to the different approaches carried out. Table 2 shows the methods of integration, the form of the solutions and the references corresponding to this study.

- (Folgueira et al., 2006)

  In this paper, we have reviewed the canonical and non-canonical variables for describing the rotation of the Earth and the relationships between them. Then, considering as the fixed reference plane the equator J2000.0, instead of the ecliptic of date, we have obtained the rigorous analytical solution in terms of sets II and III, to the first order.

- (Capitaine et al., 2006a)

  The equations of Earth rotation were obtained explicitly in terms of the celestial coordinates $(X,\ Y)$ of the CIP and of the Earth rotation angle (ERA), starting from Euler dynamical equations for a rigid Earth and using expressions for the components of the instantaneous rotation vector (set I) as functions of $(X,\ Y)$. Taking into account the order of magnitude of the different terms of these equations, we got the most appropriate form of the equations for a practical integration depending on the components of the external torque in the celestial intermediate system.

  We have investigated the possible methods of integration for providing semi-analytical solutions for the X and Y variables in the axially symmetric case and we have tested the efficiency of these methods.

  Finally, starting from Liouville equations, we have studied a possible generalization of the equations to the case of a elastic Earth based on integration constants compliant with the P03 precession.

- (Capitaine et al., 2006b)

  In this paper, we integrate the second order differential equations described above by the method of variation of constants. We solve the equations by successive approximations in order to get the semi-analytical solution for the rigid Earth in terms of $(X\,, Y)$. The semi-analytical expressions of the external torque used in the second members of the equations are computed from the theories ELP2000 for the Moon and VSOP87 for the Sun and planets. We compare the resulting semi-analytical solutions for $(X\,, Y)$ with the current IAU 2000 expression of $(X\,, Y)$ derived indirectly from the IAU 2000 solutions for the classical precession and nutation variables. For all the computations, we have used the software package GREGOIRE developed by J. Chapront (2003).

  More details on the two above studies are provided in Capitaine et al. (2006c).

- (Souchay et al., 2006)

  The equations of Earth rotation in terms of the $(X,\ Y)$ CIP coordinates and of the ERA are integrated by fifth-order adaptive step size Runge-Kutta-Fehlberg algorithm. Being a single step procedure, it is relatively stable and hence particularly suitable for the numerical simulation in different problems of Celestial Mechanics and Dynamical Astronomy. The numerical solution is also compared with the semi-analytical solution of Capitaine et al. (2006b). The comparison between these solutions allows us to test the accuracy of the integration method.

METHOD OF INTEGRATION	SOLUTIONS	REFERENCES
Hori-Deprit's averaging perturbation	analytical	(Folgueira et al., 2006)
Variation of parameters	semi-analytical	(Capitaine et al., 2006a,b,c)
Runge-Kutta-Fehlberg	numerical	(Souchay et al., 2006)

Table 2: Methods of integration, associated forms of solutions, and references corresponding to this study.

4. FUTURE PERSPECTIVES

The equations as function of the GCRS CIP (X, Y) coordinates as considered in the case of an elastic Earth will be extended to the case of a deformable Earth with a liquid core. This general case will be the aim of the other DESCARTES sub-project entitled "Geophysical effects of adopting the new solutions for the Earth's rotation in the framework of the new parameters adopted by the IAU 2000 Resolutions". The geophysical parameters will be derived from the comparison of the solutions with respect to VLBI observations.

Acknowledgments. The research was carried out in the Department of *"Systèmes de Référence Temps Espace" (SYRTE)* of Observatoire de Paris and received financial support from Descartes Prize Allowance (2004-2005) (M. Folgueira), for which we express our sincere appreciation.

REFERENCES

Capitaine, N., Chapront, J., Lambert, S., Wallace, P. T.: 2003a, A&A 400, 1145.
Capitaine, N., Wallace, P. T., Chapront, J.: 2003b, A&A 412, 567.
Capitaine, N., Folgueira, M., Souchay, J.: 2006a, A&A 445, 347.
Capitaine, N., Folgueira, M., Souchay, J.: 2006b, to be submitted to A&A.
Capitaine, N., Folgueira, M., Souchay, J.: 2006c, this issue.
Chapront, J., 2003, Notice, Paris Observatory (January 2003).
Folgueira, M., Souchay, J., Capitaine, N.: 2006, this issue.
Mathews, P.M., Herring, T.A., Buffett B.A., 2002, J. Geophys. Res. 107, B4, 10.1029/2001JB000390.
Souchay, J., Loysel, B., Kinoshita, H., and Folgueira, M., 1999, A&AS 135, 111.
Souchay, J., Capitaine, N., Folgueira, M.: 2006, to be submitted to A&A.

COMPUTATION OF THE "GEODETIC" EXCITATION FUNCTION OF NUTATION

S. BOLOTIN[1,2]
[1] Space Research Centre, PAS, Bartycka 18A, 00-716, Warsaw, Poland
[2] Main Astronomical Observatory, NASU, Zabolotnogo Str. 27, 03680, Kiev, Ukraine
e-mail: bolotin@mao.kiev.ua

ABSTRACT. Investigations concerning geophysical excitation of nutation (see Brzeziński and Bolotin, this volume) should be performed in the same way as it has been routinely applied in the polar motion excitation studies: first, compute from the time series of the observed nutation residuals the corresponding "geodetic" excitation, and then compare it to the available geophysical estimates of the excitation.

A simple digital filter for estimation of the geodetic excitation function of nutation was developed by Brzeziński (1994, 2006). A primary purpose of this paper is to assess how important are various simplifications introduced to this filter, what is the influence of the measurement errors and computer round-offs. This is achieved by applying the filter to various synthetic time series of the celestial pole offsets and then comparing its outputs to the assumed input excitations.

1. INTRODUCTION

It is commonly believed that the Free Core Nutation (FCN) and other irregular signals seen in the time series of the celestial pole offsets are mostly driven by the dynamically coupled atmosphere-ocean system.

Recent time domain comparisons of the atmospheric and oceanic excitation functions and the so-called "geodetic" excitation, derived from the nutation time series, showed that the overall correlation between them is low, below 0.3. A sliding window correlation analysis reveals the periods with high correlation, up to 0.8, but also the periods with negative correlation (Brzeziński and Bolotin, this volume).

The aim of this work is to perform numerical tests using the synthetic time series and investigate: 1) how the procedure of evaluation of the "geodetic" excitation function is sensitive to the computer round-offs; 2) how it is affected by the simplifications introduced when developing this procedure; 3) how the evaluated "geodetic" excitation is influenced by the measurements errors in nutation series; and 4) what is the level of correlations which could be expected from real data.

2. COMPUTATIONAL PROCEDURE

The excitation of the FCN by redistribution of mass within the atmosphere and the oceans manifests in offsets of the Celestial Intermediate Pole (CIP) observed by the very long baseline interferometry (VLBI).

The relation between time series of the observed CIP offsets and the celestial effective angular momentum (CEAM) function was studied in details by Brzeziński (1994, 2006). Knowing CEAM functions (mass term $\{\chi^p\}_i$ and motion term $\{\chi^w\}_i$) it is possible to evaluate the changes in nutation series (denoted $\{Nut\}_i$), and, conversely, under the assumption $\chi^w = 0$ it is possible to infer from the time series of nutation the corresponding "geodetic" excitation.

$$(\{\chi^p_{input}\}_i, \{\chi^w_{input}\}_i) \Rightarrow \{Nut\}_i; \quad (\{Nut\}_i) \Rightarrow \{\chi^p_{output}\}_i.$$

Here and below, by the "input" series we will understand a time series of CEAM mass term, synthetic or real, which is used to evaluate the corresponding time series of the CIP offsets – "nutation" series. And the "output" series will mean a time series which is inferred from a corresponding time series of the CIP (under the assumption $\chi^w = 0$).

A time domain comparison of the "input" and "output" series makes it possible to estimate the influence of measurement noise which is added to the synthetic "nutation" series. This comparison is performed using a sliding window analysis of corelation with window length equal to 2 years. Also, two integral characteristics are evaluated, the overall correlation and the relative decrease of variance ΔVar,

$$\Delta Var = \frac{(Var_{input} - Var_{input-output})}{Var_{input}} \times 100\%,$$

where Var_{input} is a variance of the "input" series and $Var_{input-output}$ is a variance of a time series composed from differences of "input" and "output" series.

3. NUMERICAL TESTS

In numerical tests we used the time interval with the available observations of the FCN signal, 1984–2005. In most cases the Gaussian noise with σ_{nut}=0.15 mas was added to nutation series to simulate the measurements errors. This value is about 3 to 4 times larger than mean uncertainties of nutation residuals reported by the VLBI analysis centers for nowadays observations.

The first simple tests were performed using a finite impulse function for the mass term of the CEAM, and zero for the motion term, without adding noise to the derived "nutation". The results show that the computer round-off errors are considerably small, on the level of 10^{-4} mas.

The synthetic time series of the CEAM mass term was then used to investigate the influence of the nutation measurements errors on the evaluating of the "geodetic" excitation function. In the (a) and (b) plots of Fig. 1 are shown the X- and Y-components of this time series. The corresponding "nutation" series derived under assumption that the motion term is zero and after adding the Gaussian noise is shown in Fig. 1, (e) and (f). The evaluated "output" series are compared to the "input" ones in Fig. 1, (c) and (d). The results of a sliding window correlation analysis between the "input" and "output" series are displayed in Fig. 1, (g) and (h). The estimated overall correlation is 0.72 and the relative decrease of variance is found to be 52%. Note, however, that the amplitudes of this synthetic time series are about two times greater than the amplitudes of the CEAM mass term calculated from the EAM functions based on the output of the NCEP-NCAR reanalysis project. Repeating this test for the mass term of the real CEAM data (NCEP-NCAR reanalysis AAM) gives the overall correlation about 0.52 and the relative decrease of variance -25% (negative ΔVar means that the variance of difference of the "input" and "output" series is greater than the variance of the "input" series). Such comparative divergence of "input" and "output" series is caused by decrease of the signal-to-noise ratio.

A similar analysis after taking into account the motion term (calculated from the effective angular atmospheric functions, NCEP-NCAR reanalysis project) is illustrated in Fig. 2. For this test the overall correlation falls down to 0.45, and the relative decrease of variance is -44%.

The last test was repeated with different values of σ_{nut} to see how the overall correlation and decrease of variances depend on the measurement noise. The results are presented in Table 1.

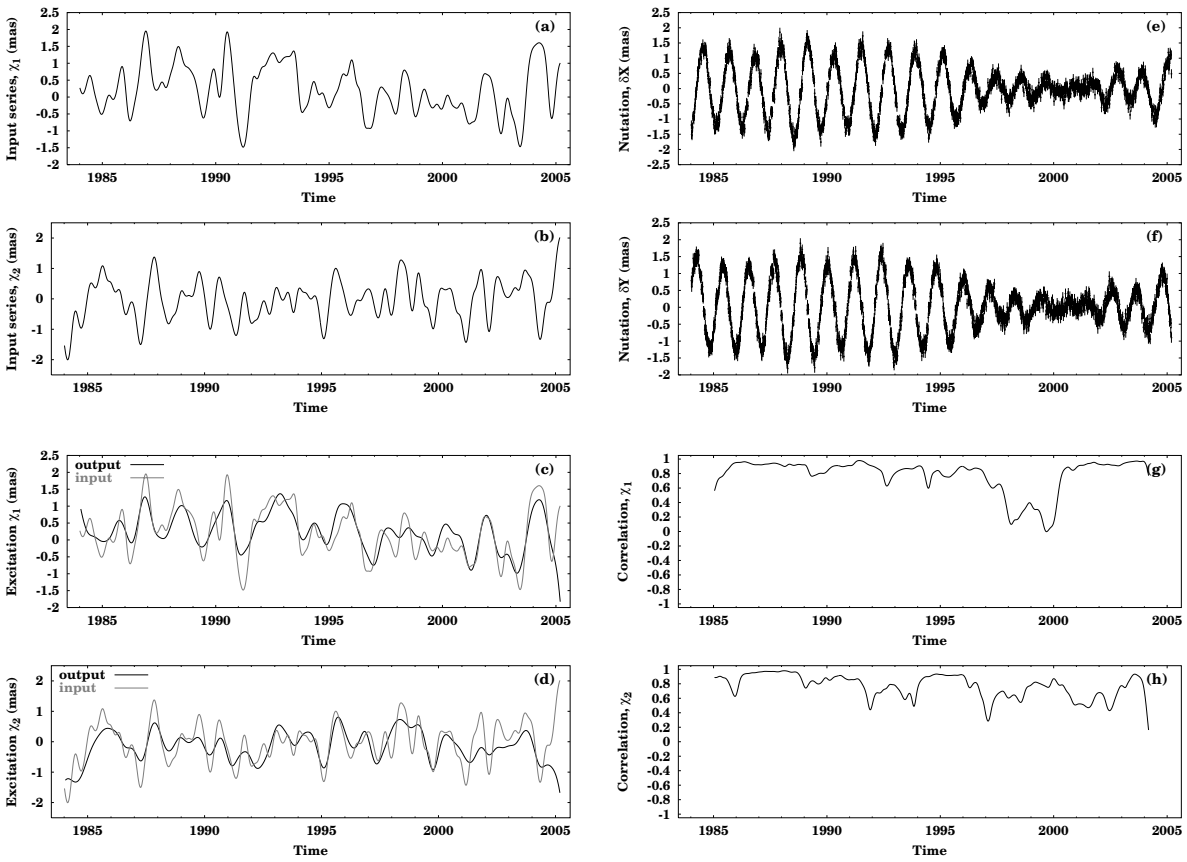

Figure 1: Artificial "input" time series. The "input" series (a) and (b), the resulting "nutation" series (e) and (f), the evaluated "output" series (c) and (d) and a sliding window correlations between the "input" and "output" series (g) and (h).

In these tests the case $\sigma_{nut} = 0$ shows how much the resulting "output" series is distorted by the assumption that the motion term has a small influence on the FCN and can be neglected.

Table 1: The changes of the overall correlation and the decrease of variances with the parameter of the Gaussian noise

σ_{nut}, mas	0.0	0.02	0.04	0.06	0.08	0.10	0.12	0.15	0.18	0.22	0.25	0.30	0.40
correlation	0.91	0.84	0.76	0.69	0.63	0.57	0.49	0.45	0.38	0.33	0.30	0.28	0.23
ΔVar, %	82	71	54	37	24	−2	−22	−60	−106	−189	−263	−383	−742

4. SUMMARY AND CONCLUSIONS

The motion term of the CEAM function has a small contribution to the excitation of the FCN; the assumption $\chi^w = 0$ in calculation of the "geodetic" excitation function does not alter the results significantly.

Calculation of the "geodetic" excitation function is also not sensitive to the computer round-offs. But, our tests show that the calculation is strongly depends on the noise contents in nutation series.

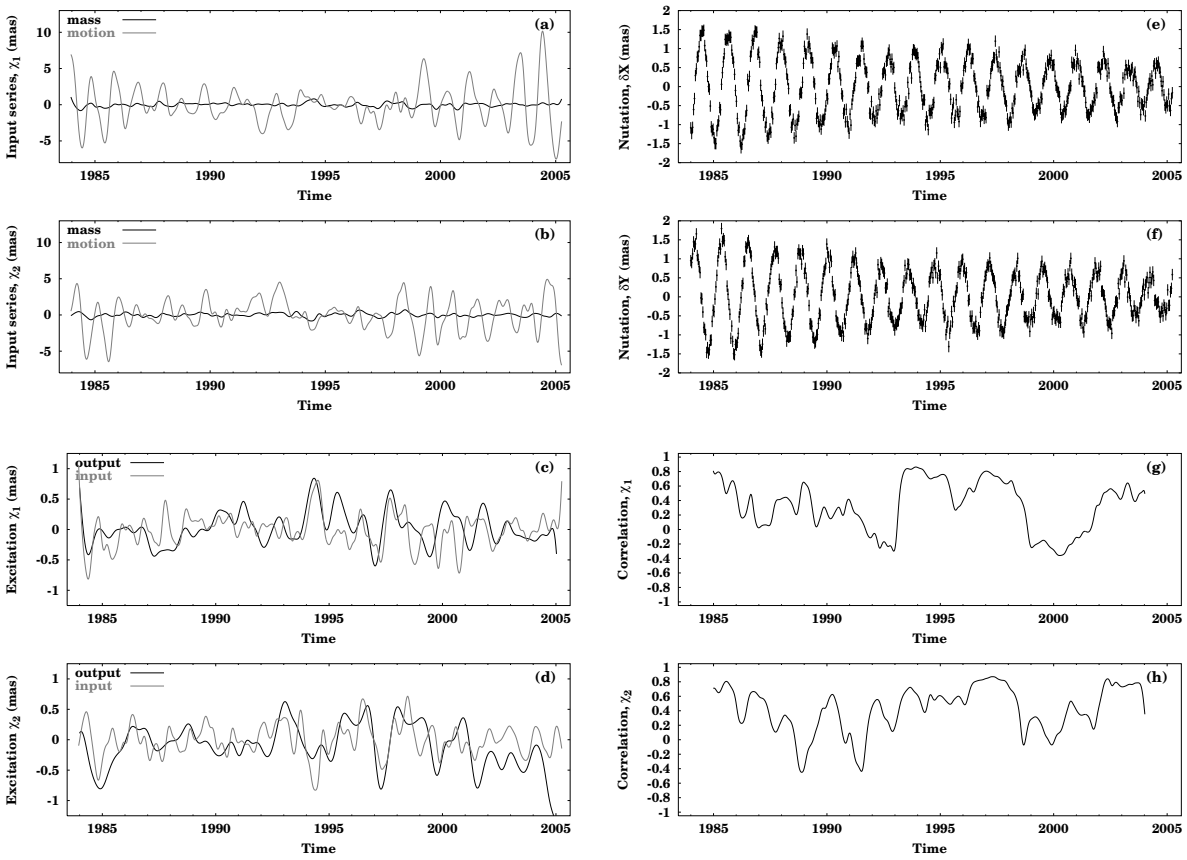

Figure 2: Mass and motion terms (from the NCEP-NCAR reanalysis project). The layout is the same as in Figure 1.

When assuming the standard deviations of the VLBI nutation series at the level of 0.15 mas or better, we can expect a reliable calculation of the "geodetic" excitation function.

Acknowledgments. This work was financed by a post-doc visiting grant in a frame of the "Descartes-Nutation" project. It was partially performed at the Space Research Centre, Polish Academy of Sciences. Author is very thankful to the collective of the Centre for cordial reception and hospitality.

This research has made use of the effective angular atmospheric functions based on results of the NCEP-NCAR reanalysis project provided by the IERS SBAAM.

REFERENCES

Brzeziński, A., 1994, Polar motion excitation by variations of the effective angular momentum function, II: Extended model, Manuscr. Geod., 19, pp. 157–171.

Brzeziński, A., 2006, A digital filter for the geophysical excitation of nutation, Journal of Geodesy, Special VLBI Issue, in press.

MODELLING AND PREDICTION OF THE FCN

M. KALARUS[1], B.J. LUZUM[2], S. LAMBERT[2] and W. KOSEK[1]
[1]Space Research Centre, Polish Academy of Sciences, Warsaw, Poland
[2]US Naval Observatory, Washington DC, USA
e-mail: kalma@cbk.waw.pl

ABSTRACT. In this paper we investigated the Free Core Nutation (FCN) which is the most significant oscillation in the celestial pole offset residuals with respect to the current IAU 2000 precession-nutation model. A wavelet phase spectrum analysis of the IERS C04 (IAU 2000) data was performed in order to determine areas of stable phase, which would be seen as times of constant period of the FCN. The results show that the retrograde period of the FCN appears to be a function of time, apparently changing between 410 and 490 days. These "changes" are correlated with Niño 4 data as well as with C_{20} coefficients of the gravity field. The wavelet modulus for the FCN period is correlated with negative change of the pressure term of the Atmospheric Angular Momentum excitation function. In order to fit the data, a combination of complex least-squares solutions was used to model and predict the FCN oscillation.

1. INTRODUCTION

Free core nutation (FCN) is a free motion of the celestial intermediate pole (CIP) in inertial space due to the interaction of the mantle and the fluid, ellipsoidal core as the Earth rotates. Because this effect is a free motion with time-varying excitation and damping resulting in a variable amplitude and phase, a FCN model was not included in the IAU 2000A nutation model. As a result, a quasi-periodic unmodeled motion of the CIP in inertial space at the 0.1–0.3 mas level still exists after the IAU 2000A model has been taken into account.

This study examined the nature of the FCN oscillation, particularly looking into the stability of the motion. A model was generated to approximate the FCN motion. Additional studies were performed in an effort to understand possible causes of the FCN.

2. WAVELET ANALYSIS

In the wavelet technique the formula for the transform coefficients are computed as the convolution of the complex-valued signal $z(t)$ and the wavelet analyzing function:

$$\hat{W}(T,t_j) = \sqrt{1/|T|} \int_{-\infty}^{+\infty} z(t)\overline{\psi}[(t-t_j)/T]dt, \tag{1}$$

where t_j is the translation parameter and T is the dilation (or period) parameter and

$$\psi(x) = \sqrt{1/(f_b\pi)}\exp(i2\pi f_c x)\exp(-x^2/f_b) \tag{2}$$

is the Morlet wavelet function applied (Chui 1992), in which $f_b > 0$ is the bandwidth parameter and f_c is the wavelet center frequency.

The wavelet transform modulus and phase are defined as $mod[\hat{W}(T, t_j)]$ and $\arg[\hat{W}(T, t_j)]$, respectively. When the gradient of the wavelet transform phase defined as

$$\hat{G}(T, t_j) = \frac{d}{dt_j}\{\arg[\hat{W}(T, t_j)] - 2\pi t_j/T\} \tag{3}$$

is equal to zero, then apparent variations of the period T can be detected.

3. DATA

The following time series were used in the analysis: 1) Nutation-precession residuals IERS C04 (1984 – August 2005) with the sampling interval of 1 day (IERS 2005), 2) Atmospheric Angular Momentum NCEP/NCAR data reanalyses (1984 – August 2005) at a sampling interval of 6 hours (Kalney et al. 1996), 3) Gravity field C_{20} (1984 – December 2002) (Cox and Chao 1998).

4. MODELLING AND PREDICTION

Initial use of the Morlet wavelet on the FCN residuals showed that there was significant power in the retrograde period range from 400 to 500 days. In an effort to isolate this phenomenon, the gradient of the phase was computed. The results of this computation are shown in the Fig. 1 below.

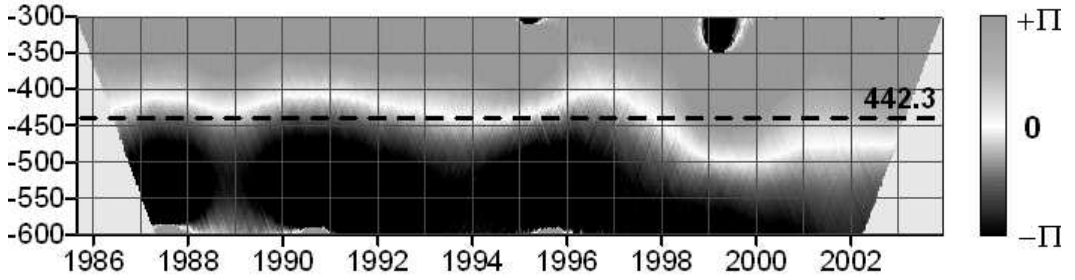

Figure 1: The gradient of the wavelet transform phase of the nutation precession corrections.

This figure shows the nonstationary character of the FCN as it was previously shown by Malkin (2004). Note that due to the way in which the FCN motion is realized, it is mathematically impossible to distinguish between a change in period with a change in the phase of the motion. In fact, from a geophysical point of view, it is unreasonable to expect that the period of the FCN could vary as is implied in the graph. Instead, it is likely that the variation is being caused by changes in the phase.

For the purposes of generating a FCN model, a constant, best-fit, period of 442.3 days is assumed. The following least-squares model similar to the model used by Lambert (2005) was fit to the IE RS C04 data set:

$$FCN(MJD) = A_n exp(i2\pi f_{FCN}) + b \cdot MJD + a. \tag{4}$$

Using this model, predictions of the FCN were made. The rms of the differences between the predictions and the IERS C04 data for various prediction lengths are shown in Fig. 2. These rms errors are of the same order as those obtained earlier by Brzeziński and Kosek (2004).

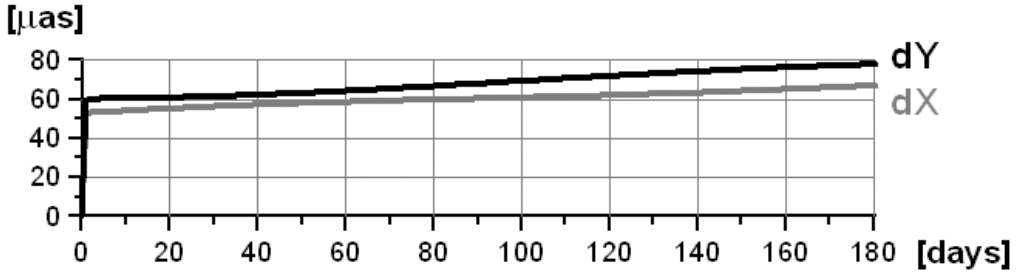

Figure 2: The RMS prediction error of the FCN model.

5. POSSIBLE EXCITATION

To understand the cause of the FCN, and therefore possibly improve the predictions, efforts were made to identify geophysical factors that were possibly related. For instance, both the Niño 4 and C_{20} coefficient show significant correlation with the calculated change in the FCN period, as shown in Fig. 3.

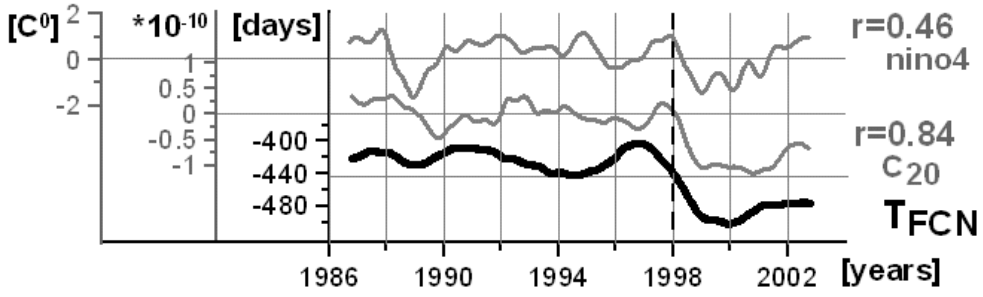

Figure 3: Niño 4 index (upper curve), gravity field C_{20} (middle curve) and the FCN period (bottom curve). The correlation coefficients are given to the right of the graph.

The AAM pressure term, on the other hand, shows a significant negative correlation with the apparent change of the FCN modulus (Fig. 4). Atmospheric and nontidal oceanic contributions of the order of $0.1mas$ to nutation was previously found by Bizouard et al. (1998).

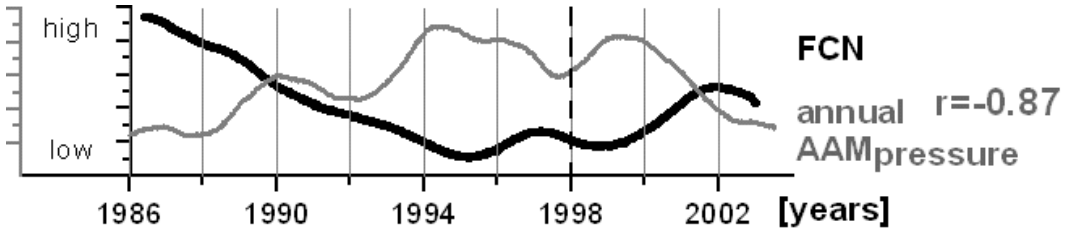

Figure 4: Wavelet transform modulus for the FCN period (black line) and for the annual oscillation in the pressure component of the AAM excitation function (grey line). The correlation coefficient is given to the right of the graph.

6. CONCLUSIONS

The general characteristic of the FCN model are that it has a variable amplitude and period (phase), a mean prediction error of roughly 70-80 μas for 180 days in the future, and an apparent relationship to geophysical phenomena.

Some possible excitation of the FCN explored in this analysis include global mass redistribution, land hydrology, and perturbations of the annual atmospheric circulation. Significant correlations were found between the apparent variations of the retrograde FCN period and C_{20} coefficients of the gravity field as well as Niño 4 data. The wavelet transform modulus for the FCN period is correlated with negative change of the pressure term of the Atmospheric Angular Momentum excitation function.

Other possible sources of excitation include subpolar glacial melting (Dickey et al. 2002), earthquakes (Shirai and Fukushima 2001), and anomalous fluctuations in the core (Cox and Chao 2002, Holme and de Viron 2005).

Acknowledgments. This research has been supported by the Descartes-Nutation project (M.K.) and by the Polish Ministry of Education and Science under the project No 4 T12E 039 29.

REFERENCES

Bizouard C., A. Brzeziński and S. Petrov, 1998, Diurnal atmospheric forcing and temporal variations of the nutation amplitudes, *J. Geod.*, 72, 561–577.

Brzeziński A. and W. Kosek, 2004, Free core nutation: Stochastic modelling versus predictability, in Proc. Journées Systèmes de Référence Spatio-Temporels 2003, A. Finkelstein and N. Capitaine (eds.), Inst. of Applied Astronomy of the Russian Acad. of Sciences, St. Petersburg, 99–106.

Chui C. K., 1992, *An Introduction to Wavelets, Wavelet Analysis and its Application. Vol.1*, Academic Press, Boston-San Diego.

Cox C. M. and B. F. Chao, 2002, Detection of a Large-Scale Mass Redistribution in the Terrestrial System Since 1998, *Science*, 297, 831–833.

Dickey J. O., S. L. Marcus, O. de Viron, and I. Fukumori, 2002, Recent Earth Oblateness Variations: Unraveling Climate and Postglacial Rebound Effects, *Science*, 298, 1975–1977.

Holme R. and O. de Viron, 2005, Geomagnetic jerks and a high-resolution length-of-day profile for core studies, *Geophys. J. Int.*, 160, 435–439.

IERS, 2005, The Earth Orientation Parameters, http://hpiers.obspm.fr/eop-pc/.

Kalnay E. et al., 1996, The NCEP/NCAR 40-year reanalysis project, *Bull. Amer. Meteor. Soc.*, 77, 437–471.

Lambert S., 2005, Empirical modelling of the free core nutation, Technical Report, Earth Orientation Department, USNO.

Malkin Z., 2004, A New Free Core Nutation Model with Variable Amplitude and Period, in IVS 2004 General Meeting Proceedings, 388–392.

Shirai T. and T. Fukushima, 2001, Detection of excitations of Free Core Nutation of the Earth and their concurrence with huge earthquakes, *Geophys. Res. Lett.*, 28(18), doi: 10.1029/2000GL012479.

ON THE APPROPRIATE SETS OF VARIABLES FOR THE RIGOROUS STUDY OF THE EARTH'S ROTATION IN THE FRAMEWORK OF IAU 2000 RESOLUTIONS

M. FOLGUEIRA[1,2], J. SOUCHAY[2] and N. CAPITAINE[2]

[1] Instituto de Astronomía y Geodesia (UCM-CSIC),
Facultad de CC. Matemáticas, Universidad Complutense de Madrid,
Plaza de Ciencias, 3. Ciudad Universitaria, 28040 Madrid, Spain.
e-mail: martafl@mat.ucm.es

[2] Observatoire de Paris, SYRTE, UMR 8630/ CNRS,
61 avenue de l'Observatoire, 75014 Paris, France.
e-mail: Jean.Souchay@obspm.fr ; n.capitaine@obspm.fr

1. VARIABLES FOR THE IAU 2000 DESCRIPTION OF THE EARTH'S ROTATION

This paper reviews the properties of different sets of canonical variables that can be used in the description of the Earth's rotational motion. The purpose is to select the most appropriate set of variables which (i) can provide a rigorous analytical solution and (ii) can be directly related to the celestial rectangular coordinates (X, Y) of the Celestial Intermediate Pole (CIP), the use of which is recommended by the IAU 2000 Resolutions on reference systems (IERS Conventions 2003). Selecting the set of variables is an important point to consider since the complexity of the differential equations as well as the method of integration to be used strongly depend on an appropriate selection of the variables. Table 1 provides the definitions of different sets of canonical variables considered in this study.

CANONICAL VARIABLES	DEFINITION
Set I: $(L_2, G_2, H_2, l_2, g_2, h_2)$ (Fukushima, 1994)	• L_2: x-component of the angular-momentum vector ($\overrightarrow{L}$) • G_2: amplitude of the angular-momentum vector • H_2: X-component of the angular-momentum vector • canonically conjugate variables to (L_2, G_2, H_2)
Set II: $(L_3, G_3, H_3, l_3, g_3, h_3)$ (new)	• L_3: y-component of the angular-momentum vector ($\overrightarrow{L}$) • G_3: amplitude of the angular-momentum vector • H_3: Y-component of the angular-momentum vector • canonically conjugate variables to (L_3, G_3, H_3)

Table 1: Sets of canonical variables for the IAU 2000 description of the Earth's rotation

The process of constructing these sets involves several canonical transformations from the initial Andoyer variables. Note that other variables can be used to establish differential equations which are appropriate for finding the semi-analytical and numerical solution of the dynamical equations of the Earth's rotation (Capitaine et al., this Volume). However, in this problem, only canonical variables can allow us to obtain a rigorous analytical solution.

2. PROPERTIES OF SETS I AND II OF CANONICAL VARIABLES

The principal characteristics and consequences of adopting the sets of variables presented in Table 1 for the IAU 2000 description of Earth's rotation are as follows:

- The canonical variables H_2 and H_3 of Table 1 are suitable variables for carrying out the rigorous analytical study of the dynamical equations of the Earth's rotation.

- These variables, H_2 and H_3, also lead to the solution of the perturbed problem, which has, at the first order, the following form that is as simple as that obtained for the classical Andoyer variables:

$$\Delta H_2 = k' \tan h_2 \sum_{i \neq 0} \frac{Q_i}{N_i} \sin \Theta_i$$

$$\Delta H_3 = k' \tan h_3 \sum_{i \neq 0} \frac{Q_i}{N_i} \sin \Theta_i$$

  where Q_i is a function of the angle I between the angular equator and the fixed equator of a given epoch, the argument Θ_i is a linear function of the mean elements of the lunar, solar and planetary orbits, k' is a constant and $N_i = \frac{d\Theta_i}{dt}$.

3. DISCUSSION

The variables of Sets I and II seem to be appropriate ones for carrying out the effective study of the dynamical equations of the Earth's rotation in the framework of the IAU 2000 Resolutions, since they contain $X-$ and $Y-$ components of the angular-momentum vector, H_2 and H_3 respectively. These variables are directly related, by geometrical relations, to the rectangular celestial coordinates of the Celestial Intermediate Pole unit vector which allow us a subsequent determination of the Oppolzer terms. Moreover, the description in terms of canonical variables offers advantages related to the integration of such equations since it is possible to apply the Hori-Deprit's averaging perturbation method, which uses the concept of canonical transformations, unquestionably one of the most powerful tools in the Hamiltonian approach.

Acknowledgments. The research was carried out in the Department of *"Systèmes de Référence Temps Espace" (SYRTE)* of Observatoire de Paris and received financial support from Descartes Prize Allowance (2004-2005) (M. Folgueira), for which we express our sincere appreciation.

REFERENCES

Capitaine, N., Folgueira, M., Souchay, J.: this Volume.

Fukushima, T.: 1994, Celest. Mech. 60, 57-68.

IERS Conventions 2003, IERS Technical Note 32, D.D. McCarthy and G. Petit (eds.), Frankfurt am Main: Verlag des Bundesamts für Kartographie und Geodäsie, 2004.

A NUTATION MODEL WITH EARTH INTERIOR PARAMETERS ESTIMATED ON THE TIME DOMAIN DATA.

L. KOOT[1], O. DE VIRON[2], V. DEHANT[1].
[1] Royal Observatory of Belgium
Avenue Circulaire 3, B-1180 Brussels, Belgium.
e-mail: laurence.koot@oma.be, veronique.dehant@oma.be
[2] Institut de Physique du Globe de Paris
Place Jussieu 4, 75252 Paris, France.
e-mail: deviron@ipgp.jussieu.fr

1. INTRODUCTION

The nutation response of the non-rigid Earth to the gravitational forcing by the Moon, the Sun, and the planets has been modeled by Mathews et al. (2002). This semi-analytic model depends on unknown Earth interior parameters (such as the dynamical ellipticities of the Earth and fluid core, e and e^f, the compliances representing elasticity effects of the whole Earth and fluid core, κ and γ, and the coupling constants at the core-mantle and inner-core boundaries, K^{CMB} and K^{ICB}) which are estimated by fitting the model to the nutation data.

The classical method used to model the nutations is to compute the nutation of a hypothetic rigid Earth with the same dynamical ellipticity as the real Earth and to convolve it with a transfer function accounting for the effects of non-rigidity. As the gravitational forcing is mainly periodic, nutation is modeled in Mathews et al. (2002) as a function of frequency:

$$\eta(\mathbf{p},\sigma) = TF(\mathbf{p},\sigma)\ .\ \eta_R(\sigma), \tag{1}$$

where $\eta = \Delta\psi \sin\epsilon_0 + i\Delta\epsilon$ is the complex amplitude of nutation, $\mathbf{p}$ is the vector of the geophysical parameters to be estimated, σ is the frequency of the nutation term, TF is the transfer function for the non-rigid Earth and η_R is the complex amplitude of the rigid Earth nutation. To adjust this model to the observations, nutation data must be transformed into a series of complex amplitudes for fixed frequencies, to which the geophysical parameters are fitted with a linearized least-squares method.

In this paper, we propose a new fitting procedure of the nutation model to the observations. We add a time dependence to the nutation model by multiplying each nutation term by the argument $\arg(\sigma,t)$ given in the rigid Earth series. We include the precession rate $P(e)$ and an empirical parameter $\frac{d\Delta\epsilon}{dt}$, accounting for the secular variation in obliquity, in the nutation model:

$$\eta(\mathbf{p},t) = \sum_{\sigma} [TF(\mathbf{p},\sigma)\ .\ \eta_R(\sigma)] \exp(i\ \ \arg(\sigma,t)) + \left(P(e)\sin(\epsilon_0) + i\frac{d\Delta\epsilon}{dt}\right) t. \tag{2}$$

We adjust this model to the nutation observations in time series and estimate the geophysical parameters with a Bayesian inversion method.

This method offers the advantages to take the time variable quality of the data into account, to allow for the estimation of non-periodic terms and, in particular, the precession and obliquity

rates, simultaneously with the geophysical parameters and to use an inversion method which does not assume a linear dependence of the model in the parameters.

2. NUMERICAL RESULTS

The geophysical parameters are estimated with the Bayesian inversion method and sampled with the Metropolis algorithm. The numerical values obtained as well as the adjustement from the values of PREM model (Dziewonski and Anderson 1981) are shown in Table 1 and compared to the results of Mathews et al. (2002).

Parameter	This Paper		Mathews et al. (2002)	
	Estimate	Adjustment	Estimate	Adjustment
e	**0.0032845456** $\pm$ 6 10^{-10}	0.000037	**0.0032845479** $\pm$ 1 10^{-9}	0.000037
e^f	**0.0026**527 $\pm$ 6 10^{-7}	0.0001048	**0.0026**456 $\pm$ 10^{-6}	0.0000973
κ	**0.0010**168 $\pm$ 7 10^{-6}	-0.0000222	**0.0010**340 $\pm$ 9 10^{-6}	-0.0000043
γ	**0.001964**3 $\pm$ 1 10^{-6}	-0.0000007	**0.001964**62 $\pm$ 1 10^{-6}	0.0000007
Im(K^{CMB})	**-0.000013**6 $\pm$ 7 10^{-7}	...	**-0.000018**5 $\pm$ 1 10^{-6}	...
Re(K^{ICB})	**0.00**0935 $\pm$ 1 10^{-4}	...	**0.00**111 $\pm$ 1 10^{-4}	...
Im(K^{ICB})	**-0.00**183 $\pm$ 2 10^{-4}	...	**-0.00**078 $\pm$ 1 10^{-4}	...

Table 1: Numerical values of the geophysical parameters.

In addition to the geophysical parameters, the secular variation of the obliquity was estimated as an empirical parameter. The correction to the IAU precession rate can be directly obtained from the estimated geophysical parameter e. Numerical results are shown in Table 2.

Parameter	This Paper (mas/y)	Herring et al. 2002 (mas/y)
$P(e)$	-3.031 $\pm$ 0.009	-2.997 $\pm$ 0.007
$\frac{d\Delta\epsilon}{dt}$	-0.254 $\pm$ 0.003	-0.252 $\pm$ 0.003

Table 2: Correction to the IAU precession rate and empirical obliquity rate.

3. CONCLUSIONS

We estimate the Earth interior parameters using all the available nutation data in time series. By using the data in the time domain, we estimate simultaneously the precession and obliquity rates and the geophysical parameters. We use a fit procedure which does not make linearizations in the parameters. The values obtained for the parameters are close to the values of Mathews et al. (2002) but are not always within their error bars.

REFERENCES

Dziewonski A. M., Anderson D. L., 1981, "Preliminary reference Earth model", Phys. Earth Planet. Inter., 25, 297-356.

Mathews P. M., Herring T. A., Buffet B. A., 2002, "Modeling of nutation and precession: New nutation series for nonrigid Earth and insights into the Earth's interior", J. Geophys. Res. , 107(B4), doi: 10.1029/2001JB000390.

ANALYSIS AND COMPARISON OF PRECISE LONG-TERM NUTATION SERIES, STRICTLY DETERMINED WITH OCCAM 6.1 VLBI SOFTWARE

G. BOURDA[1,2,3], J. BOEHM[3], R. HEINKELMANN[3], H. SCHUH[3]
[1] L3AB-UMR5804, Observatoire de Bordeaux, FRANCE
[2] SYRTE-UMR8630, Observatoire de Paris, FRANCE
[3] Institute of Geodesy and Geophysics, Vienna University of Technology, AUSTRIA
e-mail: Geraldine.Bourda@obspm.fr

1. INTRODUCTION

The IAU/IUGG Working Group on "Nutation for a non-rigid Earth", led by Véronique Dehant, won the European Descartes Prize in 2003, for its work developing a new model for the precession and the nutations of the Earth. This model (MHB2000, Mathews et al. 2002) was adopted by the IAU (International Astronomical Union) during the General Assembly in Manchester, in 2000. It is based (i) on some improvements for the precession model (with respect to the previous one of Lieske et al. 1977) owing to the VLBI technique (Very Long Baseline Interferometry), and (ii) on a very accurate nutation model, close to the observations. With this prize, the Descartes nutation project could offer for international scientists some grants, to be used for further improvements of the precession-nutation Earth model. At the IGG (Institute of Geodesy and Geophysics), with the OCCAM 6.1 VLBI analysis software and the best data and models available, we re-analyzed the whole VLBI sessions available (from 1985 till 2005) solving for the Earth Orientation Parameters (EOP). In this paper we present the results obtained for the EOP and more particularly for the nutation series. We compare them with the other IVS (International VLBI Service) analysis centers results, as well as with the IVS combined EOP series from the analysis coordinator. The series are in good agreement, except for the polar motion coordinates that show a shift with respect to the other ones and that we discuss here. Finally, we analyse the nutation series in the framework of the free core nutation (FCN) effect.

2. COMPUTATION

In this study we use 2944 VLBI sessions from 1982 till 2004, described as suitable for determining the EOP by the IVS Analysis Coordinator. They are computed at the IGG, from the NGS-format files corrected on the basis of the ECMWF meteorological data, in order to improve the height component of the stations and the determination of the tropospheric parameters. Clock breaks and reference clocks were investigated and taken into account for each session (Heinkelmann et al., 2005). The VLBI analysis software used at the IGG is OCCAM 6.1, in which the classical least-squares method based on the Gauss-Markov model (Koch, 1997) is implemented. We used (i) the terrestrial reference frame ITRF2000, (ii) the Vienna Mapping Function (VMF; Boehm & Schuh 2004), and (iii) a cut-off elevation angle for the troposphere set to 5 degrees. We estimated atmospheric gradients, clock parameters and zenith delays, as the same time we solve for the 5 EOP: one per session, and its rate for the pole and UT1. But we do not estimate the stations and sources position.

3. DISCUSSION

In Figure 1, we show the results obtained for the polar motion (x_p component) compared to the IVS combined rapid solution (series ivs03r1e). This series was obtained using the IVS-R1 and R4 sessions, very good ones for determining the EOP, occuring after the year 2000. We can notice a shift in our series with respect to the IVS combined one. We wondered if this shift could be solved removing Tigoconception station. And we can realise that it is in better agreement after removing it (see Fig. 1). This can be explained by the fact that we used ITRF2000 terrestrial reference frame, in which Tigoconception position is not well determined. But it still remains a difference at the end of the data time span. In Figure 2, we plotted the Fourier spectrum of the Celestial Pole Offsets (dψ, dϵ) we obtained, with respect to the IAU2000 nutation model. Depending on the data time span considered, we do not obtain the same periodical signals. The main ones are summarized in Table 1, investigating the longest data time span possible (between 1982 and 2004). For further studies about the Free Core Nutation effect (FCN), we will investigate a wavelet analysis on the prograde and retrograde parts of the Earth nutations. In the future, we will be able to use also the intensive VLBI sessions in our computations.

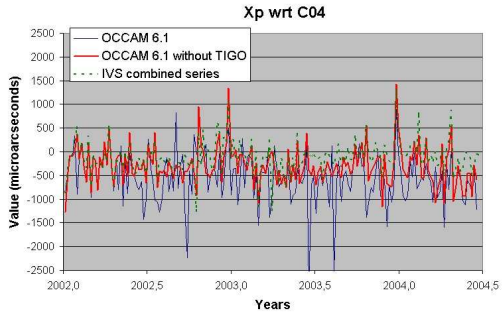

Figure 1: Polar motion x_p component, obtained with OCCAM 6.1 and compared to the IVS combined series.

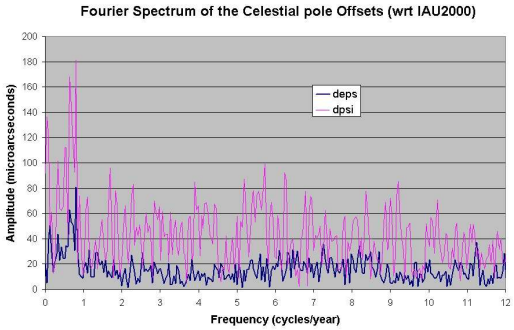

Figure 2: Fourier spectrum of the celestial pole offsets obtained with OCCAM 6.1, with respect to IAU2000 model.

Period	dϵ	dψ
450 days	81 μas	181 μas
570 days	63 μas	168 μas

Table 1: Amplitudes of the biggest periodical signals for (dψ,dϵ), with respect to IAU2000.

REFERENCES

Boehm, J., Schuh, H., 2004, "Vienna Mapping Functions in VLBI analyses", Geophys. Res. Lett., 31, doi: 10.1029/2003GL018984.

Heinkelmann, R., Boehm, J., Schuh, H., 2005, "IVS long-term series of tropospheric parameters", 6th IVS Analysis Workshop, April 21-23 2005, Noto Observatory, Sicily, Italy.

Koch, K.R., 1997, "Parameterschatzung und Hypothesentests in linearen Modellen", 3. Auflage, Ferdinand Dummlers Verlag, Bonn, pp. 381.

Mathews, P.M., Herring, T.A., Buffet, B.A., 2002, "Modeling of nutation and precession: New nutation series for nonrigid Earth and insights into the Earths's interior", J. Geophys. Res. (Solid Earth), 107, doi: 10.1029/2001JB000390.

Lieske, J.H., Lederle, T., Fricke, W., and Morando, B., 1977, "Expressions for the precession quantities based upon the IAU 1976 system of astronomical constants", A&A 58, pp. 1–16.

POLAR MOTION EXCITATION ANALYSIS DUE TO GLOBAL CONTINENTAL WATER REDISTRIBUTION *

L.I. FERNANDEZ[1,2,3], H. SCHUH[3]
[1] Consejo Nacional de Investigaciones Científicas y Técnicas (CONICET). Argentina.
[2] Facultad de Cs. Astronómicas y Geofísicas. U. N. de La Plata.
Paseo del Bosque s/n. B1900FWA. La Plata. Buenos Aires. Argentina.
e-mail: lauraf@fcaglp.unlp.edu.ar
[3] Institut für Geodäsie und Geophysik. E128/1. Technische Universität Wien.
Gußhausstraße 27-29.A-1040 Wien, Austria.
e-mail: harald.schuh@tuwien.ac.at

ABSTRACT. We present the results obtained when studying the hydrological excitation of the Earth's wobble due to global redistribution of continental water storage. This work was performed in two steps. First, we computed the hydrological angular momentum (HAM) time series based on the global hydrological model LaD (Land Dynamics model) for the period 1980 till 2004. Then, we compared the effectiveness of this excitation by analysing the residuals of the geodetic time series after removing atmospheric and oceanic contributions with the respective hydrological ones. The emphasis was put on low frequency variations. We also present a comparison of HAM time series from LaD with respect to that one from a global model based on the assimilated soil moisture and snow accumulation data from NCEP/NCAR (The National Center for Environmental Prediction/The National Center for Atmospheric Research) reanalysis. Finally, we evaluate the performance of LaD model in closing the polar motion budget at seasonal periods in comparison with the NCEP and the Land Data Assimilation System (LDAS) models.

1. COMPUTATION OF HAM TIME SERIES FROM LaD

The time series of the hydrological excitation of polar motion was computed for the period 1980 till 2004 as estimated from the Land Dynamics (LaD) model for Land Water and Energy Balance (Milly and Schmakin, 2002). The groundwater density redistribution data on a global grid is generated at the U.S. Geological Survey by the Continental Water, Climate, and Earth-System Dynamics Project. The grid is equidistant at 1° and the data outputs are available at monthly intervals. Solving the x and y component of the Liouville equations and replacing the inertia tensor components by the correspondent expression in terms of the second-order Stokes coefficients (C_{21}, S_{21}) yields (Gross et al., 2003; Chen et al., 2000)

$$(\Psi_x + \mathrm{i}\ \Psi_y)^{mass} = -1.098\,\frac{\mathrm{MR}^2}{(\mathrm{C\text{-}A})}\,(C_{21} + \mathrm{i}\ S_{21}) \qquad (1)$$

where Ψ are the excitation functions, M and R are the mass and mean radius of the Earth, C and A are the principal moments of inertia. The time series of the Stokes coefficients variations

*Poster presented by Robert Weber

can be expressed by the parameters of the LaD water storage model. Thus, replacing the Stokes coefficients in eq. (1) yields,

$$\left.\begin{array}{c}\Psi_x \\ \Psi_y\end{array}\right\} = \frac{-1.098\ \mathrm{R}^4\ (1+\mathrm{k}_l)}{(\mathrm{C\text{-}A})}\sqrt{\frac{3}{5}}\int_S \Delta s(\phi,\lambda)\, cos(\phi)\, sin^2(\phi) \left\{\begin{array}{c} cos(\lambda) \\ sin(\lambda)\end{array}\right\} \mathrm{d}\phi\, \mathrm{d}\lambda \qquad (2)$$

where k_l is the degree 2 load Love number and $\Delta s(\phi,\lambda)$ are the continental water storage values as a function of latitude (ϕ) and longitude (λ).

From eq. (2) we obtained the hydrological excitation functions time series from the LaD model by numerically solving the integral. We prior located the point at the centre of a 4-by-4 sub-block of the grid data. Afterwards, we performed a two-dimensional interpolation by using a polynomial of degree 3 in latitude and the same in longitude. The surface integrals were solved by using twice a ten-point Gauss-Legendre integration.

2. ANALYSIS OF HYDROLOGICAL POLAR MOTION EXCITATION

The equatorial components of the hydrological excitation were computed at annual, semiannual and ter-annual terms and compared with the NCEP,LDAS and LaD models in closing the polar motion budget.

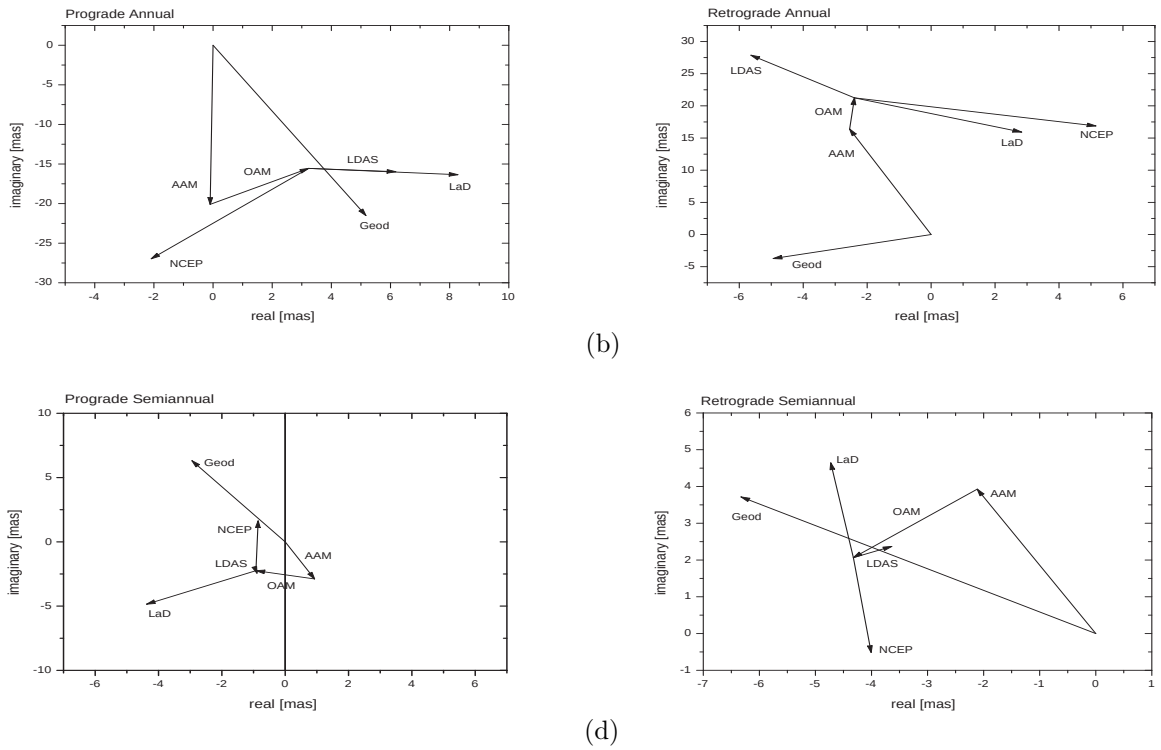

Figure 1: Phasor diagrams for the annual prograde (a), annual retrograde (b), semi-annual prograde (c) and semi-annual retrograde (d) components of the observed (geod), atmospheric (AAM), oceanic (OAM) and hydrological excitations (LaD, NCEP, LDAS)

The interannual hydrological excitation to polar motion was also computed for the whole 24-year period. The geodetic residuals were calculated by subtracting atmospheric plus oceanic contribution to the observed polar motion excitation computed from the IERS C04 series. We eliminated the high frequency components by applying a Vondrák filter (Vondrák, 1977) with ϵ

$= 1600\ y^{-6}$. Afterwards, we applied a wavelet analysis (Schmidt, 2002) in order to compute the squared cross scalogram and the normed coherence.

3. CONCLUSIONS

We computed the equatorial components of a HAM time series as estimated by the LaD model for a period of 24 years at 1-month interval. For the retrograde components, the hydrological influence with a period of 4 years can be seen, which is demonstrated by a normed coherency of .99. However the irregular variations between 5 and 8 years are not clearly explained by hydrological excitation. They should obey to oceanic or atmospheric mis-modelling.

When comparing LaD with other hydrological models at annual periods, LaD seems to overestimate the retrograde component. If one compares LaD with NCEP and LDAS in closing the annual and semi-annual polar motion budget, we can observe that LaD is close to LDAS in phase for all prograde components. Moreover, the LaD contribution approximates better to the polar motion observations in magnitude although differences in phase still exist. Finally, we also performed estimations of the ter-annual hydrological effects on polar motion.

Acknowledgments. We would like to thank M. Schmidt (DGFI) for the FORTRAN codes morlet.f and coherence.f applied in this work for performing the wavelet analysis, as well as for the support and the helpful discussions. L. Fernández is grateful to the Advisory Board of the Descartes Prize "Pinpoint positioning in a wobbly world" for the post-doctoral grant to research at the Institute of Geodesy and Geophysics of TU Wien.

REFERENCES

Chao B.F., O'Connor W.P., Chang A.T.C., Hall D.K., Foster J.L., 1987, "Snow load effect on the Earth's rotation and gravitational field, 1979-1985". J. Geophys. Res. 92 B9, pp. 9415-9422.

Chao B.F., O'Connor W.P., 1988, "Global surface-water-induced seasonal variations in the EarthŠs rotation and gravitational field". Geophysical Journal 94, pp. 263–270.

Chen J.L., Wilson C.R., Eanes R.J., Tapley B.D., 2000, "A new assessment of long-wavelength gravitational variations". J. Geophys. Res. Vol. 105, B7, pp. 16271–16277.

Chen J.L., Wilson C.R., 2005, "Hydrological excitations of polar motion, 1993-2002". Geophys. J. Int. 160, pp. 833–839.

Gross R. S.,Fukumori I., Menemenlis D., 2003, "Atmospheric and Oceanic Excitation of the Earth's Wobbles During 1980-2000". J. Geophys. Res., 108(B8), doi: 10.1029/2002JB002143, 20031992.

Hinnov L. A.,Wilson C. R., 1988, "Estimate of the water storage contribution to the excitation of polar motion", Geophys. J., R. Astr. Soc., 88, pp. 437-459.

Jochmann, H., 1999, "The influence of continental water storage on the annual wobble of polar motion estimated by inverse solution". Journal of Geodyn. 27, pp. 147–160.

Kuehne J., Wilson C. R., 1991, "Terrestrial Water Storage and Polar Motion". J. Geophys. Res., 96, B3, pp. 4337–4345.

Milly P.C.D., Shmakin A.B., 2002, "Global Modeling of Land Water and Energy Balances. Part I: The Land Dynamics (LaD) Model". Journal of Hydrometeorology. Vol. 3, pp. 283–299.

Schmidt, M., 2002, "Wavelet-Analyse von Zeitreihen". Dt. Geod. Komm., München, Reihe A, Nr. 118, pp. 46-56.

Vondrák J., 1977, "Problem of Smoothing observational data II". Bull. Astron. Inst Czech., 28, pp. 84–89.

Session 3

EXCITATION OF EARTH ROTATION BY GEOPHYSICAL FLUIDS

EXCITATION DE LA ROTATION DE LA TERRE PAR LES FLUIDES GEOPHYSIQUES

EXCITATION OF EARTH ROTATION BY GEOPHYSICAL FLUIDS

D. A. SALSTEIN[1], J. NASTULA[2]
[1]Atmospheric and Environmental Research,Inc.,
and NASA/GSFC/ University of Maryland, Baltimore County
131 Hartwell Ave., Lexington, MA 02468 USA
e-mail: salstein@aer.com
[2]Space Research Center of the PAS
Bartycka 18a, 00-716 Warsaw, Poland
e-mail: nastula@cbk.waw.pl

ABSTRACT. Among the geophysical fluids, the atmosphere and ocean are important sources of excitation for the irregularities in Earth rotation, acting on a broad range of time scales from subdiurnal to decadal. These excitations occur due to exchanges of angular momentum from these geophysical fluids to the solid Earth, and occur in both the axial direction causing changes in the length of day and in the equatorial direction leading to polar motions. In the atmosphere, angular momentum variations are due to those in the mass distribution, linked to surface pressure, and motions, namely the winds. These variations are related to the local changes occurring over many regions of the globe. Recent evaluations containing high spatial resolution decomposition of the atmosphere, over 3312 sectors, indicate the regions containing the most covariability with the global atmospheric angular momentum and the polar motion excitation itself.

1. INTRODUCTION

Various datasets that describe the angular momentum of the atmosphere are prepared through the model-data assimilation systems of the worldŠs large weather centers. They take the heterogeneous combination of meteorological observations, which are irregularly spaced, and combine them optimally with the forecasts of atmospheric prediction models. From this procedure, fields of meteorological variables are produced on regular grids. From the winds and surface pressure fields, we have been calculating the motion and mass terms of atmospheric angular momentum, which is proportional to the atmospheric excitations for Earth rotation, consisting of the equatorial terms related to polar motion and the axial terms related to length of day, and UT1, its time integral. They are archived at the Special Bureau for the Atmosphere (Salstein et al. 1993) of the International Earth Rotation and Reference Frames Service. One year of excitation data, according to the Barnes et al. (1983) framework, from the U.S. National Centers for Environmental Prediction-National Center for Atmospheric Research (NCEP-NCAR) reanalyses (Kalnay et al. 1996) for 2002 is given in Fig. 1, for the three components of angular momentum, and for the motion (wind) term and the mass (surface pressure) terms. In addition, the term related to surface pressure modified by the Inverted Barometer fluctuation is given. This term has smaller

amplitude because of the reduced variability of the atmosphere over the ocean areas.

2. HIGH-RESOLUTION SPATIAL DECOMPOSITION OF THE ANGULAR MOMENTUM FIELDS

We have decomposed the atmosphere into a network of sectors to examine the higher spatial resolutions than were heretofore available. To do so, we chose equal-area sectors bounded by 72 east-west bands (at 15 degree longitude spacing) and 46 north-south bands equally spaced in sine latitude. A map of these sectors is given in Fig. 2. We examine the variability at annual time scales in Figs. 3,4 and their contributions to the overall functions of atmospheric excitation of polar motion. It can be seen that the largest covariance with the global excitation function occurs over Asia, with relative maxima in Central Asian highlands and over far east Asia showing the finer details of the variability than was possible in Nastula and Salstein (1999). The correlation in the annual band between local and global excitations, indicating phase agreement, however, is high in other regions too, including North Africa, southeast North America, and South Africa. The same general features occur in both halves of the record, both before and after 1980, about when the satellite data were added to the mix of observations for assimilation into the atmospheric analyses. Around the same time, in fact, the geodetic data improved with the introduction of advanced space-geodetic satellite techniques. The atmospheric excitations of the pressure terms with IB forcing were also studied at different seasonal timescales, including the semiannual, terannual, Chandler, and long-period (2-5 year) bands. In each of these bands, we see the dominance of the atmosphere over Eurasia, primarily, and North America, secondarily. Central-East Asia has the largest variability in all these bands. At much higher frequencies, we examine the submonthly variability as well. Here we consider the excitations without the IB, because at the more rapid scales, the IB is less active, and we note the annual progression of such variability in one representative year. The highest variability is in the middle latitudes of each hemisphere, where the weighting functions for the excitation is large. Also, the winter months of each hemisphere show the largest submonthly variability, particularly in areas known as strong storm track regions. For example, January and February feature high values of the variability in the Iceland low region, over the Northern Pacific, and in areas across Asia and North America. The annual signal in this submonthly variability is strong, with a large winter-to-summer contrast. In the southern hemisphere, the submonthly variability in its winter months, June-September, is stronger than its winter months, but by a smaller amount than the corresponding northern hemisphere differences. Oceanic contributions to polar motion excitation, including down to rapid scales, have also been determined regionally, as has been determined by models (Ponte and Ali 2002) have their strongest variability in the middle-high latitude oceans, for example in the Northern Pacific, and across the Southern Oceans especially to the southwest of both South America and Australia.

3. SUBDAILY VARIABILITY

The variability of the atmospheric excitations of polar motion and length of day is beginning to be identified because of the question of whether the atmosphere provides any forcing at this time scale. The polar motion term has been determined four times daily, at 00, 06, 12, and 18 UT (Fig. 5) and we have computed excitation terms for a year, using some updated geophysical constants and vertical integration limits for the winds between surface and 10 hPa levels (Zhou et al. 2006). We have noted that the diurnal variability is quite large, and likely related to the tides in the atmosphere. The signatures appear to have one signature in the northern

hemisphere winter and another in the northern hemisphere summer, with the transition season months typically smaller diurnal variability. That of the axial component is relatively very small (not shown).

4. LONG-TERM VARIABILITY IN SURFACE PRESSURE

As much of the polar motion excitation depends upon the surface pressure series, we wish to note its long-term global average, which has changed since 1948, the beginning of the NCEP-NCAR reanalyses record. A running mean term is given in Fig. 6, which shows the low frequency variability, which in the earlier years of the record have approximately a decadal signature, but has stabilized since around 1980. Also, when this low-frequency term is subtracted from the series, we obtain the resulting high frequencies. Here too, the character of the high frequencies, which appears to have an annual variability, changes around 1980, giving a fairly stable size of the higher frequencies, consisting of annual and shorter.

Acknowledgments. Work has been performed under Grant ATM-0429975 of the United States National Science Foundation, which has been the source of cooperation between Atmospheric and Environmental Research, Inc., Lexington, MA, USA, and the Space Research Center in Warsaw, Poland. D. Salstein was at the National Aeronautical and Space Administration/Goddard Space Flight Center through the University of Maryland/Baltimore CountyŠs GEST program for part of the study. The research performed by J. Nastula was partly supported by the Polish State Committee for Scientific Research through project 4 T12E 04526. We thank Y.H. Zhou of Shanghai Astronomical Observatory, China, for analysis of the diurnal variability and producing Fig. 5.

REFERENCES

Barnes R.T.H., Hide R., White, A.A., and Wilson C.A., 1983, Atmospheric angular momentum fluctuations, length-of-day changes and polar motion, *Proc. R. Soc. Lond.*, A387, pp. 31-73.

Kalnay E., et al., 1996, The NMC/NCAR 40-year reanalysis project, Bull. Am. Meteorol. Soc., 77(3), pp. 437-471.

Nastula J., and Salstein D., 1999, Regional atmospheric momentum contributions to polar motion, J. Geophys. Res. , 104, pp. 7347 - 7358.

Ponte R.M., and Ali A.H., 2002, Rapid ocean signals in polar motion and length of day, *Geophys. Res. Lett.*, 29(15), doi:10.1029/2002GL015312.

Salstein D.A., Kann D.M., Miller A.J., and Rosen R.D., 1993, The Sub-bureau for atmospheric angular momentum of the International Earth Rotation Service: A meteorological data center with geodetic applications, *Bull. Amer. Meteorol. Soc.*, 74, pp. 67-80.

Zhou Y.H., Salstein D.A., and Chen J.L., 2006, Revised atmospheric angular momentum series related to Earth's variable rotation under consideration of surface topography, J. Geophys. Res. in press.

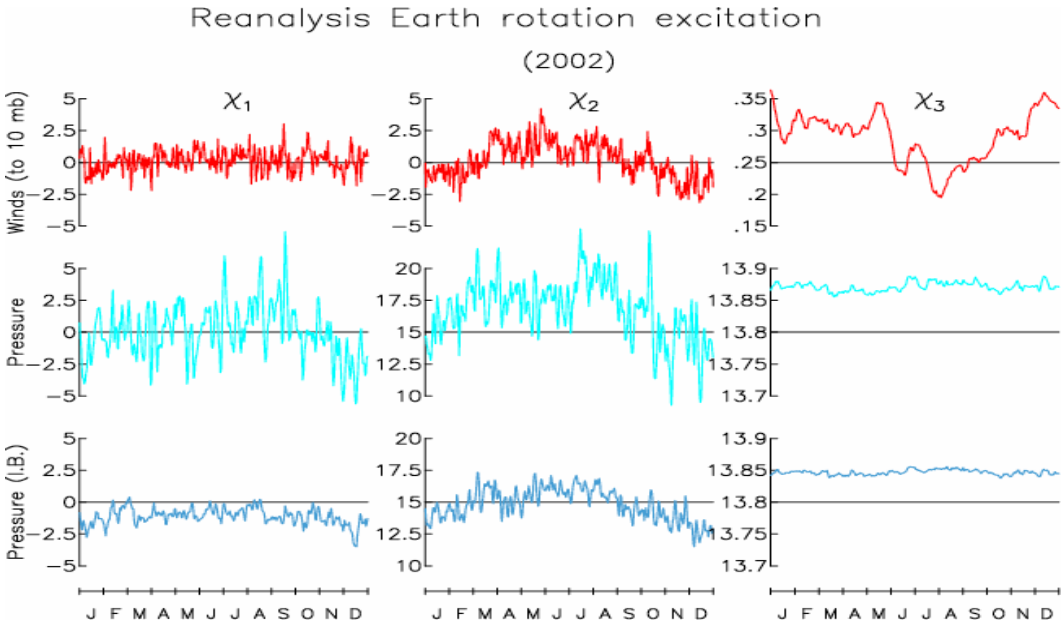

Figure 1: One year, 2002, of atmospheric excitation of Earth rotation. Columns are χ_1 and χ_2 (equatorial, related to polar motion), and χ_3 (axial, related to length of day). Rows are wind term, mass term, and mass term as modified by the Inverted Barometer.

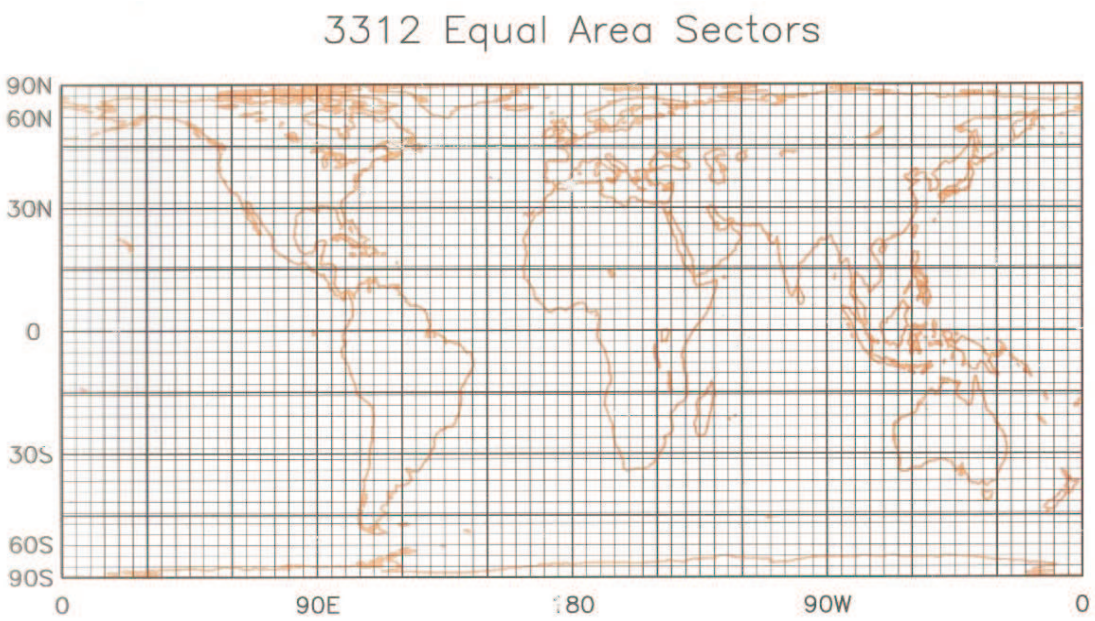

Figure 2: Map of the 3312 equal-area sectors in this study.

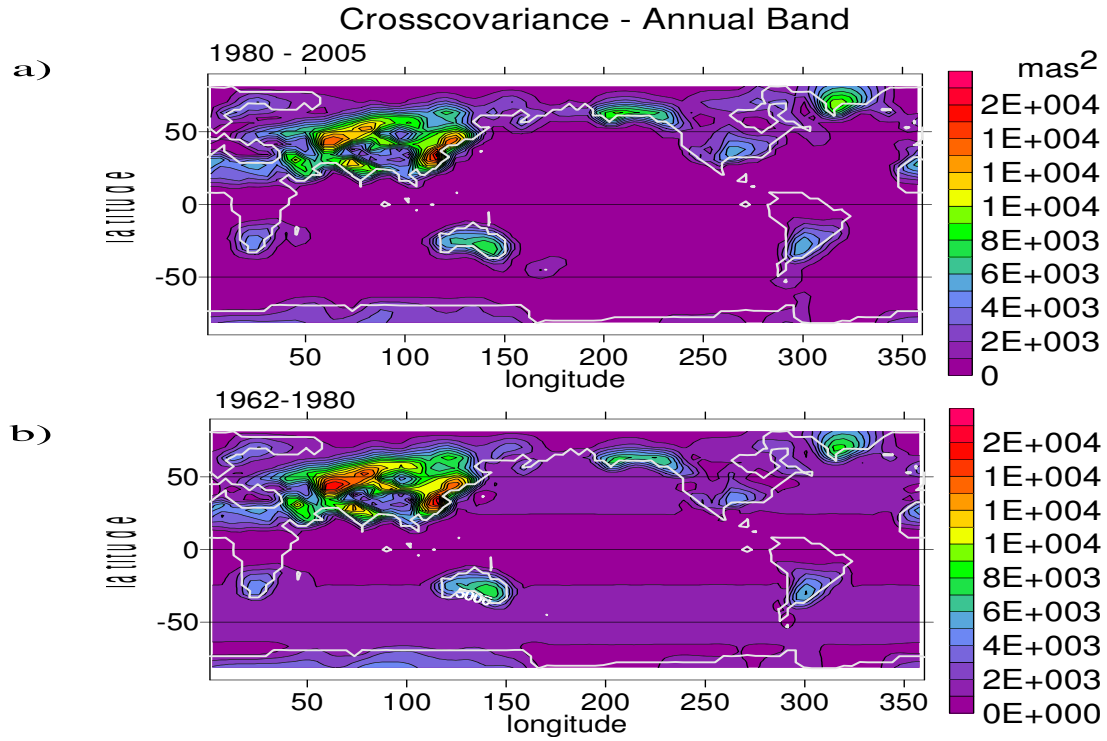

Figure 3: Cross–covariance of polar motion excitation in annual band between regional and global terms.

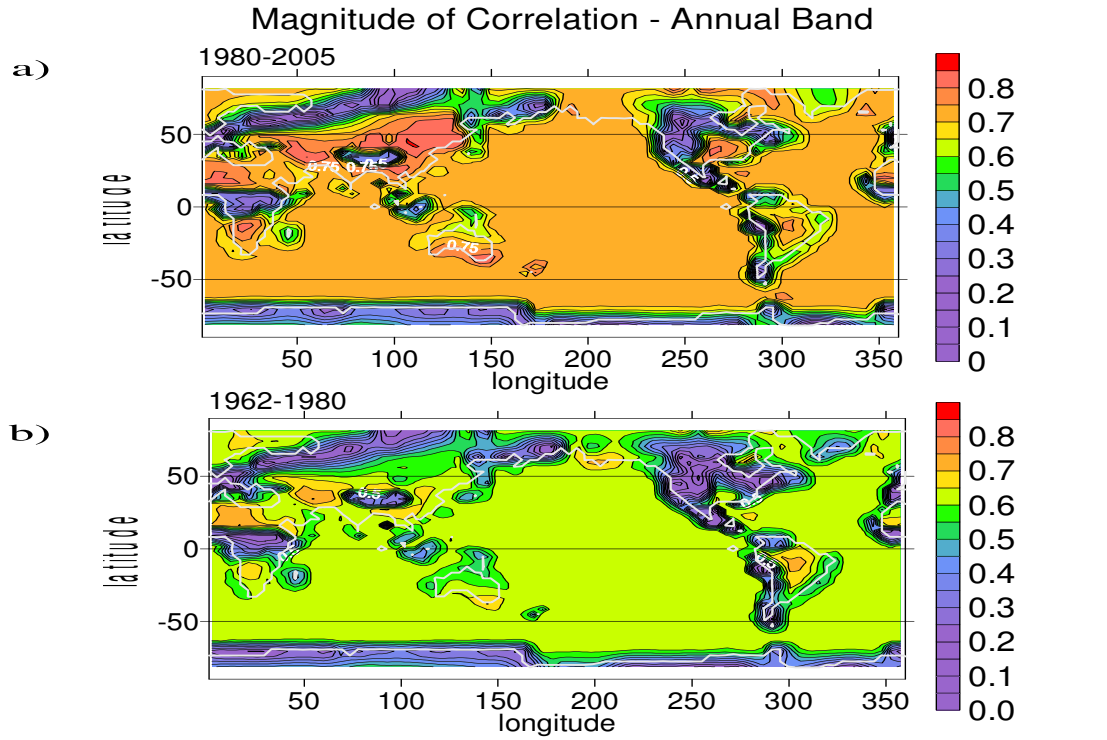

Figure 4: Correlation of polar motion excitation in annual band between regional and global terms.

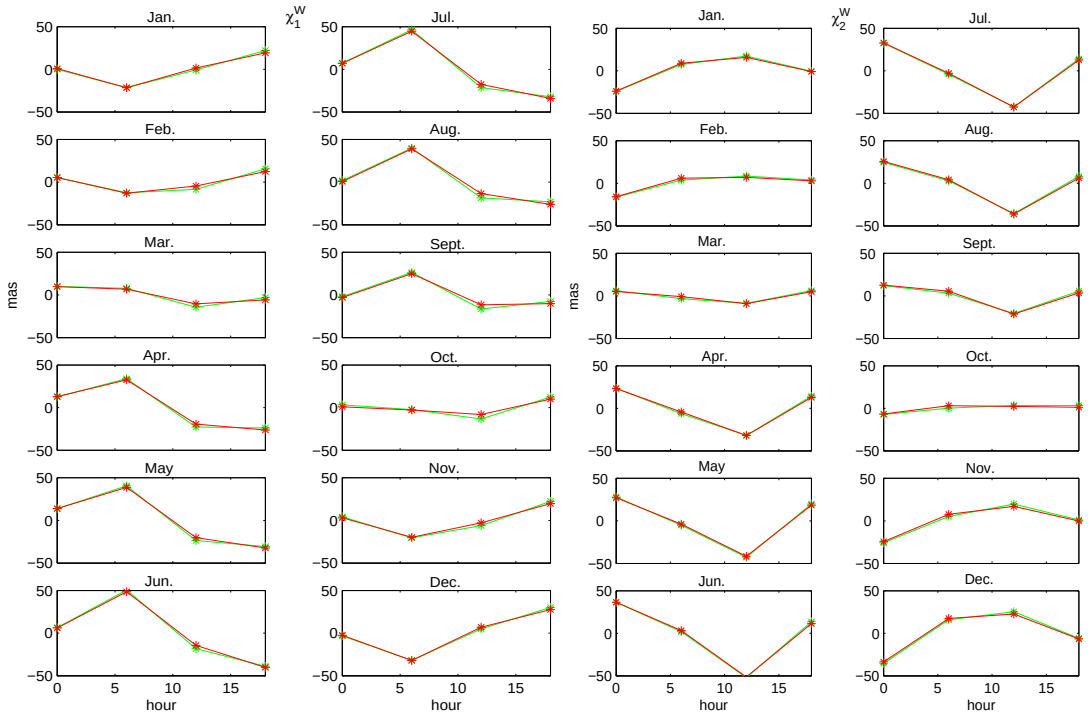

Figure 5: Four times daily excitations of two polar motion from wind terms showing seasonally modulated diurnal signature variability (Zhou et al. 2006).

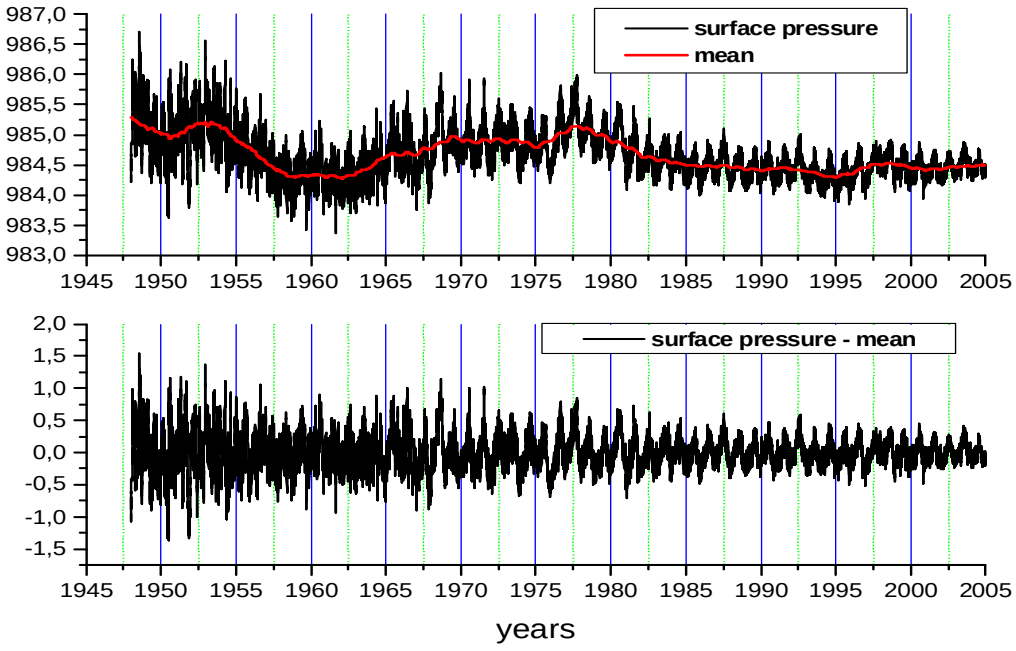

Figure 6: Values of the atmospheric surface pressure over the globe. Average denotes annual running mean. Units (hPa).

THE OCEAN'S RESPONSE TO SOLAR THERMAL AND GRAVITATIONAL TIDES AND IMPACTS ON EOP

M. THOMAS, H. DOBSLAW and M. SOFFEL
Lohrmann Observatory,
Dresden Technical University,
Mommsenstraße, 13, 01062 Dresden, Germany,
Maik.Thomas@tu-dresden.de

ABSTRACT. By means of simulations with the Ocean Model for Circulation and Tides (OMCT) the impact of oceanic mass redistributions due to pressure loading of atmospheric tides and gravitational tides on oceanic angular momentum is estimated. OMCT is forced with the luni-solar gravitational tidal potential as well as atmospheric data, i.e., heat and freshwater fluxes, wind stresses, and atmospheric surface pressure. Since no barometric approximation is applied, the ocean's response to atmospheric pressure is allowed to be dynamic as well as static. While the diurnal pressure tide is well resolved from 6-hourly analyses generally provided by meteorological centers, the semidiurnal tide aliases into a standing wave due to insufficient temporal resolution. It is demonstrated that ECMWF's 3-hourly forecasts can be used to represent atmospheric mass redistributions and corresponding oceanic responses down to semidiurnal timescales and, consequently, to determine short-term effects of the atmosphere-ocean system on Earth's rotation.

1. INTRODUCTION

This paper discusses the ocean's response to diurnal (S_1) and semi-diurnal (S_2) solar thermal tides in the atmosphere and corresponding direct gravitational tides and its impact for the calculation of Earth's Orientation Parameters (EOP). The specific interest for that kind of investigations results from the fact that pressure induced and gravitational ocean S_1 and S_2 tides cannot be separated in the observations. While gravitational tides dominate mass redistributions in the oceans, their effect can almost be neglected in the atmosphere due to the comparatively low air density. Instead, pressure variations basically forced by solar radiation are well pronounced in the atmosphere, and these pressure tides in turn cause additional tides in the ocean due to atmospheric pressure loading. To separate gravitational and pressure tides, e.g., for barometric correction in altimetry data, numerical modelling is obviously a promising way.

In general, real time atmospheric mass distributions are derived from operational data provided by meteorological data centers, e.g., the National Centers for Environment Prediction (NCEP) and the European Centre for Medium Range Weather Forecasts (ECMWF). However, the frequently used analyses with typical sampling rates of 6 and 12 hours are insufficient to resolve semidiurnal signals. Since, e.g., a sampling rate of 6 hours exactly matches the Nyquist frequency of S_2, semidiurnal tides alias into a standing wave causing unrealistic atmospheric mass redistributions and corresponding ocean responses. Thus, a priori information about the prop-

agating tidal wave is required generally provided by a time invariant model approach, although pressure tides have significant modulations on seasonal timescales [Haurwitz and Cowley, 1973; Ray and Ponte, 2003]. The central question that will be adressed here is if 3-hourly short-term forecasts provided by ECMWF can be employed to recover the semidiurnal thermal tide in the atmosphere in order to study its impact on ocean dynamics and Earth's rotation.

2. MODELING THE OCEAN'S RESPONSE TO THE DIURNAL AND SEMIDIURNAL THERMAL ATMOSPHERIC TIDES

For modeling the ocean's response to atmospheric as well as to luni-solar tidal forcing the Ocean Model for Circulation and Tides (OMCT) developed by the first author (M.T.) was employed. The numerical model is based on nonlinear balance equations for momentum, the continuity equation, and balance equations for heat and salt. The time step used is half an hour, the horizontal resolution is constant 1.875° in latitude and longitude, and 13 layers exist in the vertical. Implemented is a prognostic sea-ice model that predicts ice-thickness, compactness, and drift. Secondary effects arising from loading and self-attraction of the water column are taken into account. Atmospheric forcing enters as boundary conditions at the ocean's surface embracing atmospheric pressure, wind stresses, heat and fresh-water fluxes (precipitation and evaporation). No assumption on the ocean's response to atmospheric forcing (e.g., as inverted barometer) is applied; thus, the model allows for static as well as dynamic responses to atmospheric pressure.

To estimate the gravitational contribution to the principal diurnal and semidiurnal solar tides S_1 and S_2, a first run of OMCT was exclusively driven by the complete luni-solar tidal potential. In Figure 1 simulated mean harmonic oscillation systems of gravitational ocean tides S_1 and S_2 are given. While S_2 amplitudes reach about 30 cm in large areas, S_1 amplitudes generally do not exceed 1 cm due to adverse geometric resonance conditions.

In two further simulations gravitational forcing was turned off and only atmospheric forcing was considered to estimate circulation induced mass redistributions at S_1 and S_2 frequencies. The simulations with atmospheric forcing start from an initial climatological run that was followed by a real-time simulation for the period 1958-2000 driven by 6-hourly atmospheric fields from ECMWF's reanalysis project ERA-40. The resulting model state has been used as a common initial state for the simulations with operational atmospheric forcing. In addition to frequently used 6-hourly analyses, ECMWF operationally provides short to medium range forecasts of the transient atmospheric state. Medium range forecast runs are performed twice-daily for up to 10 days ahead and forecast fields are available with a temporal resolution of 3 hours.

Figure 2 shows rms-differences of the ocean's response to atmospheric forcing with analysis

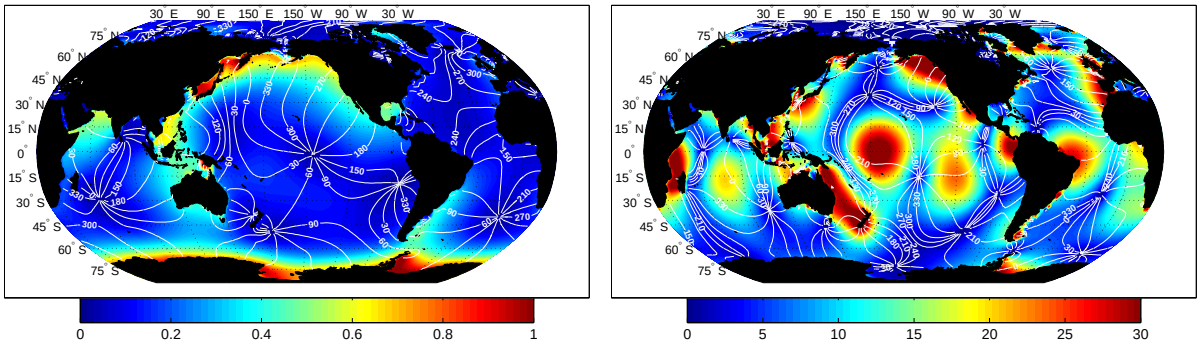

Figure 1: Simulated gravitational ocean tides S_1 (left panel) and S_2 (right panel); amplitudes are in [cm], Greenwich phases in degree.

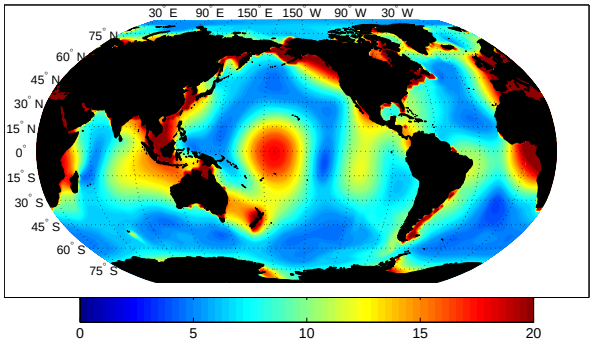

Figure 2: Total rms-differences in [cm] of the ocean's response to atmospheric forcing with analysis and forecast data.

and forecast data reaching about 20 cm in some coastal regions. These differences result from forecast errors, different wind representations (instantaneous wind velocities from analyses, accumulated wind stresses from forecasts), and different sampling rates. It can be shown that various wind representations and forecast errors are responsible for only small differences whereas the main contribution to deviations between ocean simulations driven by analyses and forecasts can be attributed to the different sampling rates.

According to Dobslaw and Thomas [2005], the mean diurnal signal in atmosphere and oceans associated with the pressure tide S_1 as deduced from 6-hourly analyses and 3-hourly forecasts and corresponding oceanic simulations are quite similar. The typical westward propagating atmospheric pressure wave is well developed, and the ocean answers, e.g., with an anticlockwise rotating wave in the Pacific with amplitudes up to about 1.5 cm. The situation is very different for S_2. Since a sampling rate of 6 hours exactly matches the Nyquist frequency, the S_2 representation within analyses aliases into an unphysical standing wave causing significant artificial momentum transfer into the oceans. In contrast to analyses, 3-hourly forecasts allow the resolution of semidiurnal waves as shown in Figure 3. The westward propagating wave in the atmosphere is well pronounced, and the corresponding oceanic response shows typical features of semidiurnal ocean tides, e.g., the anticlockwise propagating Kelvin wave around New Zealand.

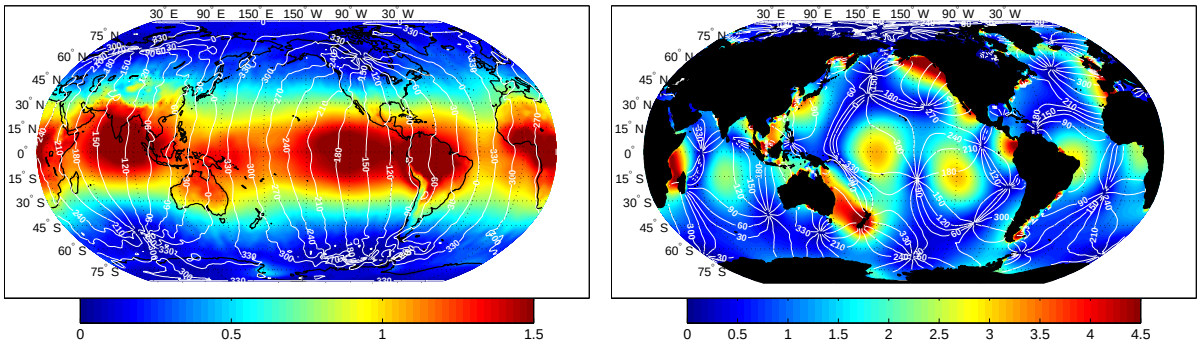

Figure 3: Pressure tide S_2 in the atmosphere (left panel, amplitudes in [hPa], phases in degree) according to 3-hourly forecasts and corresponding oceanic response (right panel, amplitudes in [cm], Greenwich phases in degree).

3. OCEANIC ANGULAR MOMENTUM

Semidiurnal and diurnal oceanic mass redistributions due to gravitational and pressure induced tides are acompanied by variations of oceanic angular momentum and, consequently, affect the Earth's rotation parameters. Corresponding mean diurnal and semidiurnal amplitudes and phases are given in Table 1. As expected for the S_1 tide the calculations with analyses and forecasts gave similar results whereas for the S_2 tide they differ significantly with deviations of order $0.25 \times 10^{24}\,\mathrm{kg\,m^2 s^{-1}}$.

Table 1: Simulated mean oceanic angular momentum amplitudes A in $[10^{24}\ \mathrm{kgm^2 s^{-1}}]$ and phases P in degree due to gravitational and pressure induced tides S_1 and S_2.

tide	x_1				x_2				x_3			
	mass		motion		mass		motion		mass		motion	
	A	P	A	P	A	P	A	P	A	P	A	P
$S_1(grav.)$	0.109	352.4	0.135	15.2	0.109	313.6	0.191	232.3	0.266	226.0	0.125	187.9
$S_1(press.)$	0.310	349.7	0.036	81.9	0.196	139.4	0.242	318.1	0.061	192.7	0.398	110.0
$S_2(grav.)$	0.820	24.9	4.869	291.4	1.320	33.0	8.002	199.4	3.111	115.3	6.9360	331.2
$S_2(press.)$	0.0751	119.3	0.488	48.8	0.123	196.3	0.804	320.2	0.221	214.6	0.568	106.8

4. CONCLUDING REMARKS

One may conclude by stating that 3-hourly operational forecasts allow the reconstruction of atmospheric mass redistributions and corresponding oceanic responses down to subdaily timescales and, consequently, to consider the transient impact of semidiurnal pressure tides, too. In contrast to previous calculations no a priori information about mean oscillations were introduced and the complete transient atmospheric dynamics could be used to force the ocean model. Thus, 3-hourly short-term forecasts provide an opportunity to determine the impact of semidiurnal signals in the coupled atmosphere-ocean system on high-resolution Earth rotation parameters, geocenter variations, and short-term gravity variations. Finally, the suggested approach allows a separation of gravitational and pressure induced tides at S_1 and S_2 frequency.

REFERENCES

Dobslaw, H., and M. Thomas, 2005, Atmospheric induced oceanic tides from ECMWF forecasts, Geophys. Res. Lett., 32, L10615, doi:10.1029/2005GL022990.

Haurwitz, B., and A. D. Cowley, 1973, The diurnal and semidiurnal barometric oscillations, global distribution and annual variation, Pure Appl. Geophys., 102, pp. 193–222.

Ray, R.D., and R. M. Ponte, 2003, Barometric tides from ECMWF operational analyses, Ann. Geophys., 21, pp. 1897–1910.

COMPARISONS OF HYDROLOGICAL ANGULAR MOMENTUM (HAM) OF THE DIFFERENT MODELS

J. NASTULA[1], B. KOLACZEK[1], W. POPIŃSKI[2]
[1]Space Research Centre
Bartycka 18a, 00-716 Warsaw, Poland
e-mail: nastula@cbk.waw.pl; e-mail: kolaczek@cbk.waw.pl
[2]Central Statistical Office
Al. Niepodległośsci 208, 00-925 Warsaw, Poland
e-mail: W.Popinski@stat.gov.pl

ABSTRACT. In the paper hydrological excitations of the polar motion (HAM) were computed from various hydrological data series (NCEP, ECMWF, CPC water storage and LaD World Simulations of global continental water). HAM series obtained from these four models and the geodetic excitation function GEOD computed from the polar motion COMB03 data were compared in the seasonal spectral band. The results show big differences of these hydrological excitation functions as well as of their spectra in the seasonal spectra band. Seasonal oscillations of the global geophysical excitation functions (AAM + OAM + HAM) in all cases besides the NCEP/NCAR model are smaller than the geodetic excitation function. It means that these models need further improvement and perhaps not only hydrological models need improvements.

1. INTRODUCTION

Excitation of polar motion is related in large measure to the redistribution of atmospheric, oceanic and hydrological masses. Up to now the influence of hydrological masses variations on polar motion has not been recognised well, due to lack of data of hydrological excitation of polar motion (Hydrological Angular Momentum - HAM). Recently several models of hydrological components, land water, snow, soil moisture have been worked out and studied (Chen and Wilson, 2005). They are available in the Special Bureau for Hydrology (SBH) of the Global Geophysical Fluid Center (GGFC). Our previous investigations of influence of HAM on the polar motion in different part of spectra show that consideration of the daily HAM data available in the SBH does not improve agreement of the geophysical excitation of polar motion containing contributions from atmosphere, oceans and hydrology (AAM+OAM+HAM) with geodetic excitation function (Nastula, Kolaczek, 2005).

In the present paper hydrological excitations of the polar motion are computed from various hydrological data series. Three of them National Centers for Environmental Prediction (NCEP), European Centre for Medium – Range Weather Forecasts (ECMWF) and Climate Prediction Center (CPC) are available from the website of the SBH. The additional hydrological data are the Land Dynamics (LaD) World Simulations of global continental water for the period from 1980 to April 2004 (Milly and Shmakin, 2002). The spectra of these HAM series obtained from the four models in seasonal spectral band are compared with the spectra of geodetic excitation function (GEOD) of polar motion, computed from the polar motion COMB03 data (Gross, 2003).

2. DATA

In this paper we investigate the polar motion excitation of geophysical fluids, atmosphere, ocean and hydrosphere. The oceanic influence on polar motion is investigated by using Oceanic Angular Momentum (OAM) derived by Gross et al. (2003) from the ECCO – JPL (Estimating the Circulation and Climate of the Ocean – Jet Propulsion Laboratory) ocean model, from 1980 to 2002.2. The data are available from the web site of the Special Bureau for the Oceans (SBO) of the GGFC. Oceanic excitation is consider as sum of the signals resulting from changes in the oceanic mass and velocity fields. The input OAM series assumes an oceanic inverted barometer correction (IB) which is response to surface atmospheric pressure signals.The atmospheric angular momentum (AAM) series is derived from 6-hour time series of the U.S. NCEP/NCAR reanalysis data (Salstein et al., 1993; Kalnay, 1996). In this study we used a sum of the wind and the pressure terms with the IB correction for the ocean response, what is consistent with the OAM series. The daily hydrological excitation function HAM is obtained by two means. The one HAM is taken from the web site of the Special Bureau for Hydrology of the GGFC for the period from 1948 -2001. This HAM is computed by the SBH from the NCEP/NCAR Reanalysis soil moisture and snow accumulation data model. The three HAM excitation functions were computed using formula given by Chen and Wilson(2005) from the three water data storage: 1. HAM-LaD (Land Dynamics) model DANUBE containing monthly solutions of snow water equivalent, shallow grand water in 1980-2004 (Milly and Shamkin, 2002); 2. HAM CPC-LDAS model containing monthly solutions of soil water storage in 1980-2004 developed by National Oceanic and Atmospheric Administration (NOAA) Climate Prediction Center (CPC); 3. HAM ECMWF model containing daily solutions of water storage defined as the sum of wetness and snow water in 1979-1993 based on the ECMWF reanalysis data. The last 2 water storage data sets are available at the SBH. The HAM ECMWF model computed in shorter period of time in 1979-1993 was not considered in further analysis.

The excitation function of polar motion referred to as "geodetic" excitation (GEOD)was computed from the polar motion COMB03 data (Gross, 2003) by applying the Kalman filter developed by Brzeziński (Brzeziński, 1992; Brzeziński et al., 2004). The input polar motion data with 12-hour sampling covers the period from 1962 to 2003.

The equatorial components of all these HAM data χ_1, χ_2 are shown in Fig. 1. It is easy to see that these functions are different and the SBH, NCEP/NCAR data are larger than others.

3. SPECTRA COMPARISONS

In order to check the character of the variations of the considered series of excitation functions of polar motion, spectra of all considered excitation functions were computed by means of the FTBPF (Fourier Transform Band Pass Filter), (Kosek, 1995). To ensure a high frequency resolution in the computation of FTBPF, appropriate values of the parameter λ, describing the filter bandwidth, have to be chosen. In this paper $\lambda = 0.02$ was chosen. The spectra of all these models show oscillations with annual, semiannual and 120 day periods both in the prograde as well as in the retrograde band (see Figures 2 and 3). It is easy to see that amplitudes of these oscillations are different in the different models. The smallest amplitudes of these oscillations are in the case of the LaD model of HAM. In the case of the NCEP/NCAR SBH model of HAM the amplitude of the annual oscillation is high and comparable with the amplitude of annual oscillation of AAM + OAM excitation function.

In the spectra of the global geophysical fluids excitation functions (AAM+OAM+HAM) the annual oscillation is the most energetic one. Amplitudes of the annual oscillation of the global geophysical fluid excitation function with the NCEP/NCAR model of HAM is much higher than in the case of the geodetic excitation function. The best agreement of the amplitudes of the annual oscillations of the global geophysical excitation function with the geodetic one is in the

case of the CPC model of HAM in prograde part of the spectrum and in the case of LaD model of the HAM in the retrograde part of spectrum. In other part of the seasonal spectrum of the global geophysical fluid excitation functions amplitudes of their oscillations are much smaller than in the case of the spectrum of geodetical excitation function. Comparison of the non-atmospheric+oceanic excitation function of polar motion with the hydrological excitation shows a nearly good agreement of amplitude of their annual oscillations in χ_1 and χ_2 and of semiannual oscillations in χ_2 only (Fig. 4).

5. CONCLUSIONS

Mass fields are important to both gravity missions and the Earth rotation, and here we considered the second.

HAM excitation functions computed from different water storage model are not homogeneous and differs greatly in temporal characteristics and in their spectra in the seasonal band.

HAM excitation functions do not improve the agreement between the observed geodetic excitation function and the global geophysical excitation function of polar motion.

The HAM models need further improvements.

Acknowledgments. The research reported here was supported by the Polish State Committee for Scientific Research through project 4 T12E 04526.

REFERENCES

Chen, J.,L., and C. R. Wilson, 2005, Hydrological excitations of polar motion, 1993-2003, *Geophys J Int.*, 160, Issue 3. pp. 833-839.

Brzeziński, A., 1992, Polar motion excitation by variations of the effective angular momentum functions: considerations concerning deconvolution problem, *Manuscr. Geodet*, 17, 3-20.

Brzeziński, A, J. Nastula, B. Kolaczek and R. M. Ponte, 2004, Ocean excitation of polar motion from intrasesonal to decadal periods, Proceedings of the 23rd IUGG General Assembly, Sapporo 2003 Japan, IAG Symposia Vol.128 A window on the future of geodesy, edited by Fernando Sanso, Springer-Verlag Berlin Heidelberg 2005, pp 591-596.

Gross, R. S., 2003, Combinatios of Earth Orientations Measurements: SPACE02, COMB2003 and POLE2002, Tech. Rep. JPL Publications 02-011, JPL, Pasadena, CA.

Kalnay, E., 1996, The NCEP/NCAR 40-year Reanalysis Project, *Bull. Amer. Meteor. Soc.*, 77, 437 - 471.

Kosek, W., 1995, Time Variable Band Pass Filter Spectrum of real and complex-valued polar motion series, *Artificial Satellites, Planetary Geodesy*, 30, 1, 27 - 43.

Milly, P.C.D. and A. B. Shmakin, 2002, Global Modelling of Land Water and Energu Balances. Part I: The Land Dynamics (LaD) Model, *J. Hydrometeor*, 3, 283-299.

Nastula, J. and B. Kolaczek, 2005, Analysis of Hydrological Excitation of Polar Motion. Proceedings of the Workshop: Forcing of polar motion in the Chandler frequency band: a contribution to understanding interannual climate variations. Centre Europeen de Geodynamique et de Seismologie, Luxembourg, 149-154.

Salstein, D. A., D. M. Kann, A. J. Miller, and R. D. Rosen, 1993, The Sub-Bureau for Atmospheric Angular Momentum of the International Earth Rotation Service: a meteorological data center with geodetic applications, *Bull. Amer. Meteor. Soc.*, 74, 67-80.

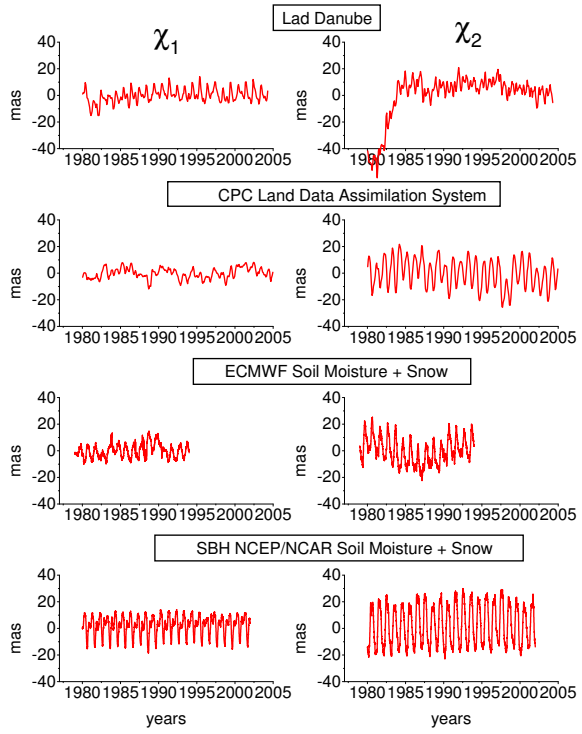

Figure 1: The equatorial excitation functions χ_1 and χ_2, computed from different hydrological data.

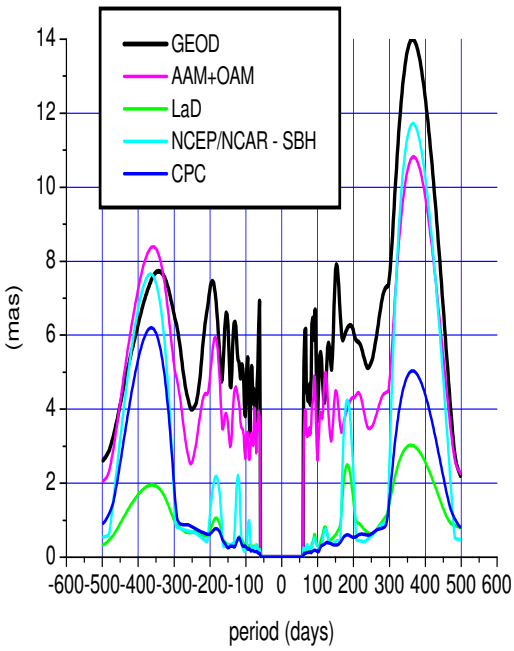

Figure 2: The FTBPF amplitude spectrum of the excitation functions in 1985-2002 filtered by the Butterworth FTBPF with the 600 day cutoff period and computed for the parameter $\lambda = 0.02$.

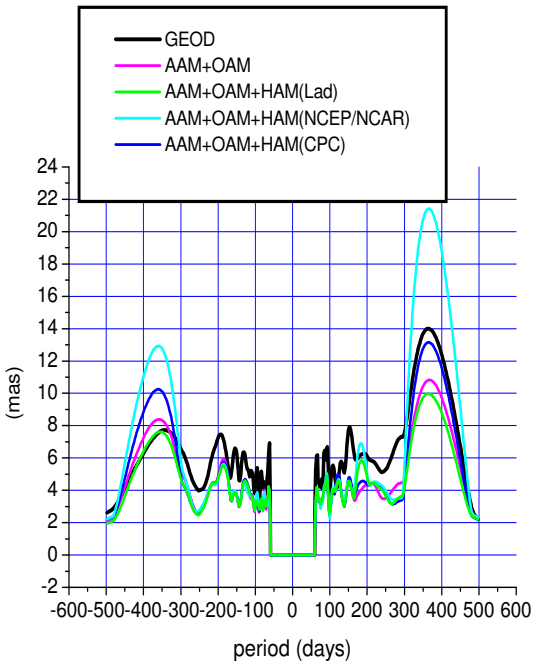

Figure 3: The FTBPF amplitude spectrum of the excitation functions in 1985-2002 filtered by the Butterworth FTBPF with the 600 day cutoff period and computed for the parameter $\lambda = 0.02$.

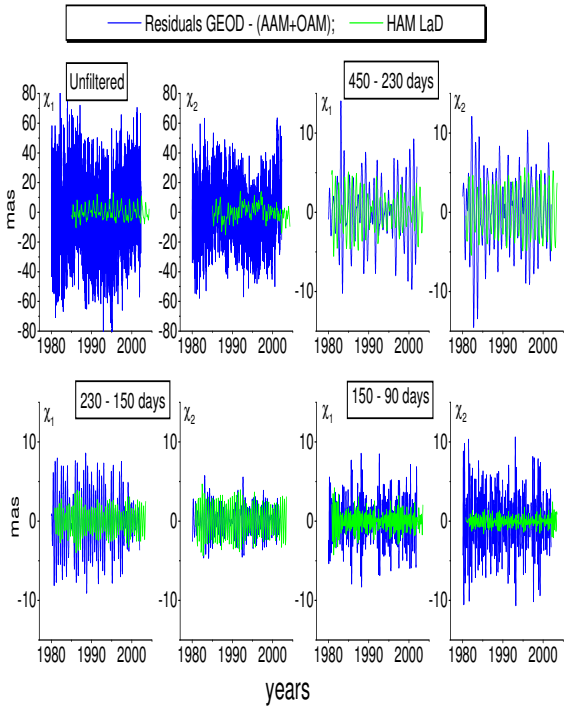

Figure 4: Comparison of the non-atmospheric + oceanic excitation function of polar motion with the hydrological excitation data in different spectral bands.

ATMOSPHERIC AND OCEANIC EXCITATION OF THE FREE CORE NUTATION: OBSERVATIONAL EVIDENCE

A. BRZEZIŃSKI and S. BOLOTIN[1]
Space Research Centre, Polish Academy of Sciences
Bartycka 18A, 00-716 Warsaw, Poland
e-mail: alek@cbk.waw.pl

ABSTRACT. The paper discusses the excitation of the observed free core nutation signal by the combination of atmospheric and oceanic processes. We compute the "geodetic" excitation from the time series of the celestial pole offsets and compare it to the subdiurnal estimates of the atmospheric and oceanic angular momenta. We find that during 1993.0 to 2000.5 the geophysical excitation contained more power at the FCN frequency, up to the factor of 10 to 30, than needed to explain the observed free motion. The cross spectral analysis shows that the observed and modeled excitations were coherent near the FCN frequency – the coherence magnitude estimates are between 0.7 and 0.8. But surprisingly, the geodetic and geophysical excitations are found to be out of phase at the FCN frequency.

1. INTRODUCTION

The celestial motion of the Earth's pole, that is precession-nutation, is dominated by the lunisolar effect which is expressed by the conventional model. The remaining part is driven by large-scale geophysical processes leading to the angular momentum exchanges between the solid Earth and its fluid environment including the dynamically coupled atmosphere-ocean system. A part of this geophysical component is the regular variation which can be expressed by the incremental amplitudes of the conventional precession-nutation model. This variation has been studied extensively by the use of the atmospheric and nontidal oceanic angular momentum (AAM, OAM) data with subdiurnal resolution by, e.g., Bizouard *et al.* (1998), Brzeziński *et al.* (2004). The remaining tiny part, below 1 milliarcsecond (mas), is the irregular fluctuation consisting of the free core nutation (FCN) and a broad-band variability with power concentrated mostly around the prograde annual frequency (Brzeziński *et al*, 2004).

Here we focus our attention on the atmospheric and oceanic excitation of the FCN signal seen in the time series of the celestial pole offsets determined from the very long baseline interferometry (VLBI) observations (Fig. 1a). Understanding the FCN and its excitation mechanism is needed for the following purposes: 1) further improvement of the conventional precession-nutation model – see (Dehant, this volume); 2) validation of the available time series of the VLBI celestial pole offsets; 3) constraining the atmospheric and oceanic global circulation models at diurnal periods.

It is commonly believed that the FCN signal is driven mostly by variability in the atmosphere and oceans associated with the daily solar heating cycle. Our earlier spectral estimation based

[1]on leave of absence from: Main Astronomical Observatory, National Academy of Sciences of Ukraine, Akademika Zabolotnoho 27, 03680 Kiev, Ukraine

on the first operational sets of 6-hourly AAM indicated that the matter term of AAM has enough power near the FCN resonant frequency to explain the observed free signal, while the contribution of the motion term is negligible (Brzeziński, 1994b). This conclusion was confirmed later on the basis of the reanalysis AAM series (Brzeziński *et al.*, 2002). A recent study based on the output of the barotropic ocean circulation model (Brzeziński *et al.*, 2004) demonstrated that adding the contribution from the nontidal OAM increased the FCN excitation power of the matter term but had a negligible contribution to the excitation by the motion term.

In this study our approach is similar to that applied successfully in the excitation study of the Chandler wobble (Brzeziński and Nastula, 2002) – from the selected series of the VLBI determinations of nutation we compute the corresponding excitation series, the "geodetic" excitation of nutation (Brzeziński, 1994a; Bolotin, this volume), which is then compared to the available subdiurnal estimates of the atmospheric and oceanic angular momentum functions. Comparison is performed in both the time domain – a sliding window correlation analysis, and in the frequency domain – the cross-spectral analysis in vicinity of the resonant FCN frequency.

2. DATA SETS AND COMPUTATIONAL PROCEDURE

Several time series of the celestial pole offsets are currently available, including individual solutions derived by different VLBI analysis centers and the combination series. Here we use the following 2 individual solutions which have been recommended by Bolotin and Brzeziński (2005) for investigations concerning the FCN signal: 1) GSF – series derived at the NASA Goddard Space Flight Center, USA, using the software CALC/SOLVE; 2) MAO – derived at the Main Astronomical Observatory of the National Academy of Sciences of Ukraine, using the software SteelBreeze. These series span the period 1979.0 to 2005.0 and are available from the International VLBI Service (GSF) or from S.B. upon request (MAO).

We use the same geophysical excitation series as Brzeziński *et al.* (2004). In case of the atmospheric excitation this is the AAM series based on results of the NCEP-NCAR reanalysis project (Kalnay *et al.*, 1996; Salstein and Rosen, 1997), available from the IERS Special Bureau for the Atmosphere. The series spans the period from 1948 to 2005 and is sampled 4 times daily. The AAM series consists of the wind (motion) and the pressure (matter) terms. In addition, there is the pressure term corrected for the ocean response using the inverted barometer (IB) model, further denoted AAMIB. The oceanic excitation is expressed by the OAM series derived from a barotropic ocean model forced by the NCEP-NCAR reanalysis fields (Ponte and Ali, 2002). The series consists of the motion and mass (matter) terms. It is sampled hourly and covers the period between 1993.0 and 2000.5. When considering the combined atmospheric and oceanic excitation this OAM series should be added to AAMIB.

In the computations we assume that only the matter term of the excitation functions (pressure term of AAM, mass term of OAM) influences the FCN signal, that is we neglect the motion term; see (Brzeziński, 1994a; Bolotin, this issue) for justification.

We process the input time series in the following way. First, we remove from the VLBI data corrections to the conventional precession-nutation model and derive the corresponding (geodetic) excitation of nutation. Then, we extract from each geophysical excitation series (AAM, AAMIB, OAM) the diurnal retrograde component by complex demodulation at -1 cycle per sidereal day (cpsd). Each demodulated excitation series is reduced by removing the best least squares fit of the model consisting of a sum of first-order polynomial and sinusoids with periods ± 1, $\pm 1/2$, $\pm 1/3$ yr. After smoothing all the series with cut-off period of 2 months, we compare the VLBI-inferred excitation to the combined atmospheric/oceanic excitation assuming three different models of the ocean response to the atmospheric forcing: 1) rigid ocean response with the aggregated excitation represented just by AAM, 2) inverted barometer response, with excitation expressed by AAMIB, and 3) dynamic response, with excitation AAMIB+OAM.

3. RESULTS AND CONCLUSIONS

From Fig. 1a it can be seen that the input VLBI data sets do not differ significantly. However, after computing the corresponding excitation functions (Fig. 1b) the differences between series became more visible. All comparisons illustrated in Figures 2 to 4 and discussed below concern only the VLBI nutation series MAO.

The time domain comparison done in Fig. 2a shows a rough agreement in size of the excitation inferred from VLBI data and the geophysical excitations AAM, AAMIB+OAM, while the variability of AAMIB is considerably lower. Overall correlation between geodetic and geophysical excitations shown in Fig. 2a is rather low: for χ_1 it is -0.206, 0.232, 0.132, for χ_2 it equals 0.068, 0.221, 0.141, where the subsequent numbers refer to AAMIB, AAM and AAMIB+OAM, respectively. The sliding-window correlation analysis (Fig. 3) reveals periods with high correlation, up to 0.8, but also periods with significant negative values.

Comparison of the power spectral densities done in Fig. 2b shows that geophysical excitation functions contain more power at the FCN frequency than the geodetic excitation, by the factor of about 10 for AAMIB and AAM, and as much as about 30 for AAMIB+OAM. But the time interval 1993.0–2000.5 used to estimate the power spectra at the FCN period of 1.18 years is relatively short. When considering the atmospheric excitation over the entire period 1984–2005 with the VLBI data (see the PSD in Fig. 1b), the discrepancy of power almost disappears. The integration of cross-power spectrum in the vicinity of the FCN frequency, yields a high coherence magnitude, between 0.7 and 0.8, for all 3 geophysical excitation series (Fig. 4). But surprisingly, the estimated argument of coherence is close to 180°, that is the geodetic and geophysical excitations are out of phase. Extending interval of comparison to 1984–2000 decreases coherence to 0.3 for AAM and to 0.2 for AAMIB, and changes the argument to about $-90°$.

In conclusion we should say that the reported results though promising in several aspects nevertheless have to be treated as preliminary. Such investigations should be continued using alternative subdiurnal estimates of the atmospheric and oceanic excitation of Earth rotation.

Acknowledgments. This research has been supported by the Polish Ministry of Scientific Research and Information Technology under grant No. 5 T12E 039 24. The work of SB was supported by the post-doc visiting grant in a frame of the Descartes–Nutation project.

REFERENCES

Bizouard Ch., A. Brzeziński and S. D. Petrov, 1998, Diurnal atmospheric forcing and temporal variations of the nutation amplitudes, *Journal of Geodesy*, 72, 561–577.

Bolotin S. and A. Brzeziński, 2005, Investigation of the atmospheric and oceanic excitation of the free core nutation, *Geophys. Res. Abstracts*, 7, 09725.

Brzeziński A., 1994a, Polar motion excitation by variations of the effective angular momentum function, II: extended model, *manuscripta geodaetica*, 19, 157–171.

Brzeziński A., 1994b, Diurnal and semidiurnal polar motions estimated from the intensive atmospheric angular momentum data, *Annales Geophysicae*, 12 (Suppl.I, Part I), C177.

Brzeziński A. and J. Nastula, 2002, Oceanic excitation of the Chandler wobble, *Adv. Space Res.*, 30, No. 2, 195–200.

Brzeziński A., Ch. Bizouard and S. Petrov, 2002, Influence of the atmosphere on Earth rotation: what new can be learned from the recent atmospheric angular momentum estimates? *Surveys in Geophys.*, 23, 33–69.

Brzeziński A., R. M. Ponte and A. H. Ali, 2004, Nontidal oceanic excitation of nutation and diurnal/semidiurnal polar motion revisited, *J. Geophys. Res.*, 109, No. B11, doi: 10.1029 / 2004JB003054.

Kalnay E., et al., 1996, The NMC/NCAR 40-year reanalysis project, *Bull. Amer. Met. Soc.*, 77 (3), 437–471.

Salstein D. A. and D. Rosen, 1997, Global momentum and energy signals from reanalysis systems, *Proc. 7th Conference on Climate Variations*, American Met. Soc., Boston, Massachusetts, 344–348.

Ponte R. M., and A. H. Ali, 2002, Rapid ocean signals in polar motion and length of day, *Geophys. Res. Lett.*, 29, doi:10.1029/2002GL015312.

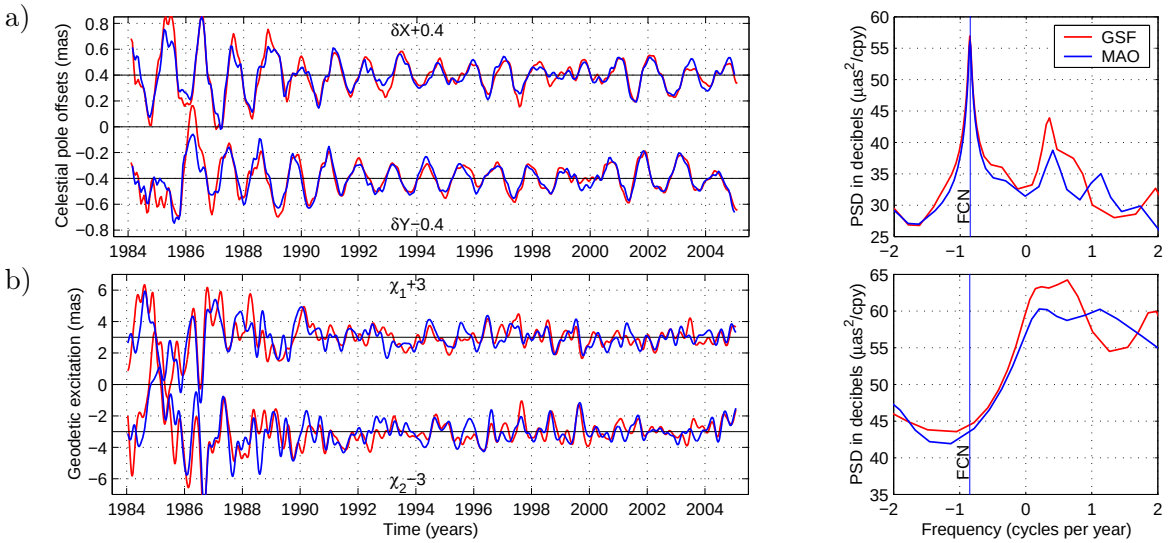

Figure 1: (a) Celestial pole offsets observed by VLBI and (b) the corresponding excitation function. The right-hand side plot show the maximum entropy method power spectra of the complex combinations $P = \delta X + i\delta Y$ and $\chi = \chi_1 + i\chi_2$.

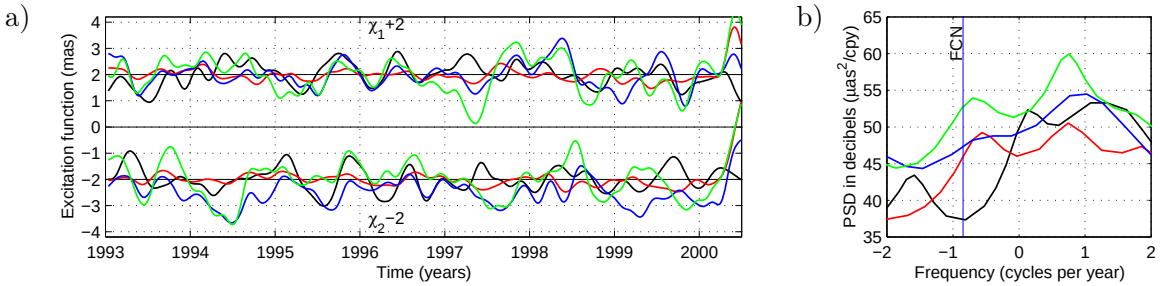

Figure 2: Comparison of the geodetic excitation of nutation (black) with geophysical excitations AAMIB (red), AAM (blue), AAMIB+OAM (green), in (a) time domain, (b) frequency domain.

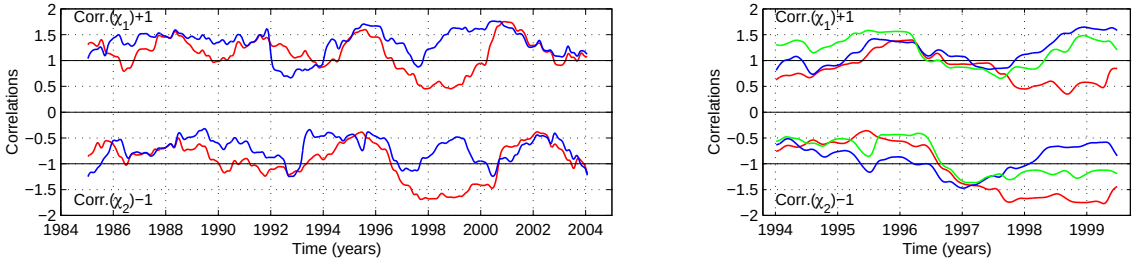

Figure 3: Sliding-window correlation between geodetic and geophysical excitations of nutation: AAMIB (red), AAM (blue) and AAMIB+OAM (green). Window length is 2 years.

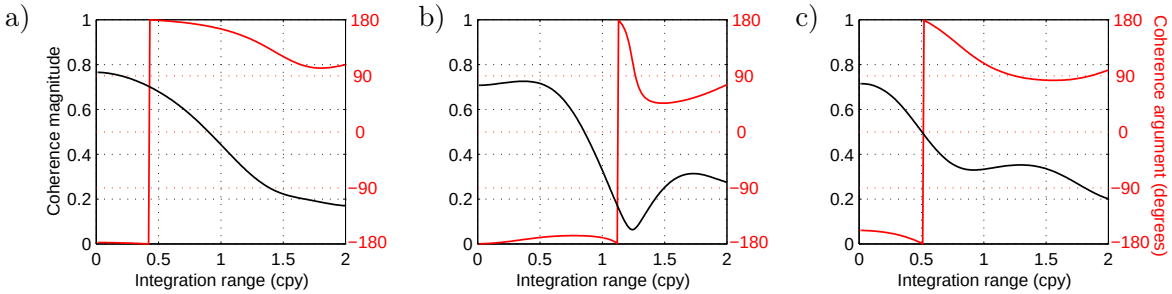

Figure 4: Coherence at the FCN frequency between geodetic and geophysical excitations of nutation (a) AAM, (b) AAMIB, (c) AAMIB+OAM, shown as a function of the length of the cross-power spectrum integration interval. Data span: 1993.0–2000.5.

RESONANCE EFFECTS AND POSSIBLE EXCITATION OF FREE CORE NUTATION

J. VONDRÁK, C. RON
Astronomical Institute, Academy of Sciences of the Czech Republic
Boční II, 141 31 Prague 4, Czech Republic
e-mail: vondrak@ig.cas.cz, ron@ig.cas.cz

ABSTRACT. From the direct analysis of VLBI observations of celestial pole offsets in the years 1982.4 – 2005.4 we found that the period of the Retrograde Free Core Nutation (RFCN) apparently grew from 425 to 470 days during the past 10–15 years. At the same period, we also derived the varying retrograde annual term of nutation that is closest to resonance. A subsequent study of indirect determination of RFCN period from this term through the resonance effects proved that the natural resonance period remained stable and was about 430 solar days. From this follows that a geophysical excitation should exist, with a terrestrial frequency close to that of RFCN (of about -1.0049 cycles per solar day), invoking the apparent changes of the directly observed RFCN period. It is demonstrated that an excitation of a very small amplitude (on the level of observation noise) is sufficient to produce such changes.

1. INTRODUCTION

We recently studied RFCN from the combined GPS/VLBI celestial pole offsets (Vondrák et al. 2005), referred to IAU2000A model of nutation, in the interval 1994.3 – 2004.6. We found that the period of RFCN as derived from the observed forced nutation terms through resonance effects remains very stable, in spite of the fact that the direct determination from the observed celestial pole offsets implies its large changes. Here we study the same problem from VLBI-only observations, in a longer time interval. To this end, we use the IVS combined solution ivs05q2X.eops (IVS 2005) covering the interval 1979.6 – 2005.4, namely the celestial pole offsets δX, δY. Prior to analysis, the data were cleaned, i.e., all offsets greater than 1mas were removed, and the sparse and scattered data before 1982.4 were rejected.

2. DIRECT AND INDIRECT ANALYSIS OF CELESTIAL POLE OFFSETS

First of all, we divided the data into three time windows (each 7 years long), and made the spectral analysis. The result is depicted in Fig. 1, from which the apparent change of the period and amplitude of the dominant peak is clear.

Now the question arises if the moving peak, determined from this direct analysis, really represents the changes of the resonant period of RFCN. From the forced nutation terms, the retrograde annual term is the closest to the resonance and therefore most sensitive to its changes. If the resonance period changes, the amplitude of the annual term must also change. Therefore

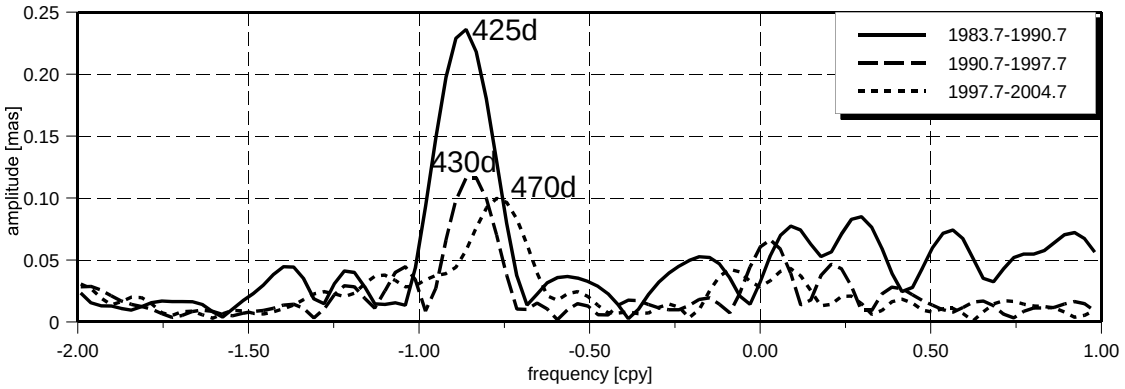

Figure 1: Spectral analysis of IVS celestial pole offsets in 3 time windows

we estimate the behavior of both RFCN and annual terms, in the running 6-year interval. We estimate both amplitude and period for RFCN, and only the amplitude for the annual term. The results are shown in Fig. 2; it is evident that all three parameters vary in time.

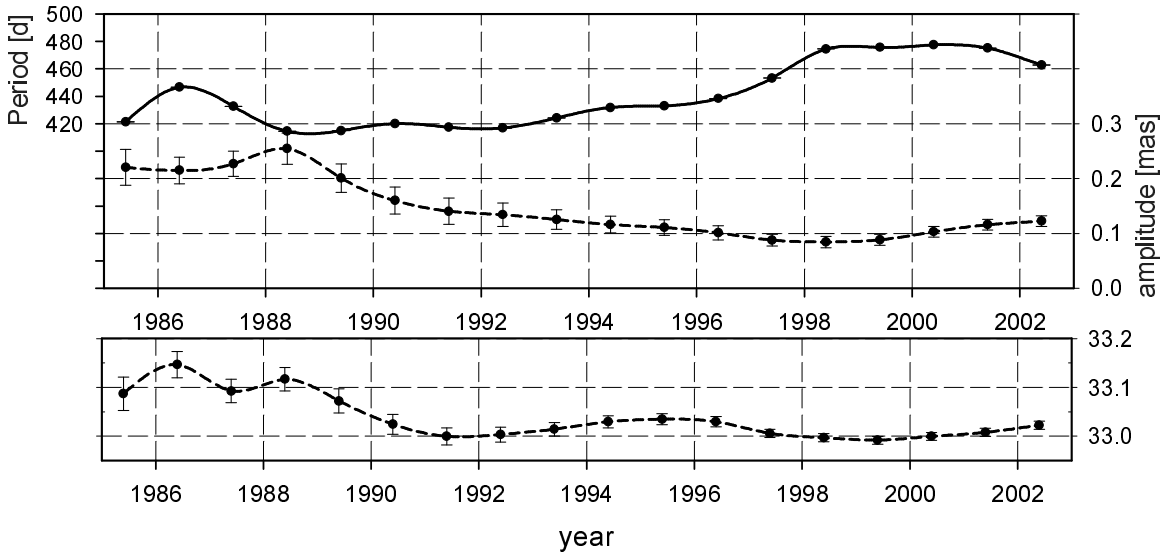

Figure 2: Variation of the period and amplitude of RFCN (upper plot) and of the amplitude of retrograde annual term (lower plot)

In order to decide if the observed variations of the annual term are in agreement with the observed variations of the RFCN period or not, we use the transfer function (giving the ratio of the amplitude of non-rigid to rigid Earth model) derived by Matthews et al. (2002)

$$T(\sigma) = \frac{e_R - \sigma}{e_R + 1} N_\circ \left[1 + (1+\sigma) \left(Q_\circ + \sum_{j=1}^{4} \frac{Q_j}{\sigma - s_j} \right) \right] \qquad (1)$$

for the indirect determination of RFCN period. Here $e_R = (C - A)/A = 0.0032845075$ is the dynamical ellipticity of the rigid Earth used to compute the 'rigid' solution. The argument σ is the terrestrial frequency in cycles per sidereal day, the other parameters are generally complex

constants, among which s_j are the resonant frequencies (of Chandler wobble, RFCN, prograde FCN and Inner Core Wobble, respectively).

In our case, only s_2 is important; the period P_{RFCN} (in celestial frame and expressed in mean solar days) is tied with s_2 by a simple relation $P_{RFCN} = 0.99727/(s_2 + 1)$. We used Eq. (1) and the rigid-Earth value of the amplitude of retrograde annual nutation term to calculate its value for a non-rigid Earth, for the periods of RFCN in the range 420–460 days. The result is shown in Fig. 3 from which follows that the possible value of resonance period, implied by variations of the annual term, keeps close to 430 days, within a fraction of a day. It is in good agreement with our previous result (Vondrák et al. 2005) – we found from 5 nutation terms, observed by VLBI and GPS in 1994.3–2004.6 that $P_{RFCN} = 430.55 \pm 0.11$ days.

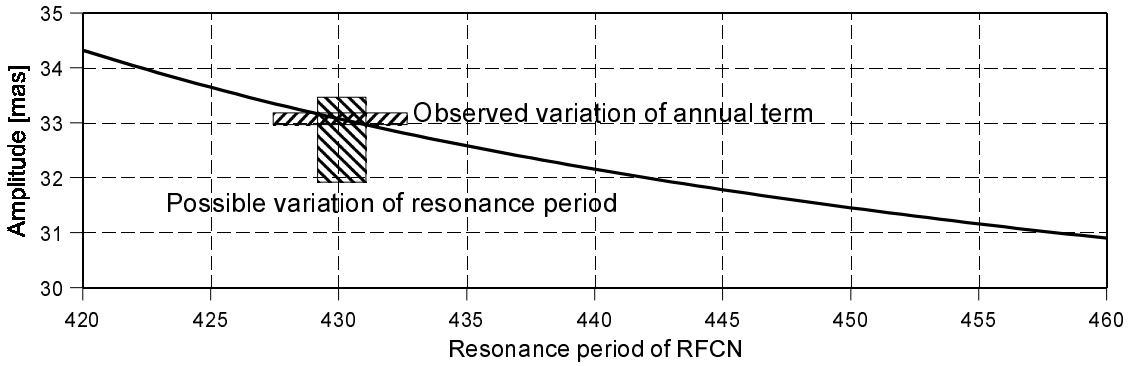

Figure 3: Amplitude of retrograde annual nutation in terms of RFCN period

3. LOOKING FOR POSSIBLE EXCITATION

The resonance frequency is given by internal structure of the Earth – mainly by the flattening of the core and electromagnetic coupling between the mantle and the core. Therefore the apparent difference between the direct and indirect determination of the RFCN period must be due to an excitation produced by outer parts of the Earth (atmosphere, ocean) – see also Dehant et al. (2003). Its period in celestial system should be in the range 420–460 days (retrograde), corresponding to terrestrial frequency around –1.0049 cycles per solar day. The amplitude of this *forced* nutation is of the order of 0.1–0.2 mas, so we must look for a very small excitation. In order to estimate its magnitude, we use Brzezinski's (1994) broadband Liouville equation in frequency domain, expressing the ratio between the amplitude of polar motion and atmospheric excitation. As the influence of atmospheric wind excitation is negligible (two orders smaller than the influence of the pressure term), we consider here the pressure term χ^P only, in complex form

$$p(\sigma) = \chi^P \left[\frac{\sigma_{CW}}{\sigma_{CW} - \sigma} + \frac{9.509 \times 10^{-2} \sigma_{CW}}{\sigma_{FCN} - \sigma} \right], \tag{2}$$

where σ_{CW} stands for Chandler frequency. The absolute value of the complex expression inside the brackets (for the periods in question) ranges from 2 to 12, so the amplitude of the excitation needed to produce the observed nutation is of about $10 - 50 \mu as$.

The spectrum of atmospheric angular momentum function (Salstein 2005), sampled at 6-hour interval (pressure term only), is depicted in Fig. 4, both with (IB) and without (NIB) inverted barometer correction. Although no evident peak is visible in the close vicinity of required frequency, the amplitude of the necessary excitation is on the same (noise) level of the spectrum.

The atmospheric pressure excitation without inverted barometer correction seem to be sufficient to produce such amplitude.

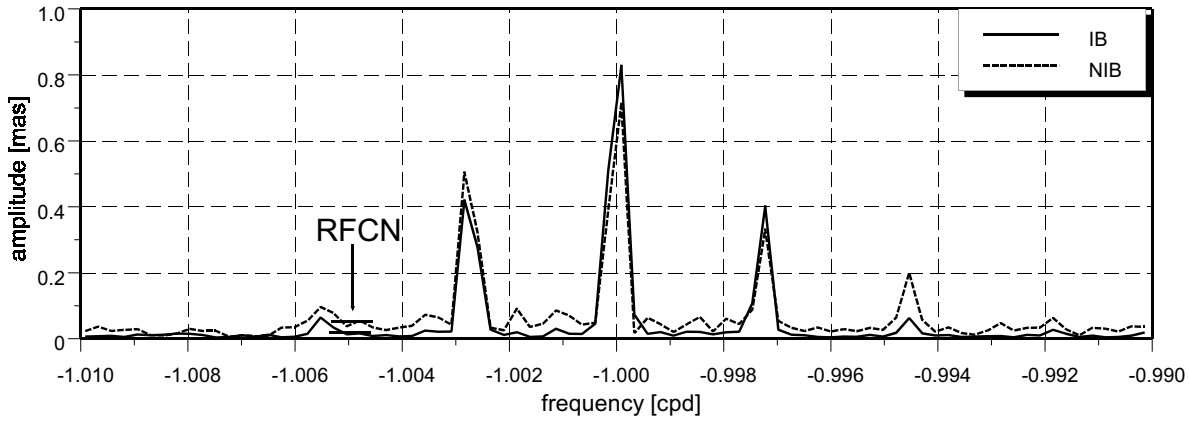

Figure 4: Spectrum of AAM pressure term (1980–2004). Required level of excitation to produce observed changes of RFCN period is marked by short horizontal lines.

4. DISCUSSION AND CONCLUSIONS

Based on indirect determination through the observed variations of the retrograde annual term of nutation, it follows that the resonance period, given by internal structure of the Earth, is relatively stable. Its variation is very small, smaller than one day, so that the period remains between 429.5 and 431.0 days. The apparently large observed change of the RFCN period (a few tens of days), obtained from direct analysis of celestial pole offsets, can be most probably ascribed to additional excitation by external parts of the Earth (atmosphere, oceans). The terrestrial period of the required excitation must be close to -23h 53min (mean solar time), and its amplitude of about $10 - 50\mu$as (i.e., close to the noise level in atmospheric data) is probably sufficient to produce the observed changes.

REFERENCES

Brzezinski A., 1994, "Polar motion excitation by variations of the effective angular momentum function: II. Extended model", Manuscripta Geodaetica, 19, 157–171.

Dehant V., Feissel-Vernier M., de Viron O., Ma C., Yseboodt M., and Bizouard Ch., 2003, "Remaining error sources in the nutation at the sub-milliarcsecond level", J. Geophys. Res. (Solid Earth), 108(B5), doi: 10.1029/2002JB001763.

IVS, 2005, "International VLBI Service products", http://ivscc.gsfc.nasa.gov/.

Mathews P.M., Herring T.A. & Buffet B.A., 2002, "Modeling of nutation and precession: New nutation series for nonrigid Earth and insights into the Earth's interior", J. Geophys. Res. , 107(B4), doi: 10.1029/2001JB000390.

Salstein D., 2005, "Computing atmospheric excitation functions for Earth rotation/polar motion", Cahiers du Centre Européen de Géodynamique et de Sésmologie, 24, 83–88.

Vondrák J., Weber R., Ron C., 2005, "Free core nutation: direct observations and resonance effects", A&A , 444, 297–303.

POLE DRIFT, NON-TIDAL ACCELERATION AND INVERSION REORGANIZATION OF THE EARTH

Yu.V.BARKIN [1,2]
[1] Alicante University, Spain
[2] Sternberg Astronomical Institute, Moscow
e-mail: yuri.barkin@ua.es

ABSTRACT. New mechanism of the Earth mass reorganization caused by the forced relative translatory-rotary oscillations of the core and mantle due to a gravitational attraction of external celestial bodies is studied and fundamental geodynamical consequences are discussed.

1. INTRODUCTION

All celestial bodies: planets, large satellites, stars and others objects are the define systems of the shells. Only in the first approximation the shells of these objects can be presented as concentric and with definite concentric distribution of densities. All shells are characterised by definite physical properties, sizes and mass distribution. They can have different physical states (rigid, elastic, non-elastic, liquid, gaseous and other). Shells are mutually interacting (including their gravitational interaction) and interact with external celestial bodies. In more detailed consideration the density of distributions of the shells are quasi-concentric and in general case the shells are non-homogeneous and non-spherical and with changing physical properties. From a mechanical point of view it means that shells are exposed by differential gravitational influence from the external celestial bodies. As result the small relative forced oscillations of the shells as celestial bodies must be observed. The centres of mass of the shells are displaced in definite rhythms including long-periodic (and secular) components. And all shells make relative rotational oscillations (small turns) with frequencies defined by the configuration of external celestial bodies and in different time-scales (Barkin, 2002). To the order by the forced oscillations should be shown and own (free) oscillations of the planet shells as celestial bodies. The main planet shells are the core and the mantle. Therefore our research on dynamics of shells have begun with two-shells models of a planet in its various treatments: a rigid core and an elastic mantle (Barkin, Shatina, 2004), a liquid core and an elastic mantle (Barkin, 2005), a rigid core and a rigid mantle separated by a visco-elastic layer (Barkin, 2001, 2002; Barkin, Vilke, 2004).

2. OSCILLATIONS OF THE EARTH CORE-MANTLE SYSTEM

The Earth, as well as many other celestial bodies, represents a system of celestial gravitating bodies - system of shells, with basic components the mantle and the core. Shells are non-spherical unbalanced bodies and, hence, are exposed to different gravitational influences on the part of external celestial bodies (the Moon, the Sun and others). In result they are forced to make small relative displacements and turns with frequencies characteristic for external actions. In result, the free oscillations and forced oscillations of the specified system are generated. The periods of

free oscillations of dynamic system "the elastic mantle - the rigid core of the Earth" have been established (Barkin, 2005): 3.47, 4.06 and 4.89 hours. Variations with the specified periods and their derivatives are observed in many geodynamic, geophysical, biological and physical processes. That specifies existence of the effective mechanism of excitation of the observed oscillations. By the study of forced relative oscillations of the core-mantle system both shells are considered as unchangeable spheroids which are subject to differential gravitational influence on the part of the Moon and the Sun and mutually interacting gravitationally and with certain elastic force and moments (Barkin, 2001, 2002; Barkin, Vilke, 2004). In this paper the mutual interaction was modeled with the help of thin elastic layer between the core and the mantle (an analog of D" layer). Here we take into account gravitational interaction of the core with the fully elastic mantle. Forced oscillations have been studied on the basis of a model problem about relative motions of a non-spherical elastic mantle and non-spherical rigid core under gravitational perturbation of the Moon and the Sun. On the basis of dynamical analytical studies of the problem (Barkin, 2002; Barkin, Vilke, 2004) we have shown that in case of the unperturbed circular orbit of the Moon, its gravitational action on the non-spherical core and mantle produces relative oscillations of their centers of mass along polar axis of the Earth according to the law

$$z = -1.519 + 0.966\cos 2M - 4.676\sin M \quad \text{(cm)} \tag{1}$$

Formula (1) describes the core oscillations with periods 13.9 days (with amplitude 0.966 cm) and with synodic period 27.8 days with amplitude 4.676 cm. Here is the mean anomaly of the circular Moon orbit. That will be coordinated to the data of precision satellite observations of the geocenter motion (Barkin, Vilke, 2004).

The angle between the polar axes of inertia of the core and mantle also oscillates with significant amplitude (Barkin, Vilke, 2004)

$$\theta_2 - \theta_1 = -0''36 \cdot 10^{-5} - 9''076\cos 2g\,. \tag{2}$$

From the formula (2) it follows, that pole of axis of symmetry of the core is displaced periodically (with period equal to a half of Moon orbital period) with amplitude about 152 m at the mantle bottom. It means, that the core "is periodically turned" relatively mantle on mentioned distance.

3. SECULAR DRIFT OF THE CORE TO THE NORTH POLE

3.1. Secular drift of center of mass

Alongside with a wide spectrum of periodic variations of position of the centre of mass of the Earth the phenomenon of its slow (secular) drift is observed. An original method (Barkin, 1995a) made us possible for the first time to evaluate a velocity of the centre of mass motion. Formally, this motion was referred to special reference system in which the coefficient of geopotential J_3 is equal zero. And effect of the center of mass motion has been interpreted as result of the change of the Earth pear-shaped form which is characterized by the known secular variations of the geopotential zonal coefficients $\dot{J}_2$ and $\dot{J}_3$. It was shown that in the given epoch the mass centre of the Earth moves to the North Pole with velocity about $1.0 \div 2.0$ cm/year. In the last years the space geodesy investigations have confirmed this phenomenon. In particular, for velocity of the center of mass drift were obtained values: 6.9 ± 3.5 mm/yr, 9.6 mm/yr (Tatevian, Kuzin, Kaftan, 2004: GPS data, 1993-2003) and others.

3.2. Core drift to North pole

For explanation of the geocenter drift (and its oscillations), the mechanism of relative translational displacements of the core and mantle of the Earth has been suggested as the main mechanism of the Earth mass redistribution (Barkin, 1995a).

For description of the geocenter drift we have used model of the homogeneous mantle and the core and on the base of PREM model we have determined superfluous mass of the core as 0.1932 of the Earth mass. The drift of this mass with theoretical velocity 4.975 cm/yr generates the center of mass drift to the North Pole with velocity 0.875 cm/yr. Relative displacements of the core and the mantle are accompanied by elastic mantle deformations. That also gives systematic component of a geocenter drift. In final solution of the problem of elasticity, the displacement vector was determined in an analytical form and additional component of the geocenter drift was evaluated as 0.25 cm/yr in direction to the North Pole also. For evaluation of the core velocity the modern data about lengthening of parallels in Southern hemisphere of the Earth have been used. In result of fulfilled studies, the following statements can be formulated (Barkin, 2005).

The main mechanism of the center of mass drift. The secular drift of the Earth center of mass is mainly a reflection of the slow drift of the mass center of the core relatively to the mass center of the mantle which occurs in the same direction as that of the mass center of the Earth.

Hypothesis about origin of the pear-shaped form of celestial bodies. The pear-shaped form of the Earth is a result of the slow redistribution of the mass (mantle deformations) caused by the core - mantle relative displacements along polar axis under the gravitation action of the external gravitating bodies (the Moon, the Sun and planets). This phenomenon is probably general for many others planets and satellites.

4. LENGTHENING (SHORTENING) OF PARALLELS IN SOUTHERN (NORTHERN) HEMISPHERE OF THE EARTH

The phenomenon of the core drift discussed here, has obtained very important confirmations on the base of the observational data: in measurements of the superconducting gravimeters and in space geodesy and VLBI data. The more important from them is a discovery of inversion geodesy phenomenon of the lengthening of the parallels of the Earth in Southern hemisphere and shortening parallels in northern hemisphere (Shuanggen Jin, Zhu Wenyao, 2002). This phenomenon has been described in an analytical form as result of solution of the problem of elasticity about mantle deformations by the secular drift of the liquid core (Barkin, Shatina, 2004; Barkin, 2005). In accordance with the last solution, the velocity $\dot{L}_p$ of lengthening of parallel φ is connected with the relative velocity of the core drift $\dot{\rho}$ by the simple relation:

$$\dot{L}_p = 2\pi 0.108021 \dot{\rho} \sin\varphi \cos\varphi = 1.5765 \sin(2\varphi) \ \ (\text{cm/yr}) \tag{3}$$

Based on results of Chinese authors on space geodesy determination of the changes of the parallel lengths we adopt $\dot{L}_p = 16.901 \pm 2.535$ mm/year for the latitude $\varphi = 45^\circ$ with formal error about 15%. By this assumption on the base of observational data, we obtain for velocity of the core trend the following evaluation:

$$\dot{\rho} = \dot{\rho}_0 = 4.6455 \pm 0.697 \ \ (\text{cm/yr})\,. \tag{4}$$

The phenomenon of the lengthening (shortening) of parallels in southern (northern) hemispheres, discovered in the Chinese works, is fully explained by the gravitational influence of the drifting core on the elastic mantle of the Earth.

5. GRAVITY CONFIRMATIONS OF THE CORE DRIFT

5.1. Love numbers of order (-2)

If the core drift is real phenomenon so many others related inversion planetary geodynamical and geophysical phenomena must be observed in the case of the Earth, it means: in gravity

measurements, in secular variations geodesic heights, in ocean and atmospheric secular mass redistributions and in many natural processes. The gravity variation in given place on the Earth surface is determined indirectly by displacement of superfluous mass of the core. The additional gravitational potential caused by the mantle deformation and height variations of gravimeters also gives contributions to gravity variation. Last two components are described with the help of the Love numbers of the order of (-2). For accepted models of the core and mantle the values of the Love numbers have been determined: $k_{-2} = -0.1423$ and $h_{-2} = 0.1419$.

5.2. Secular trend of gravity

The secular variation of gravity at the point with latitude φ is determined by formula $\dot{g} = 2g\Delta m_c\dot{\rho}(1 - h_{-2} - 0.5k_{-2})\sin\varphi/(m_\oplus r)$, where $\Delta m_c = 0.1932m_\oplus$ is the superfluous mass of the core in units of the Earth mass and r is the mean radius of the Earth. Taking into account values of parameters of problem the final expression of secular gravity variation we present in the form: $\dot{g} = 2.6182\sin\varphi$ μgal/yr.

5.3. Comparison of the theory and observations

The predicted variation of gravity at station Medsina (Zerbini et al., 2001) makes 1.82 ± 0.27 gal/yr that will well be coordinated with marked by observations secular trend in this region 1.7 ± 0.1 μgal/yr. Theoretical value of a variation of a gravity at Antarctic station Syowa -2.45 ± 0.37 μgal/yr precisely corresponds to observable here trend in 1997-2000 in -2 to -3 μgal/yr. In Potsdam for the period of 1972-1982 the variation has made about 2 to 2.5 μgal/yr that also will be coordinated to theoretical value 2.0 ± 0.3 μgal/yr.

6. HEIGHT CONFIRMATIONS OF THE CORE DRIFT

6.1. Secular height variations

A secular height variation at Earth surface on the latitude φ due to a secular trend in the relative motion of the core and the mantle is described by formula: $\delta h = -9.0487\sin\varphi$ mm/year.

6.2. Comparison of the theory and observations

As an confirmation of this result we point that the GPS height daily solutions for period July 1996 - June 2000 gives the negative linear trend of the height at a Medicine station about -7.0 ± 0.2 mm/year (Zerbini et al., 2001), that is close to a theoretical value of height trend in this region -5.4 ± 0.8 mm/year (Barkin, 2005).

7. REFLECTION OF THE CORE DRIFT IN OCEAN MASS REDISTRIBUTION

Inversion ocean tide. The luni-solar tides caused by an attraction of the Moon and the Sun, have been investigated in details. Alongside with these classical tides we ascertain existence of a new class of the tides caused by the gravitational attraction of oceanic shell by the displaced core. Obviously the gravitational attraction of the core superfluous mass moving to the North Pole must leads to formation of the special polar tide in ocean. This tide is asymmetrical. In northern hemisphere the sea level increases and in southern hemisphere it has an opposite tendency. The preliminary studies show that velocity of the sea level change (with respect to the crust) is described by the law: $\dot{\zeta} = 6.43\sin\varphi + 0.67$ mm/yr (Barkin, 2005). If the discussed fundamental phenomena of the expansion of the southern and contraction of northern hemispheres of the Earth in reality are characterized by found amplitudes (Shuanggen Jin, Zhu Wenyao, 2002) it means that the core drifts with velocity (4) and inevitably the asymmetric secular tide at global ocean should be observed on the background of many others tides of the sea. It is worth to remark that this result was obtained on the base of the classical static theory of tides and has

restricted character. In reality the formation of this inversion tide can be connected with the organization and with inversion activation of the ocean flows.

8. TO EXPLANATION OF THE NON-TIDAL ACCELERATION OF THE EARTH ROTATION

Preliminary evaluations show, that mentioned in section 7 tide (and similar cyclic inversion tides with annual and semiannual periods) causes significant secular (cyclic) variations of the moments of inertia of the Earth, geopotential coefficients and play important role for understanding of observed geodynamical phenomena. On our preliminary evaluation the described tide gives the contribution to variation of coefficient of second zonal harmonic $\dot{J}_2$ equal to 0.43. This value and all values below are given in units 10^{-9} 1/cy. The tectonic process of the plate subduction in accordance with author paper (Barkin, 1995b) gives contribution 2.00; in postglacial rebound process, Antarctica and Greenland in accordance with the model ICE1A give contributions: -8.9, 3.18 and 0.48, respectively. Others geophysical factors give the following contributions: atmosphere (0.7, 0.17), ground water (0.2), mountain glacier (0.34), reservoirs (-0.08), earthquakes (-0.022), core rotation (-0.04) and pressure at CMB (-1.3) (Cheng, 2000). So, summary effect in variation $\dot{J}_2$ is evaluated as -2.17. This variation determines secular acceleration of the Earth diurnal rotation of 4.4×10^{-9} (1/cy).

9. TO EXPLANATION OF THE POLE DRIFT

According to modern estimations the pole moves with velocity 0.351"$\pm$0.003" 1/cy in direction of meridian 79.2° W (Gross, Vondrak, 1999). Similar approach (see p. 8) can be used for explanation of this phenomenon. To describe pole drift we must determine first secular variations of geopotential coefficients caused by the all known reasons (they are mentioned in section 8). Then velocities of changes of the pole coordinates $\dot{C}_{21}$ and $\dot{S}_{21}$ can be evaluated on formulas:

$$\frac{\dot{p}}{\omega} = \left(1 - \frac{T_{CH}}{T}\right) \frac{\dot{C}_{21}}{I}, \quad \frac{\dot{q}}{\omega} = \left(1 - \frac{T_{CH}}{T}\right) \frac{\dot{S}_{21}}{I}$$

(T_{CH} is Chandler period, T is the period of the Earth rotation).

In particular we have shown that tectonic mechanism and mechanism of inversion tide give remarkable contributions to both components $\dot{p}/\omega$ and $\dot{q}/\omega$. The mechanism of plate subduction and mass accumulation give 0"139 1/cy and $-$0"153 1/cy respectively (Barkin, 1995b) and the mechanism of inversion tide gives 0"041 and 0"059 respectively.

REFERENCES

Barkin Yu.V. (1995a) About motion of the Earth center of mass, caused by global change of dynamical structure and by tidal deformations. Vestnik Moskovskogo Universiteta, Ser. 3, Physika, astronimia, Ser. 3, v.36, N5, pp.99-101. In Russian.

Barkin Yu.V. (1995b) Lithosphere Plate Motion as Mechanism of the Secular Variations of the Geopotential and Earth Rotation. Vestnik MGU. Ser.3. Fiz., Astron. 1995, T.36, No.6, p.89-94. In Russian.

Barkin, Yu.V.(2001) Dynamics of the Earth's shells and fundamental problems of celestial mechanics, astrometry, gravimetry and geodynamics. Proceedings of international conference "AstroKazan-2001". Astronomy and geodesy in new millennium (24-29 September 2001), Kazan State University: Publisher "DAS", p.59-65.

Barkin Yu.V. (2002) Explanation of endogenous activity of planets and satellites and its cyclicity. Izvestia cekzii nauk o Zemle. Rus. Acad. of Nat. Scien., Issue 9, December 2002, M.: VINITI, pp. 45-97. In Russian.

Barkin Yu.V. and V.G. Vilke (2004) Celestial mechanics of the planet shells. Astronomical and astrophysical transactions, v. 23, Issue 6 (December 2004), pp. 533-554.

Barkin Y. V. and Schatina A.V. (2004) Deformations of the mantle by moving core and geocenter motion. Abstracts of 9th Symposium on Study of the Earth's Deep Interior (SEDI 2004, July 4-9, Garmisch-Partenkirchen, Germany). P. 61.

Barkin Yu.V. (2005) Celestial geodynamics and solution of fundamental problems of geodesy, gravimetry, astrometry and geophysics. In: Metamorphism, cosmic, experimental and general issues of petrology. (Eds. Mitropfanov F.P., Fedotov Zh. A.) Proceedings of International (X All-Russian) Petrographic Conference (June 20-22, 2005, Apatity). Volume 4. - Apatity: Print. Kola Science Centre RAS, pp. 48 - 50. In Russian.

Cheng M.K. (2000) Observed and measured zonal rates. Private communication. XXV General Assembly of EGS (Nice, April 25-29, 2000).

Gross R.S. and Vondrak J. (1999) Astrometric and space-geodetic observations of polar wander. Geophysical res. Ltrs/ 1999GL900422, Vol. 26, No. 14, p. 2085.

Shuanggen Jin, Zhu Wenyao (2002) Quantitative analysis of the slowing expansion of the South hemisphere. Proceedings of colloquium "APSG-Irkutsk, 2002, Moscow, GEOS, pp. 154-162.

Tatevian S.K., Kuzin S.P., Kaftan V.I. (2004) Comparison of geocenter variations derived from GPS and DORIS data. Report of EGU (25-30 April 2004, Nice, France).

Zerbini S., Richter B. et al. (2001) Height and gravity variations by continuous GPS, gravity and environmental parameter observations in the southern Po Plain, near Bologna, Italy. Earth and planetary Science Letters, 192, pp. 267-279.

LONG-TERM CHANGES IN THE VARIANCE OF THE EARTH ORIENTATION PARAMETERS AND OF THE EXCITATION FUNCTIONS

N. SIDORENKOV
Hydrometcentre of RF
B.Predtechensky pereulok, 11-13, Moscow 123242, RUSSIA
e-mail: sidorenkov@mecom.ru

ABSTRACT. The variability in time of the Earth' Orientation Parameters (EOP) and of the Effective Atmospheric Angular Momentum (EAAM) functions is studied. The initial time series for the analysis are the daily values of the length of day from 1962 to 2005 and also the six-hour values of the EAAM functions: the wind terms χ_1^w, χ_2^w, χ_3^w, and pressure terms χ_1^P, χ_2^P, χ_3^P from 1958 to 2000. The values of variances were calculated for the annual interval that had been continuously slid from the beginning up to the end of the analyzed series. The step of the slide was equal to 1 day.

The obtained graphs of temporal changes in the variances for each analyzed time series are demonstrated. It is shown that the values of variances of the EOP and the EAAM functions change by a factor of several times. The variations are caused by the oscillations of tidal forces in the cycle of the regression of the lunar nodes (18,6 year) and also by the evolution of the phenomena of the El Nino Southern Oscillation and of the Quasy-biennial Oscillation of the atmospheric circulation.

1. INTRODUCTION

It is known that the lunisolar tide has a strong influence on the instability of the Earth rotation. The declination and geocentric distances of the Moon vary in time in a complicated way. The amplitude of monthly oscillations of the Moon declination varies from 29° up to 18° because of the regression of the lunar orbit nodes with a period of 18.61 year. The perigee of the lunar orbit moves with a period of 8.85 year, that causes the variation of the quasy-weekly period from 5 to 9 days (Sidorenkov, 2002).

The tidal oscillations of the Earth rotation have the amplitude and phase modulations due to the oscillations of the Moon declination and geocentric distance. The amplitude of the tidal oscillations varies with a period of 18.61 year, and the phase with a period of 8.85 year.

The variability of the tidal oscillations of the Earth rotation most brightly comes to light if to calculate the variance D_{td} of the tidal oscillations of the Earth angular velocity with a sliding temporal (for example, annual) interval. Figure 1 shows the temporal course of this variance D_{td}. One can see that the magnitude of the variance of the tidal oscillations varies by a factor of three from its minima in 1960, 1979, 1998 to its maxima in 1969, 1988, 2007.

The maximum (minimum) of the variance D_{td} has place when the ascending (descending)

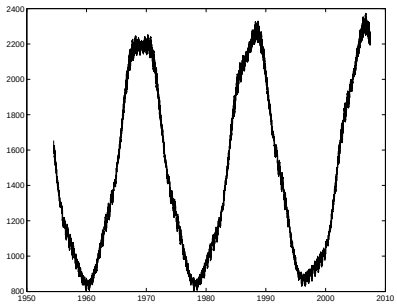

Figure 1: The variance D_{td} of the tidal oscillations of the Earth angular velocity in the sliding interval N=365 days.

node of the lunar orbit coincides with the point of the spring equinox. The long-term (zonal) tides have a strong influence on the meridianal circulation and synoptic processes of the atmosphere. We may expect that the variability of the excitation functions of the atmospheric angular momentum will reflect, along with other causes, the effect of temporal variations of the zonal lunar tides.

2. INITIAL DATA

For the analysis, we used the time series of the Earth orientation parameters C04, which were calculated in the International Earth Rotation and Reference Systems Service (IERS) with the daily discreteness from 1962 to 2005.

Also, we used the time series of the components of the atmospheric angular momentum, which are computed in the Special Bureau for the Atmosphere of the Global Geophysical Fluids Centre of the IERS. They included three wind terms: h_1, h_2 and h_3, and three terms of pressure P_1, P_2 and P_3. The wind terms were computed by integrating the winds from the Earth surface to 10 hPa, that is to the top of the atmospheric model. The pressure terms were calculated in two variants: with and without the account for the effect of the inverse barometer for pressure over the World Ocean. All these series span the period since 1948 till 2005 and have the discreteness equal to 6 hours.

Note that the inverted barometer correction involves the applying of the mean atmospheric surface pressure over the entire World Ocean to every point over the World Ocean (Salstein et al., 1993).

3. CALCULATION FORMULAS

For all series the variances D were calculated in the sliding annual interval

$$D = \frac{1}{N}\sum_{i=1}^{N}(x_i - \overline{x})^2\,,$$

where N=365 for the series with the daily discreteness, or N=1461 for the series with the 6-hour discreteness. The values of the variances were calculated for the annual interval that had been continuously slid from the beginning up to the end of the analyzed series. The step of the slide was equal to 1 day or 6 hours.

4. RESULTS AND DISCUSSION

The variance of the angular velocity ω of the Earth rotation has minima in 1962, 1979, 1999; in other words they are near to the minima of the values D_{td} of the tidal oscillations. The maxima of the variance of the angular velocity are recorded near 1969, 1988, and 2006; in other words, they coincide with the maxima of the variance D_{td} of the tidal oscillations. A sharp peak of the variance of the angular velocity near 1998 is caused by a significant acceleration of the Earth rotation at this time. The reason of such anomaly of the angular velocity ω is, probably, the El Nino phenomenon of 1997-1998. It is known that during El Nino the zonal circulation and the angular moment of the atmosphere amplify. This disturbs the usual seasonal course of the angular velocity ω. In Figure 2 it is possible to see the peaks, which are excited by the El Nino phenomenon. Smaller peaks of the variance are caused by the quasy-biennial oscillations of the atmospheric winds in the equatorial stratosphere. They conceal the course of the curve D. To suppress the quazy-biennial cyclicity, we have calculated the variances D of the angular velocity with the sliding interval N=850 days. Figure 2 shows the change in the variance D in this case. Here, oscillations D due to of the lunisolar tides (the minima in 1979 and 1998 and maxima in 1969 and 1988) are more pronounced. The peaks in 1983, 1988, and 1997 are associated with the El Nino events.

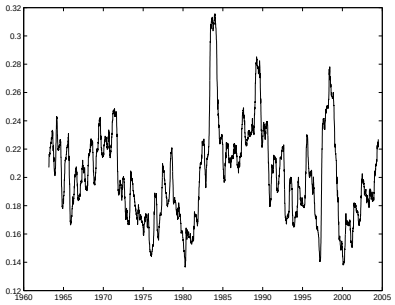

Figure 2: The variance D of the Earth angular velocity in the sliding interval N=850 days

The variances of the coordinates of the pole x and y have, apart the 6-year cyclicity, a small modulation, which is likely to be due to the phenomena of the El Nino-Southern Oscillation. Maxima of the variance of the coordinates x and y nearly coincide in time with three most strong El Nino of 1982-1983, 1987-1988, and 1997-1998. In 2003, the El Nino was developed only slightly; therefore, the variances of the coordinates x and y was minimal.

The variance of the axial component AAM h3 has peaks during the El Nino events. Thus in 1951, 1957, 1969, 1977, 1982, 1988, and 1998 there observed the El Nino phenomena and the peaks of the variances of the component AAM h3. The variance axial component AAM h3 is due to the evolution of the El Nino Southern Oscillation phenomena. Smaller peaks are caused by the quasy-biennial oscillations of winds in the equatorial stratosphere. Figure 3 shows the course of the variance of the component AAM h3 in the case of using the sliding time interval N=850 days. In this case the effect of the El Nino events became more pronounced.

The variances of the equatorial components AAM h1 and h2 had maxima in 1952, 1969 and 1982. The reason of a considerable damping of the variance in the last 20 years is not clear.

Long-term (zonal) tides have a strong influence on the meridianal circulation and the synoptic processes of the atmosphere. At increasing (decreasing) of the value D_{td} the variability of the atmospheric and oceanic processes increases (decreases).

The maximum of the lunisolar tidal forces variability in 2005 has initiated many extreme processes. For example, the catastrophic earthquake and devastating tsunami took place in December 26, 2004, i.e. they occurred exactly at the time of the winter maximum of tidal forces

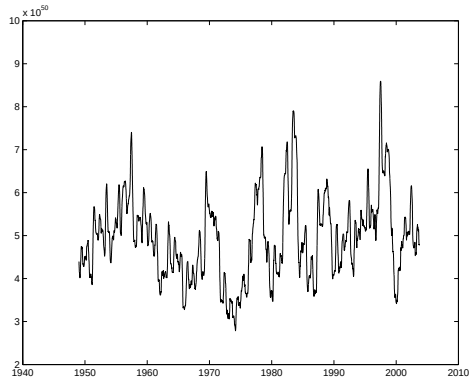

Figure 3: The variance of the atmospheric angular moment component h3 in the sliding interval N=850 days

in 2004 and of the 18.6-year maximum of tidal forces.

In 2005, the extreme activity of the tropical atmosphere was observed. Thus, the amount of hurricanes in the Atlantic Ocean in 2005 was so great that there were no enough names for them. Indeed, the name of each tropical cyclone begins with the particular letter of the Roman alphabet. According to the climatic norm, in Atlantic, in span since June till November, 9 hurricanes form, and there were 27 of them in 2005. Over the whole history of instrumental observations, such amounts of the Atlantic hurricanes were not observed.

In 2005, the blocking atmospheric highs of extremal duration were observed: in February - April - in the region of Iceland, and in September - November - over the European part of Russia. They gave rise to many extremal weather events in Europe and adjacent regions.

The statistics of hazardous hydrometeorological phenomena, which is being carried out in the Hydrometcentre of Russia, clearly reveals an increase (decrease) in their frequency with the increase (decrease) in the variance of the tidal forces.

Thus, the increased frequency of extreme natural processes in the last years, which is usually attributed to the global warming, is to a greater extent caused by the maximum variability of the tidal forces, which is presently observed.

5. CONCLUSION

The variances of the EOP and the EAAM functions changes by a factor of several times. The variations are caused by the oscillations of tidal forces in the cycle of the lunar nodes regression (18,6 years), as well as by the evolution of the El Nino Southern Oscillation and of the Quasy-biennial Oscillation phenomena of the atmospheric circulation.

Acknowledgements. This work was supported by the Russian Foundation for Basic Research (project code 05-02-27244) and the Local Organizing Committee of the "Journées 2005".

REFERENCES

Salstein, D.A., D.M. Kann, A.J. Miller, R.D. Rosen, 1993: The Sub-bureau for Atmospheric Angular Momentum of the International Earth Rotation Service: A Meteorological Data Center with Geodetic Applications. Bull. Amer. Meteor. Soc., 74, 67-80.

Sidorenkov, N.S. 2002: Fizika nestabilnostey vrashenija Zemli [Physics of the Earth's rotation instabilities.]. Moscow, Nauka, Publishing Company Fizmatlit. p. 384 [In Russian with English summary and contents.]

INFLUENCE OF THE EARTHQUAKES ON THE POLAR MOTION WITH EMPHASIS ON THE SUMATRA EVENT

Christian BIZOUARD
Observatoire de Paris, 61, av. de l'Observatoire, 75014 Paris, France
e-mail: christian.bizouard@obspm.fr

ABSTRACT. We compute the theoretical effects of the Earthquakes on polar motion from 1977 to nowadays. According to our estimates, the big Sumatra earthquake of December 26 2004 caused a polar shift below 3 cm. The polar motion observation cannot discriminate such a small amount from "normal" polar motion induced by atmosphere and oceans.

1. THE SUMATRA EARTHQUAKE

Whereas the influence of earthquakes on Earth rotation is a recurrent theme since the sixties, nothing has been ever observed. The gigantic Earthquake, that took place on 2004 December 26 at 00h 58min 51s UTC (modified Julian Date : 53365.041), about 200 km from the western coast of northern Sumatra (epicenter of latitude 3.298° and longitude 95.778°), has constituted an opportunity for recording a possible effect. Indeed its magnitude on the Richter scale reached at least $m = 9$, that makes it the third or forth biggest Earthquake ever recorded after those of Chile (1960, $m = 9.5$), Alaska (1964, $m = 9.2$), Kamchatka (1959, $m = 9$). The earthquake occurred as thrust-faulting on the interface of the India plate and the Burma microplate. In a period of minutes, the faulting released elastic strains that had accumulated for centuries from ongoing subduction of the India plate beneath the overriding Burma microplate. The ground over 1000 km fault was displaced in average by about 11 m (see Fig. 1). Probably as well excited as the Earth, some geophysicists, relieved by journalists, claimed in the following hours of the catastrophe, that a sudden polar shift had been observed. In the same time we began our investigation. We had already acquired some skill in this matter thanks to a cooperation carried out with the Seismologic Institute of Budapest (P. Varga, Z.Bus). In this paper, we shall present our own estimates of the polar wobble due to the Earthquake since 1977 with emphasis on the Sumatra event. Then, by analyzing polar motion observation, we shall attempt to answer whether the Sumatra effect has been detected or not.

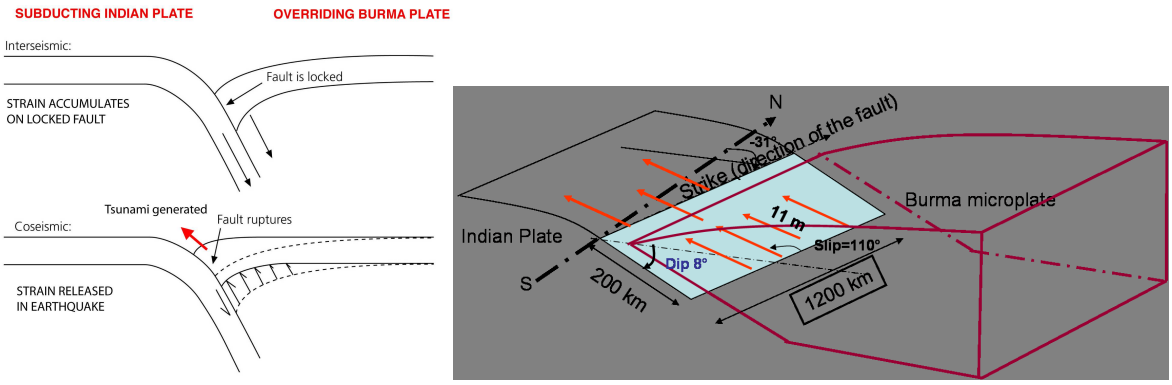

Figure 1: Left : subduction mechanism. Right : geometry of the ground displacement

2. BASIC EQUATION AND INERTIA INCREMENTS

When mass redistribution occurs inside the Earth, off-diagonal elements of the earth inertia matrix referred to the terrestrial frame $c_{13} = -\int_M xz\,\mathrm{d}m$ and $c_{23} = -\int_M yz\,\mathrm{d}m$ may change, as well as the equatorial relative angular momentum $h = h_1 + ih_2$. It follows that the Earth wobbles around the rotation axis in space, and from a terrestrial point of view the rotation axis moves with respect to the crust. For an elastic Earth model, the coordinates of the rotation axis $p = x - iy$ obey the Euler-Liouville equation :

$$p + i\frac{\dot{p}}{\sigma_C} = \frac{c}{(C-A)} + \frac{1.47h}{(C-A)\Omega} \tag{1}$$

where Ω is the mean Earth angular velocity, σ_C the Chandler pulsation ($\Omega/433$, $c = c_{13} + ic_{23}$, where C the axial inertia moment of the Earth, A the equatorial one. In the case of an earthquake, c can be modeled as a step function. The effect of relative angular momentum h is negligible, because it is not permanent. Then it can be easily shown that the consequence of the polar motion is a sudden offset of the pole, and a modification of the amplitude of the Chandler component according to :

$$\Delta p = \frac{c}{C-A} - \frac{c}{A}(\frac{\Omega}{\sigma_C} + 1)e^{i\sigma_C(t-t_0)} \tag{2}$$

We shall see that the inertia increment c can be deduced from seismic parameters. These ones are related to :1) the location of the epicenter : depth h, longitude Φ, colatitude θ) 2) the seismic displacement : it is modeled as uniform in a given plane, given by the northern azimuth α of its intersection with the earth surface (strike angle) and by its inclination with respect to the horizon δ ; the mean displacement itself is called the *slip* D, and the direction of the slip λ in this plane is reckoned from the strike direction 3) the area of the earthquake S. From the here above parameters seismologists define a quantity homogeneous to a moment of force, the seismic moment $M = \mu SD$ where μ is the shear modulus ($\approx 75Gpa$). This quantity combines the mean displacement and the surface which is concerned in relation with the shear force involved in the sliding. In Table 1 we report the seismic parameters for Sumatra Event (noted "Sum. Ev." in what follows), which are illustrated in Figure 1.

Center	Strike a	Dip angle D	Slip angle λ	Slip D	fault area S	Seismic moment M_0	Depth h
Harward CMT	329°	8°	110°	11 m	$\approx 105000km^2$	$4\,10^{22}$ Nm (up to 10^{23} Nm)	10 km
USGS	274°	13°	55°			$2.6\,10^{21}$ Nm	30 km

Table 1: Seismic parameter of the Sumatra Event

From elastic dislocation theory, Dahlen (1973) expressed the induced equatorial inertia moment increments in function of seismic parameters : seismic moment M_0, strike angle α, dip angle δ, slip angle λ, colatitude θ, longitude Φ :

$$\begin{aligned}
c_{13} = M_0\{ \quad & \Gamma_1(h) \quad [(\sin 2\alpha \sin\delta\cos\lambda + \tfrac{1}{2}\cos 2\alpha \sin 2\delta \sin\lambda)\sin 2\theta\cos\phi \\
& \qquad -2(\tfrac{1}{2}\sin 2\alpha \sin 2\delta \sin\lambda - \cos 2\alpha \sin\delta\cos\lambda)\sin\theta\sin\phi] \\
+ \quad & \Gamma_2(h) \quad (-\sin 2\delta \sin\lambda \sin 2\theta\cos\phi) \\
+ \quad & \Gamma_3(h) \quad [(\sin\alpha\cos 2\delta\sin\lambda - \cos\alpha\cos\delta\cos\lambda)\cos 2\theta\cos\phi \\
& \qquad +(\sin\alpha\cos\delta\cos\lambda + \cos\alpha\cos 2\delta\sin\lambda)\cos\theta\sin\phi]\} \\
c_{23} = M_0\{ \quad & \Gamma_1(h) \quad [(\sin 2\alpha \sin\delta\cos\lambda + \tfrac{1}{2}\cos 2\alpha \sin 2\delta \sin\lambda)\sin 2\theta \\
& \qquad +2(\tfrac{1}{2}\sin 2\alpha \sin 2\delta \sin\lambda - \cos 2\alpha \sin\delta\cos\lambda)\sin\theta\cos\phi] \\
+ \quad & \Gamma_2(h) \quad (-\sin 2\delta \sin\lambda \sin 2\theta\sin\phi) \\
+ \quad & \Gamma_3(h) \quad [(\sin\alpha\cos 2\delta\sin\lambda - \cos\alpha\cos\delta\cos\lambda)\cos 2\theta\sin\phi \\
& \qquad -(\sin\alpha\cos\delta\cos\lambda + \cos\alpha\cos 2\delta\sin\lambda)\cos\theta)\cos\phi]\}
\end{aligned} \tag{3}$$

Seismic parameters	Inertia moments 10^{26} kg m^2	Pole shift x (mas)	Pole shift $-y$ (mas)	
Harvard CMT	$c_{13} = -6.1$ $c_{23} = 0.76$	-0.68	0.09	2 cm 173° E
Hayward CMT*		-1.7	0.45	5 cm 165° E
USGS	$c_{13} = -0.47$ $c_{23} = 0.17$	-0.05	0.02	0.16 cm 160° E

* with 2.5 bigger seismic moment (Stein, Okal Nature,2005)

where $\Gamma_1(h)$, $\Gamma_2(h)$, $\Gamma_3(h)$ are function of the depth h. Without the need of considering these complicated expressions, it can be easily understood that in the case of equatorial Earthquake, the cartesian coordinate z of any mass element is closed to zero in the expression of c_{13} and c_{23}, and this make these quantities small. Therefore the very small latitude of Sumatra will preclude any large effect on polar motion. By using the Haward CMT catalogue, available on the WEB (www.seismology.harvard.edu), and giving the here-above parameters from 1977 to nowadays, we reconstituted the polar motion seismic excitation $\frac{c}{(C-A)}$. Its components in the terrestrial frame are depicted in Figure 2. Note the stability from 1964 to 1994, then the apparition of a slope these last ten years, amplified by the Sumatra earthquake. For Sumatra, the results of our

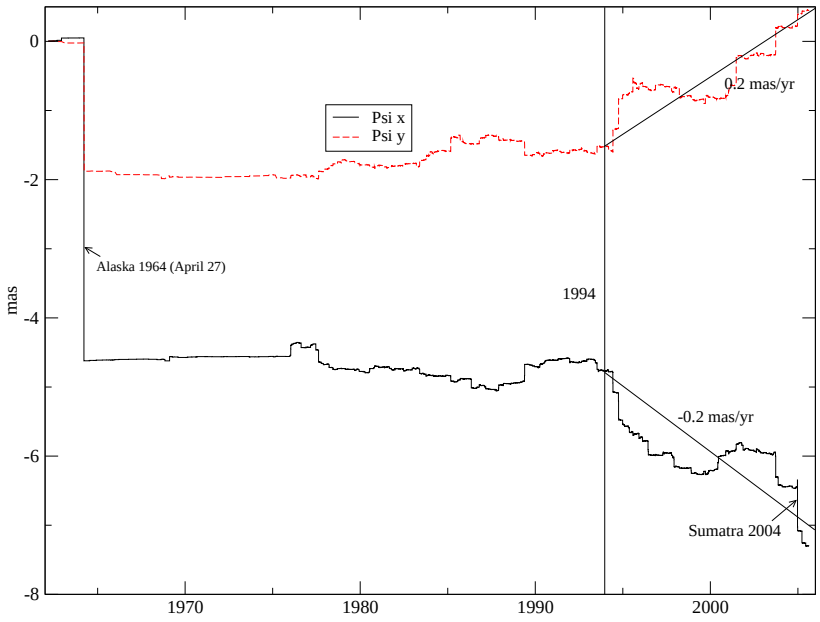

Figure 2: Co-seismic excitation of the polar motion from 1962 to 2005 (equivalently induced polar drift).

computation are reported in Table 2. The amplitude of the corresponding displacement of the rotation axis at the Earth surface varies from 0.2 cm up to 5 cm according to the estimates of the seismic moment towards $160 - 170°$ E, amount comparable to that one obtained by Gross and Chao (2005) (2.5 cm toward 145° E)

3. HAS SUMATRA EFFECT BEEN DETECTED ?

As comparison, the Alaska event (1964) of magnitude 9.2 has produced a shift of 15 cm according to the Dahlen model (see Fig. 3). With the modern techniques it would have been observed for sure, because such an displacement is much more important than the daily effect of the atmosphere and oceans, which reaches 3-9 cm per day. For the same reason, a shift of a few cm, like the one expect for Sum. Ev, is hardly detectable. Unless having hourly observations, classical daily determination of polar motion does not allow us to make difference between the

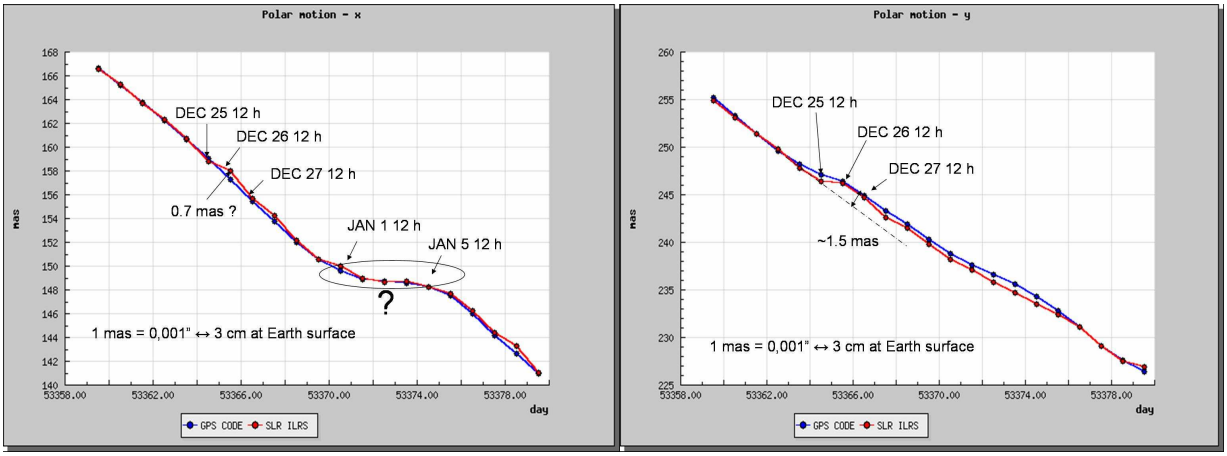

Figure 3: Polar motion around December 26. Satellite Laser Ranging Data and GPS (CODE) data slightly differ.

sudden seismic displacement and the habitual effect. Both are inextricably blended. The pole is slightly shifted ($+0.7$ mas for coordinate x, -1 mas for coordinate $-y$) from the 27th of December, as it appears the most clearly in SLR observations (see Fig. 3). But it cannot be taken as serious proof of Sumatra effect, as claimed by some of my colleagues. For essentially two reasons : 1) the observed effect is opposite to the theoretical estimate 2) centimeter shift in daily polar motion are routinely observed without any powerful earthquake taking place. For instance note the sudden stopping of pole according to the x axis from December 30th. To get the bottom of this problem, it is necessary to model the classical geophysical effects on the polar motion, and to isolate then the non explained part. For this period we have only at hand atmospheric data. The atmospheric excitation has been compared to the one found in polar motion. Around December 26th the difference between both function looks ordinary, not justifying any large episodic phenomena (larger than 10 mas). This analysis should be completed by the inclusion of oceanic angular momentum, unfortunately not yet available in public domain for December 2004. By the way the geophysical excitation is not accurately determined in order to deduced pure geodynamic excitation with the required accuracy level (0.5 mas at least!).

4. CONCLUSION

Sumatra Earthquake may have shifted the rotation axis at observable level ($2-3$ cm at the Earth surface in a few min), but such an effect is hardly distinguishable from common polar motion caused by the atmospheric/oceanic process ($6-15$ cm/day). The expected shift is for x axis, but what has been actually observed is a shift for y component (1.5 mas $\approx$ 4.5 cm). We shall conclude that Sumatra effect has not been observed. Another important conclusion of this study is that from 1964 to 1994 the excitation function is stable, but since 1994, it presents a significant drift towards 145°E, of about 0.2 mas/year (just above the accuracy level of the fit of the secular term in polar motion).

REFERENCES

Dahlen, 1973, "A correction to the Excitation of the Chandler Wobble by Earthquakes", GJR, 32, 203-217.

Gross and Chao, 2005, "Excitation of Earth Rotation and Gravitational Field Changes by the December 26 Sumatran Earthquake", Eos Trans. AGU, 86(18), Jt. Assem. Suppl., Abstract U52A-02

TIDAL INFLUENCE THROUGH LOD VARIATIONS ON THE TEMPORAL DISTRIBUTION OF EARTHQUAKE OCCURRENCES

P. VARGA[1], D. GAMBIS[2], Ch. BIZOUARD[2], Z. BUS[1], M. KISZELY[1]
[1]Geodetic and Geophysical Research Institute, Seismological Observatory
Meredek u. 18, Budapest, Hungary, H-1112
[2]International Earth Rotation Service, EOP PC, Observatoire de Paris
61, avenue de l'Observatoire, F-75014 Paris, France

ABSTRACT. Stresses generated by the body tides are very small at the depth of crustal earthquakes ($\sim 10^2$ N/m^2). The maximum value of the lunisolar stress within the depth range of earthquakes is 10^3 N/m^2 (at depth of about 600 km). Surface loads, due to oceanic tides, in coastal areas are $\sim 10^4$ N/m^2. These influences are however too small to affect the outbreak time of seismic events. Authors show the effect on time distribution of seismic activity due to ΔLOD generated by zonal tides for the case of M_f, M_m, S_{sa} and S_a tidal constituents can be much more effective to trigger earthquakes. According to this approach we show that the tides are not directly triggering the seismic events but through the generated length of day variations. That is the reason why in case of zonal tides a correlation of the lunisolar effect and seismic activity exists, what is not the case for the tesseral and sectorial tides.

1. EARTHQUAKES AND TIDES

In the second half of the 1980s correlation between seismic activity and tidal effect was described e.g. by Shierly (1988) for large earthquakes in Southern California and in the Alaska-Aleutian region, by Weems and Perry (1989) for moderate and large earthquakes in the Eastern USA. Zugravescu et al. (1989) show the distribution in time of earthquake occurrence and their correlation with lunisolar effect in two limited regions, namely in the seismic area of Vrancea (Romania) and in the eastern part of Crete (Greece). Dionysion et al. (1993) also detected significant correlation between the time of seismic events and the tide-generated stress for a small seismic region. Recently Stavinschi & Souchay (2003) found a significant correlation between the seismic activity of Vrancea area and the tidal effect in case of long-periodic zonal tides (especially for the M_f wave). Different investigators pointed out that the tidal triggering of earthquakes is connected to the type of the tectonics of the focal area: Varga and Grafarend (1996), Cochran et al. (2004) found correlations for shallow-dipping thrust events. There are authors who described the evidence of the dependence of aftershock sequences on Earth tides (Souriau et al., 1982). The most evident is the existence of tidal triggering in the case of volcanic earthquakes (Rydelek et al., 1988). Recent publications emphasize that the tides can only help to trigger earthquakes, because the stresses caused by this phenomenon are smaller by about three orders of magnitudes than those of tectonic origin (Young and Zürn, 1979, Varga and Grafarend, 1996). Stresses generated by the body tides are very small in the depth of crustal earthquakes ($\sim 10^2$ N/m^2). The maximum value of the lunisolar stress within the depth range of earthquakes is $\sim 10^3$ N/m^2.

This value is reached however at the depth of 500-600 km only. Surface loads generate stresses at and near to the Earth's surface. Stresses produced by the oceanic load in coastal areas are 10^2 N/m^2 – 10^4 N/m^2. The positive statistical correlation between tidal variations and shallow focus ($\leq$30 km) earthquake occurrences can be explained in many cases by the loading influence of oceanic tides close to coastal areas.

2. SEISMICITY AND ENERGIES OF THE EARTH

The radiated seismic energy is

$$E_R = \frac{\Delta\sigma_s}{2\mu} M_0 \tag{1}$$

and the seismic moment

$$M_0 = \mu D S \tag{2}$$

where μ - the medium's rigidity ($\sim$30 GPa), S - fault area, D - displacement offset, $\Delta\sigma_s$ - average seismic stress drop (range from 1 to 10 MPa, typically $\sim$3 MPa)

The seismic energy is related to the earthquake magnitude M is

$$\log E_R = 11.8 + 1.5M \tag{3}$$

3. INFLUENCE OF TIDES AND EXTERNAL LOADS ON THE SEISMICITY

To determine the normal (radial) and tangential (horizontal) stresses two auxiliary relations were introduced by Molodensky (1953): $N = N[r, \rho(r), \mu(r), \lambda(r)]$ and $M = M[r, \rho(r), \mu(r), \lambda(r)]$, where $\rho(r), \mu(r), \lambda(r)$ are the density and the Lamé parameters. They are increasing with depth through the depth range of interest from the viewpoint of earthquakes and reach a value of 10^3 N/m^2 at the depth of 500-600 km. Due to relatively low magnitude of Earth tide generated stresses near to the surface ($\leq 10^2$ N/m^2) the probability of their influencing effect on earthquake occurrences is small. In case of attempts to correlate the lunisolar effect to seismological events we must remember also that the lunisolar effect itself, and consequently the normal and tangential stresses produced by it, are functions of geographical latitude and significant phase shift appear between the theoretical tidal potential and the generated stresses.

Since earthquakes are shear fracture processes and therefore mainly controlled by the maximum shear stress $\tau = (N - M)/2$ in the focal area it may safely be assumed that also shear stress components of external forces have the main triggering effect. The fracture strength is dependent also on the hydrostatic pressure $p = (N + 2M)/3$. It may be taken also in consideration, but as a minor trigger effect. At the surface p can be of the same order as the surface load and their depth penetration is a function of the size of the loaded area (Figure 1). The static surface load is 10^2 N/m^2 (1 mbar).

4. INFLUENCE OF TIDES ON SEISMICITY THROUGH ΔLOD

In Section 3 it was shown that stresses generated by the solid earth tides are of the order of 10^2 N/m^2, while the loads due to oceanic tides can approach 10^4 N/m^2. On the other hand the elastic stresses accumulated in the earthquake foci and realised during seismic events are (10^6-10^7) N/m^2. The reason while the correlation between long-periodic zonal tides and the time distribution of the earthquake activity often was detected (see Section 1) by different researchers is that the tides are not directly triggering the seismic events but through the generated length of day variations.

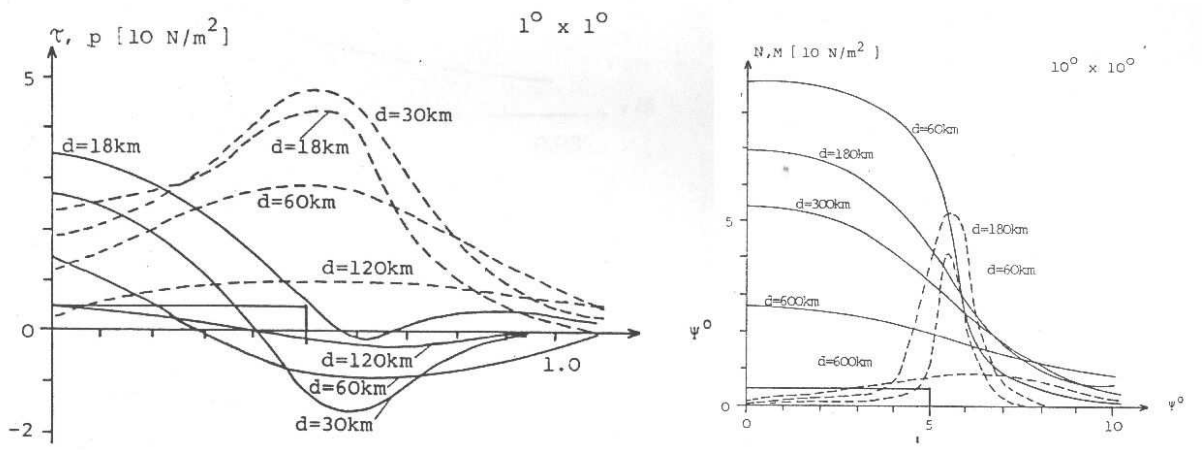

Figure 1: Hydrostatic (solid line) and maximum shear (dashed line) stresses at different depths (d) acting on different spherical segments ($1^\circ \times 1^\circ$ and $10^\circ \times 10^\circ$), Ψ^0 is the spherical distance.

In Table 1 the average ΔLOD values calculated by Defraigne & Smits (1999) are shown. Using this values the rotation energy variations (ΔE_{rot}) can be calculated with

$$\Delta E_{rot} = \frac{1}{2} C\omega^2 \Delta\omega = \frac{1}{2} C\omega^2 \frac{\Delta LOD}{LOD} \tag{4}$$

It can be seen from the last column of Table 1 that the ΔLOD variations due to zonal tides are of the order of (10^{19}-10^{21}) J. The most significant is the energy variation in case of tidal waves M_f, M_m, S_{sa} and the tidal wave with period 18.6 year. The radiated earthquake energy E_R estimated with the use (3) is in case of magnitudes M=6.0, 7.0, 8.0, 9.0 6.3×10^{13}J, 2.0×10^{15}J, 6.3×10^{16}J and 2.0×10^{16}J respectively. The comparison of ΔE_{rot} and E_R suggests that the energy variations caused by ΔLOD probably can influence the temporal distribution of the seismic activity, because they energies are significantly above the earthquake energies.

Tidal wave	**Period (days)**	**ΔLOD(10^{-4} s)**	**ΔE_{rot}(10^{20} J)**
year 18.6	6798.37	-0.1257	3.100
S_a	365.26	0.0222	0.547
S_{sa}	182.62	0.1400	3.453
M_{sm}	31.81	0.0304	0.750
M_m	27.55	0.1589	3.920
M_{sf}	14.76	0.0264	0.651
M_f	13.66	0.3008	7.4200
M_{stm}	9.56	0.0109	0.2689
M_{tm}	9.13	0.0576	1.4209
M_{sqm}	7.10	0.0092	0.2269
M_{qm}	6.86	0.0076	0.1875

Table 1: Variation of energy of rotation due to zonal tides.

As a first experimental attempt three different areas were investigated with the use of power spectra of earthquake occurrences at a frequency band 8106.7-8.0 day/cycle for the time-interval 1964-2002. The area of North France-Great Britain (3256 earthquakes) is characterised by reduced seismic activity. On the contrary the Aleutian (13ă500 earthquakes) and Honsu (6600 earthquakes) regions are very active. In every three cases the anomalies caused by zonal tidal

constituents are not significantly above the "noise level" of the power spectra. It seems to us that in the future a more detailed investigation is needed. First of all it should be remembered that different types of earthquakes are differently reacting to the triggering effect of the types (Section 3).

It is shown since long that at periods from 24 hours to some years the reaction of the Earth to external influences can be described by deformations of an elastic medium. Due to the fact that ΔLOD caused by zonal tides generates flattening variations, the elastic stress accumulation is different at different latitudes. Between the equator and latitude 48.2° (critical latitude) the azimuthal stresses are dominant above the meridional ones, while at higher latitudes the role of these two stress components is similar. It also should be remembered in case of future studies that the amplitude of vertical component of zonal tides is dependent on $\sin^2\phi$ (ϕ is the latitude), the NS component depends on $\sin^2\phi$, while the amplitude of EW component is independent from the latitude.

Acknowledgments. Research described in this contribution was completed in the frame of French-Hungarian bilateral project "Oscillations of polar motions influenced by seismic activity and another short periodic geodynamical phenomena". The Hungarian contributors enjoyed support of the Hungarian Scientific Research Found in he frame of the project OTKA K 60394 "Interaction of rotation axis with geodynamical processes".

REFERENCES

Cochran E.S., Vidale J.E., and Tanaka S., 2004, "Earth tides can trigger shallow thrust fault earthquakes", Science, 306, pp. 1164-1166.

Defraigne P., and Smits I., 1999, "Length of day variations due to zonal tides for an inelastic earth in non-hydrostatic equilibrium", Geophys. J. Int., 139, pp. 563-572.

Dionysion D.D., Sarris E.E., Tsikouras P.G., and Papadopolus G.A., 1993, "Newtonian and post-Newtonian tidal theory: variable G and earthquakes", Earth, Moon, Planets, 60, 2, pp. 127-140.

Molodensky M.S., 1953, "Elastic tides, free nutations and some questions concerning the inner structure of the Earth", Trudy Geofis. Inst. Akad. Nauk SSSR, 19 (146), pp. 3-42 (in Russian).

Rydelek P.A., Davis P.M., and Koyanagi R.Y., 1988, "Tidal triggering of earthquake swarms at Kilauea volcano", Hawai. J. Geophys. Res., 93, pp. 4401- 4411.

Shirley J.H., 1988, "Lunar and solar periodicities of large earthquakes: Southern California and Alaska-Aleutian Islands seismic region", Geophys. J., 92, pp. 403-420.

Stavinschi M., and Souchay J., 2003, "Some correlations between earthquakes and earth tides", Acta Geod. Geoph. Hung., 38(1), pp. 77-92.

Souriau M., Souriau A., and Gagnepain J., 1982, "Modelling and detecting interactions between earth tides and earthquakes with application to aftershock sequence in the Pyrenees", Bull. Seism. Soc. Am., 72, pp. 165-180.

Varga P., and Grafarend E., 1996, "Distribution of the lunisolar tidal elastic stress tensor components within the Earth's mantle", Phys. Earth Planet. Int., 93, pp. 285-297.

Weems R.E., and Perry Jr. W.H., 1989, "Strong correlation of major earthquakes with solid earth tides in parts of the Eastern United States", Geology, 17, pp. 661-664.

Young D., and Zürn W., 1979, "Tidal triggering of earthquakes in Swabian Jura?", J. Geophys., 45, pp. 171-182.

Zugravescu D., Fatullescu I., Enescu D., Danchiv D., and Haradja O., 1989, "Pecularities of the correlation between gravity tides and earthquakes", Rev. Roumanie Geol. Geophys. Geogr., 33, pp. 3-10.

EXCITATION FUNCTION RECONSTRUCTION USING OBSERVATIONS OF THE POLAR MOTION OF THE EARTH

L.V. ZOTOV
Sternberg Astronomical Institute of Moscow State University
119992, Moscow, Universitetskij prospect 13
e-mail: tempus@sai.msu.ru

ABSTRACT. Reconstruction of the excitation functions from the observations of the motion of the Earth's pole was performed with use of Jeffreys-Wilson filter, regularization, corrective smoothing in the frequency domain. Corrective smoothing procedures found preferable for solving the inverse problem of reconstruction of the excitation functions from observations. Excitation functions were reconstructed since 1900 year for chandler and annual components of the polar motion, divided from each other and separated from noise with use of singular spectral analysis (SSA). Excitation was predicted with use of SSA and neural networks (NN). Kalman filter was used for prediction of the trajectory of the pole.

1. DYNAMICAL MODELLING AND RECONSTRUCTION OF THE CAUSES

Reconstruction of the excitation functions from the observations of the Earth rotation belongs to the class of the ill-posed inverse problems. So far as different input excitations can produce the motion along the observed trajectory, a priori assumptions should be made. The errors of observations can cause a big deviation of the evaluated excitation from the real one. That's why it was recommended to use the corrective procedures for solving the ill-posed problems [Tikhonov et al., 1977]. The motion of the pole can be described by the equation [Yatskiv, 2000]

$$\frac{i}{\sigma_c}\frac{dm(t)}{dt} + m(t) = \chi(t), \tag{1}$$

where $\sigma_c = 2\pi F_c(1 + i/2Q)$. It was suggested to use the values $F_c = 0.843$ cycles per year and $Q = 175$ [Vicente, Wilson, 2002]. The frequency characteristic of the system (1) is given by the expression

$$L(f) = \frac{\sigma_c}{\sigma_c - 2\pi f}. \tag{2}$$

Fig. 1 represents the gain-frequency (GFCh) and phase-frequency (PFCh) characteristics of the system given by (2). The resonance at the chandler frequency can be well seen. When an excitation transfers from one frequency half plane to another, divided by the frequency $\sigma_c/2\pi$, the phase of the polar motion changes by π.

For reconstruction of $\chi(t)$ Wilson suggested the filter [Vicente, Wilson, 2002]

$$\chi(t) = \frac{ie^{-i\pi F_c \Delta t}}{\sigma_c \Delta t}\left[m_{t+\frac{\Delta t}{2}} - e^{i\sigma_c \Delta t} m_{t-\frac{\Delta t}{2}}\right], \tag{3}$$

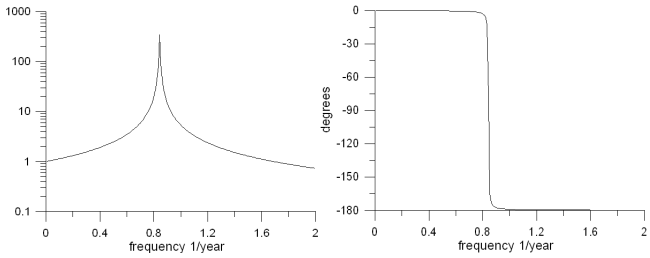

Figure 1: The gain-frequency (left) and phase-frequency (right) characteristics of the rotating Earth dynamical system.

where Δt is a time interval between the equidistant observation's read outs. This filter can be derived from the general solution of the equation (1) with use of the approximate trapezium formula for numerical integration and averaging of two neighbor read outs of excitation. Excitation reconstruction with use of (3) from observations published in EOPC01 bulletin was performed and represented by Fig. 2. It can be seen, that till the 70s years the main composition of the "excitation" is determined by the noises.

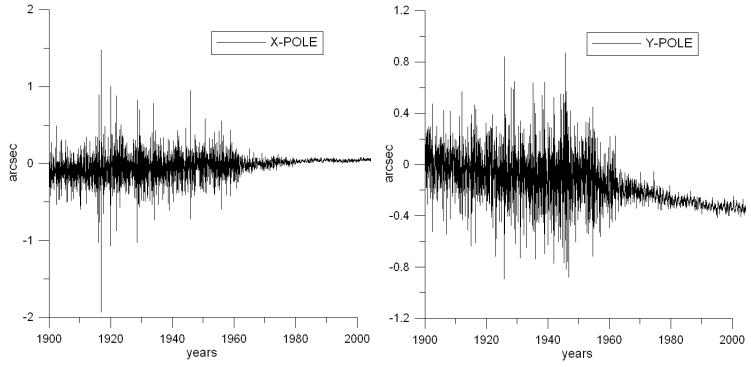

Figure 2: Excitation function reconstructed with use of Wilson filter.

Wilson filter (3) does not imply any corrective operation, if not consider averaging by two points. But it is very desirable to use it. The corrective operation is implied, for instance, by the regularization technique. In a simple assumption, that an input signal belongs to the integrated with squares function space L_2, regularizing weight function can be analytically derived

$$h_{reg}(t,\alpha) = F^{-1}\left(\frac{L'}{L'L+\alpha}\right) = \frac{1}{\alpha\tau}e^{-\frac{t}{\tau}}\cos\frac{t}{\tau\sqrt{\alpha}}, \tag{4}$$

where F^{-1} is an inverse Furier-transformation, touch denotes a complex conjugation, α is a regularization parameter, $\tau = i/\sigma_c$ - the time constant of a system. It's difficult to use the window (4) in the time domain. The regularizing procedure was performed in the frequency domain, the result converted to the time domain is represented by Fig. 3 for two values of regularization parameter [Tikhonov et al., 1977].

Other method can be used is the corrective smoothing, suggested by V.L. Panteleev [Panteleev, 2001]. We can transform the Panteleev smoothing window

$$\psi(t) = \frac{\omega_0}{2\sqrt{2}}e^{-\frac{w_0|t|}{\sqrt{2}}}\left(\cos\left(\frac{\omega_0 t}{\sqrt{2}}\right) + \sin\left(\frac{\omega_0|t|}{\sqrt{2}}\right)\right) \tag{5}$$

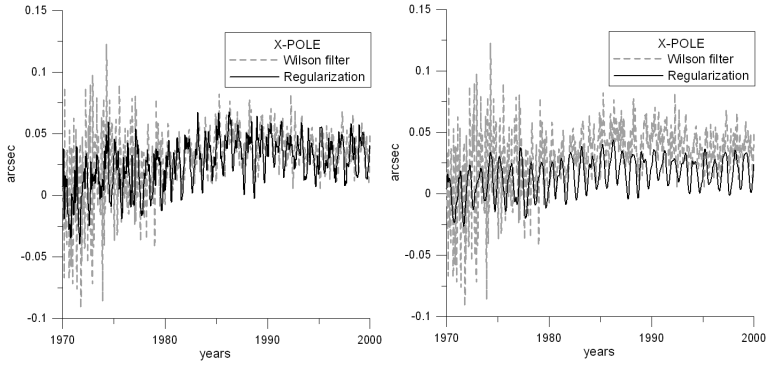

Figure 3: The X-component of the excitation function, reconstructed with use of regularization ($\alpha = 0.1$ to the left, $\alpha = 1$ to the right) and Wilson filter.

with parameter ω_0 through the system

$$\psi_{corr} = \frac{i}{\sigma_c}\dot{\psi} + \psi,$$

which gives us the corrective window. It allow us to reconstruct $\chi(t)$ resuming the influence of errors at the same time. Let's mention also that (5) transformed into the form

$$\psi(t) = \frac{a}{2} exp(-a|t|)(\cos(at) - \sin(a|t|))$$

with parameter a can be used as a wavelet basis.

The SSA method [Golyadina, 2004] allows to separate the time series of the polar motion into components: trend, chandler, annual oscillations (Fig. 4, left) and to exclude noise, which mostly determines the dispersion of excitation on Fig. 2. Reconstructed components of the annual and chandler excitation since 1900 year separated by SSA are represented by Fig. 4, right in comparison with smoothed data upon the earthquakes, evaluated from the USGS catalog. The annual excitation is mostly determined by the atmosphere processes [Salstein, 2000], and the excitation function for it does not correlates with seismicity. But correlation can be seen for the component of excitation function, which corresponds to the chandler motion. Probably, the cause of the chandler motion also influences on the regime of seismicity of the Earth.

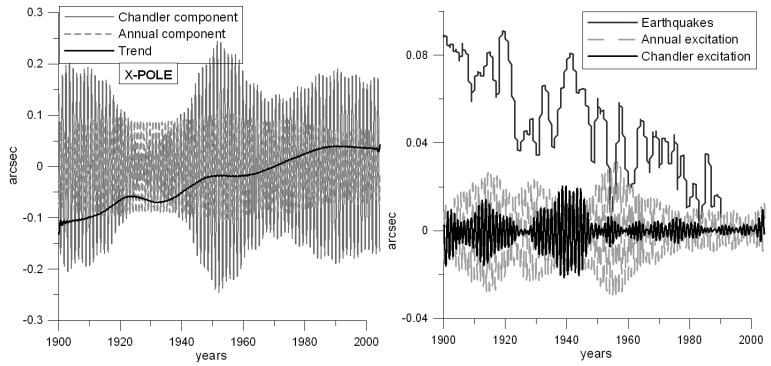

Figure 4: The components of the trend, chandler and annual oscillations of the X-coordinate of the pole picked out by SSA (to the left) and comparison of the corresponding components of the excitation function with the earthquakes (to the right).

At the next stage the forecast of excitation function with use of SSA and NN method was performed. Components freed from noise and separated from each other by SSA were predicted with use of 3-layer NN and joined together (Fig. 5, left).

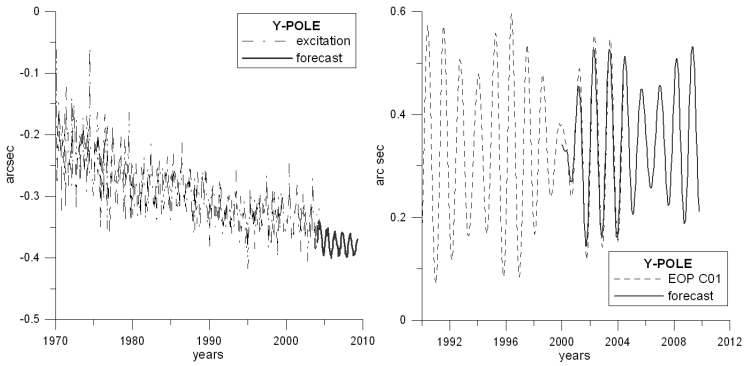

Figure 5: Forecast of the excitation by SSA and NN method (left) and prediction of the coordinates of the pole by the Kalman filter (right).

After the forecast of the excitation function $\chi(t)$ had been made, we used Kalman filter to evaluate the trajectory of the polar motion [Panteleev, 2001], [Gubanov, 1997]. The 5-year prediction is represented by Fig. 5, right. Long-time prediction for chandler component gave us possibility to suppose that it will probably relax in 2010-2020 years.

2. CONCLUSIONS

The comparison of different methods of excitation function reconstruction from the observations of the polar motion shown, that difficulties connected with this ill-posed inverse problem can be solved by using the corrective smoothing procedures. Excitation functions were reconstructed from the 1900 year for the annual and chandler components divided from each other and separated from noise with use of SSA. Their comparison with different processes can be useful for understanding the nature of the annual and chandler oscillations. It was found effective to involve singular spectral analysis, neural networks and Kalman filter for prediction of EOP.

Acknowledgements: The author is thankful to professor V.L. Panteleev for useful recommendations. The work is supported by RFBR grants No 05-02-17091 and No 04-02-16681.

REFERENCES

Tikhonov A.N., Arsenin V.Y., 1977, "Solution of ill-posed problems", John Wiley and Sons.

Yatskiv Y., 2000, "Chandler Motion Observations", ASP Conference Series, Vol. 208, p. 383.

Vicente R., Wilson C., 2002, "On long-period polar motion", Journal of Geodesy, Vol. 76, N. 4, pp. 199-208.

Golyadina S. A., 2004, "Method "Caterpillar-SSA": prediction of the time series", Saint-Petersburg, in Russian.

Gubanov V.S.,1997, "The generalized method of least squares", Saint-Petersburg, in Russian.

Panteleev V.L., 2001, "Observation and modelling of the dynamical objects", http://lnfm1.sai.msu.ru/grav/russian/lecture/lecture.htm, in Russian.

Salstein D., 2000, "Atmospheric excitation of polar motion", ASP Conference Series, Vol. 208, pp. 437-446.

COMPARISON OF TWO AAM FUNCTIONS CALCULATED FROM NCEP/DOE AND ERA-40 REANALYSIS DATA SETS

Y. MASAKI
Geographical Survey Institute
1, Kitasato, Tsukuba, Ibaraki, 305-0811, Japan
e-mail ymasaki@gsi.go.jp

ABSTRACT. We compared the AAM functions calculated from NCEP-2 and ERA-40 and found that the discrepancies between two AAMs are due to the wind term. A candidate source(s) of these discrepancies is the wind field in the upper troposphere, especially in the equatorial area and in the Southern Hemisphere.

1. INTRODUCTION

The time-varying Earth rotation is excited by the geophysical fluids, but the atmosphere plays a main role. However, atmospheric angular momentum functions calculated from different meteorological data sets have different values. What is/are the origin(s) of such differences? In this study, we examined the differences between AAM functions calculated from the two meteorological data sets; NCEP/DOE reanalysis (hereafter, NCEP-2) and ERA-40 reanalysis.

2. METHOD

We calculated AAM functions from monthly averaged meteorological reanalysis data with SP method (no wind blowing inside the mountain, after Aoyama & Naito (2000)) under the IB hypothesis. In order to examine the spatial distribution of the differences, we divided the atmospheric layer into six (surface to 850 hPa, 850-700 hPa, 700-500 hPa, 500-300hPa, 300-100hPa and 100-10hPa; hereafter, we numbered the layers from bottom to top) such that each layer contains the nearly same air-mass. Then we partitioned each layer into 15deg by 15deg blocks. We separated seasonal and non-seasonal signals from the retrieved difference signals.

3. RESULTS

Prior to the main analysis, we checked the fact that these differences are almost due to the differences in the wind AAM term.

Next, we examined which layers these wind differences came from. Figure 1(a) shows the Layer 5 (300-100hPa) contributes to large differences. From the spatial distribution of the differences in wind AAMs (Figure 1(b)), we can observe large differences in the equatorial region, also in the Southern Hemisphere. The differences are almost non-seasonal (Figure 1(c)). As we expected from Figure 1(a), large differences are observed in the upper troposphere (Layer 4 and

5, corresponding to the isobar from 100hPa to 500hPa).

Interestingly, in contrast to large wind AAM excitations in the jet streams, large differences between NCEP-2 and ERA-40 do not correspond to the jet streams; rather, correspond to the areas with sparse meteorological observation. The area near Australia shows small differences than the surrounding areas.

4. DISCUSSION

We think that these differences are due to the difficulties in wind analysis, although the wind observation from satellite images has improved the accuracy of the wind field. (For example, the Coriolis parameter, which is used in the estimation of the upper wind under the thermal wind assumption, will vanish at the equator.) This is an ironical fact that the wind at the equator most efficiently excites the Earth rotation due to the large distance from the rotational axis.

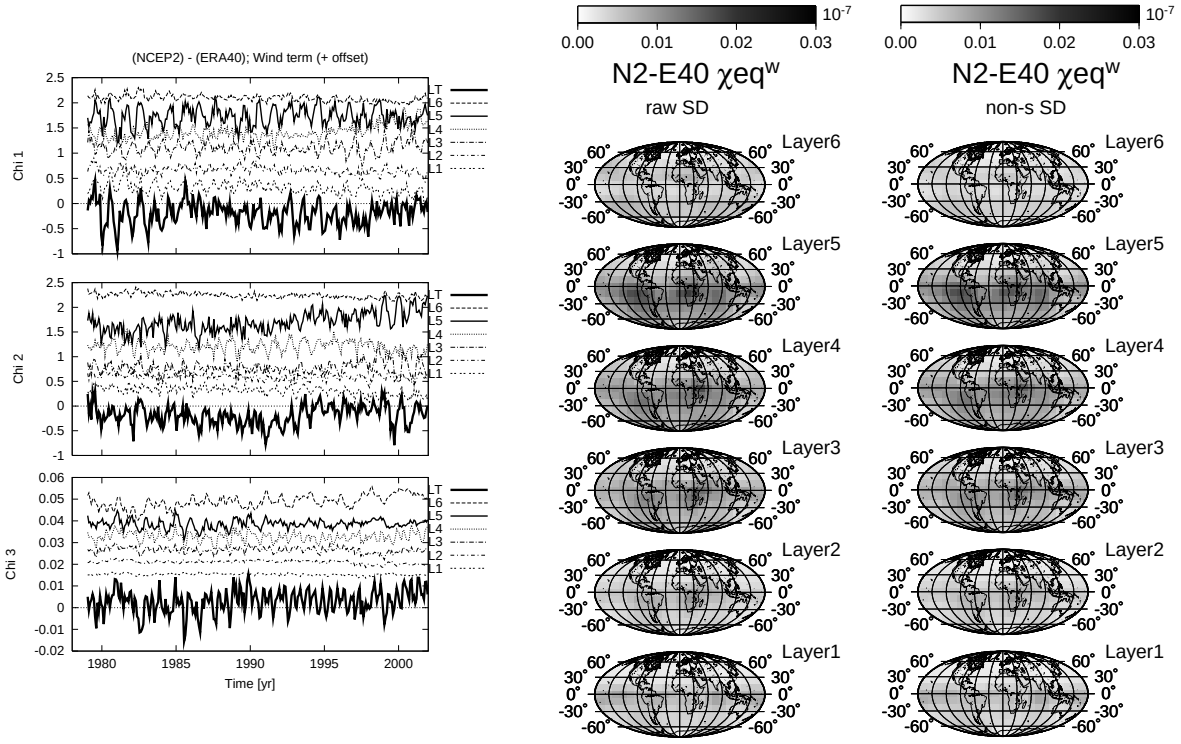

(a) (b) (c)

Figure 1: (a) Time series of the wind AAM differences of NCEP2 minus ERA40, from six vertical layers. These lines are drawn with vertical offsets. LT (the bottom series in each panel, highlighted by thick line) means the total (summed-up) differences over six layers. The difference in Layer 5 (the second series from the top in each panel, highlighted by thick line) is larger than those in other layers. Units are 10^{-7}. (b) Spatial distribution of the AAM differences of NCEP2 minus ERA-40. We only draw the equatorial component of the wind AAM (i.e. $\sqrt{(\chi 1^w)^2 + (\chi 2^w)^2}$). (c) Same as (b), but extracted only the non-seasonal components.

REFERENCES

Aoyama, Y. and Naito, I., 2000, "Wind Contributions to the Earth's Angular Momentum Budgets in Seasonal Variation", J. Geophys. Res., 105(D10), 12417-12431.

ABOUT WOBBLE EXCITATION IN THE CASE OF TRIAXIAL EARTH ROTATION

O. KUDLAY
Main Astronomical Observatory of NAS of Ukraine
Akad. Zabolotnoho Street, 27, 03680 Kyiv, Ukraine
e-mail: kudlay@mao.kiev.ua

Earth rotation theory is still challenged by an inadequate predictions for all normal modes excluding nutation. The origin of discrepancies between theory and observations we are going to show here may appears due to misunderstanding of constraints exerted on derivation of linearized Munk and Macdonald equations. They proposed two of them: 1) to replace the real Earth with 3-axis ellipsoid of inertia on the model with 2-axis ellipsoid; 2) to neglect all small terms in Liouville system.

Let's focus on the first one. An exchange of 3-axis body on 2-axis body has to make sure that trajectories of both will be close at any time because $(B - A)$ is small. Is it really true?

The answer must be sufficiently rigorous to exclude any disturbance from ordinally used mathematical procedures such as approximation, expansion, etc. The best way doing it is to analyse Euler solution for 3-axis free rigid body rotation. All the work then will be merely accurate computation of analytical solution components. Such an approach differs from well known papers of Kinoshita, Fukushima, Getino, S. Molodensky, Souchay and others by concentrating on achievement of extreme precision.

Euler system for the rotation of rigid 3-axis body

$$\left\{\begin{array}{lcl} A\dot{\omega}_1 + (C-B)\omega_2\omega_3 &=& 0, \\ B\dot{\omega}_2 - (C-A)\omega_3\omega_1 &=& 0, \\ C\dot{\omega}_3 + (B-A)\omega_1\omega_2 &=& 0 \end{array}\right. \tag{1}$$

has as it's well known the next solution

$$\left\{\begin{array}{lcl} \omega_1 &=& \sqrt{\dfrac{2EC-G^2}{A(C-A)}}cn(u), \\ \omega_2 &=& \sqrt{\dfrac{2EC-G^2}{B(C-B)}}sn(u), \\ \omega_3 &=& \sqrt{\dfrac{G^2-2EA}{C(C-A)}}dn(u), \end{array}\right. \tag{2}$$

where $sn(u)$, $cn(u)$ are elliptic sine and cosine and $dn(u) = \sqrt{1 - k^2 sn^2(u)}$ – an elliptic tangent, $k^2 = \dfrac{(B-A)(2EC-G^2)}{(B-C)(G^2-2EA)} = \text{const}$ – module of elliptical functions, E, G – integration constants.

Due to the strict limitation on paper size we save in the text only main formulae, details can be found in textbooks of Whittaker, Goldstein, Landau, etc. By the way general picture of

free motion is easy seen from (2) – properties of elliptical functions determine motion features. Here we can review only several. 1) 3-axis body pole moves along elliptical trajectory; 2) ω_3 component of 3-axis body has its own variation while 2-axis ω_3 is constant; 3) all ω_i have spectra with infinite number of discrete lines. The more is $(B - A)$ the more distinct are differences. In the case of Earth it is hard work to compute elliptical function values with high precision. The problem was solved by comparing of three various algorithm results.

The important property of motion are easy seen also from parametric expansion of elliptical functions (here for sine):

$$sn(u) = \frac{2\pi}{\sqrt{m}\,K} \sum_{n=0}^{\infty} \frac{q^{n+\frac{1}{2}}}{1 - q^{2n+1}} \sin(2n+1)\nu; \qquad m = k^2, \tag{3}$$

where $q = e^{-\pi K'/K}$ – parameter of expansion, $4K$ – period of polar motion.

Due to the very small value of q solution (2) has a very steep form of power spectra as for polar motion and LOD.

Thus, an application of constraint $A = B$ leads to an exchange of model with infinite power spectrum on the model with single line on eigenfrequency. While free rotating 3-axis body does not differ practically from 2-axis one – trajectory discrepancies are less than 1 mm, situation is drastically changed if mass motion exists. Symmetrical 2-axis body modes are excited in main resonance only, 3-axis body – on infinite set of resonances and everyone can distort as amplitude and phase of motion. Such a profound difference can not be ignored even for body with small equatorial ellipticity due to nonlinear effects.

Is it right then to ignore other small terms in Liouville equations? To validate second constraint it is necessary to perform numerical integration of perturbed 3-axis body equations. This problem is harder then previous one and will be considered elsewhere.

CONCLUSIONS

An investigation of proposal $A = B$ as constraint in derivation of Munk and MacDonald system of equations revealed that 3-axis body rotation and 2-axis body rotation are SIMILAR only while $(B-A)$ is small but NOT EQUIVALENT dynamically. Both have profoundly different excitation structures. Linear system of equations is unable to describe all properties of rotation of the real Earth.

REFERENCES

Landau L., Mechanics, Moscow, 1975.

Fukushima T., 1994, New canonical variables for orbital and rotational motions, Cel. Mech. and Dyn. Astron., 60, pp. 51-68

Souchay J., Folgueira M., Bouquillon S., 2004, Effects of triaxiality on the rotation of celestial bodies: application to the Earth, Mars and Eros, Earth, Moon and Planets, 93, pp. 107–144.

Escapa A., Getino J., Ferrandiz J., 2002, Indirect effect in the Hamiltonian theory for the rigid Earth nutations Astronomy & Astrophysics, 389, pp. 1047–1054.

Session 4

TIME AND TIME TRANSFER: RECENT DEVELOPMENTS AND PROJECTS

TEMPS ET TRANSFERT DE TEMPS : DÉVELOPPEMENTS RÉCENTS ET PROJETS

EVOLUTION OF TIME SCALES

DENNIS D. MCCARTHY
US Naval Observatory, Washington DC, USA
e-mail: dmc@maia.usno.navy.mil

ABSTRACT. Time scales evolve to meet user needs consistent with our understanding of the underlying physics. The measurement of time strives to take advantage of the most accurate measurement techniques available. As a result of improvements in both science and in measurement technology, the past fifty years has witnessed a growing number of time scales as well as the virtual extinction of some. The most significant development in timing has been the switch to frequencies of atomic transitions and away from the Earth's rotation angle as the fundamental physical phenomenon providing precise time.

1. INTRODUCTION

Time scales have continued to evolve to meet the developing needs of users in modern times. Fifty years ago time based on astronomical observations of the Earth's rotation was sufficient to meet the needs for time, both civil and technical. During that fifty-year interval, however, not only have these scales been expanded, but the advent of practical atomic clocks has led to the development of time scales based on atomic frequency transitions. In addition, the development of modern space techniques and the improvement in observational accuracy by orders of magnitude have led to the improvement of the theoretical concepts of time and the resulting relativistic definitions of time scales. The following sections provide a brief description of the chronological development of time scales since the middle of the twentieth century. A comprehensive description of time scales is presented by Nelson *et al.*, (2001).

2. MEAN SOLAR TIME

Mean solar time as derived from astronomical observations was the basis for time in the mid 1900s. It is based on the concept of a fictitious mean Sun as defined by Simon Newcomb. The mathematical expression for the right ascension of the fictitious mean Sun provides the direction to a conventional point on the equator that completes one revolution in the celestial reference frame in the same time interval as the actual Sun completes its annual path on the ecliptic. The mean solar day is the time interval between successive transits of this fiducial point, and the mean solar second, is 1/86 400 of a mean solar day (Kovalevsky, 1965; McCarthy, 1991). Apparent solar time, the time determined by using a sundial or by measuring the altitude of the Sun is defined by the motion of the observed Sun. The difference between apparent and mean solar time is called the equation of time. The maximum amount by which apparent noon precedes

mean noon is about 16.5 min around 3 November, while the maximum amount by which mean noon precedes apparent noon is about 14.5 min around 12 February (Nelson *et al.*, 2001).

3. UNIVERSAL TIME (UT)

Universal Time as designated by "UT1" is considered to be equivalent to mean solar time referred to the meridian of Greenwich and reckoned from midnight. As defined today, UT1 is a measure of the Earth's rotation angle that is used as a time scale. In practice, it is determined not by solar observations but by astronomical observations of objects in the celestial reference system with instruments fixed in a terrestrial reference system. In the middle of the twentieth century the observing instruments were optical meridian telescopes and the objects observed were stars in a galactic reference system. Very long baseline interferometry is used today to observe extragalactic radio sources to determine the Earth's rotation angle.

Observations used to determine UT1 can be made in two ways. Determinations of UT1-UTC can be determined from observed corrections to an assumed sidereal time based on a conventional expression for sidereal time. In 2000 the IAU adopted an expression for the Earth rotation angle $\theta = f(UT1)$. Observations of this angle can be used to provide corrections to an *a priori* estimate of UT1. UT0, a designation no longer in common use, is UT1 corrupted by the motion of the Earth's axis of rotation with respect to the Earth's surface, called polar motion. When observations were made using meridian instruments, UT0 was the observed quantity. However meridian instruments are no longer used for practical determination of Universal Time, and corrections to *a priori* estimates of UT1 can be observed directly. The time scale UT2 is another scale no longer in common use that attempted to provide a more uniform time scale by correcting UT1 for the known seasonal variation in the Earth's rotational speed.

Astronomical observations show that time scales based on the Earth's rotation are not uniform because of variations in the Earth's rotational speed. A wide spectrum of quasi-random and periodic fluctuations has been well documented (Lambeck, 1980). These include the secular variation due chiefly to tidal friction slowing the Earth's rotational speed and lengthening of the day by about 0.0005 to 0.0035 s per century, irregular changes apparently correlated with physical processes occurring within the Earth, and higher-frequency variations known to be largely related to the changes in the total angular momentum of the atmosphere and oceans. Periodic variations associated with tides are also present.

4. EPHEMERIS TIME (ET)

Ephemeris Time, originally suggested by G. M. Clemence (1948) is a time scale based on the period of the revolution of the Earth around the Sun, as represented by Newcomb's *Tables of the Sun*. The definition is based on Newcomb's formula for the geometric mean longitude of the Sun (Newcomb, 1895):

$$L = 279^\circ 41' 48.04'' + 129602768.13'' T + 1.089'' T^2, \quad (1)$$

where T is the time reckoned in Julian centuries of 36 525 days since January 0, 1900, 12h UT. The IAU adopted this definition in 1952 at its 8th General Assembly in Rome (*Trans. Int. Astron. Union*, 1954).

Newcomb's formula indicates that the tropical year of 1900 contains 31 556 925.9747 s. The International Committee for Weights and Measures (CIPM) in 1956, therefore, defined the second of ET to be "the fraction 1/31 556 925.9747 of the tropical year for 1900 January 0 at 12 hours ephemeris time." This definition was ratified by the General Conference on Weights and Measures (CGPM) in 1960 (*BIPM Proc.-Verb. Com. Int. Poids et Mesures*, 1956; *The*

International System of Units (SI), 1998). In 1958, the International Astronomical Union (IAU) General Assembly defined the epoch of ET by (*Trans. Int. Astron. Union*, 1960): "Ephemeris Time (ET), or Temps des Ephémérides (TE), is reckoned from the instant, near the beginning of the calendar year A.D. 1900, when the geometric mean longitude of the Sun was $279°41'48.04''$, at which instant the measure of Ephemeris Time was 1900 January 0d 12h precisely."

Although defined using Newcomb's expression, ET was realized using observations of the direction of the Moon in the celestial reference frame. These observations were used together with conventional lunar ephemerides to derive estimates of ET. This led to a set of realizations of ET based on the actual ephemeris used that were denoted ET0, ET1 and ET2 (Guinot, 1989). Although astronomical ephemerides adopted ET as the independent variable, it was inconvenient to obtain accurate, real-time estimates of ET, and it did not include relativistic effects.

5. ATOMIC TIME

Following the appearance of the first operational Caesium beam frequency standard in 1955 at the National Physical Laboratory (NPL) in the U. K. (Essen and Parry, 1957), the Royal Greenwich Observatory (RGO), U.S. Naval Observatory (USNO), and U. S. National Bureau of Standards (NBS) began to produce atomic time scales. The details of the development of these scales into the current standard TAI (International Atomic Time) is contained in Nelson *et al.*, (2001).

L. Essen and J. V. L. Parry of the NPL, in cooperation with Wm Markowitz and R. G. Hall at the USNO, determined the frequency of the NPL Caesium standard with respect to the second of ET. Photographs of the Moon and surrounding stars were taken using the USNO dual-rate Moon camera from 1955.50 to 1958.25 to determine ET from the direction of the Moon at a known UT2 determined from optical observations made at the USNO. This information was used to calibrate the Caesium beam atomic clock at NPL. The measured Caesium frequency was 9 192 631 770 Hz with a probable error of ±20 Hz (Markowitz *et al.*, 1958). In October 1967 the atomic second was adopted as the fundamental unit of time in the International System of Units. It was defined as (*Metrologia*, 1968) "the duration of 9 192 631 770 periods of the radiation corresponding to the transition between the two hyperfine levels of the ground state of the caesium 133 atom," thus making the second of atomic time equivalent to the second of ET in principle.

The Comité Consultatif pour la Définition de la Seconde (CCDS) of the CIPM recommended guidelines for the establishment of International Atomic Time (TAI) in 1970. It stated that "International Atomic Time (TAI) is the time reference coordinate established by the Bureau International de l'Heure [BIH] on the basis of readings of atomic clocks operating in various establishments in accordance with the definition of the second, the unit of time of the International System of Units" (*Metrologia*, 1971). The CCDS (*BIPM Com. Cons. Déf. Seconde*, 1970) defined the origin so that TAI would be in approximate agreement with UT2 on 1 January 1958, 0h UT2. This definition was refined in 1980 to account for relativistic concerns with the statement, "TAI is a coordinate time scale defined in a geocentric reference frame with the SI second as realized on the rotating geoid as the scale unit" (*Metrologia*, 1981). TAI, when formally adopted in 1971, was an extension of the BIH atomic time scale that had been continuous back to 1955. In 1988, the Bureau International des Poids et Mesures (BIPM) assumed responsibility for maintaining TAI. Today approximately two hundred clocks maintained in fifty laboratories contribute to the formation of TAI.

6. COORDINATED UNIVERSAL TIME (UTC)

The term "Coordinated Universal Time" was introduced in the 1950s to designate a time scale in which the adjustments to quartz crystal clocks were coordinated among participating laboratories in the U. S. and U. K. The scale evolved over the years to the state where the BIH coordinated adjustments to an internationally accepted standard Coordinated Universal Time, designated UTC, that involved adjustments in both rate and epoch to stay in step with astronomical time.

The concept of the leap second was proposed independently by G. M. R. Winkler (1968) and L. Essen (1968) at a meeting of the CIPM in 1968 (Commission Préparatoire pour la Coordination Internationale des Échelles de Temps, 1968). Steps of integer seconds were proposed to replace the steps of 100 ms or 200 ms then being used. To meet the needs of navigators, it was suggested that coded information might be incorporated in the emission of radio time signals to provide the difference between UTC and UT2.

The current UTC system is defined by ITU-R (International Telecommunications Union Ũ Radiocommunications Section, formerly International Radio Consultative Committee (CCIR)) Recommendation ITU-R TF.460-5 (*ITU-R Recommendations: Time Signals and Frequency Standards Emissions*, 1998): "UTC is the time scale maintained by the BIPM, with assistance from the IERS, which forms the basis of a coordinated dissemination of standard frequencies and time signals. It corresponds exactly in rate with TAI but differs from it by an integral number of seconds. The UTC scale is adjusted by the insertion or deletion of seconds (positive or negative leap seconds) to ensure approximate agreement with UT1." The interval between time signals of UTC is thus exactly equal to the SI second. A history of rate offsets and step adjustments in UTC is given at `http://www.iers.org`. In practice leap seconds are inserted to keep |UT1-UTC| $\leq$ 0.9s. Recently the requirement for leap seconds has been questioned. Working groups of various international scientific organizations are now investigating the need to continue the practice.

7. DYNAMICAL TIME SCALES

The concept of time scales based on the dynamics of the solar system was refined in 1976 when the International Astronomical Union (IAU) defined time-like arguments consistent with the general theory of relativity (*Trans. Int. Astron. Union*, Vol. XVI B, 1977). This led to the development of Terrestrial Dynamical Time (TDT) and Barycentric Dynamical Time (TDB) (*Trans. Int. Astron. Union*, Vol. XVII B, 1980) that distinguish coordinate systems with origins at the center of the Earth and the center of the solar system, respectively. In 1984 TDT replaced ET as the tabular argument of the fundamental geocentric ephemerides. It has an origin of 1 January 1977 0h TAI, with a unit interval equal to the SI second, and maintains continuity with ET. In 1991 the IAU renamed TDT simply Terrestrial Time (TT). A practical realization of TT in terms of the atomic time scale, TAI, is (*Explanatory Supplement to the Astronomical Almanac*, rev. ed., 1992) $TT = TAI + 32.184s$.

The constant offset represents the difference between ET and UT1 at the defining epoch of TAI on 1 January 1958. In practice any difference between TAI and TT is a consequence of the physical defects of atomic time standards. In most cases, and particularly for the publication of ephemerides, this deviation is negligible.

TDB was defined to be used as the time-like argument for ephemerides referred to the barycenter of the solar system. By adopting an appropriately chosen scaling factor, TDB varies from TT or TDT by only periodic variations, with amplitudes less than 0.002 s.

In 1991 the IAU General Assembly introduced the general theory of relativity explicitly as the theoretical basis for the celestial reference frame and the form of the space-time metric was specified (*Trans. Int. Astron. Union*, Vol. XXI B, 1992). At that time it also clarified the

definition of Terrestrial Time and defined two new time scales, Geocentric Coordinate Time (TCG) and Barycentric Coordinate Time (TCB) (Seidelmann and Fukushima 1992). The "coordinate" time scales TCG and TCB are complementary to the "dynamical" time scales TT (or TDT) and TDB. They differ in rate from TT and are related by four-dimensional space-time coordinate transformations (*IERS Conventions (1996)*). These definitions were further clarified by resolutions adopted at the IAU General Assembly in 2000 (*Trans. Int. Astron. Union*, 2001). The dynamical time scales are now used only for specialized studies and to develop astronomical ephemerides. TCG is defined by the expression

$$TCG - TT = L_G(Julian\ Date - 2443144.5) \times 86400s, \quad (2)$$

where the defining value of L_G, chosen to provide continuity with TT so that its measurement unit agrees with the SI second on the geoid is $6.969290134 \times 10^{-10}$(*IERS Conventions (2003)*).

An approximation to TCB-TCG in seconds is

$$TCB - TCG = [L_C \times (TT - TT_0) + P(TT) - P(TT_0)]/(1 - L_B) + \frac{1}{c^2}[\mathbf{v_e} \cdot (\mathbf{x} - \mathbf{x_e})] + P, \quad (3)$$

where $\mathbf{x_e}$ and $\mathbf{v_e}$ are the barycentric position and velocity of the Earth's center of mass, $\mathbf{x}$ is the barycentric position of the observer, $L_C = 1.4808268671x10^{-8}(\pm 2 \times 10^{-17})$, TT_0 is JD 2443144.5 TAI (1977 January 1, 0h) and the periodic terms, $P(TT)$, have a maximum amplitude ~ 1.6 ms. The current estimate of L_B is $1.55051976772 \times 10^{-8}(\pm 2 \times 10^{-17})$ *IERS Conventions (2003).* However, since no precise definition of TDB exists, there is no definitive value of L_B, and such an expression should be used with caution. The periodic terms can be evaluated by the "FB" analytical model (Fairhead and Bretagnon, 1990; Bretagnon, 2001), or $P(TT) - P(TT_0)$ may be provided by a numerical time ephemeris such as TE405 (Irwin and Fukushima, 1999). A series, HF2002, providing the value of $L_C \times (TT - TT_0) + P(TT) - P(TT_0)$ as a function of TT over the years 1600-2200 has been fit (Harada and Fukushima, 2002) to TE405.

8. FUTURE

Time scales will continue to evolve to meet user needs. It is likely that the definition of UTC will continue to be discussed in the next few years and that new navigational time scales will be developed. We may also expect the development of time scales to meet developments in space exploration and to take advantage of improvements in timekeeping precision. We may see the definition of a Galactic Coordinate Time.

REFERENCES

BIPM Com. Cons. Déf. Seconde, 1970, 5, 21-23; reprinted in *Time and Frequency: Theory and Fundamentals*, Natl. Bur. Stand. (U.S.) Monograph 140 (Edited by B. E. Blair), Washington, D.C., U.S. Govt. Printing Office, 1974, 19-22.

BIPM Proc.-Verb. Com. Int. Poids et Mesures, 1956, 25, 77.

Bretagnon, 2001, Personal Communication.

Clemence G. M., 1948, AJ , 53, 169-179.

Commission Préparatoire pour la Coordination Internationale des Échelles de Temps, Rapport au Comité International des Poids et Mesures, 1968, *BIPM Proc.-Verb. Com. Int. Poids et Mesures*, 36, Annexe 1, 109-113; reprinted in *BIPM Com. Cons. Déf. Seconde*, 1970, 5, Annexe S 10, 121-125.

Essen L., 1968, *Metrologia*, 4, 161-165.

Essen L., Parry J. V. L., 1957, *Philos. Trans. R. Soc. London*, 250, 45-69.
Explanatory Supplement to the Astronomical Almanac, rev. ed., 1992, (Edited by P. K. Seidelmann), Mill Valley, Calif., University Science Books, 48.
Fairhead L. and Bretagnon P., 1990, A&A , 229, 240-247.
Guinot B., 1989, "Atomic Time," in *Reference Frames for Astronomy and Geophysics* (Edited by J. Kovalevsky, I. I. Mueller and B. Kołaczek), Kluwer, Boston.
Harada W. and Fukushima T., 2003, AJ , 126, 2557-2561.
IERS Conventions (1996) (Edited by D. D. McCarthy), International Earth Rotation Service Tech. Note 21, Paris, Observatoire de Paris, 84.
IERS Conventions (2003) (Edited by D. D. McCarthy and G. Petit), International Earth Rotation Service Tech. Note 32, Verlag des Bundesamts für Kartographie und Geodäsie Frankfurt am Main, 84.
The International System of Units (SI), 7th ed., 1998, Sèvres, Bureau International des Poids et Mesures, 111-115.
Irwin A. W. and Fukushima T., 1999, A&A , 348, 642-652.
ITU-R Recommendations: Time Signals and Frequency Standards Emissions, 1998, Geneva, International Telecommunication Union, Radiocommunication Bureau, 15.
Kovalevsky J., 1965, *Metrologia*, 1, 169-180.
Lambeck K., 1980, *The Earth's Variable Rotation*, Cambridge University Press, Cambridge.
Markowitz W., Hall R. G., Essen L., Parry J. V. L., 1958, *Phys. Rev. Lett.*, 1, 105-107.
McCarthy D. D., 1991, *Proc. IEEE*, 79, 915-920.
Metrologia, 1968, 4, 43.
Metrologia, 1971, 7, 43.
Metrologia, 1981, 17, 70.
Nelson R. A., McCarthy D. D., Malys S., Levine J., Guinot B., Fliegel H. F., Beard R. L., Bartholomew T. R., 2001, *Metrologia*, 38, 509-529.
Newcomb S., 1895, *Astronomical Papers Prepared for the Use of the American Ephemeris and Nautical Almanac*, VI, Part I: *Tables of the Sun*, Washington, D.C., U.S. Govt. Printing Office, 9.
Seidelmann P. K., Fukushima T., 1992, A&A , 265, 833-838.
Trans. Int. Astron. Union, Vol. VIII, 1954, Proc. 8th General Assembly, Rome, 1952 (Edited by P. T. Oosterhoff), New York, Cambridge University Press, 66.
Trans. Int. Astron. Union, Vol. X, 1960, Proc. 10th General Assembly, Moscow, 1958 (Edited by D. H. Sadler), New York, Cambridge University Press, 72, 500.
Trans. Int. Astron. Union, Vol. XVI B, 1977, Proc. 16th General Assembly, Grenoble, 1976 (Edited by E. A. Muller and A. Jappel), Dordrecht, Reidel, 60.
Trans. Int. Astron. Union, Vol. XVII B, 1980, Proc. 17th General Assembly, Montreal, 1979 (Edited by P. A. Wayman), Dordrecht, Reidel, 71.
Trans. Int. Astron. Union, Vol. XXI B, 1992, Proc. 21st General Assembly, Buenos Aires, 1991 (Edited by J. Bergeron), Dordrecht, Reidel, 41-52.
Trans. Int. Astron. Union, Vol. XXIV B, 2001, Proc. 24th General Assembly, Manchester, 2000 (Edited by H. Rickman), San Francisco, Astron. Soc. Pacific.
Winkler G. M. R., The Future of International Standards of Frequency and Time: Memorandum submitted to the *ad hoc* group meeting at the International Bureau of Weights and Measures (BIPM), 30 May 1968.

IMPROVEMENTS IN INTERNATIONAL TIMEKEEPING

E.F. ARIAS
Bureau International des Poids et Mesures
Pavillon de Breteuil, 92310 Sèvres, France
e-mail: farias@bipm.org
Associated Astronomer to SYRTE, Observatoire de Paris
61, Av. de l'Observatoire, 75014, Paris, France

ABSTRACT. International Atomic Time and Coordinated Universal Time are calculated at the Bureau International des Poids et Mesures on the basis of international cooperation for time keeping. The process of calculation has been progressively adapted to the technology improvement in clocks and time transfer techniques, as well as to the increasing accuracy of primary frequency standards. Improvements in the last ten years are presented in this article.

1. INTRODUCTION

In 1875, seventeen countries signed in France the Metre Convention, arranged to meet every four years at the Conférence Générale des Poids et Mesures (CGPM), and created the Bureau International des Poids et Mesures (BIPM), located at Sèvres. At that epoch, the BIPM was the guardian of the two prototypes: the metre, defining the unit of length; and the kilogramme, defining the unit of mass. Short time afterwards the unit of time was added to the list of base units, but its realization and maintenance remained a task conferred to astronomers.

The original system of units grew up, and became in 1960 the International System of Units (SI), which comports seven base units. The definitions of some units evolved to render the system more accurate; in the last years efforts have been settled in different metrology institutes and in the BIPM to approach them to the fundamental constants of physics.

The definition of the unit of time has been since the beginning a responsibility of the CGPM, but this was not the case of its maintenance until the end of 1980s. The 13^{th} CGPM (1968) decided to adopt a new definition of the SI unit of time based on a transition of the caesium 133 atom; the 14^{th} CGPM (1972) introduced the use of International Atomic Time (TAI). Coordinated Universal Time (UTC) was defined for practical reasons (McCarthy, this volume); its real time representation is provided by time laboratories.

In 1988, the responsibility for maintaining the reference time scales TAI and UTC was conferred to the BIPM, with the obvious implication of insuring the consistency between the scale unit of TAI and the second of the SI. This activity is known as international time keeping, and requires coordinated activities in metrology institutes and observatories maintaining atomic clocks and primary frequency standards. For that, the BIPM organizes a network of time links on the basis of the voluntary participation of laboratories in member states and associates to the Metre Convention. Time laboratories contribute their data to be used in the construction of the reference time scales, and as a feed back their independent local time scales are traced to the international reference UTC.

The access to UTC, as well as other relevant information concerning UTC and TAI are

provided monthly via the publication of BIPM *Circular T*.

The activities of the Time section of the BIPM are focused on the maintenance of TAI and UTC, task that requires not only of the routine work of data collection and calculation, but that moreover implies research activities on algorithms, clock behaviour and techniques of comparisons of distant clocks.

2. THE REQUESTED PROPERTIES OF A TIME SCALE

A time scale is characterized by its *reliability*, *frequency stability* and *accuracy*, and *accessibility*. The algorithm used for the elaboration of a time scale will depend on what is requested for these characteristics.

The *reliability* of a time scale is closely linked with the reliability of the clocks whose measurements are used for its construction; at the same time, *redundancy* is also requested.

The *frequency stability* of a time scale is its capacity of maintaining a fixed ratio between its unitary scale interval and its theoretical counterpart.

The *frequency accuracy* of a time scale is the aptitude of its unitary scale interval to reproduce its theoretical counterpart. After the calculation of a time scale on the basis of an algorithm conferring the requested frequency stability, frequency accuracy is improved by comparing the frequency of the time scale with that of primary frequency standards, and by applying, if necessary, frequency corrections.

The *accessibility* to a worldwide time scale is its aptitude to allow all users with a means of dating events. It depends on the precision which is required. In the case of a reference time scale, where long term frequency stability is required, to attain to the ultimate precision requires a delay of a few tens of days. Furthermore, the process needs to be designed in such a way that the measurement noise is eliminated or at least minimized, this requiring a minimum of data sampling intervals.

3. INTERNATIONAL ATOMIC TIME (TAI): ITS CHARACTERISTICS

Many factors have contributed in the last ten years to the improvement of TAI. The progress in clocks and techniques for clock comparison has been accompanied at the BIPM by updates of the calculation algorithm to render it more adapted to the improvements in technology.

The increasing number of clocks, most of them with higher frequency stability and accuracy, have made TAI more reliable. The algorithm of calculation treats data over a 30-day period, during which a clock is considered to have a constant weight. The continuity with the previous period of computation is given by a prediction of the frequency of clocks, in an attempt of rendering the scale insensitive to changes in the set of participating clocks.

The calculation of TAI is based on clock differences, so requiring the use of methods of comparison of distant clocks. A prime requisite is that the methods of time transfer used for clock comparison do not degrade the frequency stability of the clocks. In fact, time transfer has been in the past a major limitation to the construction of a reference time scale. TAI relies today on a network of time links where many baselines are technique-redundant. The progress in GPS work, and the introduction of time comparisons through geostationary telecommunications satellites allows today to compare the best atomic standards over integration times of few days with nanosecond (statistical) uncertainty.

The frequency accuracy of TAI is improved by the frequency measurements of primary frequency standards developed in a few time laboratories reporting data to the BIPM. Caesium fountains provide the best representations of the SI second, with frequency accuracy of order 10^{-15} - 10^{-16}. In order to keep the unitary scale interval of TAI as close as possible to its definition, a process called frequency steering has been implemented.

The instability of TAI, is estimated today as 0.5×10^{-15} for averaging times of 20-40 days

(Petit, 2005). In the very long term, over a decade, the stability is maintained by primary frequency standards and is limited by the accuracy at the level of 10^{-15} assuming that the present performances are constant. The frequency accuracy of TAI is estimated today as better than $3x10^{-15}$.

4. THE SCHEME OF CALCULATION

The algorithm known as Algos (BIH, 1974; Guinot and Thomas, 1988; Audoin and Guinot, 2001), developed at the Bureau International de l'Heure (BIH) in 1973 has fixed the principles that are still at the basis of the construction of TAI. The quantities which intervene in the calculation are time and frequency differences at specified dates, denominated "standard dates". These dates are modified julian dates (MJD) ending by 4 and 9. Each participating laboratory k maintains a local realization of UTC denominated UTC(k); it serves as the reference for local frequency and clock differences. Clock comparison data are reported in the form of time series of $[UTC\ (k)\ -\ S\ ]$, where S is a time marker or emitter received by two or more laboratories. Comparisons of time between two laboratories (j, k) are expressed by the series of differences between their respective local realisations of UTC at the standard dates, $[UTC(j)\ -\ UTC(k)]$.

Making use of the clock and time transfer data, the algorithm calculates an averaged time scale called *Free Atomic Scale* (Echelle Atomique Libre EAL). EAL has an optimized frequency stability for a selected averaging time (20-40 days), but is not constrained to be accurate in frequency.

Frequency measurements of primary frequency standards allow to evaluate the relative deviation between the scale interval of TAI and the SI second. Depending on its value, a correction is applied to the frequency of EAL, process known as "the steering of TAI". By doing this, we obtain TAI, that benefits of the optimized frequency stability of EAL and that is accurate in frequency as a consequence of the steering procedure.

The last step consists in producing UTC by adding to TAI an integer number of seconds. The output of the process are the differences $[UTC\ -\ UTC(k)]$ published in monthly BIPM *Circular T*, providing access to UTC through its local approximations UTC(k).

5. IMPROVEMENTS IN THE REALIZATION OF THE INTERNATIONAL TIME SCALES

The improvement of TAI/UTC is a continuous process that depends on the contributing laboratories in which concern:
a) the number and quality of the participating clocks,
b) the introduction of more performing techniques of time comparison,
c) the progress in the primary frequency standards,
and on the actions of the BIPM Time section, in dialogue with the time and frequency community in issues related to:
d) international coordination for time keeping,
e) improvement of the algorithm for the calculation of TAI,
- e_1) clock weighting and clock frequency prediction,
- e_2) calculation of time links,
- e_3) TAI frequency steering.

5.1. Clocks in TAI

The number of laboratories contributing to TAI increased from 46 in 1995 to 56 in 2005. They are mostly located in national metrology institutes, but some of them are in observatories that continued with time keeping activities after the transition from astronomical to atomic time.

The number of participating clocks every month oscillates about 300, representing an increase of about 20% in ten years. 84% of clocks are commercial, high-performance caesium standards, characterized by a frequency stability of about $1x10^{-14}$ over 5 days; these clocks realize the atomic second with a relative frequency accuracy of $5x10^{-12}$, almost one order of magnitude better than the standard model mostly used in laboratories a few years before. Active, auto-tuned hydrogen masers have slightly increased in number in the mid 1990s, oscillating between 17 - 20% of the total number of participating since then. They present high frequency stability (better than 1 part in 10^{15}) over one day, but they do not realize the atomic second. Fig. 1 shows the evolution in the type of clocks that have contributed to the construction of TAI since 1995.

To improve the stability of EAL, a weighting procedure is applied to the clocks. The weight of a clock is considered constant during the 30-day period, and continuity with the previous period is assured by a prediction of the clock's frequency. These procedure renders the scale insensitive to changes in the set of participating clocks.

To avoid the possibility that very stable clocks increase their weights to the point of dominating the scale, a maximum relative weight ω_{max} is fixed. The choice of the value for ω_{max} has evolved accordingly with the evolution of clocks in TAI. Fig. 2 shows an histogram with the percentage (averaged for a year) of clocks of different types having reached the maximum relative weight since 1995.

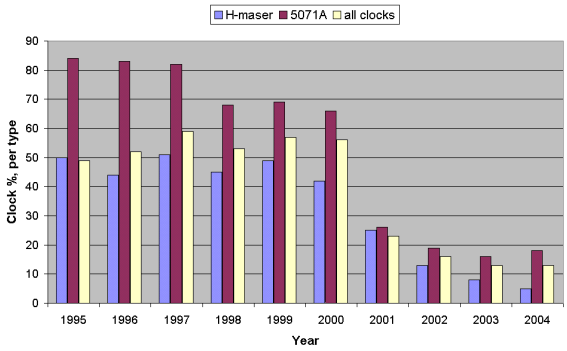

Figure 1: Clocks having contributed to TAI since 1995.

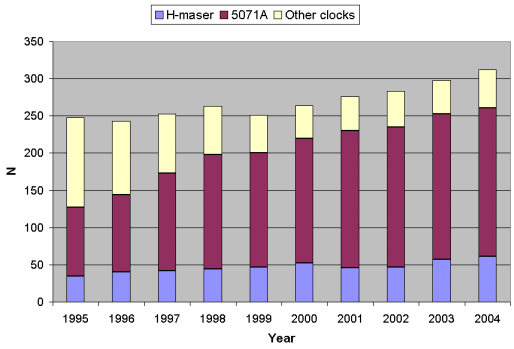

Figure 2: Evolution of the maximum weight of clocks in TAI.

5.2. Clock comparison in TAI

The calculation of TAI and UTC is based on clock comparison data. Since clocks are located in different laboratories, it is required to use methods of comparison of distant clocks. The methods of time transfer should not contaminate the frequency stability of the clocks; this has been in the past the major limitation in the construction of a reference time scale. At the state of art in commercial clock technology, this is not a constraint today. The uncertainty of clock comparison is today between a few tens of nanoseconds and a nanosecond for the best links, a priori sufficient to compare the best atomic standards over integration times of a few days. This assertion is strictly valid for frequency comparisons, where only statistical uncertainty affects the process. In the case of time comparisons, the systematic uncertainty coming from the equipment calibration should be considered in addition. In the present situation, calibration contributes with an uncertainty that surpasses the statistical component, and that can reach 20 ns for non calibrated equipment. It can be inferred that repeated equipment calibrations are indispensable for clock comparison.

The use of GPS satellites in time comparisons introduced a major improvement in the 1980s in the construction and dissemination of time scales. It consists in using the signal broadcast by GPS satellites, which contains timing and positioning information. It is a one-way method, the signal being emitted by a satellite and received by specific equipment installed in a laboratory. For this purpose, GPS receivers have been developed and commercialized to be used specifically for time transfer. The Russian satellite system of global navigation GLONASS is not used for time comparison in TAI on a routine basis, since the satellite constellation is not yet complete and stable, and the time laboratories are at present completing their equipments for GLONASS reception. Nevertheless, studies conducted at the BIPM and in other laboratories prove (Bogdanov et al., 2002; Lewandowski et al., 2005) that the system is potentially useful for accurate time transfer.

Modern GPS and GPS/GLONASS receivers installed in national time laboratories that contribute to the calculation of TAI provide in an automated way time transfer data.

Thanks to new hardware and to improvements in data treatment and modelling, the uncertainty of clock synchronization via GPS fell from a few hundreds of nanoseconds at the beginning of the 1980s to 1 ns today. Old single-channel, single-frequency C/A Ũ code receivers are being replaced in time laboratories by multi-channel receivers, which allow the simultaneous observation of all satellites over the horizon. The effects of ionospheric delay introduce one of the most significant errors in GPS time comparison and in particular, in the case of clocks compared over long baselines. GPS observations with single-frequency receivers used in regular TAI calculations are corrected for ionospheric delays by making use of ionospheric maps produced by the International GPS Service (IGS) (Wolf and Petit, 1999). Dual-frequency receivers installed in some of the participating laboratories permit the removal of the delay introduced by the ionosphere, thus increasing the accuracy of time transfer. All GPS links are corrected for satellite positions using IGS post-processed precise satellite ephemerides.

Precise-code data from GPS geodetic-type, multi-channel, dual-frequency receivers has been introduced since June 2004 in the calculation of TAI (Defraigne and Petit, 2003). These links, denominated by GPS P3 links, provide ionosphere-free data and allow clock comparisons with nanosecond uncertainty or better.

After about 25 years of experimentation, the method of two-way satellite time and frequency transfer (TWSTFT) is currently used in TAI since 1999 (Lewandowski and Azoubib, 2000). The TWSTFT technique utilizes a telecommunication geostationary satellite to compare clocks located in two receiving-emitting stations. Two-way observations are scheduled between pairs of laboratories so that their clocks are simultaneously compared at both ends of the baseline. The clocks are directly compared, using the transponder of the satellite. It has the advantage of a two-way method over the one-way method of eliminating or reducing some sources of systematic error such as ionospheric and tropospheric delays, uncertainty on the positions of the satellite and the ground stations. The differences between two clocks placed in the two stations are directly computed. Until the mid-2004, intervals of 5-minute measurements were made three days per week, impeding the technique to reach its highest potential performance, which is sub-nanosecond uncertainty. With the installation of automated stations in most laboratories, some of the TWSTFT link observations in TAI are at daily or even sub-daily intervals, with the consequence of setting the uncertainty below the nanosecond.

For two decades, GPS C/A-code observations have provided a unique tool for clock comparison in TAI, rendering impossible any test of its performance with respect to other methods. The present situation is quite different. For the links where the two techniques are available, both GPS and TWSTFT links are computed; the best being used in the calculation of TAI, the other kept as a backup. The GPS P3 links have further increased the reliability of the system of time links, providing a method of assessing the performance of the TWSTFT technique. Comparison of results obtained on the same baselines with the different techniques (Arias et al., 2005)

shows equivalent performances for GPS geodetic-type dual-frequency receivers and TWSTFT equipment, when two-way sessions have a daily regularity (1 ns or less).

At the moment, 80% of the links in TAI are obtained by using GPS equipment (65% with GPS time-receivers; 15% with GPS geodetic-type receivers) and about 14% of the links are provided by TWSTFT observations.

Calibration of the laboratory's equipment for time transfer is fundamental for the stability of TAI and for its dissemination. Campaigns of GPS time equipment differential calibration are organised by the BIPM to compensate for internal delays in laboratories by comparing their equipment with travelling GPS equipment.

A network of international time links has been established by the BIPM to organise these comparisons (see Fig. 3). It is a star-like scheme with links from laboratories to a pivot laboratory in each continent, and long baselines providing the links between the pivot points.

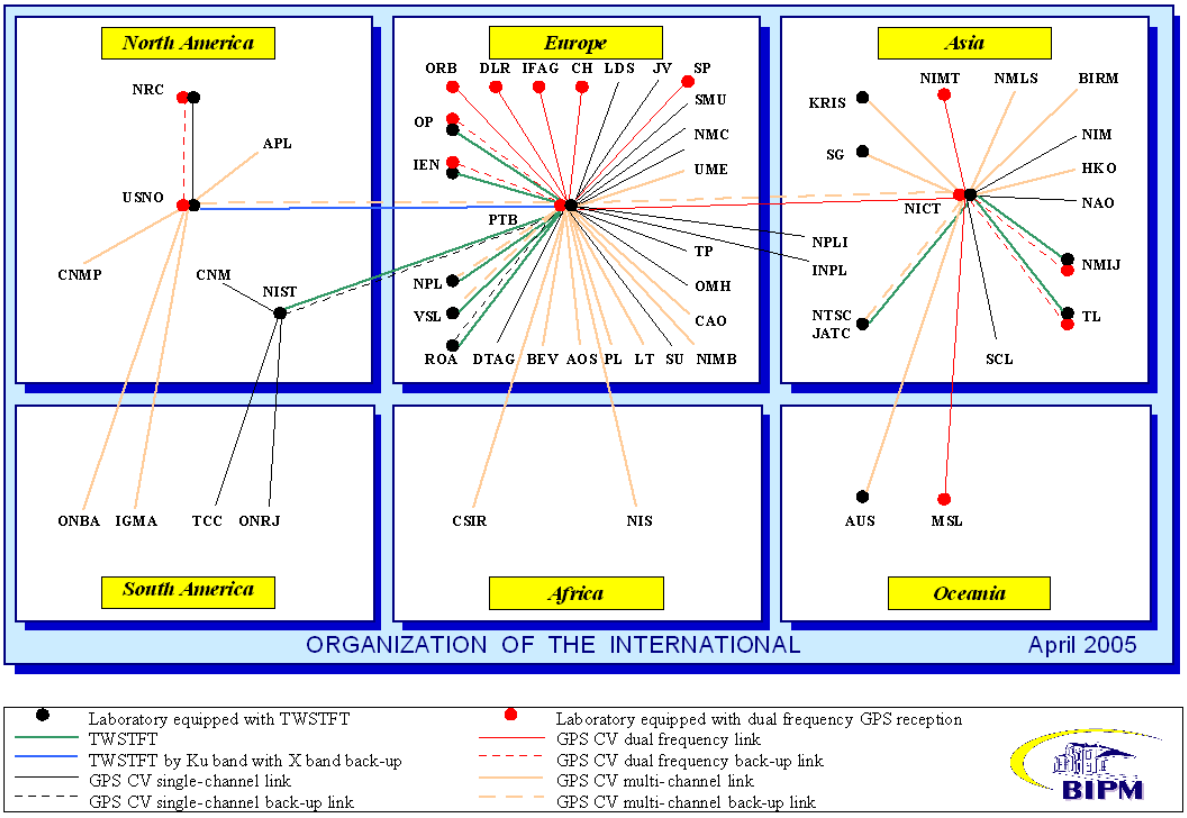

Figure 3: Network of international time links for TAI as in April 2005.

5.3. Improvement of the frequency accuracy of TAI

The frequency accuracy of TAI is assured by the primary frequency standards developed in some laboratories reporting their frequency measurements to the BIPM. A report of a PFS includes the measurement of the frequency of the standard relative to that of a clock participating in TAI, and a complete characterization of its uncertainty as published in a peer-reviewed journal. Five caesium fountains and two optically pumped caesium beam standards have contributed, more or less regularly, in the last two years to TAI with measurements over 10 to 30-day intervals. Two magnetically deflected caesium beam standards of the PTB (CS1 and CS2) are operated in a continuous manner and contribute permanently to both the accuracy of TAI and the stability of

EAL. In 2005, the definition of the second of the SI is realised, at best, by the primary frequency standards with an accuracy of order 10^{-15}.

Based on the frequency measurements of the PFS reported to the BIPM during a 12-month period, the fractional deviation d of the unitary scale interval of TAI from its theoretical value (the unitary scale interval of TT) is evaluated, together with its uncertainty.

In order to keep the unitary scale interval of TAI as close as possible to its definition, a process called *frequency steering* has been implemented. It consists in applying a correction to the frequency of EAL when d exceeds a tolerance value, generally fixed to 2.5 times its uncertainty. These frequency corrections should be smaller than the frequency fluctuations of the time scale in order to preserve its long term stability. Over the period 1998-2004, frequency steering corrections of $+/-$ 1x10^{-15} have been applied, when necessary, for intervals of two months at least. The values of d demonstrated that the unitary scale interval of TAI had significantly deviated from its definition and that the steering procedure was in need of revision. A different strategy for the frequency steering was adopted in July 2004. A frequency correction of variable magnitude, up to 0.7x10^{-15} is applied for intervals of one month at least, if the value of d reach 2.5 times its uncertainty.

5.4. Dissemination of TAI/UTC

The time scales TAI and UTC are disseminated every month by *Circular T* (BIPMa). Access to UTC is provided in the form of differences [UTC - $UTC(k)$] making at the same time the local approximations UTC(k) traceable to UTC; starting in January 2005, their uncertainties are also published (Lewandowski et al., 2005).

The values of the frequency corrections on TAI and their intervals of validity are regularly reported. This information is needed for the laboratories to steer the frequency of their UTC(k) to UTC.

Circular T provides wide access to the best realisation of the second through the estimation of the fractional deviation d of the scale interval of TAI with respect to its theoretical value based on the SI second. The values of d for the individual contributions of PFS are also published, giving access to the second as realised by each of the primary standards.

Within *Circular T*, the time links used for the calculation of one month, with their respective uncertainties are detailed, accompanied by information about the technique used in the calibration of the time transfer equipment or link.

The ftp server of the BIPM time section gives access to clock data, time transfer files provided by the participating laboratories, results of link comparisons, as well as the rates and weights for clocks in TAI in each month of calculation. This information is particularly useful for laboratories in the study of their clocks behaviour (www.bipm.org).

Results for a complete year are published in the *Annual Report of the BIPM Time Section* (BIPMb), together with information about the laboratories' equipment, time signals and time dissemination services, as reported by the laboratories to the BIPM.

Data used for the calculation of TAI, *Circular T*, some tables of the *Annual Report* and all relevant results and information are available on the ftp server of the BIPM Time section.

REFERENCES

13^{th} Conférence Générale des Poids et Mesures, *Metrologia*, 1968, 4, 43.

14^{th} Conférence Générale des Poids et Mesures, *Metrologia*, 1972, 8, 35.

Annual Report of the BIPM Time Section, published annually by the BIPM.

Arias E.F., Jiang Z., Lewandowski W., Petit G., 2005, *Proc. 2005 Joint FCS and PTTI meeting*, 213-315.

Audoin C , Guinot B., 2001, *The measurement of time*, Cambridge University Press.

Bogdanov P., Zholnerov S., Kovita S., Lewandowski W., Azoubib J., de Jong G., Imae M., Nawrocki J., 2002, *Proc. 16th EFTF*.

Bureau International de l'Heure, *BIH Annual Report for 1973*, 1974, Observatoire de Paris.

Bureau International des Poids et Mesures, *Circular T*, a monthly publication of the BIPM.

Defraigne P., Petit G., 2003, *Metrologia*, 38, 184-188.

Guinot B., Thomas C., 1988, *Establishment of International Atomic Time*, *Annual Report of the BIPM Time Section*, 1, D1-D22.

Lewandowski W., Azoubib J., 2000, *Proc. of IEEE/EIA International Frequency Control Symposium*, 586-597.

Lewandowski W., Foks A., Jiang Z., Nawrocki J., Nogas P., 2005, *Proc. Joint IEEE FCS and PTTI meeting*, 728-734.

Lewandowski W., Matsakis D., Panfilo G., Tavella P., 2005, *Proc. 36th PTTI meeting*, 247-262.

Petit G., 2005, *Proc. 19th EFTF*, 79-82.

Wolf P., Petit G., 1999, *Proc. 31st PTTI meeting*, 419-428.

GPS TIME AND FREQUENCY TRANSFER: STATE OF THE ART

P. DEFRAIGNE, C. BRUYNINX
Royal Observatory of Belgium
Avenue Circulaire, 3, B-1180 Brussels
e-mail: p. defraigne@oma.be, c.bruyninx@oma.be

ABSTRACT. The comparison of clocks located in different laboratories, called Time and Frequency Transfer, can be obtained from the common view of GPS satellites. This method consists in determining the clock offsets between the laboratory clocks and a common time scale associated with the GPS system; this can be either the satellite clocks, or the GPS time scale, or the IGS time scale. The last developments in GPS data analysis for time transfer, in collaboration with the geodetic community associated with the IGS, have improved significantly the capabilities of the technique. The paper presents the state of the art of the performances and limitations of the GPS time and frequency transfer.

1. USING GEODETIC RECEIVERS FOR TIME TRANSFER

The GPS signal is presently composed of two carriers (L1 and L2) modulated by two pseudo-random noise codes. Geodetic GPS receivers measure in addition to the C/A-code also the precise P1 and P2 codes as well as the carrier phases on the L1 and L2 frequencies. Time transfer benefits from geodetic-like GPS receivers because their dual frequency measurements allow eliminating the first order ionospheric delay. As the ionospheric perturbation on an electromagnetic wave is frequency-dependent, a combination of two signals with different frequencies can be used to cancel the first order ionospheric delays. Rather than using the C/A code, which is the only available information on the classical time receivers, the geodetic receivers allow to use the so-called 'ionospheric-free' code observable P3, corresponding to a combination of the two GPS precise codes P1 and P2 (Defraigne and Petit, 2003). Users limited to the C/A code observable correct the ionospheric delay using the ionospheric maps issued by the International GNSS Service (IGS). These IGS IONEX maps only correct for the long wavelength and long term variations (above 2 hours), while the ionospheric-free combination eliminates both the short and long wavelength behavior of the ionosphere as well as short and long term variations.

Figure 1 shows the time transfer between two Hydrogen masers, the first one located NPLD (UK) and the second one located at USNO (Washington), when using on one hand the C/A code and correcting for the ionospheric delays using the IGS IONEX maps and when using on the other hand the P3 code. In both cases the precise satellite ephemeredes provided by the IGS have been used for the determination of the geometric distances satellites-station and for the satellite clock synchronization errors. This use of P3 improves the Allan deviation by a factor of 2 on a transatlantic baseline.

Next to the availability of dual frequency observations, the geodetic GPS receiver also provide carrier phase observables (L1, L2) which have a noise about 100 times smaller than the code measurements. For this reason, the carrier phases have been used since '80 for different geodetic applications requiring very high precision. During the last years, the potential of GPS carrier

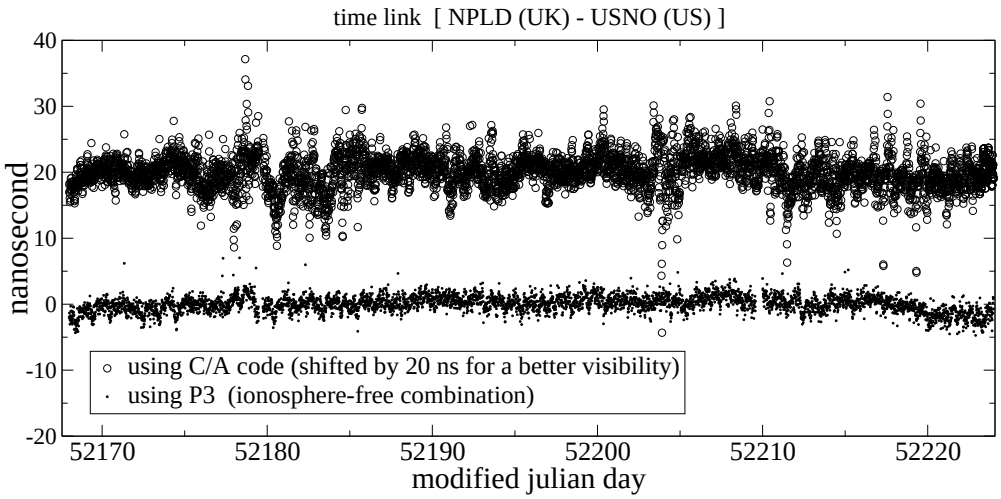

Figure 1: Time transfer between two Hydrogen Masers located in stations NPLD and USNO, using either the C/A code corrected for the ionosphere with the IONEX maps, or the P3 code.

phases for time transfer was recognized and demonstrated by different authors (Larson et al., 1999, Bruyninx et al., 1999). Carrier phases have been shown to be extremely interesting for averaging times smaller than 5 days. However, due to the presence of the initial ambiguities, the carrier phases are ambiguous and are not able to determine the absolute offset between the remote clocks. It is therefore necessary to process the code observations together with the phase observables. The absolute offset between the remote clocks is then only determined by the code information, while the carrier phases allow to give a precise signal evolution. Due to the use of daily data batches for the data processing, day boundary jumps appear in the clock solution obtained with the combined code/carrier phase data analysis. For each data batch (each day in our case) the evolution obtained from carrier phases has to be "calibrated" with the absolute offset obtained with the code data, and this within the noise level of the code measurements, i.e. about 1 ns. This leads to day boundary jumps up to 500 ps in the solution. In order to avoid these jumps, several ideas have been tested: either an overlap of the data files (Bruyninx and Defraigne, 1999), or the use of a longer data batch (Orregazzi et al., 2005) in order to have less jumps (one jump between 2 data batches); or the use ambiguities obtained from the previous data batch (Dach et al., 2004). The concatenation of the results is probably the worse solution as it can introduce some trend in the result (Ray and Senior, 2005).

2. LIMITATIONS OF CARRIER PHASE RESULTS

Environmental effects

Among the hardware considerations, one has to account for the hardware delays of the GPS equipment, which have to be determined by calibration. These hardware delays are sensitive to the ambient temperature variations; this is the reason why it is important to have temperature stabilization in the laboratories. Some experiments have been performed to test the sensitivity of the equipment (receiver, amplifiers, ...) to the temperature variations and the results showed the importance to keep the temperature constant within 0.1°C. Concerning the GPS antenna, the experiments show maximum diurnal variations (for diurnal variations of 20°C) of 40 ps for the carrier phases (Ray and Senior, 2001), while up to 2 ns for the code measurements (Smolarski et

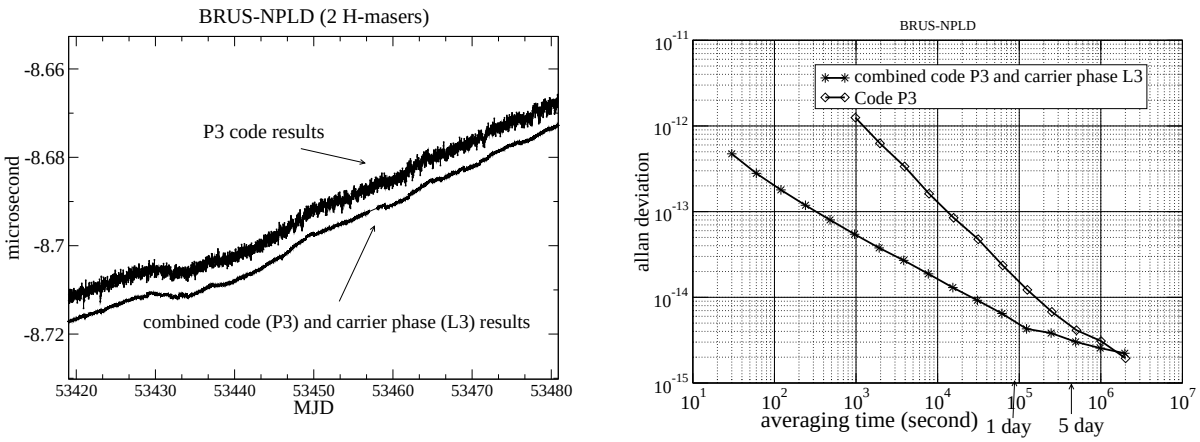

Figure 2: left : Comparison between the time transfer results obtained with precise codes (ionosphere free combination P3) or combined code-carrier phases (ionosphere free combination L3) analysis; the two curves have been separated by 5 nanoseconds in order to improve the visibility. right: allan deviation of the two curves.

al., 2002); some GPS antenna cables exist with very small sensitivity to temperature variations and should be used for precise time and frequency transfer.

Troposphere (zenith total delay)

As the troposphere activity varies rapidly, the troposheric delay must be corrected using either Water Vapor Radiometer (WVR) measurements or by an estimation of the parameters of a given tropospheric model. In that case, there will be a correlation between the tropospheric parameters determined and the clock solution, because both appear in the equation to be solved. As shown by Hackman and Levine (2004), this can lead to differences up to 300 ps in the clock solution between the solutions obtained either using WVR data for the troposphere delay or using an estimation of the tropospheric parameters. This is illustrated in Figure 3.

Reaction of the receiver to frequency changes

We recently tested the fidelity of GPS receivers to the external frequency standard used to drive them (Defraigne and Bruyninx, 2005). For this, we connected two GPS receivers to the same antenna and to two separate atomic frequency standards. The time and frequency transfer results obtained from the GPS code and carrier phase data analysis were then compared with the measurements of a phase comparator connected to the two frequency standards. The numerical differences obtained in this study were of course related to the receiver type. On the short term, we measured differences of tens of picoseconds between the GPS results and the phase comparator. On the long term, 3 weeks in our case, the maximum differences reached 180 picoseconds peak-to-peak, after correction for the day boundary jumps. These differences between the GPS timing results and the phase comparator seemed to be caused by a smoothing of the phase measurements within the GPS receiver.

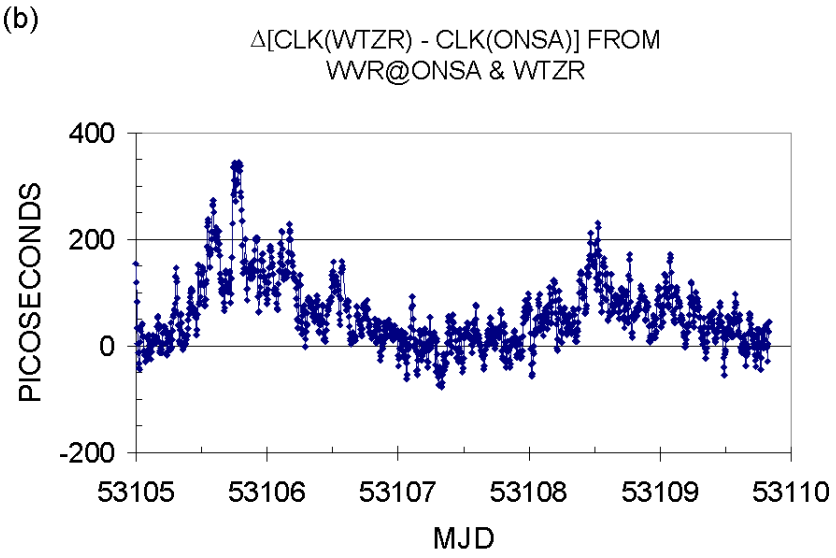

Figure 3: (from Hackman and Levine, 2004) Difference between the time transfer results obtained with estimated tropospheric delay and those obtained using Water Vapor Radiometer data. The stwo stations used are in Wettzel (Germany) and Onsala (Sweden).

GPS analysis strategy

The clock solutions can be obtained either through a network analysis or in a PPP (Precise Point Positioning) process. In the first case, all the station clocks are determined in a global solution, and these clock solutions correspond to the clock synchronization errors with respect to a reference time scale which can be either one clock in the network, or a combination of the network clocks. In the PPP analysis, the clock solutions of one single station are determined with respect to a reference time scale (GPS time or IGS time scale). In that case, the satellite orbits and clocks are taken from some external source, as for example the IGS products.

To compare the PPP and network results we express them both with respect to the IGS time scale. This time scale is provide by the IGS with a 1-day delay. IGST (or IGRT for the rapid version) is realized from the IGS clock combinations, i.e. satellite and receiver clock offsets (Kouba and Springer, 2001; Senior et al., 2003, Ray and Senior, 2003), and is based on code/phase time transfer between IGS receiver and/or satellite clocks.

Figure 4 shows the differences between the PPP and network solutions. The differences obtained between both kinds of analysis can be up to 400 picosecond peak-to-peak in the clock solutions, depending on the analysis software used among the existing tools. For longer data batches, the differences can reach 800 ps due to the day boundary jumps mentioned above. Also the final IGS clock solution which gives the clock synchronization errors of all the station clocks with respect to the IGST or IGRT is shown in this Figure. This IGS clock solution can be used by the IGS stations for a short term monitoring of their clocks.

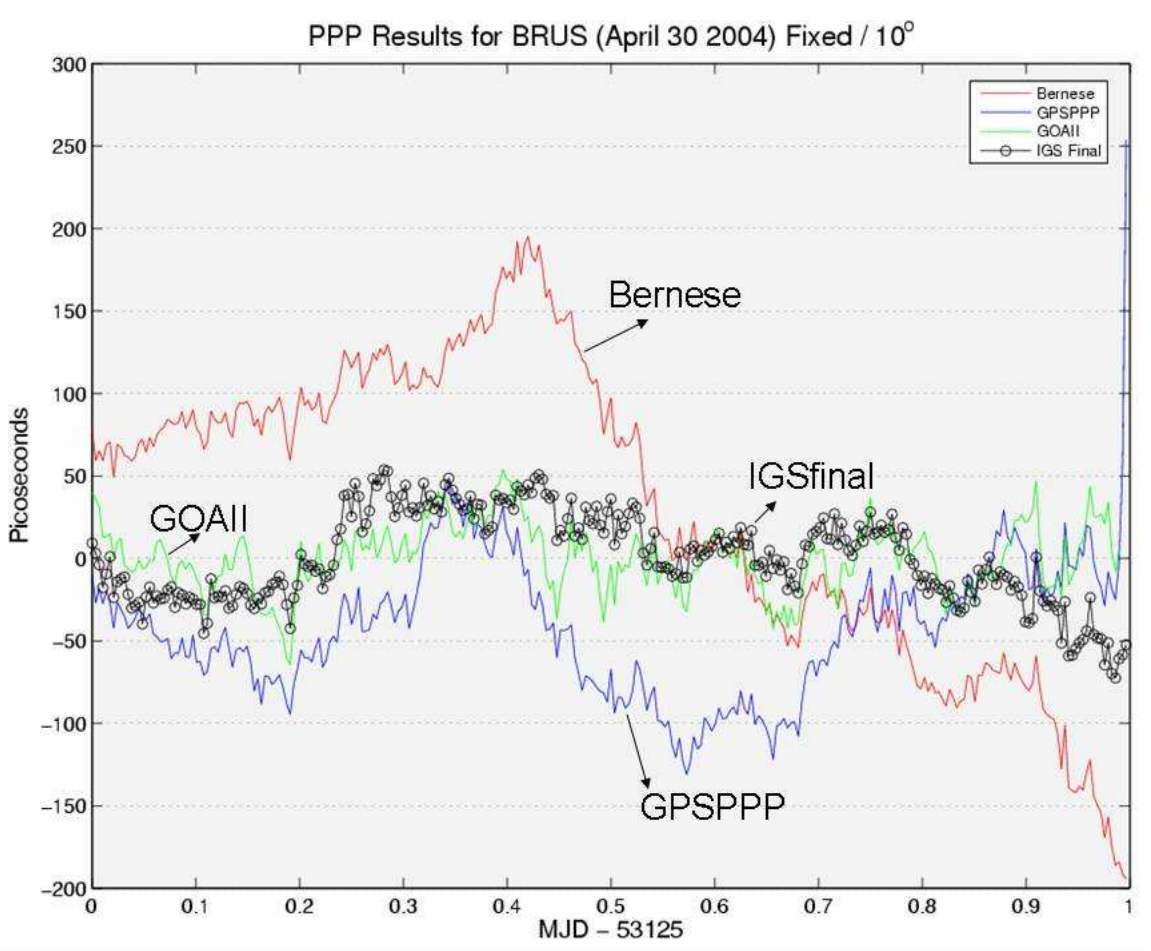

Figure 4: Results obtained for the clock solution BRUS-IGST with either a PPP solution, using different software tools, or the network solution computed by IGS (final).

3. CONCLUSIONS

This paper presented a summary of the capabilities and limitations of the present GPS data analysis for time and frequency transfer. The carrier phases are a very efficient tool for short term clock comparisons. The major factor limiting their use is the day boundary jumps, as illustrated by the Figure 5 which presents the different uncertainty sources in the combined GPS code-carrier phase data analysis for time and frequency transfer. These jumps can reach 500 ps or even more for some receivers. One parameter not yet tested in detail is the network geometry, and should be the subject of a further study. Furthermore, the accuracy of the calibration was not mentioned in this study. This calibration presently limits the determination of the absolute offset between the remote clocks to an uncertainty of 2.5 ns. However the hardware delay should not deteriorate the frequency comparisons as it is constant with time (for instruments in temperature stabilized rooms).

REFERENCES

Bruyninx C.,Defraigne P., 1999, "Frequency Transfer Using GPS Codes and Phases : Short and Long Term Stability", *Proc. of the 31th PTTI meeting, Dana Point, California, décembre 1999,* pp. 471-478.

Bruyninx C., Defraigne P., and Sleewagen J.-M., 1999,"Time and Frequency transfer using GPS

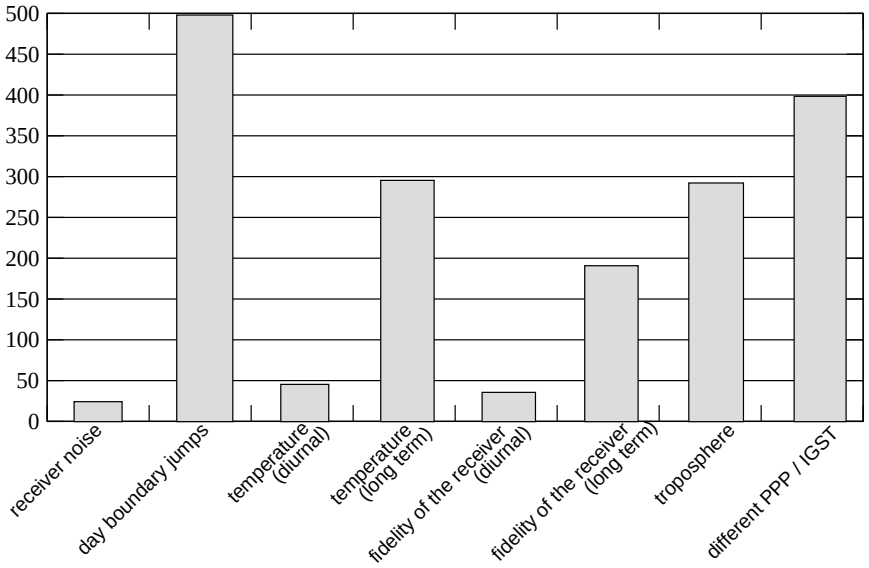

Figure 5: Summary of the uncertainty sources on combined GPS code-carrier phase data analysis for time and frequency transfer.

Code and Carrier Phases: Onsite Experiments", *GPS Solutions*, 3, 1-10.

Dach R., Schildnecht T., Hugentobler U., Bernier L.-G. and Dudle G., 2004, "Continuous geodetic time transfer analysis methods", *Proc. IEEE Trans. Ultrason. Ferroelect. Freq. Contr.*.

Defraigne P., Petit G., 2003. "Time Transfer to TAI using geodetic receivers", *metrologia* , 40, pp. 184-188.

Defraigne P., Bruyinx C., 2005. "Testing the capabilities of GPS receivers for time transfer", *Proc. PTTI 2005, Vancouver*, august 2005.

Hackman K., Levine J., 2004, "Adding water vapor radiometer data to GPS carrier-phase time transfer" *Proc. 36th PTTI, Washington*, 2004.

Kouba and Springer, 2001, "New IGS station and satellite clock combination", *GPS Solutions*, 4(4), 31-36.

Larson K., Levine J., Nelson L. and Parker T., 2000, "Assessment of GPS carrier-phase stability for time-transfer aplications", *IEEE Trans. Ultrason. Ferroelect. Freq. Contr.* 47(2), 484-494.

Orregazzi D., Tavella P., Lahaye F., 2005, "Experimental Assesment of the Time Transfer Capability of Precise Point Positioning (PPP)", *Proc.Joint IEEE Intern. Freq. Contr. Symp. and PTTI, Vancouver.*

Ray J. and Senior K., 2001, "Temperature sensitivity of timing measurements using Dorne Margolin antennas",*GPS Solutions*, 2(1), 24-30.

Ray J. and Senior K., 2003, "IGS/BIPM Pilot Project: GPS carrier phase for time/frequency transfer and time scale formation", *Metrologia*, 40(3), S270-S288.

Ray J. and Senior K., 2005, "Geodetic techniques for time and frequency comparisons using GPS phase and code measurements", *Metrologia*, 42, 215-232.

Smolarski A., Lisowiec A., Nawrocki J., 2002, "Improving the accuracy of GPS Time Transfer by Thermal Stabilization of GPS Antenna and Receiver",*Proc. 16th EFTF, St. Petersburg*, march 2002.

Senior K., Koppang P., and Ray J., 2003. Developing an IGS time scale, *IEEE Trans. Ultrason., Ferroelect., Freq. Contr.*, 50(6), 585-593.

SATELLITE TIME-TRANSFER: RECENT DEVELOPMENTS AND PROJECTS

W. LEWANDOWSKI [1] and J. NAWROCKI [2]
[1] Bureau International des Poids et Mesures, Sèvres, France
e-mail: wlewandowski@bipm.org
[2] Astrogeodynamical Observatory, Space Research Centre, Borowiec, Poland
e-mail: nawrocki@cbk.poznan.pl

ABSTRACT. Global Navigation Satellite Systems (GNSS) keep a central role in the international timekeeping. American Global Positioning System (GPS) is a navigation system that has proven itself to be a reliable source of positioning for both the military community and the civilian community. But, little known by many, is the fact that GPS has proven itself to be an important and valuable utility to the timekeeping community (Lewandowski et al. 1999). GPS is a versatile and global tool which can be used to both *distribute time* to an arbitrary number of users and *synchronise clocks* over large distances with a high degree of precision and accuracy. Similar performance can be obtained with Russian Global Navigation Satellite System (GLONASS). It is expected in the near future satellites of a new European navigation system GALILEO might bring some important opportunities for international timekeeping. This paper after a brief introduction to international timekeeping focuses on the description of recent progress in time transfer techniques using GNSS satellites.

1. INTRODUCTION

Construction of International Atomic Time (TAI) and Coordinated Universal Time (UTC) relies on a network of satellite time links encircling the Earth. For a quarter of century the American Global Positioning System (GPS) has served the principal needs of national timing laboratories for regular comparisons of remote atomic clocks. From about ten years Two-Way Satellite Time and Frequency transfer (TWSTFT) through telecommunication satellites plays an increasing role. Russian GLONASS P-code shows an outstanding performance, although is not yet used operationally. A possible common use of GPS+GLONASS has also been demonstrated. GPS and GLONASS augmentation satellites such as WAAS, EGNOS, MSAS and GAGAN appear to be convenient for time transfer. It is expected that the European project Galileo will provide new opportunities. The timing community is developing time transfer standards for all available and upcoming global navigation satellite systems (GNSS). The interoperability of all GNSS is a major issue, implying coordination of time scales and reference frames.

Until now the major research work focused on GPS time transfer. This resulted in improvement of GPS time transfer reaching now accuracy of 1ns when using multichannel and P3 techniques. A major part of this progress is due to new generations of satellite receivers, often geodetic. However the TWSTFT technique has the best performance approaching right now 0.2 ns and having a great potential of further improvements.

The Bureau International des Poids et Mesures (BIPM), located in Sèvres near Paris, is on charge of computing and publishing international reference time scale. A practical scale

of time for world-wide use has two essential elements: a realization of the unit of time and a continuous temporal reference. The reference used is International Atomic Time (TAI), a time scale calculated at the BIPM using data from some two hundred atomic clocks in over fifty national laboratories. The long-term stability of TAI is assured by a judicious way of weighting the participating clocks. The scale unit of TAI is kept as close as possible to the SI second by using data from those national laboratories which maintain the best primary caesium standards. TAI is a uniform and stable scale which does not, therefore, keep in step with the slightly irregular rotation of the Earth. For public and practical purposes it is necessary to have a scale that, in the long term, does. Such a scale is Coordinated Universal Time (UTC), which is identical with TAI except that from time to time a leap second is added to ensure that, when averaged over a year, the Sun crosses the Greenwich meridian at noon UTC to within 0.9 s. The dates of application of the leap second are decided by the International Earth Rotation Service (IERS). At present TAI is 32 s ahead of UTC (see Figure 1 and http://www.bipm.org/en/scientific/tai/tai.html).

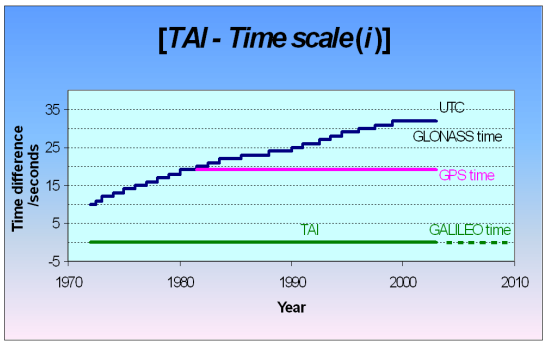

Figure 1: Differences between TAI, UTC, 'GPS time', 'GLONASS time', 'Galileo time' (project).

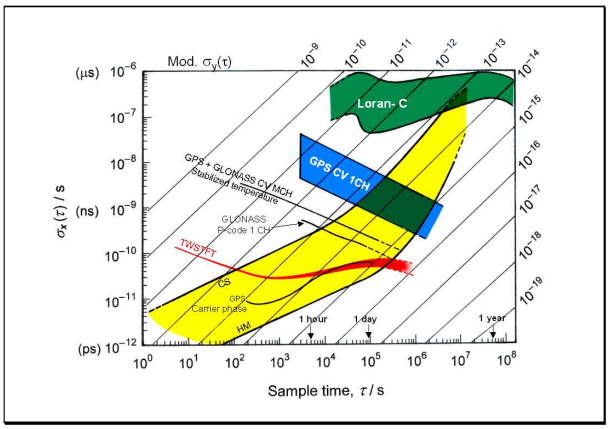

Figure 2: Comparison of some newer techniques with classical GPS single-channel common-view time transfer. Also indicated are typical clock performances.

This presentation reviews the above mentioned techniques as well as their potential impact on UTC and TAI.

UTC is computed and made available every month in the BIPM *Circular T* through the publication of [*UTC - UTC(k)*]. UTC is the reference time scale for world-wide time coordination. It serves as the basis of legal time in the different countries. Local realizations of UTC named UTC(k) are broadcast by time signals in some countries.

The GNSS are using 'internal' reference time scales. GPS uses 'GPS time', which was set in 1980 to have zero second difference with UTC, and to be 19 s behind TAI. 'GPS time' is, like TAI, a uniform time scale, it means that it does not follow leap seconds. GLONASS uses 'GLONASS time' which does follow leap seconds. According to the information available in September 2004, 'Galileo time' will be set to have zero second difference with TAI, and will be uniform time scale so not following leap seconds (see Figure 1). Each of these systems is programmed to broadcast a prediction of UTC, so a time scale using leap seconds. It happens, however, that for some applications it is suggested to use uniform time scales as TAI or 'GPS time', instead of UTC 'suffering' from leap seconds. Such proliferation of various time scales may cause major problems.

The utility of leap seconds is under discussion within International Astronomical Union (IAU) and International Telecommunications Union (ITU). A colloquium on future of UTC was organized by the ITU at the IEN Galileo Ferraris, Turin, Italy, in May 2003.

2. TIME TRANSFER TECHNIQUES

For the timekeeping community, GPS is today a significant contributor to solving the traditional problems of timekeeping; it is a reliable source of time and it is a reliable time transfer system. Russian global satellite navigation system GLONASS although not as well known as the GPS possesses comparable capabilities for navigation, precise geodetic positioning and time-transfer applications (Gouzhva et al. 1992).

Over the years, the clocks by which we have kept time have become not only more precise but also more accurate and the timekeeping community has sought more precise and more stable systems to help them with synchronisation. Time metrology began to use GPS signals about fifteen years ago at the National Bureau of Standards, NBS (now National Institute of Standards and Technology, NIST). A system using common-view observations of GPS satellites for accurate time and frequency transfer was suggested (Allan and Weiss 1980), and receivers especially designed for this purpose were built first at the NBS and then in several commercial companies. These were single-channel one-frequency C/A-code receivers capable of tracking only one satellite at a time. To operate them it was essential to issue periodic schedules of common-view observations. The common-view method was clever and far-reaching: it not only reduced some uncertainties of physical origin, but went on to cancel the deliberate degradation of GPS Time introduced in 1990 under the name of Selective Availability (SA).

The introduction of GPS brought about a significant improvement in time and frequency transfer. With uncertainties ranging from 10 ns to 20 ns for time comparisons during early stages of the use of GPS, it was possible, for the first time, to compare the best atomic standards in the world at their full level of performance using integration times of about 10 days. Since then a number of improvements have been introduced, including the use of ultra-accurate antenna coordinates, precise ephemerides and measurements of the ionosphere. These led at the beginning of 1990s to time comparison uncertainties of about 3 ns, which corresponds to a few parts in 10^{14} in frequency transfer. This paralleled improvements in atomic standards, which advanced by an order of magnitude, and made possible the comparison of the new clocks, e.g., HP5071A Cesium Beam Frequency Standards, at their full level of performances for averaging times of several days.

Today, in metrology, we are witnessing the birth of a number of new and innovative frequency standards. These devices have accuracy of about 1×10^{-15} and seem to have short term instability approaching 1×10^{-16}. This corresponds to a clock having the capability to maintain a level of performance corresponding to 10 picoseconds/day. Since the newest devices are not transportable and do not operate continuously, it is important to compare them in a reasonable time in order to determine the existence of systematic differences among them. A measurement with a precision of 1 nanosecond over a 24 hour period corresponds to 1×10^{-14} in frequency. Therefore, at today's present levels, it would take weeks to compare two such devices. That is why it is important to develop and improve time transfer methods to allow these comparisons to be made within a reasonable amount of time. For this reason the timing community is engaged in the development of new approaches to time and frequency comparisons. Among them are GNSS techniques based on multi-channel GPS C/A-code measurements, GPS carrier-phase (Schildknecht et al. 1990), GPS P3 (Defraigne and Petit 2003) and GLONASS P-code measurements (Azoubib and Lewandowski 2000; Lewandowski et al. 2000), temperature-stabilised antennas and standardisation of receiver software.

The performances of various methods of time transfer are illustrated in Figure 2. It has been

shown that the stability of time and frequency transfer is improved by a factor of about 3 when GPS common-view time transfer is carried out in multi-channel mode (Lewandowski et al. 1997). The use of GLONASS P-code shows a reduction in noise level by a factor of 5 in comparison with GPS C/A-code. It is now well documented that satellite-receiving equipment is subject to significant systematic effects due to environmental conditions; the use of TSA antennas and better cables reduces these effects and improves the accuracy of time transfer. The GPS carrier-phase technique allows frequency comparisons at a level of 1 part in 10^{15} and should soon be a useful tool for the comparison of primary frequency standards. Difficulties in calibration of GPS carrier-phase equipment remain unresolved, however, and this technique can not yet be used for operational time transfer. The Two-Way Satellite Time and Frequency Transfer (TWSTFT) technique (Kirchner 1999), which has a similar performance to that of carrier phase, is already operational and used in TAI for several time links.

3. EVOLUTION OF CLOCKS AND TIME LINKS AND TIME LINKS CONTRIBUTING TO TAI

The international time scales computed at the BIPM - TAI and UTC - are based on data from some 220 atomic clocks located in about 50 time laboratories around the world. The number of clocks fluctuates a little but remains roughly constant. The quality of the clocks, however, has been improving dramatically. In 1992 the first HP 5071A caesium clocks with high-performance tubes were introduced into the TAI computation, and the number of hydrogen masers has also been increasing steadily. In 1999 about 65% of the participating clocks were HP 50701A with a high-performance tube and about 17% were hydrogen masers. Other commercial caesium clocks (including HP 5071A clocks with a low-performance tube, and continuously operating primary frequency standards) account for only 18%. This progress has of course contributed to a significant improvement in the stability of TAI.

The quality of the clocks, although an important issue, is not the only factor contributing to the stability of TAI. Another important factor is the quality of the time links used to compare the clocks. Prior to 1981 only LORAN-C and TV links were used to compare clocks contributing to TAI. In 1981 the first GPS common-view single-channel C/A-code links were introduced. These allowed, for the first time, comparison of the stability of remote atomic clocks within an averaging time of several days. The proportion of GPS common-view links has increased steadily over the years and reached almost 100% in 1999 (see Figure 3). A new technique was then entered into TAI: that of TWSTFT. As of September 2004 nine TWSTFT links are used for TAI, and several others are in preparation.

To illustrate the impact of the improved quality of the time links on the frequency stability of TAI, we have analysed the period mid-1986-1993, during which the number of GPS links steadily increase but there was no dramatic change in the nature of the participating clocks. The frequency stability of EAL (the échelle atomic libre) against the primary frequency standard PTB CS2 is indicated in Figure 4 for the three periods mid-1986-mid-1988, 1988-1989 and 1992-1993. EAL is the free atomic time scale from which TAI is derived using steering corrections. We observe a significant improvement in the frequency stability of EAL for each consecutive period for averaging times up to a few tens of days (for these averaging times the white phase noise due to the time-transfer methods by which EAL was affected is drastically reduced). The evaluation of the frequency stability of EAL is here limited by the frequency stability of PTB CS2.

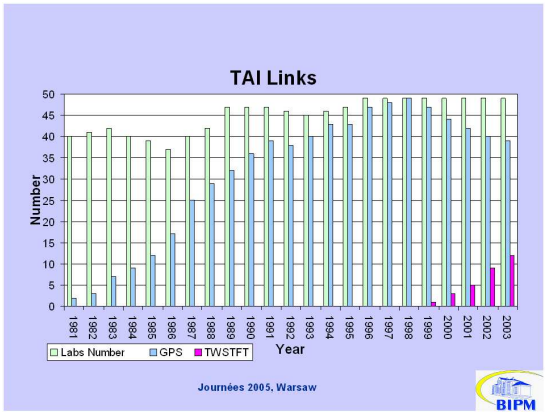

Figure 3: DTAI time links.

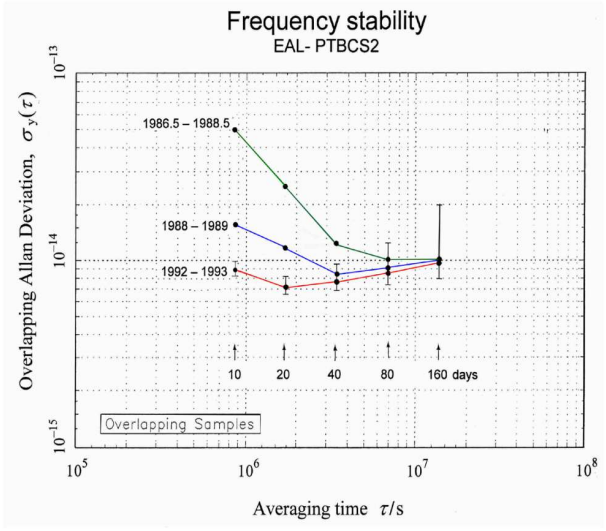

Figure 4: Frequency stability of [*EAL–PTB Cs2*].

4. SUMMARY

The construction of TAI requires time-transfer techniques that allow participating clocks to be compared at their full level of performance for intervals at which TAI is computed. In the pre-GPS era this was impossible because the technology of atomic clocks was always ahead of that of time transfer. This resulted in an annual term in TAI. The replacement of LORAN-C links by GPS C/A-code common-view links during the years 1981-1998 has progressively reduced the impact of white phase noise on TAI, improving its stability up to about 80 days. During the 1980s, GPS allowed for the first time the comparison of remote atomic clocks at their full level of performance for averaging times of just a few days, fully satisfying needs of TAI, computed at this epoch at intervals of 10 days.

However, with the improvements in clock technology made during the 1980s and the resulting dramatic increase in the quality of the clocks contributing to TAI in the 1990s, intercontinental GPS C/A-code single-channel common-view measurements need to be averaged sometimes over up to 20 days in order to smooth out measurement noise. This is no longer sufficient for TAI, computed at five-day intervals from 1 January 1996. However, the GPS multi-channel C/A-code and P3 measurements are showing better performance.

Analysis of the performance of TWSTFT, which is now in use for several TAI links, shows that clocks located on different continents can be compared by this technique at five-day intervals at their full level of performance, without being affected by time-transfer measurement noise. Thus, if TWSTFT were used for all TAI links, the stability of TAI would be improved for periods of up to 20 days.

The introduction of TWSTFT into TAI has brought about another important change for the better: TAI is not longer reliant on a single technique, because TWSTFT links are backed-up by GPS links and vice versa. Also, for the first time, two transatlantic links are used for its construction, and each of these links is performed by two independent techniques. This very new situation increases the robustness of TAI construction.

The international timekeeping, despite using for some links TWSTFT, still relies heavily on the use of sole GPS satellites. The use of other GNSS satellites as GLONASS and GALILEO is expected to bring more reliability and some further improvements in the performance of time links. A particular problem is the uniformization of reference time scales used by different GNSS systems.

REFERENCES

Lewandowski W., Azoubib J., Klepczynski W.J. (1999): GPS: Primary Tool for Time Transfer, Proceedings of the IEEE, Vol. 87, No. 1, pp. 163 - 172.

Gouzhva J. et al. (July/August 1992): High-Precision Time and Frequency Dissemination with GLONASS, GPS World, pp. 40-49.

Allan D.W., Weiss M.A. (1980): Accurate Time and Frequency Transfer During Common-View of a GPS Satellite, Proc. 1980 Frequency Control Symposium, pp. 334-336.

Schildknecht T., Beutler G., Gurtner W., Rothacher M. (1990): Towards subnanosecond GPS time transfer using geodetic GPS processing techniques, Proc. 4th European Frequency and Time Forum, pp. 335-346.

Defraigne P., Petit G. (2003): Time transfer to TAI using geodetic receivers, Metrologia, 40, pp. 184-188.

Azoubib J., Lewandowski W. (2000): Test of GLONASS precise-code time transfer, Metrologia 37, pp. 55-59.

Lewandowski W. Nawrocki J., Azoubib J. (2000): First use of IGEX precise ephemerides for international GLONASS P-code time transfer, Journal of Geodesy, 75, pp. 620-625.

Lewandowski W., Azoubib J., de Jong G., Nawrocki J., Danaher J. (1997): A new approach to international time and frequency comparisons: "all-in-view" multi-channel GPS+GLONASS observations, Proc. ION GPS-97, pp 1085-1091.

Kirchner D. (1999): Two-Way Satellite Time and Frequency Transfer (TWSTFT): Principle, Implementation and Current Performance, Review of Radio Science, Oxford University Press.

LOCAL ATOMIC TIME TA(UA)

V. SOLOVYOV[1], O. TKACHUK[1], A. KORSUN'[2]
[1] National Scientific Centre "Institute of Metrology"
42 Mironositska Str., 61002 Kharkiv, Ukraine
e-mail: solovyov@metrology.kharkov.ua
[2] Main Astronomical Observatory, National Academy of Sciences of Ukraine
27 Zabolotnoho Str., 03680 Kyiv, Ukraine
e-mail: akorsun@mao.kiev.ua

The standard of the units of time and frequency, which was realized at the National Scientific Centre "Institute of Metrology", was confirmed as the national standard of Ukraine in 1997.

It consists of the following groups of measurement technique means:

- the equipment of realization and keeping the units of timefrequency, which includes the hydrogen standards of frequency, formed into the main and the reserve groups. The main group consists of not less than three standards as a rule;
- the equipment of keeping the scale of time and the standard frequencies, which includes the system of forming the working scale of time, the system of forming the standard frequencies, the system of amplification and multiplication of the standard signals of time and frequency;
- the equipment of internal comparisons including frequency and phase comparators and automated measurement system;
- the equipment of external comparisons, which includes the equipment of standards comparisons by means of the signals of satellite navigation systems GPS and GLONASS (the specialized time receivers Acutime-2000, Navior-T and geodetic receiver by the company Trimble 4000 SSI); the equipment of comparisons of standards by radio meteoric channel by means of the equipment "Metka"; the equipment of comparisons of standards by TV channels;
- the equipment of standard assurance including the following:
  - the system of reserved power supply;
  - the system of conditioning and thermostating of the working rooms;
  - the system of measurement the environment parameters in the working rooms.

The standard has the following features:

- the metrological characteristics:
  - the standard provides realization of the units of time and frequency with the average square deviation of the measurement result, which doesn't exceed $5{\cdot}10^{-14}$;

– instability of the standard is not more than $2{\cdot}10^{-14}$ within the measurement interval of 1000 s to one day;

– the non-excluded systematic error is not more than $1{\cdot}10^{-13}$.

Mean fractional deviations of the UTC (UA) scale interval from that of UTC and UTC(SU) are presented in Table:

MJD	$\Delta f/f$[UTC(UA)–UTC], $\times 10^{-14}$	$\Delta f/f$ [UTC(UA)–UTC(SU)], $\times 10^{-14}$
53014...53043	2.6	2.3
53044...53073	2.1	2.5
53074...53103	0.8	1.6
53104...53133	1.0	1.6
53134...53163	−0.6	−0.5
53164...53193	−0.8	−0.7
53194...53223	−2.0	−0.8
53224...53253	−3.6	−1.6
53254...53283	−1.6	−0.5
53284...53313	−2.2	−0.5
53314...53343	−1.5	−0.5
53344...53373	−0.6	−4.6
Θ	−0.5	−0.1
σ	1.9	2.0

Θ is the constant difference, σ is the standard deviation

The tasks of the time scale TA(UA):

a) to insert in set of the primary cesium frequence standard,

b) to renovate the set of the hydrogen standards,

c) to enter the international set of the laboratories which collaborate with the BIPM (Bureau International des Poids et Mesures). As a results of these tasks, the accuracy of determination of the differences between the scales UTC and UTC(UA) and so the metrological safety of the time scale TA(UA) will be increased. To solve this problem it is necessary to acquire a special receiver of the GPS and GLONASS signal.

TTS-3, MULTI-CHANNEL, MULTI-SYSTEM GPS/GLONASS/WAAS/EGNOS RECEIVER

J. NAWROCKI, P. NOGAŚ, R. DIAK, A. FOKS, D. LEMAŃSKI
Space Research Centre of Polish Academy of Sciences,
Astrogeodynamic Observatory, Borowiec, Poland
e-mail: nawrocki@cbk.poznan.pl

1. INTRODUCTION

The Astrogeodynamic Observatory (AOS) of the Space Research Centre, following a popular TTS-2, has developed a new high-performance Time Transfer System - 3 (TTS-3).
The TTS-3 allows observations of GPS, GLONASS, EGNOS and WAAS satellites simultaneously in multi-channel, multi-frequency mode. The following codes are used: C/A-code for GPS, WAAS, EGNOS and GLONASS, P-code for GLONASS, and reconstructed P-code for GPS. In future the receiver will be a base for a new generation TTS-4, observing also GALILEO satellites. The receiver hardware, the treatment of the observations, and the output data fulfil the recommendations of the CCTF Group on GNSS Time Transfer Standards (CGGTTS). Data in RINEX format are also provided.

2. THE TTS-3 PERFORMANCE

The TTS-3 consists of a PC industrial computer, a PC card time interval counter, a GNSS 40-channel, appropriate software, an antenna and connecting cables.
Main technical specifications of the receiver are:
- full conformability to CCTF recommendations for common-view multi-channel, multi-system and multi-code GNSS time transfer technology;
- 40 channels, all-in-view, L1 GPS, L1/L2 GPS, L1/L2 GLONASS, WASS, EGNOS;
- full-duplex 10BASE-T Ethernet port;
- two 1 PPS output (LVTTL) synchronized to GPS time, GLONASS time or UTC;
- two Event Marker inputs;
- time interval resolution of the counter: 100 ps;
- external reference frequency 10 MHz;
- local 1 PPS input connector.

On request the TTS-3 can be equipped with a temperature-stabilized chamber for the GNSS board, and a temperature stabilized antenna.

3. APPLICATIONS OF TTS-3

The present applications of TTS-3 include comparisons of very stable (1e-15) atomic clocks between the NMI, UTC laboratories participating to TAI, military and research precise time and frequency centers. TTS-3 will be used by the Galileo Time Service Provider and the Galileo Precise Time Facility.

4. TTS-3 EVALUATION

The on-site comparisons and multi-system time-transfers between the AOS and the BIPM prove the high performance of TTS-3. The time transfer results:
- GPS C/A RMS 2.0 ns,
- GPS P3 RMS 0.6 ns,
- GLONASS P RMS 0.5 ns.

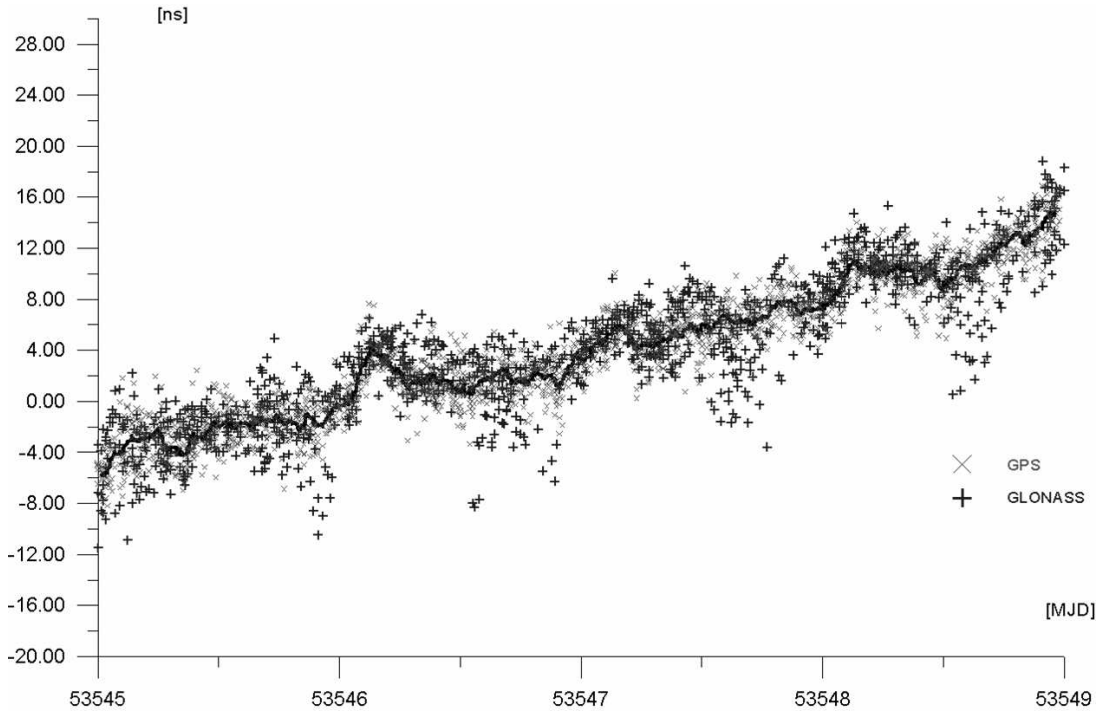

Figure 1: AOS/BIPM common-view, GPS+GLONASS P1 CODE

5. SUMMARY

The TTS-3 receiver integrates observations of all available navigation satellites: GPS, GLONASS, WAAS and EGNOS. Besides it serves as a base for TTS-4 observing also Galileo (under development). It uses GPS and GLONASS C/A-code, GLONASS P-code, GPS reconstructed P-code and P3 modes. The precision in multi-channel reconstructed GPS P-code mode, when using measurements of ionosphere and precise ephemerides should reach 1 ns for intercontinental and continental time links.

The system works under LINUX, providing multitasking and integration with networks and Internet and allows an easy upgrade of presently available and future options.

Session 5

GLOBAL REFERENCE FRAMES AND EARTH ROTATION :
Impact of the gravitational satellite missions (CHAMP, GRACE, GOCE),
new techniques (ring laser etc.), new international projects
(IAG-GGOS, GALILEO)

SYSTÈMES DE RÉFÉRENCE GLOBAUX ET ROTATION DE LA TERRE :
Impacts des missions des satellites gravitationels (CHAMP, GRACE, GOCE),
nouvelles techniques (ring laser etc.), nouveaux projets internationaux
(IAG-GGOS, GALILEO)

ESTIMATION OF DIURNAL POLAR MOTION TERMS USING RING LASER DATA

T. KLÜGEL[1], U. SCHREIBER[2], W. SCHLÜTER[1], A. VELIKOSELTSEV[2], M. ROTHACHER[3]
[1] Bundesamt für Kartographie und Geodäsie
Fundamentalstation Wettzell, Sackenrieder Str. 25, D-93444 Kötzting
e-mail: kluegel@wettzell.ifag.de, schlueter@wettzell.ifag.de
[2] Forschungseinrichtung Satellitengeodäsie, TU München
Fundamentalstation Wettzell, Sackenrieder Str. 25, D-93444 Kötzting
e-mail: schreiber@wettzell.ifag.de
[3] GeoForschungsZentrum Potsdam
Telegrafenberg, D-14473 Potsdam
e-mail: rothacher@gfz-potsdam.de

1. INTRODUCTION

Today, Earth rotation parameters are routinely obtained using the geodetic space techniques VLBI (Very Long Baseline Interferometry), SLR (Satellite Laser Ranging), GPS (Global Positioning System) und DORIS (Doppler Orbitography by Radiopositioning Integrated on Satellite). Technical progress over the last decades resulted in a precision of recently 0.01 milliseconds in length of day and 0.1 milliarcseconds in pole coordinates. The common principle is the relative measurement of rotation by observing reference points, stars or satellites, outside the rotating Earth. All these techniques require global networks and structures for the observation and data handling, which are coordinated by the international services IVS, ILRS, IGS and IDS.

The absolute measurement of rotation using inertial rotation sensors is a completely different approach. Mechanical gyroscopes measuring the coriolis force are by far not sensitive enough to detect Earth rotation variations. Instruments measuring the centrifugal acceleration as a part of the total gravity vector, gravimeters and tiltmeters, are basically sensitive to Earth rotation variations, but even the excellent resolution of superconducting gravimeters of 10^{-11} g is not sufficient to resolve short-period Earth rotation variations. In contrast, laser gyroscopes use the Sagnac effect, where the small wavelength of the laser light allows an extreme high resolution. An adequate sensitive laser gyroscope attached to the Earth gives us instantaneous access to the spin of the Earth and the orientation component of its axis in the observed direction. For the determination of the complete rotation vector, three linear independent laser gyroscopes are required.

The basic goals of laser gyroscopes for Earth rotation monitoring are:

- Detection of short-term spin fluctuations with a resolution of 10^{-9}
- Detection of short-term polar motions with a resolution of 0.2 mas or 6 mm
- Near real time acquisition with a temporal resolution of 1 hour or less

It is not expected that laser gyroscopes will ever reach the excellent long-term stability of the geodetic space techniques. However, the increasing interesting short-time range is poorly covered by these techniques. Furthermore ring laser measurements are quasi continuous, while VLBI and SLR usually have a resolution of one day, with gaps of some days.

2. THE WETTZELL RING LASER "G"

Ring lasers are inertial rotation sensors using the Sagnac effect, which is the frequency splitting of two counter-rotating laser beams due to rotation (Sagnac 1913). Four mirrors form a closed light path in a ring resonator. The resonator cavity is filled with the laser medium, a helium/neon gas mixture. The plasma is excited at one location by an alternating electrical field generating two counter-propagating laser beams. When this assembly is rotating, the (also rotating) observer sees a frequency difference between the co-rotating and the counter-rotating beam being proportional to the rotation rate. This beat frequency or Sagnac frequency Δf is described by the Sagnac formula for active resonators:

$$\Delta f = \frac{4A}{\lambda P}\vec{n} \cdot \vec{\Omega}$$

- A enclosed area
- P perimeter (beam path length)
- λ optical wavelength
- $\vec{n}$ normal vector to A
- $\vec{\Omega}$ rotation vector

The task is to measure the frequency of the optical interference pattern, approximately 12 magnitudes below the optical frequency, with a relative precision of 10^{-9}.

The large ring laser "G" has been developed on behalf of the Research Group Satellite Geodesy (FGS) by the Bundesamt für Kartographie und Geodäsie (BKG) and the Forschungseinrichtung Satellitengeodäsie of the Technical University Munich (FESG) in close cooperation with the University of Canterbury in Christchurch, New Zealand. "G" is in operation since 2001. The unique resolution and stability was reached by its size of 4 m x 4 m, its extreme mechanical and thermal stability resulting from the use of the glass ceramic Zerodur as base material, and the use of dielectric mirrors with minimum losses. The instrument operates under stable thermal conditions (annual variation less than 0.6 deg C in an underground laboratory at the Fundamentalstation Wettzell, Bavaria. A detailed description of the "G" ring laser is given in Klügel et al. (2005) or at http://www.wettzell.ifag.de/LKREISEL/G/LaserGyros.html. Table 1 shows the basic properties of three large ring lasers. Due to its construction, the "G" ring laser is the most stable instrument which is an important condition for monitoring Earth rotation variations.

Ring	Location	Area $[m^2]$	Δf $[Hz]$	Resolution $[rad/(s\sqrt{Hz})]$	Stability $[\Delta f/f]$
C-II	Christchurch	1	79.4	$4.8 \cdot 10^{-10}$	$1.0 \cdot 10^{-6}$
G	Wettzell	16	348.6	$9.1 \cdot 10^{-11}$	$1.0 \cdot 10^{-8}$
UG1	Christchurch	366	1512.8	$7.3 \cdot 10^{-12}$	$1.0 \cdot 10^{-7}$

Table 1: Properties of the 3 most sensitive ring lasers.

3. ORIENTATION CHANGES

A horizontally installed ring laser being rigidly attached to the Earth measures the projection of the Earth rotation vector onto the laser plane normal vector. Considering the orientation the inner product between the rotation and the normal vector can be expressed as:

$$\vec{n} \cdot \vec{\Omega} = |\Omega| \cdot \sin(\phi + \delta_N) \cdot \cos \delta_E$$

where ϕ is the geographic latitude and δ_N and δ_E are small angular variations towards North and East, respectively. Consequently, both local tilts of the instrument and motions of the Earth rotation axis affect the ring laser signal. As an example, an angular variation of 1 μrad (200 mas) towards North results in a Sagnac frequency variation of $1 \cdot 10^{-6}$, whereas the same variation towards East alters the Sagnac frequency by only $5 \cdot 10^{-13}$, which ist negligible.

As local tilts due to ground deformations cannot be avoided, the orientation of the ring laser has to be monitored. For this purpose a set of six specially designed platform tiltmeters are employed on the ring laser body measuring in different directions. The high resolution of these vertical pendulums and the excellent environmental conditions allow the detection of tilts at the nanorad level. In the case of tidal effects, the ring laser feels only the geometric part of tidal deformation, while tiltmeters are additionally sensitive to tidal attraction. However, not only the direct attraction of the tidal bodies, but also the change of the potential due the shifted masses of the tidally deformed Earth has to be taken into account. This is expressed by the Love number k, that gives the fraction of the additional deformation potential V_d relative to the tidal potential of the attracting bodies V_t:

$$V_{at} = V_t + V_d = (1 + k)V_t$$

The total attraction potential V_{at} is subtracted from the tiltmeter timeseries before being transformed into variations of the Sagnac frequency.

4. DIURNAL POLAR MOTION

The torques of Sun and Moon on the ellipsoidal and tilted Earth cause a circular motion of the instantaneous rotation pole in an Earth-fixed frame. The same physical cause generates precession and nutation of the Earth's axis in space. In an Earth-fixed frame these motions have diurnal periods, because the observer rotates with the Earth. In a space-fixed frame the periods are identical to the nutation periods (14 d, 28 d, 0.5 y, 1 y, 18.6 y, ...) and also known as Oppolzer terms. Earth rotation parameter estimations using space geodetic techniques yield the complete rotation matrix of the Earth and are basically not able to distinguish between space-related (nutation terms) and Earth-related (Oppolzer terms) components. The Oppolzer terms have to be introduced in the analysis.

Ring lasers on the other hand are only sensitive to Earth-related motions of the rotation axis and provide the only technique to directly measure diurnal polar motion. Fourier spectra of ring laser timeseries clearly show the presence of this signal (fig. 2). The diurnal polar motion is superimposed on the Chandler/annual wobble. A comparison of the expected timeseries with the measured Sagnac frequency shows that it is recently not possible to identify the Chandler/annual wobble in the data due to instrumental drifts (fig. 1).

A detailed theoretical investigation of diurnal polar motion for an elastically deformable Earth has been carried out by McClure (1973). The model extension for an anelastic Earth with liquid core (Wahr 1981, Brzezinski 1986, Frede & Dehant 1999) did not result in a major difference

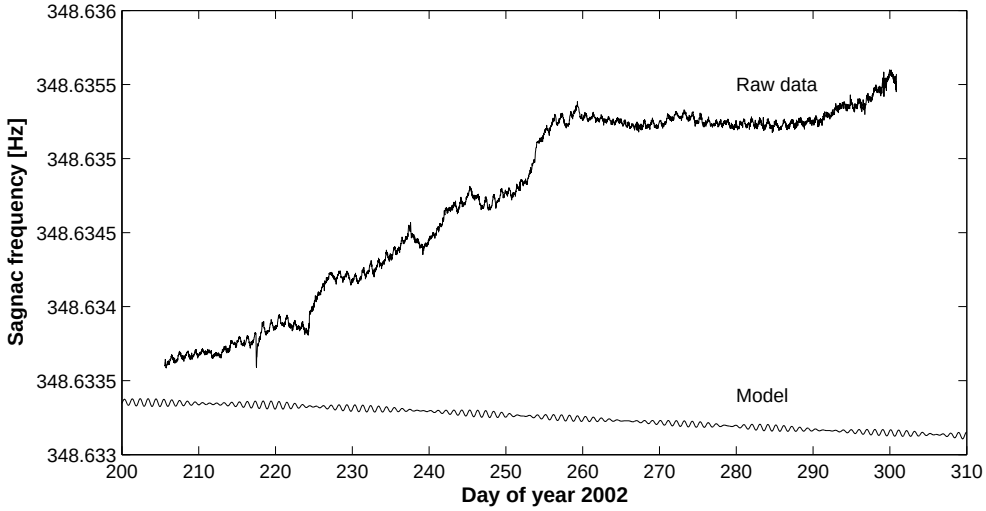

Figure 1: "G" ring laser raw timeseries (top) and predicted timeseries (bottom) from diurnal polar motion model plus Chandler/annual wobble.

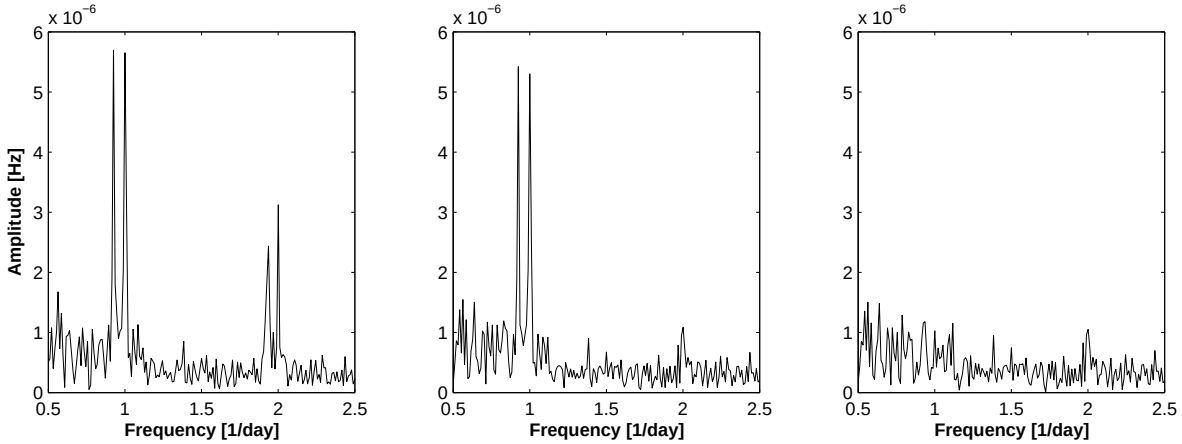

Figure 2: Fourier spectra of "G" ring laser data. Left: raw timeseries, middle: after removal of tidal tilt effects, right: after removal of diurnal polar motion model.

for the motion of the rotation axis. The diurnal polar motion terms are expressed in terms of fundamental arguments corresponding to particular orbital parameters. The procedure for the generation of the model timeseries is given in Scheiber et al. (2004).

For the estimation of the amplitudes of the diurnal polar motion components, the Bernese GPS software 5.0 has been modified for processing ring laser data in order to use the ERP estimation routines. Six continuous timeseries between 35 and 96 days long and a concatenated set of these data with a total contents of 401 days were analyzed. The data was resampled to 30-min averages and corrected for local and tidal tilts using attraction-corrected tiltmeter data. Only the amplitudes of the 8 strongest components were estimated. The formal errors of the individual solutions (table 2) are less than 1.2 mas for the group of shorter and less than 0.4 for the group of longer timeseries. The solution of the total data set shows formal errors of less than 0.2 mas. The estimated amplitudes (table 3) show in some cases good agreement with the expected model value, in other cases the amplitudes deviate from the model by more than 3 sigma. The total data set, however, yields amplitudes matching well the model.

Astron. arguments						wave	2002a	2002b	2003a	2003b	2004a	2004b	Total
l	l'	F	D	Ω	Θ		35 d	96 d	76 d	53 d	91 d	50 d	401 d
0	0	0	0	0	-1	K1	1.16	0.27	0.22	0.53	0.37	0.42	0.14
0	0	2	0	2	-1	O1	0.39	0.21	0.22	0.47	0.30	0.37	0.13
0	0	2	-2	2	-1	P1	1.16	0.25	0.23	0.53	0.27	0.42	0.12
1	0	2	0	2	-1	Q1	0.40	0.20	0.20	0.46	0.21	0.37	0.12
0	0	2	0	1	-1			0.21	0.22		0.30		0.13
0	0	0	0	1	-1			0.22	0.25		0.37		0.14
1	0	0	0	0	-1	M1		0.20	0.20		0.21		0.11
-1	0	0	0	0	-1	J1		0.20	0.20		0.21		0.11

Table 2: Formal errors in milliarcseconds.

Astron. arguments						wave	2002a	2002b	2003a	2003b	2004a	2004b	Total	Model
l	l'	F	D	Ω	Θ		35 d	96 d	76 d	53 d	91 d	50 d	401 d	
0	0	0	0	0	-1	K1	-7.70	-8.92	-5.67	-5.81	-8.75	-8.13	-7.44	-8.71
0	0	2	0	2	-1	O1	6.25	6.96	5.70	7.25	7.65	10.91	6.96	6.87
0	0	2	-2	2	-1	P1	0.89	2.99	1.89	2.87	3.90	1.72	2.40	3.00
1	0	2	0	2	-1	Q1	1.32	1.89	0.74	-0.38	1.55	3.47	1.56	1.36
0	0	2	0	1	-1			1.36	-0.03		1.13		1.39	1.30
0	0	0	0	1	-1			-2.35	-1.33		-0.25		-1.15	-1.18
1	0	0	0	0	-1	M1		-1.44	-0.03		0.25		-0.44	-0.52
-1	0	0	0	0	-1	J1		0.20	-0.10		-1.30		-0.40	-0.50

Table 3: Estimated amplitudes in milliarcseconds. Model amplitudes from Brzezinski (1986).

5. SUMMARY AND OUTLOOK

Among the inertial rotation sensors, only large ring lasers are recently able to monitor the rotation of the Earth continuously and with a resolution high enough for geodetic and geophysical applications. The world's most precise rotation sensor, the Wettzell "G" ring laser, resolves 10^{-8} of the Earth rotation rate, which is equivalent to 1 ms length of day or 2 mas polar motion. The minimum in the Allan deviation plot (fig. 3), which is adequate to describe resolution and stability, is reached after an integration time of 3 hours. Longer integration times suffer from instrumental drifts. The operation requires stable thermal and mechanical conditions and orientation monitoring in order to eliminate signals coming from local tilting.

Unlike for the geodetic space techniques, polar motion can directly be measured by ring lasers. From 6 timeseries covering 401 days of observations, the 8 largest diurnal polar motion terms were estimated with a formal error of less than 0.2 mas. A technical upgrade to improve resolution (shifts left branch of Allan deviation plot downwards) and stability (shifts minimum towards right) is in progress. This means that smaller signals like the effect of ocean tides or the atmosphere on Earth rotation may be detectable in future.

However by using one ring laser alone, one can not distinguish between variations of the Earth rotation rate and polar motions. Three linear independent instruments would eventually be required for the determination of the complete Earth rotation vector.

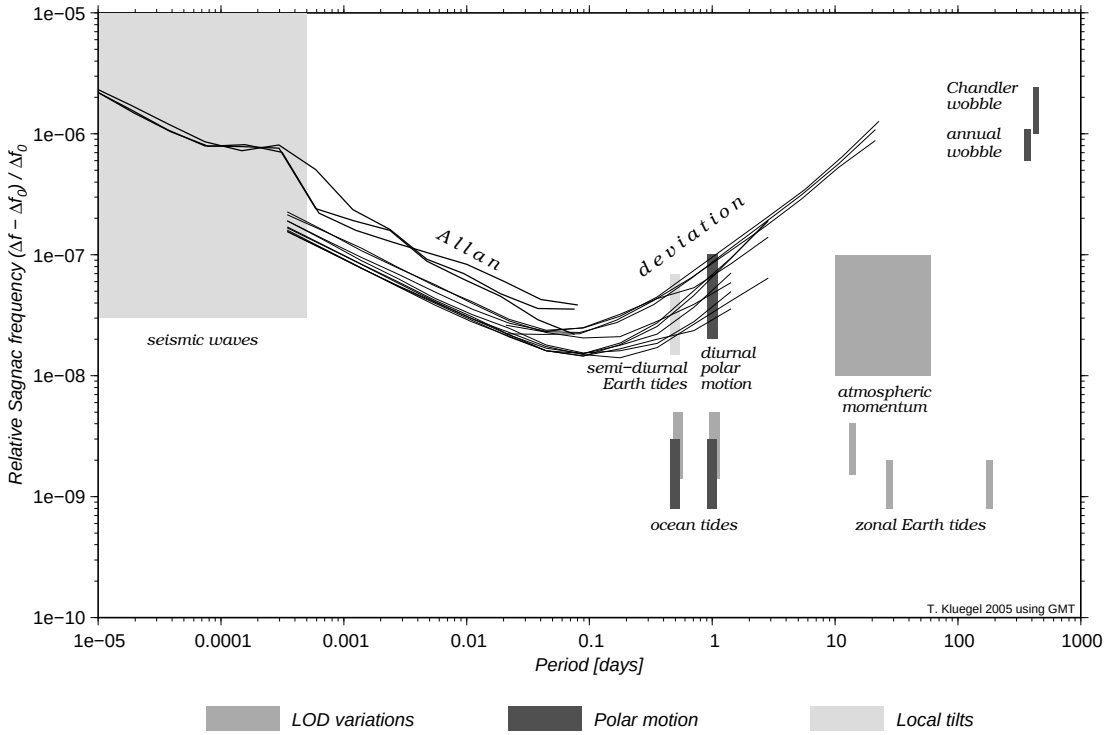

Figure 3: Resolution and stability of the "G" ring laser with respect to Earth rotation signals.

REFERENCES

Brzezinski A., 1986, "Contribution to the theory of polar motion for an elastic earth with liquid core", Manuscripta Geodaetica, 11, pp. 226–241.

Frede V., and Dehant V., 1999, "Analytical versus semi-analytical determinations of the Oppolzer terms for a non-rigid Earth", J. Geodesy, 73, pp. 94–104.

Klügel T., Schlüter W., Schreiber U., and Schneider M., 2005, "Grossringlaser zur kontinuierlichen Beobachtung der Erdrotation", Zeitschrift für Vermessungswesen, 130(2), pp. 99–108.

McClure P., 1973, "Diurnal polar motion", GSFC Rep. X-529-73-259, Goddard Space Flight Center, Greenbelt.

Sagnac M.G., 1913, "La démonstration de l'existence de l'éther lumineux a travers les mesures d'un intérferomètre en rotation", Comptes-Rendus de l'Académie des Sciences, 157, pp. 708–718.

Schreiber U., Velikoseltsev A., Rothacher M., Klügel T., Stedman G.E., and Wiltshire D.L., 2004, "Direct measurement of diurnal polar motion by ring laser gyroscopes", J. Geophys. Res., 109 (B6), 10.1029/2003JB002803, B06405.

Wahr J.M., 1981, "The forced nutations of an elliptical, rotating, elastic and oceanless earth", Geophys. J. R. Astr. Soc., 64, pp. 705–727.

PRESENT STATUS AND FUTURE OF THE IAG PROJECT GGOS

M. ROTHACHER
GeoForschungsZentrum Potsdam
Telegrafenberg, D-14473 Potsdam
e-mail: rothacher@gfz-potsdam.de

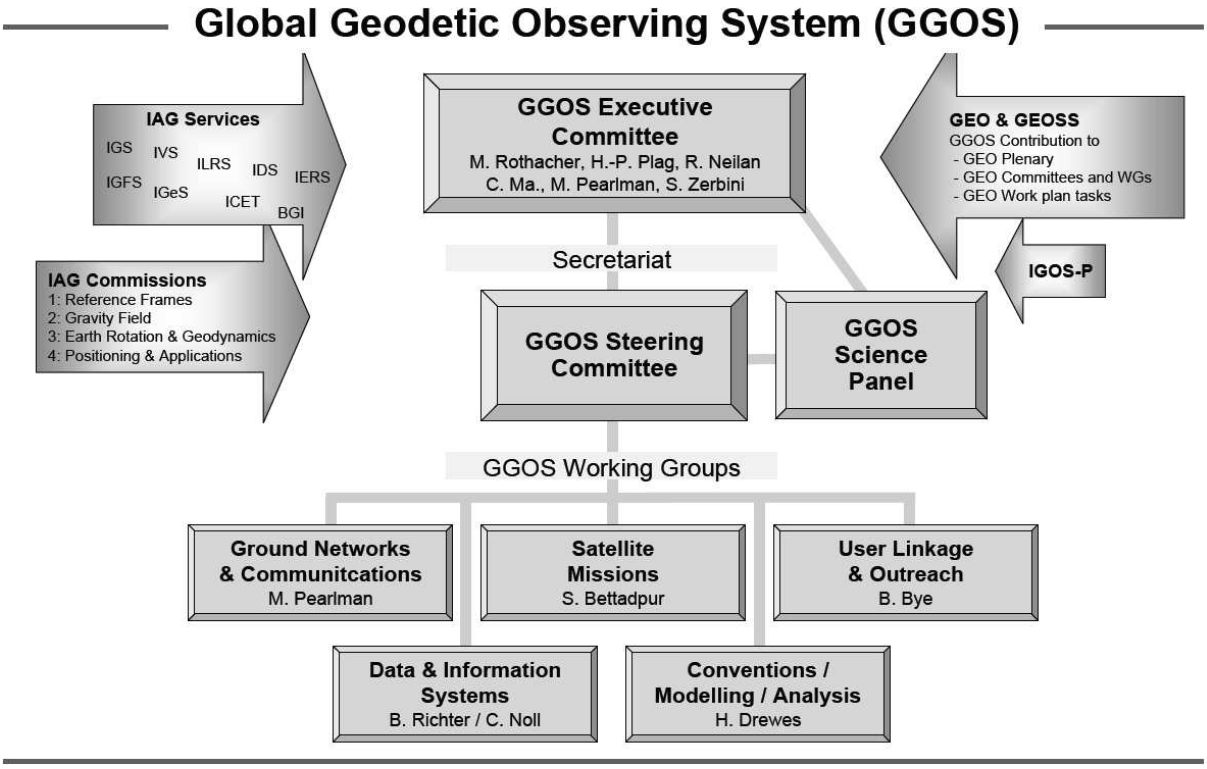

REFERENCES

Rothacher M., 2006, GGOS: the IAG contribution to Earth observation, *IGS Workshop 2006 "Perspectives and Visions for 2010 and beyond", May 8-12, Darmstadt, Germany.*

http://nng.esoc.esa.de/ws2006/GGOS2.pdf

SOME PROPERTIES OF EMISSION COORDINATES

J.M. POZO
SYRTE, Observatoire de Paris – CNRS
61, Avenue de l'Observatoire. F-75014 Paris, France
Departament de Física Fonamental, Universitat de Barcelona
Martí i Franquès, 1. E-08028 Barcelona, Spain
e-mail: jose-maria.pozo@obspm.fr

ABSTRACT. 4 emitters broadcasting an increasing electromagnetic signal generate a system of relativistic coordinates for the space-time, called emission coordinates. Their physical realization requires an apparatus similar to the one of the Global Navigation Satellite Systems (GNSS). Several relativistic corrections are utilized for the current precisions, but the GNSS are conceived as classical (Newtonian) systems, which has deep implications in the way of operating them. The study of emission coordinates is an essential step in order to develop a fully relativistic theory of positioning systems. This talk presents some properties of emission coordinates. In particular, we characterize how any observer sees a configuration of satellites giving a degenerated system and show that the trajectories of the satellites select a unique privileged observer at each point and, for any observer, a set of 3 orthogonal spatial axes.

1. INTRODUCTION

Practically all experiments in general relativity and all the uses of relativity in any application are done from a classical (Newtonian) conceptual framework. In this framework, the "relativistic effects" are added with the same status as any non-desired perturbation (gravitational influence of other planets, effects of the atmosphere ...). This is made with corrections of first order, coming from general relativity when compared with classical mechanics, in weak gravitational fields and with small velocities (PostNewtonian formalism). Typically, this is what is done in the Global Navigation Satellite Systems (GNSS), as the GPS or the future GALILEO, where the corrections from both special and general relativity cannot be neglected.

This approach is perfectly justified from a practical and numerical point of view. However, if the resolutions are increased (more accurate clocks), it will be necessary to consider corrections of third or higher order. Then, it can be wondered if it would not be more convenient to change the framework to an exact formulation in general relativity. This would imply to abandon the classical framework. Obviously, this is a jump with many implications and difficulties of many different kinds: from technical to sociological. The first one is that such a relativistic theory of positioning systems has not been developed. Our project is aimed to develop a theory of positioning systems in the framework of general relativity. This is a long term project which is still in a state of theoretical construction.

Four emitters broadcasting an increasing electromagnetic signal generate a system of space-time coordinates, the so called *emission coordinates*. The most natural case is the one in which the emitted signal is the proper time of the emitter. The emission coordinates of an event (the 4 signals received) can be immediately known by this event, thus they constitute an immediate

relativistic positioning system. Its physical construction is very similar to the one realized by the GNSS, where the emitters are satellites. But the way of operating and conceiving the positioning systems is very different. This is reflected in the fact that the 4 signals emitted by the satellites are not considered as primary space-time coordinates, but the satellites are used as mere beacons to obtain separately the time and the position in some predefined coordinates for the Earth. The study of emission coordinates is aimed to develop a fully relativistic theory of positioning and reference systems. A complete theory should be able to substitute the nowadays classical perturbative approach to the satellite navigation and to provide a different framework for experimental tests of general relativity.

Emission coordinates and the associated positioning systems has been extensively studied in 2-dimensional space-times, where several strong analytic results have been obtained (Coll 2001, Coll 2002). Unfortunately, they are not trivially generalizable for the real case of 4-dimensional space-times, where a more deep study is needed. But, some very interesting global and local properties have been already obtained for 3 and 4 dimensions (Derrick 1981, Coll and Morales 1991, Rovelli 2002, Blagojević et al. 2002, Pozo and Coll 2005). In this work we briefly explain some local properties of 4-dimensional emission coordinates.

2. EMISSION COORDINATES. A DEFINING DESCRIPTION

The first ingredient in our approach to positioning systems is the use of the 4 electromagnetic signals emitted by each set of 4 satellites, directly as coordinates for the domain of interest of the space-time. This type of coordinates are called *emission coordinates*. The usual treatments of any relativistic problem, takes a somehow classical description of the space-time, using one time-like coordinate which defines the instantaneous 3-dimensional spaces (synchronization) and 3 space-like coordinates to coordinate this sequence of spaces. This description is very adapted to our intuition about space and time. However, when relativity is not negligible, the needed synchronization is a convention which is not absolutely defined. For inertial observers in flat space-time we can use the Einstein convention, which is dependent on the observer chosen. For general observers, even in flat space-time, this is still worse since no standard synchronization is well defined.

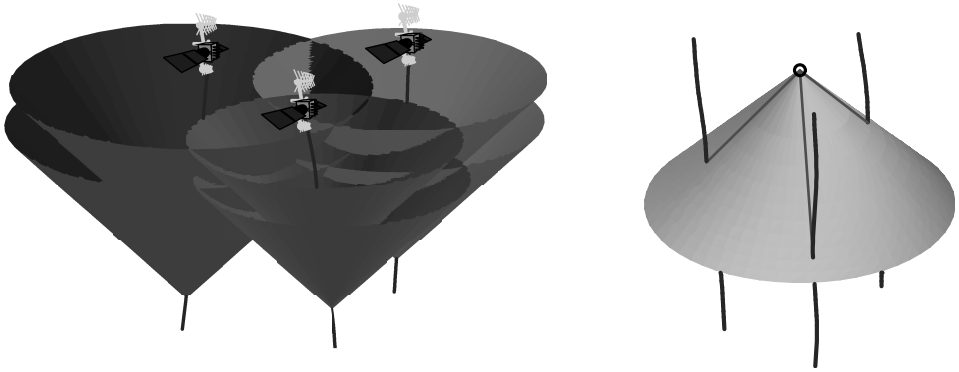

Figure 1: Representation of 3 emitters in a 3-dimensional space-time (time vertical). The lines are the space-time trajectories (world-lines) of the emitters. The left figure shows the space-time surfaces visited by each value of the signals emitted (future light-cones), which defines the grid of emission coordinates. The right figure shows the past light-cone of an event. Its intersection with the trajectories of the emitters gives the emission coordinates of this event.

The 4 families of hypersurfaces defining emission coordinates are light-like. This means that the natural covectors $\{\mathrm{d}\tau^1, \mathrm{d}\tau^2, \mathrm{d}\tau^3, \mathrm{d}\tau^4\}$ are light-like: $\mathrm{d}\tau^A \cdot \mathrm{d}\tau^A = 0$. In fact the metrically associated vectors $\vec{\ell}^A = g^*(\mathrm{d}\tau^A)$ (or with index notation, $(\vec{\ell}^A)^\mu = g^{\mu\nu}(\mathrm{d}\tau^A)_\nu$) are the directions defined by the light-like geodesics followed by the signals (rays). Observe that this class of

coordinates is radically different from the usual decomposition into space and time, where we have 1 time-like coordinate and 3 space-like coordinates.

3. PROPERTIES OF THE METRIC

The light-like nature of the covectors implies that the contravariant metric in emission coordinates has vanishing diagonal elements:

$$(g^{AB}) = \begin{pmatrix} 0 & g^{12} & g^{13} & g^{14} \\ g^{12} & 0 & g^{23} & g^{24} \\ g^{13} & g^{23} & 0 & g^{34} \\ g^{14} & g^{24} & g^{34} & 0 \end{pmatrix}$$

And, since the covectors $\mathrm{d}\tau^A$ are future oriented, the extra-diagonal elements are all positive $g^{AB} > 0$. Besides, the Lorentzian signature of the space time implies the triangular inequalities

$$A < B+C, \quad B < A+C, \quad C < A+B \quad \text{where} \quad A \equiv \sqrt{g^{14}g^{23}}, \quad B \equiv \sqrt{g^{24}g^{13}}, \quad C \equiv \sqrt{g^{34}g^{12}}\,.$$

The determinant of the metric can be factorized into

$$|g^{AB}| = (A+B+C)(A-B-C)(B-A-C)(C-A-B)\,.$$

Given an observer u (that is, a field of unit time-like vectors representing the *4-velocity* of a local laboratory) the light-like vector $\vec{\ell}^A$ is split into

$$\vec{\ell}^A = \nu^A(u + \hat{n}^A),$$

where ν^A is a positive scalar representing the *frequency* of the signal seen by the observer, and $\hat{n}^A$ is a space-like unitary vector, $\hat{n}^A \cdot \hat{n}^A = -1$, representing the direction toward which the observer sees the propagation of the signal in its space.

The angle θ^{AB} between the directions $\hat{n}^A$ and $\hat{n}^B$ of two different signals (the apparent angle between the two signals) are given by

$$c^{AB} \equiv \cos\theta^{AB} = -\hat{n}^A \cdot \hat{n}^B\ .$$

Result *Given an arbitrary observer at an event, 4 light-like directions, $d\tau^A$, are linearly dependent at this event if and only if the observer sees the apparent sources of the signals τ^A arranged in a circle in its celestial sphere.*

4. THE INTRINSIC SPLITTING OF THE METRIC AND THE CENTRAL OBSERVER

Given a system of emission coordinates we can ask if there exists some observers who see the constellation of satellites arranged in some special configuration. For instance, in 3 dimensions we can ask for an observer who see the 3 satellites in his celestial *circumference* with all the angles equal: $\theta^{12} = \theta^{13} = \theta^{23} = 2\pi/3$. This property can be generalized to 4 dimensions by asking for the 6 angles θ^{AB} between the 4 emitters to be equal. This would correspond to an observer who would see the 4 emitters arranged in a regular tetrahedron in its celestial sphere. This property is too restrictive. A different generalization is to ask for the 4 solid angles defined by the trihedral of each 3 emitters to be equal: $\theta^{123} = \theta^{124} = \theta^{134} = \theta^{234} = \pi$. This corresponds to an observer who sees the 4 emitters in an *equifacial tetrahedron* in its celestial sphere. This property can be equivalently characterized by asking for the angle between each pair of directions to be equal to the angle formed by the complementary pair: $\theta^{12} = \theta^{34}$, $\theta^{13} = \theta^{24}$ and $\theta^{23} = \theta^{14}$. An observer seeing the four emitters in this configuration will be called a *Central observer*. Let us remark that (although called central) this property does not selects a position or an event in the space-time, but a velocity at each event.

Result *Given any system of emission coordinates the Central observer exists and is unique.*

An equifacial tetrahedron defines 3 orthogonal axes in the space. This implies that the 4 trajectories of the emitters also select 3 orthogonal spatial directions, orthogonal to the central observer. In addition, since any two observers define a pure boost that relate both, by applying this boost to the spatial axes we obtain the following:

Result *For any observer, the trajectories of the 4 emitters select 3 privileged orthogonal axis in its space.*

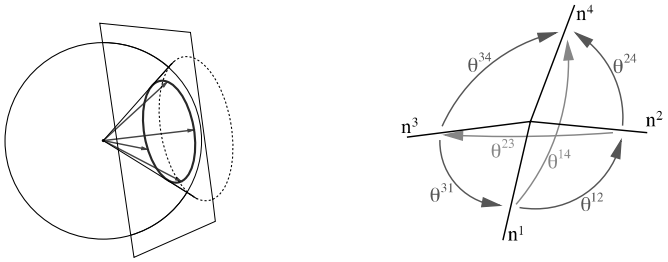

Figure 2: The left figure represents 4 points in the celestial sphere of an observer which lie in a unique circle (the directions lie in a cone). The system of emission coordinates is degenerate at the events where any observer see the 4 emitters in this configuration. The right figure represents 4 directions and the six planar angles between them.

This result is intimately related with the existence of the following splitting of the metric:

$$(g^{AB}) = \begin{pmatrix} \mu^1 & 0 & 0 & 0 \\ 0 & \mu^2 & 0 & 0 \\ 0 & 0 & \mu^3 & 0 \\ 0 & 0 & 0 & \mu^4 \end{pmatrix} \begin{pmatrix} 0 & \hat{C} & \hat{B} & \hat{A} \\ \hat{C} & 0 & \hat{A} & \hat{B} \\ \hat{B} & \hat{A} & 0 & \hat{C} \\ \hat{A} & \hat{B} & \hat{C} & 0 \end{pmatrix} \begin{pmatrix} \mu^1 & 0 & 0 & 0 \\ 0 & \mu^2 & 0 & 0 \\ 0 & 0 & \mu^3 & 0 \\ 0 & 0 & 0 & \mu^4 \end{pmatrix}$$

Here, the 6 degrees of freedom of the metric are split into two types of parameters, which behave in clearly different ways when the series broadcasted by the emitters is changed (that is, when the clocks on board the satellites are modified):

- 4 parameters $\{\mu^A\}$ which scale, each of them, linearly with the series broadcasted by the corresponding satellite and are independent of the others.
- 3 parameters (2 degrees of freedom) $\hat{A}, \hat{B}, \hat{C}$ which are invariant respect to the change of the series broadcasted. They only dependent on the satellite world-lines.

This splitting is a promising tool in order to study the consequences of the derive of the clocks, the election of different corrections for this, and the possible role that some arbitrary or geometrically justified synchronization could have in the positioning system.

5. REFERENCES

Blagojević M., Garecki J., Hehl F.W., and Obukhov Yu.N., 2002, "Real null coframes in general relativity and GPS type coordinates", Phys. Rev. D, 65, pp. 044018.

Coll B., and Morales J.A., 1991, "Symmetric frames on Lorentzian spaces", J. Math. Phys., 32, pp. 2450–2455.

Coll B., 2001, "Elements for a theory of relativistic coordinate systems. Formal and physical aspects", Reference Frames and Gravitomagnetism, Proc. of the Spanish Relativistic Meeting ERE2000, eds. J. F. Pascual-Sanchez et al., World Scientific, Singapore, pp. 53–65.

Coll B., 2002, "A principal positioning system for the Earth", JSR 2002, eds. N. Capitaine and M. Stavinschi, Pub. Observatoire de Paris, pp. 34–38.

Derrick G.H., 1981, "On a completely symmetric choice of space-time coordinates", J. Math. Phys., 22, pp. 2896–2902.

Pozo J.M., and Coll B., 2005, Intern. school: Relativistic Coordinates, Reference and Positioning Systems, held in Salamanca, February 2005. The results will be collected in a series of papers in preparation.

Rovelli C., 2002, "GPS observables in general relativity", Phys. Rev. D, 65, pp. 044017.

WAVELET ANALYSIS OF TEC MEASUREMENTS OBTAINED USING DUAL FREQUENCY SPACE AND SATELLITE TECHNIQUES

A. KRANKOWSKI[1], T. HOBIGER[2], H. SCHUH[2], W. KOSEK[3] and W. POPIŃSKI[4]
[1]Institute of Geodesy, University of Warmia and Mazury in Olsztyn, Poland
[2]Institute of Geodesy and Geophysics, Vienna University of Technology, Austria
[3]Space Research Centre, Polish Academy of Sciences, Warsaw, Poland
[4]Central Statistical Office, Warsaw, Poland
e-mail: kand@uwm.edu.pl

ABSTRACT. An extensive database of Total Electron Content (TEC) measurements has become available from both ground- and space-based observations. Global Positioning System (GPS) and Very Long Baseline Interferometry (VLBI) observations collected at the IGS (International GNSS Service) and the IVS (International VLBI Service for Geodesy and Astrometry) stations over Europe were used to obtain TEC data during the time interval 1995 till 2003. In this paper, the wavelet analysis is used to determine the wavelet time-frequency spectra of TEC data above one European collocation station - Wettzell. The GPS and VLBI TEC time series of quiet and disturbed ionospheric conditions, utilized in this study, cover one solar cycle. A very good agreement between semidiurnal, diurnal, semiannual, and annual oscillations of TEC estimated using GPS and VLBI observations was obtained. The diurnal and annual oscillations are the most energetic and clearly visible ones especially during increasing and maximum solar activity.

1. INTRODUCTION

The wavelet analysis is a mathematical technique which is very useful for numerical analysis and manipulation of multidimensional discrete data sets. Originally applied in geophysics, analyzing the Earth orientation parameters and atmospheric angular momentum, the wavelet transforms were better and broadly formalized thanks to mathematicians', physicists', and engineers' efforts (Morlet 1983, Popiński et al. 2002). Therefore, the use of wavelet techniques in data analysis has grown, since it represents a synthesis of old techniques associated with robust mathematical results and efficient computational algorithms under the interest of a broad community (Daubechies et al. 1992). In a rapidly developing field, overview papers are particularly useful, and several good ones concerning wavelets are already available (Daubechies et al. 1992, Chui 1992). In atmospheric science applications, the main characteristic of the wavelet technique is the introduction of the time-frequency decomposition. A well known example of such a feature can be found in the musical structure, where it has been interpreted as events localized in time. Although it belongs to a more complex structure, a piece of music can be understood as a set of musical notes characterized by four parameters: frequency, time of occurrence, duration and intensity (Daubechies et al.1992, Lau and Weng 1995).

In the last decades, the wavelet technique has been extensively adopted in atmospheric science (Gambis 1992, Krankowski et al. 2005). In the last years numerous attempts were made to compare TEC values obtained from different ground- and space-based observations (Codrescu et al. 2001, Orús et al. 2002, Balehaki et al. 2003). Over the last decade, an extensive database of TEC measurements has become available from GPS and VLBI. The GPS satellites

continuously provide TEC data (since 1994) through the world-wide network of GPS ground receivers. Earlier than GPS the VLBI technique has provided TEC data for more than 20 years (since 1984), collected at IVS (Hobiger et al. 2005).

In this work, the Morlet wavelet transform (MWT) is used to determine the wavelet time-frequency spectra of TEC data above one European collocation station - Wettzell. The GPS and VLBI TEC time series of quiet and disturbed ionospheric conditions, utilized in this study, cover one solar cycle (from 1995 to 2003).

2. DATA

The absolute TEC and instrumental biases were estimated using a single site algorithm (Baran et al. 1997). The relationship between the ionospheric delay and TEC, and the difference between the dual-frequency code (P) and phase (Φ) measurements may be written:

$$\Delta P[m] = M \cdot TEC/cos(z') + A_P + \varepsilon_P \qquad \Delta\Phi[m] = M \cdot TEC/cos(z') + A_\Phi + \varepsilon_\Phi, \quad (1)$$

where the scaling factor M converts units of distance (m) to units of TEC (el/m^2), z' is the zenith angle, ε_P , ε_Φ are noise terms, A_P and A_Φ are equipment biases (A_Φ contains the phase ambiguity).

The diurnal variation of the vertical TEC (VTEC) is expressed as the series of harmonic terms:

$$VTEC = a_1 + a_2\Delta\phi + (a_3 + a_4)cos(s) + (a_5 + a_6)cos(2s) + ... + (a_{13} + a_{14})cos(6s) + a_{15}\Delta\phi^2 s, \quad (2)$$

where $s = \pi(LT - 14)/12$ and LT is the local solar time, $\Delta\phi$ is the latitudinal difference between the coordinates of the receiver and the sub-ionospheric point.

The VLBI observables at two different frequencies (2.3 and 8.4 GHz, S- and X-band) are performed in order to calculate the ionospheric delay and consequently to model the ionosphere above each station (Kondo 1991). In the Vienna TEC Model $VTEC_i(t)$ is calculated as a piecewise linear function (Hobiger et al. 2005):

$$VTEC_{VIENNA,i} = offset_i + rate_{i1}(t_1 - t_0) + rate_{i12}(t_2 - t_1) + ... + rate_{in}(t_n - t), \quad (3)$$

where $t \leq t_n$. After calculating the partial derivatives ($\frac{\delta TEC_{VIENNA,i}}{\delta offset_i}$; $\frac{\delta TEC_{VIENNA,i}}{\delta rate_{i,j}}$) a least-squares adjustment allows separation of the VTEC values from constant instrumental offset $\tau_{offset,i}$.

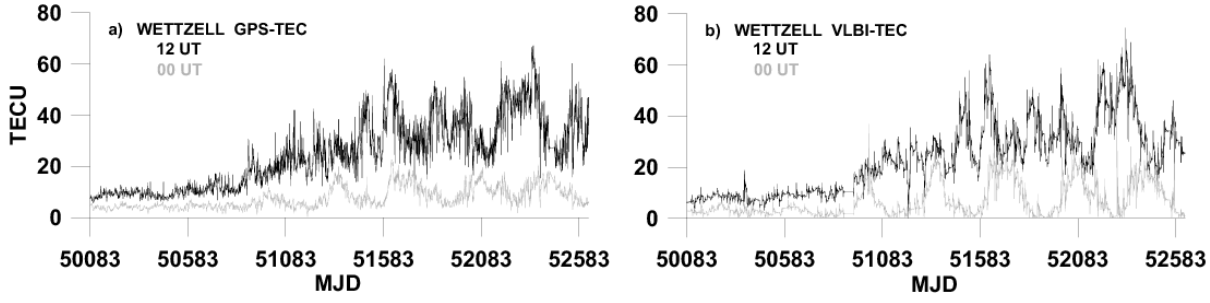

Figure 1: GPS (a) and VLBI TEC (b) measurements observed at noon (black line) and at midnight (grey line) over Wettzell during 1996 till 2002.

The accuracy of the TEC determined from GPS and VLBI data is of the order of 1-3 TECU ($TECU = 10^{16} electrons \cdot m^{-2}$). Figure 1 shows an example of TEC monitoring using GPS

and VLBI measurements over the mid-latitude European station Wettzell, i.e. TEC observed at noon and midnight for the period of 1996 to 2002. The day by day variation in TEC shows a strong dependence on solar activity; a very good agreement between diurnal variations of GPS and VLBI TEC observations was obtained.

3. WAVELET ANALYSIS

The wavelet transform coefficients are computed using the inverse discrete Fourier transform (DFT) by the following approximate formula (Chui 1992):

$$S(T,b) \simeq \frac{1}{n}\sqrt{|T|}\sum_{\nu=-n/2+1}^{n/2} \tilde{s}(\nu)\breve{\psi}(2\pi T\nu/n)\exp(i2\pi b\nu/n), \tag{4}$$

where T and $b = 0, 1, ..., n-1$, are the dilation (period) and translation (time shift) parameters, respectively, $\tilde{s}(\nu) = \sum_{k=0}^{n-1} s(k)\exp(-i2\pi\nu k/n)$ is the DFT of the analyzed signal $s(k), k = 0, 1, ..., n-1$, of the total length n, and

$$\breve{\psi}(\omega) = \sigma[\exp(-(\omega-2\pi)^2\sigma^2/2) - \exp(-(\omega-2\pi)^2\sigma^2/4)\exp(-\pi^2\sigma^2)] \tag{5}$$

denotes the continuous Fourier transform (CFT) of the Morlet wavelet function (Schmitz-Hübsch and Schuh 1999) with parameter $\sigma > 0$ which controls the frequency resolution of the wavelet transform. The corresponding time-frequency spectrum is defined as $|S(T,b)|^2$.

4. RESULTS

The MWT time-frequency spectra are shown in Figures 2 - 3. Figure 2 presents the MWT time-frequency spectra of TEC obtained using GPS (left panel) and VLBI (right panel) during the period March till June 2001. The semidiurnal and diurnal oscillations are clearly visible in these spectra. The time-frequency spectrum shows that the diurnal oscillation is more energetic than the semidiurnal one. Figure 3 presents the MWT time-frequency spectra of TEC data over Wettzell station during one period of solar activity (between 1996 and 2002). Semiannual and annual oscillations, respectively, can be seen in these Figures. The annual oscillation was energetic and clearly visible especially during periods of increasing and maximum solar activity. The semiannual oscillation was less energetic than annual oscillation, but it is also easy to distinguish in periods of increasing and maximum solar activity. From Figures 2 and 3 you can see that the time-frequency spectra of GPS-TEC and VLBI-TEC data over Wettzell station from one period of solar activity (between 1996 and 2002) show the same pattern for semidiurnal, diurnal, semiannual and annual oscillations. Results obtained using GPS and VLBI TEC measurements agree very well for all oscillations.

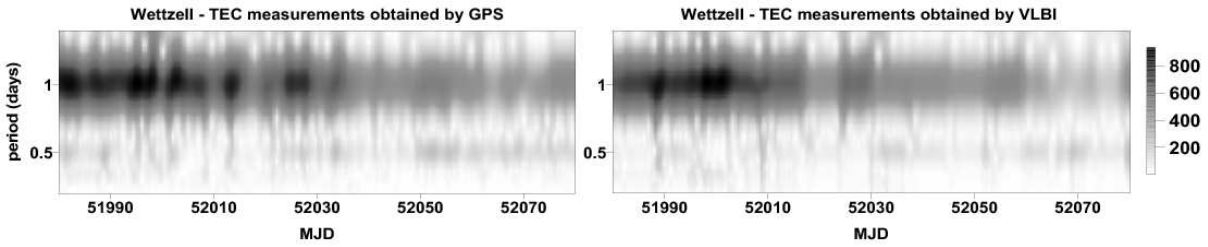

Figure 2: Wavelet time-frequency spectrum of the TEC data obtained using GPS (left panel)and VLBI (right panel) measurements over Wettzell during the period March till June 2001.

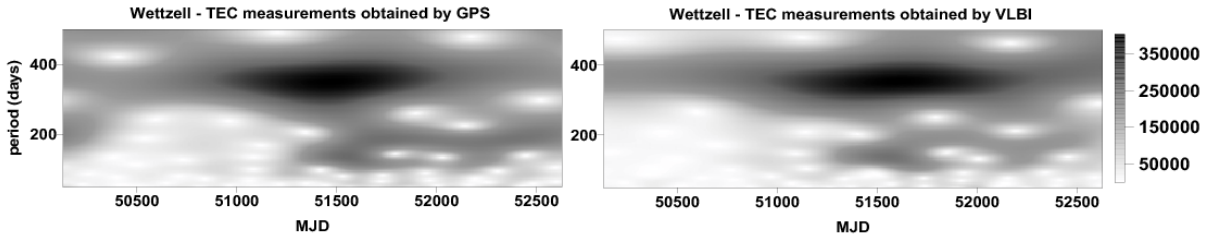

Figure 3: Wavelet time-frequency spectrum of the TEC data obtained using GPS (left panel) and VLBI (right panel) measurements over Wettzell for the period 1996 till 2002.

5. CONCLUSIONS

Information from time-frequency analysis of the TEC time series is very useful for investigation of the irregular variations in these data and also for the comparison of different time series. The time-frequency spectra of GPS-TEC and VLBI-TEC data over one collocation station Wettzell, computed by the MWT method, during one period of solar activity (between 1996 and 2002) show the same portrait for all detected oscillations: semidiurnal, diurnal, semiannual and annual. The information from time-frequency analysis can explain big prediction errors of these data especially during the ionospheric storms. GPS or VLBI TEC measurement will be used in further investigations aiming at creating the predicted TEC maps over Europe.

Acknowledgments. This study has been partly supported by grant 5T12E 033 23 of the Polish State Committee for Scientific Research. The Austrian Science Fund is acknowledged for funding project P16136-N06.

REFERENCES

Baran, L.W., Shagimuratov, I.I., Tepenitsina, N.J., 1997, Artificial Satellites 32, 1, 49–60.

Belehaki, A., Jakowski, N., Reinisch, B.W., 2003, Radio Science 38 6, 1105.

Codrescu, M.V., Beierle, K. L., Fuller-Rowell, T J., Palo, S.E., Zhang, X., 2001, Radio Science 36, 2, 325–333.

Chui, C.K., 1992, An Introduction to Wavelets, Wavelet Analysis and its Application - Vol. 1, Academic Press, Boston-San Diego.

Daubechies, I., Mallat, S., Willsky, A., 1992, IEEE Transactions on Information Theory 38 (2), 528–531.

Gambis, D., 1992, Annales-Geophysicae 10, 429–437.

Hobiger, T., Boehm, J., Schuh, H., 2005, in: Sanso, F. (ed), A Window on the Future Geodesy, International Association of Geodesy Symposia, Springer, Vol. 128, 131–136.

Kondo, T., 1991, Journal of the Communications Research Laboratory 38, 3, Japan, 613–622.

Krankowski, A., Kosek, W., Baran, L.W., Popiński W., 2005, Journal of Atmospheric and Solar-Terrestrial Physics 67, 12, 1147–1156.

Lau, K.M., Weng, H., 1995, Bulletin of the American Meteorological Society 76 (12), 2391–2402.

Morlet, J., 1983, in: Chen, C.H. (Ed.), Acoustic Signal/Image Processing and Recognition, No. 1 in NATO ASI. Springer-Verlag, New York, 233–261.

Orús, R., Hernández-Pajares, M., Juan, J.M., Sanz, J., García-Fernández, M., 2002, Journal of Atmospheric and Solar-Terrestrial Physics 64, 18, 2055–2062.

Popiński, W., Kosek, W., Schuh H., Schmidt, M., 2002, Studia geophysica et geodetica, 45, 455–468.

Schmitz-Hübsch, H., Schuh, H., 1999, in: F. Krumm and V.S. Schwarze (eds), Geodesy. The E. Grafarend Challenge of the Third Millennium, Springer, 125–135.

POTENTIAL CONTRIBUTION OF GALILEO TO THE TRF AND THE DETERMINATION OF ERPs

R. WEBER, S. ENGLICH
Institute of Geodesy and Geophysics, Univ. of Technology Vienna, Austria
e-mail: rweber@mars.hg.tuwien.ac.at

1. INTRODUCTION

In addition to the existing GPS and GLONASS systems the EC and ESA plan to launch an European Satellite Navigation System (GALILEO) till end of 2009. 30 GALILEO satellites will populate three orbital planes with an inclination of about 56^o. This paper strives to summarize potential improvements in geodetic point positioning and especially in the determination of Earth Rotation gained from the combined use of all three systems or at least of GPS+GALILEO.

We made use of continuous measurements of a global GPS reference station network (about 95 stations, constrained to IGSb00) and estimated Earth Rotation Parameters with daily and hourly resolution. Subsequently we added simulated observations of the upcoming European GALILEO Satellite Navigation System and investigated their impact (decrease of formal errors due to number of observations and geometry) on geodetic point determination, on derived tropospheric delays and on the ERPs. This calculations are performed with the Bernese V5.0 Software and are based on two-frequency GALILEO signals (L1 and L5 frequency bands).

As a first result the geodetic point determination by means of GPS can be improved by about 55% by adding data from a largely interoperable GALILEO system with all remaining intersystem biases modelled correctly. Thus the well-known accuracy currently achievable with GPS positioning in 24 hour sessions of about 2mm in plane and 4mm in height will decrease roughly by a factor of two.

2. CONTRIBUTION OF GALILEO TO THE DETERMINATION OF POLAR MOTION, LOD, NUTATION RATES

Because of the higher altitude (about 23 600 km) of the GALILEO satellites the revolution period is about 14 hours and 5 minutes and far outside of the unpleasant 2:1 resonance of the GPS satellites with Earth Rotation. Thus, the GALILEO data may help to distinguish between orbital effects propagating into the ERP estimates and geophysical variations in high- frequency Earth rotation.

The relations between LOD and Nutation Offset Rates and the time derivatives of the orbital elements read:

$$
\begin{aligned}
(UT1 \dot{-} UTC) &= -LOD = -\rho \cdot (\dot{\Omega} + \cos i \cdot \dot{u}_0) \\
\delta\dot{\Delta}\epsilon &= \cos\Omega \cdot \dot{i} + \sin i \sin\Omega \cdot \dot{u}_0 \\
\delta\dot{\Delta}\psi \cdot \sin\epsilon &= -\sin\Omega \cdot \dot{i} + \sin i \cdot \cos\Omega \cdot \dot{u}_0
\end{aligned}
$$

LOD :

> LOD estimates are related to changes in the orbital nodes Ω and changes in the argument of latitude u_0. Therefore a drift in the node common to all satellites or

a common drift in the argument of latitude will directly propagate into the LOD estimates. Due to the similar inclination of the orbital planes of GPS and GALILEO this effect maps into LOD with almost the same factor for both systems.

Nutation Rates :

For nutation rates changes in u_0 from unmodelled perturbing forces are even more critical ($\sin i \approx 0.82$) but may average out because of the different node values for the different orbital planes. GALILEO offers 3 additional planes sometimes matching the GPS planes, sometimes expanding the variety of orbital nodes.

In summary all parameters are affected by unmodelled perturbing forces most likely stemming from deficiencies in the applied solar radiation pressure models. The quality of the solar radiation pressure model available for the GALILEO satellites will be of crucial importance for the contributions of this Satellite Navigation System to the estimation of LOD and Nutation Rates. Errors in the Earth potential model (possible node drift) affects the higher GALILEO orbits less than the lower GPS orbits.

3. CONCLUSIONS

The future GALILEO satellite navigation system will offer another powerful tool for point positioning and the determination of ERPs. Together with the already existing GPS and GLONASS systems about 80 satellites in MEO orbits will be available for geodynamic studies. GALILEO satellites are not in deep resonance with Earth Rotation.

GALILEO will offer about the same number of observations as GPS. The GPS based point determination can be improved by about 55% if data from a fully interoperable GALILEO system is additionally used.

The GALILEO data may help to distinguish between orbital effects propagating into the ERP estimates and geophysical variations in high- frequency Earth rotation. Especially Ocean Tidal Terms close to the diurnal frequency will be better determined than with GPS.

The quality of the solar radiation pressure model available for the GALILEO satellites will be of crucial importance for the contributions of GALILEO to the estimation of LOD and Nutation Rates.

REFERENCES

Rothacher M.,G. Beutler, T.A. Herring and R.Weber, 1999a, Estimation of Nutation Using the Global Positioning System, Journal of Geophysical Research, Vol.104, No.B3, pp. 4835-4859.

Van der Marel H., 2004, Impact of GALILEO and Modernized GPS on Height Determination, Geowissenschaftliche Mitteilungen, TU-Wien, Heft 69, pp. 44-54.

POSTFACE

JOURNÉES 2007 SYSTÈMES DE RÉFÉRENCE SPATIO-TEMPORELS

"The Celestial Reference Frame for the Future"

Observatoire de Paris (France), 17-19 September 2007 (dates to be confirmed)

Scientific Organizing Committee

A. Brzeziński, Poland; N. Capitaine, France (Chair); P. Defraigne, Belgium; T. Fukushima, Japan; D.D. McCarthy, USA; M. Soffel, Germany; J. Vondrák, Czech R.; Ya. Yatskiv, Ukraine

Local Organizing Committee

P. Baudoin, O. Becker, C. Bizouard, S. Bouquillon, D. Gambis (Chair), A-M. Gontier, S. Lambert, J. Souchay

Conference location : Observatoire de Paris (probably on its Meudon site), France

Scientific objectives

The Journées 2007 "Systèmes de référence spatio-temporels", with the sub-title "The Celestial Reference Frame for the Future", will be organized at Paris Observatory. These Journées will be the eighteenth conference in this series whose main purpose is to provide a forum for discussion of researchers in the fields of celestial and terrestrial reference systems, Earth rotation, astrometry and time. The Journées 2007 will be focused on the issues related to the recent developments, perspectives of future realizations and scientific applications of the Celestial Reference Frame.

There will be presentations and discussions related to the new Division 1 Commission 52 "Relativity in Fundamental astronomy" and Working Groups on "Numerical standards in Fundamental astronomy" and "The Celestial Reference Frame" that have been established at the 26th IAU GA and also on the recent evolution in the concepts, terminology and results in fundamental astronomy. There will be a special session dedicated to nutation (organized by V. Dehant), 30 years after the IAU Colloquium No 78 on "Nutation and the Earth's rotation" that was organized in Kiev in 1977.

Scientific programme

The Scientific programme of the Journées 2007 will include topics related to:

Plans for the new ICRF
Plans for the analysis of VLBI data
Precession-nutation
Geophysical excitation of Earth rotation
Relativistic considerations in the new ICRF
Models incorporated in the new ICRF
Connecting the new ICRF to other wavelengths
Connecting the dynamical reference frame to the new ICRF
Gaia and the new ICRF

Contact : Nicole Capitaine, SYRTE, Observatoire de Paris,
61, avenue de l'Observatoire, 75014, Paris, France;
phone : 33 1 40 51 22 31; fax : 33 1 40 51 22 91; e-mail : n.capitaine@obspm.fr;

or see the web page of the Journées 2007 at: http://syrte.obspm.fr/journees2007/
(will be available in January 2007)

Printed and bound by:
Printing Division of the Space Research Centre PAS
Bartycka 18A, 00-716 Warsaw, Poland